

Puspendu Barik
Samiran Mondal *Editors*

Application of Quantum Dots in Biology and Medicine

Recent Advances

 Springer

Application of Quantum Dots in Biology and Medicine


Puspendu Barik · Samiran Mondal
Editors


Application of Quantum Dots in Biology and Medicine

Recent Advances

 Springer

Editors

Puspendu Barik 
S. N. Bose National Centre for Basic
Sciences
Kolkata, West Bengal, India

Samiran Mondal 
Department of Chemistry
Rammohan College
University of Calcutta
Kolkata, West Bengal, India

ISBN 978-981-19-3143-7 ISBN 978-981-19-3144-4 (eBook)
<https://doi.org/10.1007/978-981-19-3144-4>

© The Editor(s) (if applicable) and The Author(s), under exclusive license to Springer Nature Singapore Pte Ltd. 2022

This work is subject to copyright. All rights are solely and exclusively licensed by the Publisher, whether the whole or part of the material is concerned, specifically the rights of translation, reprinting, reuse of illustrations, recitation, broadcasting, reproduction on microfilms or in any other physical way, and transmission or information storage and retrieval, electronic adaptation, computer software, or by similar or dissimilar methodology now known or hereafter developed.

The use of general descriptive names, registered names, trademarks, service marks, etc. in this publication does not imply, even in the absence of a specific statement, that such names are exempt from the relevant protective laws and regulations and therefore free for general use.

The publisher, the authors, and the editors are safe to assume that the advice and information in this book are believed to be true and accurate at the date of publication. Neither the publisher nor the authors or the editors give a warranty, expressed or implied, with respect to the material contained herein or for any errors or omissions that may have been made. The publisher remains neutral with regard to jurisdictional claims in published maps and institutional affiliations.

This Springer imprint is published by the registered company Springer Nature Singapore Pte Ltd. The registered company address is: 152 Beach Road, #21-01/04 Gateway East, Singapore 189721, Singapore

*This one is for you.
With you know what, and you probably know
why.*

Foreword by Dr. Soumitra Kumar Choudhuri

Quantum dots (QDs) are currently being used for various research purposes as they are nanocrystals of semiconductors wherein an electron-hole pair can be trapped. The application of QDs or nanoparticles (NPs) is thriving in the biomedical field, and plenty of books have been published, but there is a dearth of books covering the details of the application of QDs from bio-imaging to theragnostic applications, from synthesis to their optical characterization, and from specific QDs systems to their cytotoxicity.

The present book describes the above aspects in an elaborate manner. The contributing authors offer their profound knowledge related to the colloidal synthesis, optical characterizations, and biomedical applications of various water-soluble QDs. I recommend this book, as it illustrates the progress, significant research developments in the field, and its prospects. During the last two decades, scientists have achieved significant progress in understanding and refining many aspects and facts related to various groups of QD systems and their applications in the biomedical

field, both in vitro and in vivo. The editors of this book have done an excellent job for the readers who are (and will be) interested in applying QDs in the biomedical field.



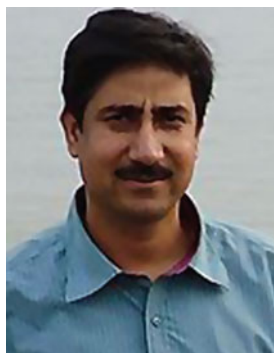
Dr. Soumitra Kumar Choudhuri
Former Head, Department of IVCCC
and Emeritus Medical Scientist (EMS, ICMR)
Chittaranjan National Cancer Institute (CNCI)
Kolkata, India

Foreword by Prof. Pranab Sarkar

In 1959, in his prophetic talk titled *There's Plenty of Room at the Bottom: An Invitation to Enter a New Field of Physics*, the great Physicist Feynman predicted that the time would come when one can arrange the atoms at his/her will. Now, we are in the era when the researchers made possible the prediction of this great scientist a reality. Quantum dots or semiconductor nanoparticles have emerged as a class of fascinating materials with a wide spectrum of tailor-made properties. The photoluminescent quantum dots are being exploited in a wide range of fields, e.g., developing sophisticated and high-accuracy biomedical tools and targeted drug delivery vehicles, etc. In this context, the two young and budding scientists, Dr. Puspendu Barik and Dr. Samiran Mondal, have made an extraordinary effort to bring about such spectacular and massive applications of quantum dots in a single volume of their edited book, *Application of Quantum Dots in Biology and Medicine*.

Throughout the thirteen chapters of this book, the readers will be acquainted with the tremendous flurry of activities going on in the synthesis and applications of quantum dots in biomedical fields. This book is indeed a very good attempt by Dr. Barik and Dr. Mondal, where various researchers worldwide shared their knowledge, expertise, and views on the recent developments regarding the fundamentals of luminescent and biocompatible quantum dots, their synthetic protocols, and potential applications in biology and medicine. Each of the thirteen chapters in this book is comprehensive, well-referenced, and represents a current and systematic as well as coherent portrayal of the synthesis, characterization, properties, and biomedical applications of luminescent quantum dots.

It is noteworthy that this book would be useful as a general introduction to luminescent and biocompatible quantum dots, which will attract novice readers, and simultaneously, it will also draw the attention of the experts seeking in-depth information in the field of quantum dots. I am sure that this book will be extremely valuable and expedient to the scientific community. I would like to extend my heartfelt congratulations to Puspendu and Samiran for their outstanding effort and contribution.



Prof. Pranab Sarkar
Department of Chemistry
Siksha-Bhavana (Institute of Science)
Visva-Bharati
Santiniketan, West Bengal, India

Preface

Quantum dots (QDs) or nanoparticles (NPs) are nanoscale semiconductor materials with tunable optical and electrical properties due to the quantum confinement effect. QDs are currently utilized in a wide range of optoelectronic devices, in many in vivo and in vitro imaging, single-molecule tracking, labeling, therapeutic, and energy transfer-based sensing techniques since their first synthesis. During the last two decades, many QDs have been developed and enriched with superior photophysical properties due to the advancement of synthesis strategy (both hydrophobic and hydrophilic) and in-depth analysis of their exciting properties. However, a complete risk assessment arising from QDs is still in its infancy stage due to the lack of knowledge of all the relevant toxicological mechanisms for all QDs.

We have brought together eleven contributed chapters from some leading researchers worldwide in this edited book. The book comprises thirteen chapters. In the chapter “[Introduction to Quantum Dots](#)”, Mondal starts with a brief introduction of QDs as a potential candidate in the biomedical field and summarizes each chapter in this book. Chapter “[Synthetic Developments of Semiconductor Quantum Dot for Biological Applications](#)” describes the synthesis methodologies of QDs and their surface modifications for application in biomedical fields. In the chapter “[All-Optical Detection of Biocompatible Quantum Dots](#)”, Barik will discuss the photophysical properties of QDs and the fundamentals of the origin of unique optical properties to characterize QDs. In the chapter “[A Toxicologic Review of Quantum Dots: Recent Insights and Future Directions](#)”, Guha reviews the pharmacology of QDs, the cellular uptake mechanism, and review of the assessment techniques of QD toxicity. In the chapter “[Advantages and Disadvantages of Using Quantum Dots in Lateral Flow and Other Biological Assay Formats](#)”, Bruno describes the advantages and disadvantages of using quantum dots, including toxicity and toxicity management in various assay formats, with some real-world examples. In the chapter “[Recent Developments in Quantum Dots Technologies as Effective Theranostic Tools Against Cancer](#)”, Mukherjee and Sarkar discuss the recent developments in QDs technologies as effective theranostic tools against cancer. In the chapter “[The Underlying Mechanism of Quantum Dot-Induced Apoptosis: Potential Application in Cancer Therapy](#)”, Mondal et al. presents the underlying mechanism of QD-induced apoptosis

and its application in cancer therapy with various cell lines of malignant cells in mice and humans. In the chapter “[Fluorescent Quantum Dots, A Technological Marvel for Optical Bio-imaging: A Perspective on Associated in Vivo Toxicity](#)”, Poddar portrays the fluorescent QDs as a technological marvel for optical bio-imaging. In the chapter “[Quantum Dots in Biosensing, Bioimaging, and Drug Delivery](#)”, Mondal and Pan cover applications of different QDs in drug delivery, bio-sensing, and bio-imaging. In the chapter “[Quantum Dots: Potential Cell Imaging Agent](#)”, Mallick et al. depict the supreme characteristics features of different QDs and their applications in vitro and in vivo cell imaging. In the chapter “[Quantum Dot: A Boon for Biological and Biomedical Research](#)”, Pandit and Chandra review QD’s synthetic approaches, biological relevance, and potential in clinical applications like targeted molecular therapy, cancer cell imaging, as well as the left-over issues and future perspectives. In the chapter “[Upconversion and Downconversion Quantum Dots for Biomedical and Therapeutic Applications](#)”, Dutta and Barik comprehensively discuss the fundamentals of upconversion (UC) and downconversion (DC) QDs/NPs and their biomedical and therapeutic applications. In the last chapter “[Present Status and Future Perspective](#)”, Mondal concludes with the present status of QDs in the biomedical field and a future perspective.

We hope that this book will benefit a wide range of physicists, chemists, biologists, and material scientists working in the science and application of QDs. In particular, those who work with the application QDs in bio-imaging, apoptosis, drug delivery, and cancer therapy will find the book helpful. This book consists of two dedicated chapters for UC and DC mechanisms and toxicity arising from QDs. In addition, the book will assist graduate students who are working in these fields in building an understanding of the fundamental of QD’s properties, various types of QDs, synthesis methodologies, and their immediate applications in biomedical fields. We want to thank the contributing authors for their excellent contributions. We sincerely thank Dr. Soumitra Kumar Choudhuri and Professor Pranab Sarkar for writing the book’s foreword. Finally, we thank Sunny Guo for her assistance in completing this book project.

Kolkata, India
March 2022

Dr. Puspendu Barik
Dr. Samiran Mondal

Contents

Introduction to Quantum Dots	1
Samiran Mondal	
Synthetic Developments of Semiconductor Quantum Dot for Biological Applications	9
Puspendu Barik	
All-Optical Detection of Biocompatible Quantum Dots	35
Puspendu Barik and Manik Pradhan	
A Toxicologic Review of Quantum Dots: Recent Insights and Future Directions	67
Arun Guha and Debasree Ghosh	
Advantages and Disadvantages of Using Quantum Dots in Lateral Flow and Other Biological Assay Formats	91
John G. Bruno	
Recent Developments in Quantum Dots Technologies as Effective Theranostic Tools Against Cancer	103
Aniket Mukherjee and Nandini Sarkar	
The Underlying Mechanism of Quantum Dot-Induced Apoptosis: Potential Application in Cancer Therapy	125
Jishu Mandal, Mriganka Mandal, Tamanna Mallick, and Samiran Mondal	
Fluorescent Quantum Dots, A Technological Marvel for Optical Bio-imaging: A Perspective on Associated In Vivo Toxicity	143
Santosh Podder	
Quantum Dots in Biosensing, Bioimaging, and Drug Delivery	165
Somrita Mondal and Animesh Pan	
Quantum Dots: Potential Cell Imaging Agent	191
Tamanna Mallick, Abhijit Karmakar, and Zinnia Sultana	

Quantum Dot: A Boon for Biological and Biomedical Research	209
Palash Pandit and Arpita Chandra	
Upconversion and Downconversion Quantum Dots for Biomedical and Therapeutic Applications	229
Riya Dutta and Puspendu Barik	
Present Status and Future Perspective	265
Samiran Mondal	

Introduction to Quantum Dots



Samiran Mondal

Abstract Quantum dots (QDs) or luminescent semiconductor nanocrystals possess size-tunable elegant electro-optical properties, broad absorption spectra, and narrow emission ranging from UV to NIR region, high fluorescent quantum yields, fluorescence intermittency, resistance to photobleaching, and significant Stoke shift, which are the prerequisites for the application in vitro and in vivo bioimaging, biomarker, molecular pathology, drug delivery, and many more. The suitable applicability of QDs in the biomedical field needs to understand the science behind the QDs and their fundamental properties, which are most relevant to biology and medicine. In recent years, QDs have shown a wide variety of possibilities in the biomedical field due to their recent development of synthetic procedures and biocompatibility. The chapters will focus on the fundamentals of QDs. The chapter also includes a brief description of chapters in the book, which may help readers understand the topics' overview.

Keywords Quantum dots (QDs) · Fundamentals and applications of QDs · Biomedical field

QDs are nanometer-scale (typically 2–10 nm in diameter) semiconductor nanocrystals composed of Groups II (e.g., Zn, Cd),-VI (e.g., Se, S) or III (e.g., Ga, I),-V (e.g., N, P) or IV (e.g., Pb)-VI (e.g., Se, S) elements of Mendeleev periodic table that exhibit size-dependent optical properties, including absorbance and photoluminescence [1, 2]. Unique optoelectronic, catalytic, and semiconductor properties of QDs are arising due to their three-dimensional quantum confinement regime, i.e., the size of the QDs in the range of exciton Bohr radius [3, 4]. Valence and conduction bands are separated by a band gap in the semiconductor material. On photon absorption, electrons from the lower electronic energy state (valence band) are promoted to the higher electronic energy state (conduction band), producing a hole in the valence band. Bandgap energy becomes higher for the smaller QDs, and

S. Mondal (✉)

Department of Chemistry, Rammohan College, 102/1-Raja Rammohan Sarani, Kolkata, West Bengal 700009, India

e-mail: samiran1985@gmail.com; samiran@rammohancollege.ac.in

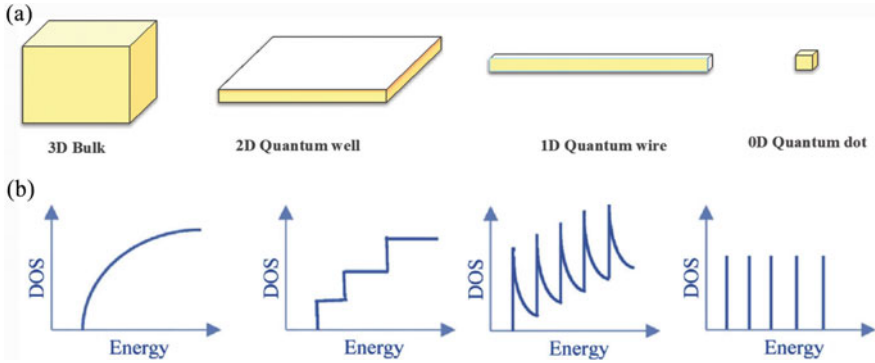


Fig. 1 a Representation of different types of quantum confinement as 0D, 1D, 2D, and 3D b density of states (DOS) (schematically) for bulk semiconductor, quantum wells, quantum wires, and quantum dots

therefore, an electron will require more energy to become excited. Consequently, QD's fluorescence is emitted when the excited electron returns to the valence band from the conduction band [5] and the wavelength range of the emitted light in the ultraviolet (UV) to the infrared (IR) region [6]. QDs were first identified in solids (glass crystals) in the 1980s, more than three decades ago by Ekimov et al. [7], and significant advancement in the field of QDs was driven after 1984 when L. E. Brus discovered the same phenomenon in colloidal solutions [8]. He discovered that the wavelength of light emitted or absorbed by a quantum dot changed over time as the crystal grew and concluded that the confinement of electrons gave the particle quantum properties [9]. Unique characteristics of QDs involve a typical size range of 2–10 nm in diameter, high photostability, broad range excitation, size-tunable narrow emission spectra, making them potential materials in promising applications in nanodiagnosics, bioimaging, targeted drug delivery, and photodynamic therapy [10, 11].

A quantum dot is a semiconductor nanocrystal with unique properties distinct from bulk semiconductors or discrete molecules. The different types of quantum confinements are used during the design of QDs, shown in Fig. 1. Depending on the spatial confinement of electron–hole pairs (excitons), one may classify the confinement nature of nanostructures as (i) one-dimension confinement: quantum well; (ii) two-dimension confinement: quantum wire; (iii) three-dimension confinement: quantum dot.

The quantum-confined properties of any material are determined by the quantum nature of electrons and holes [12, 13]. The size and shape of the individual QDs altered the conductive properties of the QDs. The semiconductor bandgap increases with a decrease in nanocrystal size, as depicted in Fig. 2a, hence the difference in energy between the highest valence band and the lowest conduction band will be higher [14]. Consequently, more energy will be required to excite the dot, and when the crystal returns to its resting state, more energy is released [15]. The size governs

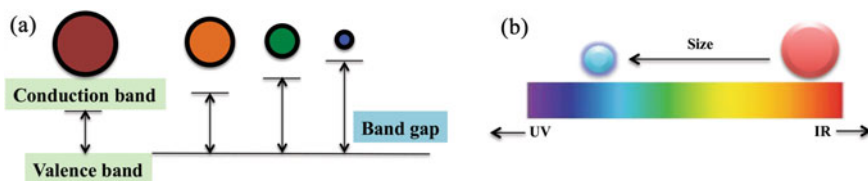
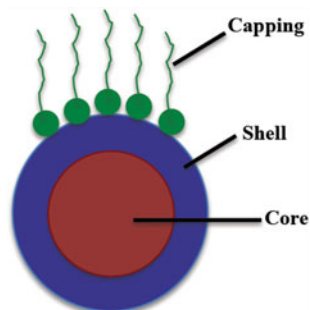


Fig. 2 **a** Schematic representation of bandgap; smaller QDs have a large band gap. **b** Dependence of emission (in the visible light) from the size of quantum dots

Fig. 3 Schematic representation of core-shell QDs: a core in the center (brown), over it a shell (blue), above a QD is functionalized by different molecules



the wavelength of the emission from QDs; as the size decreases, there is a color shift from red to blue in the light emitted (shown in Fig. 2b).

Structurally, QDs consist of a semiconductor core overcoated by a shell to improve the biocompatibility, photoluminescence (PL) quantum yield (QY) of fluorescence, and stability of these core nanocrystals, as depicted in Fig. 3. PLQY can be altered via passivation of the surface of QD by a shell of a larger bandgap semiconductor and the leaching of the metal ions from the core of QD [15, 16]. At first, CdSe/ZnS and CdSe/CdS were most intensively studied [17, 18]. Later, many more QDs of “core-shell” type were developed, such as CdSe/ZnSe, CdTe/CdS, CdTe/ZnS, and even CdTe/CdS/ZnS “core/shell/shell” QDs [18–22].

Here, we summarize the essential physicochemical properties of QDs:

- QDs are comparatively more resistant to degradation and photostable to traditional dyes due to their inorganic composition and fluorescence intensity and also having a high signal to noise compared to organic dyes [23, 24].
- QDs absorb over a broad range and have fluorescence emission over a narrow range with excellent photoresistance capacity [25, 26].
- The photoluminescence behavior of QDs can be tuned depending on the material and the size [26].
- The surface of QDs can be coated with different chemical entities and biomaterials owing to their easily molded shape [27].

- The photoluminescence follows the quantum confinement effect, where smaller quantum dots emit at higher energy (lower wavelength) and larger quantum dots emit at lower energy (higher wavelength) [14].

QDs have shown outstanding advantages in a long time, from detection to diagnosis to treatment. Recently, QDs have been designed in many biological applications (e.g., diagnosis of disease, single protein tracking, drug delivery, intracellular, and therapy) [28]. Because of the unique physical, optical, and exciting electrical properties of QDs, they are extensively applied in other applications such as diagnostics, bioimaging, tissue engineering, cancer treatment, photo-thermal therapy, biosensing, and especially drug delivery. Due to the high photostability and less photobleaching properties of QDs are used as fluorescence probes for all types of labeling studies and in cell marking [29]. Nowadays, the core shell structure has opened an excellent window of research to use in broad fields, such as catalysis, optics, electronics, biomedical, pharmaceutical, and drug delivery [30]. In the field of diagnosis, magnetic resonance imaging (MRI), optical, and nuclear imaging based on the optical properties of fluorescent QDs seems to be the critical imaging techniques [31, 32]. Recent progress in surface modification and bioconjugation have expanded their use as suitable probes for live-cell applications [33]. The development of multi-functional nanoparticle probes based on semiconductor QDs is now used widely in vitro (biomolecular tracking in cells, cellular imaging, and tissue staining) as well as in vivo (QD biodistribution, vascular imaging, tracking, and tumor imaging) [34]. One of the most critical applications of QDs is cancer detection, diagnosis, management, and treatment [35, 36]. Biocompatibility and toxicity are extremely important to use QDs in biology. ZnS or CdS capping improved the quantum yield of the QDs and protected them against photo-oxidation, which provides photostability and minimizes cytotoxicity. Absorption, distribution, metabolism, excretion and toxicity of QDs depend on physicochemical and environmental factors [37]. The size, charge, concentration, outer coating bioactivity (capping material and functional groups), and oxidative, photolytic, and mechanical stability have been associated as determining factors in QD toxicity.

This book aims to provide basic information on the properties of QDs, and then explore their potential in advanced biological and medical strategies. The book consists of eleven chapters showing the important properties, synthesis procedures, all-optical detection techniques, and the applications of QDs in biology and medicine. First two chapters, Barik et al. discussed the synthetic developments of semiconductor QDs for biological application and all-optical detection of biocompatible QDs. Biocompatibility is one of the prerequisites for using QDs in biological and biomedical research. In one of the chapters, Barik et al. addressed a more green synthetic approach of QDs preparation with less toxicity, making QDs more water-soluble and biofunctionalization of chemically synthesized QDs. In another chapter, Barik et al. focus on the basics and the all-optical detection techniques for biocompatible QDs, considering their various application toward bioimaging, biomolecule sensing, and their interaction with biomolecules. The article also includes recently explored optical detection techniques for QDs. John G. Bruno has discussed the advantages and

disadvantages of using QDs, including toxicity and toxicity management in various assay formats with real-world examples. Sarkar et al. presented recent developments in quantum dots technologies as effective theranostic tools against certain cancers and their drawbacks like cytotoxicity. Moving to the review concerning the application of QDs in cancer therapy, Mandal et al. discussed the multimodal application of QDs in cancer treatment and cellular mechanism initiated by apoptotic and autophagy cell death after application of QDs in various cell lines of malignant cells. S. Poddar has elaborately discussed the utility of QDs as an excellent fluorescent probe for a wide range of fluorescence microscopy technologies ranging from conventional epifluorescence, confocal, multiphoton to super-resolution microscopy for in vitro cell and tissue imaging to in vivo deep tissue and whole animal imaging and their relevant toxicity issues associated with using QDs in vivo investigations. In the next chapter, Mondal et al. aim to focus on applications of different quantum dots in drug delivery, biosensing, and bioimaging. On the other hand, Mallick et al. have depicted the supreme characteristics features of different QDs and their applications in vitro and in vivo cell imaging. Chandra et al. provide the background for QDs, including their synthetic approaches, biological relevance, and potentials in clinical applications like bioimaging (cancer cell imaging) and targeted molecular therapy (drug delivery). In one separate chapter, Dutta et al. summarize the chemical and optical properties and the functionalization of different up-conversion (UC) and down-conversion (DC) QDs. The chapter focuses on the recent advances of each category of UCQDs and DCQDs in bioimaging, biosensing, disease diagnostics, and light-controlled drug and gene delivery. Finally, S. Mondal concluded with the present status and some possible future development of the applicability of QDs in the biomedical field. In recent years, the availability of green and biocompatible QDs demands progressively more application in the biomedical field owing to the unique properties of QDs. Furthermore, QDs provide a suitable platform for engineering multifunctional nanodevices with the capabilities of exploiting multiple imaging modalities or merging imaging and therapeutic functionalities within a single nanoparticle. Recently, QDs have been safely used in advanced clinical research and are a promising diagnostic tool that will open up a new direction. This book is exciting and valuable to a wide variety of readership communities (students, early-stage researchers, and scientists) in the various fields of chemistry, physics, biology, and medicine.

References

1. Alivisatos AP. Semiconductor clusters, nanocrystals, and quantum dots. *Science*. 1996;271(5251):933–7.
2. Medintz IL, Uyeda HT, Goldman ER, Mattoussi H. Quantum dot bioconjugates for imaging, labelling and sensing. *Nat Mater*. 2005;4(6):435–46.
3. Reimann SM, Manninen M. Electronic structure of quantum dots. *Rev Mod Phys*. 2002;74(4):1283–342.
4. Bawendi MC, Steigerwald ML, Brus LE. Mechanics of larger semiconductor clusters (“quantum dots”). *Annu Rev Phys Chem*. 1990;41(1):477–96.

5. Fomenko V, Nesbitt DJ. Solution control of radiative and nonradiative lifetimes: a novel contribution to quantum dot blinking suppression. *Nano Lett.* 2008;8(1):287–93.
6. Jamieson T, Bakhshi R, Petrova D, Pocock R, Imani M, Seifalian AM. Biological applications of quantum dots. *Biomaterials.* 2007;28(31):4717–32.
7. Ekimov AI, Onushchenko AA. Quantum size effect in three-dimensional microscopic semiconductor crystals. *JETP Lett.* 1981;34(6):345–9.
8. Brus LE. Electron-electron and electron-hole interactions in small semiconductor crystallites: The size dependence of the lowest excited electronic state. *J Chem Phys.* 1984;80(9):4403–9.
9. Brus L. Electronic wave functions in semiconductor clusters: experiment and theory. *J Phys Chem.* 1986;90(12):2555–60.
10. Samia ACS, Chen X, Burda C. Semiconductor quantum dots for photodynamic therapy. *J Am Chem Soc.* 2003;125(51):15736–7.
11. Viana OS, Ribeiro MS, Fontes A, Santos BS. Quantum dots in photodynamic therapy. In: Batinić-Haberle I, Rebouças J, Spasojević I, editors. *Redox-active therapeutics, oxidative stress in applied basic research and clinical practice.* Cham: Springer; 2016. https://doi.org/10.1007/978-3-319-30705-3_23.
12. Siegel RW. Synthesis and processing of nanostructured materials. In: Nastasi M, Nastasi M, Parkin DM, Gleiter H, editors. *Mechanical properties and deformation behavior of materials having ultrafine microstructures, NATO-ASI, vol. E233.* Dordrech: Kluwer Academic; 1993. p. 508–36.
13. Chowdhury S, Barik P. Nanocrystal materials, fabrications, and characterizations, nanocrystals in nonvolatile memory; 2018. p. 1–73.
14. Maksym P, Chakraborty T. Quantum dots in a magnetic field: role of electron-electron interactions. *Phys Rev Lett.* 1990;65:108–11.
15. Mínnich A, Dresselhaus M, Ren ZF, Chen G. Bulk nanostructured thermoelectric materials: current research and future prospects. *Energy Environ Sci.* 2009;2:466–79.
16. Hines MA, Guyot-Sionnest P. Synthesis and characterization of strongly luminescing ZnS-capped CdSe nanocrystals. *J Phys Chem.* 1996;100(2):468–71.
17. Dabbousi BO, Rodriguez-Viejo J, Mikulec FV, Heine JR, Mattoussi H, Ober R, Jensen KF, Bawendi MG. (CdSe)/ZnS core-shell quantum dots: synthesis and characterization of a size series of highly luminescent nanocrystallites. *J Phys Chem B.* 1997;101(46):9463–75.
18. Peng X, Schlamp MC, Kadavanich AV, Alivisatos AP. Epitaxial growth of highly luminescent CdSe/CdS core/shell nanocrystals with photostability and electronic accessibility. *J Am Chem Soc.* 1997;119(30):7019–29.
19. Reiss P, Bleuse J, Pron A. Highly luminescent CdSe/ZnSe core/shell nanocrystals of low size dispersion. *Nano Lett.* 2002;2(7):781–4.
20. He Y, Lu HT, Sai LM. Microwave-assisted growth and characterization of water-dispersed CdTe/CdS core-shell nanocrystals with high photoluminescence. *J Phys Chem B.* 2006;110(27):13370–4.
21. Zhao D, He Z, Chan WH, Choi MMF. Synthesis and characterization of high-quality water-soluble near-infrared-emitting CdTe/CdS quantum dots capped by N-Acetyl-L-cysteine via hydrothermal method. *J Phys Chem C.* 2009;113(4):1293–300.
22. Chakravarthy KV, Davidson BA, Helinski JD, Ding H, Law WC, Yong KT, et al. Doxorubicin-conjugated quantum dots to target alveolar macrophages and inflammation. *Nanomedicine.* 2011;7:88–96.
23. He Y, Lu HT, Sai LM, Su YY, Hu M, Fan CH, Huang W, Wang LH. Microwave synthesis of water-dispersed CdTe/CdS/ZnS core-shell-shell quantum dots with excellent photostability and biocompatibility. *Adv Mater.* 2008;20(18):3416–21.
24. Dabbousi BO, Rodriguez-Viejo J, Mikulec FV, Heine JR, Mattoussi H, Ober R, et al. (CdSe) ZnS core-shell quantum dots: synthesis and characterization of a size series of highly luminescent nanocrystallites. *J Phys Chem B.* 1997;101:9463–75.
25. Ghasemi Y, Peymani P, Afifi S. Quantum dot: magic nanoparticle for imaging, detection and targeting. *Acta Biomed.* 2009;80:156–65.

26. Bera D, Qian L, Tseng TK, Holloway PH. Quantum dots and their multimodal applications: a review. *Materials*. 2010;3:2260–345.
27. Dubertret B, Skourides P, Norris DJ, Noireaux V, Brivanlou AH, Libchaber A. In vivo imaging of quantum dots encapsulated in phospholipid micelles. *Science*. 2002;298:1759–62.
28. Field LD, Walper SA, Susumu K, Lasarte-Aragones G, Oh E, Medintz IL, Delehanty JB. A quantum dot-protein bioconjugate that provides for extra-cellular control of intracellular drug release. *Bioconjug Chem*. 2018;29:2455–67.
29. Derfus AM, Chan WC, Bhatia SN. Intracellular delivery of quantum dots for live cell labeling and organelle tracking. *Adv Mat*. 2004;16:961–6.
30. He D, Zhang C, Zeng G, Yang Y, Huang D, Wang L, Wang H. A multifunctional platform by controlling of carbon nitride in the core-shell structure: from design to construction, and catalysis applications. *Appl Catal B Environ*. 2019;258: 117957.
31. Kroutvar M, Ducommun Y, Heiss D, Bichler M, Schuh D, Abstreiter G, Finley JJ. Optically programmable electron spin memory using semiconductor quantum dots. *Nature*. 2004;432:81–4.
32. Cassidy PJ, Radda GK. Molecular imaging perspectives. *J Royal Soc Interface*. 2005;2:133–44.
33. Sapmaz S, Jarillo-Herrero P, Kouwenhoven LP, vander Zant HSJ. Quantum dots in carbon nanotubes. *Semicond Sci Technol*. 2006;21:S52–63.
34. Schnee VP, Woodka MD, Pinkham D. Quantum dot material for the detection of explosive-related chemicals. In: SPIE defense, security, and sensing, international society for optics and photonics, vol. XVII; 2012. p. 83571J. <https://doi.org/10.1117/12.921403>.
35. Biju V, Mundayoor S, Omkumar RV, Aaas A, Ishikawa M. Bioconjugated quantum dots for cancer research: present status, prospects and remaining issues. *Biotechnol Adv*. 2010;28:199–213.
36. Gao X, Cui Y, Levenson RM, Chung LWK, Nie S. In vivo cancer targeting and imaging with semiconductor quantum dots. *Nat Biotechnol*. 2004;22:969–76.
37. Hardman R. *Environ Health Perspect*. 2006;114:165.

Synthetic Developments of Semiconductor Quantum Dot for Biological Applications



Puspendu Barik

Abstract To date, numerous varieties of semiconductor quantum dots (QDs) have been successfully synthesized with proper control over size and shape. Some have shown good biocompatibility, which is one of the prerequisites for using QDs in biological and biomedical research. However, chemically processed QDs show their non-biocompatibility issue in most cases, limiting their direct use in biological and biomedical research. Various types of QDs, their synthesis methodologies, surface passivation techniques for biocompatibility, and biofunctionalization will be addressed in this chapter.

Keywords QDs · Classification · Synthesis methodologies · Biofunctionalization · Surface passivation

1 Introduction

Semiconductor Quantum Dots (QDs) are gaining importance due to their potential applications in medicine, biotechnology, and catalysis in recent years. In the past 30 years, the development of colloidal synthesis techniques modifies the electrical, optical, magnetic, and chemical properties of QDs compared to their bulk counterparts, enabling enormous technological applications and cultivating fundamental scientific knowledge. QDs are nanocrystals with dimensions less than exciton Bohr radius in three space dimensions. After its first demonstration [1, 2], colloidal QDs make their path in the biomedical field because of their excellent physicochemical properties, fluorescence stability, and biocompatibility. However, the biotoxicity, solubility, and blinking properties have been criticized. The stability and emission properties of QDs depend on the characteristics of the chemical bonds of the composting materials. However, semiconductor QDs can also lose their unique optical and electrical properties due to the ruptured surface. Hence, the surface of

P. Barik (✉)

Technical Research Centre, S. N. Bose National Centre for Basic Sciences, JD Block, Sector-III, Salt Lake City, Kolkata 700106, India

e-mail: pbarik_mid1983@yahoo.co.in; puspendub@bose.res.in

QDs must be protected besides developing a new synthesis method for the homogeneous distribution of QDs. In most cases, semiconducting shells or ligands or coating of polymers perform the surface passivation of QDs efficiently.

Numerous recent reviews describe the synthesis methods to efficiently produce high-quality QDs in both aqueous and organic solvents. This chapter does not include all the synthesis methods elaborately; instead, the chapter describes the fundamentals behind the synthesis techniques. The chapter includes a brief overview of different types of QDs and their surface passivation techniques so that QDs can be favorable to many biomedical applications. Reiss et al. discuss the fundamental properties and synthesis methods of II–VI, IV–VI, III–V QDs [3], and nontoxic QDs [4]. Pietryga et al. review synthesis methods of QDs elaborately and discuss tuning the properties beyond traditional size manipulation, the concept of “Stokes shift engineering,” and interface engineering to obtain high-quality QDs [5]. Hühn et al. describe selected standard protocols for the synthesis, surface modification via ligand exchange reactions, purification, and characterization of various types of colloidal QDs in organic solvents and aqueous solutions [6]. Embden et al. provide an overview of the vast array of QDs synthesized successfully using heat-up approaches, including detailed discussions of controlled precursor chemistry, reaction additives, and heating conditions on their crystallinity, defect density, and surface passivation [7]. Boles et al. elaborate on the bonding, electronic structure, and chemical transformations at QD’s surfaces due to surface ligands for their importance for biomedical (imaging, diagnostics, and therapeutics) applications [8]. Zhao et al. summarize basic structures, the related synthetic methods, the functionalization and surface bioconjugation of NIR QDs, and their biomedical applications in biosensing, bioimaging, and drug delivery [9]. Pu et al. present a comprehensive overview of the synthesis of colloidal QDs synthesized via chemical approaches in the solution phase, emphasizing green routes aiming for reproducible and large-scale production [10]. Makkar et al. discuss the advantages and challenges involved in impurity doping in semiconductor QDs arising from colloidal synthesis methods [11]. Agarwal et al. summarize the recent advances in the exfoliation and synthesis of single-layered transition metal dichalcogenides and their biomedical applications [12]. Wagner et al. review the recent advances and challenges in the molecular design of QDs for drug delivery, theranostic, and imaging [13]. Molaei et al. review carbon QDs, their synthesis routes, optical properties, and recent advances in biomedical applications like bioimaging (in vivo and in vitro), drug delivery, cancer therapy, gene delivery [14]. Bian et al. discuss the research progress in the microfluidic synthesis of QDs, the design of microfluidic synthesis devices, and their nanomedical application [15]. Heuer-Jungemann et al. provide a comprehensive review on the role of the ligands in designing QDs for desired morphology, colloidal stability, and function toward the applications ranging from biomedicine to sensing and energy [16]. Algar et al. provide a comprehensive overview of the development and application of luminescent QDs, including II–VI, IV–VI, III–V, I–III–VI, I–VI, and IV QDs for chemical and biological analysis and imaging [17]. Peng et al. describe doped semiconductor QDs, their synthesis approaches and techniques, and their current biomedical applications [18]. Shi et al.

detail the advanced progress of biomedical applications of biosynthesized QDs and their synthesis methods via low-cost and eco-friendly biosynthesis approaches [19].

Classification of QDs by their composition will be reviewed in the first section of the chapter. In the following section, physicochemical principles of nucleation and growth, the chemistry of the inorganic core, and interaction with organic surface ligands will be discussed elaborately. In the third section, various surface modification techniques will be reviewed, emphasizing the biological applications. Finally, a perspective on remaining challenges and future directions for the biomedical applications of QDs will be presented. Interested readers are encouraged to explore further reviews/articles cited throughout the text for specific QDs.

2 Classification of QDs by Their Composition

Quantum confinement of electrons and holes in QDs defines quantization of energy levels where the level spacing decreases with the confinement length in general. The spatially confined electron–hole pair (i.e., exciton) inside QDs control the optical and electro-optical properties. The distance between the electron and hole probability distributions in an exciton is called the exciton Bohr radius, a_B (see Chapter “[All-Optical Detection of Biocompatible Quantum Dots](#)” for more details) that resembles a simple H-atom system. The electronic structure of semiconductor materials can be altered by confining the spatial distribution of the exciton, electron, or even hole wavefunctions in all three physical dimensions. The strong, intermediate, and weak confinement depends on the specific size in each dimension relative to the exciton Bohr radius, a_B . In a strong confinement regime, the size of QDs is less than a_B and in a weak confinement regime, it is greater than a_B . In the intermediate regime, the size of QDs is comparable to a_B . The electrical and optical properties of QDs strongly depend on the confinement regime, and thus their properties are somewhere between the individual atoms/molecules and the bulk materials.

Further, QDs can be classified according to their elemental composition. Table 1 summarize the various types of QDs and their respective uses in the biomedical field. However, robust and good-quality QDs are the prerequisites for biomedical fields. An important strategy to enhance the electrical and optical properties of QDs is the surface passivation with a shell of a second semiconductor (shell) or a strong coating of ligands. According to the shell material, the QDs can be divided into core, core/shell, and alloyed core/shell. Another type of QDs, i.e., core/shell/ligand, will be discussed in the following subsections. Core/shell and alloyed shell structures are the most favorable QDs variants for the application in biomedical fields due to low cytotoxicity (even if the presence of toxic core), enhanced dispersibility, prone to bio-, and cytocompatibility, improved conjugation ability to other bioactive molecules, enhanced thermal and chemical stability, resistant to photobleaching, and increased affinity to bind with drugs, receptors, ligands.

Table 1 Classification of QDs according to the elemental composition

Type	Examples	Application	References
I-I-III-VI	Ag-Cu-Ga-Se	Imaging	[20]
I-II-IV-VI	$\text{Ag}_2\text{ZnSnS}_4$, $\text{Cu}_2\text{ZnSn}(\text{S}_{1-x}\text{Se}_x)_4$	NIR luminescence	[21–23]
I-III-VI	CuInSe_2 , CuInS_2 , AgInS_2 , AgInSe_2 , AgGaS_2	Real-time tumor-targeted bioimaging, drug carriers, FRET	[24–28]
I-III-III-VI	Ag-In-Ga-S, Ag-In-Ga-Se, Cu-In-Ga-Se	Bioimaging	[27, 29, 30]
I-VI	Cu_2S , Ag_2X (X=S, Se, Te)	Chemodynamic therapy, fluorescence imaging, inhibit protein fibrosis	[9, 31, 32]
I-VII	AgBr	Biomedical, food detection, and environmental analysis	[28, 33, 34]
II-I-III-VI	Zn-Ag-In-Se, Zn-Cu-In-S	Biomedical imaging	[35–37]
II-II-VI	$\text{Cd}_x\text{Zn}_{1-x}\text{S}$, $\text{Cd}_{1-x}\text{Zn}_x\text{Se}$	Biological labeling	[38]
II-VI	ZnTe, ZnSe, ZnS, ZnO, CdS, CdSe, CdTe, HgTe, HgSe, HgS	FRET, gene technology, fluorescent labeling of cellular proteins, pathogen and toxin detections, drug carriers, Anticancer applications, bioimaging	[18, 39–42]
II-VI-VI	$\text{CdSe}_x\text{Te}_{1-x}$, $\text{CdS}_x\text{Se}_{1-x}$	NIR bioimaging, high QY, artificial photosynthesis	[43–45]
III-V	InP, InAs, GaAs, InSb	Bioimaging, NIR bioimaging	[42, 46, 47]
III-V-V	$\text{InAs}_{1-x}\text{Sb}_x$	Infrared detector	[48]
IV	Si, C	Bioimaging, targeted drug delivery, nanomedicine, biosensing, photocatalysis	[14, 49–53]
IV-VI	PbSe, PbS	NIR bioimaging	[9, 54, 55]
V	P	Photothermal therapy, photodynamic therapy, drug delivery, bioimaging, biosensing, and combined immunotherapy	[56–58]
2D	Graphene, Graphitic carbon nitride (g- C_3N_4), Hexagonal boron nitride (h-BN), phosphorene, MXene	Biosensing, implants, tissue engineering, antimicrobial and antifouling, reactive oxygen species generation and scavenging, cancer phototherapy	[59–66]

(continued)

Table 1 (continued)

Type	Examples	Application	References
TMDC (2D)	Transition metal dichalcogenide, e.g., TiS_2 , TiSe_2 , TaS_2 , MoS_2 , MoSe_2 , WS_2 , WSe_2 , ReS_2	Drug delivery, anticancer photothermal therapy, photodynamic therapy, combined phototherapy, bioimaging, biosensing, theranostics, toxicity, tissue engineering, and antimicrobials	[17, 62, 67, 68]
Pdots	Semiconducting polymer dots	NIR bioimaging, image-guided tumor surgery, molecular imaging, multicolor imaging, cell tracking, combinational phototherapy	[67, 69–72]
Perovskite	MPbX_3 (M=Cs or CH_3NH_3 ; X=Cl, Br or I)	Therapeutic and energy storage applications, biosensing, bioimaging, photocatalysis	[73–75]

QY quantum yield

2.1 Core Type QDs

Core QDs or bare QDs means semiconductor QDs without any shell material or robust polymer coating. Initially, core QDs were synthesized. However, they have a high density of surface defects/traps, low PL lifetime, low quantum yield and poor chemical, thermal, and photochemical/physical stability in a biological environment, and high toxicity. For example, bare CdSe QDs fail to maintain their properties under different environments, including argon, oxygen, air, water vapor, wet oxygen, and under different excitation conduction, even if they are stored in an inert gas atmosphere [3, 76]. Hence, bare QDs can not be used in the biomedical field. Therefore, coating shell materials is essential to preserve their properties for application in various fields.

2.2 Core–Shell Type QDs

The shell (obviously of semiconductor origin) can have different functions in core/shell QDs depending on the bandgaps and the relative position of electronic energy levels of the involved semiconductors, the thickness of the shell compared to core, and the number of different shells in core/shell/shell QDs. The schematic in Fig. 1 shows the electronic-band alignment for different core/shell QD systems (light gold color for electron and red color for hole wave functions). According to the relative alignment of conduction and valence band edges of core and shell materials, core/shell QDs are divided into type-I (Fig. 1a), where both the charge carriers (electron and hole) remain confined within the core (e.g., CdSe/CdS, CdSe/ZnS,

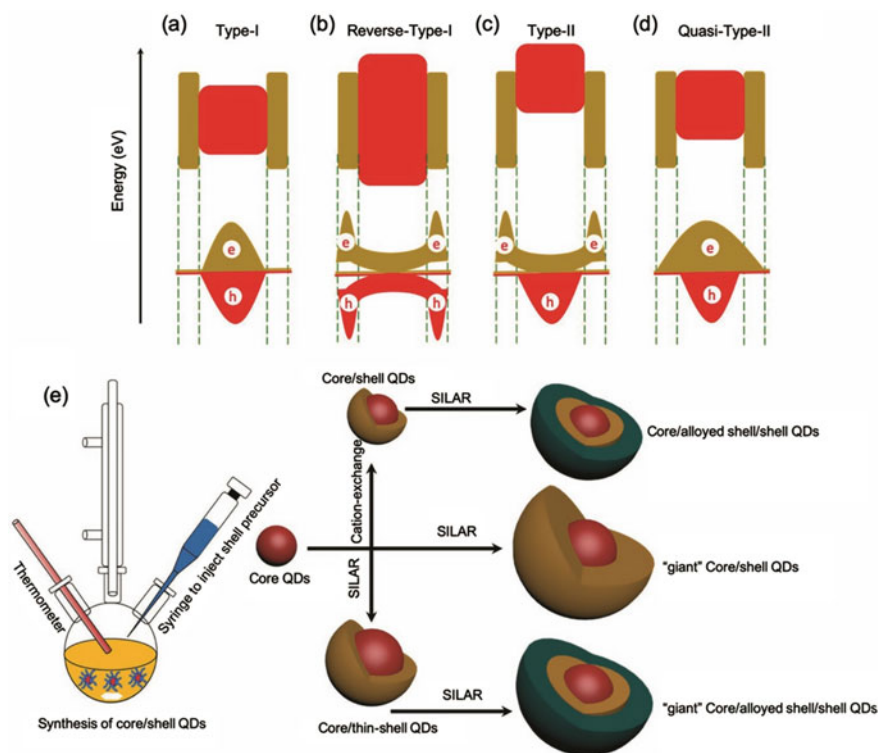


Fig. 1 The schematic shows the electronic-band alignment for different classes of core/shell QD system (light gold color for electron and red color for hole wave functions): **a** type-I, **b** reverse type-I, **c** type-II, **d** quasi-type-II. **e** Schematic representation of the synthesis of colloidal core/shell QDs. The core can be synthesized via a hot injection or cation exchange approach, and the shell can be developed on the core via cation exchange/SILAR or a combination of both. Reproduced from Ref. [77]. Copyright © 2020 WILEY-VCH Verlag GmbH & Co. KGaA, Weinheim

InAs/CdSe) and Type-II (Fig. 1c), where one carrier is confined in shell and the other in the core (e.g., ZnTe/CdSe, CdS/ZnSe). Schematic representation of the synthesis of colloidal core/shell QDs and multiple shell formation is shown in Fig. 1e, where SILAR represents successive ionic layer adsorption and reaction. Type-I QDs generally emit red-shifted light upon radiative recombination relative to the core. The shell in type-I QDs is used to passivate the surface of the core to protect them from the surrounding medium and improve its optical properties. Moreover, type-I QDs have more stability against photodegradation and higher fluorescence quantum yield (QY) by reducing the number of surface dangling bonds during shell formation. In reverse Type-I QDs (e.g., CdS/HgS, CdS/CdSe, ZnSe/CdSe, InP/ZnS, PbSe/PbS), the bandgap of the core is larger than the shell material. Exciton energy separation will be minimum when charge carriers are confined in the shell, and emission wavelength can be altered by changing the thickness of the shell. Adding one more shell formation of a larger bandgap semiconductor on the reverse type-I QDs may enhance

the photostability and fluorescence QY. In type-II QDs (CdSe/CdTe, ZnSe/CdS), the emission wavelength's significant redshift occurs due to staggered band alignment than the constituting core and shell materials. However, Type-II QDs effectively tune the emission spectral range, varying the shell thickness, e.g., in particular for near-infrared emission. Comparatively, the amount of redshift in emission wavelength occurs relative to the core as Type-I < reverse Type-I < Type-II. In contrast, the photoluminescence decay time of Type-II QDs is much more than the others. In quasi-type II QDs (e.g., CdSe/CdS, PbSe/CdSe, and CuInS₂/CdS), the core and shell must have similar conduction band edge levels or valence band edge levels (i.e., small offsets) without the interfacial defects.

2.3 Alloyed Shell Type QDs

An alloyed shell means a composite or mixed semiconducting or continuously graded shell around the core rather than a single semiconducting shell. The graded shells have severely impacted the dynamics of multiexcitons and charged QDs to obtain superior fluorescence quantum yield, low lattice strain, and high performance in applications. CdSe/Cd_xPb_{1-x}S, CdSeTeS/ZnS, ZnSeTe/ZnSe/ZnS, CdSeZnS/ZnS, CdSe/AgZnS, CdS/AgZnSe, CdTe/CdTeSe/CdSe, Zn-Ag-In-Se, InZnPS, Cd_xZn_{1-x}Se_yS_{1-y}/ZnS are few examples of alloyed shell QDs.

3 Synthetic Strategies

3.1 Physicochemical Principles of Nucleation and Growth

According to the classical theory, the nucleation and growth of QDs involve two distinct processes—burst nucleation by LaMer's theory [78, 79] and Ostwald ripening [80] to describe the particle size change. The key idea of the LaMer mechanism is the conceptual separation of two stages of nucleation and growth. The process of nucleation and growth can be divided into three distinct stages: (a) rapid increase of monomer concentration in solution, (b) a burst of the self-nucleation process reduces the concentration of free monomers in solution, (c) growth process occurs under the control of the diffusion of the monomers. The variation of monomer concentration with time is schematically plotted in Fig. 2. However, LaMer's conditions for nucleation are not sufficient conditions for mono-dispersity but play an essential role in deciding the particle size and size distribution. For example, in most of the synthetic procedures of QDs, the reactants are mixed or often one of the components mixed to another within a short duration, ensuring the nucleation process in a short time followed by a much slower growth process. The nucleation process can be divided into heterogeneous and homogeneous nucleation processes and can be explained by

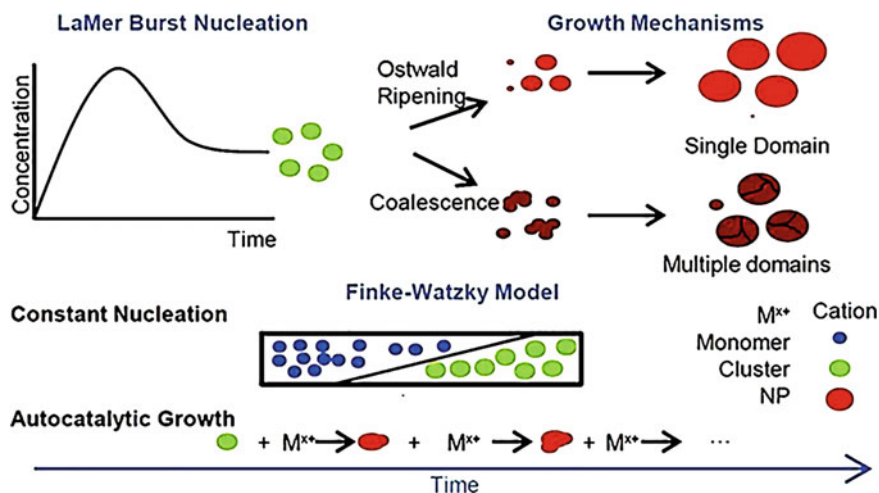


Fig. 2 The schematic shows the nucleation and growth process of QDs. Different classical theories can explain the nucleation and growth processes—LaMer Mechanism, Ostwald Ripening, Finke-Watzky Two-Step Mechanism, Coalescence, and Orientated Attachment, Intraparticle Growth. Reproduce from Ref. [84] under ACS AuthorChoice with CC-BY license

classical nucleation theory because the thermodynamic system tends to minimize its Gibbs free energy. The seeded growth method is a prototype reaction for the heterogeneous nucleation process [81]. The seeded growth of Au nanoparticles is an example of heterogeneous nucleation. However, the seeded growth method is a robust technique for synthesizing spherical core/shell semiconductor heterostructures varying in size and shape. Heterogeneous nucleation requires lower activation energy than homogeneous nucleation, and preferential growth can be possible. Therefore, the whole process can be summarized as precursors \rightarrow monomers/seeds \rightleftharpoons QDs.

According to the Gibbs–Thompson equation, the chemical potential of a particle increases with decreasing particle size, i.e., smaller particles have increased solubility and surface energy owing to their high surface-to-volume ratio. Therefore, in the solution initially not in thermodynamic equilibrium, larger particles form at the cost of smaller particles controlled by mass transport or diffusion. As a result, the concentration gradients lead to the transport of the solute from the small particles to the larger particles and, in turn, allow the larger particles to grow even more, as shown in Fig. 2. The process is often called the Ostwald ripening process and hence plays a crucial role in the growth of nanocrystals. The mathematical formulation of Ostwald ripening is the basis of Lifshitz–Slyozov–Wagner (LSW) theory and post-LSW theory [82–84], where the growth mechanism was first quantified. Digestive ripening is effectively the inverse of Ostwald ripening. Smaller particles grow in the solution where the larger particles redissolve, governed by the surface energy of the particles within the solution.

According to Finke-Watzky's two-step mechanism, the nucleation and growth process happens simultaneously in the solution, where the autocatalytic surface growth follows a slow nucleation process [85]. However, this process is not diffusion-controlled and follows a critical size described in a classical nucleation framework [84]. The growth process of iridium, platinum, ruthenium, and rhodium follow Finke-Watzky's two-step mechanism. Coalescence and orientated attachment are similar except randomly orientated lattice planes within coalescence, whereas a perfect alignment of the planes in orientated attachment. Coulombic and van der Waals interactions play a vital role in these processes.

During the last three decades, numerous synthesis methods for QDs have been developed to understand how these particles nucleate and grow within the solution. Several reviews summarize the method and study the properties of QDs [4, 6, 7, 10, 18, 86]. The hot injection (HI) and the heat-up method (HU) are the most studied synthesis methods to obtain monodisperse QDs by separating nucleation and growth in organic solvents.

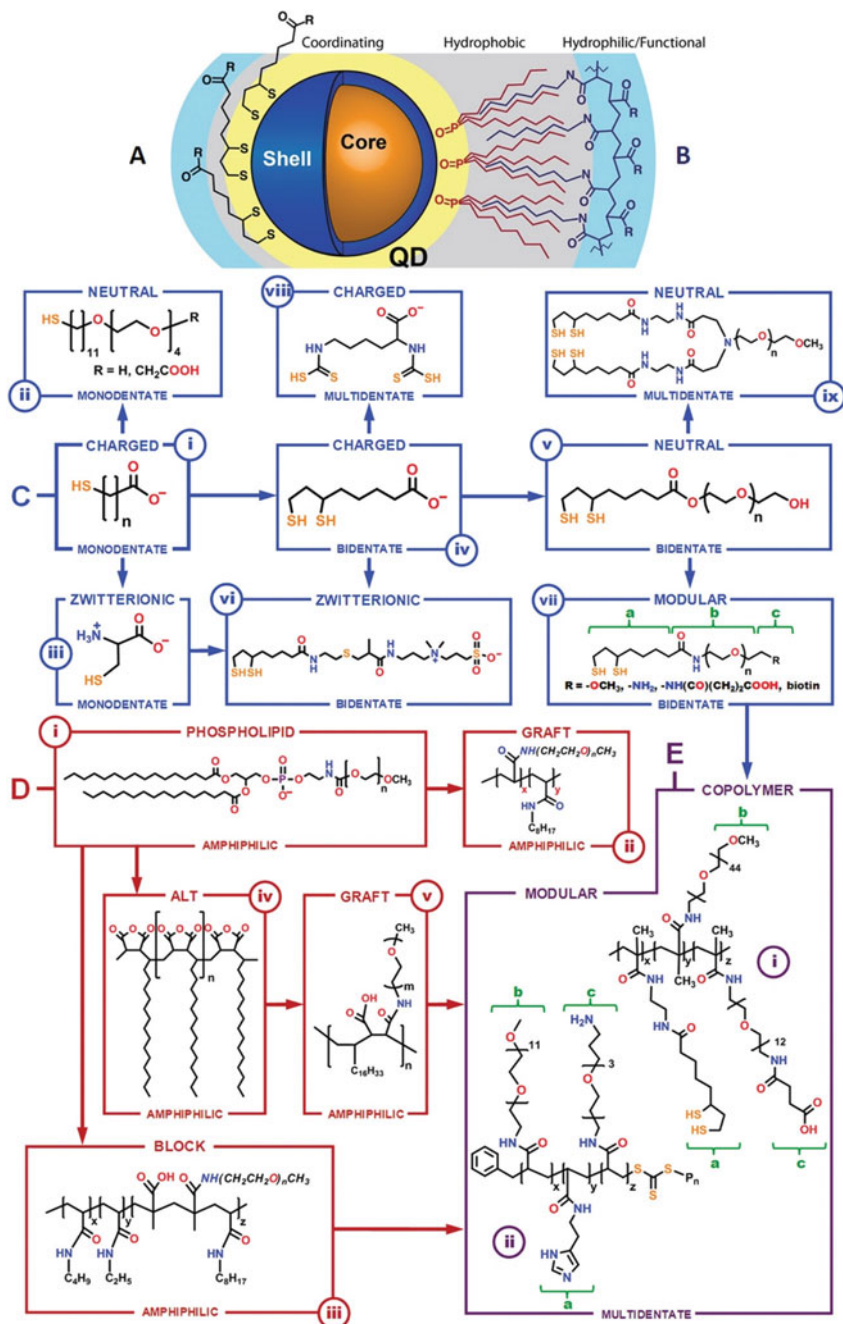
Till today, the HI approach remains the most common method to obtain monodisperse QDs. The HI method involves homogeneous nuclei via the rapid injection of organometallic reagents into a hot solvent. The reaction solution contains surfactant molecules/ligands (typically alkylphosphine, alkyl phosphine oxides, long-chain carboxylic acids, and long-chain amines) to prevent QDs agglomeration. The nucleation process is rapid enough to generate large quantities of small nuclei within a short period. After nucleation, a homogeneous diffusion-controlled growth happens to grow the size of the QDs, where larger QDs grow slower than the smaller ones. Ostwald ripening occurs during the growth, where smaller QDs redissolve due to their higher chemical potential, and larger QDs continue to grow. Thus the average size of QDs increase, and the concentration of QDs decrease until the saturation point. The HI method effectively obtains high quality and size tuneable QDs varying the temperature, concentration of the surfactants, and reaction time by separating nucleation from the growth stage to reduce particle polydispersity. The HI methods are successfully employed for the synthesis of cadmium- and lead-based QDs, all-inorganic cesium lead halide perovskite (CsPbX_3 , $X=\text{Cl, Br, I}$), CuInX_2 ($X=\text{S, Se}$), InP , and various alloyed shell QDs [7]. Embden et al. elaborately describe analytical and numerical aspects of nanocrystal formation mechanisms to elucidate the concepts and governing equations to understand the nucleation and growth process of QDs in solution [7]. They derive the expression for the temperature-dependent precursor to monomer conversion rate, the nucleation rate varying the supersaturation, surface energy, temperature, and the growth rate.

The main difference between HU and HI methods is that the nucleation and growth times are similar for the HU method. During the HU method, monomers are produced progressively faster as heated linearly (Arrhenius behavior). The nucleation process goes slowly after its trigger, and the supersaturation lasts for a long time before the decrease in the monomer concentration in the solution. Thus, lengthening the nucleation event is unique to the HU method to design a practical synthesis approach. The overlap between the nucleation and growth process of QDs restricts obtaining narrow particle size distribution.

3.2 *Chemistry of the Inorganic Core, Interaction with Organic Surface Ligands*

The choice of surface ligands is the crucial parameter to obtain defined morphologies and photophysical properties of QDs. Ligands play an essential role in regulating the solubility, colloidal stability, the availability of anchoring groups during synthesis and post-synthesis ligand exchange, and QD's functionality. Ligands are the key parameters to control the properties of QDs to preferentially bind to functional biomolecules such as peptides, proteins, and oligonucleotides. The quality of the QDs can be determined with the ability to attach different types of ligands or conjugation to secondary ligands for application in drug delivery, biomedical field, bioimaging, and many more. The strength of ligand binding is critical to assess the long-term colloidal stability and can be enhanced by using multidentate anchoring groups on ligands. Ligand binding must be strong enough to remain bound in complex biological media and buffers with different pH values and interacting biomolecules. Ligands play an essential role in determining the dispersibility in solution, colloidal stability, the ability to complexate with active components, inherent size-dependent emission, photoluminescence quantum yield (PLQY), and moderating agent for the exciton relaxation, Auger recombination, or energy transfer to ligands [8, 16, 87–89]. For example, σ - and π -donating ligands (e.g., alkylamines, thiolates) can modify the PLQY of QDs up to 50% due to the effective passivation and thus ligands must be carefully selected to control the PL emissions [90–92].

In most synthesis methods, common anchoring groups for ligand conjugation are phosphine oxide ($\text{O}=\text{PR}_3$), thiol ($-\text{SH}$), phosphonyl ($-\text{PO}(\text{OR})_2$), carboxyl ($-\text{COOH}$). Most high-quality QDs are synthesized using hot-injection methods which involve the pyrolysis of organometallic precursors in nonpolar coordinating solvents. Figure 3 shows various ligands and anchoring groups available for colloidal QDs. This figure also depicts the ligand chemistry, and surface ligand strategies of QDs applied for biological applications. However, the use of different sizes of ligands may affect the overall hydrodynamic radius, especially in a biological context for bioconjugation of functional molecules to the QD. During the last decade, aqueous syntheses of QDs (e.g., CdS, CdTe, CdSe, ZnSe, HgTe, PbS) have been intensely studied of good quality, defect-free emission, and large polydispersity in size [16]. The synthesis process generally involves metal-thiol complexes and metal-chalcogenide precursors in water by adjusting the pH, temperature, and injection time into the reaction solution, which induces the nucleation and growth process. A short alkyl chain thiols and phosphates like thioglycolic acid, mercaptopropionic acid, thio-glycerol, mercaptoethylamine, glutathione, and L-cysteine, mercaptobenzoic acid, per-6-thio- α -cyclodextrin, and per-7-thio- β -cyclodextrin are common ligands in the aqueous synthesis of QDs.



◀**Fig. 3** **A** The schematic shows the ligand binding at the QD surface. **B** The right-hand side shows the hydrophilic/functional ligand (blue) with the native QD ligands (red). **C** Ligand chemistries (i) thioalkyl acids, (ii) PEGylated ligands, (iii) zwitterionic ligands, (iv) dihydrolipoic acid ligands and (v) PEGylated, (vi) zwitterionic and (vii) modular derivatives thereof, (viii) multidentate charged, and (ix) multidentate PEGylated ligands. **D** Amphipol coatings (i) phospholipid micelles, (ii) hydrophilic polymer backbones grafted with alkyl chains, (iii) triblock copolymers, and (iv) alternating copolymers that hydrolyze to acids or (v) are grafted with PEG chains. **E** Copolymers with pendant PEG oligomers and (i) dithiol or (ii) imidazole groups. Discrete moieties for (a) QD binding, (b) solubility, and (c) bioconjugation are identified where applicable (green). The arrows illustrate a conceptual progression and not synthetic pathways or chronological development. Reprinted from Ref. [93] under standard ACS AuthorChoice/Editors' Choice usage agreement, American Chemical Society

4 Surface Modification of QDs for Biological Applications

The successful application of QDs requires preserving their unique properties even if interacting with different environments. A large fraction of constituent atoms of QDs reside on the surface, and hence any exposure to the surface with the environment may lead to loss of photophysical properties. It is critical to control these surface atoms to prevent the trapping of electrons, quenching of fluorescence emission, and charge transfer. For all biological applications of QDs, these surface atoms must be attached to coordinating ligands that dictate how the QD interacts with the biological fluid. The interface between atoms of a crystalline solid and ligands coordinated to the surface atoms is chemically heterogeneous. In most cases, chemisorption occurs to form the ligand layer on the surface of QDs during synthesis, and the post-synthetic ligand exchange can modify the surface ligand. Water solubilization of QDs is a fundamental criterion for biological applications. QDs must be coated in biocompatible ligands to survive and create less toxicity with aqueous biological media because bare surfaces are highly reactive and adsorb the constituents of biological solutions [94] composed of water molecules, ions, small molecules (like sugars), and macromolecules (like proteins). Ligands play a vital role in determining the hydrodynamic size, optical and chemical stability, and nonspecific interactions for the applications of QDs in molecular imaging and labeling. Different strategies are adopted to make QDs water-soluble, described in the following sections.

QDs are typically synthesized in an organic solution containing surface ligands with a head-group bound to the QD surface and a hydrocarbon tail directed away. QDs are typically synthesized in an organic solvent containing surface ligands such as trioctyl phosphine oxide (TOPO), trioctyl phosphine (TOP), tetradecylphosphonic acid (TDPA), oleic acid with a head-group bound to the QD surface, and a hydrocarbon tail directed away. Water-soluble bifunctional molecules such as mercapto-carbonic acids $[\text{HS}-(\text{CH}_2)_n-\text{COOH}$, $n = 1-15]$, 2-aminoethanethiol, dithiothreitol, dihydrolipoic acid, oligomeric phosphines, peptides, crosslinked dendrons connects to QDs surface in one end, and the other end is hydrophilic. The hydrophilic group not only imparts water solubility but can also be used for the conjugation of biomolecules. Different ligand exchange strategies will be adopted to achieve bright and compact

QDs with homogeneous monodisperse population, retain high fluorescence quantum yield long-term stability, minimize nonspecific interaction, retain synthetic reactivity.

4.1 Surface Coating

Encapsulation with phospholipids is one of the fundamental methods to solubilize QDs [95, 96]. Amphiphilic phospholipids overcoat the existing organic ligands where aliphatic phospholipid chains can organize within the organic ligands on the surface of QDs due to the hydrophobic interactions. The composition of the phospholipid formulations can be tailored to yield fairly monodisperse QDs for biological applications for specific applications. Due to the aggregation and reduced cytoplasmic mobility of the phospholipids-coated QDs, the octylamine-modified poly-acrylic acid-based polymer can be used to coat QDs [97]. Guo et al. recently demonstrated that the QDs encapsulated with Canine Parvovirus-like particles modified using 3-mercaptopropanoic acid can significantly improve the cellular-targeted labeling that could expand these encapsulated applications of QDs in biological medicine [98].

Silicon-containing ligands are the most widely used in functional QDs for biomedical applications due to hydrophilic properties, dispersibility, biocompatibility, minimum particle aggregation, and colloidal stability. Silica coating on the QD reduces oxidation and its toxicity too. Several strategies have been reported to make QDs/SiO₂ core/shell structure the sol-gel synthesis of silica from an alkoxy-silane: $\text{Si}(\text{OR})_4 + 2\text{H}_2\text{O} \rightarrow \text{SiO}_2 + 4\text{ROH}$. However, silica-coated QDs with shells less than ~5 nm have not been widely implemented due to silane chemistry's complex and unpredictable nature [99]. Silica encapsulated QDs have been used to overcome many of the problems concerning bioapplication. Gofman et al. fabricated silica nanoparticles encapsulated CdSe/CdS/ZnS core-shell QDs through water-in-oil reverse microemulsion process and used for the immunoassay detection of the mycotoxin deoxynivalenol in food and feed [100]. Bardi et al. developed NH₂ functionalized CdSe/ZnS QD-doped silica nanoparticles having imaging and gene carrier capabilities both in vitro and in vivo [101].

4.2 Encapsulation of Amphiphilic Ligands

Amphiphilic ligands, comprised of a hydrophobic backbone and hydrophilic alkyl chains, are appreciated for their ability to facilitate organometallic reactions in the presence of water; the hydrophobic part intercalates the hydrophobic stabilizing agent during the synthesis of QDs, while the hydrophilic portion offers aqueous solubility. For example, poly(maleic anhydride-alt-1-octadecene) (PMAO)-PEG, (1,2-distearoyl-sn-glycero-3-phosphoethanolamine-*N*-[carboxy(polyethylene glycol)-2000] (PE-PEG), poly(maleic anhydride alt-1-tetradecene) (PMAT), poly(styrene-co-maleic anhydride) (PSMA), phospholipids,

polystyrene-*b*poly(acrylic acid), poly(methyl methacrylate)-poly(ethyleneoxide), poly(isoprene)-*b*poly(ethylene glycol) (PI-*b*-PEG), poly(isoprene-*block*-ethylene oxide) (PI-*b*-PEO) are common amphiphilic ligands for QDs synthesis [102–107]. These polymers are flexible for functionalization in terms of tuned type and number of functional groups that have a barrier to control the permeability of the QDs. The nontoxicity and water solubility of PEO, PI-*b*-PEO, and PI-*b*-(PEO)₂ reduce unspecific protein absorption and provide good biocompatibility [95]. PEG-PEO amphiphilic polymer-based micelle encapsulation processes are more effective at reducing QD cytotoxic responses to QDs, making them excellent candidates for bioimaging, biosensing, and therapeutic applications [96].

The amphiphilic phospholipid vesicles or liposomes with hollow spherical structures and high loading capacity are advantageous for packaging QDs for delivery applications. Using liposomes in vivo applications leads to dramatic instability and high sensitivity toward the external medium, while it can be overcome by using an extra layer of silica on QDs [97]. Lopes et al. demonstrated a process of hydroxyapatite-coated liposomes for the controlled release of QDs and bupivacaine [98]. The amphiphilic block polymers approach has been previously proposed to encapsulate QDs for the biomedical field, and one can manipulate size tunability, composition, and chemical properties [100]. During the last decade, a wide range of amphiphilic block polymers has been developed to improve the solubility and biocompatibility of QDs; however, common drawbacks of the increase of hydrodynamic radius remain in comparison to simple organic ligands [95].

4.3 Multidentate Ligands for Ligands Exchange

Small organic molecules, which allow only one interaction site to bind QDs surface, are called monodentate ligands. In contrast, the multidentate ligands have multi-coordinating groups, which can bind by complementing the chelate effect on the surface, can enhance the colloidal stability of QDs. Theoretically, it was shown that the equilibrium constant of ligand adsorption to the QD surface could increase exponentially by increasing the number of ligating groups per molecule [101, 108], e.g., binding strengths are slightly higher for ligands containing two thiols to QDs [109]. Optimizing ligands on QDs surface can be complex due to non-independent contributions from ligand affinity, packing density, conformation, hydrophobicity, and solubility [94]. In this perspective, researchers have attracted much attention to polymeric multidentate ligands in recent years to overcome the limited aqueous stability of QDs coated with thiolate ligands maintaining a small hydrodynamic size. QDs coated with polymers containing few binding groups show dramatically increased colloidal stability, i.e., stable for years without ligand loss after extensive purification and dilution, without the need of any hydrophobic solvent [110–114]. These ligands comprise a linear polymeric backbone decorated with groups that act either as anchor groups bound to the QD facets or as a functional group to interact with the solvent. For example, X-type thiolates, L-type imidazole, and pyridine groups yield high

stability at neutral pH; however, imidazole and pyridine ligands are independently unstable in an acidic environment ($\text{pH} < 6$) [115, 116]. If a polymer contains both thiol and imidazole groups, QDs show high stability over a pH range of 3–13 [117]. However, it is challenging to attach multidentate polymeric ligands to QD surfaces with a stable and compact conformation despite their high binding affinity, as some unbound groups can crosslink QDs [118–120]. Total coordination is not practical as the QDs surfaces are not atomically flat. Complete removal or replacement of the original hydrophobic ligands with some weakly bound hydrophilic ligands must be satisfied to achieve homogeneous products. Talapin group screened a variety of metal-free and intermediate ligands for colloidal nanocrystals [121]. They found that weakly bound X-type ions (hydroxide) are optimal for yielding compact and homogeneous products. Small QD clusters can be dissociated by heating ($\sim 110^\circ\text{C}$), and it yields densely packed homogeneously polymer coated QDs showing high QY and stability in an aqueous environment with a hydrodynamic size of 7–12 nm [111, 113]. Bidentate ligands such as folic acid (FA), ethylenediamine tetra-acetic acid (EDTA), succinic acid (SA), and glutamic acid (GA) can be effective to develop efficient water-compatible perovskite QDs with good optical properties as compared to oleic acid (OA) and all other ligands [122, 123].

A modular ligand based on poly(ethylene glycol) (PEG, single-chain to promote hydrophilicity) and a dihydrolipoic acid (DHLA) unit connected to one end of the PEG chain for strong anchoring onto the QD surface, providing QDs with significant stability from pH 5 to 12 for over one year under the broad range pH solubility of the polymers segment [124]. The multidentate polymer ligands, which contain binding motifs, can overcome the colloidal stability, photobleaching and minimize the hydrodynamic size of QDs [111, 116]. For example, the pyridine polymer-coated QDs show biocompatibility and long-term stability through cellular delivery, intracellular single QD tracking studies, and cytotoxicity testing. A poly(isobutylene-alt-maleic anhydride) (PIMA) is used to synthesize multidentate polymer amphiphilic ligands that maintain PL intensity in water like that in hexane and long-term stability in a broad pH range of 3–13 at a nanomolar concentration under ambient conditions [117, 125]. Giovanelli et al. discussed that the significant advantage of multidentate polymer ligands over bidentate zwitterionic ligands is the higher affinity for long-term bioimaging [112]. However, a comprehensive study of multidentate polymers and small-molecular ligands is essential for biological applications. Mattoussi et al. reported a general strategy for lipoic acid (LA) based on zwitterionic ligands-controlled phase transfer of QDs, providing high PL QY and high colloidal stability over an extensive pH range and excess salt concentration [126], allowing QDs to conjugate globular proteins in acidic and basic conditions. The polymers containing multiple coordinating sites such as thiols, imidazole, or pyridine groups act as multidentate small molecular substrates which exhibit stronger resistance against photo-oxidation. His-Tag-based self-assembly [116, 117, 127] and metal-free strain-promoted click chemistry of high selectivity [125, 128, 129] are helpful for coupling biomolecules.

5 Conclusion

QDs are already well recognized for the current state-of-the-art bioimaging applications as an alternative label to molecular dyes; however, the regular application is limited due to the lack of understanding of bioconjugation chemistry. Recent research for bioanalytical development is rapidly improving, and it will overcome the challenges of using QDs in biomedical fields. Polymeric multidentate ligands coated QDs are colloidally stable and yield high PL QY; however, further comprehensive research must be needed to minimize the ligand coating size with chemical inertness. Multidentate ligands cause the monolayer porosity to increase, and hence the core of the QDs may be exposed to chelating solutes, which is a common problem during protein stabilization. Amorphous silica (SiO_2) shell may solve the problem, but it is not accessible to the formation of silica shell less than ~ 5 nm due to silane chemistry's complex and unpredictable nature. In summary, the development of new QDs is still going on, and a vast pace of research is waiting for researchers to develop biocompatible QDs and the techniques for introducing outstanding properties of QDs in bioanalysis. The cost of commercial QD materials and the complex synthesis techniques are conventional obstructions for applying QDs in biomedical fields. Besides, most medical scientists and biologists are unaware of complex synthesis with desired properties. Collaborative work would produce fruitful results.

Acknowledgements I acknowledge the Technical Research Centre (TRC) [No. All1/64/SNB/2014(C)] of the S. N. Bose National Centre for Basic Sciences, Kolkata, for funding this work.

References

1. Brus LE. On the development of bulk optical properties in small semiconductor crystallites. *J Lumin* [Internet]. 1984;31–32:381–4. Available from: <https://linkinghub.elsevier.com/retrieve/pii/0022231384903028>.
2. Rossetti R, Ellison JL, Gibson JM, Brus LE. Size effects in the excited electronic states of small colloidal CdS crystallites. *J Chem Phys* [Internet]. 1984;80(9):4464–9. Available from: <http://scitation.aip.org/content/aip/journal/jcp/80/9/10.1063/1.447228>.
3. Reiss P, Protière M, Li L. Core/shell semiconductor nanocrystals. *Small* [Internet]. 2009;5(2):154–68. Available from: <http://doi.wiley.com/10.1002/sml.200800841>.
4. Reiss P, Carrière M, Linceneau C, Vaure L, Tamang S. Synthesis of semiconductor nanocrystals, focusing on nontoxic and earth-abundant materials. *Chem Rev* [Internet]. 2016;116(18):10731–819. Available from: <https://pubs.acs.org/doi/10.1021/acs.chemrev.6b00116>.
5. Pietryga JM, Park Y-S, Lim J, Fidler AF, Bae WK, Brovelli S, et al. Spectroscopic and device aspects of nanocrystal quantum dots. *Chem Rev* [Internet]. 2016;116(18):10513–622. Available from: <https://pubs.acs.org/doi/10.1021/acs.chemrev.6b00169>.
6. Hühn J, Carrillo-Carrion C, Soliman MG, Pfeiffer C, Valdeperez D, Masood A, et al. Selected standard protocols for the synthesis, phase transfer, and characterization of inorganic colloidal nanoparticles. *Chem Mater* [Internet]. 2017;29(1):399–461. Available from: <https://pubs.acs.org/doi/10.1021/acs.chemmater.6b04738>.

- van Embden J, Chesman ASR, Jasieniak JJ. The heat-up synthesis of colloidal nanocrystals. *Chem Mater* [Internet]. 2015;27(7):2246–85. Available from: <https://pubs.acs.org/doi/10.1021/cm5028964>.
- Boles MA, Ling D, Hyeon T, Talapin DV. The surface science of nanocrystals. *Nat Mater* [Internet]. 2016;15(2):141–53. Available from: <http://www.nature.com/articles/nmat4526>.
- Zhao P, Xu Q, Tao J, Jin Z, Pan Y, Yu C, et al. Near infrared quantum dots in biomedical applications: current status and future perspective. *Wiley Interdiscip Rev Nanomedicine Nanobiotechnology* [Internet]. 2018;10(3):e1483. Available from: <https://onlinelibrary.wiley.com/doi/10.1002/wnan.1483>.
- Pu Y, Cai F, Wang D, Wang J-X, Chen J-F. Colloidal synthesis of semiconductor quantum dots toward large-scale production: a review. *Ind Eng Chem Res* [Internet]. 2018;57(6):1790–802. Available from: <https://pubs.acs.org/doi/10.1021/acs.iecr.7b04836>.
- Makkar M, Viswanatha R. Frontier challenges in doping quantum dots: synthesis and characterization. *RSC Adv* [Internet]. 2018;8(39):22103–12. Available from: <http://xlink.rsc.org/?DOI=C8RA03530J>.
- Agarwal V, Chatterjee K. Recent advances in the field of transition metal dichalcogenides for biomedical applications. *Nanoscale* [Internet]. 2018;10(35):16365–97. Available from: <http://xlink.rsc.org/?DOI=C8NR04284E>.
- Wagner AM, Knipe JM, Orive G, Peppas NA. Quantum dots in biomedical applications. *Acta Biomater* [Internet]. 2019;94:44–63. Available from: <https://linkinghub.elsevier.com/retrieve/pii/S1742706119303393>.
- Molaei MJ. Carbon quantum dots and their biomedical and therapeutic applications: a review. *RSC Adv* [Internet]. 2019;9(12):6460–81. Available from: <http://xlink.rsc.org/?DOI=C8RA08088G>.
- Bian F, Sun L, Cai L, Wang Y, Zhao Y. Quantum dots from microfluidics for nanomedical application. *WIREs Nanomed Nanobiotechnol* [Internet]. 2019;11(5). Available from: <https://onlinelibrary.wiley.com/doi/10.1002/wnan.1567>.
- Heuer-Jungemann A, Feliu N, Bakaimi I, Hamaly M, Alkilany A, Chakraborty I, et al. The role of ligands in the chemical synthesis and applications of inorganic nanoparticles. *Chem Rev* [Internet]. 2019;119(8):4819–80. Available from: <https://pubs.acs.org/doi/10.1021/acs.chemrev.8b00733>.
- Algar WR, Massey M, Rees K, Higgins R, Krause KD, Darwish GH, et al. Photoluminescent nanoparticles for chemical and biological analysis and imaging. *Chem Rev* [Internet]. 2021;121(15):9243–358. Available from: <https://pubs.acs.org/doi/10.1021/acs.chemrev.0c01176>.
- Peng X, Ai F, Yan L, Ha E, Hu X, He S, et al. Synthesis strategies and biomedical applications for doped inorganic semiconductor nanocrystals. *Cell Reports Phys Sci* [Internet]. 2021;2(5):100436. Available from: <https://linkinghub.elsevier.com/retrieve/pii/S2666386421001314>.
- Shi K, Xu X, Li H, Xie H, Chen X, Zhan Y. Biosynthesized quantum dots as improved biocompatible tools for biomedical applications. *Curr Med Chem* [Internet]. 2021;28(3):496–513. Available from: <https://www.eurekaselect.com/178019/article>.
- Wei J, Hu Z, Zhou W, Qiu Y, Dai H, Chen Y, et al. Emission tuning of highly efficient quaternary Ag–Cu–Ga–Se/ZnSe quantum dots for white light-emitting diodes. *J Colloid Interface Sci* [Internet]. 2021;602:307–15. Available from: <https://linkinghub.elsevier.com/retrieve/pii/S002197972100789X>.
- Saha A, Konstantatos G. Ag₂ZnSnS₄–ZnS core–shell colloidal quantum dots: a near-infrared luminescent material based on environmentally friendly elements. *J Mater Chem C* [Internet]. 2021;9(17):5682–8. Available from: <http://xlink.rsc.org/?DOI=D1TC00421B>.
- Saha A, Figueroba A, Konstantatos G. Ag₂ZnSnS₄ nanocrystals expand the availability of RoHS compliant colloidal quantum dots. *Chem Mater* [Internet]. 2020;32(5):2148–55. Available from: <https://pubs.acs.org/doi/10.1021/acs.chemmater.9b05370>.
- Singh A, Singh S, Levchenko S, Unold T, Laffir F, Ryan KM. Compositionally tunable photoluminescence emission in Cu₂ZnSn(S_{1-x}Se_x)₄ nanocrystals. *Angew Chem Int Ed* [Internet].

- 2013;52(35):9120–4. Available from: <https://onlinelibrary.wiley.com/doi/10.1002/anie.201302867>.
24. Dutková E, Bujňáková ZL, Sphotyuk O, Jakubíková J, Cholujová D, Šišková V, et al. SDS-stabilized CuInSe₂/ZnS multianocomposites prepared by mechanochemical synthesis for advanced biomedical application. *Nanomaterials* [Internet]. 2020;11(1):69. Available from: <https://www.mdpi.com/2079-4991/11/1/69>.
 25. Lian W, Tu D, Hu P, Song X, Gong Z, Chen T, et al. Broadband excitable NIR-II luminescent nano-bioprobes based on CuInSe₂ quantum dots for the detection of circulating tumor cells. *Nano Today* [Internet]. 2020;35:100943. Available from: <https://linkinghub.elsevier.com/retrieve/pii/S1748013220301122>.
 26. Muñoz R, Santos EM, Galan-Vidal CA, Miranda JM, Lopez-Santamarina A, Rodriguez JA. Ternary quantum dots in chemical analysis. Synthesis and detection mechanisms. *Molecules* [Internet]. 2021;26(9):2764. Available from: <https://www.mdpi.com/1420-3049/26/9/2764>.
 27. Kameyama T, Yamauchi H, Yamamoto T, Mizumaki T, Yukawa H, Yamamoto M, et al. Tailored photoluminescence properties of Ag(In,Ga)Se₂ quantum dots for near-infrared in vivo imaging. *ACS Appl Nano Mater* [Internet]. 2020;3(4):3275–87. Available from: <https://pubs.acs.org/doi/10.1021/acsnm.9b02608>.
 28. Borovaya M, Horiunova I, Plokhovska S, Pushkarova N, Blume Y, Yemets A. Synthesis, properties and bioimaging applications of silver-based quantum dots. *Int J Mol Sci* [Internet]. 2021;22(22):12202. Available from: <https://www.mdpi.com/1422-0067/22/22/12202>.
 29. Rismaningsih N, Yamauchi H, Kameyama T, Yamamoto T, Morita S, Yukawa H, et al. Photoluminescence properties of quinary Ag–(In,Ga)–(S,Se) quantum dots with a gradient alloy structure for in vivo bioimaging. *J Mater Chem C* [Internet]. 2021;9(37):12791–801. Available from: <http://xlink.rsc.org/?DOI=D1TC02746H>.
 30. Peng W, Du J, Pan Z, Nakazawa N, Sun J, Du Z, et al. Alloying strategy in Cu–In–Ga–Se quantum dots for high efficiency quantum dot sensitized solar cells. *ACS Appl Mater Interfaces* [Internet]. 2017;9(6):5328–36. Available from: <https://pubs.acs.org/doi/10.1021/acsmi.6b14649>.
 31. Li S-L, Jiang P, Hua S, Jiang F-L, Liu Y. Near-infrared Zn-doped Cu₂S quantum dots: an ultrasmall theranostic agent for tumor cell imaging and chemodynamic therapy. *Nanoscale* [Internet]. 2021;13(6):3673–85. Available from: <http://xlink.rsc.org/?DOI=D0NR07537J>.
 32. Li S-L, Yang Q-Q, Liu X-Y, Jiang F-L, Xiong J, Jiang P, et al. Zn-doped Cu₂S quantum dots as new high-efficiency inhibitors against human insulin fibrillation based on specific electrostatic interaction with oligomers. *Int J Biol Macromol* [Internet]. 2021;179:161–9. Available from: <https://linkinghub.elsevier.com/retrieve/pii/S0141813021005298>.
 33. Bajorowicz B, Kobylański MP, Gołabiewska A, Nadolna J, Zaleska-Medynska A, Malankowska A. Quantum dot-decorated semiconductor micro- and nanoparticles: a review of their synthesis, characterization and application in photocatalysis. *Adv Colloid Interface Sci* [Internet]. 2018;256:352–72. Available from: <https://linkinghub.elsevier.com/retrieve/pii/S0001868617303676>.
 34. Hao N, Zhang X, Zhou Z, Hua R, Zhang Y, Liu Q, et al. AgBr nanoparticles/3D nitrogen-doped graphene hydrogel for fabricating all-solid-state luminol-electrochemiluminescence *Escherichia coli* aptasensors. *Biosens Bioelectron* [Internet]. 2017;97:377–83. Available from: <https://linkinghub.elsevier.com/retrieve/pii/S0956566317304001>.
 35. Deng D, Qu L, Zhang J, Ma Y, Gu Y. Quaternary Zn–Ag–In–Se Quantum dots for biomedical optical imaging of RGD-modified micelles. *ACS Appl Mater Interfaces* [Internet]. 2013;5(21):10858–65. Available from: <https://pubs.acs.org/doi/10.1021/am403050s>.
 36. Guo W, Chen N, Tu Y, Dong C, Zhang B, Hu C, et al. Synthesis of Zn–Cu–In–S/ZnS core/shell quantum dots with inhibited blue-shift photoluminescence and applications for tumor targeted bioimaging. *Theranostics* [Internet]. 2013;3(2):99–108. Available from: <http://www.thno.org/v03p0099.htm>.
 37. Saatsakis G, Michail C, Fountzoula C, Kalyvas N, Bakas A, Ninos K, et al. Fabrication and luminescent properties of Zn–Cu–In–S/ZnS quantum dot films under UV excitation. *Appl Sci* [Internet]. 2019;9(11):2367. Available from: <https://www.mdpi.com/2076-3417/9/11/2367>.

38. Fitzmorris BC, Pu Y-C, Cooper JK, Lin Y-F, Hsu Y-J, Li Y, et al. Optical properties and exciton dynamics of alloyed core/shell/shell Cd_{1-x}Zn_xSe/ZnSe/ZnS quantum dots. *ACS Appl Mater Interfaces* [Internet]. 2013;5(8):2893–900. Available from: <https://pubs.acs.org/doi/10.1021/am303149r>.
39. Torchynska T, Vorobiev Y. Semiconductor II–VI quantum dots with interface states and their biomedical applications. In: *Advanced biomedical engineering* [Internet]. InTech; 2011. Available from: <http://www.intechopen.com/books/advanced-biomedical-engineering/semiconductor-ii-vi-quantum-dots-with-interface-states-and-their-biomedical-applications>.
40. Abbasi E, Kafshdooz T, Bakhtiary M, Nikzamir N, Nikzamir N, Nikzamir M, et al. Biomedical and biological applications of quantum dots. *Artif Cells Nanomed Biotechnol* [Internet]. 2015;1–7. Available from: <http://www.tandfonline.com/doi/full/10.3109/21691401.2014.998826>.
41. Yadav AN, Singh AK, Singh K. Synthesis, properties, and applications of II–VI semiconductor core/shell quantum dots; 2020. p. 1–28. Available from: http://link.springer.com/10.1007/978-3-030-46596-4_1.
42. Granada-Ramírez DA, Arias-Cerón JS, Rodríguez-Fragoso P, Vázquez-Hernández F, Luna-Arias JP, Herrera-Perez JL, et al. Quantum dots for biomedical applications. In: *Nanobiomaterials* [Internet]. Elsevier; 2018. p. 411–36. Available from: <https://linkinghub.elsevier.com/retrieve/pii/B9780081007167000167>.
43. Elibol E. Synthesis of near unity photoluminescence CdSeTe alloyed quantum dots. *J Alloys Compd* [Internet]. 2020;817:152726. Available from: <https://linkinghub.elsevier.com/retrieve/pii/S0925838819339726>.
44. Li Z, Zhang Q, Huang H, Ren C, Pan Y, Wang Q, et al. RGDS-conjugated CdSeTe/CdS quantum dots as near-infrared fluorescent probe: preparation, characterization and bioapplication. *J Nanoparticle Res* [Internet]. 2016;18(12):373. Available from: <http://link.springer.com/10.1007/s11051-016-3669-6>.
45. Nie R, Ma W, Dong Y, Xu Y, Wang J, Wang J, et al. Artificial photosynthesis of methanol by Mn:CdS and CdSeTe quantum dot cosensitized titania photocathode in imine-based ionic liquid aqueous solution. *ChemCatChem* [Internet]. 2018;10(15):3342–50. Available from: <https://onlinelibrary.wiley.com/doi/10.1002/cctc.201800190>.
46. Kirkwood N, Monchen JO V., Crisp RW, Grimaldi G, Bergstein HAC, du Fossé I, et al. Finding and fixing traps in II–VI and III–V colloidal quantum dots: the importance of Z-type ligand passivation. *J Am Chem Soc* [Internet]. 2018;140(46):15712–23. Available from: <https://pubs.acs.org/doi/10.1021/jacs.8b07783>.
47. Li C, Hosokawa C, Suzuki M, Taguchi T, Murase N. Preparation and biomedical applications of bright robust silica nanocapsules with multiple incorporated InP/ZnS quantum dots. *New J Chem* [Internet]. 2018;42(23):18951–60. Available from: <http://xlink.rsc.org/?DOI=C8NJ02465K>.
48. Zhou W, Coleman JJ. Semiconductor quantum dots. *Curr Opin Solid State Mater Sci* [Internet]. 2016;20(6):352–60. Available from: <https://linkinghub.elsevier.com/retrieve/pii/S1359028616300729>.
49. Singh P, Srivastava S, Singh SK. Nanosilica: recent progress in synthesis, functionalization, and biomedical applications. *ACS Biomater Sci Eng* [Internet]. 2019;5(10):4882–98. Available from: <https://pubs.acs.org/doi/10.1021/acsbiomaterials.9b00464>.
50. Sivasankarapillai VS, Jose J, Shanavas MS, Marathakam A, Uddin MS, Mathew B. Silicon Quantum dots: promising theranostic probes for the future. *Curr Drug Targets* [Internet]. 2019;20(12):1255–63. Available from: <http://www.eurekaselect.com/171354/article>.
51. Zhang H, Wang H, Yang H, Zhou D, Xia Q. Luminescent, protein-binding and imaging properties of hyper-stable water-soluble silicon quantum dots. *J Mol Liq* [Internet]. 2021;331:115769. Available from: <https://linkinghub.elsevier.com/retrieve/pii/S0167732221004943>.
52. Zhu C, Chen Z, Gao S, Goh BL, Samsudin I Bin, Lwe KW, et al. Recent advances in non-toxic quantum dots and their biomedical applications. *Prog Nat Sci Mater Int* [Internet].

- 2019;29(6):628–40. Available from: <https://linkinghub.elsevier.com/retrieve/pii/S1002007119306963>.
53. Alaghmandfard A, Sedighi O, Tabatabaei Rezaei N, Abedini AA, Malek Khachatourian A, Toprak MS, et al. Recent advances in the modification of carbon-based quantum dots for biomedical applications. *Mater Sci Eng C* [Internet]. 2021;120:111756. Available from: <https://linkinghub.elsevier.com/retrieve/pii/S0928493120336754>.
 54. Yang F, Zhang Q, Huang S, Ma D. Recent advances of near infrared inorganic fluorescent probes for biomedical applications. *J Mater Chem B* [Internet]. 2020;8(35):7856–79. Available from: <http://xlink.rsc.org/?DOI=D0TB01430C>.
 55. Krajnik B, Golacki LW, Fiedorczyk E, Bański M, Noculak A, Hołodnik KM, et al. Quantitative comparison of luminescence probes for biomedical applications. *Methods Appl Fluoresc* [Internet]. 2021;9(4):045001. Available from: <https://iopscience.iop.org/article/10.1088/2050-6120/ac10ae>.
 56. Miao Y, Wang X, Sun J, Yan Z. Recent advances in the biomedical applications of black phosphorus quantum dots. *Nanoscale Adv* [Internet]. 2021;3(6):1532–50. Available from: <http://xlink.rsc.org/?DOI=D0NA01003K>.
 57. Gaddam SK, Pothu R, Saran A, Boddula R. Biomedical applications of black phosphorus; 2020. p. 117–38. Available from: http://link.springer.com/10.1007/978-3-030-29555-4_6.
 58. Zeng G, Chen Y. Surface modification of black phosphorus-based nanomaterials in biomedical applications: strategies and recent advances. *Acta Biomater* [Internet]. 2020;118:1–17. Available from: <https://linkinghub.elsevier.com/retrieve/pii/S1742706120305845>.
 59. Liu X, Gaihre B, George MN, Li Y, Tilton M, Yaszemski MJ, et al. 2D phosphorene nanosheets, quantum dots, nanoribbons: synthesis and biomedical applications. *Biomater Sci* [Internet]. 2021;9(8):2768–803. Available from: <http://xlink.rsc.org/?DOI=D0BM01972K>.
 60. Nguyen EP, de Carvalho Castro Silva C, Merkoçi A. Recent advancement in biomedical applications on the surface of two-dimensional materials: from biosensing to tissue engineering. *Nanoscale* [Internet]. 2020;12(37):19043–67. Available from: <http://xlink.rsc.org/?DOI=D0NR05287F>.
 61. Wang L, Li Y, Zhao L, Qi Z, Gou J, Zhang S, et al. Recent advances in ultrathin two-dimensional materials and biomedical applications for reactive oxygen species generation and scavenging. *Nanoscale* [Internet]. 2020;12(38):19516–35. Available from: <http://xlink.rsc.org/?DOI=D0NR05746K>.
 62. Liu M, Zhu H, Wang Y, Sevensan C, Li BL. Functionalized MoS₂-based nanomaterials for cancer phototherapy and other biomedical applications. *ACS Mater Lett* [Internet]. 2021;3(5):462–96. Available from: <https://pubs.acs.org/doi/10.1021/acsmaterialslett.1c00073>.
 63. Erol O, Uyan I, Hatip M, Yilmaz C, Tekinay AB, Guler MO. Recent advances in bioactive 1D and 2D carbon nanomaterials for biomedical applications. *Nanomed Nanotechnol Biol Med* [Internet]. 2018;14(7):2433–54. Available from: <https://linkinghub.elsevier.com/retrieve/pii/S1549963417300898>.
 64. Niu Y, Li J, Gao J, Ouyang X, Cai L, Xu Q. Two-dimensional quantum dots for biological applications. *Nano Res* [Internet]. 2021;14(11):3820–39. Available from: <https://link.springer.com/10.1007/s12274-021-3757-5>.
 65. Chen Y, Tan C, Zhang H, Wang L. Two-dimensional graphene analogues for biomedical applications. *Chem Soc Rev* [Internet]. 2015;44(9):2681–701. Available from: <http://xlink.rsc.org/?DOI=C4CS00300D>.
 66. Lu B, Zhu Z, Ma B, Wang W, Zhu R, Zhang J. 2D MXene nanomaterials for versatile biomedical applications: current trends and future prospects. *Small* [Internet]. 2021;17(46):2100946. Available from: <https://onlinelibrary.wiley.com/doi/10.1002/sml.202100946>.
 67. Gupta R, Peveler WJ, Lix K, Algar WR. Comparison of semiconducting polymer dots and semiconductor quantum dots for smartphone-based fluorescence assays. *Anal Chem* [Internet]. 2019;91(17):10955–60. Available from: <https://pubs.acs.org/doi/10.1021/acs.analchem.9b02881>.

68. Christopherson CJ, Paisley NR, Xiao Z, Algar WR, Hudson ZM. Red-emissive cell-penetrating polymer dots exhibiting thermally activated delayed fluorescence for cellular imaging. *J Am Chem Soc* [Internet]. 2021;143(33):13342–9. Available from: <https://pubs.acs.org/doi/10.1021/jacs.1c06290>.
69. Shou K, Tang Y, Chen H, Chen S, Zhang L, Zhang A, et al. Diketopyrrolopyrrole-based semiconducting polymer nanoparticles for in vivo second near-infrared window imaging and image-guided tumor surgery. *Chem Sci* [Internet]. 2018;9(12):3105–10. Available from: <http://xlink.rsc.org/?DOI=C8SC00206A>.
70. Pu K, Shuhendler AJ, Valta MP, Cui L, Saar M, Peehl DM, et al. Phosphorylcholine-coated semiconducting polymer nanoparticles as rapid and efficient labeling agents for in vivo cell tracking. *Adv Healthc Mater* [Internet]. 2014;3(8):1292–8. Available from: <https://onlinelibrary.wiley.com/doi/10.1002/adhm.201300534>.
71. Pu K, Chattopadhyay N, Rao J. Recent advances of semiconducting polymer nanoparticles in in vivo molecular imaging. *J Control Release* [Internet]. 2016;240:312–22. Available from: <https://linkinghub.elsevier.com/retrieve/pii/S0168365916300037>.
72. Xu M, Zhang C, Zeng Z, Pu K. Semiconducting polymer nanoparticles as activatable nanomedicines for combinational phototherapy. *ACS Appl Polym Mater* [Internet]. 2021;3(9):4375–89. Available from: <https://pubs.acs.org/doi/10.1021/acsapm.1c00695>.
73. Veeramani V, Bao Z, Chan M-H, Wang H-C, Jena A, Chang H, et al. Quantum dots for light conversion, therapeutic and energy storage applications. *J Solid State Chem* [Internet]. 2019;270:71–84. Available from: <https://linkinghub.elsevier.com/retrieve/pii/S0022459618304912>.
74. Luo J, Zhang W, Yang H, Fan Q, Xiong F, Liu S, et al. Halide perovskite composites for photocatalysis: a mini review. *EcoMat* [Internet]. 2021;3(1). Available from: <https://onlinelibrary.wiley.com/doi/10.1002/eom2.12079>.
75. Talianov PM, Peltek OO, Masharin M, Khubezhov S, Baranov MA, Drabavičius A, et al. Halide perovskite nanocrystals with enhanced water stability for upconversion imaging in a living cell. *J Phys Chem Lett* [Internet]. 2021;12(37):8991–8. Available from: <https://pubs.acs.org/doi/10.1021/acs.jpcllett.1c01968>.
76. Regulacio MD, Han M-Y. Composition-tunable alloyed semiconductor nanocrystals. *Acc Chem Res* [Internet]. 2010;43(5):621–30. Available from: <https://pubs.acs.org/doi/10.1021/ar900242r>.
77. Selopal GS, Zhao H, Wang ZM, Rosei F. Core/shell quantum dots solar cells. *Adv Funct Mater* [Internet]. 2020;30(13):1908762. Available from: <https://onlinelibrary.wiley.com/doi/10.1002/adfm.201908762>.
78. La Mer VK, Dinegar RH. Theory, production and mechanism of formation of monodispersed hydrosols. *J Am Chem Soc* [Internet]. 1950;72(11):4847–54. Available from: <https://pubs.acs.org/doi/abs/10.1021/ja01167a001>.
79. La Mer VK. Nucleation in phase transitions. *Ind Eng Chem* [Internet]. 1952;44(6):1270–7. Available from: <https://pubs.acs.org/doi/abs/10.1021/ie50510a027>.
80. Ostwald W. Über die vermeintliche Isomerie des roten und gelben Quecksilberoxyds und die Oberflächenspannung fester Körper. *Zeitschrift für Phys Chemie* [Internet]. 1900;34U(1):495–503. Available from: <https://www.degruyter.com/document/doi/10.1515/zpch-1900-3431/html>.
81. Zsigmondy R. Über amikroskopische Goldkeime. I. *Z Phys Chem* [Internet]. 1906;56U(1):65–76. Available from: <https://www.degruyter.com/document/doi/10.1515/zpch-1906-5605/html>.
82. Lifshitz IM, Slyozov VV. The kinetics of precipitation from supersaturated solid solutions. *J Phys Chem Solids* [Internet]. 1961;19(1–2):35–50. Available from: <https://linkinghub.elsevier.com/retrieve/pii/0022369761900543>.
83. Wagner C. Theorie der Alterung von Niederschlägen durch Umlösen (Ostwald-Reifung). *Z Elektrochem Ber Bunsenges Phys Chem* [Internet]. 1961;65(7–8):581–91. Available from: <https://onlinelibrary.wiley.com/doi/abs/10.1002/bbpc.19610650704>.

84. Thanh NTK, Maclean N, Mahiddine S. Mechanisms of nucleation and growth of nanoparticles in solution. *Chem Rev* [Internet]. 2014;114(15):7610–30. Available from: <https://pubs.acs.org/doi/10.1021/cr400544s>.
85. Watzky MA, Finke RG. Nanocluster size-control and “magic number” investigations. experimental tests of the “living-metal polymer” concept and of mechanism-based size-control predictions leading to the syntheses of iridium(0) nanoclusters centering about four sequential magic. *Chem Mater* [Internet]. 1997;9(12):3083–95. Available from: <https://pubs.acs.org/doi/10.1021/cm9704387>.
86. de Mello Donegá C, Liljeroth P, Vanmaekelbergh D. Physicochemical evaluation of the hot-injection method, a synthesis route for monodisperse nanocrystals. *Small* [Internet]. 2005;1(12):1152–62. Available from: <https://onlinelibrary.wiley.com/doi/10.1002/sml.200500239>.
87. Peterson MD, Cass LC, Harris RD, Edme K, Sung K, Weiss EA. The role of ligands in determining the exciton relaxation dynamics in semiconductor quantum dots. *Annu Rev Phys Chem* [Internet]. 2014;65(1):317–39. Available from: <https://www.annualreviews.org/doi/10.1146/annurev-physchem-040513-103649>.
88. Zhou J, Liu Y, Tang J, Tang W. Surface ligands engineering of semiconductor quantum dots for chemosensory and biological applications. *Mater Today* [Internet]. 2017;20(7):360–76. Available from: <https://linkinghub.elsevier.com/retrieve/pii/S1369702116303510>.
89. Chakraborty I, Jimenez de Aberasturi D, Pazos-Perez N, Guerrini L, Masood A, Alvarez-Puebla RA, et al. Ion-selective ligands: how colloidal nano- and micro-particles can introduce new functionalities. *Z Phys Chem* [Internet]. 2018;232(9–11):1307–17. Available from: <https://www.degruyter.com/document/doi/10.1515/zpch-2018-1172/html>.
90. Munro AM, Jen-La Plante I, Ng MS, Ginger DS. Quantitative study of the effects of surface ligand concentration on CdSe nanocrystal photoluminescence. *J Phys Chem C* [Internet]. 2007;111(17):6220–7. Available from: <https://pubs.acs.org/doi/10.1021/jp068733e>.
91. Jeong S, Achermann M, Nanda J, Ivanov S, Klimov VI, Hollingsworth JA. Effect of the thiol–thiolate equilibrium on the photophysical properties of aqueous CdSe/ZnS nanocrystal quantum dots. *J Am Chem Soc* [Internet]. 2005;127(29):10126–7. Available from: <https://pubs.acs.org/doi/10.1021/ja042591p>.
92. Talapin D V., Lee JS, Kovalenko MV, Shevchenko EV. Prospects of colloidal nanocrystals for electronic and optoelectronic applications. *Chem Rev* [Internet]. 2010;110(1):389–458. Available from: <https://doi.org/10.1021/cr900137k>.
93. Algar WR, Susumu K, Delehanty JB, Medintz IL. Semiconductor quantum dots in bioanalysis: crossing the valley of death. *Anal Chem* [Internet]. 2011;83(23):8826–37. Available from: <https://pubs.acs.org/doi/10.1021/ac201331r>.
94. Lim SJ, Ma L, Schleife A, Smith AM. Quantum dot surface engineering: toward inert fluorophores with compact size and bright, stable emission. *Coord Chem Rev* [Internet]. 2016;320–321:216–37. Available from: <https://linkinghub.elsevier.com/retrieve/pii/S0010854516300352>.
95. Ostermann J, Merkl J-P, Flessau S, Wolter C, Kornowksi A, Schmidtke C, et al. Controlling the physical and biological properties of highly fluorescent aqueous quantum dots using block copolymers of different size and shape. *ACS Nano* [Internet]. 2013;7(10):9156–67. Available from: <https://pubs.acs.org/doi/10.1021/nn4037859>.
96. Fan Q, Dehankar A, Porter TK, Winter JO. Effect of micelle encapsulation on toxicity of CdSe/ZnS and Mn-doped ZnSe quantum dots. *Coatings* [Internet]. 2021;11(8):895. Available from: <https://www.mdpi.com/2079-6412/11/8/895>.
97. Beloglazova N V., Goryacheva IY, Shmelin PS, Kurbangaleev V, De Saeger S. Preparation and characterization of stable phospholipid–silica nanostructures loaded with quantum dots. *J Mater Chem B* [Internet]. 2015;3(2):180–3. Available from: <http://xlink.rsc.org/?DOI=C4TB01662A>.
98. Lopes FF, de Freitas CF, de Paula E, Lourenço SA, Florian M, Cabeça LF. Hydroxyapatite-coated liposomes for the controlled release of quantum dots and bupivacaine. *J Mater Res* [Internet]. 2021;36(14):3021–30. Available from: <https://link.springer.com/10.1557/s43578-021-00292-5>.

99. Hu X, Gao X. Silica–polymer dual layer-encapsulated quantum dots with remarkable stability. *ACS Nano* [Internet]. 2010;4(10):6080–6. Available from: <https://pubs.acs.org/doi/10.1021/nn1017044>.
100. Tasso M, Giovanelli E, Zala D, Bouccara S, Fragola A, Hanafi M, et al. Sulfobetaine–vinylimidazole block copolymers: a robust quantum dot surface chemistry expanding bioimaging’s horizons. *ACS Nano* [Internet]. 2015;9(11):11479–89. Available from: <https://pubs.acs.org/doi/10.1021/acsnano.5b05705>.
101. Wang W, Zhang S, Chinwangso P, Advincula RC, Lee TR. Electric potential stability and ionic permeability of SAMs on gold derived from bidentate and tridentate chelating alkanethiols. *J Phys Chem C* [Internet]. 2009;113(9):3717–25. Available from: <https://pubs.acs.org/doi/10.1021/jp808957r>.
102. Zhang Y, Clapp A. Overview of stabilizing ligands for biocompatible quantum dot nanocrystals. *Sensors* [Internet]. 2011;11(12):11036–55. Available from: <http://www.mdpi.com/1424-8220/11/12/11036>.
103. Schmidtke C, Kreuziger A-M, Alpers D, Jacobsen A, Leshch Y, Eggers R, et al. Glycoconjugated amphiphilic polymers via click-chemistry for the encapsulation of quantum dots. *Langmuir* [Internet]. 2013;29(40):12593–600. Available from: <https://pubs.acs.org/doi/10.1021/la402826f>.
104. Schmidtke C, Pösel E, Ostermann J, Pietsch A, Kloust H, Tran H, et al. Amphiphilic, cross-linkable diblock copolymers for multifunctionalized nanoparticles as biological probes. *Nanoscale* [Internet]. 2013;5(16):7433. Available from: <http://xlink.rsc.org/?DOI=c3nr01520c>.
105. Schmidtke C, Lange H, Tran H, Ostermann J, Kloust H, Bastús NG, et al. Radical initiated reactions on biocompatible CdSe-based quantum dots: ligand cross-linking, crystal annealing, and fluorescence enhancement. *J Phys Chem C* [Internet]. 2013;117(16):8570–8. Available from: <https://pubs.acs.org/doi/10.1021/jp402929j>.
106. Pösel E, Schmidtke C, Fischer S, Peldschus K, Salamon J, Kloust H, et al. Tailor-made quantum dot and iron oxide based contrast agents for in vitro and in vivo tumor imaging. *ACS Nano* [Internet]. 2012;6(4):3346–55. Available from: <https://pubs.acs.org/doi/10.1021/nn300365m>.
107. Anderson RE, Chan WCW. Systematic investigation of preparing biocompatible, single, and small ZnS-capped CdSe quantum dots with amphiphilic polymers. *ACS Nano* [Internet]. 2008;2(7):1341–52. Available from: <https://pubs.acs.org/doi/10.1021/nn700450g>.
108. Mammen M, Choi S-K, Whitesides GM. Polyvalent interactions in biological systems: implications for design and use of multivalent ligands and inhibitors. *Angew Chem Int Ed* [Internet]. 1998;37(20):2754–94. Available from: [https://onlinelibrary.wiley.com/doi/10.1002/\(SICI\)1521-3773\(19981102\)37:20%3C2754::AID-ANIE2754%3E3.0.CO;2-3](https://onlinelibrary.wiley.com/doi/10.1002/(SICI)1521-3773(19981102)37:20%3C2754::AID-ANIE2754%3E3.0.CO;2-3).
109. Aldana J, Lavelle N, Wang Y, Peng X. Size-dependent dissociation pH of thiolate ligands from cadmium chalcogenide nanocrystals. *J Am Chem Soc* [Internet]. 2005;127(8):2496–504. Available from: <https://doi.org/10.1021/ja047000+>.
110. Zhan N, Palui G, Safi M, Ji X, Mattoussi H. Multidentate zwitterionic ligands provide compact and highly biocompatible quantum dots. *J Am Chem Soc* [Internet]. 2013;135(37):13786–95. Available from: <https://pubs.acs.org/doi/10.1021/ja405010v>.
111. Smith AM, Nie S. Minimizing the hydrodynamic size of quantum dots with multifunctional multidentate polymer ligands. *J Am Chem Soc* [Internet]. 2008;130(34):11278–9. Available from: <https://pubs.acs.org/doi/10.1021/ja804306c>.
112. Giovanelli E, Muro E, Sitbon G, Hanafi M, Pons T, Dubertret B, et al. Highly enhanced affinity of multidentate versus bidentate zwitterionic ligands for long-term quantum dot bioimaging. *Langmuir* [Internet]. 2012;28(43):15177–84. Available from: <https://pubs.acs.org/doi/10.1021/la302896x>.
113. Duan H, Kuang M, Wang YA. Quantum dots with multivalent and compact polymer coatings for efficient fluorescence resonance energy transfer and self-assembled biotagging. *Chem Mater* [Internet]. 2010;22(15):4372–8. Available from: <https://pubs.acs.org/doi/10.1021/cm100442x>.

114. Muro E, Pons T, Lequeux N, Fragola A, Sanson N, Lenkei Z, et al. Small and stable sulfobetaine zwitterionic quantum dots for functional live-cell imaging. *J Am Chem Soc* [Internet]. 2010;132(13):4556–7. Available from: <https://pubs.acs.org/doi/10.1021/ja1005493>.
115. Liu W, Greytak AB, Lee J, Wong CR, Park J, Marshall LF, et al. Compact biocompatible quantum dots via RAFT-mediated synthesis of imidazole-based random copolymer ligand. *J Am Chem Soc* [Internet]. 2010;132(2):472–83. Available from: <https://pubs.acs.org/doi/10.1021/ja908137d>.
116. Susumu K, Oh E, Delehanty JB, Pinaud F, Gemmill KB, Walper S, et al. A new family of pyridine-appended multidentate polymers as hydrophilic surface ligands for preparing stable biocompatible quantum dots. *Chem Mater* [Internet]. 2014;26(18):5327–44. Available from: <https://pubs.acs.org/doi/10.1021/cm502386f>.
117. Wang W, Kapur A, Ji X, Safi M, Palui G, Palomo V, et al. Photoligation of an amphiphilic polymer with mixed coordination provides compact and reactive quantum dots. *J Am Chem Soc* [Internet]. 2015;137(16):5438–51. Available from: <https://pubs.acs.org/doi/10.1021/jacs.5b00671>.
118. Han H-S, Niemeyer E, Huang Y, Kamoun WS, Martin JD, Bhaumik J, et al. Quantum dot/antibody conjugates for in vivo cytometric imaging in mice. *Proc Natl Acad Sci* [Internet]. 2015;112(5):1350–5. Available from: <http://www.pnas.org/lookup/doi/10.1073/pnas.1421632111>.
119. Pelaz B, Jaber S, de Aberasturi DJ, Wulf V, Aida T, de la Fuente JM, et al. The state of nanoparticle-based nanoscience and biotechnology: progress, promises, and challenges. *ACS Nano* [Internet]. 2012;6(10):8468–83. Available from: <https://pubs.acs.org/doi/10.1021/nn303929a>.
120. Kim C, Galloway JF, Lee KH, Searson PC. Universal antibody conjugation to nanoparticles using the Fcγ receptor I (FcγRI): quantitative profiling of membrane biomarkers. *Bioconjug Chem* [Internet]. 2014;25(10):1893–901. Available from: <https://pubs.acs.org/doi/10.1021/bc5003778>.
121. Nag A, Kovalenko MV, Lee J-S, Liu W, Spokoyny B, Talapin DV. Metal-free inorganic ligands for colloidal nanocrystals: S₂⁻, HS⁻, Se₂⁻, HSe⁻, Te₂⁻, HTe⁻, TeS₃₂⁻, OH⁻, and NH₂⁻ as surface ligands. *J Am Chem Soc* [Internet]. 2011;133(27):10612–20. Available from: <https://pubs.acs.org/doi/10.1021/ja2029415>.
122. Sanjayan CG, Jyothi MS, Sakar M, Balakrishna RG. Multidentate ligand approach for conjugation of perovskite quantum dots to biomolecules. *J Colloid Interface Sci* [Internet]. 2021;603:758–70. Available from: <https://linkinghub.elsevier.com/retrieve/pii/S0021979721009620>.
123. Ruzicka-Ayoush M, Kowalik P, Kowalczyk A, Bujak P, Nowicka AM, Wojewodzka M, et al. Quantum dots as targeted doxorubicin drug delivery nanosystems in human lung cancer cells. *Cancer Nanotechnol* [Internet]. 2021;12(1):8. Available from: <https://cancer-nano.biomedcentral.com/articles/10.1186/s12645-021-00077-9>.
124. Susumu K, Uyeda HT, Medintz IL, Pons T, Delehanty JB, Mattoussi H. Enhancing the stability and biological functionalities of quantum dots via compact multifunctional ligands. *J Am Chem Soc* [Internet]. 2007;129(45):13987–96. Available from: <https://pubs.acs.org/doi/10.1021/ja0749744>.
125. Zhan N, Palui G, Merkl J-P, Mattoussi H. Bio-orthogonal coupling as a means of quantifying the ligand density on hydrophilic quantum dots. *J Am Chem Soc* [Internet]. 2016;138(9):3190–201. Available from: <https://pubs.acs.org/doi/10.1021/jacs.5b13574>.
126. Zhan N, Palui G, Grise H, Tang H, Alabugin I, Mattoussi H. Combining ligand design with photoligation to provide compact, colloiddally stable, and easy to conjugate quantum dots. *ACS Appl Mater Interfaces* [Internet]. 2013;5(8):2861–9. Available from: <https://pubs.acs.org/doi/10.1021/am302788q>.
127. Speranskaya ES, Beloglazova NV, Lenain P, De Saeger S, Wang Z, Zhang S, et al. Polymer-coated fluorescent CdSe-based quantum dots for application in immunoassay. *Biosens Bioelectron* [Internet]. 2014;53:225–31. Available from: <https://linkinghub.elsevier.com/retrieve/pii/S0956566313006635>.

128. Zhang P, Liu S, Gao D, Hu D, Gong P, Sheng Z, et al. Click-functionalized compact quantum dots protected by multidentate-imidazole ligands: conjugation-ready nanotags for living-virus labeling and imaging. *J Am Chem Soc* [Internet]. 2012;134(20):8388–91. Available from: <https://pubs.acs.org/doi/10.1021/ja302367s>.
129. Ma L, Tu C, Le P, Chitoor S, Lim SJ, Zahid MU, et al. Multidentate polymer coatings for compact and homogeneous quantum dots with efficient bioconjugation. *J Am Chem Soc* [Internet]. 2016;138(10):3382–94. Available from: <https://pubs.acs.org/doi/10.1021/jacs.5b12378>.

All-Optical Detection of Biocompatible Quantum Dots



Puspendu Barik and Manik Pradhan

Abstract Quantum dots (QDs) or luminescent semiconductor nanocrystals possess size-tunable elegant electro-optical properties, broad absorption spectra and narrow emission ranging from UV to NIR region, high fluorescent quantum yields, fluorescence intermittency, resistance to photobleaching, and significant Stoke shift, which are the prerequisite for the application in vitro and in vivo bioimaging, biomarker, and many more. The suitable applicability of QDs in the biomedical field needs to understand the science behind the QDs and the fundamental properties which may be tuned to achieve the desired optical properties. Therefore, the knowledge of optical detection techniques is desirable to explore the surface chemistry, the interactions with biomolecules, bioconjugation, energy transfer mechanisms, disease identification, and drug delivery, single biomolecule tracking, intracellular reporting, cellular imaging, and trace metal ion detection. This review focuses on the basics and the all-optical detection techniques for biocompatible QDs, considering their various application toward bioimaging, biomolecule sensing, and their interaction with biomolecules. The chapter also includes recently explored optical detection techniques for QDs.

Keywords QDs · Biocompatible QDs · Optical detection technique · SERS · Fluorescence

1 Introduction

The applicability of quantum dots (QDs), which are tiny semiconductor nanocrystals, has been growing day by day since it was first discovered in the early 1980s. QDs are currently utilized in a wide range of optoelectronic devices, in many in vitro

P. Barik (✉) · M. Pradhan

Technical Research Centre, S. N. Bose National Centre for Basic Sciences, JD Block, Sector-III, Salt Lake City, Kolkata 700106, India
e-mail: puspendub@bose.res.in

M. Pradhan

Department of Chemical, Biological and Macromolecular Sciences, S. N. Bose National Centre for Basic Sciences, JD Block, Sector-III, Salt Lake City, Kolkata 700106, India

and *in vivo* imaging, single-molecule tracking, labeling, therapeutic, and energy transfer-based sensing techniques [1–7] since their first synthesis [8]. In the glass matrix, Alexei Ekimov first observed that semiconductor microcrystals like CdS, CdSe, CuCl, and CuBr could absorb light at much lower wavelengths than bulk [9]. Ekimov, with the theoretician Alexander Efros, subsequently demonstrated the size-dependent optical properties of these semiconductor nanocrystals. Size-dependent absorption spectra were demonstrated independently for QDs in glass [9, 10] and an aqueous solution [8, 11]. Murphy and Coffey published the first review of its kind on QDs in 2002 [12].

During the last two decades, many QDs have been developed and enriched with superior photophysical properties due to the advancement of synthesis strategy (both hydrophobic and hydrophilic) and in-depth analysis of their exciting properties. Initially, QDs were synthesized with an organic ligand on the surface to protect from agglomeration, the decay of quantum efficiency, and the reduction of optical properties over time. Over the time, formation of shells on the surface of core QDs solves these problems to some extent. Still, the QDs cannot be used in the biological system due to nonpolar organic ligands, which restricts their solubility in a buffer. An original approach to this problem is to exchange nonpolar ligands with polar ligands using a thiol functional group [13, 14]. However, the thiol ligand on the surface is not stable and emission properties of QDs decay over time. An amphiphilic polymer strategy was developed to encapsulate the dot in a “plastic bag” that was water-soluble [15]. The demonstration of QDs in biological imaging as fluorescent biological labels was first introduced in 1998 [13, 16]. Bruchez et al. demonstrated CdSe/ZnS QDs (2- to 6-nm size range) with a spectral emission range from 400 nm to 2 μ m for fluorescent probes in biological staining and diagnostics [16] and covalently coupled to biomolecules for use in ultrasensitive biological detection [13]. After that, the application of QDs in the biomedical field was flourished exponentially in several applications, including molecular biotechnology and bioengineering [17], medical diagnostics [18], biological labeling [13]. Many recent reports and review articles discuss the vast applications of QDs in the biomedical field for different uses like cancer imaging agents [19], biosensing, imaging, drug delivery and therapeutics [20–22], and biomedical application [23–27]. The demand for nontoxic QDs has been growing for biomedical applications to avoid serious safety concerns for their undesired environmental or healthy impact [2, 28–31]. Recent reports on the modification of QDs by using nontoxic shells and biocompatible ligands or polymers are efficient techniques to effectively minimize the toxicity effects of traditional QDs [2, 3, 25, 32, 33].

This chapter will discuss the photophysical properties of QDs and the fundamentals of the origin of unique optical properties. In the following sections, the optical techniques will be discussed to characterize the QDs and discuss an essential question for the applicability of QDs in a biomedical perspective—how will these properties be necessary for the biomedical field?

2 Basic Properties of QDs

Here, we would like to recapitulate the basic concepts of quantum mechanics to understand the properties of QDs and their detection mechanism optically. QDs are semiconductor nanostructures that consist of $\sim 10^2$ – 10^5 atoms. QDs are typically between 2 and 20 nm in size and have discrete energy levels like an atom. The optical bandgap of QDs is always more significant than its bulk counterpart. Size-tunable photophysical properties of the QDs and their emission from the ultraviolet to the infrared region are shown in Fig. 1.

Structural composition: The QDs are composed of an inorganic core and an outer shell composed of organic ligands or some inorganic compound. The inorganic core controls the optical and electrical properties. At the same time, ligands or inorganic shells in the QDs play an essential role in developing the solubility, stability, particle morphology, and particle size distribution. The core part of the QDs is composed of several elements of the periodic table, for example, group IV (Si, C), groups II–VI (CdSe, ZnS, CdTe), group II–VI–VI or II–II–VI (alloyed QDs, e.g., $\text{CdSe}_x\text{Te}_{1-x}$, $\text{CdS}_x\text{Se}_{1-x}$, $\text{Cd}_x\text{Zn}_{1-x}\text{S}$, $\text{Cd}_{1-x}\text{Zn}_x\text{Se}$), groups III–V (InP, InAs, GaAs, InSb), group III–V–V ($\text{InAs}_{1-x}\text{Sb}_x$), groups IV–VI (PbSe, PbS), groups

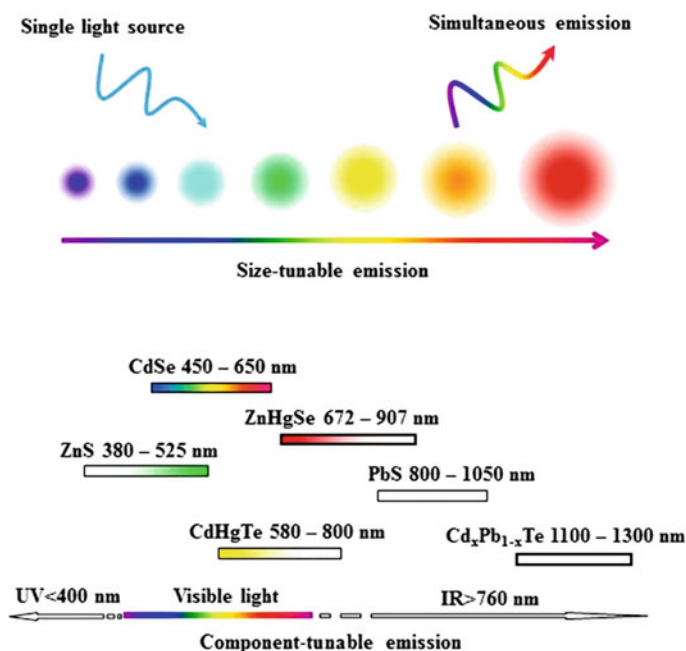


Fig. 1 Photophysical properties of the QDs with size-tunable properties. The emission of QDs consists of a broad spectral window from the ultraviolet to infrared region. Reprinted with permission from Ref. [3]. Copyright © 2015, American Chemical Society

I–III–VI (CuInSe₂, CuInS₂, AgInS₂, AgInSe₂) and groups II–I–III–VI (Zn–Ag–In–Se, Ag–In–Ga–S). The most common ligands for QDs are carboxyl (–COOH), hydroxyl (–OH), primary amines (–NH₂), phosphine oxide (O=PR₃), phosphonyl (–PO(OR)₂), and thiols (–SH). The inorganic shell materials are generally of group II–VI and IV–VI elements (ZnO, ZnS, MgO, HgS, CdSe, CdS). Moreover, the shell structure can be a single shell, multi-shell, and graded shell.

Quantum Mechanical Concepts: Quasiparticle (QP) is a purely mathematical concept that tackles the many-body problem of fundamental quantum particles and makes them comprehensible in a simple way. The concept of QPs was first developed in the 1940s and 1950s. A system of bosonic QPs, e.g., phonons, plasmons, excitons, are primarily discussed in solids [34]. An example of QP is “hole,” which represents the absence of an electron and has a positive charge. In the theory of many-body systems, physicists consider a small number of noninteracting QPs instead of a large number of interacting particles. Commonly, an electron–hole pair is bound with a characteristic length in a bulk semiconductor, called the exciton Bohr radius, with the analogy of a hydrogen atom. The bound state of electrons and holes occurs due to Columbic attraction between them. When the size of a semiconductor crystal becomes comparable to the material’s exciton Bohr radius (a_B), the electron energy levels should be treated as discrete, and it is called quantum confinement. Quantum confinement in QDs implies the confinement of the electron motion in all three directions of crystalline nanoparticles (nanocrystals) with their size, no more than a few nanometers. Exciton Bohr radius (a_B) is calculated with the analogy of the hydrogen atom:

$$a_B = \frac{\hbar^2 \varepsilon}{e^2} \left(\frac{1}{m_e^*} + \frac{1}{m_h^*} \right)$$

where \hbar is the reduced Plank’s constant, m_e^* and m_h^* are the effective masses of the electron and hole, respectively, ε is the effective permittivity of the semiconductor, e is the charge of the electron. The value of effective mass represents the interaction of the particle with the periodic crystal lattice, i.e., the increased or decreased mobility of a charge carrier (electron or hole) in a semiconductor compared to an electron in a vacuum. Therefore, $m_{e,h}^* > m_0$, implies that low carrier mobility whereas $m_{e,h}^* < m_0$, reflects higher carrier mobility for an interaction. The degree of delocalization is inversely proportional to the effective mass of charge carriers, i.e., lighter carriers are more delocalized [35]. For example, the values of effective masses for PbS QDs are $m_e^* = 0.085m_0$ and $m_h^* = 0.085m_0$ at 300 K where m_0 is the rest mass of the electron [36]. The dielectric constant of PbS is $\varepsilon_\infty = 17.2$ and $\varepsilon_0 = 161$ [36, 37]. Putting all the value in the above expression, the exciton Bohr radius (a_B) for PbS will be ~ 18 nm. However, the above expression shows that the magnitude of a_B is of the order of 2–50 nm for most semiconductors [38–40].

Several quantum mechanical concepts like Bohr radius, de Broglie wavelength or Heisenberg’s uncertainty formalism, and infinite square well potential approximation are employed to understand the quantum confinement regime. We can

explain the quantum size effect using these concepts, i.e., the size dependence of optical bandgap in various semiconductor nanoparticles. Moreover, the quantum confinement depends on the effective electron and hole masses and the dielectric constant. However, the confinement of electrons in QDs can be categorized into two distinct regimes—strong confinement and weak confinement regime. Strong quantum confinement takes place at the size of the QDs much smaller than a_B , i.e., at least several times smaller in size. The confinement potential in a strong confinement regime becomes more significant than the Coulomb interaction, much larger than in a bulk crystal. But, in a weak confinement regime (the size of QDs is larger than a_B), the rise in exciton energy is observed because of the quantization of the exciton center-of-mass motion where exciton behaves like a particle in a spherical potential. The confinement effect vanishes when the size of the QDs becomes more than 2–3 times of a_B . In both cases, the quantum confinement effects support the formation of discrete energy levels and more significant energy gaps with decreasing sizes in QDs.

According to Heisenberg's uncertainty principle, the quantum confinement effect can be observed when the diameter (d) of the QDs has the same order of magnitude as the thermal de Broglie wavelength of the electron wave function ($d \approx \lambda_e, \lambda_h$).

$$\lambda_e = \frac{\hbar}{\sqrt{2m_e^*k_B T}} \quad \text{and} \quad \lambda_h = \frac{\hbar}{\sqrt{2m_h^*k_B T}}$$

For an electron in a vacuum, the above equation gives the de Broglie wavelength of 7.3 nm. For PbS QDs at 300 K, $R = \lambda_e \cong \lambda_h \cong 4$ nm and hence strong confinement limit for PbS QDs is ~ 4 nm, i.e., the diameter of the QDs. The confinement energy will be considered if it is equal to or greater than the thermal energy, and we can derive the condition for the quantum confinement as

$$d \approx \frac{\hbar}{\sqrt{2m_{e,h}^*k_B T}}$$

The electronic structure of QDs with spherical shape can be described by the effective mass approximation using a simple model “particle in a quantum box” where the electron's motion is limited in all three dimensions [10, 41, 42]. The condition will be applicable when the size of the QDs (d) obeys the condition, $d_L \ll d \ll \lambda_{em}$, where d_L is the crystal lattice constant, λ_{em} is the photon wavelength corresponding to the lowest possible optical transition. Quantum size effect can be effective when the energy separation is greater than the thermal energy $k_B T$. Brus has introduced a theoretical insight on the size dependence of the bandgap energy of QDs considering effective mass model and neglecting spatial correlation effects [43]. The bandgap energy can be expressed as

$$E_g = (E_g)_{\text{Bulk}} + E_{\text{Confinement}} + E_{\text{Coulomb}}$$

$$E_g = (E_g)_{\text{Bulk}} + \frac{\pi^2 \hbar^2}{2R^2} \left(\frac{1}{m_e^*} + \frac{1}{m_h^*} \right) - \frac{1.8e^2}{4\pi \epsilon_0 \epsilon R}$$

where E_g is the bandgap energy of the QDs, R is the radius of QDs, ϵ is the dielectric constant of the material of QDs, and ϵ_0 is the permittivity of free space. We neglect the electron–hole spatial correlation effect [44]. Considering all the parameters for PbS QDs (diameter ~ 4 nm), the bandgap energy will be $E_g = 0.41 \text{ eV} + 2.21 \text{ eV} - 0.08 \text{ eV} = 2.54 \text{ eV}$.

Quantum confinement effects are also observed in the optical absorption spectra of QDs. The material’s composition and physical dimensions influence the quantum confinement effects. In bulk semiconductor materials, bandgap energy (E_g) is defined as the difference between the valence band’s highest occupied energy state and the conduction band’s lowest unoccupied state, as depicted in Fig. 2. a_B determines the transition point between the different properties observed in the bulk and quantum confined states. Therefore, the size of the QDs controls the optical properties.

Absorption and emission: QDs offer excellent photoelectronic properties, including broad excitation spectra, tunable fluorescence, and multicolor fluorescence compared to dye molecules. The significant absorption coefficients make QDs excellent solar absorbers when QD layers combine with a metal contact (form a Schottky junction)

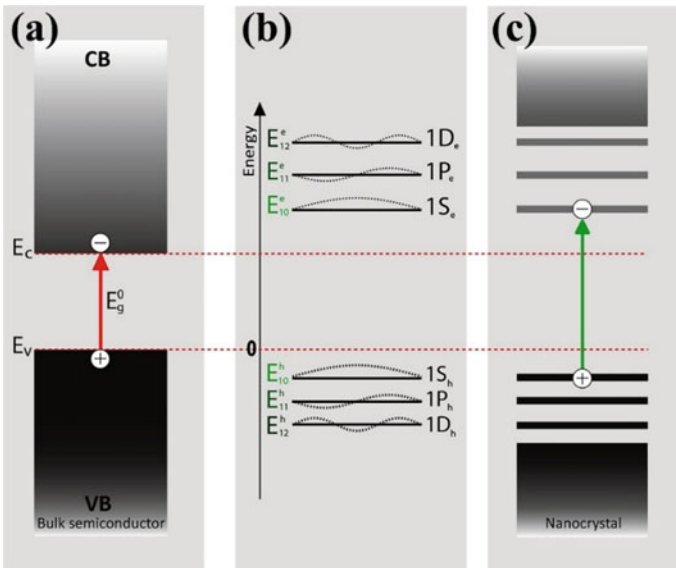


Fig. 2 The figure shows the effect of quantum confinement on the electronic structure of Semiconductor nanocrystals or QDs. The arrows indicate the lowest energy absorption transition for **a** Bulk semiconductors. **b** The energy levels and corresponding wave functions in semiconductor nanocrystals or QDs, and **c** Semiconductor nanocrystals or QDs (CB = conduction band; VB = valence band). Reproduced from Ref. [42] under CC BY 4.0

or another semiconductor (form a heterostructure). QDs exhibit high fluorescence intensity with higher stability, which is helpful for in vivo and in vivo imaging. QDs are an effective sensitizer coupled with organic chromophores due to their strong absorption properties. Lanthanide doped QDs can down-convert one high-energy photon to multiple lower-energy photons, i.e., quantum cutting. QDs can convert optical energy into chemical energy when carrier density increases at the interface of QDs and nearby molecular acceptors, owing to a strong confinement regime.

Stokes shift: The Stokes shift is named after Irish physicist George Gabriel Stokes and is the difference between the wavenumber/wavelength/energy of the incident light and the scattered light or emitted light after an interaction [45]. It is an essential concept in both fluorescence and Raman spectroscopy. Stokes' Law states that the fluorescence emission occurs at a longer wavelength (redshift) than the incident light wavelength (absorption). However, the emission occurs at a lower wavelength (i.e., higher energy or blueshift) than the incident light wavelength (absorption) in up-conversion photoluminescence. The shift to a longer wavelength is called the Stokes shift in his honor. In fluorescence spectroscopy, the Stokes shift is the difference between the spectral position of the first absorption maxima and the maxima of fluorescence emission in either wavelength (nm) or wavenumber units (cm^{-1}) or in an informal way of energy unit (meV) [46, 47]. The size-dependent redshift of emission peaks is an exciting feature of QDs. Stokes shift changes with the nature of QDs, and the solvents owing to dielectric mismatch between QDs and the surrounding medium, e.g., more polar solvents typically produce more significant Stokes shifts. Moreover, the Stokes shift for QDs depends on several factors like size [48], polydispersity [49, 50], ligands, defects [50, 51], and dopants [52, 53].

Fluorescence quantum yield (QY): The fluorescence quantum yields (Φ_f) are defined as the ratio of the number of emitted photons (N_{em}) from QDs and the number of absorbed photons (N_{abs}) at the excitation wavelength (λ_{ex}). The QY represents the spectral sensitivity, photo-emissive efficiency, photostability, and brightness of the QDs. Its value remains in the range of 0–1.

Synthesis of QDs: According to synthesis techniques, the QDs are divided into two broad groups—(i) Colloidal QDs [32, 54–60]—formed by the wet chemical synthesis technique. The size and shape of the QDs can be controlled by varying several reaction conditions. In most cases, the passivating organic ligands on the surface of the QDs form an energy barrier between QDs and the surrounding medium, (ii) Epitaxial or self-assembled QDs [61–66]—QDs are grown by epitaxy technique. These are nearly defect-free as compared to colloidal QDs. The molecule- and/or solid-like structures are possible with synthesis techniques. In contrast to epitaxial QDs, the colloidal QDs assembly is much more flexible as it is accomplished in solution, and functionalizing QDs with organic molecules is much more effective. It is worth mentioning that the fabrication costs of the colloidal QDs, which benefit from self-purification, are certainly cheaper than the epitaxial growth of QDs, which requires ultra-high vacuum equipment and expensive high purity materials. However, considering the advanced integration in the micro-optoelectronic device, epitaxial

QDs demand its applicability for precise deposition processability, quantum light sources, quantum well formation, and many more. Nevertheless, in terms of the applicability of QDs in biological systems or conjugation to biomolecules, colloidal QDs are superior to epitaxial QDs as it is possible to synthesize QDs to cover the whole visible spectral range and near-infrared (NIR) just by varying the size. In this chapter, we will consider colloidal QDs and all-optical detection of them. Some of the unique properties of QDs and their corresponding applicability are presented in Table 1.

Biocompatibility of QDs: QDs must have appropriate physical and optical properties to be applied for bio-applications. QDs must show high quantum yield (QY), good thermal and photostability, low cytotoxicity, and excellent biocompatibility with proper surface functionalization. The size, shape, composition, and surface are the critical factors for different bio-applications of QDs. Above all, the surface must be carefully designed to obtain the proper QDs functionality, e.g., targeting specific epitopes, making stealth to the environments to circumvent the immune system, and high biomolecules loading capability [60, 67]. Several surface functionalization processes complete via ligand exchange procedure or through steric stabilization have been demonstrated to improve the biocompatibility of QDs and reduce toxicity in vivo and in vivo applications [60]. QD bioconjugation is very versatile, and the size of QDs is large compared to conventional dye molecules, which leads to alterations in the biological function of the QD-bioconjugate. Moreover, charged surfaces of QDs provide ample space for non-specific interactions and control the specific recognition of the QD-bioconjugates [68]. Figure 3 summarizes the different surface coating strategies and functionalization pathways of QDs. Many reviews discussed different kinds of surface coating strategies and functionalization pathways of QDs and their application in biomedical fields [3, 7, 20, 69]. The large surface of QDs offers efficient surface modification to render QDs biocompatible. The biocompatibility of QDs can be improved by functionalizing it by some standard, nontoxic, highly hydrophilic polymer ligands, such as polyethylene glycol (PEG) [70–74], polyvinylpyrrolidone (PVP) [73, 75], mercaptopropionic acid (MPA), bovine serum albumin (BSA) [74, 76–79], zwitterionic polymer ligands [80], phospholipid [81–83], amphiphilic polymer [84, 85], polypeptides [86], and block copolymer micelles [87, 88], to name just a few.

3 Optical Techniques for the Detection of QDs

QDs can be regarded as large molecules from the viewpoint of molecular physics. QDs show nonhomogeneous broadened absorption and emission spectra owing to their distribution of sizes, defect concentrations, shape variations, surrounding inhomogeneities, and other factors. Therefore, the most efficient way to characterize QDs is the luminescence spectroscopy technique. As discussed in the previous sections, the effect of quantum confinement is clearly observed in the optical properties of

Table 1 Notable properties and possible application area for QDs

	Description	Application
<i>Physical properties</i>		
Size	The size of a typical QDs is in the range of 1–20 nm and may contain between 100 and 100,000 atoms	Solar cells, ultrafast all-optical switches, quantum computing, and many others
Color	The emission wavelength covers from UV to NIR region depending on the size and material of QDs	Biosensor, bioimaging, labeling
Solubility or dispersibility	Soluble in aqueous and non-aqueous solvents depending on the nature of the capping molecules/ligands	Biocompatibility, heteroconjugation
Thermal stability	Excellent resistance to photobleaching; observation time of minutes to hours	Bioimaging, labeling
<i>Optical properties</i>		
Absorption spectra	QDs absorb over a broad range	Useful to determine size and concentration
Emission spectra	Tunable emission from UV to NIR, Symmetric, Gaussian profile; FWHM: 30–90 nm	Enables deeper tissue imaging
Stokes shift	Up to >150 nm. Typically <50 nm only for visible wavelength-emitting QDs	Enables simultaneous multiplexed imaging with a single excitation source
Quantum yield (QY)	It determines a QD's photo-emissive efficiency. 0–0.25 (NIR region) and 0–1.0 (visible region)	High imaging contrast
Fluorescence lifetimes	Long photoluminescence lifetime, Decay in 10–100 ns, typically multiexponential	Allows time-gate detection for reducing auto-fluorescence
Energy transfer	(1) Förster resonance energy transfer (FRET), (2) Chemiluminescence resonance energy transfer (CRET), and (3) Bio-luminescence resonance energy transfer (BRET)	Biosensing
<i>Chemical properties</i>		
Photochemical stability	Resistant to photobleaching and other environmental factors	Allows for long-term exposure

(continued)

Table 1 (continued)

	Description	Application
Toxicity	Compatible with biomolecular functionalization and show enhanced permeation and retention (EPR) effect by proper surface modifications	Capable of targeting a tumor or lymphatics, compatibility to biomedical diagnostics and therapeutics
Light to chemical energy conversion	Convert optical energy into chemical energy that can be stored in useful chemical bonds	Photocatalytic H ₂ evolution, CO ₂ /N ₂ reduction
Compatible with biomolecular functionalization	It can be done using ligand chemistry, and several biomolecules can bind to a single QD	Capable of targeting a tumor or lymphatics or other biomolecules of interest
Reproducibility of labels	Limited due to the complex structure and also due to surface chemistry	Labeling

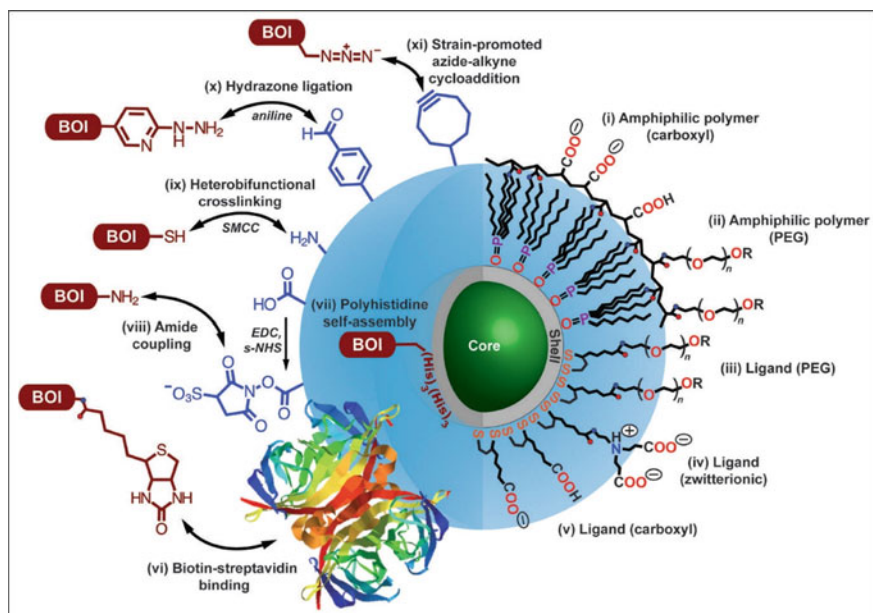


Fig. 3 Overview of bioconjugation (left side, BOI = biomolecule of interest) and surface coating (right side) strategies for QDs. The double arrows are intended to represent conjugation between the functional groups. They are not drawn to scale. Reprinted with permission from Refs. [68, 89]. Copyright 2013 Society for Applied Spectroscopy

QDs. A simple interpretation of a two-level system can be considered to understand the optical transitions in QDs [35, 90]. Recent biological applications of QDs rely on spectroscopic techniques, including absorption spectroscopy measuring the absorption coefficient; emission spectroscopy measuring intensity, polarization, or lifetime; quantifying energy and charge transfer; fluorescence enhancement employing photonic crystals and plasmon coupling; confocal and two-photon excitation (TPE) microscopy; single-particle tracking and fluorescence correlation spectroscopy; and super-resolution imaging and near-field scanning optical microscopy [89].

3.1 Absorption and Emission Spectroscopy

The absorption and emission spectroscopy can quantify the light absorption and emission by a QD in the cell environment or a solvent. Here, we discuss the basic mathematical understanding of absorption spectroscopy, which can apply to QDs. Since absorbance (A) depends on the thickness (L) of the sample, absorbance is a sample property rather than a material's property. We can express the attenuation of light intensity $I(x)$ as it travels a distance x , by (at a wavelength λ , the complex refractive index, $n = n + ik$, where k is the extinction coefficient of the material, n is the real part of refractive index).

$$I(x) = I(0)e^{-\frac{4\pi k}{\lambda} \cdot x}$$

Now, we can define a thickness independent absorption coefficient (α), an intrinsic property of the medium.

$$\alpha = \frac{4\pi k}{\lambda}$$

The above relation connects the experimentally accessible A to the property of material, i.e., the extinction coefficient k . For composite medium, e.g., suspended QDs in a solvent, the relation will be valid by replacing the k by k_{eff} . Hence, the absorption coefficient of the composite medium is expressed as

$$\mu = \frac{\ln 10A}{L} = \frac{4\pi k_{\text{eff}}}{\lambda}$$

A colloidal dispersion of QDs contains both solid QDs and the solvent (organic or inorganic). The composition can be described by volume fraction (f , the volume occupied by the QDs per unit of sample volume) and the molar concentration of QDs (c , the amount of QDs in mole per unit sample volume). Considering the QDs as polarizable point dipoles in the solvent, the effective (complex) dielectric function $\tilde{\epsilon}_{\text{eff}}$ of the colloidal solution of QDs can be related to the polarizability (a) of an individual

QD employing the Clausius–Mossotti relation (N_A is the Avogadro's number) [91–93]

$$\frac{\tilde{\epsilon}_{\text{eff}} - \epsilon_s}{\tilde{\epsilon}_{\text{eff}} + 2\epsilon_s} = \frac{1}{3}cN_A a$$

where ϵ_s is the dielectric function of solvent. For a spherical QDs in a solvent, the polarizability can be written as

$$a = 4\pi r^3 \epsilon_s \beta = 4\pi r^3 \epsilon_s \left(\frac{\epsilon_{\text{QD}} - \epsilon_s}{\epsilon_{\text{QD}} + 2\epsilon_s} \right)$$

ϵ_{QD} is the dielectric function of QDs. From these above two equations, $\tilde{\epsilon}_{\text{eff}}$ can be expressed as (i.e., the well-known Maxwell Garnett mixing rule)

$$\tilde{\epsilon}_{\text{eff}} = \frac{1 - 2\beta f}{1 - \beta f} \cdot \epsilon_s$$

For a diluted colloidal solution of QDs (i.e., $f \ll 1$), $(\tilde{\epsilon}_{\text{eff}})_{\text{Real}}$, ϵ_s and $(\tilde{\epsilon}_{\text{eff}})_{\text{Im}}$ $\frac{9\epsilon_s^2}{|\epsilon_{\text{QD}} + 2\epsilon_s|^2} f (\epsilon_{\text{QD}})_{\text{Im}}$. $(\tilde{\epsilon}_{\text{eff}})_{\text{Im}}$ represent the idea of local field factor f_{LF} , which is defined as the ratio between the external driving field E_0 and the resulting local field E_{loc} . For spherical QDs, local field factor can be expressed as, $f_{\text{LF}} = \frac{3\epsilon_s}{\epsilon_{\text{QD}} + 2\epsilon_s}$. Thus, the absorption coefficient μ for dispersion of QDs as (considering Maxwell Garnett composites for spherical particles approximation, $(\tilde{\epsilon}_{\text{eff}})_{\text{Im}} = 2n_{\text{eff}}k_{\text{eff}}$),

$$\mu = \frac{2\pi}{\lambda n_s} \cdot |f_{\text{LF}}|^2 \cdot f (\epsilon_{\text{QD}})_{\text{Im}} = \frac{n}{n_s} \cdot |f_{\text{LF}}|^2 \cdot f \alpha$$

According to the above equation, the local field effect strongly modifies the absorption of a material when it is dispersed in another medium. Since μ increases proportionally to f , one can define intrinsic absorption coefficient μ_i as:

$$\mu_i = \frac{\mu}{f} = \frac{2\pi}{\lambda n_s} \cdot |f_{\text{LF}}|^2 \cdot (\epsilon_{\text{QD}})_{\text{Im}}$$

The intrinsic absorption coefficient only depends on the optical constant of QDs, the local field factor, and the solvent. At incident light energies, a strong dielectric screening of the external electric field occurs and hence the reduction of the absorption of QDs compared to bulk. The substantial enhancement of the absorbance at high energy is due to an increase in f_{LF} at these energies. The intrinsic absorption coefficient μ_i can be measured experimentally by the following relation knowing the value of volume fraction f (i.e., the total number of atoms and the lattice constants)

$$\mu_i = \frac{\ln 10A}{fL}$$

The above equation helps us to quantify and understand the QD light absorption by knowing μ_i, f , and vice versa. Beer's Law states that A is proportional to c and the path length L ($A \propto cL$). The proportionality constant (ϵ) is defined as the molar extinction or molar absorption coefficient ($A = \epsilon cL$). The absorption cross-section σ of a single QD can be derived as $\sigma = V_{\text{QD}}\mu_i$. The QD band structure consists of a discrete set of energy levels. According to the quantum mechanical description of light absorption and emission, the optical properties can be realized starting from the oscillator strength and corresponding exciton emission rate of a two-level system. The description in detail is out of the scope of the book chapter. Cadmium selenide (CdSe) QDs show size-tunable fluorescence throughout the visible light spectrum, as depicted in Fig. 4.

Absorption spectroscopy is a technique that performs quantitative and qualitative analysis through the absorption of light by QDs. The electron-hole pair (exciton) in a QDs absorb a photon in absorption spectrum measurements with the excitation by a source, whereas in emission spectrum measurements, a photon is emitted, which is measured. Photoluminescence (PL) spectroscopy is a technique where the emission properties of a material are measured by varying the excitation energy. Photoluminescence excitation (PLE) spectroscopy is a complementary technique to get insights into the absorption properties. Absorption spectra are acquired in transmission configuration by varying the incident energy, whereas in PLE, detection is carried out in reflection configuration, and the detection energy is fixed. In general, PLE must be a replica of absorption spectra, but the size distribution of QDs and the dependence of luminescence quantum efficiency on the excitation energy may alter

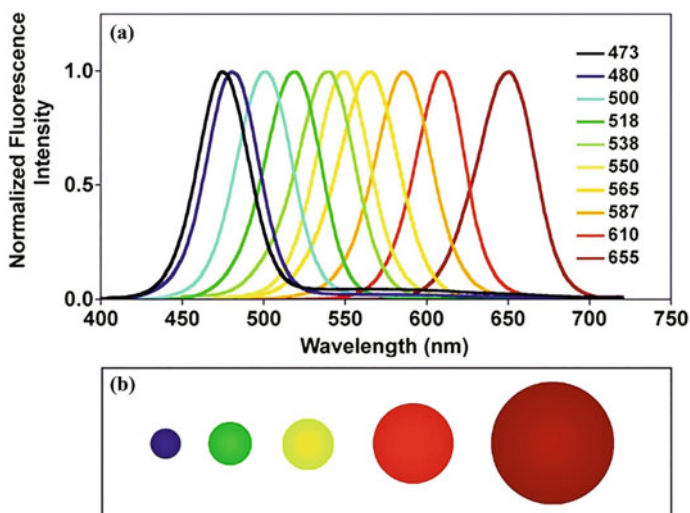


Fig. 4 **a** Size-tunable fluorescence spectra of CdSe QDs, **b** a representative illustration of the relative particle sizes (not in size ratio). The particle diameters are 2.1 nm, 2.5 nm, 2.9 nm, 4.7 nm, and 7.5 nm from left to right. Reproduced from Ref. [94] with permission from The Royal Society of Chemistry

the characteristics of the PLE spectra [95]. However, PLE shows a better signal-to-noise ratio, i.e., a better energy resolution than absorption spectra. Ultraviolet–visible (UV–Vis) absorption spectroscopy is a routine analytical technique to characterize QDs in a colloidal dispersion that is based on the variation of the position of the first excitonic absorption peak with the size of QDs of narrow size distribution. The average size and concentration of QDs can be approximately estimated from the absorption spectra.

Photoluminescence (phosphorescence and fluorescence) is triggered by the absorption of a photon with high energy, resulting in emission with a low energy photon (Stoke emission). In chemistry, it is termed fluorescence spectroscopy. The relaxation processes can be studied using time-resolved fluorescence spectroscopy. Photoluminescence (PL) imaging techniques map the intensity (confocal microscopy) or the lifetime (fluorescence-lifetime imaging microscopy) across a sample (biological sample marked with fluorescent QDs). After the absorption of a photon by the QDs (considering a two-level system), the excited electron typically goes to the bottom of excited states after successive vibrational relaxation in a picosecond time range (ps). Now, the electron quickly recombines with the vacancy/hole in the ground state, i.e., fluorescence resulting in an emission of a photon at a time delay in the range of nanosecond (ns). Otherwise, the electron will go to a metastable state and relax to the ground state with a longer recombination time (microseconds (μs) to minutes), i.e., phosphorescence. PL spectra of QDs in solution or QDs solid provide several important information about QDs: (i) the size of QDs and the bandgap energy, (ii) impurity levels and defect detections, (iii) surface structure and excited states, (iv) recombination mechanisms, and (v) molecular structure and crystallinity. Charges can be created inside QDs by Auger autoionization or injection from outside, leading to nonradiative recombination of excitons. Therefore, time-resolved photoluminescence (TRPL) spectroscopy of QDs ensembles can identify the nature of the suppression of light emission, and hence, TRPL can identify the individual ionized particles.

3.2 Fluorescence Microscopy

Fluorescence microscopy plays a crucial role in bioimaging to visualize biological samples. Fluorescence imaging can offer real-time imaging with high contrast and resolution and is an alternative modality for imaging like magnetic resonance imaging (MRI), computed tomography (CT), positron emission tomography (PET), single-photon emission computed tomography (SPECT), and ultrasound. Fluorescence imaging involves three main steps: an external fluorescent probe to allow for signal generation, optical excitation, and collection of fluorescent light emissions. These imaging techniques are advantageous for medical diagnosis, single-cell tracking, studying the immune system, fluorescence-guided surgery, and many more. The fluorescent probe must be selective for the target, possess low toxicity,

and have excellent fluorescent properties, i.e., high photoluminescent QY, photostability, and tunable emission. In this perspective, QDs with emission bands at the near-infrared (NIR) region of the electromagnetic spectrum can be employed as the fluorescent probe for fluorescence imaging where scattering, absorption, and autofluorescence from tissues have a minimum effect in obtaining high image quality and greater tissue penetration. The interference of the biological media is lowest for two NIR regions, i.e., NIR biological windows: NIR-I (650–950 nm) and NIR-II (between 1000 and 1400 nm). During the last decades, QDs are crucial for imaging applications compared to dye molecules due to the high brightness (QY \times absorptivity) caused by high QYs and significant molar extinction coefficients [68, 96]. Another advantage of QDs is a more significant two-photon cross-section (10^3 – 10^4 Goeppert-Mayer units (GM)) for in vivo applications with NIR excitation and advantageous for multiphoton excitation. The in vivo two-color fluorescence molecular imaging of an essential immune cell, myeloid-derived suppressor cell (MDSC), was achieved using QD-based nanoprobes in the second near-infrared window (NIR-II, 1000–1700 nm), confirming the successful binding of two separate receptors on MDSCs, as shown in Fig. 5.

Confocal microscopy is one of the essential derivatives of the wide-field microscopy technique, and implementing a pinhole in confocal microscopy is the main difference. A pinhole can filter away the fluorescence photons coming from out-of-focus points to obtain a background-free image. The resolution of the confocal microscopy (the optical diffraction limit) can be expressed as

$$R = \frac{0.61\lambda}{\text{N.A.}} = \frac{0.61\lambda}{n \sin \theta}$$

where n is the refractive index, λ is the emission maxima, N.A. is the numerical aperture, θ is half the light collection angle, and R is the closest distance between two neighbor locations that can be resolved. However, confocal laser scanning microscope (CLSM) or resonant scanning confocal microscopy, the derivatives of confocal microscopy are generally used in biomedical imaging. Super-resolution microscopy has been developed to overcome the resolution limit beyond its optical diffraction limit for studying single molecules and the dynamics of biomolecules. So far, stimulated emission depletion microscopy (STED), stochastic optical reconstruction microscopy (STORM), photoactivated localization microscopy (PALM), and saturated structured illumination microscopy (SSIM) are used in the biomedical field. By separating spontaneous emission and stimulated emission in STED, localization of fluorescence molecules on a nanometer scale can be achieved. QDs have been effectively employed for STED microscopy to study biological phenomena. The fluorescent probes like QDs can be distributed evenly, making them excellent for the STORM technique. Recently, super-resolution microscopies, including 3D-STED, 3D-STORM, or iPALM, have been developed in 3D-bioimaging for three-dimensional (3D) construction of tissues or the progression of cell development. QD blinking was employed to achieve three-dimensional (3D) super-resolution imaging with nm resolution [97]. Likewise, light-sheet fluorescence microscopy (LSFM) can

be employed to obtain deep-tissue imaging. Many other optical microscopy techniques can resolve the biological tissue with an outstanding signal-to-noise ratio, e.g., universal point accumulation for imaging in nanoscale topography (PAINT), conical diffraction microscopy (CoDiM), differential interference contrast (DIC) microscopy, phase contrast microscopy, and total internal reflection fluorescence microscopy (TIRF).

Fluorescence microscopy-related techniques: QDs have been extensively used in bioassays, immunoassays, and bioimaging as probes to detect pathogens, medical

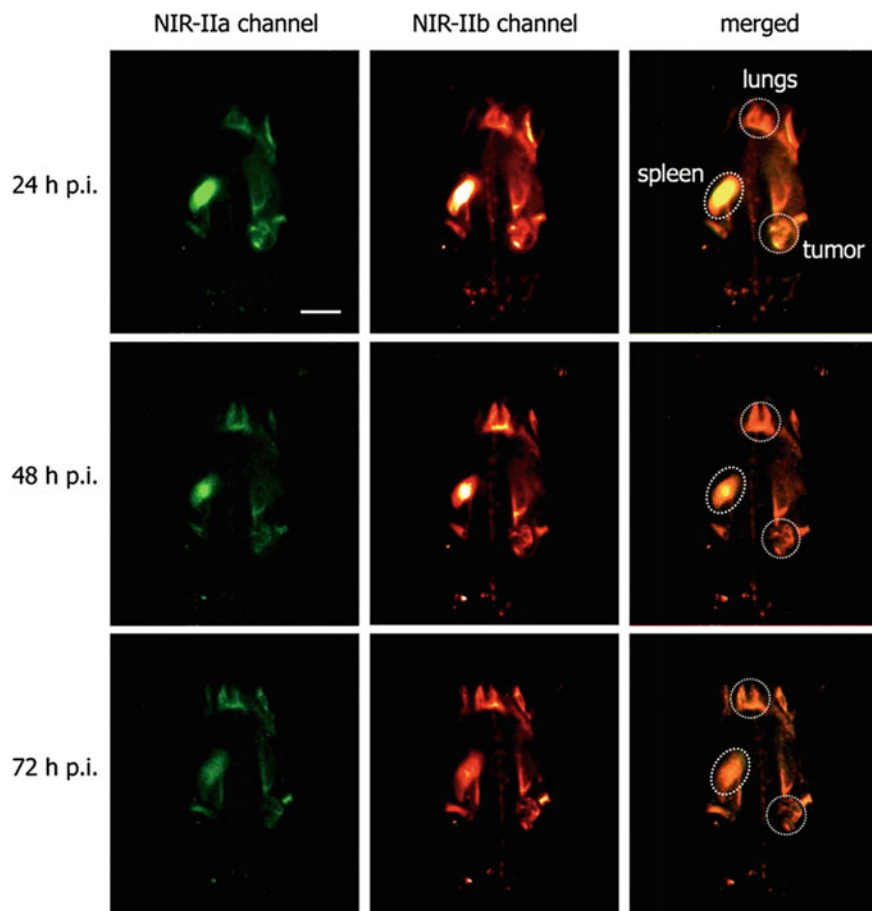


Fig. 5 In vivo non-invasive two-color fluorescence imaging of mouse in the NIR-II window. Two kinds of PbS/CdS QDs emitting in NIR-IIa and NIR-IIb regions with the combination of long-pass (LP) and short-pass (SP) emission filters by using a NIR-II imaging setup equipped with an InGaAs CCD camera ($1\times$ magnification objective, 808 nm laser excitation, laser power ~ 20 mW/cm², and exposure time of 200 ms). Reprinted with permission from Ref. [98]. Copyright © 2019, American Chemical Society

imaging, biosensing, assay labeling, optical barcoding, bio-analytes, and heavy metal ions during the last decades [99–105]. The biosensors involve three key components: the probe, the analyte, and the capturing agent (primary antibody, aptamer, peptides. QDs act as the probe attached to a revealing agent (secondary antibody, aptamer, monoclonal antibody). The interaction between revealing agents and the analytes will reflect the nature of the fluorescence. Photon-induced energy transfers phenomena affect the fluorescence and pave a pathway for sensing an analyte molecule. There are three classes of energy transfer mechanisms [106, 107]: (1) Förster resonance energy transfer (FRET), (2) Chemiluminescence resonance energy transfer (CRET), and (3) Bio-luminescence resonance energy transfer (BRET). The mechanism of FRET involves a donor fluorophore (QDs) in an excited electronic state on the absorption of photons via external optical excitation, which may transfer its excitation energy to the ground state of a nearby acceptor chromophore (light-sensitive biomolecules) through nonradiative emissions due to long-range dipole–dipole interactions. The change in fluorescence quantifies that moieties have been attached to QDs and can be used as a sensor. The applications of FRET in biological investigations are the measurement of distances between two sites on a macromolecule (protein or nucleic acid) or the examination of *in vivo* interaction between two biomolecular objects. Biosensors can detect multiple biomolecules based on the fluorescence sensor model, including DNAs, microRNAs, proteins, enzymes, and small molecules [103]. QD-based fluorescent biosensors are extensively utilized due to their high sensitivity, and the FRET technique is frequently adopted. The detection of target biomolecules is possible in a homogeneous manner without any washing and separation steps. Fluorescent probes like QDs can label the protein to serve as the donor and acceptor. Significant Förster distance can be possible for QDs due to their high quantum yield. Size-tunable properties of QDs also help to adjust the Förster distance by tuning the spectral overlap over a range of values exciting with lower intensity and minimizing or even avoiding photobleaching. Moreover, QDs also act as acceptors during FRET when organic chromophore [108–110].

Fluorescence correlation spectroscopy (FCS) is another essential optical modality to study single biomolecules. Combining FCS with optical microscopy techniques like STED, FRET, and confocal microscopy is quite powerful for biological sample sections to obtain the fluorescence signal of molecules from precisely selected areas. Fluorescence-activated cell sorting (FACS) uses fluorescence signal detection to sort out labeled cells by charging biological particles and morphology. Near-field scanning optical microscopy (NSOM) can obtain simultaneous topographic and fluorescence images to identify nanosized domains of molecules (R 50 nm) on the cell surface [111–113].

These optical imaging techniques were demonstrated to understand biological processes and their dynamics like single-molecule recognition, investigating cellular structures and functions, *in vivo* (cell movement, cell delivery, muscle contraction, cell migration, intracellular transport), and *in vivo* (investigations of the lymphatic system, tumors, and metastases) imaging applications. However, a more profound investigation of QDs-biomolecule conjugates has been necessary to quantify the

molecular interactions on the cellular and subcellular level at higher multiplexing dimensions (considering intensity, lifetime, color, and polarization of PL).

3.3 Dynamic Light Scattering (DLS) Technology

The light scattering cross-section is comparable to r^6 , where r is the radius of the particles present in the solution. Elastic scattering happens when the particle size is less than 1/10th of the incident light wavelength (i.e., $\sim\lambda/10$), and it is not angle-dependent. Dynamic light scattering (DLS), also called photon correlation spectroscopy (PCS) or quasi-elastic light scattering (QELS), relies on detecting and analyzing the interference of electric fields scattered by inhomogeneities in a medium caused by dispersed objects (e.g., polymers or colloidal nanoparticles or QDs) subject to electromagnetic irradiation [114–116]. PCS and QELS are standard in older literature. DLS is based on the Brownian motion of dispersed particles, and the DLS instruments measure the intensity of the light scattered over time. The scattered intensities are similar in the beginning and lose similarity over time due to Brownian motion. Now, let us consider QDs scatter electromagnetic waves in all directions, depending on QDs' size isotropically or anisotropically. Scattering intensity patterns correlate with themselves (auto-correlation) after short time delay intervals (τ), depending on how fast QDs are diffusing. The exponential auto-correlation function (ACF) expresses the continuous decay of correlation. The photon correlation is lost faster for small particles than large ones. One can determine the hydrodynamic diameter by measuring the speed of the particles where smaller particles will move at higher speeds than larger particles. The Stokes–Einstein equation gives the hydrodynamic particle radius (R_H) with known temperature (T) and viscosity of the fluid (η).

$$D = \frac{k_B T}{6\pi \eta R_H}$$

where D is the translational diffusion coefficient ($\text{m}^2 \text{s}^{-1}$)—represent the speed of the particles, k_B is the Boltzmann constant ($\text{m}^2 \text{kg s}^{-2} \text{K}^{-1}$). An ACF of scattered light at time point t is generated during a DLS experiment depending on the correlation time delay τ so that a second order ACF is generally given by:

$$g_2(\tau) = \frac{I(t)I(t + \tau)}{I(t)^2}$$

Multi-channel DLS allows us to characterize the solution of QDs solution or suspension efficiently. Alternatively, diffusing-wave spectroscopy (DWS) is most suitable for highly dense colloidal suspensions or highly scattering media, e.g., gels or biological media. The applications of DLS include the study of the homogeneity of proteins, RNA, and their complexes, reliable estimates of the quality of biomolecular preparations (both degradation and aggregation), protein–protein interaction studies,

the study of size and shape macromolecules. However, the DLS experiments have some notable limits like being very sensitive to temperature and solvent viscosity, hard to resolute monomer and dimer, restricted to transparent sample.

Zeta potential (ζ), also called electrokinetic potential, is the potential at the shear plane of a colloid particle moving under an electric field and routinely measured using the technique of micro-electrophoresis [116, 117]. The ζ reflects the potential difference between the EDL (electric double layer) of electrophoretically mobile particles and the dispersant layer around them at the slipping plane. ζ can be assessed by the electrophoretic mobility of charged particles under an applied electric field. The electrophoretic mobility (μ_e) of the particles is calculated by Henry's equation [116]

$$\mu_e = \frac{\varepsilon_r \varepsilon_0 \zeta f}{3\eta}$$

where ε_r is the relative permittivity/dielectric constant of the medium, ε_0 is the permittivity of vacuum, f (1 or 1.5, for organic medium or aqueous medium, respectively) is the Henry's or Helmholtz-Smoluchowski function. Zeta potential depends on pH, the concentration of the solution, and ionic strength. pH is perhaps the most influential parameter in Zeta potential measurements. Colloids of QDs fail to retain their stability and agglomerate/flocculate when the pH is close to the isoelectric point. Concentration alters both surface adsorption and the effect of EDL by complex relationship. According to drug delivery perspective, the values of ζ of the order of $\pm 0-10$ mV, $\pm 10-20$ mV, $\pm 20-30$ mV, and $> \pm 30$ mV represent as highly unstable, relatively stable, moderately stable, and highly stable, respectively. As Zeta potential does not include the contribution of van der Waals attractive forces, the low potential value may show for a stable solution like colloidal silica [118]. Surface functionality, the colloidal stability of dispersed QDs in a medium, and the interaction of QDs with the solid surface can be characterized by measuring the zeta potential. Zeta potential provides indicative evidence of the nature of the surface charge (positive/negative) in nanoparticles. Usually, naturally occurring surfaces or molecules show negative charge (e.g., cell membrane, proteins, lipids, mucus), and synthetic molecules or surfaces are often cationic. The zero value of Zeta potential cannot claim to have "neutral" nanoparticles due to unavoidable charge build-up on their surfaces in dispersion. Both DLS and Zeta potential techniques rely on the scattering of light. Hence the inability to handle high concentrations ($> 100 \mu\text{g/ml}$) and nonhomogeneous solution are major weakness of both these techniques. Therefore, they are not independently conclusive in vivo circumstances. However, they are excellent tools to characterize QDs at their initial stages of development.

3.4 FTIR Spectroscopy

Fourier transform infrared (FTIR) spectroscopy technique can identify the variations in the composition of biomolecules and their QDs-conjugates by determining changes in functional groups in biomolecules. FTIR spectroscopy is a common analytical technique in pharmaceutical, medical, and forensic laboratories for qualitative and quantitative analysis [119–122]. It measures the vibration and rotation of molecules influenced by infrared radiation at a specific wavelength. It measures the absorption of infrared radiation by each bond in the molecule and produces a transmittance spectrum (%) versus wavenumber (cm^{-1}). It is an essential technique to investigate the ion–dipole interactions, characterize the surface chemistry of biomaterials, the quantitative analysis of complex mixtures, the qualitative verification of functional groups, and investigate surface and interfacial phenomena. Moreover, FTIR spectroscopy overcomes the limitations encountered with dispersive instruments, i.e., slow scanning process, measuring intensity at a single wavelength at a time, by employing a simple optical device called an interferometer and a well-known mathematical technique called the Fourier transformation. In comparison to UV–Vis spectroscopy, the FTIR spectrum supplies a rich array of absorption bands and gives us more insight into the structure of molecules in all three physical states (i.e., gas, liquid and solid). The FTIR spectrum covers near-IR ($\sim 15,000 \text{ cm}^{-1}$ to 3000 cm^{-1}), mid-IR ($\sim 4000 \text{ cm}^{-1}$ to 400 cm^{-1}), and far-IR ($\sim 200 \text{ cm}^{-1}$ to 10 cm^{-1}). However, the most used spectrum range is 4000 cm^{-1} to 400 cm^{-1} to analyze common molecules in biomedical fields.

Symmetrical molecules are not IR sensitive as it has no net dipole moment (e.g., H_2 , O_2). Two molecules with different structures always produce different infrared spectrums, although some frequencies might be the same. Every bond (predominantly covalent for organic molecules) has a natural vibrational frequency, and the amplitude of vibrational modes of the molecules increases when the natural vibrational frequencies are matched with the incident IR frequencies. Moreover, all molecular bonds absorb specific IR radiation (frequencies) and do not affect by the adjacent bonds. The movement of the bonds in a molecule has two main vibrational modes—stretching and bending vibrational mode. Stretching mode is further divided into symmetric and asymmetric vibrations modes while wagging, twisting (out of plane bending vibration) and rocking, scissoring (in-plane bending vibration) are the characteristic modes of bending vibrations. FTIR spectroscopy can be helpful for the structural determination of protein where X-ray crystallography or multidimensional NMR spectroscopy techniques cannot be appropriately applied.

Attenuated Total Reflection (ATR) sampling revolutionized FTIR spectroscopy in several ways—simplicity in sample handling and applicability for any form of samples. ATR-FTIR spectroscopy has been used to investigate biomedical samples, protein crystallization, surface interaction with proteins, and the behavior of proteins [123, 124]. IR radiation gets internally reflected and attenuated at an interface between a high refractive index material (an internal reflection element such as diamond, Ge, Si, and ZnSe) and an infrared absorbing low refractive index material

(the sample). Hence, generated evanescent wave at the interface can penetrate with the depth of penetration (d_p) in the sample in the range between 0.2 and 5 μm . Therefore, it can characterize the surface and a depth of a few micrometer samples adjacent to the surface of the ATR crystal within the imaging field of view. The generation of amide vibrational bands in the FTIR spectra of proteins are very useful for determining changes in the secondary structure, disordered regions, and aggregated β -sheets in the protein. As ATR-FTIR spectroscopy analyzes only the surface molecules, it can be free from the issue of complete absorption of the IR radiation by the aqueous phase. Thus, the ATR-FTIR imaging technique is label-free, nondestructive, and can distinguish between protein and nonprotein crystals, proving a viable alternative to X-ray crystallography and dye-based fluorescence. Protein aggregation of purified protein *in vivo*, which has a significant impact on biotherapeutics, can be effectively visualized using ATR-FTIR spectroscopic imaging compared to other techniques, including size-exclusion chromatography (SEC), dynamic light scattering, and circular dichroism. The combination of two nondestructive vibrational spectroscopy—Raman and FTIR—are complementary techniques or fingerprint spectroscopic techniques that allow real-time analysis or the identification (qualitative analysis) and structural elucidation of molecules of interest in biomedical samples with excellent sensitivity with relatively low detection limit.

3.5 Raman Spectroscopy

Raman scattering, a feeble effect, occurs during an inelastic collision of photons with molecules. Typical Raman cross-sections are between 10^{-30} and 10^{-25} cm^2 per molecule in comparison with fluorescence spectroscopy (between 10^{-17} and 10^{-16} cm^2 per molecule), infrared absorption (between 10^{-19} and 10^{-20} cm^2 per molecule). However, surface-enhanced Raman scattering (SERS) is an ultrasensitive technique for detecting molecules on or in the vicinity of metal nanostructures owing to the resonances between optical fields and surface plasmons leading to strongly enhanced Raman scattering signals of molecules. The SERS effect can improve the Raman signal by 10^4 – 10^{10} times and detect trace concentrations of specific analytes. SERS is superior to conventional optical spectroscopic techniques such as fluorescence and UV/Vis absorption spectroscopy. Over the last two decades, SERS has become one of the most promising analytical techniques in biomedical and agri-food applications [125–130]. A labeled SERS approach can detect biomolecules efficiently and provide high specificity. A multiplex detection uses encoding nanoprobe with a unique code to identify the attached ligand molecules. SERS—fluorescence dual-encoded nanoprobe (layer-by-layer assembly—SERS layer consisting of Raman reporters and a fluorescent layer composed by QDs) guarantees the high-throughput sensing and imaging technologies (e.g., clinical diagnosis, biosensing, and imaging) and high stability inhibiting the signal cross-talk [131–134]. QDs bioconjugate is covalently linked with proteins,

antibodies, and DNA eliminating the need for biomarker and labeling in biomedical imaging. Here, SERS biosensing plays a vital role in the potential of a cancer diagnosis using Si-based semiconductor material [135].

4 Conclusion

QDs attract much attention in the biomedical field owing to their excellent photophysical properties. However, QDs may show the following drawbacks: poorly controlled growth rate and difficulties in high-throughput synthesis, aggregation in the cell environment, single QDs blinking, reduction of QY owing to surface traps, complicated surface chemistry, relatively large size, and toxicity. In the present scenario, we could not use the QDs to supplant the other fluorophores (e.g., dye) in labeling and imaging; instead, we successfully have deployed them in combination with other types of fluorophores. Therefore, more research (both *in vitro* and *in vivo*) must be needed to thoroughly investigate the possible effects of the applicability of QDs for clinical applications (still questionable). Most of the QDs are not biodegradable, and the long-term effect of the accumulation of QDs inside the body of animals is unknown based on the present knowledge. However, QDs have proved effective for *in vitro* studies, e.g., diagnostics, imaging, and biomarker. Multiple functionalities of QDs are already established as fluorescent labels for bioimaging, specific capture molecules for targeted delivery, and therapy. More investigation of the influence of QDs in the pharmacokinetic properties and functional activity of drugs must be performed to explore more possibilities in the biomedical field. Tunable emissions of NIR QDs have become an attractive tool for deep-tissue, high-resolution *in vivo* imaging. FRET is an excellent biosensing tool where QDs act as donors for detecting biomolecules. Nevertheless, spectroscopy and DLS provide accurate data about QDs surface properties for accurate identification of bioconjugates with retaining of biological activity of conjugated molecules. Hence, all-optical detection of the surface properties of QDs is desirable for application in the biomedical field.

Acknowledgements We acknowledge the Technical Research Centre (TRC) [No. All1/64/SNB/2014(C)] of the S. N. Bose National Centre for Basic Sciences, Kolkata, for funding this work.

References

1. Farzin MA, Abdoos H. A critical review on quantum dots: from synthesis toward applications in electrochemical biosensors for determination of disease-related biomolecules. *Talanta* [Internet]. 2021;224:121828. Available from: <https://linkinghub.elsevier.com/retrieve/pii/S003991402031119X>.
2. Zhu C, Chen Z, Gao S, Goh BL, Samsudin I Bin, Lwe KW, et al. Recent advances in non-toxic quantum dots and their biomedical applications. *Prog Nat Sci Mater Int* [Internet].

- 2019;29(6):628–40. Available from: <https://linkinghub.elsevier.com/retrieve/pii/S1002007119306963>.
- Zhou J, Yang Y, Zhang C. Toward biocompatible semiconductor quantum dots: from biosynthesis and bioconjugation to biomedical application. *Chem Rev* [Internet]. 2015;115(21):11669–717. Available from: <https://pubs.acs.org/doi/10.1021/acs.chemrev.5b00049>.
 - Castro RC, Ribeiro DSM, Santos JLM. Visual detection using quantum dots sensing platforms. *Coord Chem Rev* [Internet]. 2021;429:213637. Available from: <https://linkinghub.elsevier.com/retrieve/pii/S0010854520307335>.
 - Tajik S, Dourandish Z, Zhang K, Beitollahi H, Le Q Van, Jang HW, et al. Carbon and graphene quantum dots: a review on syntheses, characterization, biological and sensing applications for neurotransmitter determination. *RSC Adv* [Internet]. 2020;10(26):15406–29. Available from: <http://xlink.rsc.org/?DOI=D0RA00799D>.
 - Yu Y, Li M, Yu Y. Tracking single molecules in biomembranes: is seeing always believing? *ACS Nano* [Internet]. 2019;13(10):10860–8. Available from: <https://pubs.acs.org/doi/10.1021/acsnano.9b07445>.
 - Kargozar S, Hoseini SJ, Milan PB, Hooshmand S, Kim H, Mozafari M. Quantum dots: a review from concept to clinic. *Biotechnol J* [Internet]. 2020;15(12):2000117. Available from: <https://onlinelibrary.wiley.com/doi/10.1002/biot.202000117>.
 - Rossetti R, Nakahara S, Brus LE. Quantum size effects in the redox potentials, resonance Raman spectra, and electronic spectra of CdS crystallites in aqueous solution. *J Chem Phys* [Internet]. 1983;79(2):1086–8. Available from: <http://aip.scitation.org/doi/10.1063/1.445834>.
 - Ekimov AI, Efros AL, Onushchenko AA. Quantum size effect in semiconductor microcrystals. *Solid State Commun* [Internet]. 1985;56(11):921–4. Available from: <https://linkinghub.elsevier.com/retrieve/pii/S0038109885800259>.
 - Ekimov AE, Onushchenko AA. Quantum size effect in three-dimensional microscopic semiconductor crystals. *J Exp Theor Phys Lett*. 1981;35(6):345.
 - Rossetti R, Ellison JL, Gibson JM, Brus LE. Size effects in the excited electronic states of small colloidal CdS crystallites. *J Chem Phys* [Internet]. 1984;80(9):4464–9. Available from: <http://scitation.aip.org/content/aip/journal/jcp/80/9/10.1063/1.447228>.
 - Murphy CJ, Coffey JL. Quantum dots: a primer. *Appl Spectrosc* [Internet]. 2002;56(1):16A–27A. Available from: <http://journals.sagepub.com/doi/10.1366/0003702021954214>.
 - Chan WC. Quantum dot bioconjugates for ultrasensitive nonisotopic detection. *Science* (80–) [Internet]. 1998;281(5385):2016–8. Available from: <https://www.sciencemag.org/lookup/doi/10.1126/science.281.5385.2016>.
 - Pathak S, Choi S-K, Arnheim N, Thompson ME. Hydroxylated quantum dots as luminescent probes for in situ hybridization. *J Am Chem Soc* [Internet]. 2001;123(17):4103–4. Available from: <https://pubs.acs.org/doi/10.1021/ja0058334>.
 - Wu X, Liu H, Liu J, Haley KN, Treadway JA, Larson JP, et al. Immunofluorescent labeling of cancer marker Her2 and other cellular targets with semiconductor quantum dots. *Nat Biotechnol* [Internet]. 2003;21(1):41–6. Available from: <http://www.nature.com/articles/nbt764>.
 - Bruchez Jr. M. Semiconductor nanocrystals as fluorescent biological labels. *Science* (80–) [Internet]. 1998;281(5385):2013–6. Available from: <https://www.sciencemag.org/lookup/doi/10.1126/science.281.5385.2013>.
 - Chan WC., Maxwell DJ, Gao X, Bailey RE, Han M, Nie S. Luminescent quantum dots for multiplexed biological detection and imaging. *Curr Opin Biotechnol* [Internet]. 2002;13(1):40–6. Available from: <https://linkinghub.elsevier.com/retrieve/pii/S095816690202823>.
 - Han M, Gao X, Su JZ, Nie S. Quantum-dot-tagged microbeads for multiplexed optical coding of biomolecules. *Nat Biotechnol* [Internet]. 2001;19(7):631–5. Available from: http://www.nature.com/articles/nbt0701_631.
 - McHugh KJ, Jing L, Behrens AM, Jayawardena S, Tang W, Gao M, et al. Biocompatible semiconductor quantum dots as cancer imaging agents. *Adv Mater* [Internet]. 2018;30(18):1706356. Available from: <http://doi.wiley.com/10.1002/adma.201706356>.

20. Banerjee A, Pons T, Lequeux N, Dubertret B. Quantum dots–DNA bioconjugates: synthesis to applications. *Interface Focus* [Internet]. 2016;6(6):20160064. Available from: <https://royalsocietypublishing.org/doi/10.1098/rsfs.2016.0064>.
21. Pandey S, Bodas D. High-quality quantum dots for multiplexed bioimaging: a critical review. *Adv Colloid Interface Sci* [Internet]. 2020;278:102137. Available from: <https://linkinghub.elsevier.com/retrieve/pii/S0001868619302969>.
22. Zhao P, Xu Q, Tao J, Jin Z, Pan Y, Yu C, et al. Near infrared quantum dots in biomedical applications: current status and future perspective. *Wiley Interdiscip Rev Nanomedicine Nanobiotechnol* [Internet]. 2018;10(3):e1483. Available from: <https://onlinelibrary.wiley.com/doi/10.1002/wnan.1483>.
23. Wagner AM, Knipe JM, Orive G, Peppas NA. Quantum dots in biomedical applications. *Acta Biomater* [Internet]. 2019;94:44–63. Available from: <https://linkinghub.elsevier.com/retrieve/pii/S1742706119303393>.
24. Wang X, Zhong X, Li J, Liu Z, Cheng L. Inorganic nanomaterials with rapid clearance for biomedical applications. *Chem Soc Rev* [Internet]. 2021;50(15):8669–742. Available from: <http://xlink.rsc.org/?DOI=D0CS00461H>.
25. Mahle R, Kumbhakar P, Nayar D, Narayanan TN, Kumar Sadasivuni K, Tiwary CS, et al. Current advances in bio-fabricated quantum dots emphasising the study of mechanisms to diversify their catalytic and biomedical applications. *Dalt Trans* [Internet]. 2021;50(40):14062–80. Available from: <http://xlink.rsc.org/?DOI=D1DT01529J>.
26. Li C, Li Y, Zhang Y, Zhang C. Single-molecule fluorescence resonance energy transfer and its biomedical applications. *TrAC Trends Anal Chem* [Internet]. 2020;115753. Available from: <https://linkinghub.elsevier.com/retrieve/pii/S0165993619304923>.
27. Wang B, Kostarelos K, Nelson BJ, Zhang L. Trends in micro-/nanorobotics: materials development, actuation, localization, and system integration for biomedical applications. *Adv Mater* [Internet]. 2021;33(4):2002047. Available from: <https://onlinelibrary.wiley.com/doi/10.1002/adma.202002047>.
28. Younis MR, He G, Lin J, Huang P. Recent advances on graphene quantum dots for bioimaging applications. *Front Chem* [Internet]. 2020;8. Available from: <https://www.frontiersin.org/article/10.3389/fchem.2020.00424/full>.
29. Das A, Snee PT. Synthetic developments of nontoxic quantum dots. *ChemPhysChem* [Internet]. 2016;17(5):598–617. Available from: <https://onlinelibrary.wiley.com/doi/10.1002/cphc.201500837>.
30. Hai X, Feng J, Chen X, Wang J. Tuning the optical properties of graphene quantum dots for biosensing and bioimaging. *J Mater Chem B* [Internet]. 2018;6(20):3219–34. Available from: <http://xlink.rsc.org/?DOI=C8TB00428E>.
31. Molaei MJ. Carbon quantum dots and their biomedical and therapeutic applications: a review. *RSC Adv* [Internet]. 2019;9(12):6460–81. Available from: <http://xlink.rsc.org/?DOI=C8R A08088G>.
32. Hühn J, Carrillo-Carrion C, Soliman MG, Pfeiffer C, Valdeperez D, Masood A, et al. Selected standard protocols for the synthesis, phase transfer, and characterization of inorganic colloidal nanoparticles. *Chem Mater* [Internet]. 2017;29(1):399–461. Available from: <https://pubs.acs.org/doi/10.1021/acs.chemmater.6b04738>.
33. Zhao N, Yan L, Zhao X, Chen X, Li A, Zheng D, et al. Versatile types of organic/inorganic nanohybrids: from strategic design to biomedical applications. *Chem Rev* [Internet]. 2019;119(3):1666–762. Available from: <https://pubs.acs.org/doi/10.1021/acs.chemrev.8b00401>.
34. Wölfle P. Quasiparticles in condensed matter systems. *Reports Prog Phys* [Internet]. 2018;81(3):032501. Available from: <https://iopscience.iop.org/article/10.1088/1361-6633/aa9bc4>.
35. Koole R, Groeneveld E, Vanmaekelbergh D, Meijerink A, de Mello Donegá C. Size effects on semiconductor nanoparticles. In: *Nanoparticles* [Internet]. Berlin, Heidelberg: Springer; 2014. p. 13–51. Available from: http://link.springer.com/10.1007/978-3-662-44823-6_2.

36. Wang Y, Suna A, Mahler W, Kasowski R. PbS in polymers. From molecules to bulk solids. *J Chem Phys* [Internet]. 1987;87(12):7315–22. Available from: <http://aip.scitation.org/doi/10.1063/1.453325>.
37. Nanda KK, Kruijs FE, Fissan H, Behera SN. Effective mass approximation for two extreme semiconductors: band gap of PbS and CuBr nanoparticles. *J Appl Phys* [Internet]. 2004;95(9):5035–41. Available from: <http://aip.scitation.org/doi/10.1063/1.1691184>.
38. Gaponenko SV. Optical properties of semiconductor nanocrystals [Internet]. Cambridge University Press; 1998. Available from: <https://www.cambridge.org/core/product/identifier/9780511524141/type/book>.
39. Alivisatos AP. Perspectives on the physical chemistry of semiconductor nanocrystals. *J Phys Chem* [Internet]. 1996;100(31):13226–39. Available from: <https://pubs.acs.org/doi/10.1021/jp9535506>.
40. Gaponenko S V. Introduction to nanophotonics [Internet]. Cambridge University Press; Cambridge; 2010. Available from: <http://ebooks.cambridge.org/ref/id/CBO9780511750502>.
41. Pietryga JM, Park Y-S, Lim J, Fidler AF, Bae WK, Brovelli S, et al. Spectroscopic and device aspects of nanocrystal quantum dots. *Chem Rev* [Internet]. 2016;116(18):10513–622. Available from: <https://pubs.acs.org/doi/10.1021/acs.chemrev.6b00169>.
42. Groeneveld E. Synthesis and optical spectroscopy of (hetero)-nanocrystals: an exciting interplay between chemistry and physics. Utrecht University; 2012.
43. Brus LE. Electron–electron and electron-hole interactions in small semiconductor crystallites: the size dependence of the lowest excited electronic state. *J Chem Phys* [Internet]. 1984;80(9):4403–9. Available from: <http://link.aip.org/link/JCPSA6/v80/i9/p4403/s1&Agg=doi>.
44. Kayanuma Y. Quantum-size effects of interacting electrons and holes in semiconductor microcrystals with spherical shape. *Phys Rev B* [Internet]. 1988;38(14):9797–805. Available from: <https://link.aps.org/doi/10.1103/PhysRevB.38.9797>.
45. Stokes GG. On the change of refrangibility of light. *Philos Trans R Soc London* [Internet]. 1852;142:463–562. Available from: <https://royalsocietypublishing.org/doi/10.1098/rstl.1852.0022>.
46. Verhoeven JW. Glossary of terms used in photochemistry (IUPAC recommendations 1996). *Pure Appl Chem* [Internet]. 1996;68(12):2223–86. Available from: <https://www.degruyter.com/document/doi/10.1351/pac19966812223/html>.
47. Valeur B, Berberan-Santos MN. Molecular fluorescence [Internet]. Wiley-VCH Verlag GmbH & Co. KGaA, Weinheim, Germany; 2012. Available from: <http://doi.wiley.com/10.1002/9783527650002>.
48. Brennan MC, Zinna J, Kuno M. Existence of a size-dependent stokes shift in CsPbBr₃ perovskite nanocrystals. *ACS Energy Lett* [Internet]. 2017;2(7):1487–8. Available from: <https://pubs.acs.org/doi/10.1021/acsenerylett.7b00383>.
49. Flores-Pacheco A, Sánchez-Zeferino R, Saavedra-Rodríguez G, Contreras-Rascón JI, Díaz-Reyes J, Álvarez-Ramos ME. Enhanced Stokes-shift and dispersibility in non-polar PMMA solvent of CdTe quantum dots by silica coating. *Chem Phys* [Internet]. 2021;544:111102. Available from: <https://linkinghub.elsevier.com/retrieve/pii/S0301010421000136>.
50. Liu Y, Kim D, Morris OP, Zhitomirsky D, Grossman JC. Origins of the stokes shift in PbS quantum dots: impact of polydispersity, ligands, and defects. *ACS Nano* [Internet]. 2018;12(3):2838–45. Available from: <https://pubs.acs.org/doi/10.1021/acsnano.8b00132>.
51. Han N, Liu C, Zhao Z, Zhang J, Xie J, Han J, et al. Quantum dots in glasses: size-dependent stokes shift by lead chalcogenide. *Int J Appl Glas Sci* [Internet]. 2015;6(4):339–44. Available from: <https://onlinelibrary.wiley.com/doi/10.1111/ijag.12138>.
52. Yadav AN, Singh AK, Chauhan D, Solanki PR, Kumar P, Singh K. Evaluation of dopant energy and Stokes shift in Cu-doped CdS quantum dots via spectro-electrochemical probing. *New J Chem* [Internet]. 2020;44(32):13529–33. Available from: <http://xlink.rsc.org/?DOI=D0NJ03004J>.
53. Avidan A, Oron D. Large blue shift of the biexciton state in tellurium doped CdSe colloidal quantum dots. *Nano Lett* [Internet]. 2008;8(8):2384–7. Available from: <https://pubs.acs.org/doi/10.1021/nl801241m>.

54. Reiss P, Carrière M, Lincineau C, Vaure L, Tamang S. Synthesis of semiconductor nanocrystals, focusing on nontoxic and earth-abundant materials. *Chem Rev* [Internet]. 2016;116(18):10731–819. Available from: <https://pubs.acs.org/doi/10.1021/acs.chemrev.6b00116>.
55. van Embden J, Chesman ASR, Jasieniak JJ. The heat-up synthesis of colloidal nanocrystals. *Chem Mater* [Internet]. 2015;27(7):2246–85. Available from: <https://pubs.acs.org/doi/10.1021/cm5028964>.
56. Reiss P, Protière M, Li L. Core/shell semiconductor nanocrystals. *Small* [Internet]. 2009;5(2):154–68. Available from: <http://doi.wiley.com/10.1002/smll.200800841>.
57. Mourdikoudis S, Liz-Marzán LM. Oleylamine in nanoparticle synthesis. *Chem Mater* [Internet]. 2013;25(9):1465–76. Available from: <https://pubs.acs.org/doi/10.1021/cm4000476>.
58. Yamauchi M, Masuo S. Self-assembly of semiconductor quantum dots using organic templates. *Chem A Eur J* [Internet]. 2020;26(32):7176–84. Available from: <https://online.library.wiley.com/doi/abs/10.1002/chem.201905807>.
59. Agrawal A, Cho SH, Zandi O, Ghosh S, Johns RW, Milliron DJ. Localized surface plasmon resonance in semiconductor nanocrystals. *Chem Rev* [Internet]. 2018;118(6):3121–207. Available from: <https://pubs.acs.org/doi/10.1021/acs.chemrev.7b00613>.
60. Coughlan C, Ibáñez M, Dobrozhan O, Singh A, Cabot A, Ryan KM. Compound copper chalcogenide nanocrystals. *Chem Rev* [Internet]. 2017;117:5865–6109. Available from: <http://pubs.acs.org/doi/10.1021/acs.chemrev.6b00376>.
61. Bhattacharya A, Bansal B. Self-assembly in semiconductor epitaxy. In: *Handbook of crystal growth* [Internet]. Elsevier; 2015. p. 1057–99. Available from: <https://linkinghub.elsevier.com/retrieve/pii/B9780444633040000263>.
62. Petroff PM, Lorke A, Imamoglu A. Epitaxially self-assembled quantum dots. *Phys Today* [Internet]. 2001;54(5):46–52. Available from: <http://physicstoday.scitation.org/doi/10.1063/1.1381102>.
63. Nemcsics A. Quantum dots prepared by droplet epitaxial method. In: *Quantum dots—theory and applications* [Internet]. InTech; 2015. Available from: <http://www.intechopen.com/books/quantum-dots-theory-and-applications/quantum-dots-prepared-by-droplet-epitaxial-method>.
64. Wang YR, Han IS, Jin C-Y, Hopkinson M. Precise arrays of epitaxial quantum dots nucleated by in situ laser interference for quantum information technology applications. *ACS Appl Nano Mater* [Internet]. 2020;3(5):4739–46. Available from: <https://pubs.acs.org/doi/10.1021/acsnm.0c00738>.
65. Bayer M. Bridging two worlds: colloidal versus epitaxial quantum dots. *Ann Phys* [Internet]. 2019;1900039. Available from: <https://onlinelibrary.wiley.com/doi/abs/10.1002/andp.201900039>.
66. Fafard S, Wasilewski ZR, Allen CN, Picard D, Piva PG, McCaffrey JP. Self-assembled quantum dots: five years later. *Superlattices Microstruct* [Internet]. 1999;25(1–2):87–96. Available from: <https://linkinghub.elsevier.com/retrieve/pii/S074960369890619X>.
67. Nel AE, Mädler L, Velegol D, Xia T, Hoek EM V., Somasundaran P, et al. Understanding biophysicochemical interactions at the nano–bio interface. *Nat Mater* [Internet]. 2009;8(7):543–57. Available from: <http://www.nature.com/articles/nmat2442>.
68. Wegner KD, Hildebrandt N. Quantum dots: bright and versatile in vivo and in vivo fluorescence imaging biosensors. *Chem Soc Rev* [Internet]. 2015;44(14):4792–834. Available from: <http://xlink.rsc.org/?DOI=C4CS00532E>.
69. Zrazhevskiy P, Sena M, Gao X. Designing multifunctional quantum dots for bioimaging, detection, and drug delivery. *Chem Soc Rev* [Internet]. 2010;39(11):4326. Available from: <http://xlink.rsc.org/?DOI=b915139g>.
70. Liu W, Howarth M, Greytak AB, Zheng Y, Nocera DG, Ting AY, et al. Compact biocompatible quantum dots functionalized for cellular imaging. *J Am Chem Soc* [Internet]. 2008;130(4):1274–84. Available from: <https://pubs.acs.org/doi/10.1021/ja076069p>.
71. Howard MD, Jay M, Dziubla TD, Lu X. PEGylation of nanocarrier drug delivery systems: state of the art. *J Biomed Nanotechnol* [Internet]. 2008;4(2):133–48. Available

- from: <http://openurl.ingenta.com/content/xref?genre=article&issn=1550-7033&volume=4&issue=2&spage=133>.
72. Wenger WN, Bates FS, Aydil ES. Functionalization of cadmium selenide quantum dots with poly(ethylene glycol): ligand exchange, surface coverage, and dispersion stability. *Langmuir* [Internet]. 2017;33(33):8239–45. Available from: <https://pubs.acs.org/doi/10.1021/acs.langmuir.7b01924>.
 73. Sabah A, Tasleem S, Murtaza M, Nazir M, Rashid F. Effect of polymer capping on photonic multi-core-shell quantum dots CdSe/CdS/ZnS: impact of sunlight and antibacterial activity. *J Phys Chem C* [Internet]. 2020;124(16):9009–20. Available from: <https://pubs.acs.org/doi/abs/10.1021/acs.jpcc.9b11656>.
 74. Hong E, Liu L, Li C, Shan D, Cao H, Wang B. Study on cytotoxicity of polyethylene glycol and albumin bovine serum molecule-modified quantum dots prepared by hydrothermal method. *J Mater Res* [Internet]. 2020;35(9):1135–42. Available from: <http://link.springer.com/10.1557/jmr.2020.78>.
 75. Jung H-S, Cho K-J, Ryu S-J, Takagi Y, Roche PA, Neuman KC. Biocompatible fluorescent nanodiamonds as multifunctional optical probes for latent fingerprint detection. *ACS Appl Mater Interfaces* [Internet]. 2020;12(5):6641–50. Available from: <https://pubs.acs.org/doi/10.1021/acsami.9b19245>.
 76. Zhang C, Fu Y-Y, Zhang X, Yu C, Zhao Y, Sun S-K. BSA-directed synthesis of CuS nanoparticles as a biocompatible photothermal agent for tumor ablation in vivo. *Dalt Trans* [Internet]. 2015;44(29):13112–8. Available from: <http://xlink.rsc.org/?DOI=C5DT01467K>.
 77. Li H, Yang X. Bovine serum albumin-capped CdS quantum dots as an inner-filter effect sensor for rapid detection and quantification of protamine and heparin. *Anal Methods* [Internet]. 2015;7(19):8445–52. Available from: <http://xlink.rsc.org/?DOI=C5AY01817J>.
 78. Abha K, Sumithra IS, Suji S, Anjana RR, Anjali Devi JS, Nebu J, et al. Dopamine-induced photoluminescence quenching of bovine serum albumin-capped manganese-doped zinc sulphide quantum dots. *Anal Bioanal Chem* [Internet]. 2020;412(23):5671–81. Available from: <http://link.springer.com/10.1007/s00216-020-02787-2>.
 79. Song C, Luo H, Lin X, Peng Z, Weng L, Tang X, et al. Study on AgInZnS-graphene oxide non-toxic quantum dots for biomedical sensing. *Front Chem* [Internet]. 2020;8. Available from: <https://www.frontiersin.org/article/10.3389/fchem.2020.00331/full>.
 80. Zhan N, Palui G, Mattoussi H. Preparation of compact biocompatible quantum dots using multicoordinating molecular-scale ligands based on a zwitterionic hydrophilic motif and lipoic acid anchors. *Nat Protoc* [Internet]. 2015;10(6):859–74. Available from: <http://www.nature.com/articles/nprot.2015.050>.
 81. Zheng W, Liu Y, West A, Schuler EE, Yehl K, Dyer RB, et al. Quantum dots encapsulated within phospholipid membranes: phase-dependent structure, photostability, and site-selective functionalization. *J Am Chem Soc* [Internet]. 2014;136(5):1992–9. Available from: <https://pubs.acs.org/doi/10.1021/ja411339f>.
 82. Guo X, Zhang Y, Liu J, Yang X, Huang J, Li L, et al. Red blood cell membrane-mediated fusion of hydrophobic quantum dots with living cell membranes for cell imaging. *J Mater Chem B* [Internet]. 2016;4(23):4191–7. Available from: <http://xlink.rsc.org/?DOI=C6TB01067A>.
 83. Li J, Zhang Y, Ai J, Gao Q, Qi H, Zhang C, et al. Quantum dot cluster (QDC)-loaded phospholipid micelles as a FRET probe for phospholipase A 2 detection. *RSC Adv* [Internet]. 2016;6(19):15895–9. Available from: <http://xlink.rsc.org/?DOI=C5RA25292J>.
 84. Fowley C, McCaughan B, Devlin A, Yildiz I, Raymo FM, Callan JF. Highly luminescent biocompatible carbon quantum dots by encapsulation with an amphiphilic polymer. *Chem Commun* [Internet]. 2012;48(75):9361. Available from: <http://xlink.rsc.org/?DOI=c2c34962k>.
 85. Zhang C, Palui G, Zeng B, Zhan N, Chen B, Mattoussi H. Non-invasive characterization of the organic coating of biocompatible quantum dots using nuclear magnetic resonance spectroscopy. *Chem Mater* [Internet]. 2018;30(10):3454–66. Available from: <https://pubs.acs.org/doi/10.1021/acs.chemmater.8b01033>.

86. Zhang H, Chen J, Xiao C, Tao Y, Wang X. A multifunctional polypeptide via ugi reaction for compact and biocompatible quantum dots with efficient bioconjugation. *Bioconjug Chem* [Internet]. 2018;29(4):1335–43. Available from: <https://pubs.acs.org/doi/10.1021/acs.bioconjchem.8b00072>.
87. Zhu S, Zhao F, Deng M, Zhang T, Lü C. Construction of β -cyclodextrin derived CDs-coupled block copolymer micelles loaded with CdSe/ZnS QDs via host-guest interaction for ratiometric fluorescence sensing of metal ions. *Dye Pigment* [Internet]. 2019;168:369–80. Available from: <https://linkinghub.elsevier.com/retrieve/pii/S0143720819301688>.
88. He X, Jia K, Marks R, Hu Y, Liu X. 3D confined self-assembling of QD within super-engineering block copolymers as biocompatible superparticles enabling stimulus responsive solid state fluorescence. *Nano Res* [Internet]. 2021;14(1):285–94. Available from: <http://link.springer.com/10.1007/s12274-020-3086-0>.
89. Petryayeva E, Algar WR, Medintz IL. Quantum dots in bioanalysis: a review of applications across various platforms for fluorescence spectroscopy and imaging. *Appl Spectrosc* [Internet]. 2013;67(3):215–52. Available from: <http://journals.sagepub.com/doi/10.1366/12-06948>.
90. Henderson B, Imbusch GF. *Optical spectroscopy of inorganic solids*. Oxford University Press; 1989. 645 p.
91. Hens Z, Moreels I. Light absorption by colloidal semiconductor quantum dots. *J Mater Chem* [Internet]. 2012;22(21):10406. Available from: <http://xlink.rsc.org/?DOI=c2jm30760j>.
92. Maxwell Garnett JC. VII. Colours in metal glasses, in metallic films, and in metallic solutions.—II. *Philos Trans R Soc Lond Ser A Contain Pap A Math Phys Charact* [Internet]. 1906;205(387–401):237–88. Available from: <https://royalsocietypublishing.org/doi/10.1098/rsta.1906.0007>.
93. Maxwell Garnett JC. XII. Colours in metal glasses and in metallic films. *Philos Trans R Soc Lond Ser A Contain Pap A Math Phys Charact* [Internet]. 1904;203(359–371):385–420. Available from: <https://royalsocietypublishing.org/doi/10.1098/rsta.1904.0024>.
94. Smith AM, Nie S. Chemical analysis and cellular imaging with quantum dots. *Analyst* [Internet]. 2004;129(8):672. Available from: <http://xlink.rsc.org/?DOI=b404498n>.
95. Tonti D, van Mourik F, Chergui M. On the excitation wavelength dependence of the luminescence yield of colloidal CdSe quantum dots. *Nano Lett* [Internet]. 2004;4(12):2483–7. Available from: <https://pubs.acs.org/doi/10.1021/nl0486057>.
96. Leatherdale CA, Woo W-K, Mikulec F V., Bawendi MG. On the absorption cross section of CdSe nanocrystal quantum dots. *J Phys Chem B* [Internet]. 2002;106(31):7619–22. Available from: <https://pubs.acs.org/doi/10.1021/jp025698c>.
97. Wang Y, Fruhwirth G, Cai E, Ng T, Selvin PR. 3D super-resolution imaging with blinking quantum dots. *Nano Lett* [Internet]. 2013;13(11):5233–41. Available from: <https://pubs.acs.org/doi/10.1021/nl4026665>.
98. Yu G-T, Luo M-Y, Li H, Chen S, Huang B, Sun Z-J, et al. Molecular targeting nanoprobe with non-overlap emission in the second near-infrared window for in vivo two-color colocalization of immune cells. *ACS Nano* [Internet]. 2019;13(11):12830–9. Available from: <https://pubs.acs.org/doi/10.1021/acsnano.9b05038>.
99. Medintz IL, Uyeda HT, Goldman ER, Mattoussi H. Quantum dot bioconjugates for imaging, labelling and sensing. *Nat Mater* [Internet]. 2005;4(6):435–46. Available from: <http://www.nature.com/articles/nmat1390>.
100. Mukherjee A, Shim Y, Myong Song J. Quantum dot as probe for disease diagnosis and monitoring. *Biotechnol J* [Internet]. 2016;11(1):31–42. Available from: <https://onlinelibrary.wiley.com/doi/10.1002/biot.201500219>.
101. Sapsford K, Pons T, Medintz I, Mattoussi H. Biosensing with luminescent semiconductor quantum dots. *Sensors* [Internet]. 2006;6(8):925–53. Available from: <http://www.mdpi.com/1424-8220/6/8/925>.
102. Kumar YR, Deshmukh K, Sadasivuni KK, Pasha SKK. Graphene quantum dot based materials for sensing, bio-imaging and energy storage applications: a review. *RSC Adv* [Internet]. 2020;10(40):23861–98. Available from: <http://xlink.rsc.org/?DOI=DORA03938A>.

103. Ma F, Li C, Zhang C. Development of quantum dot-based biosensors: principles and applications. *J Mater Chem B* [Internet]. 2018;6(39):6173–90. Available from: <http://xlink.rsc.org/?DOI=C8TB01869C>.
104. Cui L, He X-P, Chen G-R. Recent progress in quantum dot based sensors. *RSC Adv* [Internet]. 2015;5(34):26644–53. Available from: <http://xlink.rsc.org/?DOI=C5RA01950H>.
105. Bilan R, Nabiev I, Sukhanova A. Quantum dot-based nanotools for bioimaging, diagnostics, and drug delivery. *ChemBioChem* [Internet]. 2016;17(22):2103–14. Available from: <https://onlinelibrary.wiley.com/doi/10.1002/cbic.201600357>.
106. Chandan HR, Schiffman JD, Balakrishna RG. Quantum dots as fluorescent probes: synthesis, surface chemistry, energy transfer mechanisms, and applications. *Sens Actuators B Chem* [Internet]. 2018;258:1191–214. Available from: <https://linkinghub.elsevier.com/retrieve/pii/S0925400517323201>.
107. Jones GA, Bradshaw DS. Resonance energy transfer: from fundamental theory to recent applications. *Front Phys* [Internet]. 2019;7. Available from: <https://www.frontiersin.org/article/10.3389/fphy.2019.00100/full>.
108. Härmä H, Soukka T, Shavel A, Gaponik N, Weller H. Luminescent energy transfer between cadmium telluride nanoparticle and lanthanide(III) chelate in competitive bioaffinity assays of biotin and estradiol. *Anal Chim Acta* [Internet]. 2007;604(2):177–83. Available from: <https://linkinghub.elsevier.com/retrieve/pii/S0003267007016777>.
109. Hildebrandt N, Charbonnière LJ, Beck M, Ziessel RF, Löhmansröben H-G. Quantum dots as efficient energy acceptors in a time-resolved fluoroimmunoassay. *Angew Chem Int Ed* [Internet]. 2005;44(46):7612–5. Available from: <https://onlinelibrary.wiley.com/doi/10.1002/anie.200501552>.
110. Boulesbaa A, Huang Z, Wu D, Lian T. Competition between energy and electron transfer from CdSe QDs to adsorbed rhodamine B. *J Phys Chem C* [Internet]. 2010;114(2):962–9. Available from: <https://pubs.acs.org/doi/10.1021/jp909972b>.
111. Bazylewski P, Ezugwu S, Fanchini G. A review of three-dimensional scanning near-field optical microscopy (3D-SNOM) and its applications in nanoscale light management. *Appl Sci* [Internet]. 2017;7(10):973. Available from: <http://www.mdpi.com/2076-3417/7/10/973>.
112. Chen J, Wu Y, Wang C, Cai J. Nanoscale organization of CD₄ molecules of human T helper cell mapped by NSOM and quantum dots. *Scanning* [Internet]. 2008;30(6):448–51. Available from: <https://onlinelibrary.wiley.com/doi/10.1002/sca.20128>.
113. Ke C, Chen J, Guo Y, Chen ZW, Cai J. Migration mechanism of mesenchymal stem cells studied by QD/NSOM. *Biochim Biophys Acta Biomembr* [Internet]. 2015;1848(3):859–68. Available from: <https://linkinghub.elsevier.com/retrieve/pii/S0005273614004416>.
114. Carvalho PM, Felício MR, Santos NC, Gonçalves S, Domingues MM. Application of light scattering techniques to nanoparticle characterization and development. *Front Chem* [Internet]. 2018;6. Available from: <https://www.frontiersin.org/article/10.3389/fchem.2018.00237/full>.
115. Bhattacharjee S. DLS and zeta potential—what they are and what they are not? *J Control Release* [Internet]. 2016;235:337–51. Available from: <https://linkinghub.elsevier.com/retrieve/pii/S0168365916303832>.
116. Kaszuba M, Corbett J, Watson FM, Jones A. High-concentration zeta potential measurements using light-scattering techniques. *Philos Trans R Soc A Math Phys Eng Sci* [Internet]. 2010;368(1927):4439–51. Available from: <https://royalsocietypublishing.org/doi/10.1098/rsta.2010.0175>.
117. Delgado AV, González-Caballero F, Hunter RJ, Koopal LK, Lyklema J. Measurement and interpretation of electrokinetic phenomena (IUPAC technical report). *Pure Appl Chem* [Internet]. 2005;77(10):1753–805. Available from: <https://www.degruyter.com/document/doi/10.1351/pac200577101753/html>.
118. An SSA, Kim K, Kim HM, Lee W, Lee C, Kim T, et al. Surface treatment of silica nanoparticles for stable and charge-controlled colloidal silica. *Int J Nanomed* [Internet]. 2014;29. Available from: <http://www.dovepress.com/surface-treatment-of-silica-nanoparticles-for-stable-and-charge-control-peer-reviewed-article-IJN>.

119. Khan SA, Khan SB, Khan LU, Farooq A, Akhtar K, Asiri AM. Fourier transform infrared spectroscopy: fundamentals and application in functional groups and nanomaterials characterization. In: Handbook of materials characterization [Internet]. Cham: Springer International Publishing; 2018. p. 317–44. Available from: http://link.springer.com/10.1007/978-3-319-92955-2_9.
120. Sala A, Anderson DJ, Brennan PM, Butler HJ, Cameron JM, Jenkinson MD, et al. Biofluid diagnostics by FTIR spectroscopy: a platform technology for cancer detection. *Cancer Lett* [Internet]. 2020;477:122–30. Available from: <https://linkinghub.elsevier.com/retrieve/pii/S0304383520300835>.
121. Bunaciu AA, Aboul-Enein HY. Adulterated drug analysis using FTIR spectroscopy. *Appl Spectrosc Rev* [Internet]. 2021;56(5):423–37. Available from: <https://www.tandfonline.com/doi/full/10.1080/05704928.2020.1811717>.
122. Talari ACS, Martinez MAG, Movasaghi Z, Rehman S, Rehman IU. Advances in Fourier transform infrared (FTIR) spectroscopy of biological tissues. *Appl Spectrosc Rev* [Internet]. 2017;52(5):456–506. Available from: <https://www.tandfonline.com/doi/full/10.1080/05704928.2016.1230863>.
123. Byrne B, Beattie JW, Song CL, Kazarian SG. ATR-FTIR spectroscopy and spectroscopic imaging of proteins. In: *Vibrational spectroscopy in protein research* [Internet]. Elsevier; 2020. p. 1–22. Available from: <https://linkinghub.elsevier.com/retrieve/pii/B9780128186107000013>.
124. Rohman A, Windarsih A, Lukitaningsih E, Rafi M, Betania K, Fadzillah NA. The use of FTIR and Raman spectroscopy in combination with chemometrics for analysis of biomolecules in biomedical fluids: a review. *Biomed Spectrosc Imaging* [Internet]. 2020;8(3–4):55–71. Available from: <https://www.medra.org/servelet/aliasResolver?alias=iospress&doi=10.3233/BSI-200189>.
125. Perumal J, Wang Y, Attia ABE, Dinish US, Olivo M. Towards a point-of-care SERS sensor for biomedical and agri-food analysis applications: a review of recent advancements. *Nanoscale* [Internet]. 2021;13(2):553–80. Available from: <http://xlink.rsc.org/?DOI=D0NR06832B>.
126. Liang X, Li N, Zhang R, Yin P, Zhang C, Yang N, et al. Carbon-based SERS biosensor: from substrate design to sensing and bioapplication. *NPG Asia Mater* [Internet]. 2021;13(1):8. Available from: <http://www.nature.com/articles/s41427-020-00278-5>.
127. Lane LA, Qian X, Nie S. SERS nanoparticles in medicine: from label-free detection to spectroscopic tagging. *Chem Rev* [Internet]. 2015;115(19):10489–529. Available from: <https://pubs.acs.org/doi/10.1021/acs.chemrev.5b00265>.
128. Langer J, Jimenez de Aberasturi D, Aizpuru J, Alvarez-Puebla RA, Auguie B, Baumberg JJ, et al. Present and future of surface-enhanced raman scattering. *ACS Nano* [Internet]. 2020;14(1):28–117. Available from: <https://pubs.acs.org/doi/10.1021/acsnano.9b04224>.
129. Pérez-Jiménez AI, Lyu D, Lu Z, Liu G, Ren B. Surface-enhanced Raman spectroscopy: benefits, trade-offs and future developments. *Chem Sci* [Internet]. 2020;11(18):4563–77. Available from: <http://xlink.rsc.org/?DOI=D0SC00809E>.
130. Wang Z, Zong S, Wu L, Zhu D, Cui Y. SERS-activated platforms for immunoassay: probes, encoding methods, and applications. *Chem Rev* [Internet]. 2017;117(12):7910–63. Available from: <https://pubs.acs.org/doi/10.1021/acs.chemrev.7b00027>.
131. Wang Z, Zong S, Li W, Wang C, Xu S, Chen H, et al. SERS-fluorescence joint spectral encoding using organic–metal–QD hybrid nanoparticles with a huge encoding capacity for high-throughput biodetection: putting theory into practice. *J Am Chem Soc* [Internet]. 2012;134(6):2993–3000. Available from: <https://pubs.acs.org/doi/10.1021/ja208154m>.
132. Wang Z, Zong S, Chen H, Wang C, Xu S, Cui Y. SERS-fluorescence joint spectral encoded magnetic nanoprobes for multiplex cancer cell separation. *Adv Healthc Mater* [Internet]. 2014;3(11):1889–97. Available from: <https://onlinelibrary.wiley.com/doi/10.1002/adhm.201400092>.
133. Fang P-P, Lu X, Liu H, Tong Y. Applications of shell-isolated nanoparticles in surface-enhanced Raman spectroscopy and fluorescence. *TrAC Trends Anal Chem* [Internet]. 2015;66:103–17. Available from: <https://linkinghub.elsevier.com/retrieve/pii/S0165993615000096>.

134. Alvarez-Puebla RA, Pazos-Perez N, Guerrini L. SERS-fluorescent encoded particles as dual-mode optical probes. *Appl Mater Today* [Internet]. 2018;13:1–14. Available from: <https://linkinghub.elsevier.com/retrieve/pii/S235294071830249X>.
135. Keshavarz M, Tan B, Venkatakrishnan K. Label-free SERS quantum semiconductor probe for molecular-level and in vivo cellular detection: a noble-metal-free methodology. *ACS Appl Mater Interfaces* [Internet]. 2018;10(41):34886–904. Available from: <https://pubs.acs.org/doi/10.1021/acsami.8b10590>.

A Toxicologic Review of Quantum Dots: Recent Insights and Future Directions



Arun Guha and Debasree Ghosh

Abstract An engineered nanoscale product such as quantum dots (QDs) attracts the fascination and attention of scientists due to simultaneous targeting and imaging potential in drug delivery in fields of pharmaceutical and biomedical applications. The absorption, distribution, metabolism, excretion, and toxicity of QDs, i.e., the pharmacology, depends on QDs' inherent physicochemical properties of QDs (size, charge, concentration, capping materials, and functional groups) and environmental conditions (temperature, surrounding medium). Therefore, understanding the pharmacology of QDs becomes essential for researchers to elucidate the adverse effects of in vivo and in vitro studies in recent years. The first part of the chapter describes the cellular uptake mechanism and reviews the QD toxicity assessment techniques. The following sections will focus on exposure to toxicity and the key factors that decide the toxicity level. The following section will discuss the possible approaches to reduce the toxicity of QDs during the processes of imaging and therapeutic applications. An overview of the present status and a future perspective of the toxicity of QDs will be discussed.

Keywords Quantum dots · Toxicity · Toxicology · Cellular uptake · Pharmacology

1 Introduction

QDs are semiconductor nanocrystals having size-dependent optical properties. The physicochemical properties of QDs depend on the size, composition/structure, and material used during synthesis. In general, at least one spatial dimension of the QDs must be below the Bohr radius (the value is different for every QDs) to fulfill the quantum confinement regime. However, the other spatial dimensions may be ~ 100 nm for asymmetric structures, like nanorods. By altering the size, size distribution, composition, and crystal structure of QDs, one can tune the emission spectra in the electromagnetic spectrum. Solubility or dispersibility of QDs in water or organic

A. Guha (✉) · D. Ghosh

Department of Health & Family Welfare, Government of West Bengal, Kolkata, India

e-mail: arunvbu@gmail.com

solvent depends on the surface ligand or capping molecules. Thermal stability also depends on the nature/composition of shell and surface ligands.

Toxicity is an adverse health effect caused by many substances (e.g., a drug, chemical, toxin or poison, nanomaterials, and many more substances) ranging from a minor unpleasant side effect to a significant threat to an organism, life quality, and health. Cytotoxicity, toxicity at the cellular level, is often caused by direct chemical toxicity, inflammatory reactions, or immune responses to the materials. Systemic toxicity involves excessive or severe cytotoxicity, inflammatory reactions, or immune responses affecting organs or organ systems. Cytotoxicity or nonimmune systemic toxicity depends on the dose of the material and a threshold below which the material exposes little toxicity ascertained by *in vitro* and *in vivo* studies. However, determination of such a threshold is extremely difficult for systemic immune toxicity as it depends on the individual materials' properties, dosage, and implantation location. Due to their intrinsic properties, nanoparticles (NPs) or quantum dots (QDs) are commonly used in various areas, like electronics, photovoltaics, catalysis, engineering, cosmetics, therapy, medicine, and pharmacy. However, a complete risk assessment arising from QDs is still in its infancy stage due to the lack of knowledge of all the relevant toxicological mechanisms for all QDs. The leading portals of entry for NPs or QDs are the respiratory, digestive, ocular, cutaneous (skin), and direct injections into the blood circulation in the human body.

Numerous studies in different *in vivo* and *in vitro* systems result in various endpoints with different toxic effects due to QDs. However, oxidative stress, i.e., the formation and release of reactive oxygen species (ROS), is one of the central mechanisms inducing toxicity that damage pathological consequences such as lipid peroxidation, protein damage, deactivation of enzymatic activities, DNA modification, DNA modification, and standard pro-inflammatory processes [1–7]. This chapter elaborates a general understanding of toxicity, QDs/NPs cytotoxicity mechanism, and some methodology to mitigate the toxicity.

2 General Comments on the Toxicity of QDs

Currently, the knowledge of the toxicity of QDs is an inadequate due limited number of in-depth cytotoxicity studies on QDs like Cd, Pb-based, and C-based QDs. It is impossible to provide a generalized assumption on the toxicity that arises from QDs. However, various reports published in the last decade have made several important observations. The nanoparticles (NPs), nanocrystals, including QDs, are compared with various biological molecules in Fig. 1 according to their respective size. The size and surface energy of QD are the most important properties which govern the toxicity at large. QDs with sizes 1–20 nm may accommodate roughly ~ 100–20,000 atoms that affect the associated chemical and physical properties compared to bulk counterparts. Due to the small size, QDs possess large surface areas, typically $100\text{--}1000\text{ m}^2\text{g}^{-1}$. In addition, QDs have dangling (i.e., unsaturated) bonds on the surface and carry partial charges, increasing the surface's energy. Thus, various properties of QDs,

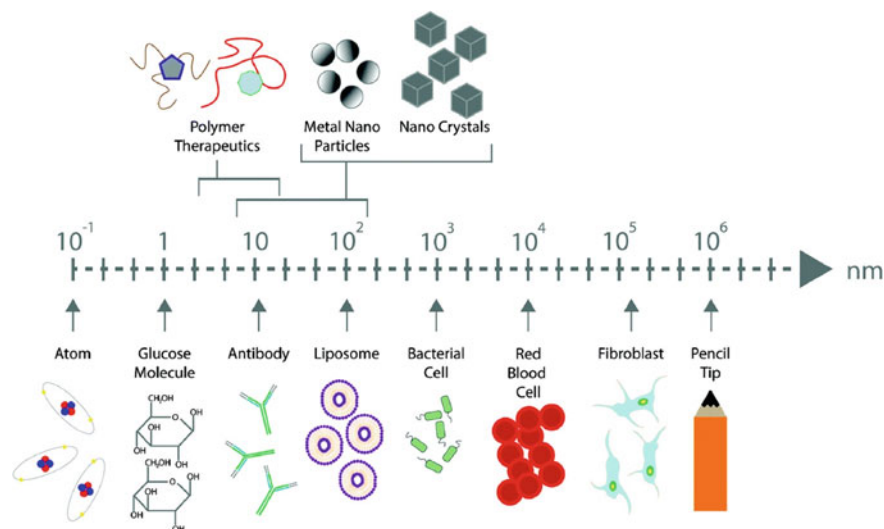


Fig. 1 Schematic representation of nanomaterial size in comparison to other biological molecules. Reproduced with permission from Ref. [9]. Copyright 2020 © The Royal Society of Chemistry

e.g., surface functionalization, grafting, adsorption, agglomeration, and reactivity with the environment, are affected. The toxicity studies of QDs consider only the chemical composition and substance dose (in mg per kg of body weight) in sterile laboratory conditions, and the tests are generally performed on animals, such as rats, mice, and hamsters [8].

2.1 Identifying Hazards

There is only limited information about the impact or the potential technical risks of QDs on non-human/human species, ecosystems, or the global environment. After several years of toxicology research, how different QDs interact within the human body or the environment is still uncertain. Regulatory bodies, like the International Organization for Standardization (ISO), European Committee for Standardisation (CEN), Organisation for Economic Co-operation and Development (OECD), the U.S. National Institute for Occupational Safety and Health (NIOSH), Occupational Safety and Health Administration (OSHA), provide objective and reliable information to the public on innovation and safety aspects of nanomaterials [10]. Identifying hazards is the first step in determining the risk and exposure of QDs. This step involves identifying chemicals or QDs, and the specific effect of surface chemistry, shape, size, and morphology on toxicity caused to various organs. Table 1 summarizes primary hazard categories that may be considered when assessing the risk associated with QDs.

Table 1 Primary hazard categories associated with QDs

Categories	Descriptions	Effects
Morphology	Sphere, rod, tube, star, oval, and various asymmetric shapes	One can modify their surface properties in several emerging technologies
Particle size	~ 1–100 nm	QDs have a greater chance of deposition by translocating to other organs or absorbing through the blood. It can penetrate the membrane barriers resulting in significant damage
Surface charge	+ Ve or –Ve or neutral	Nonspecifically bound to opposite polarity rather than the target
Surface ligand	Alkyl thiol, polyethylene glycol (PEG), alkylthiol-PEG, amino acid, aminothiols, amphiphilic-polymer, aminothiols, lipid, polyol, silica	Surface ligands may interact with the biomolecules and may induce unpredictable effects
Surface modification	Drug, polymer, amino acid, protein, toxin, unmodified	QDs can be applied to a specific target location and bind to particular molecules. Also, it minimizes QD exposure to the biological environment
Solubility	In general, as-prepared QDs are hydrophobic. However, hydrophilic QDs may be synthesized, or surface functionalization can make them hydrophilic	Poorly soluble inhaled QDs can cause oxidative stress, leading to inflammation, fibrosis, or cancer
Exposure time	Long-term exposure with external light excitation happens during bioimaging and in vivo study	Cell damage due to long time excitation via external light source due to rise in temperature
Toxic hazards	QDs toxicity is not well-understood	Threshold limit values (TLV) or permissible exposure limits (PEL) helps in determining proper safety precautions

2.2 Routes of Exposure to QDs

Various routes may introduce QDs into the body as a part of treatment, diagnostic purposes, and environmental pollution or accidental release. In the case of the biomedical field, the routes are termed gastrointestinal (GI), intravenous (IV), intra-dermal (ID), intramuscular (IM), and peritoneal injections (IP) [8], as depicted in Fig. 2a. The smaller size of QDs may cause a high chance of pulmonary uptake and deposition followed by transportation to systemic sites. The ability of QDs (compared to metal NPs) to cross the dermal barrier is different for various test subjects [11, 12]. QDs injected via the IV route are quickly distributed by the bloodstream, primarily to the liver and spleen, kidneys, heart, lungs, bone marrow, and brain. A biocompatible

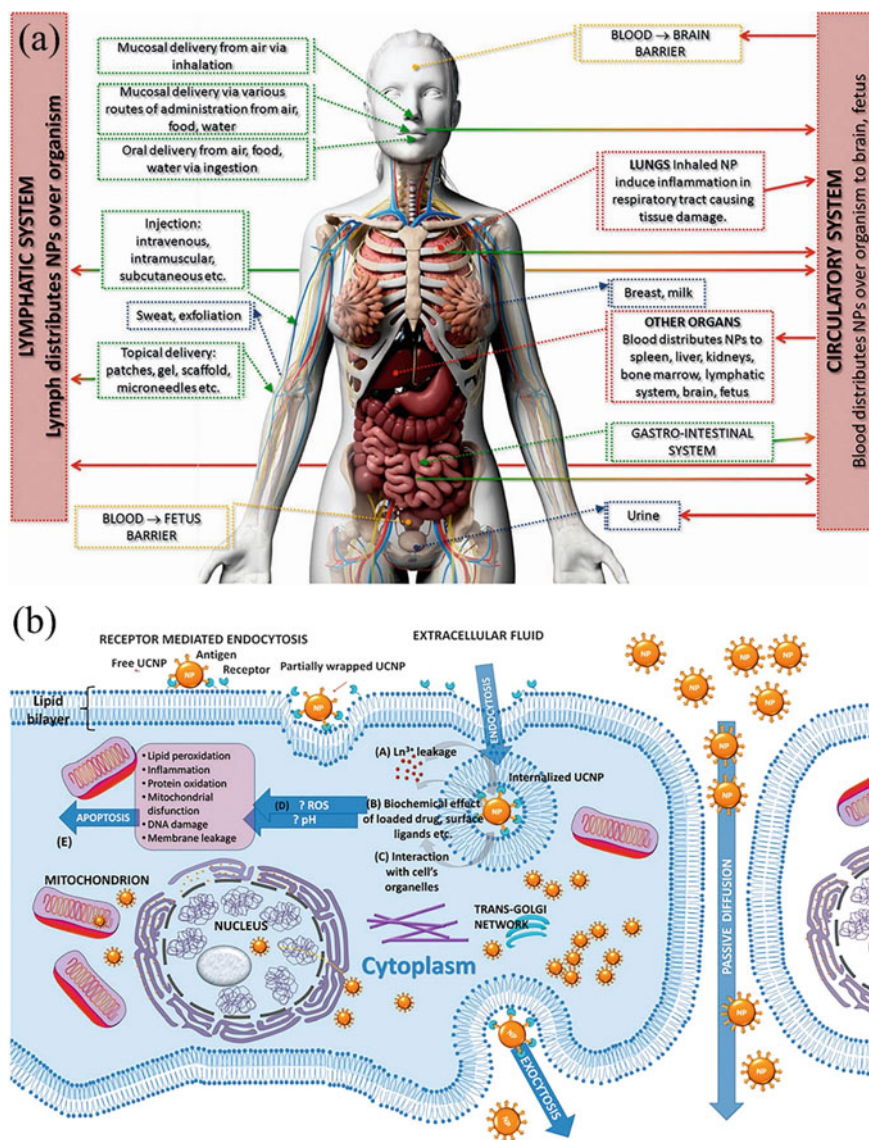


Fig. 2 **a** The nanoparticles (NPs) may enter the human body via various routes (green arrows) and, after translocation (red arrows), with the help of blood and lymph, transported to other organs. Most colloidal NPs are removed from the organism through urine and sweat (blue arrows), but some aggregation may happen. **b** The NPs can be invisible to the immune system and thus can be efficiently adopted by the endocytic pathway like phagocytosis, pinocytosis, clathrin-mediated endocytosis, and caveolae-mediated endocytosis. Potential interactions with cellular organelles include (A) Ln^{3+} leakage, (B) interaction ligands with proteins enzymes, (C) cellular structures, (D) potential ROS generation, and variation of the cellular environment, which may cause apoptosis. Reproduced with permission from Ref. [8]. Copyright 2014 ©The Royal Society of Chemistry

coating like polyethylene glycol (PEG) may reduce the circulation of such QDs in the bloodstream [8]. However, QDs less than ~ 5 nm in size can easily be excreted by renal filtration. The nature of the surface coating of QDs controls the retention of blood and organs.

2.3 Factors Affecting NPs-Cell Interactions

The chemical nature of the QD itself has primary influences on the QD-cell interactions. However, particle size, shape, texture, rigidity, charge, functional groups, and surface properties can affect cellular uptake and interaction with cellular counterparts. Upon entering the human or animal body, QDs/NPs interact with the serum and extracellular matrix (ECM) proteins, generating a 'protein corona' around them [13] that can prevent agglomeration, reduce toxicity, and restrict them from entering the cytoplasm [14]. The corona also modifies biological (antibacterial, antioxidant activity, or ROS generation) and physical (fluorescence, surface plasmon resonance, or magnetic) properties [15].

The specific surface area of NPs depends exclusively on the size and shape of NPs, essentially determining high reaction capacity and catalytic activity, the unique mechanism of NP interaction with living systems. The sizes of NPs (from 1 to 100 nm) are comparable to many biomolecules and membranes like protein globules (2–10 nm), DNA (2 nm), and cell membranes (10 nm), as shown in Fig. 1. Macrophage engulfment of NPs depends on particle size, and they can only recognize relatively large NPs, not all smaller particles like QDs [16]. The size of NPs/QDs also influences cellular uptake and intracellular distribution [17, 18]. ECM controls the movement of NPs across it due to mesh-like structure (20–40 nm); small size QDs can penetrate easily, but larger NPs are restricted [19]. However, the hydrodynamic diameter and surface charge of QDs also modify the mobility through the ECM [20]. Nanomaterials (e.g., QDs, single-walled carbon nanotubes (SWNT)) with a large surface-to-volume ratio successfully penetrate the cell membrane to enter the cells after passing through the ECM barrier [21]. The optimal particle size for cellular uptake is determined by competition between receptor diffusion kinetics and thermodynamic driving forces [22, 23]. The size distribution (polydispersity index) and agglomeration behavior of NPs impact interactions and subsequent cellular responses [24]. NPs can reach the cell nucleus by passive diffusion and active transport by supporting a cytoplasmic protein named importins. The ability of active transport is inversely dependent on the size of the QD. Due to such low dimensions, NPs can easily penetrate through cell and cell organelles. The size and shape also determine the kinetics of their distribution and accumulation in the body. NPs smaller than ~ 5 nm typically overcome cell barriers via translocation, whereas NPs larger than ~ 5 nm may cross cell barriers by phagocytosis, macropinocytosis, and other transport mechanisms [25]. Various *in vivo* studies observed that NPs (< 10 nm) are rapidly circulated among all organs and tissues upon intravenous administration; however, larger NPs (> 50 nm) are found in the liver, spleen, and blood [26]. Larger NPs like mesoporous silica may cause

erythrocyte destruction (hemolysis) and deform the membrane [27]. The shape of NPs is crucial in determining toxicity [28, 29]. For example, spherical NPs are more prone to endocytosis than nanotubes and nanofibers; plate-like and needle-like NPs may cause more cell death than spherical and rod-like NPs. Thereby changing the shape of the NPs can prevent the damage of cell membranes to some extent. The shape of NPs influences the uptake, distribution, interactions with cellular components, e.g., elongated NPs generally show higher uptake than spherical ones due to their easily adhering to the cell membranes [30], rod, disc, discoid, cylinder, triangle, and quasi-ellipsoidal NPs showed more effective internalization than spherical-shaped ones [31–33].

The chemistry of base materials for the synthesis of QDs may have severe influences on their interactions with the cells and cellular components. The use of biopolymers or non-toxic chemicals during synthesis produces mostly cell-friendly and bioactive QDs [34]. Hydrophilic QDs with functional groups (e.g., hydroxyl, carboxyl, amino, and acetamido groups) or synthesized with biopolymers (e.g., polyvinyl alcohol, polycaprolactone, polylactic acid) are beneficial for the biomedical field and also compatible with mammalian cells [35]. Solubility and ionization of metallic or metal-containing QDs have unique impacts on the cellular response and toxicity at the molecular, cellular, tissue, and systemic level. Surface topography and stiffness of QDs affect QD-cell interaction and the subsequent cellular responses [24]. ECM holds a net negative charge owing to glycosaminoglycans (GAGs) chains. The penetration of QDs through ECM is controlled by a charge-dependent mechanism, i.e., interaction filtering [36]. Protein corona formation over the QDs may change the net charge, and mostly QDs with a net positive charge are internalized by cells vigorously. Cationic QDs can provide relatively robust interaction with cell membranes and result in their quick internalization with potential membrane distortions, disorganizing the phospholipids bilayer followed by the generation of “holes” in the cell membranes [37, 38]. In this perspective, neutral and anionic QDs are less harmful, have a low affinity with cells, and thus result in less internalization [23].

Apart from all the parameters, various functional groups on the surface of QDs can modify their interactions with cells and subsequent cellular responses. For example, poly-L-lysine (PLL) has shown superior cell membrane affinity, and polyethylene glycol (PEG) linkers reduce the targeted receptor's binding affinity and minimize nonspecific membrane interactions. However, the functionalization of QDs can reduce cytotoxicity. The functionalization of QDs with ligands such as proteins, peptides, antibodies, small molecules, and nucleic acids is the easiest way to target specific cells or intracellular components [39]. Specific charged QDs or simultaneously functionalized with multiple groups having different surface charges can be possible via surface functionalization [40]. QDs/NPs with hydrophilic surface groups exhibited an extended circulation period due to the resistance to phagocytosis [41]. Macrophage polarization depends on the hydrophilic or hydrophobic nature of the QD surface, e.g., medium hydrophilicity favors cell adhesion and proliferation [42].

2.4 Mechanisms of Cellular and Tissue Transport of QDs

In most cases, the NPs can be invisible to the immune system and thus can be efficiently adopted by the endocytic pathway like phagocytosis, pinocytosis, clathrin-mediated endocytosis, and caveolae-mediated endocytosis. Potential interactions with cellular organelles include Ln^{3+} leakage, interaction ligands with proteins enzymes, cellular structures, potential ROS generation, and variation of the cellular environment, which may cause apoptosis, as shown in Fig. 2(b). QDs can be internalized into the cell via processes requiring energy or by passive transport, as depicted in Fig. 2(b). QDs are transported into the cell interior via cargo, i.e., the process is called endocytosis. Endocytosis can be classified into several types, varying the mechanism, size, and type of cargo. Phagocytosis, clathrin-mediated endocytosis, caveolae-mediated endocytosis, pinocytosis, and clathrin/caveolae-independent endocytosis, are significant types of endocytosis. Endocytosis may occur via a receptor-mediated process or a nonspecific process, pinocytosis.

Caveolin-mediated endocytosis is responsible for the cellular uptake of NPs (20–100 nm), and clathrin-mediated endocytosis is mainly responsible for the cellular uptake of submicron particles (100–350 nm) [40, 43, 44]. Phagocytosis and pinocytosis are responsible for NPs internalization [45]. The clathrin- and caveolae-mediated endocytosis and physical adhesion-subsequent penetration are responsible for the cellular internalization of small-sized NPs due to surface charge. An energy-dependent endocytosis mechanism played a more prominent role for larger NPs. Carbon-based nanomaterials such as fullerenes, graphene, and carbon nanotubes (CNTs) can penetrate the cell membrane by spontaneous insertion/penetration across the membrane or by endocytosis [46–51]. Size, surface chemistry, and shape of NPs have adverse effects on nano-bio interactions, adverse effects, and toxicity [52, 53].

NPs may interact with the organ or tissue after entering the body and may subsequently translocate and enter the bloodstream to access distant organs/tissues via systemic transport [5], leading to cause toxicity at cellular and subcellular levels. The NPs mainly interact with various biomolecules, including proteins, carbohydrates, lipids, and nucleic acids, resulting in the formation of a biomolecular nanoparticle surface corona, i.e., protein corona. The formation of protein corona may cause protein unfolding [54, 55], which may induce the loss of protein function and cause immunotoxicity [56, 57]. Moreover, the alteration of protein configuration can have adverse effects and toxicity owing to cell signaling pathway activation, enzyme function loss, protein fibrillation, new antigenic site formation, and NPs aggregation [54, 55, 58–61]. NPs may directly interact with cells and result in physical damage of cell membrane structures and cause cytoskeletal dysfunction and abnormal morphological stretching owing to various morphology of NPs [62–64]. NPs can indirectly disturb normal cellular bio-functions and homeostasis by blocking cell membrane receptors and membrane ion channels.

Most of the nanotoxicity mechanism relies on generating ROS, e.g., singlet oxygen, superoxide anion radicals ($\text{O}_2^{\text{@@}^-}$), oxygen radicals (O_2^1), peroxide ions (O_2^{2-}), hydrogen peroxide (H_2O_2), and hydroxyl radicals ($\text{HO}^{\text{@@}}$). ROS generates

through one-electron oxidation reactions with transition metals (e.g., Fe, Cu, Ca, Co, Cr, Si, Zn, V) through Fenton and Haber–Weiss reaction mechanisms [65–68] or NP's surface groups [69, 70]. NPs may induce ROS overproduction, causing harmful oxidative stress by perturbing the cellular balance between ROS and antioxidants [5, 71–73]. Besides, the surface group of NPs may induce hypersensitivity reactions and anaphylaxis mediated by anti-PEG antibodies in humans, where PEG is widely used in biomedical studies for surface modification of nanomedicines [74–76]. In addition, the NPs may interfere with cell differentiation, protein synthesis, activation of pro-inflammatory genes, and synthesis of inflammatory mediators [63]. For example, superparamagnetic iron oxide NPs can disturb or entirely suppress osteogenic differentiation of stem cells and activate the synthesis of signal molecules and tumor antigens [77, 78]. NP's interaction with the cells may enhance the expression of the genes responsible for the formation of lysosomes and inhibit protein synthesis [79, 80].

In summary, the most common mechanisms of NP cytotoxicity are the following: (a) oxidation via the formation of ROS and other free radicals, (b) cell membranes damage via perforation, (c) damaging cytoskeleton, which leads to disruption in intracellular transport and cell division, (d) affect transcription and damage DNA, accelerating mutagenesis, (e) harm mitochondria and hence metabolism, causing a cell energy imbalance, (f) restrict the formation of lysosomes, thus hindering autophagy and degradation of macromolecules and triggering the apoptosis, (g) affecting standard mechanisms of cell metabolism, via formation of inflammatory mediators. Therefore, it is necessary to define and classify the mechanism of the toxic effect of NPs, which is a function of their physical and chemical properties.

2.5 Dose Assessment for Nanotoxicology

A concept for dose assessment of QDs in the same way the dose concept developed within radiation protection over the decades will be presented here. The deposited dose is defined as the total deposited or agglomerated QDs surface area (SA) per tissue mass or volume (m^2/kg , or m^2/m^3 or m^{-1}), which can induce biological effects. The equivalent dose is defined as the weighted deposited dose quantifying the effects of several other physicochemical properties of the QDs, e.g., the specific SA, surface texture, surface charge (zeta-potential), and morphology (shape, surface roughness, aspect ratio). Table 2 shows the dose quantities with the analogy from the dose assessment for ionizing radiation. Similar approaches can be followed for nanotoxicology to determine the dose factors for QDs.

Table 2 Dose assessment for QDs in nanotoxicology

Dose quantities	Dosimetry for QDs
Absorbed/deposited dose	The deposited or absorbed dose of QD (D_{QD}) is the total deposited SA of QD per mass of living matter dm , m^2/kg : $D_{QD} = \frac{d(SA)}{dm}$
Dose rate	The mean absorbed QD dose rate in T at time t : $D_{QD,T}(t)$
Committed tissue dose	The quantity of absorbed QD dose (uptake) per unit time: $D_{QD,T} = \int_0^T D_{QD,T}(t) dt$
Equivalent dose	Absorbed dose weighted by QD property (material) dependent reactivity weighting factor (s) $w_{p,i}$ ($i = 1, 2, \dots$) for different physicochemical properties of QD: $H_T = \prod_i w_{p,i} \cdot D_{QD,T}$
Effective dose	The tissue-weighted sum of H_T in all specified tissues and organs of the body: $E = \sum_T w_T \cdot H_T = \prod_i w_{p,i} \sum_T w_T \cdot D_{QD,T}$

2.6 The Biological Relevance of Nanotoxicology

The safety of the extensive use of biofunctionalized QDs must be considered from a technological or biomedical perspective, retaining the desirable properties of QDs. These properties may lead to hazardous, unexpected toxicities within cells and tissues. A straightforward strategy to reduce the toxicity effect of QDs and induce bio-incompatibility is to make a coating of polymers, ligands, and detergents to block access to the QD surface. In this way, cellular uptake, bioavailability, and limiting the spreading of QDs can be possible by changing or adapting the physicochemical characteristics. Depositing a shell of silica, ZnS, or a polymer on the surface of bare QD may overcome poor biocompatibility. However, an increase of their hydrodynamic radius by the coating of SiO_2 or polymer results in aggregation, leading to an obstruction of blood flow and capillary vessel blockage. In general, toxicity due to QDs may be analyzed/quantified, which associates specific phenomena, processes, or test methodology. Figure 2 shows exposure and internalization schematically. Cellular level understanding requires analysis of apoptosis, necrosis, growth arrest, abnormal morphology, undesired cell signaling, or secretory activity. Molecular-level cytotoxicity involves failure of cell signaling or mitochondrial electron transport deregulation, misfolding, disruption, aggregation of the protein, inactivation of enzymes, cell stress due to reactive oxygen species (ROS), ROS mediated detrimental effects, e.g., DNA damage, mRNA degradation, gene expression perturbation [8].

Moreover, subcellular toxicity includes various effects, like membrane disruption or permeability changes and mitochondrial activity perturbations leading to apoptosis. Organ level toxicity means the toxic effects on different organs (mainly kidney, spleen, liver, heart, brain, lungs, skin), which is assessed or observed after a certain

exposure period, measuring its physiological parameters, morphology, and histology. Due to its complexity, environmental toxicity is possibly the most challenging area of nanotoxicology research. The dissolution and release of potentially toxic ions from QDs or chemical coating may produce other chemical adverse effects.

2.7 Nanotoxicity Assessment

Toxicity assessments are defined as the cell culture and animal toxicity tests adapted to evaluate the safety of QDs. Table 3 summarizes commonly used nanotoxicity assessment tools with a few examples. Cell culture studies are advantageous over others due to their simplicity, scalability, low cost, and throughput for nanotoxicity evaluation of various model animals and human cell lines [5]. In recent years, computational nanotoxicity methods have been popular in toxicity assessment for cell culture, animal models, and human subjects, reducing the need, cost, and time required for animal and cell nanotoxicity testing. However, published studies demonstrate significant discrepancies in QD's characterization, dose metrics,

Table 3 The table summarizes commonly used nanotoxicity assessment tools with a few references

Toxicity tests	Assessment tool(s)	Reference(s)
<i>Cell culture level</i>		
Cell morphology	AFM, SEM, TEM, QPM, SLIM	[81–84]
Cell membrane integrity	LDH assay, flow cytometry	[85–87]
Cell necrosis and apoptosis	Flow cytometry, TUNEL method	[88]
Cell viability and cell death	Tetrazolium salts (MTT, MTS, XTT, WST-1), neutral red assay, flow cytometry, trypan blue, WST	[89–92]
DNA damage and gene expression	Apoptosis assays like DNA laddering, Comet Assay, TUNEL assay, ELISA, qPCR, LMPCR, TDPCR	[93–95]
Hemoglobin release	Hemolysis assay	[96–98]
Inflammation and immune responses	ELISA, qPCR	[99–101]
Ion channel disruption	Patch-clamp experiment	[102]
Mitochondrial damage	Mitochondrial membrane potential measurements	[103–105]
Protein structure	CD, DSC, FTIR, NMR, cryo-EM, AlphaFold (CASPI4), Ab initio	[106–112]
ROS generation	Oxidative stress assay, DCFH assay, FLIM, EPR, lipid peroxidation, plasmid assay	[113–116]
<i>Animal and human level</i>		

(continued)

Table 3 (continued)

Toxicity tests	Assessment tool(s)	Reference(s)
Biochemistry	biomarkers (ALP, ASAT, LDH, ALAT), cytokine analysis	[117–119]
Hematology	Hemoglobin content, RBCs, PCV, total erythrocyte, platelets, and leukocyte counts	[120, 121]
Histopathology	Tissue sections (hematoxylin/eosin, immunohistochemistry)	[122, 123]
Pharmacokinetics and pharmacodynamics	MRI, PET, SPECT, CT, ICP-MS, fluorescence, biodistribution	[124–127]
Skin test	Skin penetration and skin allergic reactions	[122, 128, 129]
Survival studies	Kaplan–Meier analysis, survival curves, median survival, LC ₅₀ , LD ₅₀	[130–132]
Clinical trials (phase I–IV)	Safety and toxicity data on human subjects	[133, 134]

Abbreviation *AFM* Atomic force microscopy; *ALAT* alanine aminotransferase; *ALP* alkaline phosphatase; *ASAT* aspartate aminotransferase; *CD* circular dichroism; *cryo-EM* cryogenic electron microscopy; *CT* X-ray computed tomography; *CASP14* 14th Critical Assessment of protein Structure Prediction; *DCFH* 2,7-dichlorofluorescein; *DSC* differential scanning calorimetry; *ELISA* enzyme-linked immunosorbent assay; *EPR* Electronparamagnetic resonance; *Fpg* formamidopyrimidine-DNA glycosylase; *FLIM* fluorescence lifetime imaging microscopy; *FTIR* Fourier transform infrared spectroscopy; *ICP-MS* inductively coupled plasma mass spectrometry; *LC₅₀* lethal concentration 50%; *LD₅₀* lethal dose 50%; *LDH* lactate dehydrogenase; *LMPCR* ligation-mediated PCR; *MRI* magnetic resonance imaging; *MTT* 3-(4,5-dimethylthiazol-2-yl)-2,5-diphenyltetrazolium bromide; *MTS* 3-(4,5-dimethylthiazol-2-yl)-5-(3-carboxymethoxyphenyl)-2-(4-sulfophenyl)-2H-tetrazolium, inner salt; *NMR* nuclear magnetic resonance; *PCV* packed cell volume; *PET* positron emission tomography; *qPCR* quantitative polymerase chain reaction; *QPM* quantitative phase microscopy; *RBCs* Red blood corpuscles; *SLIM* spatial light interference microscopy; *SPECT* single-photon emission computed tomography; *SEM* scanning electron microscope; *TDPCR* terminal transferase-dependent PCR; *TEM* transmission electron microscopy; *TUNEL* Terminal deoxynucleotidyl transferase dUTP(deoxyuridine triphosphate) nick end labeling; *WST* water-soluble tetrazolium salt; *WST-1* 2-(4-iodophenyl)-3-(4-nitrophenyl)-5-(2,4-disulfophenyl)-2H-tetrazolium; *XTT* sodium(2,3-bis(2-methoxy-4-nitro-5-sulphophenyl)-2H-tetrazolium-5-carboxanilide, inner salt

experimental methods, data completeness, and the lack of standardized protocols, lowering computational models' overall statistical power and accuracy for nanotoxicity predictions.

3 Strategies to Mitigate the Toxicity of QDs

The detailed study on the physicochemical properties of QDs with the rate of cellular absorption is the prerequisite in designing QDs with ideal biological performance [135]. However, numerous studies are already performed on their uptake, accumulation, and transport in biological conditions; still, comprehensive research must be

done before using QDs in biomedical fields. Biotransformation and fate of biodegradable, dissolvable, nondissolved, and nonbiodegradable NPs/QDs, as shown in the schematic in Fig. 3. In the following subsections, the overall strategies will be discussed to mitigate the toxicity of QDs to some extent.

Designing QDs with ideal biological performance is a fundamental issue to the scientist at the present-day understanding of the relationship between the physical and chemical properties of QDs and the amount and rate of cellular absorption to improve the effectiveness of QDs in therapeutic utility and safety. Cellular uptake and transport of NPs can be regulated by altering the size and shape. However, it is more complicated to predict the effect of size exclusively as a limited number of demonstrations to resolve the issue. Rod-like structures with different aspect ratios may be advantageous over other morphologies of QDs/NPs.

Another factor affecting cytotoxicity is the core composition and charges of QDs/NPs. The most common QDs with excellent optical properties are composed of Cd-element. Cd-ions can produce various ROS and can easily bind to the sulfhydryl groups on various intracellular proteins, weakening many subcellular organelles' functions [3]. Therefore, the shell formation (e.g., ZnS) may reduce the toxicity; however, their toxicity and functionality have yet to be fully characterized. A double-layer of polymer/silica layer formation can also reduce QDs toxicity and retain their optical properties in the biological environment. Surface charges are also essential elements to stabilize the QDs from agglomeration, and the adsorption of proteins happens owing to the toxic effects of anions (e.g., carboxyl) and cations (e.g., amine) of secondary coatings on QDs. Cationic QDs are more prone to attach to the cell membrane than neutral or anionic QDs [136]. However, cationic QDs have high stability and excellent emission properties. In cationic QD, amine groups may cause

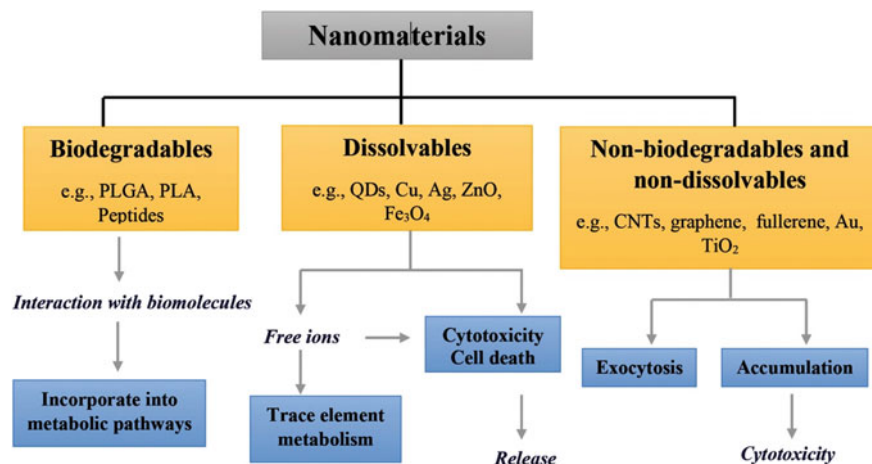


Fig. 3 Biotransformation and fate of biodegradable, dissolvable, nondissolved, and nonbiodegradable NPs/QDs. PLGA—poly(D,L-lactide-co-glycolide); PLA—polylactide; Cu—copper; CNTs—carbon nanotubes; TiO₂—titanium dioxide; ZnO—zinc oxide

buffering and amplification of proton pump activity, which results in osmotic swelling and lysosomal rupture [24, 137]. Therefore, optimizing the concentration of positive charges may balance the internalization efficiency and potential toxicity.

The surface of QDs must be modified to inhibit the formation of protein corona and hence, regulate the uptake, ROS levels, lipid peroxidation, cellular toxicity, and apoptosis. In this perspective, the secondary coating of biocompatible polymer (e.g., PEG) on the surface of QDs may decrease the toxicity. Selecting proper coating materials and surface functionalization techniques can diminish or eliminate the adverse effects of QDs. The surface coating also modifies the colloidal stability and quality of QDs. Researchers must consider during the control modification of the surface. Researchers also demonstrated that the aggregation of QDs is dependent on the surface properties or coating, leading to their toxicity and increasing the chance of deposition in cells or organs. Various studies indicate that the cellular viability decreases slightly with the ligands used in the order Poly(acrylic acid) (PAA); Poly(ethylene imine) (PEI) > AA; 6-Aminohexanoic acid (AHA); Folic acid (FA); oleic acid (OA) > Arginine–glycine–aspartate tripeptide (RGD) > citrate > PEG > SiO₂. However, it is not easy to draw a general conclusion due to the various sizes, doping, shape, crystallographic structure, ligands, and composition of NPs/QDs, different incubation times, and the variety of cells used in vitro and in vivo studies.

Reduction of QDs toxicity can be possible using greener or biocompatible QDs. For example, AgSe QDs accumulate in the liver and spleen after the intravenous injection into mice [138]. The AgSe QDs decompose into Ag and Se within a week. The existence of Ag and Se does not cause damage to the tissue. The optimal surface modification with different surface functional groups (-COOH, -OH) of InP/ZnS QDs may reduce potential toxicity in biological applications [139]. Black phosphorus quantum dots (BP QDs) can cause acute toxicities by oxidative stress but do not give rise to long-term appreciable toxicological responses [140]. Cadmium-free QDs, such as silicon, carbon/graphene, Ag₂Se, and Ag₂S, are the current research interest for biomedical applications with reduced toxicity. However, stability and toxicity are inversely proportional to each other. Therefore, more comprehensive demonstrations are needed to understand the interconnections between them.

4 Conclusion and Future Perspectives

Numerous studies show that the general impact of engineered nanomaterials or QDs on human health is not well-documented, and risk assessment studies on hazard and exposure need to be done to assess the toxicity of QDs. Nanotoxicity mechanisms and the origin of toxicity due to specific QDs on the cells and subcellular structures are still in their infancy. More comprehensive research and demonstration (both in vivo and in vitro) are the prerequisites for the proper toxicity assessment. The complex nature of QDs and their various properties, including chemical compositions, surface state (i.e., surface charge, functionality, porosity, surface area, hydrophilicity, hydrophobicity), physical properties (primary and hydrodynamic size, shape, size distribution,

structure, agglomeration, and concentration), local environmental factors (temperature, pH, dissolution rate) and presence of other chemicals or electromagnetic field, predicting the potential toxicity of QDs is a significant challenge for researchers. First, understanding the interaction of QDs with the living cells is critical to evaluating the processes and reactivity, and hence the toxicity. In this perspective, there is an open question: How should we define the toxic dose for various QDs to evaluate the adverse health and environmental effects? Because the present research methodology relies on the results obtained concerning particular concentration, composition, and time of exposure of QDs. The lack of standardized protocol for cytotoxicity assessment is one major obstacle before properly assessing QD toxicity. Identifying the relationship between physicochemical properties and QDs toxicity effects will be beneficial with the advancement of detection techniques and methodologies, e.g., in-situ, real-time, and rapid quantitative analysis methods, in future.

Moreover, it is challenging to compare toxicity assessments for similar studies on various cell lines under different conditions. Controlling the inherent toxicity originating from the synthesis protocol and the same protocols available for handling highly toxic chemicals, followed by different research groups, is still challenging to maintain the same amount of toxicity coming from nanostructure. Ultimately, more and more research will catalyze the generation of frameworks to exploit the full potential of safe QDs exposure and application in humans.

Acknowledgements No competing financial support to acknowledge.

References

1. Filali S, Pirot F, Miossec P. Biological applications and toxicity minimization of semiconductor quantum dots. *Trends Biotechnol* [Internet]. 2020 Feb;38(2):163–77. Available from: <https://linkinghub.elsevier.com/retrieve/pii/S0167779919301878>
2. Gidwani B, Sahu V, Shukla SS, Pandey R, Joshi V, Jain VK, et al. Quantum dots: Prospectives, toxicity, advances and applications. *J Drug Deliv Sci Technol* [Internet]. 2021 Feb;61:102308. Available from: <https://linkinghub.elsevier.com/retrieve/pii/S1773224720315975>
3. Hu L, Zhong H, He Z. Toxicity evaluation of cadmium-containing quantum dots: A review of optimizing physicochemical properties to diminish toxicity. *Colloids Surfaces B Biointerfaces* [Internet]. 2021 Apr;200:111609. Available from: <https://linkinghub.elsevier.com/retrieve/pii/S0927776521000539>
4. Huang X, Tang M. Research advance on cell imaging and cytotoxicity of different types of quantum Dots. *J Appl Toxicol* [Internet]. 2021 Mar 9;41(3):342–61. Available from: <https://onlinelibrary.wiley.com/doi/10.1002/jat.4083>
5. Yang W, Wang L, Mettenbrink EM, DeAngelis PL, Wilhelm S. Nanoparticle Toxicology. *Annu Rev Pharmacol Toxicol* [Internet]. 2021 Jan 6;61(1):269–89. Available from: <https://www.annualreviews.org/doi/10.1146/annurev-pharmtox-032320-110338>
6. Simkó M, Nosske D, Kreyling W. Metrics, dose, and dose concept: The need for a proper dose concept in the risk assessment of nanoparticles. *Int J Environ Res Public Health* [Internet]. 2014 Apr 14;11(4):4026–48. Available from: <http://www.mdpi.com/1660-4601/11/4/4026>

7. Eşref D, Vincent C. Evaluation of the potential genotoxicity of quantum dots. A Review. *Asp Nanotechnol* [Internet]. 2017 Mar 20;1(1). Available from: <https://scholars.direct/Articles/nanotechnology/ant-1-001.php?jid=nanotechnology>
8. Gnach A, Lipinski T, Bednarkiewicz A, Rybka J, Capobianco JA. Upconverting nanoparticles: assessing the toxicity. *Chem Soc Rev* [Internet]. 2015;44(6):1561–84. Available from: <http://xlink.rsc.org/?DOI=C4CS00177J>
9. Foulkes R, Man E, Thind J, Yeung S, Joy A, Hoskins C. The regulation of nanomaterials and nanomedicines for clinical application: current and future perspectives. *Biomater Sci* [Internet]. 2020;8(17):4653–64. Available from: <http://xlink.rsc.org/?DOI=D0BM00558D>
10. Allan J, Belz S, Hoeveler A, Hugas M, Okuda H, Patri A, et al. Regulatory landscape of nanotechnology and nanoplastics from a global perspective. *Regul Toxicol Pharmacol* [Internet]. 2021 June;122:104885. Available from: <https://linkinghub.elsevier.com/retrieve/pii/S0273230021000258>
11. Zoabi A, Touitou E, Margulis K. Recent advances in nanomaterials for dermal and transdermal applications. *Colloids and Interfaces* [Internet]. 2021 Mar 18;5(1):18. Available from: <https://www.mdpi.com/2504-5377/5/1/18>
12. Yu Z, Meng X, Zhang S, Chen Y, Zhang Z, Zhang Y. Recent progress in transdermal nanocarriers and their surface modifications. *Molecules* [Internet]. 2021 May 21;26(11):3093. Available from: <https://www.mdpi.com/1420-3049/26/11/3093>
13. Marichal L, Giraudon--Colas G, Cousin F, Thill A, Labarre J, Boulard Y, et al. Protein–nanoparticle interactions: What are the protein–Corona thickness and organization? *Langmuir* [Internet]. 2019 Aug 20;35(33):10831–7. Available from: <https://pubs.acs.org/doi/10.1021/acs.langmuir.9b01373>
14. Tenzer S, Docter D, Kuharev J, Musyanovych A, Fetz V, Hecht R, et al. Rapid formation of plasma protein corona critically affects nanoparticle pathophysiology. *Nat Nanotechnol* [Internet]. 2013 Oct 22;8(10):772–81. Available from: <http://www.nature.com/articles/nnano.2013.181>
15. Kobos L, Shannahan J. Biocorona—induced modifications in engineered nanomaterial–cellular interactions impacting biomedical applications. *WIREs Nanomed Nanobiotechnol* [Internet]. 2020 May;12(3). Available from: <https://onlinelibrary.wiley.com/doi/10.1002/wnan.1608>
16. Sohaebuddin SK, Thevenot PT, Baker D, Eaton JW, Tang L. Nanomaterial cytotoxicity is composition, size, and cell type dependent. *Part Fibre Toxicol* [Internet]. 2010 Dec 21;7(1):22. Available from: <https://particleandfibretoxicology.biomedcentral.com/articles/10.1186/1743-8977-7-22>
17. Aggarwal P, Hall JB, McLeland CB, Dobrovolskaia MA, McNeil SE. Nanoparticle interaction with plasma proteins as it relates to particle biodistribution, biocompatibility and therapeutic efficacy. *Adv Drug Deliv Rev* [Internet]. 2009 June;61(6):428–37. Available from: <https://linkinghub.elsevier.com/retrieve/pii/S0169409X0900101X>
18. Saw WS, Ujihara M, Chong WY, Voon SH, Imae T, Kiew LV, et al. Size-dependent effect of cystine/citric acid-capped confeito-like gold nanoparticles on cellular uptake and photothermal cancer therapy. *Colloids Surfaces B Biointerfaces* [Internet]. 2018 Jan;161:365–74. Available from: <https://linkinghub.elsevier.com/retrieve/pii/S0927776517307142>
19. Tomasetti L, Breunig M. Preventing Obstructions of Nanosized Drug Delivery Systems by the Extracellular Matrix. *Adv Healthc Mater* [Internet]. 2018 Feb;7(3):1700739. Available from: <https://onlinelibrary.wiley.com/doi/10.1002/adhm.201700739>
20. Pons T, Uyeda HT, Medintz IL, Mattoussi H. Hydrodynamic dimensions, electrophoretic mobility, and stability of hydrophilic quantum dots. *J Phys Chem B* [Internet]. 2006 Oct 1;110(41):20308–16. Available from: <https://pubs.acs.org/doi/https://doi.org/10.1021/jp065041h>
21. Donkor DA, Tang XS. Tube length and cell type-dependent cellular responses to ultra-short single-walled carbon nanotube. *Biomaterials* [Internet]. 2014 Mar;35(9):3121–31. Available from: <https://linkinghub.elsevier.com/retrieve/pii/S0142961213015718>

22. Gao H, Shi W, Freund LB. From The Cover: Mechanics of receptor-mediated endocytosis. *Proc Natl Acad Sci* [Internet]. 2005 July 5;102(27):9469–74. Available from: <http://www.pnas.org/cgi/doi/https://doi.org/10.1073/pnas.0503879102>
23. Verma A, Stellacci F. Effect of Surface Properties on Nanoparticle–cell interactions. *Small* [Internet]. 2010 Jan 4;6(1):12–21. Available from: <https://onlinelibrary.wiley.com/doi/10.1002/sml.200901158>
24. Nel AE, Mädler L, Velegol D, Xia T, Hoek EM V., Somasundaran P, et al. Understanding biophysicochemical interactions at the nano–bio interface. *Nat Mater* [Internet]. 2009 July 14;8(7):543–57. Available from: <http://www.nature.com/articles/nmat2442>
25. Zhang S, Gao H, Bao G. Physical principles of nanoparticle cellular endocytosis. *ACS Nano* [Internet]. 2015 Sept 22;9(9):8655–71. Available from: <https://pubs.acs.org/doi/10.1021/acs.nano.5b03184>
26. De Jong WH, Hagens WI, Krystek P, Burger MC, Sips AJAM, Geertsma RE. Particle size-dependent organ distribution of gold nanoparticles after intravenous administration. *Biomaterials* [Internet]. 2008 Apr;29(12):1912–9. Available from: <https://linkinghub.elsevier.com/retrieve/pii/S014296120701071X>
27. Zhao Y, Sun X, Zhang G, Trewyn BG, Slowing II, Lin VS-Y. Interaction of mesoporous silica nanoparticles with human red blood cell membranes: Size and surface effects. *ACS Nano* [Internet]. 2011 Feb 22;5(2):1366–75. Available from: <https://pubs.acs.org/doi/10.1021/nn103077k>
28. Hamilton RF, Wu N, Porter D, Buford M, Wolfarth M, Holian A. Particle length-dependent titanium dioxide nanomaterials toxicity and bioactivity. Part Fibre Toxicol [Internet]. 2009 Dec 31;6(1):35. Available from: <https://particleandfibretoxicology.biomedcentral.com/articles/10.1186/1743-8977-6-35>
29. Champion JA, Mitragotri S. Role of target geometry in phagocytosis. *Proc Natl Acad Sci* [Internet]. 2006 Mar 28;103(13):4930–4. Available from: <https://pnas.org/doi/full/10.1073/pnas.0600997103>
30. Huang X, Teng X, Chen D, Tang F, He J. The effect of the shape of mesoporous silica nanoparticles on cellular uptake and cell function. *Biomaterials* [Internet]. 2010 Jan;31(3):438–48. Available from: <https://linkinghub.elsevier.com/retrieve/pii/S0142961209009922>
31. Salatin S, Maleki Dizaj S, Yari Khosroushahi A. Effect of the surface modification, size, and shape on cellular uptake of nanoparticles. *Cell Biol Int* [Internet]. 2015 Aug;39(8):881–90. Available from: <https://onlinelibrary.wiley.com/doi/10.1002/cbin.10459>
32. Gratton SEA, Ropp PA, Pohlhaus PD, Luft JC, Madden VJ, Napier ME, et al. The effect of particle design on cellular internalization pathways. *Proc Natl Acad Sci* [Internet]. 2008 Aug 19;105(33):11613–8. Available from: <http://www.pnas.org/cgi/doi/10.1073/pnas.0801763105>
33. Kolhar P, Anselmo AC, Gupta V, Pant K, Prabhakar Pandian B, Ruoslahti E, et al. Using shape effects to target antibody-coated nanoparticles to lung and brain endothelium. *Proc Natl Acad Sci* [Internet]. 2013 June 25;110(26):10753–8. Available from: <http://www.pnas.org/cgi/doi/10.1073/pnas.1308345110>
34. Augustine R, Hasan A. Emerging applications of biocompatible phytosynthesized metal/metal oxide nanoparticles in healthcare. *J Drug Deliv Sci Technol* [Internet]. 2020 Apr;56:101516. Available from: <https://linkinghub.elsevier.com/retrieve/pii/S1773224719315308>
35. Zhao H, Lin ZY, Yildirim L, Dhinakar A, Zhao X, Wu J. Polymer-based nanoparticles for protein delivery: Design, strategies and applications. *J Mater Chem B* [Internet]. 2016;4(23):4060–71. Available from: <http://xlink.rsc.org/?DOI=C6TB00308G>
36. Cho EJ, Holback H, Liu KC, Abouelmagd SA, Park J, Yeo Y. Nanoparticle characterization: State of the art, challenges, and emerging technologies. *Mol Pharm* [Internet]. 2013 June 3;10(6):2093–110. Available from: <https://pubs.acs.org/doi/10.1021/mp300697h>
37. Wu Y-L, Putcha N, Ng KW, Leong DT, Lim CT, Loo SCJ, et al. Biophysical responses upon the interaction of nanomaterials with cellular interfaces. *Acc Chem Res* [Internet]. 2013 Mar 19;46(3):782–91. Available from: <https://pubs.acs.org/doi/10.1021/ar300046u>

38. Xia T, Kovochich M, Liong M, Zink JI, Nel AE. Cationic polystyrene nanosphere toxicity depends on cell-specific endocytic and mitochondrial injury pathways. *ACS Nano* [Internet]. 2008 Jan 22;2(1):85–96. Available from: <https://pubs.acs.org/doi/10.1021/nn700256c>
39. Rizzo LY, Theek B, Storm G, Kiessling F, Lammers T. Recent progress in nanomedicine: therapeutic, diagnostic and theranostic applications. *Curr Opin Biotechnol* [Internet]. 2013 Dec;24(6):1159–66. Available from: <https://linkinghub.elsevier.com/retrieve/pii/S0958166913000347>
40. Augustine R, Hasan A, Primavera R, Wilson RJ, Thakor AS, Kevadiya BD. Cellular uptake and retention of nanoparticles: Insights on particle properties and interaction with cellular components. *Mater Today Commun* [Internet]. 2020 Dec;25:101692. Available from: <https://linkinghub.elsevier.com/retrieve/pii/S2352492820327033>
41. Otsuka H, Nagasaki Y, Kataoka K. PEGylated nanoparticles for biological and pharmaceutical applications. *Adv Drug Deliv Rev* [Internet]. 2012 Dec;64:246–55. Available from: <https://linkinghub.elsevier.com/retrieve/pii/S0169409X12002827>
42. Mager MD, LaPointe V, Stevens MM. Exploring and exploiting chemistry at the cell surface. *Nat Chem* [Internet]. 2011 Aug 22;3(8):582–9. Available from: <http://www.nature.com/articles/nchem.1090>
43. Gustafson HH, Holt-Casper D, Grainger DW, Ghandehari H. Nanoparticle uptake: The phagocytosis problem. *Nano Today* [Internet]. 2015 Aug;10(4):487–510. Available from: <https://linkinghub.elsevier.com/retrieve/pii/S1748013215000766>
44. Bouallegui Y, Ben Younes R, Oueslati R, Sheehan D. Redox proteomic insights into involvement of clathrin-mediated endocytosis in silver nanoparticles toxicity to *Mytilus galloprovincialis*. In: Mukherjee A, editor. *PLoS One* [Internet]. 2018 Oct 29;13(10):e0205765. Available from: <https://dx.plos.org/10.1371/journal.pone.0205765>
45. Behzadi S, Serpooshan V, Tao W, Hamaly MA, Alkawareek MY, Dreaden EC, et al. Cellular uptake of nanoparticles: journey inside the cell. *Chem Soc Rev* [Internet]. 2017;46(14):4218–44. Available from: <http://xlink.rsc.org/?DOI=C6CS00636A>
46. Zhang Y, Ali SF, Dervishi E, Xu Y, Li Z, Casciano D, et al. Cytotoxicity effects of graphene and single-wall carbon nanotubes in neural pheochromocytoma-derived PC12 cells. *ACS Nano* [Internet]. 2010 June 22;4(6):3181–6. Available from: <https://pubs.acs.org/doi/10.1021/nn1007176>
47. Yang K, Ma Y-Q. Computer simulation of the translocation of nanoparticles with different shapes across a lipid bilayer. *Nat Nanotechnol* [Internet]. 2010 Aug 25;5(8):579–83. Available from: <http://www.nature.com/articles/nnano.2010.141>
48. Shi X, Kong Y, Gao H. Coarse grained molecular dynamics and theoretical studies of carbon nanotubes entering cell membrane. *Acta Mech Sin* [Internet]. 2008 Apr 6;24(2):161–9. Available from: <http://link.springer.com/10.1007/s10409-007-0131-0>
49. Qiao R, Roberts AP, Mount AS, Klaine SJ, Ke PC. Translocation of C 60 and its derivatives across a lipid bilayer. *Nano Lett* [Internet]. 2007 Mar 1;7(3):614–9. Available from: <https://pubs.acs.org/doi/10.1021/nl062515f>
50. Shi X, von dem Bussche A, Hurt RH, Kane AB, Gao H. Cell entry of one-dimensional nanomaterials occurs by tip recognition and rotation. *Nat Nanotechnol* [Internet]. 2011 Nov 18;6(11):714–9. Available from: <http://www.nature.com/articles/nnano.2011.151>
51. Li Y, Yuan H, von dem Bussche A, Creighton M, Hurt RH, Kane AB, et al. Graphene microsheets enter cells through spontaneous membrane penetration at edge asperities and corner sites. *Proc Natl Acad Sci* [Internet]. 2013 Jul 23;110(30):12295–300. Available from: <http://www.pnas.org/cgi/doi/10.1073/pnas.1222276110>
52. Albanese A, Tang PS, Chan WCW. The effect of nanoparticle size, shape, and surface chemistry on biological systems. *Annu Rev Biomed Eng* [Internet]. 2012 Aug 15;14(1):1–16. Available from: <https://www.annualreviews.org/doi/10.1146/annurev-bioeng-071811-150124>
53. Elsaesser A, Howard CV. Toxicology of nanoparticles. *Adv Drug Deliv Rev* [Internet]. 2012 Feb;64(2):129–37. Available from: <https://linkinghub.elsevier.com/retrieve/pii/S0169409X11002328>

54. Dominguez-Medina S, Kiskeya L, Tauzin LJ, Hoggard A, Shuang B, D. S. Indrasekara AS, et al. Adsorption and unfolding of a single protein triggers nanoparticle aggregation. *ACS Nano* [Internet]. 2016 Feb 23;10(2):2103–12. Available from: <https://pubs.acs.org/doi/10.1021/acs.nano.5b06439>
55. Deng ZJ, Liang M, Monteiro M, Toth I, Minchin RF. Nanoparticle-induced unfolding of fibrinogen promotes Mac-1 receptor activation and inflammation. *Nat Nanotechnol* [Internet]. 2011 Jan 19;6(1):39–44. Available from: <http://www.nature.com/articles/nnano.2010.250>
56. Saptarshi SR, Duschl A, Lopata AL. Interaction of nanoparticles with proteins: Relation to bio-reactivity of the nanoparticle. *J Nanobiotechnology* [Internet]. 2013 Dec 19;11(1):26. Available from: <https://jnanobiotechnology.biomedcentral.com/articles/10.1186/1477-3155-11-26>
57. Neagu M, Piperigkou Z, Karamanou K, Engin AB, Docea AO, Constantin C, et al. Protein bio-corona: critical issue in immune nanotoxicology. *Arch Toxicol* [Internet]. 2017 Mar 20;91(3):1031–48. Available from: <http://link.springer.com/10.1007/s00204-016-1797-5>
58. Lin H, Bu Q, Cen X, Zhao Y-L. Current methods and research progress in nanomaterials risk assessment. *Curr Drug Metab* [Internet]. 2012 Apr 1;13(4):354–63. Available from: <http://www.eurekaselect.com/openurl/content.php?genre=article&issn=1389-2002&volume=13&issue=4&spage=354>
59. Gatoo MA, Naseem S, Arfat MY, Mahmood Dar A, Qasim K, Zubair S. Physicochemical properties of nanomaterials: Implication in associated toxic manifestations. *Biomed Res Int* [Internet]. 2014;2014:1–8. Available from: <http://www.hindawi.com/journals/bmri/2014/498420/>
60. Pustulka SM, Ling K, Pish SL, Champion JA. Protein nanoparticle charge and hydrophobicity govern protein Corona and macrophage uptake. *ACS Appl Mater Interfaces* [Internet]. 2020 Oct 28;12(43):48284–95. Available from: <https://pubs.acs.org/doi/10.1021/acsami.0c12341>
61. Walkey CD, Chan WCW. Understanding and controlling the interaction of nanomaterials with proteins in a physiological environment. *Chem Soc Rev* [Internet]. 2012;41(7):2780–99. Available from: <http://xlink.rsc.org/?DOI=C1CS15233E>
62. Wang Y, Tang M. Dysfunction of various organelles provokes multiple cell death after quantum dot exposure. *Int J Nanomedicine* [Internet]. 2018 May;13:2729–42. Available from: <https://www.dovepress.com/dysfunction-of-various-organelles-provokes-multiple-cell-death-after-q-peer-reviewed-article-IJN>
63. Sukhanova A, Bozrova S, Sokolov P, Berestovoy M, Karaulov A, Nabiev I. Dependence of nanoparticle toxicity on their physical and chemical properties. *Nanoscale Res Lett* [Internet]. 2018 Dec 7;13(1):44. Available from: <https://nanoscalereslett.springeropen.com/articles/10.1186/s11671-018-2457-x>
64. Akhavan O, Ghaderi E. Toxicity of graphene and graphene oxide nanowalls against bacteria. *ACS Nano* [Internet]. 2010 Oct 26;4(10):5731–6. Available from: <https://pubs.acs.org/doi/10.1021/nn101390x>
65. Rodrigo-Moreno A, Poschenrieder C, Shabala S. Transition metals: A double edge sword in ROS generation and signaling. *Plant Signal Behav* [Internet]. 2013 Mar 28;8(3):e23425. Available from: <http://www.tandfonline.com/doi/abs/10.4161/psb.23425>
66. Pospíšil P. The role of metals in production and scavenging of reactive oxygen species in photosystem II. *Plant Cell Physiol* [Internet]. 2014 July;55(7):1224–32. Available from: <https://academic.oup.com/pcp/article-lookup/doi/10.1093/pcp/pcu053>
67. Riley PA. Free radicals in biology: Oxidative stress and the effects of ionizing radiation. *Int J Radiat Biol* [Internet]. 1994 Jan 3;65(1):27–33. Available from: <http://www.tandfonline.com/doi/full/10.1080/09553009414550041>
68. Knaapen AM, Borm PJA, Albrecht C, Schins RPF. Inhaled particles and lung cancer. Part A: Mechanisms. *Int J Cancer* [Internet]. 2004 May 10;109(6):799–809. Available from: <https://onlinelibrary.wiley.com/doi/10.1002/ijc.11708>
69. Fu PP, Xia Q, Hwang H-M, Ray PC, Yu H. Mechanisms of nanotoxicity: Generation of reactive oxygen species. *J Food Drug Anal* [Internet]. 2014 Mar;22(1):64–75. Available from: <https://linkinghub.elsevier.com/retrieve/pii/S1021949814000064>

70. Qiu TA, Gallagher MJ, Hudson-Smith N V., Wu J, Krause MOP, Fortner JD, et al. Research highlights: unveiling the mechanisms underlying nanoparticle-induced ROS generation and oxidative stress. *Environ Sci Nano* [Internet]. 2016;3(5):940–5. Available from: <http://xlink.rsc.org/?DOI=C6EN90021F>
71. von Moos N, Slaveykova VI. Oxidative stress induced by inorganic nanoparticles in bacteria and aquatic microalgae—state of the art and knowledge gaps. *Nanotoxicology* [Internet]. 2014 Sept 19;8(6):605–30. Available from: <http://www.tandfonline.com/doi/full/10.3109/17435390.2013.809810>
72. Manke A, Wang L, Rojanasakul Y. Mechanisms of nanoparticle-induced oxidative stress and toxicity. *Biomed Res Int* [Internet]. 2013;2013:1–15. Available from: <http://www.hindawi.com/journals/bmri/2013/942916/>
73. Sharifi S, Behzadi S, Laurent S, Laird Forrest M, Stroeve P, Mahmoudi M. Toxicity of nano-materials. *Chem Soc Rev* [Internet]. 2012;41(6):2323–43. Available from: <http://xlink.rsc.org/?DOI=C1CS15188F>
74. Shiraishi K, Yokoyama M. Toxicity and immunogenicity concerns related to PEGylated-micelle carrier systems: A review. *Sci Technol Adv Mater* [Internet]. 2019 Dec 31;20(1):324–36. Available from: <https://www.tandfonline.com/doi/full/10.1080/14686996.2019.1590126>
75. Ingen-Housz-Oro S, Pham-Ledard A, Brice P, Lebrun-Vignes B, Zehou O, Reitter D, et al. Immediate hypersensitivity reaction to pegylated liposomal doxorubicin: Management and outcome in four patients. *Eur J Dermatology* [Internet]. 2017 May;27(3):271–4. Available from: <http://www.john-libbey-eurotext.fr/medline.md?doi=10.1684/ejd.2017.2986>
76. Szebeni J, Simberg D, González-Fernández Á, Barenholz Y, Dobrovolskaia MA. Roadmap and strategy for overcoming infusion reactions to nanomedicines. *Nat Nanotechnol* [Internet]. 2018 Dec 22;13(12):1100–8. Available from: <http://www.nature.com/articles/s41565-018-0273-1>
77. Chen Y-C, Hsiao J-K, Liu H-M, Lai I-Y, Yao M, Hsu S-C, et al. The inhibitory effect of superparamagnetic iron oxide nanoparticle (Ferucarbotran) on osteogenic differentiation and its signalling mechanism in human mesenchymal stem cells. *Toxicol Appl Pharmacol* [Internet]. 2010 June;245(2):272–9. Available from: <https://linkinghub.elsevier.com/retrieve/pii/S0041008X10000979>
78. Kostura L, Kraitman DL, Mackay AM, Pittenger MF, Bulte JWM. Feridex labeling of mesenchymal stem cells inhibits chondrogenesis but not adipogenesis or osteogenesis. *NMR Biomed* [Internet]. 2004 Nov;17(7):513–7. Available from: <https://onlinelibrary.wiley.com/doi/10.1002/nbm.925>
79. Kedziorek DA, Muja N, Walczak P, Ruiz-Cabello J, Gilad AA, Jie CC, et al. Gene expression profiling reveals early cellular responses to intracellular magnetic labelling with superparamagnetic iron oxide nanoparticles. *Magn Reson Med* [Internet]. 2010 Apr;63(4):1031–43. Available from: <https://onlinelibrary.wiley.com/doi/10.1002/mrm.22290>
80. Poirier M, Simard J-C, Antoine F, Girard D. Interaction between silver nanoparticles of 20 nm (AgNP 20) and human neutrophils: induction of apoptosis and inhibition of de novo protein synthesis by AgNP 20 aggregates. *J Appl Toxicol* [Internet]. 2014 Apr;34(4):404–12. Available from: <https://onlinelibrary.wiley.com/doi/10.1002/jat.2956>
81. Tang W-B, Ji Y, Zhang M-M, Chen Z-Y, Xu Y-Y, Wang Y-W. A rapid detection method for morphological characteristics of biological cells based on phase imaging. *Biomed Res Int* [Internet]. 2018;2018:1–9. Available from: <https://www.hindawi.com/journals/bmri/2018/4651639/>
82. Franz CM, Puech P-H. Atomic force microscopy: A versatile tool for studying cell morphology, adhesion and mechanics. *Cell Mol Bioeng* [Internet]. 2008 Dec 6;1(4):289–300. Available from: <http://link.springer.com/10.1007/s12195-008-0037-3>
83. M. J. Advanced-microscopy techniques for the characterization of cellulose structure and cellulose-cellulase interactions. In: *Cellulose—Fundamental Aspects* [Internet]. InTech; 2013. Available from: <http://www.intechopen.com/books/cellulose-fundamental-aspects/advanced-microscopy-techniques-for-the-characterization-of-cellulose-structure-and-cellulose-cellula>

84. Malenica M, Vukomanović M, Kurtjak M, Masciotti V, dal Zilio S, Greco S, et al. Perspectives of microscopy methods for morphology characterisation of extracellular vesicles from human biofluids. *Biomedicines* [Internet]. 2021 May 26;9(6):603. Available from: <https://www.mdpi.com/2227-9059/9/6/603>
85. Bowman AM, Nesin OM, Pakhomova ON, Pakhomov AG. Analysis of plasma membrane integrity by fluorescent detection of Tl⁺ uptake. *J Membr Biol* [Internet]. 2010 July 11;236(1):15–26. Available from: <http://link.springer.com/10.1007/s00232-010-9269-y>
86. Smith SM, Wunder MB, Norris DA, Shellman YG. A simple protocol for using a LDH-based cytotoxicity assay to assess the effects of death and growth inhibition at the same time (Roemer K, editor). *PLoS One* [Internet]. 2011 Nov 17;6(11):e26908. Available from: <https://dx.plos.org/10.1371/journal.pone.0026908>
87. Aeschbacher M, Reinhardt CA, Zbinden G. A rapid cell membrane permeability test using fluorescent dyes and flow cytometry. *Cell Biol Toxicol* [Internet]. 1986 June;2(2):247–55. Available from: <http://link.springer.com/10.1007/BF00122693>
88. Fink SL, Cookson BT. Apoptosis, pyroptosis, and necrosis: Mechanistic description of dead and dying eukaryotic cells. *Infect Immun* [Internet]. 2005 Apr;73(4):1907–16. Available from: <https://journals.asm.org/doi/10.1128/IAI.73.4.1907-1916.2005>
89. Mosmann T. Rapid colorimetric assay for cellular growth and survival: Application to proliferation and cytotoxicity assays. *J Immunol Methods* [Internet]. 1983 Dec;65(1–2):55–63. Available from: <https://www.ncbi.nlm.nih.gov/books/NBK144065/>
90. Riss TL, Moravec RA, Niles AL, Duellman S, Benink HA, Worzella TJ, et al. Cell viability assays. *Assay Guid Man* [Internet]. 2016 July 1 [cited 2022 Jan 22]; Available from: <https://www.ncbi.nlm.nih.gov/books/NBK144065/>
91. Goodwin CJ, Holt SJ, Downes S, Marshall NJ. Microculture tetrazolium assays: A comparison between two new tetrazolium salts, XTT and MTS. *J Immunol Methods* [Internet]. 1995 Jan;179(1):95–103. Available from: <https://linkinghub.elsevier.com/retrieve/pii/0022175994002774>
92. Präbst K, Engelhardt H, Ringgeler S, Hübner H. Basic colorimetric proliferation assays: MTT, WST, and Resazurin. In 2017. p. 1–17. Available from: http://link.springer.com/10.1007/978-1-4939-6960-9_1
93. Figueroa-González G, Pérez-Plasencia C. Strategies for the evaluation of DNA damage and repair mechanisms in cancer. *Oncol Lett* [Internet]. 2017 June;13(6):3982–8. Available from: <https://www.spandidos-publications.com/10.3892/ol.2017.6002>
94. Furda AM, Bess AS, Meyer JN, Van Houten B. Analysis of DNA damage and repair in nuclear and mitochondrial DNA of animal cells using quantitative PCR. In 2012. p. 111–32. Available from: http://link.springer.com/10.1007/978-1-61779-998-3_9
95. Ribas-Maynou J, García-Peiró A, Fernández-Encinas A, Abad C, Amengual MJ, Prada E, et al. Comprehensive analysis of sperm DNA fragmentation by five different assays: TUNEL assay, SCSA, SCD test and alkaline and neutral Comet assay. *Andrology* [Internet]. 2013 Sept;1(5):715–22. Available from: <https://onlinelibrary.wiley.com/doi/10.1111/j.2047-2927.2013.00111.x>
96. Neun BW, Ilinskaya AN, Dobrovolskaia MA. Updated method for in vitro analysis of nanoparticle hemolytic properties. In 2018. p. 91–102. Available from: http://link.springer.com/10.1007/978-1-4939-7352-1_9
97. Dobrovolskaia MA, Clogston JD, Neun BW, Hall JB, Patri AK, McNeil SE. Method for analysis of nanoparticle hemolytic properties in vitro. *Nano Lett* [Internet]. 2008 Aug 13;8(8):2180–7. Available from: <https://pubs.acs.org/doi/10.1021/nl0805615>
98. Tsamesidis I, Pouroutzidou GK, Lympiraki E, Kazeli K, Lioutas CB, Christodoulou E, et al. Effect of ion doping in silica-based nanoparticles on the hemolytic and oxidative activity in contact with human erythrocytes. *Chem Biol Interact* [Internet]. 2020 Feb;318:108974. Available from: <https://linkinghub.elsevier.com/retrieve/pii/S0009279719315443>
99. Leng SX, McElhaney JE, Walston JD, Xie D, Fedarko NS, Kuchel GA. ELISA and multiplex technologies for cytokine measurement in inflammation and aging research. *Journals Gerontol Ser A Biol Sci Med Sci* [Internet]. 2008 Aug 1;63(8):879–84. Available from: <https://academic.oup.com/biomedgerontology/article-lookup/doi/10.1093/gerona/63.8.879>

100. Chen L, Liu J, Zhang Y, Zhang G, Kang Y, Chen A, et al. The toxicity of silica nanoparticles to the immune system. *Nanomedicine* [Internet]. 2018 Aug 1;13(15):1939–62. Available from: <https://www.futuremedicine.com/doi/10.2217/nmm-2018-0076>
101. Germolec DR, Shipkowski KA, Frawley RP, Evans E. Markers of inflammation. In 2018. p. 57–79. Available from: http://link.springer.com/10.1007/978-1-4939-8549-4_5
102. Pun RYK, Lecar H. Patch-clamp techniques and analysis. In: *Cell physiology source book* [Internet]. Elsevier; 1995. p. 279–92. Available from: <https://linkinghub.elsevier.com/retrieve/pii/B9780126569704500269>
103. Hussain S. Measurement of nanoparticle-induced mitochondrial membrane potential alterations. In 2019. p. 123–31. Available from: http://link.springer.com/10.1007/978-1-4939-8916-4_7
104. Teodoro JS, Simões AM, Duarte F V., Rolo AP, Murdoch RC, Hussain SM, et al. Assessment of the toxicity of silver nanoparticles in vitro: A mitochondrial perspective. *Toxicol Vitro* [Internet]. 2011 Apr;25(3):664–70. Available from: <https://linkinghub.elsevier.com/retrieve/pii/S0887233311000063>
105. Sun L, Li Y, Liu X, Jin M, Zhang L, Du Z, et al. Cytotoxicity and mitochondrial damage caused by silica nanoparticles. *Toxicol Vitro* [Internet]. 2011 Dec;25(8):1619–29. Available from: <https://linkinghub.elsevier.com/retrieve/pii/S0887233311001809>
106. Jumper J, Evans R, Pritzel A, Green T, Figurnov M, Ronneberger O, et al. Highly accurate protein structure prediction with AlphaFold. *Nature* [Internet]. 2021 Aug 26;596(7873):583–9. Available from: <https://www.nature.com/articles/s41586-021-03819-2>
107. Deng H, Jia Y, Zhang Y. Protein structure prediction. *Int J Mod Phys B* [Internet]. 2018 Jul 20;32(18):1840009. Available from: <https://www.worldscientific.com/doi/abs/10.1142/S021797921840009X>
108. Hardin C, Pogorelov T V, Luthey-Schulten Z. Ab initio protein structure prediction. *Curr Opin Struct Biol* [Internet]. 2002 Apr;12(2):176–81. Available from: <https://linkinghub.elsevier.com/retrieve/pii/S0959440X02003068>
109. Marzolf DR, Seffernick JT, Lindert S. protein structure prediction from NMR hydrogen–deuterium exchange data. *J Chem Theory Comput* [Internet]. 2021 Apr 13;17(4):2619–29. Available from: <https://pubs.acs.org/doi/10.1021/acs.jctc.1c00077>
110. Haris PI, Severcan F. FTIR spectroscopic characterization of protein structure in aqueous and non-aqueous media. *J Mol Catal B Enzym* [Internet]. 1999 Sept;7(1–4):207–21. Available from: <https://linkinghub.elsevier.com/retrieve/pii/S1381117799000302>
111. De Meutter J, Goormaghtigh E. FTIR imaging of protein microarrays for high throughput secondary structure determination. *Anal Chem* [Internet]. 2021 Mar 2;93(8):3733–41. Available from: <https://pubs.acs.org/doi/10.1021/acs.analchem.0c03677>
112. Micsonai A, Wien F, Kernya L, Lee Y-H, Goto Y, Réfrégiers M, et al. Accurate secondary structure prediction and fold recognition for circular dichroism spectroscopy. *Proc Natl Acad Sci* [Internet]. 2015 Jun 16;112(24):E3095–103. Available from: <http://www.pnas.org/lookup/doi/10.1073/pnas.1500851112>
113. Olowe R, Sandouka S, Saadi A, Shekh-Ahmad T. Approaches for reactive oxygen species and oxidative stress quantification in epilepsy. *Antioxidants* [Internet]. 2020 Oct 14;9(10):990. Available from: <https://www.mdpi.com/2076-3921/9/10/990>
114. Dikalov SI, Harrison DG. Methods for detection of mitochondrial and cellular reactive oxygen species. *Antioxid Redox Signal* [Internet]. 2014 Jan 10;20(2):372–82. Available from: <http://www.liebertpub.com/doi/10.1089/ars.2012.4886>
115. Griendling KK, Touyz RM, Zweier JL, Dikalov S, Chilian W, Chen Y-R, et al. Measurement of reactive oxygen species, reactive nitrogen species, and redox-dependent signalling in the cardiovascular system. *Circ Res* [Internet]. 2016 Aug 19;119(5). Available from: <https://www.ahajournals.org/doi/10.1161/RES.000000000000110>
116. Shahidi F, Zhong Y. Measurement of antioxidant activity. *J Funct Foods* [Internet]. 2015 Oct;18:757–81. Available from: <https://linkinghub.elsevier.com/retrieve/pii/S175646461500511>

117. WM A, DW N. Biochemical markers of in vivo hepatotoxicity. *J Clin Toxicol* [Internet]. 2016;06(02). Available from: <https://www.omicsonline.org/open-access/biochemical-markers-of-in-vivo-hepatotoxicity-2161-0495-1000297.php?aid=72597>
118. Dorsaf H, Sabrine M, Houda BL, Khémais BR, Mohsen S, Olfa T. Pecan pericarp extract protects against carbon tetrachloride-induced liver injury through oxidative mechanism in rats. *Toxicol Res (Camb)* [Internet]. 2020 Oct 29;9(5):652–60. Available from: <https://academic.oup.com/toxres/article/9/5/652/5910622>
119. Yang Y, Qin Z, Zeng W, Yang T, Cao Y, Mei C, et al. Toxicity assessment of nanoparticles in various systems and organs. *Nanotechnol Rev* [Internet]. 2017 Jun 27;6(3):279–89. Available from: <https://www.degruyter.com/document/doi/10.1515/ntrev-2016-0047/html>
120. Heatley JJ, Russell KE. Hematology. In: *Mader's Reptile and Amphibian Medicine and Surgery* [Internet]. Elsevier; 2019. p. 301–318.e3. Available from: <https://linkinghub.elsevier.com/retrieve/pii/B9780323482530000337>
121. WM A, DW N. Hematological markers of in vivo toxicity. *J Hematol Thromboembolic Dis* [Internet]. 2016;04(02). Available from: <http://www.esciencecentral.org/journals/hematological-markers-of-in-vivo-toxicity-2329-8790-1000236.php?aid=70754>
122. Jatana S, Palmer BC, Phelan SJ, DeLouise LA. Immunomodulatory effects of nanoparticles on skin allergy. *Sci Rep* [Internet]. 2017 Dec 21;7(1):3979. Available from: <http://www.nature.com/articles/s41598-017-03729-2>
123. Al-Harbi NS, Alrashood ST, Siddiqi NJ, Arafah MM, Ekhzaimy A, Khan HA. Effect of naked and PEG-coated gold nanoparticles on histopathology and cytokines expression in rat liver and kidneys. *Nanomedicine* [Internet]. 2020 Feb;15(3):289–302. Available from: <https://www.futuremedicine.com/doi/10.2217/nmm-2019-0220>
124. Castro-Balado A, Mondelo-García C, González-Barcia M, Zarra-Ferro I, Otero-Espinar FJ, Ruibal-Morell Á, et al. Ocular biodistribution studies using molecular imaging. *Pharmaceutics* [Internet]. 2019 May 16;11(5):237. Available from: <https://www.mdpi.com/1999-4923/11/5/237>
125. Mitchell N, Kalber TL, Cooper MS, Sunassee K, Chalker SL, Shaw KP, et al. Incorporation of paramagnetic, fluorescent and PET/SPECT contrast agents into liposomes for multimodal imaging. *Biomaterials* [Internet]. 2013 Jan;34(4):1179–92. Available from: <https://linkinghub.elsevier.com/retrieve/pii/S0142961212010939>
126. Hong H, Chen F, Cai W. Pharmacokinetic issues of imaging with nanoparticles: Focusing on carbon nanotubes and quantum dots. *Mol Imaging Biol* [Internet]. 2013 Oct 29;15(5):507–20. Available from: <http://link.springer.com/10.1007/s11307-013-0648-5>
127. Chen C, Li Y-F, Qu Y, Chai Z, Zhao Y. Advanced nuclear analytical and related techniques for the growing challenges in nanotoxicology. *Chem Soc Rev* [Internet]. 2013;42(21):8266. Available from: <http://xlink.rsc.org/?DOI=c3cs60111k>
128. Gautam R, Yang S, Maharjan A, Jo J, Acharya M, Heo Y, et al. Prediction of skin sensitization potential of silver and zinc oxide nanoparticles through the human cell line activation test. *Front Toxicol* [Internet]. 2021 May 28;3. Available from: <https://www.frontiersin.org/articles/10.3389/ftox.2021.649666/full>
129. Rice RH, Mauro TM. Toxic responses of the skin. In: *Casarett and Doull's Toxicology: The Basic Science of Poisons*, 8e [Internet]. New York, NY: McGraw-Hill Education; 2012. Available from: accesspharmacy.mhmedical.com/content.aspx?aid=1100089236
130. Kishore J, Goel M, Khanna P. Understanding survival analysis: Kaplan-Meier estimate. *Int J Ayurveda Res* [Internet]. 2010;1(4):274. Available from: <http://www.ijaronline.com/text.asp?2010/1/4/274/76794>
131. Messori A, Damuzzo V, Agnoletto L, Leonardi L, Chiumente M, Mengato D. A model-independent method to determine restricted mean survival time in the analysis of survival curves. *SN Compr Clin Med* [Internet]. 2020 Jan 5;2(1):66–8. Available from: <http://link.springer.com/10.1007/s42399-019-00199-7>
132. Jain S, Coulter JA, Butterworth KT, Hounsell AR, McMahon SJ, Hyland WB, et al. Gold nanoparticle cellular uptake, toxicity and radio sensitisation in hypoxic conditions. *Radiother Oncol* [Internet]. 2014 Feb;110(2):342–7. Available from: <https://linkinghub.elsevier.com/retrieve/pii/S0167814013006592>

133. Huang H, Feng W, Chen Y, Shi J. Inorganic nanoparticles in clinical trials and translations. *Nano Today* [Internet]. 2020 Dec;35:100972. Available from: <https://linkinghub.elsevier.com/retrieve/pii/S1748013220301419>
134. Bobo D, Robinson KJ, Islam J, Thurecht KJ, Corrie SR. Nanoparticle-based medicines: A review of FDA-approved materials and clinical trials to date. *Pharm Res* [Internet]. 2016 Oct 14;33(10):2373–87. Available from: <http://link.springer.com/10.1007/s11095-016-1958-5>
135. Zhu M, Nie G, Meng H, Xia T, Nel A, Zhao Y. Physicochemical properties determine nanomaterial cellular uptake, transport, and fate. *Acc Chem Res* [Internet]. 2013 Mar 19;46(3):622–31. Available from: <https://pubs.acs.org/doi/10.1021/ar300031y>
136. Qiu Y, Liu Y, Wang L, Xu L, Bai R, Ji Y, et al. Surface chemistry and aspect ratio mediated cellular uptake of Au nanorods. *Biomaterials* [Internet]. 2010 Oct;31(30):7606–19. Available from: <https://linkinghub.elsevier.com/retrieve/pii/S0142961210008318>
137. Iversen T-G, Skotland T, Sandvig K. Endocytosis and intracellular transport of nanoparticles: Present knowledge and need for future studies. *Nano Today* [Internet]. 2011 Apr;6(2):176–85. Available from: <https://linkinghub.elsevier.com/retrieve/pii/S1748013211000181>
138. Lu J, Tang M, Zhang T. Review of toxicological effect of quantum dots on the liver. *J Appl Toxicol* [Internet]. 2019 Jan;39(1):72–86. Available from: <https://onlinelibrary.wiley.com/doi/10.1002/jat.3660>
139. Lin G, Chen T, Pan Y, Yang Z, Li L, Yong K, et al. Biodistribution and acute toxicity of cadmium-free quantum dots with different surface functional groups in mice following intratracheal inhalation. *Nanotheranostics* [Internet]. 2020;4(3):173–83. Available from: <http://www.ntno.org/v04p0173.htm>
140. Mu X, Wang J-Y, Bai X, Xu F, Liu H, Yang J, et al. Black phosphorus quantum dot induced oxidative stress and toxicity in living cells and mice. *ACS Appl Mater Interfaces* [Internet]. 2017 Jun 21;9(24):20399–409. Available from: <https://pubs.acs.org/doi/10.1021/acsami.7b02900>

Advantages and Disadvantages of Using Quantum Dots in Lateral Flow and Other Biological Assay Formats



John G. Bruno

Abstract The use of quantum dots in fluorescence assays has presented some unique advantages in terms of extreme fluorescence intensity, assay sensitivity, and multiplexing via different emission wavelengths (colors) based on the size of the quantum dots with a single ultraviolet or blue light source. However, quantum dots have also presented several key disadvantages in terms of structural and photonic stability, susceptibility to certain buffer compositions and possibly fats that may lead to blinking or complete loss of fluorescence some assay matrices. The loss of fluorescence is perhaps due to stripping of the ZnS or other coating materials which then prevent photon capture and re-emission. In this review, we explore the advantages and disadvantages of using quantum dots including toxicity and toxicity management in various assay formats with some real world examples from the author's own research and the work of others.

Keywords Autofluorescence · Carbon dots · Electrochemiluminescence · Giant quantum dots · Multiplex · Stoke's shift

1 Introduction

As with any useful technology, quantum dots have some very worthwhile advantages, but also some significant limitations. The discovery of semiconductor quantum dots is attributed to both Ekimov in glass matrices and Brus in colloidal solutions in the early 1980s. Quantum dots were initially studied and developed for their unique physical properties of exceptional fluorescence intensity due to narrow wavelength emission ranges, very long Stoke's shifts from the ultraviolet (UV) or blue excitation range to green, yellow or even red emissions and multiple colored emissions based on quantum dot diameter (2–10 nm). These properties made quantum dots of use in solar cells, TV screens, lasers, LEDs, and quantum computing, but some of these same traits were not exploited for biological applications in diagnostics until the

J. G. Bruno (✉)

Department of Biotechnology, Nanohmics Inc., 6201 E. Oltorf Street, Austin, TX, USA

e-mail: jbruno@nanohmics.com

early 2000s [1–4]. The need for ultrasensitive and multiplexed assays drove the initial biological applications of quantum dots and continues to drive quantum dot biological applications today [5, 6].

Although most types of quantum dots are composed of toxic metallic amalgams such as cadmium and selenium (Cd/Se) with zinc sulfide (Zn/S) or other shell coating materials to achieve 3-dimensional quantum confinement of incoming photons. Quantum dots can be relatively bio-compatible with the proper shell materials and therefore used for very sensitive intracellular and in vivo tracking of various targets [7–10]. In this mini-review, the author will discuss the pros and cons of quantum dots such as the aforementioned intracellular and in vivo imaging considerations for use in various diagnostic formats.

2 Quantum Dot Use in Biological and Diagnostic Assays

Due to their already documented highly fluorescent and multi-colored fluorescence emissions from a single UV or blue excitation source, quantum dots have been adopted in virtually all assays or diagnostics in which fluorescence is already used with conventional fluorescent dyes and latex or other fluorescent nanoparticles. To be more specific, quantum dots have already found applications in: immunocytochemical and immunohistochemical staining of cells and tissues [11], flow cytometry [12–16], lateral flow (LF) or immunochromatographic (IC) test strips [17–33], fluorescence resonance energy transfer (FRET) assays [34–38], Western or other forms of blotting [39–43], etc.

2.1 Advantages of Quantum Dots

2.1.1 Ultrasensitivity

As already mentioned, quantum dots exhibit extreme fluorescence intensity or brightness which has led to ultrasensitive immunological or DNA aptamer-based assays capable of detecting between one and ten bacterial cells [44–46] or one to a few hundred viral particles [47–49] or specific single molecules within cells [50] due to the very high fluorescence signal-to-noise ratios (SNRs).

While extreme sensitivity is often unnecessary for detection of many target analytes, there are instances where the user or government regulators require or desire ultrasensitivity. For example, in the food safety testing industry, there is a policy of “zero tolerance” for foodborne pathogens such as Shiga toxin-producing *E. coli* (STEC) serotypes, *Listeria* and *Salmonella* bacteria, meaning that if even one colony of these bacteria can be detected after enrichment culture, the food from which it came, must be rejected. This extreme level of sensitivity is not driven by infectious dose values. Indeed, one pathogenic bacterium is quite unlikely to induce

disease, but the testing industry exerts extreme caution to avoid costly food recalls, potential human illness, and bankruptcy for the food producer.

Quantum dots have been demonstrated to increase the sensitivity of most assays at least tenfold. A prime example of this can be seen in the author’s own work in which an *E. coli* lateral flow test strip assay had a limit of detection (LOD) of about 3000 *E. coli* cells per sample was shown to clearly increase its sensitivity to 300 *E. coli* cells per test as illustrated in Fig. 1 [17].

Another infectious disease diagnostic area that could really benefit from ultrasensitivity is that of rapid viral testing. In recent times, the public has become acutely aware that testing for pandemic viruses such as SARS-CoV-2, its variants or potentially pandemic strains of influenza A or B is broken into two types of tests: (1) polymerase chain reaction (PCR) or reverse transcriptase (RT)-PCR-based nucleic acid (DNA or RNA) tests that are ultrasensitive, but generally require more time for detection and can suffer from some false positives, if too many rounds of PCR amplification are used and (2) rapid (~15 min) LF test strips such as the well-known Abbott Laboratories’ BinaxNOW™ colloidal gold LF tests which exhibit much lower sensitivity than PCR-based tests, but can be conducted on site to enable businesses,

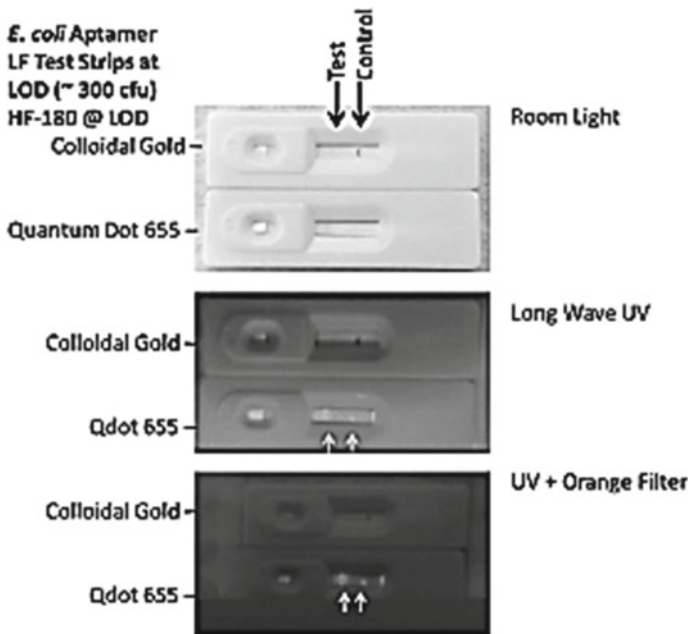


Fig. 1 Author’s demonstration that an aptamer-based *E. coli* LF test strip assay which had exhibited an LOD of 3000 cells per test when colloidal gold was used as the reporter tag, improved to 300 cells (ten-fold increase) when red Qdot 655 tags from Invitrogen were used on the reporter aptamer as shown in this side-by-side comparison with and without ultraviolet (UV) excitation and an orange emission filter. Reproduced from Ref. [17], licensed under an open access Creative Commons CC BY 4.0 license

schools, restaurants, and other public venues to remain open during a pandemic by testing individuals at building entrances. Unfortunately, the lateral flow tests are not being used as widely as they could be due to their lower sensitivity.

Ideally, one would like to combine the sensitivity of PCR-based diagnostic technologies with the speed, convenience, and portability of LF test strips. Companies such as Quidel have taken steps toward improving LF test strip sensitivity in their Sophia[®] line of products that utilize fluorescent nanoparticles to enhance detection of viruses versus colloidal gold. Most recently, Ellume Corporation from Brisbane, Australia in conjunction with Qiagen has begun to market an LF test strip for SARS-CoV-2 which Ellume claims on their website to be 95–96% as sensitive and accurate as the major COVID-19 RT-PCR tests, because they use quantum dots as their fluorescent tags.

In the author's own research and development of an influenza A/B LF test strip (funded by the Centers for Disease Control; CDC contract no. 75D30119P05866), the use of red-emitting quantum dots (Qdot 655 from Invitrogen to avoid blue-green autofluorescence from clinical oral or nasopharyngeal samples) which were covalently attached to reporter antibodies from HyTest (Finland), yielded ultrasensitive detection of various influenza viruses to levels of 0.1 hemagglutination (HA) units, comparable to the Quidel Sofia[®] or other published results by Wu et al. [51]. To maximize sensitivity in IC-based test strips, the author found that use of click chemistry kits from Invitrogen were quite useful, because click chemistry ensures covalent bonding of quantum dots to the heavy chain terminal sugars of IgG or other antibodies, thereby preventing potential binding of the antibody's hypervariable antigen binding sites to the quantum dots which would sterically hinder or completely block virus binding to antibodies [52].

When designing an assay for a small molecule target analyte having only one epitope per target, which disallows a sandwich assay, competitive displacement may be the only LF test strip option. Also in the case of competitive displacement assays, achievement of high sensitivity may be nearly impossible due to the nature of the affinity or equilibrium constants which resist displacement of the fluorescently tagged target bound to the capture antibody line. In such cases, relatively high concentrations of the target analyte is required to compete or "push" the fluorescently tagged target off of the capture antibody line, thus severely limiting sensitivity. However, by using quantum dots, the assay developer is able to achieve higher sensitivity, because higher initial fluorescence intensity or brightness levels give a greater dynamic range of detection and small changes in brightness are more noticeable. Such was the case in the author's own National Oceanic and Atmospheric Administration (NOAA)-funded grant (NA20OAR0210085) for saxitoxin (Stx)-red quantum dot-based LF competitive displacement test strip development which achieved an LOD of 0.5–1 parts per billion (ppb or ng/ml) sensitivity as illustrated in Fig. 2 [53].

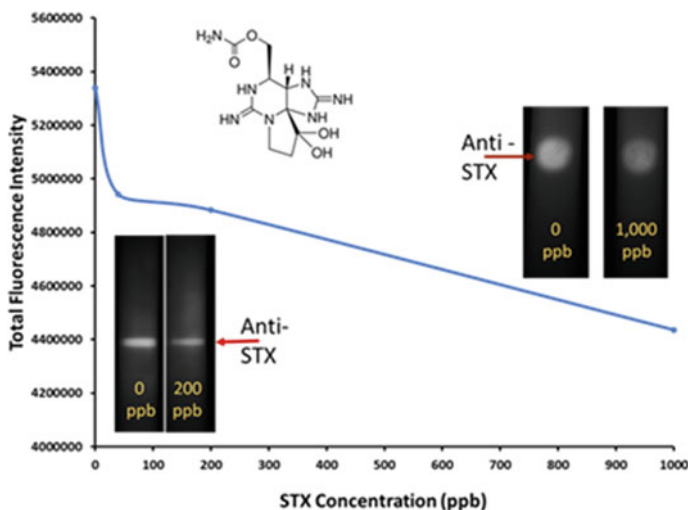


Fig. 2 Competitive fluorescence dipstick assay format in which free saxitoxin (Stx) molecules from the sample can competitively displace red saxitoxin-quantum dot 655 conjugates pre-loaded onto an antibody capture line to quantitatively diminish fluorescence as a function of increasing saxitoxin concentration. The optimized assay demonstrated a LOD between 0.5 and 1 part per billion (ppb or ng/ml) with a dynamic range up to 20,000 ppb. Reproduced with permission from Ref. [53]. Copyright © 2020 American Scientific Publishers

2.1.2 Electrochemiluminescence (ECL); Alternative Excitation Method for Ultrasensitivity

An alternative electrical excitation method for some types of quantum dots that further suppresses optical background is electroluminescence (EL) as in some TV screens or electrochemiluminescence (ECL), because excitation occurs due to electrical stimulation instead of photonic excitation, thus keeping background at nearly zero (i.e., a completely black background) with very high SNR when ECL is induced electrically. Indeed, Cao et al. [6] have demonstrated sensitivity of Cd/Se or Cd/S core Zn/S-coated quantum dots that is a million times greater by ECL than by fluorescence excitation.

2.1.3 Multiplexing/Multi-colored Emissions

One of the other key advantages of quantum dots is their ability to emit several fluorescent colors across the visible spectrum from blue to red and even into the near infrared based on size of the quantum dots in the range from 2 to 10 nm with a single excitation source in the ultraviolet or blue range. With conventional fluorescent dyes having very narrow Stoke's shifts, several different excitation sources

with wavelengths close to the dye's emission maximum are required, thus complicating multiplexed fluorescence optical systems that need several different excitation sources operating at different wavelengths. The single light source for quantum dots with multiple emission colors property of quantum dots is enabled by the extremely long Stoke's shifts of various sized quantum dots (e.g., excitation in the UV at ~300 nm with red emission at >600 nm). And discrimination of different quantum dots and analytes or cell populations is further enabled by the very narrow emission peaks of quantum dots (10–15 nm wide peaks) that clearly discriminate different colors with little or no emission spectrum overlap between various colored quantum dots. Perhaps nowhere is the property of a single light source with multiple colored emissions more valuable than in fluorescence microscopy and flow cytometry where the ability to excite in the UV or blue region and detect several different cell types simultaneously based on different colored emissions from green to red because this property can cut complexity and costs for assays and instrumentation [12–16, 54, 55].

2.2 Disadvantages of Quantum Dots and Remedies

2.2.1 Blinking and Loss of Fluorescence

From the beginning of quantum dot usage in the biosciences, it was noticed that quantum dots exhibited fluorescence “blinking” in which fluorescence emission levels appeared to fluctuate rapidly in some cases. Of course for biological assays, one wishes to have steady fluorescence levels against which to make accurate comparisons of target analyte fluorescence levels as a function of analyte concentration. And in the author's own work, red shifting [4] and complete loss of quantum dot fluorescence in some fatty food matrices [44, 56] presented unacceptable problems. In both blinking and red shifting or complete loss of fluorescence, the culprit was suspected to be the shell, because thin or absent coatings would limit or prevent quantum confinement, thus inhibiting or eliminating fluorescence emissions. In the author's case, fatty food matrices appeared to dissolve the shell and lead to a total loss of fluorescence [56]. The solution to this problem was to make the Zn/S or other shell thicker and more robust. Dr. Jennifer Hollingsworth's group at Los Alamos National Laboratory solved this problem by developing much thicker shells surrounding their “giant” quantum dots [57–64].

It has also been noted that long-term storage of quantum dots even in a refrigerator in some common physiologic buffers such as phosphate buffered saline (PBS at pH 7.2–7.4) can lead to a loss of fluorescence over time. Manufacturers such as Invitrogen deliver their quantum dots in 50 mM borate buffer at pH 8.2 and recommend storage in the same buffer. So clearly, researchers need to be aware and conscious of potential buffer effects on quantum dots and to examine the effects of any new buffers on quantum dot fluorescence over time.

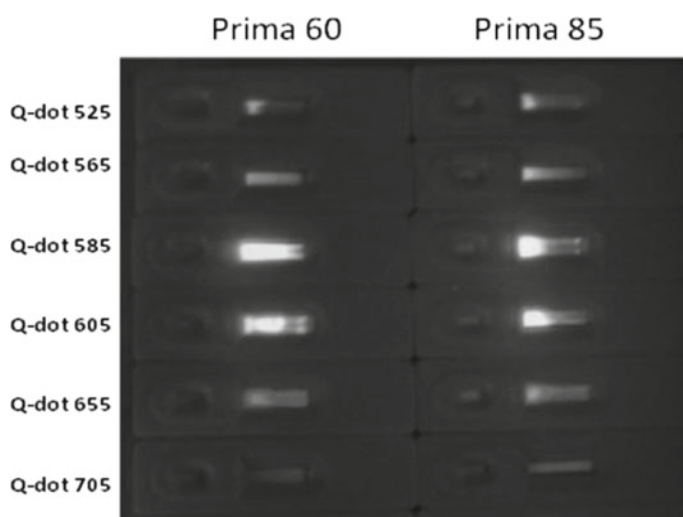


Fig. 3 Illustration of various types of quantum dot clumping and poor mobility problems in even the fastest (Prima 60 and 85 s transit time) lateral flow test strips in the absence of high levels of detergents such as 5% Tween 20 from Refs. [17, 29, 65]. Reproduced from Ref. [17] under an open access Creative Common CC BY license

A final problem that can occur with quantum dots is aggregation or clumping of the quantum dots either in their conjugated or unconjugated states which will undoubtedly impede wicking even in faster or more porous analytical membranes such as Prima 60 or 85 s transit membranes and performance of quantum dots in LF test strips as shown in Fig. 3 [17].

In order to prevent such clumping, Berlina et al. [29, 65] recommended a ridiculously high level 5% Tween 20 detergent in the dried antibody-quantum dot reporter complex in the conjugate pad of LF test strips and perhaps even in the assay running buffer. Such a high level of detergent may form micelles around the reporter complexes to prevent aggregation. It may not need to be as high as 5% in all cases, but in the author's experience 5% Tween 20 will almost always prevent quantum dot clumping if used in the conjugate pad and running buffer [17, 29, 65].

2.2.2 Quantum Dot Toxicity and Management

Various types of quantum dots can be quite toxic to human and other animal life especially those containing cadmium ions including cadmium selenide (CdSe), cadmium telluride (CdTe), indium phosphide (InP), zinc selenide (Zn/Se), lead sulfide (PbS), etc., which can leach toxic ions into the environment and ground water [66, 67]. The daily intake limit of cadmium established by the Agency for Toxic Substances and Disease Registry (ATSDR) is a mere 200 ng per kg per day based on its renal toxicity suggesting that most quantum test strips or other quantum dot assays should not be

discarded carelessly, but rather collected and disposed of in compliance with EPA standards for hazardous materials.

One general solution for quantum dot toxicity may be the use of newer and much less cytotoxic fluorescent carbon (graphene) quantum dots or simply “carbon dots.” Outside of photo-induced cytotoxicity, carbon dots appear to be well tolerated by cells at relatively high concentrations [68]. Not only are carbon dots relatively nontoxic, but they are highly fluorescent and also exhibit multiple fluorescent colored emissions that are based on the amount of oxygen-containing “defects” in the dots instead of size-dependence as with traditional metallic quantum dots. The more oxidized defects in carbon dots, the more reddish the fluorescence emissions [69–71].

3 Discussion

This article has outlined the primary advantages and disadvantages of using quantum dots in biological fluorescence assays, especially those involving lateral flow test strip formats. Among the main advantages of using quantum dots are ultrasensitivity and a broad dynamic range due to the very intense brightness of quantum dots that aid both sandwich and competitive displacement LF assays. Simultaneous multiplexed discrimination of various analytes also provides quantum dots with a key advantage in that multiple colored emissions are possible due to very long Stoke’s shifts in all types of quantum dots with a single light source in the ultraviolet or blue region to simplify optical instrument designs for fluorescence microscopic and flow cytometric applications.

Disadvantages of using quantum dots in biological assays include blinking and loss of fluorescence if the shell is damaged or lost. However, the use of thicker coatings on giant quantum dots can avoid blinking and loss of fluorescence. Aggregation into visible clumps will also lead to loss of quantum dot utility in LF test strips which cannot transit the analytical membrane by wicking easily and would precipitate in other types of tube assays. The solution to this dilemma is to add less than or equal to 5% Tween 20 or high levels of other detergents to the conjugate pads and running buffers [17, 29, 65].

4 Conclusions

While the knowledge of quantum dot advantages and disadvantages in biological assays is available in the open literature, it is obscure in some cases such as the solutions to clumping issues. Thus, it was the author’s intention to bring together this knowledge of quantum dot pros, cons, and pragmatic application tips in one concise article which hopefully this article has accomplished.

Acknowledgements Some of the data shown in this article was funded by the following U.S. Small Business Innovative Research (SBIR) grants or contracts: Centers for Disease Control (CDC) SBIR Contract No. 75D30119P05866 and National Oceanic and Atmospheric Administration (NOAA) SBIR Grant No. NA20OAR0210085.

References

1. Tan CY, Liang RQ, Ruan KC. Application of quantum dot to life science. *Sheng Wu Hua Xue Yu Sheng Wu Wu Li Xue Bao Acta Biochim Biophys Sin.* 2002;34(1):1–5.
2. Kaul Z, Yaguchi T, Kaul SC, Hirano T, Wadhwa R, Taira K. Mortalin imaging in normal and cancer cells with quantum dot immuno-conjugates. *Cell Res.* 2003;13(6):503–7.
3. Lim YT, Kim S, Nakayama A, Stott NE, Bawendi MG, Frangioni JV. Selection of quantum dot wavelengths for biomedical assays and imaging. *Mol Imaging.* 2003;2(1):50–64.
4. Dwarakanath S, Bruno JG, Shastry A, Phillips T, John AA, Kumar A, et al. Quantum dot-antibody and aptamer conjugates shift fluorescence upon binding bacteria. *Biochem Biophys Res Commun.* 2004;325(3):739–43.
5. Bai Z, Wei H, Yang X, Zhu Y, Peng Y, Yang J, et al. Rapid enrichment and ultrasensitive detection of influenza A virus in human specimen using magnetic quantum dot nanobeads based test strips. *Sens Actuators B Chem.* 2020;325:128780.
6. Cao Z, Shu Y, Qin H, Su B, Peng X. Quantum dots with highly efficient, stable, and multicolor electrochemiluminescence. *ACS Cent Sci.* 2020;6(7):1129–37.
7. Kosaka N, Mitsunaga M, Choyke PL, Kobayashi H. In vivo real-time lymphatic draining using quantum-dot optical imaging in mice. *Contrast Media Mol Imaging.* 2013;8(1):96–100.
8. Li Y, Li Z, Wang X, Liu F, Cheng Y, Zhang B, et al. In vivo cancer targeting and imaging-guided surgery with near infrared-emitting quantum dot bioconjugates. *Theranostics.* 2012;2(8):769–76.
9. Yaghini E, Turner H, Pilling A, Naasani I, MacRobert AJ. In vivo biodistribution and toxicology studies of cadmium-free indium-based quantum dot nanoparticles in a rat model. *Nanomed Nanotechnol Biol Med.* 2018;14(8):2644–55.
10. Zhu Y, Hong H, Xu ZP, Li Z, Cai W. Quantum dot-based nanoprobes for in vivo targeted imaging. *Curr Mol Med.* 2013;13(10):1549–67.
11. Caldwell ML, Moffitt RA, Liu J, Parry RM, Sharma Y, Wang MD. Simple quantification of multiplexed quantum dot staining in clinical tissue samples. In: Annual international conference of the IEEE engineering in medicine and biology society IEEE engineering in medicine and biology society annual international conference 2008; 2008. p. 1907–10.
12. Chattopadhyay PK. Quantum dot technology in flow cytometry. *Methods Cell Biol.* 2011;102:463–77.
13. Chattopadhyay PK, Perfetto SP, Yu J, Roederer M. The use of quantum dot nanocrystals in multicolor flow cytometry. *Wiley Interdisc Rev Nanomed Nanobiotechnol.* 2010;2(4):334–48.
14. Mittal R, Bruchez MP. Calibration of flow cytometry for quantitative quantum dot measurements. *Curr Protoc Cytom.* 2009;49(1):6–26 (Chapter 6: Unit 6.26).
15. Smith RA, Giorgio TD. Quantitative measurement of multifunctional quantum dot binding to cellular targets using flow cytometry. *Cytom Part A J Int Soc Anal Cytol.* 2009;75(5):465–74.
16. Wu Y, Campos SK, Lopez GP, Ozbun MA, Sklar LA, Buranda T. The development of quantum dot calibration beads and quantitative multicolor bioassays in flow cytometry and microscopy. *Anal Biochem.* 2007;364(2):180–92.
17. Bruno JG. Application of DNA aptamers and quantum dots to lateral flow test strips for detection of foodborne pathogens with improved sensitivity versus colloidal gold. *Pathogens.* 2014;3(2):341–55.

18. Frohnmeyer E, Tuschel N, Sitz T, Hermann C, Dahl GT, Schulz F, et al. Aptamer lateral flow assays for rapid and sensitive detection of cholera toxin. *Analyst*. 2019;144(5):1840–9.
19. Bruno JG, Richarte A. Aptamer-quantum dot lateral flow test strip development for rapid and sensitive detection of pathogenic *E. coli* via intimin, O157-specific LPS and Shiga toxin 1 aptamers. *Curr BioNanotechnol*. 2015;1(2):80–6.
20. Gui C, Wang K, Li C, Dai X, Cui D. A CCD-based reader combined with CdS quantum dot-labeled lateral flow strips for ultrasensitive quantitative detection of CagA. *Nanoscale Res Lett*. 2014;9(1):57.
21. Yan X, Wang K, Lu W, Qin W, Cui D, He J. CdSe/ZnS quantum dot-labeled lateral flow strips for rapid and quantitative detection of gastric cancer carbohydrate antigen 72–4. *Nanoscale Res Lett*. 2016;11(1):138.
22. Meng HM, Chen J, Qu L, Li Z. Detection of tetanus antibody applying a Cu–Zn–In–S/ZnS quantum dot-based lateral flow immunoassay. *Methods Mol Biol*. 2020;2135:285–92.
23. Bruno JG, Sivils JC. Development and selection of specific listeria monocytogenes p60 aptamers for quantum dot-based lateral flow test strips. *J Bionanosci*. 2017;11(6):567–72.
24. Chen Y, Fu Q, Xie J, Wang H, Tang Y. Development of a high sensitivity quantum dot-based fluorescent quenching lateral flow assay for the detection of zearalenone. *Anal Bioanal Chem*. 2019;411(10):2169–75.
25. Bruno J. Evaluation of pathogenic big 7 *E. coli* aptamer-quantum dot lateral flow test strips. *J Bionanosci*. 2017;11(2):148–52.
26. Li X, Lu D, Sheng Z, Chen K, Guo X, Jin M, et al. A fast and sensitive immunoassay of avian influenza virus based on label-free quantum dot probe and lateral flow test strip. *Talanta*. 2012;100:1–6.
27. Wang C, Shen W, Rong Z, Liu X, Gu B, Xiao R, et al. Layer-by-layer assembly of magnetic-core dual quantum dot-shell nanocomposites for fluorescence lateral flow detection of bacteria. *Nanoscale*. 2020;12(2):795–807.
28. Wu R, Zhou S, Chen T, Li J, Shen H, Chai Y, et al. Quantitative and rapid detection of C-reactive protein using quantum dot-based lateral flow test strip. *Anal Chim Acta*. 2018;1008:1–7.
29. Berlina AN, Taranova NA, Zherdev AV, Vengerov YY, Dzantiev BB. Quantum dot-based lateral flow immunoassay for detection of chloramphenicol in milk. *Anal Bioanal Chem*. 2013;405(14):4997–5000.
30. Liang ZY, Deng YQ, Tao ZZ. A quantum dot-based lateral flow immunoassay for the rapid, quantitative, and sensitive detection of specific IgE for mite allergens in sera from patients with allergic rhinitis. *Anal Bioanal Chem*. 2020;412(8):1785–94.
31. Savin M, Mihailescu CM, Matei I, Stan D, Moldovan CA, Ion M, et al. A quantum dot-based lateral flow immunoassay for the sensitive detection of human heart fatty acid binding protein (hFABP) in human serum. *Talanta*. 2018;178:910–5.
32. Zhao Y, Zhang Q, Meng Q, Wu F, Zhang L, Tang Y, et al. Quantum dots-based lateral flow immunoassay combined with image analysis for semiquantitative detection of IgE antibody to mite. *Int J Nanomed*. 2017;12:4805–12.
33. Wang S, Liu Y, Jiao S, Zhao Y, Guo Y, Wang M, et al. Quantum-dot-based lateral flow immunoassay for detection of neonicotinoid residues in tea leaves. *J Agric Food Chem*. 2017;65(46):10107–14.
34. Bhuckory S, Lefebvre O, Qiu X, Wegner KD, Hildebrandt N. Evaluating quantum dot performance in homogeneous FRET immunoassays for prostate specific antigen. *Sensors*. 2016;16(2):197.
35. Goryacheva OA, Beloglazova NV, Vostrikova AM, Pozharov MV, Sobolev AM, Goryacheva IY. Lanthanide-to-quantum dot forster resonance energy transfer (FRET): application for immunoassay. *Talanta*. 2017;164:377–85.
36. Ma Y, Zhang H, Liu F, Wu Z, Lu S, Jin Q, et al. Highly sensitive detection of DNA methylation levels by using a quantum dot-based FRET method. *Nanoscale*. 2015;7(41):17547–55.
37. Mattera L, Bhuckory S, Wegner KD, Qiu X, Agnese F, Lincheneau C, et al. Compact quantum dot-antibody conjugates for FRET immunoassays with subnanomolar detection limits. *Nanoscale*. 2016;8(21):11275–83.

38. Wu YT, Qiu X, Lindbo S, Susumu K, Medintz IL, Hober S, et al. Quantum dot-based FRET immunoassay for HER2 using ultrasmall affinity proteins. *Small*. 2018;14(35):e1802266.
39. Bakalova R, Zhelev Z, Ohba H, Baba Y. Quantum dot-based western blot technology for ultrasensitive detection of tracer proteins. *J Am Chem Soc*. 2005;127(26):9328–9.
40. Chen W, Xu D, Liu L, Peng C, Zhu Y, Ma W, et al. Ultrasensitive detection of trace protein by Western blot based on POLY-quantum dot probes. *Anal Chem*. 2009;81(21):9194–8.
41. Gilroy KL, Cumming SA, Pitt AR. A simple, sensitive and selective quantum-dot-based western blot method for the simultaneous detection of multiple targets from cell lysates. *Anal Bioanal Chem*. 2010;398(1):547–54.
42. Makrides SC, Gasbarro C, Bello JM. Bioconjugation of quantum dot luminescent probes for Western blot analysis. *Biotechniques*. 2005;39(4):501–6.
43. Scholl B, Liu HY, Long BR, McCarty OJ, O'Hare T, Druker BJ, et al. Single particle quantum dot imaging achieves ultrasensitive detection capabilities for Western immunoblot analysis. *ACS Nano*. 2009;3(6):1318–28.
44. Bruno JG, Phillips T, Carrillo MP, Crowell R. Plastic-adherent DNA aptamer-magnetic bead and quantum dot sandwich assay for *Campylobacter* detection. *J Fluoresc*. 2009;19(3):427–35.
45. Bruno JG, Phillips T, Montez T, Garcia A, Sivils JC, Mayo MW, et al. Development of a fluorescent enzyme-linked DNA aptamer-magnetic bead sandwich assay and portable fluorometer for sensitive and rapid listeria detection. *J Fluoresc*. 2015;25(1):173–83.
46. Chalmers NI, Palmer RJ Jr, Du-Thumm L, Sullivan R, Shi W, Kolenbrander PE. Use of quantum dot luminescent probes to achieve single-cell resolution of human oral bacteria in biofilms. *Appl Environ Microbiol*. 2007;73(2):630–6.
47. Bruno JG, Francis K, Ikanovic M, Rao P, Dwarakanath S, Rudzinski WE. Reovirus detection using immunomagnetic-fluorescent nanoparticle sandwich assays. *J Bionanosci*. 2007;1(2):84–9.
48. Herod MR, Pineda RG, Mautner V, Onion D. Quantum dot labelling of adenovirus allows highly sensitive single cell flow and imaging cytometry. *Small*. 2015;11(7):797–803.
49. Hou W, Li Y, Kang W, Wang X, Wu X, Wang S, et al. Real-time analysis of quantum dot labeled single porcine epidemic diarrhea virus moving along the microtubules using single particle tracking. *Sci Rep*. 2019;9(1):1307.
50. Ishihama Y, Funatsu T. Single molecule tracking of quantum dot-labeled mRNAs in a cell nucleus. *Biochem Biophys Res Commun*. 2009;381(1):33–8.
51. Wu F, et al. Ultra sensitive detection of influenza A virus based on Cdse/Zns quantum dots immunoassay. *SOJ Biochem*. 2016;2(3):6.
52. Bruno JG. Antibody specificity can be altered by nonspecific quantum dot conjugation chemistries, but preserved by click chemistry attachment to heavy chain saccharides. *J Bionanosci*. 2018;12(2):206–10.
53. Bruno JG, John J. Preliminary development of a competitive fluorescent quantum dot-based immunochromatographic test strip for sensitive saxitoxin detection. *Sens Lett*. 2020;18:459–63.
54. Kerman K, Endo T, Tsukamoto M, Chikae M, Takamura Y, Tamiya E. Quantum dot-based immunosensor for the detection of prostate-specific antigen using fluorescence microscopy. *Talanta*. 2007;71(4):1494–9.
55. Robelek R, Niu L, Schmid EL, Knoll W. Multiplexed hybridization detection of quantum dot-conjugated DNA sequences using surface plasmon enhanced fluorescence microscopy and spectrometry. *Anal Chem*. 2004;76(20):6160–5.
56. Bruno JG, Sivils JC, Phillips T. Aptamer-magnetic bead quantum dot sandwich assays for foodborne pathogen detection: pros, cons, and lessons learned. *J AOAC Int*. 2017;100(4):895–9.
57. Chen Y, Vela J, Htoon H, Casson JL, Werder DJ, Bussian DA, et al. “Giant” multishell CdSe nanocrystal quantum dots with suppressed blinking. *J Am Chem Soc*. 2008;130(15):5026–7.
58. Dennis AM, Mangum BD, Piryatinski A, Park YS, Hannah DC, Casson JL, et al. Suppressed blinking and Auger recombination in near-infrared type-II InP/CdS nanocrystal quantum dots. *Nano Lett*. 2012;12(11):5545–51.
59. DeVore MS, Stich DG, Keller AM, Ghosh Y, Goodwin PM, Phipps ME, et al. Three dimensional time-gated tracking of non-blinking quantum dots in live cells. *Proc SPIE Int Soc Opt Eng*. 2015;9338.

60. Hanson CJ, Hartmann NF, Singh A, Ma X, DeBenedetti WJI, Casson JL, et al. Giant PbSe/CdSe/CdSe quantum dots: crystal-structure-defined ultrastable near-infrared photoluminescence from single nanocrystals. *J Am Chem Soc.* 2017;139(32):11081–8.
61. Hollingsworth JA, Vela J, Chen Y, Htoon H, Klimov VI, Casson AR. ‘Giant’ multishell CdSe nanocrystal quantum dots with suppressed blinking: novel fluorescent probes for real-time detection of single-molecule events. *Proc SPIE Int Soc Opt Eng.* 2009;7189:718904.
62. Keller AM, Ghosh Y, DeVore MS, Phipps ME, Stewart MH, Wilson BS, et al. 3-Dimensional tracking of non-blinking “giant” quantum dots in live cells. *Adv Func Mater.* 2014;24(30):4796–803.
63. Kundu J, Ghosh Y, Dennis AM, Htoon H, Hollingsworth JA. Giant nanocrystal quantum dots: stable down-conversion phosphors that exploit a large stokes shift and efficient shell-to-core energy relaxation. *Nano Lett.* 2012;12(6):3031–7.
64. Vela J, Htoon H, Chen Y, Park YS, Ghosh Y, Goodwin PM, et al. Effect of shell thickness and composition on blinking suppression and the blinking mechanism in “giant” CdSe/CdS nanocrystal quantum dots. *J Biophotonics.* 2010;3(10–11):706–17.
65. Berlina AN, Taranova NA, Zherdev AV, Sankov MN, Andreev IV, Martynov AI, et al. Quantum-dot-based immunochromatographic assay for total IgE in human serum. *PLoS ONE.* 2013;8(10):e77485.
66. Rafati Rahimzadeh M, Rafati Rahimzadeh M, Kazemi S, Moghadamnia AA. Cadmium toxicity and treatment: an update. *Casp J Intern Med.* 2017;8(3):135–45.
67. Winnik FM, Maysinger D. Quantum dot cytotoxicity and ways to reduce it. *Acc Chem Res.* 2013;46(3):672–80.
68. Esfandiari N, Bagheri Z, Ehtesabi H, Fatahi Z, Tavana H, Latifi H. Effect of carbonization degree of carbon dots on cytotoxicity and photo-induced toxicity to cells. *Heliyon.* 2019;5(12):e02940.
69. Nguyen HA, Srivastava I, Pan D, Gruebele M. Unraveling the fluorescence mechanism of carbon dots with sub-single-particle resolution. *ACS Nano.* 2020;14(5):6127–37.
70. Wang Y, Zhu Y, Yu S, Jiang C. Fluorescent carbon dots: rational synthesis, tunable optical properties and analytical applications. *RSC Adv.* 2017;7(65):40973–89.
71. Yan F, Sun Z, Zhang H, Sun X, Jiang Y, Bai Z. The fluorescence mechanism of carbon dots, and methods for tuning their emission color: a review. *Microchim Acta.* 2019;186(8):583.

Recent Developments in Quantum Dots Technologies as Effective Theranostic Tools Against Cancer



Aniket Mukherjee and Nandini Sarkar

Abstract Cancer, being a condition of unhindered cell growth ultimately leading to the death of the patient, is very prominent in modern society. Despite all the colloquial therapies to stop or prevent or cure cancer, it's not curable to a full extent. These colloquial therapies used in the treatment of cancer involve chemotherapy, radiation therapy, etc., leading to very prominent side effects and more often than not, the recurrence of the disease. Thus, the need for an alternative to the treatment of cancer is of utmost and urgent requirement; in lieu of this fact, the quantum dots, which are semiconductor nanocrystals in the range of 1–10 nm are employed as a complete theranostic tool for the same. Recent progress in the quantum dots technology allows us to both image and kill cancer cells with high target specificity and minimum or no side effects. Various organic, as well as inorganic quantum dots, are being employed to cure cancer as it is or in conjugation with various biomarkers like peptides, transferrin, folic acid, etc. to increase target specificity and minimize side effects. Though a lot of research review, have been written over the past few years in the last decade, in this review we will be focusing on certain types of cancers and the treatments generally employed and their drawbacks, and the development with the current status of the quantum dots technology in the treatment of cancer and its drawbacks like cytotoxicity.

Keywords Cancer · Quantum dots · Transferrin · Folic acid · Theranostic

1 Introduction

Cancer is a specific condition of the human cells which directly affects the growth and multiplication of cells in such a manner that cells keep on multiplying without a stop phase which results in the tumor with the ability to affect the surrounding tissues. Now the problem is with cancer being one of the deadliest medical conditions worldwide in recent decades, with around 1,688,780 new cases and 600,920 cancer

A. Mukherjee · N. Sarkar (✉)

Department of Biotechnology and Medical Engineering, National Institute of Technology Rourkela, Rourkela, Odisha 769008, India
e-mail: sarkam@nitrkl.ac.in

deaths were projected for 2017. Over the next few years, the number of new cases is projected to increase by about 70%. GLOBOCAN has estimated about 12.7 million cases of cancer and 7.6 million deaths due to cancer to have occurred in 2008, out of which, 56% of the total cases and 64% of the cancer-related deaths have occurred in the economically developing world [1]. Thus we can draw a relation of the socio-economic status to the cancer occurrence. Over the past few decades, researchers have been studying cellular properties like cell adhesion, cytoskeletal dynamics etc. to understand the mechanism of cancer though all the studies were not very effective in determining a cure for cancer [2–4]; thus a complete treatment to cancer is yet to be determined. At present, cancer progression is considered to be cellular as well as tissue-driven process; it has been found that the cancer progression is pretty adaptive along the path of progression [5]. There is a tumor microenvironment which responds to the growing tumor cells, the surrounding components like endothelial cells, fibroblasts etc. secrete functional factors which may or may not help the growing tumor [6–8]. Thus, it can be concluded that tumor progression is controlled by the influences of the tumor microenvironment and its interaction with the tumor cells [9, 10]. Thus to understand the cancer mechanisms in order to determine the cure, the tumor biology is needed to be understood first.

Nanotechnology has been a boon so far to the human race; since its development, it has been used in various fields mainly in the electronics field. Well, for the past few decades, nanotechnology is finding its application in the biomedical field in various forms, for example, in the treatment of cancer as well as other incurable diseases like Parkinson [11], Alzheimer [12] etc. as well as for cancer the nanostics or both diagnostic as well as therapy. As the problem has been discussed, with cancer being one of the deadliest diseases, we need to find a cure as soon as possible. In the quest to do so, researchers have discovered quantum dots which are being effectively employed as tools for imaging and early detection of cancer. Both the organic as well as inorganic quantum dots are being extensively studied to find a way to diagnose cancer at a very early and treatable state due to their unique optical and electronic properties, which are predominantly the result of their size as well as to overcome the problems faced by the quantum dots like biocompatibility, low cytotoxicity etc. [13–19]. QDs are semiconductor nanocrystal whose electronic conductivity lies between the bulk and amorphous materials and have a size ranging from 2 to 10 nm in diameter and consisting of elements from groups II to VI or III to V in the periodic table [20]. Quantum dots are known to show higher advantages over the regular fluorescent dyes in the fields of a longer lifetime, higher resistance to photo bleaching as well as high fluorescent intensity [20]. Quantum dots, when conjugated with some biomolecular agents they can specifically target an organ inside the body in order to image or deliver drug. Not only for imaging, quantum dots are also used for the preparation of drugs as well as siRNA delivery systems [21]. Though with all the various functions of the quantum dots (inorganic), more often than not, these are highly cytotoxic resulting in harmful side effects. In this context, fluorescent carbon-based nanomaterials has drawn increasing attention in recent years owing to exceptional advantages such as high optical absorptivity, chemical stability, biocompatibility, and very low toxicity. Carbon dots or carbon quantum dots were first discovered by Xu et al. in the year

2004 [22] accidentally and since then extensive research are being carried out and successfully c-dots have been found to be applicable in fields of biomedical imaging [23, 24], sensor development [25] as well as electronics [26]. Due to ease with which carbon dots can cross blood brain barrier it's likely to be used for the treatment of brain cancer [27, 28]. Carbon dots are emerging as platform for attaching receptors as well as dugs which helps it to be target-specific causes minimal side effects to the surrounding cells. The main reasons for the emergence of carbon dots as primary theranostic tool against various ailments are its high biocompatibility, low cytotoxicity as well as ease of preparation thus essentially minimizing the requirement for complex processes and it is also cost-effective. C-dots are also found to provide more effective receptor binding affinity and better cell penetration [29]. Thus, carbon dots have been widely studied as it is as well as in conjugation with various other entities like Transferrin, Folic acid etc. as theranostic tool against cancer. A complete treatment for cancer would require public interventions, awareness etc., but for the time being the mortality rate can only be reduced by better and early detection of malignancy but target specific imaging, targeted therapy using nanotechnology thus significantly reducing the risk of death of healthy cells. Thus in this review paper, we will discuss certain types of cancer and the existing therapies of treating them along with the development of the quantum dots technology in imaging, detection and therapy of cancer.

2 Cancer: Selective Types and Properties

2.1 Breast Cancer

Typically, the breast cancer forms either in the lobules or in the ducts of the breast where lobules are present, the glands that produce milk, and ducts are the pathways that transport the milk from the glands to the nipple. Breast cancer may also occur in the fatty tissue or the fibrous connective tissue within the breast. TNBC or the Triple Negative Breast Cancer is responsible for 15% of the total cases in females. In a study performed by Sherri Sheinfeld Gorin et al., in the year 2006, it was reported that African American women experience the maximum delay in diagnosis of the breast cancer [30]. Lack of the Estrogen Receptor, Progesterone Receptor, and HER2, increases difficulty to diagnosing TNBC with a high relapse rate [31] (Tables 1 and 2). Metastasis makes the TNBC more fatal among the subtypes of breast cancer. In early stages, often the BC doesn't show any symptoms but generally, it's detected in a mammogram. Though, Human epidermal growth factor receptor 2 (HER2) is overexpressed in approximately 25–30% BC patients and has an important function in cancer progression. Recent studies have validated the value of HER2 detection for BC treatment and prognosis [42, 43]. With the advancement in the technologies and the fact that breast cancer is heterogeneous, scientist has evolved the diagnosing process by looking for morphological as well as immune histochemical changes of prognostic

Table 1 Selective examples of inorganic quantum dots, their modifications and functionality

Quantum dots	Modifier	Functionality	References
Zns capped CdSe	Peptide coating	In vivo targeting of lungs endothelium, brain endothelial cell, as well as breast cancer	[32]
CdTe	Silica coated	Biocompatibility on human embryonic kidney 293 cells (HEK293)	[33]
pH sensitive ZnO	Loaded with doxorubicin	Targeted drug delivery for lung cancer	[34]
CdTe/CdSe	RGD peptide conjugated, functionalized with Mercaptosuccinic Acid (MSA)	Target marker for human pancreatic carcinoma cell (SW1990)	[35]
CdSe/Fe ₂ O ₃ magnetic qd	Silica coated	Live cell imaging	[36]

Table 2 Selective examples of carbon nanoparticles, their modifications and functionality

Carbon Nanoparticles	Modifier	Functionality	References
c-dots	–	Optical in-vivo imaging	[37]
SWCNT	Folic acid conjugated and loaded with doxorubicin	Targeted drug delivery for cancer	[38]
MWCNT	Transferrin conjugated and loaded with docetaxel	Targeted drug delivery for lung cancer	[39]
c-dots	Folic acid conjugated	Targeted cellular imaging	[40]
c-dots	Folic acid conjugated and doxorubicin loaded	FA mediated targeted drug delivery	[41]
c-dots	Transferrin and doxorubicin conjugated	Targeted drug delivery into SJGBM2 cells (pediatric glioblastoma cells)	[28]

significance [44]. According to Decker et al., some of the important prognostic factors are lymph node status, tumor diameter and histological differentiation stage, NPI or the Nottingham Prognostic Index indexes some of the most vital prognostic factor thus delivering a reliable diagnosis [45].

2.2 Liver Cancer

Liver cancer or hepatocellular cancer (HCC), has grown to be the third most common cause for cancer related deaths, late diagnosis or even at times the absence of it is the major case for the above reason and the liver is the general metastasis site for

colorectal carcinoma [1, 46–48]. The available treatment options for HCC remain quite exquisite, with Sorafenib as the only prospective agent to have shown to increase overall survival [49]. Due to lack of any set of rules, it is best to serve the patient with a multidisciplinary approach as adopted by multiple consensus guidelines, including the National Comprehensive Cancer Network (NCCN) and the European Association for the Study of the Liver (EASL) [50–52]. Other methods, including surgical resection, have shown significant survival rates thus are being employed whenever feasible for both primary and secondary hepatocellular carcinoma [52, 53]. While comparing the five year survival rates or both surgical as well as for the people undergoing just chemotherapy for curative hepatectomy for colorectal metastases (CRM) it was seen that > 50% of the people survive in the medicinal group undergoing surgical resection, as compared to 15% in the other group [53, 54]. However, there is a very high chance of an unhealthy state of liver causing problems such as cirrhosis due to prolonged use of chemotherapy. As the HCC is increasing over the past two decades, methods of imaging have also been improved which include certain non-invasive or minimally invasive local treatments for both primary and metastatic liver tumors. Thus all in all we need better and more targeted localized therapies like quantum dots imaging in case of liver cancer to treat it with minimal damage to the surrounding cells in the liver area.

2.3 Gastric Cancer

Stomach cancer or gastric cancer is the fourth most common cause of cancer-related deaths [55–57]. Treatment of gastric cancer is significantly challenging, as most patients are diagnosed with the late stage of cancer, thus the requirement for early detection of gastric cancer is of utmost necessity. Early gastric cancer cells could be detected using multi-mode targeting techniques [33, 58–62]. As is known, there are very few clinical markers for the early detection, though in recent years carcinoembryonic antigen (CEA) is known to be primarily used as a biomarker to treat or diagnose early cancer [63, 64], though due to low sensitivity and specificity, CEA based detections are not always accurate and there is a need to find a different biomarker for the early detection and diagnosis of gastric cancer. A study of 2001 by Marelli et al., has presented in their article about gastric cancer-related antigen carbohydrate antigen 72-4 (CA72-4) showing higher sensitivity than CEA in early detection as well as recurrent cases of cancer [65]. Nowadays, in the last decade, Immuno-Chromatographic Test Strips (ICTS) is being prepared for early detection of cancer, which uses the antigen–antibody interaction to detect the quantity of both antigens as well as the antibody [66–68]. Similarly in another study in 2016, performed by Xinyu Yan et al., where they prepared CdSe/ZnS quantum dots to flow strips which have shown promising results in early detection of gastric cancer using the CA72-4 biomarker [69]. Among modern gastric cancer treatments, while in some treatments imaging and therapy is based on subcutaneous cancer models, even fewer numbers of therapies are based on in-situ gastric cancer models. By using invisible

NIR light and fluorescent quantum dots, a sensitive and real-time intra-operative SLN (sentinel lymph node) mapping of the gastrointestinal tract has also been done in a recent study [70]. Along with this, tumor and normal human colorectal tissues have also been successfully labeled using zinc oxide (ZnO) and zinc oxide (ZnO) with a coating of titanium oxide (TiO₂) core-shell QDs [71]. Next, in 2012, safe and effective nanoprobe for targeted imaging and selective therapy for in-situ gastric cancer was synthesized by Jing Ruan et al. [72]. They used one of a kind HER2 conjugated RNase-A-associated CdTe quantum dots cluster (HER2-RQD) which was synthesized by the method [73] elucidated by Kong Y. Chen et al., in the year 2010 and these clusters have proved to be an excellent therapeutic agent.

2.4 Lung Cancer

Lung cancer, also known as bronchogenic carcinoma, is among the top causes of fatalities by cancer-related deaths in South East Asia. Lung cancer contributes to 11.6% of all the recently diagnosed cancer cases and 18.4% of the total mortality rate as of 2018 [74]. This kind of cancer is very prevalent in third world countries which are yet not developed or are developing ones and the occurrence of this kind of cancer is related to the socio-economic condition of the population [75]. The two main types of lung cancer that can be identified histologically are the NSLC (non-small cell lung cancer), representing about 80% of the total cases, while the other type is SCLC (small cell lung cancer) representing about 20% of the total no of cases. It is also considered to be a heterogeneous disease clinically, histologically, biologically and molecularly. NSLC can be further divided into adenocarcinoma, squamous cell carcinoma, large cell carcinoma as well as the mixed histology's like adenosquamous carcinoma. And moreover lung adenocarcinoma is considered one of the best genetic characterizations of human malignancies. The primary cause for misdiagnosis or misidentification of the disease at an early stage is due to its symptoms being very similar to any chronic pulmonary disease [76]. The screening technique currently in clinical use is a low dose computed tomography (LDCT) [77]. However, the LDCT isn't a very efficient technique owing to the fact that it doesn't have any significant effect on the mortality rate [78]. In addition to its insignificant nature, the LDCT is having a high cost and an exposure risk to a high amount of radiation [50, 79–81]. Thus, there is a need for selective biomarkers that can detect malignancy at an early stage.

3 Nanoparticles Used in Cancer Therapy: Focus on Quantum Dots

Cancer is not a disease but a condition of exponential cell growth skipping the lag phase which causes lumps of cells, known as tumors which can either be malignant or benign, and depending on its nature, treatments are prescribed. Most of the existing cancer therapies involve intrusive method including the application of catheter to allow chemotherapy or surgical removal of the tumor, these procedures, however effective, causes damage to the surrounding healthy tissue or lifelong use of certain medicines which has harsh side effects. Several investigations and studies have shown that tissue, as well as cell distribution profiles of the anti-cancer drug, can be regulated by encapsulation of the former in submicronic colloid matrix (nanoparticles) [82]. Semiconductor nanocrystals systems or quantum dots which are governed by the quantum confinement effect constitutes a very important role in biological contrast agent for diagnosis via imaging, sensing of various biomarkers, as well as drug carriers [83]. The first-micron level particle employed in the treatment of cancer were liposomes, which are 30 nm to several microns in diameter, consisting of a lipid bilayer surrounding a water core hosting the drug. Certain kinds of nanoparticles as known as theranostic molecules, which can be used for both diagnostics and therapy simultaneously [84]. Pamujula et al., devised a biodegradable nanoparticle suitable for cellular delivery of chemotherapeutic drugs. They synthesized the PLGA using a modified solvent evaporation method. Since the past decade or so, magnetic nanoparticles are being used for contrast agents in MRI for local hyperthermia are now being employed as drug carriers to utilize their full potential. Magnetic nanoparticles can be placed or positioned inside the body by an external magnetic field, and can be used to invoke local hyperthermia by heating up the same by an external magnetic field. Magnetic nanoparticles are generally used in the superparamagnetic state for their application in the biomedical field. Some of the standard imaging techniques include Magneto acoustic technique (MAT) [85], Computed tomography (CT) [86], Magnetic resonance imaging (MRI) [87] and Near IR imaging (NIR) [88], out of which one of the most effective technique in early detection of cancer is the MRI and magnetic nanoparticles are being used as contrast agent [89]. This is the age for modern and much newer techniques to tackle the growing cancer fatalities, and for this, we require quantum dots that can specifically target the cancerous cells [34]. Quantum dots are semiconducting nanoparticles whose dimensions are within 10nm. Upon excitation in the UV-NIR region of the light spectrum, QDs of different sizes and materials emit a narrow tunable spectrum of light that is harnessed for the tumor imaging [90, 91]. Compared with organic dyes like rhodamine, these quantum dots are like 20 times brighter and 100 times more stable towards photo bleaching, are biocompatible (not all the QDs) and water soluble [92, 93]. Quantum dots or these fluorescent nanoparticles are a perfect fit for intravascular transportation as well as accumulation over various tumor beds [84]. Further, these quantum dots can be classified as organic, inorganic, and magnetic depending on their constituent elements.

3.1 *Inorganic Quantum Dots*

Inorganic quantum dots are semiconducting nanoparticle in the range of 1–10 nm which differ in electrical and optical properties from their bulk material giving them an edge in the field of imaging and treatment of tumor-related cases, these nanoparticles comprise of inorganic material. One of the very first studies were performed by Ackerman et al., in the year 2002, where they have demonstrated peptide coated quantum dots having high target specificity for lung cancer using peptide coated ZnS capped CdSe quantum dots which opened the gate for further research into the area of targeting size-controlled organic/inorganic hybrid quantum dots [32]. In 2010 Md. Narunnabi et al., synthesized CdSe/CdTe quantum dots which were coated by PEG-PCDA which was further stabilized by UV irradiation which was tested on MDA-MB-231 tumor model and has shown high therapeutic efficiency [94]. Surface Plasmonic resonating nanoparticles such as gold are being used for diagnosis and treatment of cancer, owing it to their non-cytotoxicity, high affinity towards biomolecules and good chemical stability [95, 96]. Among the various nanoparticles (np) used in cancer treatment in recent times like polymeric np, magnetic np, or quantum dots, the major advantage of these surface plasmonic nanomaterials is in its use, both as a contrast agent as well as drug delivery agents for cancer therapy. X. Huang et al., in 2006 explained a phenomena called surface plasmon resonance [97] by which gold particles can scatter visible or near-infrared light depending on the size and shape of the particle which makes it feasible for gold to be used in various kinds of microscopic techniques like confocal scanning optical microscopy [98], multi-photon plasmon resonance microscopy [99], optical coherence microscopy [100], for optical imaging and diagnostics. Jing Liang Li et al., in 2008 used the fact that gold nanoparticles converts the absorbed photon from the light source into thermal energy and can be used to kill tumors, so they prepared gold nanoparticles by a seeding growth method and was coated with SDS (Sodium Dodecyl Sulphate) and functionalized it with transferrin, which is a glycoprotein present on the surface of the cell and it is related to cell proliferation [101], which is more expressed in malignant tissue rather than normal tissue owing to more iron demand for faster cell growth, cytotoxic studies were performed using Hs 578 T cells and 3T3 cells and PEG-Tf-NPs and PEG-NPs, the cytotoxicity, as well as the cellular uptake, were found to be higher in case of the transferrin conjugated gold nanoparticles. Zhaowu Zhang et al., in 2010, synthesized gold nanoparticles which were capped with glutathione (GSH) containing carboxyl group over its surface and then FA (folic acid) was conjugated with the GNPs through the reaction between the amino group of the FA and the carboxyl group of the GSH and these conjugates were stable over a wide range of pH and ionic strength values, the targeting of FA-GSH-GNP in human cervix carcinoma cell (HeLa cells) with a high level of folate expression were shown through TEM and CLSM, while in A549 cells no cellular uptake was seen due to lack of folate receptors.

3.1.1 Peptide Conjugated Inorganic Quantum Dots

Conjugation of the inorganic quantum dots with biomaterials is of grave importance to make them biocompatible. Various materials like folic acid, transferrin, hyaluronan, etc. are conjugated with the quantum dots in order to make them biocompatible as well as to target them to a particular tumor in study or therapy. The integrin $\alpha_v\beta_3$ receptor, which is known to bind with several extracellular proteins, is not generally expressed in the normal healthy cell, while it is overly expressed in the blood vessels going through angiogenesis, or the new blood vessel formation. This overexpression has been shown in the pancreatic cells and plays a significant role in the development of the tumor [102, 103]. Due to the overexpression of $\alpha_v\beta_3$ receptor in both the tumor vasculature as well as the cell lines makes it ideal for using it as a biomarker for quantum dots probes conjugated with the RGD peptide (arginine-glycine-aspartic acid) to detect cancer in early stages. In a study in the year 2008 performed by Cai et al., RGD peptides were conjugated with PEG-coated QD with the help of a heterobifunctional linker, 4-maleimidobutyric acid N-succinimidyl ester and they used human glioblastoma cells and the breast cancer cells as positive and negative controls for the experiment, and the competitive cell-binding assay was performed using radio ligand and live staining was performed to confirm the binding of the peptides with the quantum dots [104]. DNA functionalized CdTe quantum dots were prepared by the one-step synthesis in the year 2009 for photoluminescence [105, 106]. In another study in the year 2013, He et al., prepared a one-step synthesis of the peptide conjugated quantum dots at room temperature. In this study, $Zn_xHg_{1-x}Se$ QD was synthesized in an aqueous solution and was completed in a sec and the product exhibited strong red to NIR photoluminescence which was essential for bio imaging [107]. Li et al. in the year 2016, conjugated RGD peptides with inorganic quantum dots to act as target markers for human pancreatic carcinoma cells, where CdTe/CdS qds were functionalized with MSA (mercaptosuccinic acid) and then EDC/NHS chemistry was applied before mixing it with the RGD peptide in 1:2 ratio and the resulting product has shown significantly low cytotoxicity found using the MTT assay and good photoluminescence [35].

3.2 Magnetic Quantum Dots or Magnetic Nanoparticles

Based on the nature of the constituent elements of the quantum dots, apart from organic and inorganic, they can also be classified as magnetic quantum dots. Magnetic nanoparticles are very common in the biological system where applications range from geomagnetic navigational aid in migratory birds to ferritin, one of the most common storage protein which is known to contain about 3000 ferric ions in a paramagnetic oxyhydroxide core [108]. Mostly superparamagnetic iron oxide nanoparticles (SPION) are used for imaging and therapy. Due to their small volumes, these magnetic nanoparticles or the quantum dots show superparamagnetic behavior and they can convert the magnetic field energy to thermal energy locally thus killing the

cancer cells. Loss of any remnant magnetism after the field is being withdrawn is utilized for biomedical applications, which enables them to prevent the formation of agglomerates in turn maintaining stability. A new phenomena Photodynamic Therapy (PDT), has been studied or explained by various to be helpful in anti-cancer therapy at both primary as well as the advanced stages of cancer, this photodynamic therapy not only helps in cancer treatment but also helps in various cardiovascular, endodontic and ophthalmic diseases [109–111]. In 2007, S. Tamil Selvan et al., studied magnetic quantum dots, in which they have synthesized Fe_2O_3 –CdSe nanocomposite via a facile synthesis method, which has produced high quantum yield over a broad range of color without the use of ZnS capping, keeping the toxicity in mind, it was made biocompatible using a silica coating; these MQD's properties both magnetic and optical can be tuned separately which was used to image tumor cells [36]. Park et al., in the year 2008, prepared micellar hybrid nanoparticles that contain iron oxide magnetic nanoparticles, quantum dots, doxorubicin with single PEG-modified phospholipid micelle, which can be used for both ex vivo and in vivo imaging as well as for MRI [112]. In another study, Surinder P. Singh in the year 2011, synthesized Fe_3O_4 –ZnO core–shell magnetic quantum dots at room temperature by the seed-mediated approach and controlling the aging time, which could provide a combination of radiation therapy and PDT while simultaneously being used in MR imaging, thus providing to be a multifunctional platform for cancer treatment [113]. In 2014, Fei Ye et al., prepared a biodegradable vesicle (PLGA) containing SPIOs, Cd free Mn-doped ZnS quantum dots and anti-cancer drugs for in vivo imaging and drug delivery, which showed promising results as an anti-cancer theranostic tool and it needs to be studied further controlled drug release as well as organ targeting [114].

The use of nanotechnology for medicinal purposes is the most successful application of pure nanotechnology; though, however useful nanotechnology might be, there is always a risk of toxicity of these nanoparticles. Elements such as cadmium and selenium comprise a major part of quantum dots used for imaging are known to be acutely and chronically toxic to cells and organisms, especially they are taken up by the calcium membrane, for example, cadmium mutates the chromosome, breaks down the DNA strands as well as it inhibits the synthesis of DNA, RNA and protein [115–118]. The earliest known toxicity study was performed by Derfus et al., in the year 2004, where they probed the cytotoxicity of CdSe quantum dots using primary hepatocytes as a liver model. They concluded that the CdSe quantum dots are indeed cytotoxic under a certain condition such as surface oxidation through various pathways causes the Cd to get reduced on the surface of QD thus releasing Cd ion in the cell subsequently causing cell death [119]. Various methods are applied like surface coating with ZnO and BSA (Bovine serum albumin), which significantly reduced but did not eliminate cytotoxicity. Some studies also have shown the use of ZnS capping, using CdO as a precursor to form highly luminescent CdSe quantum dots that doesn't need an inorganic capping [120, 121]. Certain groups of researchers focus on reducing the size of shell or simply using uncapped CdSe or CdS QD for biological labeling/imaging [122, 123] where an organic capping plays the role of preventing the surface oxidation thus eliminating or reducing the cytotoxicity.

3.3 Organic Quantum Dots

Carbon is one of the most abundant materials available on the earth, has unique properties due to its hybrid orbitals, which leads to the formation of various allotropes of carbon, which are also called different forms of carbon. All these together make carbon one of the most studied elements of the planet as said by Nathan P. Guisinger and Michael S Arnold in their review in the year 2010 [124]. The accidental discovery of the carbon quantum dots while X Y. Xu et al., was purifying and separating the single-walled Carbon Nanotubes from the arc discharged soot in the year 2004 triggered further studies in the area of organic quantum dots [22]. In 2006, Sun et al., renamed the fluorescent carbon nanoparticles previously discovered by X. Y. Xu et al., in their study as Carbon quantum dots, where they synthesized carbon quantum dots by laser ablation route which was previously unknown. Carbon quantum dots are quasi-spherical nano particle consisting of amorphous as well as nano crystalline cores with graphitic or turbostratic carbon (sp^2 hybridized carbon) or graphene and graphene oxide sheets fused by diamond-like sp^3 hybridized carbon insertions [37, 125, 126]. Organic quantum dots are synthesized using two approaches namely the top-down approach [127–129] and the bottom-up approach [130–132] and could be easily surface passivated to emit greater fluorescence. In the year 2016, Noha A. El Essawy et al., devised a novel one-step synthesis of highly luminescent carbon quantum dots from PET (Polyethylene Terephthalate) bottle waste by thermal decomposition of PET followed by heating at 800 °C gave the carbon dots [133]. In earlier reviews the scenario for surface functionalization and its effects on the brightness, the quantum yield has been discussed [134], in which Changqin Ding et al., have shown that the radiative recombination of the surface-confined electrons and holes are responsible for the photoluminescence shown by the carbon dots. The photoluminescence of the carbon dots from cheap sources like candle soot was found to be around 15% [130] while that from oils was found to be 53% [131] at room temperature which is the highest yet to be recorded. Carbon dots have been prepared from any material having carbon in their molecular backbone like glucosamine, ascorbic acid, ethanol, citric acid, saccharides, carbon quantum dots are also termed as organic quantum dots, which are recently being used in cancer cell imaging and killing of cancer cells due to high quantum yield and biocompatibility. Photo-luminescent (PL) nanomaterials, such as carbon dots (CDs), up-conversion nanoparticles and luminescent metal complexes offers unique tunable chemical and physical characteristics suitable for various application in STEM field [135–140]. Carbon dots are being used in chemical biological, physical scientific applications including sensors, imaging, drug carries, catalysis, even in white light emitting diodes etc. These carbon quantum dots are being loaded with drugs or are surface functionalized and then loaded with drugs in order to target specific cancer cells. Synthesis of carbon dots with high QY and good biocompatibility still remains a challenge [141–143]. Various novel methods of synthesis are being devised for the synthesis of carbon quantum dots with good quantum yield, high target specificity, solubility as well as biocompatibility, over the past decade. Fluorescent carbon dots are conjugated with targeting ligands such as

transferrin [28], folic acid (FA) [144], peptides [145], to observe the ligand-biomarker binding visually. Carbon quantum dots are found as complete therapeutic solution to the cancer treatment.

3.3.1 Carbon Quantum Dots Conjugated with Folic Acid

Folic acid is a synthetic form of the naturally occurring vitamin B, which is found in certain food products. Folic acid helps regulate the cell division and growth by assisting in synthesis of purines and pyrimidines. Lemon and Lou in the year 1991, first conceived the idea of using the folate receptors for targeted delivery of drugs into cells, which proved to be very essential in the case of treatment of cancer as well as other inflammatory diseases and further studies were performed since then on this topic [146]. The folate receptors are overly expressed in ovarian, breast, epithelial, cervical, lung, kidney, colorectal and brain tumors [147]. Carbon dots conjugated with folic acid shows more affinity towards getting endocytosed into a tumorous cell more than a healthy cell thus potentially increasing the efficiency of the detection and subsequently, elimination of the same without having much side effects on the neighboring healthy cells. FA conjugated c-dots are known to be endocytosed at a higher rate in the tumor cell than in the normal cell thus have greater efficiency in determining the cancerous cell [40, 148]. Also, it helps in killing the tumor cell when loaded with the doxorubicin, where the bovine serum albumen is employed to increase drug loading as well as improve biocompatibility [41]. Folic acid is known to have amine attached to its aromatic rings which enables them to easily conjugate with carboxylic group enriched carbon dots. EDC/NHS chemistry can be used to functionalize c-dots to conjugate FA to the carbon dots [38], in a study Shong Y. et al., in the year 2012, the functionalized folic acid with NHS and then filtered with DCC and the mixed with c-dots at pH 10, in the same study the conjugation was characterized by using UV-Vis spectroscopy where a prominent mark at 283 nm was observed for FA which doesn't overlap the c-dot's mark as well as other tools like AFM or the atomic force microscopy, Transmission Electron Microscopy or TEM were used to ensure complete conjugation [148].

3.3.2 Carbon Quantum Dots Conjugated with Transferrin

Transferrins are glycoproteins present in the blood plasma, helps regulate the level of free iron in the body by binding to them. Being a very large molecule with 79 kDa mass transferrin can easily be purified and conjugated with carbon dots containing amine groups over its surface. The site of binding can't be pinpointed as there are multiple sites for binding. Based on binding, the entire molecule can be inactivated. So in order to check the binding mass spectroscopy can be performed as the size is quite large. Transferrins are itself not very highly fluorescent material with a peak around 364 nm. It is a part of the innate immune system, the binding of the iron-bound transferrin to the transferrin receptor 1 on the cell surface starts with the

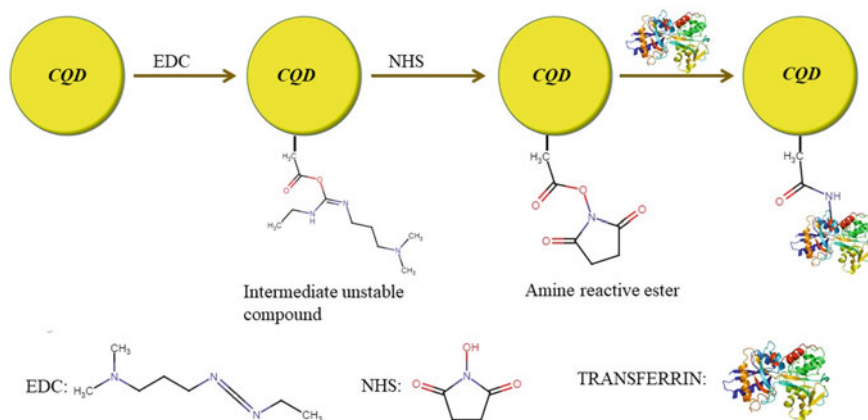


Fig. 1 Simplified schematic representation of reaction mechanism of carbon dots-transferrin conjugation

clathrin-coated pits and internalization into the cytoplasm and ends with apotransferrin formation (after the intake of iron the transferrins are recycled back into the cell surface) [149]. In 2016 a study conducted by Shanghao li et al., it is concluded that transferrin conjugated cq d is being used for drug delivery in pediatric brain cancer patients. The regular known chemotherapy might affect the proper functioning of the healthy cells thus a transferrin mediated drug delivery is very essential. Very often the transferrin receptors are well expressive in the brain tumor cells which can be utilized to deliver carbon quantum dots containing doxorubicin into the cell [28] and they can pass the blood–brain barrier which is unpassable by many known delivery vehicles [150]. By virtue of this property, we can target the carbon quantum dots functionalized with transferrins directly to the affected cells. Transferrin conjugated chemotherapeutic drugs have shown the promising percentage of tumor cell death in carcinoma, leukemia as well as glioblastoma as compared to the conventional techniques [151–153]. With pediatric brain tumor c-dots conjugated with dox and transferrin have shown better tumor cell death as compared with the free drug alone [28]. Since the Transferrins are able to carry iron they might also be useful in magnetic resonance imaging. A schematic for the conjugation of transferrin with the carbon quantum dots is shown in Fig. 1.

4 Conclusion

We know not so much about the cancer condition thus as of recent times cancer is becoming a highly researched field, with respect to that many quantum dot's technologies are recently going into clinical trials which increasingly kills the tumor

cells with higher efficiency than their normal chemotherapeutic counterpart. Inorganic as well as magnetic quantum dots on itself are fairly toxic so they need to be conjugated with certain biomaterials in order to reduce their cytotoxicity. Peptides conjugated inorganic quantum dots have proven to be highly biocompatible and have shown good photoluminescence, mostly in the tumor vasculature imaging. Magnetic quantum dots are being used for the MRI scans. Now carbon quantum dots have time and again proved to be highly biocompatible with less or no cytotoxicity and high fluorescence property much better than the heavy metal inorganic or magnetic quantum dots. Conjugating the c-dots with various cancer biomarkers has proven to be more effective in selectively targeting thus destroying the tumor cells with very high efficiency. Due to the tunable fluorescence property, we can use the carbon dots for the excretion off the c-dots from the system which enables us to maintain the body's internal environment. Drugs can be loaded on the quantum dots conjugated with the various biomarkers. Continuation of the research will help us understand the cancer condition better as well as development of a complete theranostic tool with lower side effects. There is very little research on the conjugation of peptides with the carbon dots, in the future, this conjugation might prove to be very successful in treating cancer with higher efficacy and lower side effects.

Acknowledgements The authors acknowledge the infrastructural facilities provided by NIT Rourkela.

Conflict of Interest The authors declare no conflict of interest.

References

1. Jemal A, Bray F, Center MM, Ferlay J, Ward E, Forman D. Global cancer statistics. *CA Cancer J Clin.* 2011;61(2):69–90.
2. Sanz-Moreno V, Marshall CJ. The plasticity of cytoskeletal dynamics underlying neoplastic cell migration. *Curr Opin Cell Biol.* 2010;22(5):690–6.
3. Ridley AJ, Schwartz MA, Burridge K, Firtel RA, Ginsberg MH, Borisy G, et al. Cell migration: Integrating signals from front to back. *Science.* 2003;302(5651):1704–9.
4. Lauffenburger DA, Horwitz AF. Cell migration: A physically integrated molecular process. *Cell.* 1996;84(3):359–69.
5. Friedl P, Alexander S. Cancer invasion and the microenvironment: Plasticity and reciprocity. *Cell.* 2011;147(5):992–1009.
6. Egeblad M, Rasch MG, Weaver VM. Dynamic interplay between the collagen scaffold and tumor evolution. *Curr Opin Cell Biol.* 2010;22(5):697–706.
7. Alexander S, Friedl P. Cancer invasion and resistance: Interconnected processes of disease progression and therapy failure. *Trends Mol Med.* 2012;18(1):13–26.
8. Yao H, Zeng ZZ, Fay KS, Veine DM, Staszewski ED, Morgan M, et al. Role of $\alpha(5)\beta(1)$ integrin up-regulation in radiation-induced invasion by human pancreatic cancer cells. *Transl Oncol.* 2011;4(5):282–92.
9. Nelson CM, Khauv D, Bissell MJ, Radisky DC. Change in cell shape is required for matrix metalloproteinase-induced epithelial-mesenchymal transition of mammary epithelial cells. *J Cell Biochem.* 2008;105(1):25–33.

10. Xu R, Boudreau A, Bissell MJ. Tissue architecture and function: Dynamic reciprocity via extra- and intra-cellular matrices. *Cancer Metastasis Rev.* 2009;28(1–2):167–76.
11. Kim D, Yoo JM, Hwang H, Lee J, Lee SH, Yun SP, et al. Graphene quantum dots prevent α -synucleinopathy in Parkinson's disease. *Nat Nanotechnol.* 2018;13(9):812–8.
12. Chung YJ, Kim K, Lee BI, Park CB. Carbon nanodot-sensitized modulation of Alzheimer's β -amyloid self-assembly. *Disassembly Toxicity.* 2017;13(34):1700983.
13. Bentolila LA, Ebenstein Y, Weiss S. Quantum dots for in vivo small-animal imaging. *J Nucl Med Official Publ Soc Nucl Med.* 2009;50(4):493–6.
14. Hilderbrand SA, Weissleder R. Near-infrared fluorescence: Application to in vivo molecular imaging. *Curr Opin Chem Biol.* 2010;14(1):71–9.
15. Wang Y, Chen L. Quantum dots, lighting up the research and development of nanomedicine. *Nanomedicine.* 2011;7(4):385–402.
16. Tholouli E, Sweeney E, Barrow E, Clay V, Hoyland JA, Byers RJ. Quantum dots light up pathology. *J Pathol.* 2008;216(3):275–85.
17. Byers RJ, Hitchman ER. Quantum dots brighten biological imaging. *Prog Histochem Cytochem.* 2011;45(4):201–37.
18. True LD, Gao X. Quantum dots for molecular pathology: Their time has arrived. *J Mol Diagn.* 2007;9(1):7–11.
19. He X, Gao J, Gambhir SS, Cheng Z. Near-infrared fluorescent nanoprobe for cancer molecular imaging: Status and challenges. *Trends Mol Med.* 2010;16(12):574–83.
20. Fang M, Peng CW, Pang DW, Li Y. Quantum dots for cancer research: Current status, remaining issues, and future perspectives. *Cancer Biol Med.* 2012;9(3):151–63.
21. Medarova Z, Pham W, Farrar C, Petkova V, Moore A. In vivo imaging of siRNA delivery and silencing in tumors. *Nat Med.* 2007;13(3):372–7.
22. Xu X, Ray R, Gu Y, Ploehn HJ, Gearheart L, Raker K, et al. Electrophoretic analysis and purification of fluorescent single-walled carbon nanotube fragments. *J Am Chem Soc.* 2004;126(40):12736–7.
23. Li S, Skromne I, Peng Z, Dallman J, Al-Youbi AO, Bashammakh AS, et al. "Dark" carbon dots specifically "light-up" calcified zebrafish bones. *J Mater Chem B.* 2016;4(46):7398–405.
24. Peng Z, Miyanji EH, Zhou Y, Pardo J, Hettiarachchi SD, Li S, et al. Carbon dots: promising biomaterials for bone-specific imaging and drug delivery. *Nanoscale.* 2017;9(44):17533–43.
25. Gao X, Du C, Zhuang Z, Chen W. Carbon quantum dot-based nanoprobe for metal ion detection. *J Mater Chem C.* 2016;4(29):6927–45.
26. Margraf JT, Strauss V, Guldi DM, Clark T. The electronic structure of amorphous carbon nanodots. *J Phys Chem B.* 2015;119(24):7258–65.
27. Zhou Y, Peng Z, Seven ES, Leblanc RM. Crossing the blood-brain barrier with nanoparticles. *J Controlled Release: Official J Controlled Release Soc.* 2018;270:290–303.
28. Li S, Amat D, Peng Z, Vanni S, Raskin S, De Angulo G, et al. Transferrin conjugated nontoxic carbon dots for doxorubicin delivery to target pediatric brain tumor cells. *Nanoscale.* 2016;8(37):16662–9.
29. Yu B, Tai HC, Xue W, Lee LJ, Lee RJ. Receptor-targeted nanocarriers for therapeutic delivery to cancer. *Mol Membr Biol.* 2010;27(7):286–98.
30. Gorin SS, Heck JE, Cheng B, Smith SJ. Delays in breast cancer diagnosis and treatment by racial/ethnic group. *Arch Intern Med.* 2006;166(20):2244–52.
31. Mustacchi G, De Laurentiis M. The role of taxanes in triple-negative breast cancer: literature review. *Drug Des Devel Ther.* 2015;9:4303–18.
32. Åkerman ME, Chan WCW, Laakkonen P, Bhatia SN, Ruoslahti E. Nanocrystal targeting in vivo. *Proc Natl Acad Sci.* 2002;99(20):12617.
33. Ruan J, Wang K, Song H, Xu X, Ji J, Cui D. Biocompatibility of hydrophilic silica-coated CdTe quantum dots and magnetic nanoparticles. *Nanoscale Res Lett.* 2011;6(1):299.
34. Cai X, Luo Y, Zhang W, Du D, Lin Y. pH-sensitive ZnO quantum dots-doxorubicin nanoparticles for lung cancer targeted drug delivery. *ACS Appl Mater Interfaces.* 2016;8(34):22442–50.
35. Li S, Yang J, Lei X, Zhang J, Yang H, Li K, et al. Peptide-conjugated quantum dots act as the target marker for human pancreatic carcinoma cells. *Cell Physiol Biochem.* 2016;38(3):1121–8.

36. Selvan ST, Patra PK, Ang CY, Ying JY. Synthesis of silica-coated semiconductor and magnetic quantum dots and their use in the imaging of live cells. *Angew Chem.* 2007;119(14):2500–4.
37. Yang S-T, Cao L, Luo PG, Lu F, Wang X, Wang H, et al. Carbon dots for optical imaging in vivo. *J Am Chem Soc.* 2009;131(32):11308–9.
38. Zhang X, Meng L, Lu Q, Fei Z, Dyson PJ. Targeted delivery and controlled release of doxorubicin to cancer cells using modified single wall carbon nanotubes. *Biomaterials.* 2009;30(30):6041–7.
39. Singh RP, Sharma G, Sonali, Singh S, Patne SCU, Pandey BL, et al. Effects of transferrin conjugated multi-walled carbon nanotubes in lung cancer delivery. *Mater Sci Eng C.* 2016;67:313–25.
40. Zhao X, Zhang J, Shi L, Xian M, Dong C, Shuang S. Folic acid-conjugated carbon dots as green fluorescent probes based on cellular targeting imaging for recognizing cancer cells. *RSC Adv.* 2017;7(67):42159–67.
41. Mewada A, Pandey S, Thakur M, Jadhav D, Sharon M. Swarming carbon dots for folic acid mediated delivery of doxorubicin and biological imaging. *J Mater Chem B.* 2014;2(6):698–705.
42. Moasser MM. The oncogene HER2: its signaling and transforming functions and its role in human cancer pathogenesis. *Oncogene.* 2007;26(45):6469–87.
43. Goldhirsch A, Wood WC, Gelber RD, Coates AS, Thurlimann B, Senn HJ. Meeting highlights: updated international expert consensus on the primary therapy of early breast cancer. *J Clin Oncol.* 2003;21(17):3357–65.
44. Leong ASY, Zhuang Z. The changing role of pathology in breast cancer diagnosis and treatment. *Pathobiology.* 2011;78(2):99–114.
45. Decker T, Hungermann D, Böcker W. Prognostic and predictive factors of invasive breast cancer: Update 2009. *Pathologe.* 2009;30(1):49–55.
46. Altekruse SF, McGlynn KA, Reichman ME. Hepatocellular carcinoma incidence, mortality, and survival trends in the United States from 1975 to 2005. *J Clin Oncol.* 2009;27(9):1485–91.
47. Simard EP, Ward EM, Siegel R, Jemal A. Cancers with increasing incidence trends in the United States: 1999 through 2008. *CA Cancer J Clin.* 2012;62(2):118–28.
48. Parkin DM, Bray F, Ferlay J, Pisani P. Global cancer statistics, 2002. *CA Cancer J Clin.* 2005;55(2):74–108.
49. Li D, Kang J, Golas BJ, Yeung VW, Madoff DC. Minimally invasive local therapies for liver cancer. *Cancer Biol Med.* 2014;11(4):217–36.
50. Goulart BH, Bensink ME, Mummy DG, Ramsey SD. Lung cancer screening with low-dose computed tomography: costs, national expenditures, and cost-effectiveness. *J Nat Compr Cancer Netw JNCCN.* 2012;10(2):267–75.
51. Al BB, Tanius B-S, Emily C, Yi-Jen C, Michael AC, Harry SC, et al. Metastatic colon cancer, version 3.2013. *J Nat Compr Cancer Netw.* 2013;11(2):141–52.
52. Benson A, Abrams T, Ben-Josef E, Bloomston M, Clary B, Covey A, et al. Hepatobiliary cancers. *J Nat Compr Cancer Netw JNCCN.* 2009;7.
53. Brouquet A, Abdalla EK, Kopetz S, Garrett CR, Overman MJ, Eng C, et al. High survival rate after two-stage resection of advanced colorectal liver metastases: Response-based selection and complete resection define outcome. *J Clin Oncol.* 2011;29(8):1083–90.
54. <Local Therapies for Hepatic Metastases.pdf>.
55. Hohenberger P, Gretschel S. Gastric cancer. *The Lancet.* 2003;362(9380):305–15.
56. Parkin DM. International variation. *Oncogene.* 2004;23(38):6329–40.
57. Parkin DM, Bray FI, Devesa SS. Cancer burden in the year 2000. The global picture. *Eur J Cancer (Oxford, England: 1990).* 2001;37 Suppl 8:S4–66.
58. Huang P, Xu C, Lin J, Wang C, Wang X, Zhang C, et al. Folic acid-conjugated graphene oxide loaded with photosensitizers for targeting photodynamic therapy. *Theranostics.* 2011;1:240–50.
59. Huang P, Bao L, Zhang C, Lin J, Luo T, Yang D, et al. Folic acid-conjugated silica-modified gold nanorods for X-ray/CT imaging-guided dual-mode radiation and photo-thermal therapy. *Biomaterials.* 2011;32(36):9796–809.

60. Tian B, Wang C, Zhang S, Feng L, Liu Z. Photothermally enhanced photodynamic therapy delivered by nano-graphene oxide. *ACS Nano*. 2011;5(9):7000–9.
61. Ma LL, Feldman MD, Tam JM, Paranjape AS, Cheruku KK, Larson TA, et al. Small multi-functional nanoclusters (Nanoroses) for targeted cellular imaging and therapy. *ACS Nano*. 2009;3(9):2686–96.
62. He M, Huang P, Zhang C, Hu H, Bao C, Gao G, et al. Dual phase-controlled synthesis of uniform lanthanide-doped NaGdF₄ upconversion nanocrystals via an OA/ionic liquid two-phase system for in vivo dual-modality imaging. *Adv Func Mater*. 2011;21(23):4470–7.
63. Lee EC, Yang JY, Lee KG, Oh SY, Suh YS, Kong SH, et al. The value of postoperative serum carcinoembryonic antigen and carbohydrate antigen 19–9 levels for the early detection of gastric cancer recurrence after curative resection. *J Gastric Cancer*. 2014;14(4):221–8.
64. Asao T, Fukuda T, Yazawa S, Nagamachi Y. Carcinoembryonic antigen levels in peritoneal washings can predict peritoneal recurrence after curative resection of gastric cancer. *Cancer*. 1991;68(1):44–7.
65. Marrelli D, Pinto E, De Stefano A, Farnetani M, Garosi L, Roviello F. Clinical utility of CEA, CA 19–9, and CA 72–4 in the follow-up of patients with respectable gastric cancer. *Am J Surg*. 2001;181(1):16–9.
66. Duan D, Fan K, Zhang D, Tan S, Liang M, Liu Y, et al. Nanozyme-strip for rapid local diagnosis of Ebola. *Biosens Bioelectron*. 2015;74:134–41.
67. Sudjaroen Y. Efficiency assessment of immunochromatographic strip test for the diagnosis of alpha-thalassemia-1 carriers. *J Lab Physicians*. 2015;7(1):4–10.
68. Vyas SS, Jadhav SV, Majee SB, Shastri JS, Patravale VB. Development of immunochromatographic strip test using fluorescent, micellar silica nanosensors for rapid detection of B. abortus antibodies in milk samples. *Biosens Bioelectron*. 2015;70:254–60.
69. Yan X, Wang K, Lu W, Qin W, Cui D, He J. CdSe/ZnS quantum dot-labeled lateral flow strips for rapid and quantitative detection of gastric cancer carbohydrate antigen 72–4. *Nanoscale Res Lett*. 2016;11(1):138.
70. Soltesz EG, Kim S, Kim SW, Laurence RG, De Grand AM, Parungo CP, et al. Sentinel lymph node mapping of the gastrointestinal tract by using invisible light. *Ann Surg Oncol*. 2006;13(3):386–96.
71. Parungo CP, Ohnishi S, Kim SW, Kim S, Laurence RG, Soltesz EG, et al. Intraoperative identification of esophageal sentinel lymph nodes with near-infrared fluorescence imaging. *J Thorac Cardiovasc Surg*. 2005;129(4):844–50.
72. Ruan J, Song H, Qian Q, Li C, Wang K, Bao C, et al. HER2 monoclonal antibody conjugated RNase-A-associated CdTe quantum dots for targeted imaging and therapy of gastric cancer. *Biomaterials*. 2012;33(29):7093–102.
73. Kong Y, Chen J, Gao F, Li W, Xu X, Pandoli O, et al. A multifunctional ribonuclease-A-conjugated CdTe quantum dot cluster nanosystem for synchronous cancer imaging and therapy. *Small*. 2010;6(21):2367–73.
74. Bray F, Ferlay J, Soerjomataram I, Siegel RL, Torre LA, Jemal A. Global cancer statistics 2018: GLOBOCAN estimates of incidence and mortality worldwide for 36 cancers in 185 countries. *CA Cancer J Clin*. 2018;68(6):394–424.
75. Wong MCS, Lao XQ, Ho KF, Goggins WB, Tse SLA. Incidence and mortality of lung cancer: global trends and association with socioeconomic status. *Sci Rep*. 2017;7(1):14300.
76. Bjerager M, Palshof T, Dahl R, Vedsted P, Olesen F. Delay in diagnosis of lung cancer in general practice. *Br J Gen Pract*. 2006;56(532):863–8.
77. Singh RD, Shandilya R, Bhargava A, Kumar R, Tiwari R, Chaudhury K, et al. Quantum dot based nano-biosensors for detection of circulating cell free mirnas in lung carcinogenesis: From biology to clinical translation. *Front Genet*. 2018;9:616.
78. Reduced lung-cancer mortality with low-dose computed tomographic screening. *New England J Med*. 2011;365(5):395–409.
79. Wildstein KA, Faustini Y, Yip R, Henschke CI, Ostroff JS. Longitudinal predictors of adherence to annual follow-up in a lung cancer screening programme. *J Med Screen*. 2011;18(3):154–9.

80. Brenner DJ. Radiation and chest CT scans: Are there problems? What should we do? *Chest*. 2012;142(3):549–50.
81. McCunney RJ, Li J. Radiation risks in lung cancer screening programs. *Chest*. 2014;145(3):618–24.
82. Brigger I, Dubernet C, Couvreur P. Nanoparticles in cancer therapy and diagnosis. *Adv Drug Deliv Rev*. 2012;64:24–36.
83. Schroeder KL, Goreham RV, Nann T. Graphene quantum dots for theranostics and bioimaging. *Pharm Res*. 2016;33(10):2337–57.
84. Alessandro A, Giuseppa P, Andrea A, Vincenzo R, Sabina R, Caterina M. Nanoparticles in oncology: The new theragnostic molecules. *Anticancer Agents Med Chem*. 2011;11(7):669–86.
85. Mariappan L, Shao Q, Jiang C, Yu K, Ashkenazi S, Bischof JC, et al. Magneto acoustic tomography with short pulsed magnetic field for in-vivo imaging of magnetic iron oxide nanoparticles. *Nanomedicine*. 2016;12(3):689–99.
86. FitzGerald PF, Butts MD, Roberts JC, Colborn RE, Torres AS, Lee BD, et al. A proposed computed tomography contrast agent using carboxybetaine Zwitterionic tantalum oxide nanoparticles: Imaging, biological, and physicochemical performance. *Invest Radiol*. 2016;51(12):786–96.
87. Lu A-H, Zhang X-Q, Sun Q, Zhang Y, Song Q, Schüth F, et al. Precise synthesis of discrete and dispersible carbon-protected magnetic nanoparticles for efficient magnetic resonance imaging and photothermal therapy. *Nano Res*. 2016;9(5):1460–9.
88. Stone RC, Fellows BD, Qi B, Trebatoski D, Jenkins B, Raval Y, et al. Highly stable multi-anchored magnetic nanoparticles for optical imaging within biofilms. *J Colloid Interface Sci*. 2015;459:175–82.
89. Zhou Q, Wei Y. for better or worse, iron overload by superparamagnetic iron oxide nanoparticles as a MRI contrast agent for chronic liver diseases. *Chem Res Toxicol*. 2017;30(1):73–80.
90. Michalet X, Pinaud FF, Bentolila LA, Tsay JM, Doose S, Li JJ, et al. Quantum dots for live cells, in vivo imaging, and diagnostics. *Science*. 2005;307(5709):538–44.
91. Alivisatos AP, Gu W, Larabell C. Quantum dots as cellular probes. *Annu Rev Biomed Eng*. 2005;7:55–76.
92. Chan WC, Nie S. Quantum dot bioconjugates for ultrasensitive nonisotopic detection. *Science*. 1998;281(5385):2016–8.
93. Li ZG, Yang K, Cao YA, Zheng G, Sun DP, Zhao C, et al. In vivo study of the effects of peptide-conjugated near-infrared fluorescent quantum dots on the tumorigenic and lymphatic metastatic capacities of squamous cell carcinoma cell line Tca8113 and U14. *Int J Mol Sci*. 2010;11(4):1413–22.
94. Nurunnabi M, Cho KJ, Choi JS, Huh KM, Lee YK. Targeted near-IR QDs-loaded micelles for cancer therapy and imaging. *Biomaterials*. 2010;31(20):5436–44.
95. Huisman HJ, Fütterer JJ, van Lin ENJT, Welmers A, Scheenen TWJ, van Dalen JA, et al. Prostate cancer: Precision of integrating functional MR imaging with radiation therapy treatment by using fiducial gold markers. *Radiology*. 2005;236(1):311–7.
96. Ackerson CJ, Sykes MT, Kornberg RD. Defined DNA/nanoparticle conjugates. *Proc Natl Acad Sci U S A*. 2005;102(38):13383–5.
97. Huang X, El-Sayed IH, Qian W, El-Sayed MA. cancer cell imaging and photothermal therapy in the near-infrared region by using gold nanorods. *J Am Chem Soc*. 2006;128(6):2115–20.
98. Sokolov K, Follen M, Aaron J, Pavlova I, Malpica A, Lotan R, et al. Real-time vital optical imaging of precancer using anti-epidermal growth factor receptor antibodies conjugated to gold nanoparticles. *Can Res*. 2003;63(9):1999–2004.
99. Yelin D, Oron D, Thiberge S, Moses E, Silberberg Y. Multiphoton plasmon-resonance microscopy. *Opt Express*. 2003;11(12):1385–91.
100. Troutman TS, Barton JK, Romanowski M. Optical coherence tomography with plasmon resonant nanorods of gold. *Opt Lett*. 2007;32(11):1438–40.

101. Trowbridge IS, Omary MB. Human cell surface glycoprotein related to cell proliferation is the receptor for transferrin. *Proc Natl Acad Sci U S A*. 1981;78(5):3039–43.
102. Reynolds AR, Hart IR, Watson AR, Welti JC, Silva RG, Robinson SD, et al. Stimulation of tumor growth and angiogenesis by low concentrations of RGD-mimetic integrin inhibitors. *Nat Med*. 2009;15(4):392–400.
103. Ji S, Xu J, Zhang B, Yao W, Xu W, Wu W, et al. RGD-conjugated albumin nanoparticles as a novel delivery vehicle in pancreatic cancer therapy. *Cancer Biol Ther*. 2012;13(4):206–15.
104. Cai W, Chen X. Preparation of peptide-conjugated quantum dots for tumor vasculature-targeted imaging. *Nat Protoc*. 2008;3(1):89–96.
105. Tikhomirov G, Hoogland S, Lee PE, Fischer A, Sargent EH, Kelley SO. DNA-based programming of quantum dot valency, self-assembly and luminescence. *Nat Nanotechnol*. 2011;6(8):485–90.
106. Ma N, Sargent EH, Kelley SO. One-step DNA-programmed growth of luminescent and bifunctionalized nanocrystals. *Nat Nanotechnol*. 2009;4(2):121–5.
107. He X, Gao L, Ma N. One-step instant synthesis of protein-conjugated quantum dots at room temperature. *Sci Rep*. 2013;3:2825.
108. Gillis P, Koenig SH. Transverse relaxation of solvent protons induced by magnetized spheres: Application to ferritin, erythrocytes, and magnetite. *Magn Reson Med*. 1987;5(4):323–45.
109. Felsher DW. Cancer revoked: Oncogenes as therapeutic targets. *Nat Rev Cancer*. 2003;3(5):375–80.
110. Triesscheijn M, Baas P, Schellens JH, Stewart FA. Photodynamic therapy in oncology. *Oncologist*. 2006;11(9):1034–44.
111. Pagonis TC, Chen J, Fontana CR, Devalapally H, Ruggiero K, Song X, et al. Nanoparticle-based endodontic antimicrobial photodynamic therapy. *J Endod*. 2010;36(2):322–8.
112. Park JH, von Maltzahn G, Ruoslahti E, Bhatia SN, Sailor MJ. Micellar hybrid nanoparticles for simultaneous magnetofluorescent imaging and drug delivery. *Angew Chem Int Ed Engl*. 2008;47(38):7284–8.
113. Singh SP. Multifunctional magnetic quantum dots for cancer theranostics. *J Biomed Nanotechnol*. 2011;7(1):95–7.
114. Ye F, Barrefelt A, Asem H, Abedi-Valugerdi M, El-Serafi I, Saghaian M, et al. Biodegradable polymeric vesicles containing magnetic nanoparticles, quantum dots and anticancer drugs for drug delivery and imaging. *Biomaterials*. 2014;35(12):3885–94.
115. Stohs SJ, Bagchi D. Oxidative mechanisms in the toxicity of metal ions. *Free Radical Biol Med*. 1995;18(2):321–36.
116. Prakash AS, Rao KS, Dameron CT. Cadmium inhibits BPDE alkylation of DNA in the major groove but not in the minor groove. *Biochem Biophys Res Commun*. 1998;244(1):198–203.
117. Hossain Z, Huq F. Studies on the interaction between Cd²⁺ ions and DNA. *J Inorg Biochem*. 2002;90:85–96.
118. Beyersmann D, Hechtenberg S. Cadmium, gene regulation, and cellular signalling in mammalian cells. *Toxicol Appl Pharmacol*. 1997;144(2):247–61.
119. Derfus AM, Chan WCW, Bhatia SN. Probing the cytotoxicity of semiconductor quantum dots. *Nano Lett*. 2004;4(1):11–8.
120. Dabbousi BO, Rodriguez-Viejo J, Mikulec FV, Heine JR, Mattoussi H, Ober R, et al. (CdSe)ZnS core–shell quantum dots: Synthesis and characterization of a size series of highly luminescent nanocrystallites. *J Phys Chem B*. 1997;101(46):9463–75.
121. Qu L, Peng ZA, Peng X. Alternative routes toward high quality CdSe nanocrystals. *Nano Lett*. 2001;1(6):333–7.
122. Yong KT, Hu R, Roy I, Ding H, Vathy LA, Bergey EJ, et al. Tumor targeting and imaging in live animals with functionalized semiconductor quantum rods. *ACS Appl Mater Interfaces*. 2009;1(3):710–9.
123. Winter JO, Liu TY, Korgel BA, Schmidt CE. Recognition molecule directed interfacing between semiconductor quantum dots and nerve cells. *Adv Mater*. 2001;13(22):1673–7.
124. Guisinger NP, Arnold MS. Beyond silicon: Carbon-based nanotechnology. *MRS Bull*. 2010;35(4):273–9.

125. Demchenko AP, Dekaliuk MO. Novel fluorescent carbonic nanomaterials for sensing and imaging. *Methods Appl Fluoresc.* 2013;1(4): 042001.
126. Baker SN, Baker GA. Luminescent carbon nanodots: Emergent nanolights. *Angew Chem Int Ed Engl.* 2010;49(38):6726–44.
127. Sun Y-P, Zhou B, Lin Y, Wang W, Fernando KAS, Pathak P, et al. Quantum-sized carbon dots for bright and colorful photoluminescence. *J Am Chem Soc.* 2006;128(24):7756–7.
128. Zheng L, Chi Y, Dong Y, Lin J, Wang B. Electrochemiluminescence of water-soluble carbon nanocrystals released electrochemically from graphite. *J Am Chem Soc.* 2009;131(13):4564–5.
129. Li X, Wang H, Shimizu Y, Pyatenko A, Kawaguchi K, Koshizaki N. Preparation of carbon quantum dots with tunable photoluminescence by rapid laser passivation in ordinary organic solvents. *Chem Commun (Camb).* 2011;47(3):932–4.
130. Liu H, Ye T, Mao C. Fluorescent carbon nanoparticles derived from candle soot. *Angew Chem.* 2007;119(34):6593–5.
131. Wang F, Pang S, Wang L, Li Q, Kreiter M, Liu C. One-step synthesis of highly luminescent carbon dots in noncoordinating solvents. *Chem Mater.* 2010;22(16):4528–30.
132. Wang X, Qu K, Xu B, Ren J, Qu X. Microwave assisted one-step green synthesis of cell-permeable multicolor photoluminescent carbon dots without surface passivation reagents. *J Mater Chem.* 2011;21(8).
133. El Essawy NA, Konsowa AH, Elnouby M, Farag HA. A novel one-step synthesis for carbon-based nanomaterials from polyethylene terephthalate (PET) bottles waste. *J Air Waste Manag Assoc.* 2017;67(3):358–70.
134. Ding C, Zhu A, Tian Y. Functional surface engineering of C-dots for fluorescent biosensing and in vivo bioimaging. *Acc Chem Res.* 2014;47(1):20–30.
135. Zhu S, Song Y, Zhao X, Shao J, Zhang J, Yang B. The photoluminescence mechanism in carbon dots (graphene quantum dots, carbon nanodots, and polymer dots): current state and future perspective. *Nano Res.* 2015;8(2):355–81.
136. Ma DL, Lin S, Wang W, Yang C, Leung CH. Luminescent chemosensors by using cyclometalated iridium(III) complexes and their applications. *Chem Sci.* 2017;8(2):878–89.
137. Liu J, Zhang P, Yang X, Wang K, Guo Q, Huang J, et al. Aptamer-mediated indirect quantum dot labeling and fluorescent imaging of target proteins in living cells. *Nanotechnology.* 2014;25(50): 505502.
138. DuChene JS, Sweeny BC, Johnston-Peck AC, Su D, Stach EA, Wei WD. Prolonged hot electron dynamics in plasmonic-metal/semiconductor heterostructures with implications for solar photocatalysis. *Angew Chem Int Ed Engl.* 2014;53(30):7887–91.
139. Wang N, Yu X, Zhang K, Mirkin CA, Li J. Upconversion nanoprobe for the ratiometric luminescent sensing of nitric oxide. *J Am Chem Soc.* 2017;139(36):12354–7.
140. Jiang Y, Wang M, Hardie J, Tonga GY, Ray M, Xu Q, et al. Chemically engineered nanoparticle-protein interface for real-time cellular oxidative stress monitoring. *Small.* 2016;12(28):3775–9.
141. Li H, Shao F-Q, Zou S-Y, Yang Q-J, Huang H, Feng J-J, et al. Microwave-assisted synthesis of N, P-doped carbon dots for fluorescent cell imaging. *Microchim Acta.* 2015;183(2):821–6.
142. Cai QY, Li J, Ge J, Zhang L, Hu YL, Li ZH, et al. A rapid fluorescence “switch-on” assay for glutathione detection by using carbon dots-MnO₂ nanocomposites. *Biosens Bioelectron.* 2015;72:31–6.
143. Dong Y, Pang H, Yang HB, Guo C, Shao J, Chi Y, et al. Carbon-based dots co-doped with nitrogen and sulfur for high quantum yield and excitation-independent emission. *Angew Chem Int Ed Engl.* 2013;52(30):7800–4.
144. Tang F, Wang C, Wang X, Li L. Facile synthesis of biocompatible fluorescent nanoparticles for cellular imaging and targeted detection of cancer cells. *ACS Appl Mater Interfaces.* 2015;7(45):25077–83.
145. Qiu J, Zhang R, Li J, Sang Y, Tang W, Rivera Gil P, et al. Fluorescent graphene quantum dots as traceable, pH-sensitive drug delivery systems. *Int J Nanomedicine.* 2015;10:6709–24.

146. Leamon CP, Low PS. Delivery of macromolecules into living cells: A method that exploits folate receptor endocytosis. *Proc Natl Acad Sci U S A*. 1991;88(13):5572–6.
147. Parker N, Turk MJ, Westrick E, Lewis JD, Low PS, Leamon CP. Folate receptor expression in carcinomas and normal tissues determined by a quantitative radioligand binding assay. *Anal Biochem*. 2005;338(2):284–93.
148. Song Y, Shi W, Chen W, Li X, Ma H. Fluorescent carbon nanodots conjugated with folic acid for distinguishing folate-receptor-positive cancer cells from normal cells. *J Mater Chem*. 2012;22(25).
149. Elliott RL, Head JF. Cancer: Tumor iron metabolism, mitochondrial dysfunction and tumor immunosuppression; “A tight partnership—Was warburg correct?” *J Cancer Ther*. 2012;03(04):278–311.
150. Tortorella S, Karagiannis TC. Transferrin receptor-mediated endocytosis: A useful target for cancer therapy. *J Membr Biol*. 2014;247(4):291–307.
151. Fritzer M, Barabas K, Szüts V, Berczi A, Szekeres T, Faulk WP, et al. Cytotoxicity of a transferrin-adriamycin conjugate to anthracycline-resistant cells. *Int J Cancer*. 1992;52(4):619–23.
152. Lubgan D, Jozwiak Z, Grabenbauer GG, Distel LV. Doxorubicin-transferrin conjugate selectively overcomes multidrug resistance in leukaemia cells. *Cell Mol Biol Lett*. 2009;14(1):113–27.
153. Fritzer M, Szekeres T, Szüts V, Jarayam HN, Goldenberg H. Cytotoxic effects of a doxorubicin-transferrin conjugate in multidrug-resistant KB cells. *Biochem Pharmacol*. 1996;51(4):489–93.

The Underlying Mechanism of Quantum Dot-Induced Apoptosis: Potential Application in Cancer Therapy



Jishu Mandal, Mriganka Mandal, Tamanna Mallick, and Samiran Mondal

Abstract Quantum dots (QDs) are a popular agent to use in a wide range of scientific and industrial applications because the molecules consist of an excellent biophysical and optical property, later varies with the compositions from a wide range of visible to infrared wavelength. Being an established fluorescent probe QDs are useful in the long-term, multiplexed and quantitative imaging and detection is governed wonderfully by QDs. Here we represent the present trends of the multidimensional use or applications of QDs in the field of biological science to achieve disease diagnostics, control over it and in particular cancer treatments and cellular mechanisms induced by QDs. The QDs are small in size with a high surface ratio, capable of potentially changing the therapeutic and pharmacological efficacy towards a good dimension of disease management. These are unique anti-cancer activities like apoptotic cell death and autophagy cell death, different types of molecular path-ways and mechanism of apoptosis has been focused hereafter application of quantum dots in various cell lines of malignant cells of mice and humans.

Keywords Quantum dots · Apoptosis · Cancer therapy

Jishu Mandal, Mriganka Mandal—Both the authors have equal contributions.

J. Mandal

CIF Division Biophysical Laboratory, CSIR-Indian Institute of Chemical Biology, 4, Raja S. C. Mullick Road, Kolkata, West Bengal 700032, India

M. Mandal

Department of Botany, Dr. Kanailal Bhattacharyya College, 15, Kona Road, Santragachi, Howrah, West Bengal 711104, India

T. Mallick

Department of Chemistry, Viswa Bharat University, Santiniketan, West Bengal 731235, India

S. Mondal (✉)

Department of Chemistry, Rammohan College, 102/1-Raja Rammohan Sarani, Kolkata, West Bengal 700009, India

e-mail: samiran1985@gmail.com; samiran@rammohancollege.ac.in

1 Introduction

One of the most important nano-particle which is used in cancer cell biology nowadays is quantum dots. The Quantum dots are semiconductor nanocrystal which is excited in different dimension three dimensions. In 1988 Alexia Ekimov and Louis E. Brus had discovered the importance of quantum dot significantly promoted fluorescent imaging in both in vitro and in vivo conditions. The discovery of quantum dots are still in the infancy stage, biologically it was first applied in 1998. The preparation of quantum dots is improved several times. Quantum dots are conjugated in different biologically active molecules to probe cancer. In breast cancer detection quantum dot is used for its binding nature with Her-2 marker on the surface of the malignant cells. In this case, the quantum dot is binds with immunoglobulin G and streptoviridin. Quantum dots are used in coupled with oligo-nucleotides for in situ hybridization. They can be binds with different biomolecules. These properties are used for the detection of cancer therapy, they have enabled their usages in targeting drug delivery. Quantum dots have different extraordinary binding capacities with the cellular molecules and give authentic florescent activity which is brighter than commonly used organic dyes like FITC, TRITC, RITC, etc. [1, 2]. Polyelectrolyte microcapsule interacts with cellular surface molecules which can be recognised by various antibodies then helps to drug internalization into the target cells. Quantum dots induce different cytotoxicity in various malignant cell lines. Oxidative stress is important for apoptotic cell death as well as necrotic cell death.

2 Properties of QDs

QDs are nanometre-sized crystalline clusters (3–10 nm) that are synthesized from a variety of semiconductor materials and also carbon like non-metal, for detailed reviews on the synthesis and properties of QDs see reference [3, 4]. Laboratory level synthesis of QDs in small scales, QDs retain some of the bulk properties of the material from which they are derived but also adopt new properties that directly depend on their size. In terms of photophysics, this translates into according to the composition-, shape- and size-dependent luminescence with absorption and emission band quality. The wavelength of the fluorescence depends strongly on the size of QDs.

Quantum dots (QDs) have an advanced effect on traditional fluorescence spectroscopy/organic molecular chromophore of scientific study over biology and biomedical science research, due to its unique optical electromagnetic response where ever it may be required for the application. The QDs are exhibiting size and composition-dependent optical and electronic properties i.e., these particles are ultra-electronic and varies in size of 1.5–10 nm in dimensions. In recent science, the QDs are successfully been introduced into many kinds of applications including biology and medical science also. QDs have several advantages like a size-dependent optoelectric agent, high extinction coefficient, brightness and large stokes shifts. It

generates a large surface area that allows binding various kinds of molecules to deliver the target place.

QDs of most semiconductor metal ions are not safe for the body or organs of a target, in some reports people showed that small or zwitterionic QDs can be excreted into the urine to safeguard the body while the experiment was done in mice model, but in contrary QDs are not going out of the body in most of the cases of semiconductor, metals. We have two major pathways of out of QDs from the body are through the urine while another is liver's biliary systems into faeces.

3 Apoptosis: A Basic Biological Phenomenon

Cell death is the default. But deliberate attempt to attain death or initiate processes leading to self-destruction is known as suicide. In case of suicide in human beings it is considered as either impulsive or irrational, not in balanced behaviour. But suicidal cell death is pervasive and organised as well as rational in stress condition. In case of multicellular organisms homeostasis is maintained by suicidal cell death, where ordered metabolic changes are happened in normal development, environmental stress as well as in pathogenic attack. This gene regulated cell suicidal process is called apoptosis [5]. Apoptosis is thus a process of deliberate life sacrifice by a cell. A sequential series of biochemical series is happened during apoptosis process. The cell suicidal phase is occurred in such a way that all cellular fragments and cell corpses are removed very safely [6]. In normal multicellular life number of cells must be constant and it is maintained by cell division and death. Cells must be replaced when they become diseased or malfunctioning; but proliferation must be compensated by cell death [7]. Homeostasis is a part of living organisms, it necessary to keep the balance state to stable the multicellular organisms. So, it is only maintained simultaneously by cell division and death.

3.1 Characteristics of Cell Apoptosis

A cell undergoing apoptosis shows a characteristic morphology that can be observed with a microscope (Fig. 1) [8].

- (i) Cytoskeleton proteins break down after activation of caspase, and then cell shrinks which are the hall marks of apoptosis.
- (ii) Cellular organelles tightened and cytoplasm becomes dense.
- (iii) Chromatin condensation in nucleus occurs, it is known as pyknosis; important hall marks of apoptosis [9].
- (iv) The nuclear covering breaks down; inside it DNA fragmented which is known as karyorrhexis, another features of apoptosis [10].
- (v) The cell membrane shows irregular buds known as blebs.

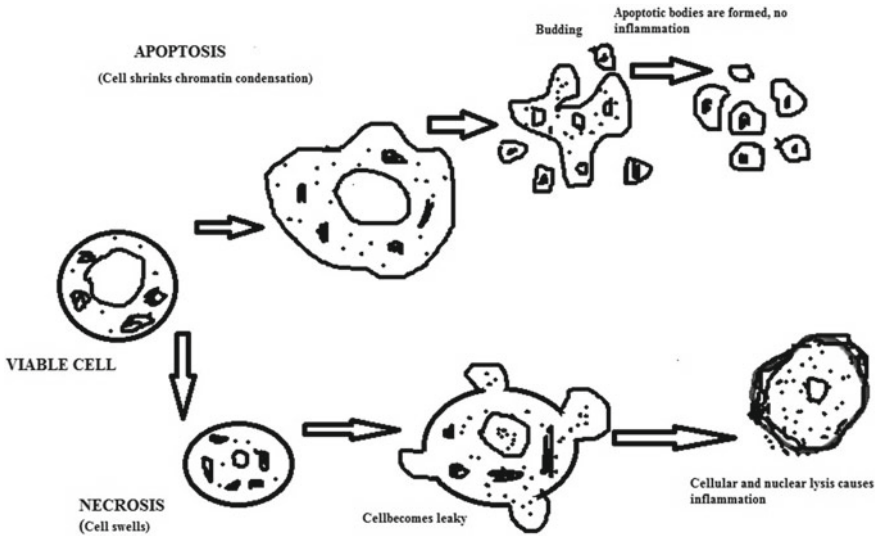


Fig. 1 Morphology of cells under apoptosis at the various stages

- (vi) Apoptotic bodies are formed due to cell breaks, these apoptotic bodies later phagocytosed.

3.2 Intrinsic and Extrinsic Apoptotic Pathways

The death signals are linked to the execution programmes via an integration stage, which acts as a control stage. It uses both positive and negative regulatory molecules which will ‘inhibit, stimulate or forestall apoptosis’ i.e. determining whether the cell is committed to death or allowed to live. Two main integration pathways exist and converge to a common execution phase: (i) the extrinsic apoptotic pathway; and (ii) the intrinsic apoptotic pathway.

I. The extrinsic apoptotic pathway (Fig. 2)

This pathway is typically engaged in the immune system and is the process used to delete activated T-cells at the end of an immune response. It is triggered by the death factors e.g. TNF, Fas L (Fas Ligand) binding with the death-receptor superfamily e.g. TNF receptor (TNFR) and Fas receptor (also known as Apo-1 or CD95) [11]. Binding to the receptor induces receptors to cluster and trimerise. FADD (Fas-associated death domain) protein is engaged through the death domains. The DED (death effector domain) of FADD recruits pro-caspase 8 via its DED. The complex brings multiple pro-caspase 8 molecules in close proximity, leading to their activation through ‘induced proximity’ (the aggregation of pro-caspase 8 molecules results in their cross-activation). This is

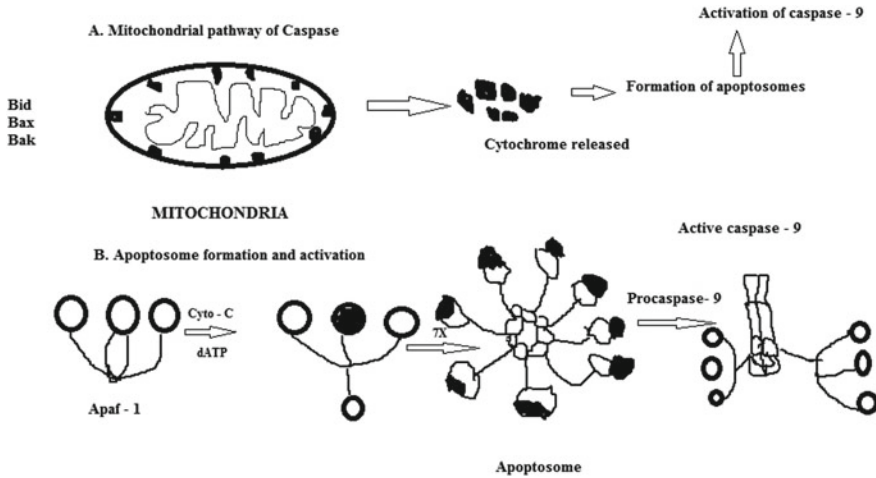


Fig. 2 Caspase activation in the extrinsic apoptotic pathway

the death-inducing signalling complex (DISC). Activated caspase-8 (a heterotetramer) is released from DISC into the cytoplasm where it functions as an initiator caspase, activating downstream executioner caspase, primarily via pro-caspase-3. Few number of cells (type I) caspase—8 is directly initiated the apoptosis process by activating other caspase proteins and then apoptotic cell death takes pace. The Fas—DISC in some cells (type II) forms a loop which is responsible for releasing some proapoptotic factors from mitochondria. These proapoptotic factors increased the activity of caspase-8 [11]. In case of mammal cells proapoptotic factors (BAX, BID, BAK or BAD) [12] and some anti apoptotic factors (Bcl-Xl and Bcl-2) simultaneously maintained a balance which is proportion to homodimers of proapoptotic factors established on outer membrane of mitochondria.

II. **The intrinsic apoptotic pathway**

The mitochondria are essential to multicellular life, without them a cell ceases to respire aerobically and quickly dies—a fact exploited by some apoptotic pathways (Fig. 3). The mitochondrial pathway is usually activated in response to lethal stimuli such as DNA damage, oxidative stress and hypoxia [13]. Apoptotic proteins which target mitochondria affect them in different ways; they may cause mitochondrial swelling through the formation of membrane pores, or they may increase the permeability of the mitochondrial membrane and cause apoptotic effectors to leak [14]. Mitochondria contain pro-apoptotic factors such as cytochrome c and apoptosis-inducing factors (AIF). These are harmless whilst safely sequestered within the mitochondria but lend to activation of the caspase cascade once released into the cytoplasm. Cytochrome c is released from mitochondria due to increased permeability of the outer mitochondrial membrane and serves a regulatory function as it precedes morphological change

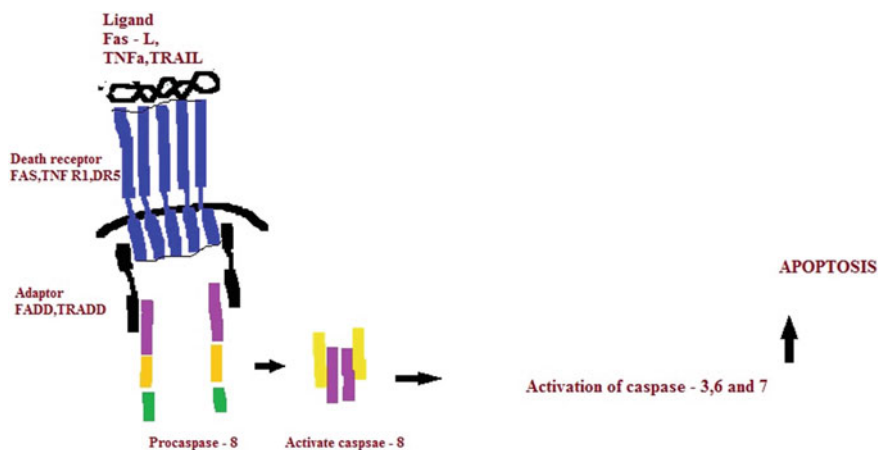


Fig. 3 Caspase activation in the intrinsic apoptotic pathway

associated with apoptosis [14]. The Bcl-2 family members control the release of cytochrome c etc. The family consists of pro- and anti-apoptotic members, which regulates mitochondrial ‘pores’ by an as yet uncharacterized mechanism. Bcl-2 proteins can promote or inhibit apoptosis by either direct action on mitochondrial permeability, or indirectly through other proteins. Importantly, the actions of some Bcl-2 proteins can halt apoptosis even if cytochrome C has been released by the mitochondria coupled to extrinsic signals [14]. Cytochrome C associates with both apoptosis protease activating factor-1 (Apaf-1) and procaspase-9 to form active caspase-9. The active enzyme complex is called the apoptosome. Mitochondrial proteins known as SMACs (second mitochondria-derived activator of caspases) are also released into the cytosol following an increase in permeability.

4 Applications of QDs and Their Potential Toxicity

4.1 Quantum Dots Induced Cell Death

Recent studies have shown that Quantum dots induce toxicity modified by an antioxidant N-acetyl cysteine which up-regulates the Fas receptors, lipid peroxidation and breakdown of mitochondrial membrane potential [15]. In this context, the graphene quantum dot has special attention for autophagy and apoptotic death in different cell lines. It has been found that graphene quantum dot induces cell death in human glioma cells U251 by creating oxidative stress. The photoexcited graphene quantum dots (GQD) are produced by electrochemical oxidation of graphites with an average particle diameter 56.6 ± 8.7 which induce ROS generation inside the cell. GQD

have the highest luminescence 460 nm this photoluminescence enhances the oxidative stress into the cell [12]. They observed that temperature did not increase in cell suspension after photo excitation of GQD. So, it was clear that this material did not show any toxicity into the cell. After the irradiation with GQD the apoptotic cell death occurs when it was justified by FACS analysis, numbers of both early (propidium iodide) and late (propidium iodide) apoptotic cells expressing phosphatidylserine (Annexin+). DNA fragmentation in sub G level during cell cycle observed. Activation of a caspase protein family involved after photo excitation of GQD component [12]. Mitochondrial membrane potential breaks down are another phenomenon for apoptotic cell death [16], after the application of photo excited GQD they also showed the mitochondrial membrane potential breakdown in human glioma cell line U251. Another cell death-like autophagy also they have noticed after irradiation by photo excited GQD. This type 2 cell death is also related to the photo excited GQD. According to this experiment, hairpin RNA was used for silencing the autophagy essential protein. After irradiation by photo excited GQD cells were significantly protected by the irradiation.

4.2 In Osteosarcoma Cell Line Carbon Dot Induces Apoptotic Cell Death

Carbon-based nanoparticles are very crucial for biomedicine nowadays in several complicated disease treatments like cancer. These carbon-based nanoparticles are more effective than any other nanoparticle due to their low cost, low toxicity, compatibility with living cells and easily penetrating through the cell membrane [17]. The osteosarcoma cell line 143B showed the effective apoptotic cell death after the treatment of carbon-based nanoparticles (CQDs) in particular doses. At highest doses (276 $\mu\text{g/ml}$) cell death occurred very significantly. Mitochondrial membrane potential breakdown is an important phenomenon for apoptotic cell death [18]. CQDs play the master role for mitochondrial membrane potential breakdown and induce ROS generation. This carbon-based nanoparticle showed the dose-dependent mitochondrial dysfunction and breakdown of MMP [19].

Inhibition of tumour growth was noticed after the treatment of these CQDs in mice (276 $\mu\text{g/ml}$). After the treatment by 4 weeks, a significant decrease of tumour volume was noticed without a significant change of body weight of mice [19]. Some anti apoptotic proteins like Bcl2, Bcl—XL inhibit cell death when they bind with proapoptotic proteins like caspase—3. Caspase -3 is known as important protein factor; it is cleaved and activated during apoptosis [20]. Caspase-3, then several types of cellular factors are also cleaved, among this PARP is an important factor it acts as a DNA repairing unit. So, cleaved PARP is a important apoptotic marker [21].

4.3 A Carbon Dot Induces DNA Damage and Cell Cycle Arrest in MCF7 (Breast Cancer Cell Line)

Due to the intrinsic fluorescence properties, carbon dots have a great attention for studying cell death in various cancer cell lines. Even anti-tumour activity has also been recorded by several researchers' in vivo studies. The excellent biocompatible nature of this carbon dots compound gives it a special interest for cytotoxicity in the different malignant cells. Recently carbon dots showed the real-time cytotoxicity of super tiny CDs (2.05 ± 0.22 nm) in human breast cancer cell MCF7 [22]. In their study, they have shown that tiny particles of carbon dots affect the viability of MCF7 cells and HDFa cells together induced genotoxicity, cell cycle progression, and clastogenicity of these cell lines. They showed that the highest concentration of CDs did not show any cytotoxic effects on a normal cell. In this case, cell cycle arrest was happened in G_0/G_1 phase respectively and induces apoptosis and dramatic changes took place after the treatment of CDs in different doses in MCF7 cells. A significant increase of DNA damage i.e. clastogenic has occurred at 48 h after the treatment of CDs.

4.4 Quantum Dots Induces Apoptotic Biochemical Changes in Human Neuroblastoma Cells (IMR32)

We have already learnt that quantum dots have typical luminescence properties, for this reason, quantum dots are used in the different cell lines to show the mechanism of cell death. It has been demonstrated that QD treated neuroblastoma cells undergoes apoptosis after their treatment in a dose-dependent manner [23].

4.5 Animated Graphene QDs Uptake by Alveolar Macrophage of Rat Cells Induced Cell Death

Graphene Quantum dots are the smallest in size, they can be easily entered through the cells and they showed less cytotoxicity in normal cells. Due to their excellent stable photoluminescence, chemical inertness, and compatible functionalization with biomolecules, they are extensively used in different biomedical research purposes. Animated graphene QDs are a very effective agent of DNA damage and proapoptotic death of alveolar macrophage cells of rats. It has been shown that 100 and 200 $\mu\text{g/ml}$ concentrations of AG-QD (animated graphene quantum dots showed very effective results in cell death. Animated graphene quantum dots entered through the nuclear pore complex and interacts with the DNA chain, as a result, a significant breakdown of DNA in different sizes occurred.

4.6 Multi-walled Carbon Nano Tubes (MWCNTs) Induced Apoptosis in Pancreatic Cancer Cells

Pancreatic cancer is the most serious disease where the survival rate of the patient is only 5%. It has been investigated by some researchers that thermally active multi-walled carbon nanotubes gave promising results after the treatment of these polyethene glycated carbon nanotubes on pancreatic cancer cells (PANC-1). It was justified from molecular and cellular parameters. The polyether compound (PEG) is used to coat the particles in different medicine to increase their biocompatibility. There are many data about laser-induced carbon-based materials photo-excitation to generate necrosis of malignant cells [24]. All the data have shown that laser-induced carbon-based materials cause thermal-based necrotic cell death. Carbon nanotube mediated necrotic cell death after laser induction converted photo energy to heat energy in cancer cells of a tumour. In this experiment, it has been shown that multi-walled carbon nanotubes induce apoptosis in the pancreatic cancer cell (PANC-1) [25]. Many chemotherapeutics are used for the treatment of cancer based on the breakdown of mitochondrial membrane potential and induces ROS generation, which ultimately causes apoptotic cell death. In this experiment, the above group have shown that MWCNTs combined with laser beam induces apoptosis by activating early apoptotic pathway. Internalization of CTNs into the pancreatic cells produces oxidative stress inside it; flow cytometric analysis showed that ROS generation occurred in a dose-dependent manner. These groups studied that ROS generated cells were less in case of control (0.2%), in 5 $\mu\text{g/ml}$ it was 36.2% and in 10 $\mu\text{g/ml}$ concentration ROS generated cells were 50%. Exposer of a laser beam (3 min, 808 nm, 2 W/cm^2) followed by the treatment of MWCNTs. showed the breakdown of mitochondrial membrane potentiality. Where they have shown that at 50 $\mu\text{g/ml}$ concentration MWCNTs maximum cells have green fluorescent which is the indication of mitochondrial electron transport chain disruption.

4.7 Cytotoxic Effects of Copper Quantum Dots

Copper oxide quantum dot has cytotoxic effects on the different cell lines. It has been shown that copper oxide quantum dot induces apoptosis in different caspase-mediated pathways in mouse cell line C2C12. The CuO-quantum dots were synthesized by using copper acetate and hexamethylenetetramine. Quantum dots are very tiny particles which are having strong fluorescence properties without any photobleaching [26]. Copper metals have a very important use in different fields over centuries like disinfectants of drinking water, solids and human tissues [27]. It has been shown caspase—3 and—7 are the key mediators for apoptotic cell death [28]. CuO quantum dots have cytotoxicity in a dose-dependent manner in the case of C2C12 mice cells [29]. They have also shown that at the high dose of CuO quantum dot (20 $\mu\text{g/ml}$) cells become shrinks and lost their original shape. The expressions of

caspases were also evaluated by them followed by the RT-PCR method. Treatment of CuO quantum dots at the highest level (20 $\mu\text{g/ml}$). Metal oxide has potential effects on DNA damage [30, 31]. This research group has extensively studied the DNA damage after the treatment of CuO quantum dots. In this study mouse myoblast cells C2C12 have demonstrated that copper oxide quantum dots have potential biological activity for the breaking of DNA via caspase-mediated pathways. So, cytotoxicity effects of metal oxide quantum dots are very important for the treatment of tumour prognosis, and especially in the field of biomedical research like treatment of cancer for prospects.

4.8 Cadmium Telluride Quantum Dots Induces Apoptotic Cell Death in Human Umbilical Vein Endothelial Cells

Semiconductor quantum dots have excellent fluorescent properties, they have wide spectra range properties and 1000 times brighter and narrower emission. Many researchers have established intercellular tracking and biomedical diagnosis and drug designing by utilizing these types of nanoparticles. QDs are important for biodistribution, drug transportation through the vascular system. Due to their multicolour, multiplex nature in different vascular systems researchers can be able to identify easily the intricate blood circulation networks within organs and tissues. Endothelial cells of the vascular system are very important for the entry of different drugs, toxicants and other pathogens like bacteria and viruses. When QDs injected, it directly interacts with the luminal surface of endothelial cells (EC). QDs would also expect the cellular dysfunction of different organs. Endothelial cells also maintain homeostasis through the secretion of vasoactive factors, which regulates angiogenesis, thrombosis and atherogenesis etc. [32]. Different types of cytotoxic and pathological conditions may arise due to the exposure of QDs on endothelial cell lumen and cause ER stress. The ER stress activates different kinds of factors like protein kinase, RNA like ER-kinase (PERK), activating transcription factors. In severe cases, ER stress causes cellular damage, and then damaged cells are eliminated by apoptosis. In human umbilical vein ECs (HUVECs) cadmium telluride quantum dots causes cell hazards after treatment of these QDs [33]. This group showed that the average size of cadmium telluride QDs (3.492 ± 0.87 nm) had symmetrical emission spectra near about 60 nm and the emission peak was 599 nm with negatively charged carboxyl groups. The treatment of CdTe QDs in different doses on HUVECs cell line like 0, 1, 10, 20 and 50 $\mu\text{g/ml}$ the percentage of CdTe QDs holding into the cell were increased both dose and time-dependent manner. They have evaluated cytotoxicity in different ways. However, they have shown that ER stress is the key point of cellular damage in the case of HUVECs cell lines. According to their proposed model ER stress activates the transmembrane PERK factor, the eIF2 α phosphorylated by PERK. Then it introduces the apoptosis signalling pathways by activating ATF3 and CHOP/GADD153 genes. As earlier, it has been explored that transmembrane effector PERK bypass the

ATF4 factor and eIF2 α phosphorylation, which initiates the apoptosis signalling pathways [34]. Some genes like ATF3 and CHOP/GADD153 are responsible for apoptosis. This group also demands that CdTe QDs mediated apoptosis in this HUVECs cell by the involvement of before mentioned factors. As a whole, they concluded that CdTe QDs mediated cell death and the level of toxicity revealed the potential cytotoxic effects on HUVECs cells especially the risk factors for future use of this cadmium telluride QDs in the different biological research fields.

4.9 Nitrogen Phosphorus Doped Carbon Dots Regulates Apoptosis and Autophagy in B16F10 Mouse Melanoma Cells Imaging Application

Melanoma is a highly dreadful cancer in the malignant stage; there are no drugs to treat this malignant melanoma. It occurs worldwide only 4% but 80% of death is occurred due to skin cancer [35]. All drugs which are used for treating skin cancer has adverse effects and cytotoxicity in a normal cell. The nitrogen phosphorus-doped carbon dots have a very effective role. The multi emissive carbon QDs has a very good potential for imaging purpose due to their core structure and with rich surface functional species [36]. The properties of CDs can be increased in different ways, like doping by heteroatom or metal ion (e.g. with N, B, P etc.) individually [37], or multiple doping can be effective for this purpose [38]. Nitrogen and phosphorus doping gives the carbon dots specific physiochemical properties that are surface defects which are improved the optical properties [39]. The multi heteroatom (N-P) co-doped CDs (NPCDs) in which single-step thermal treatment was applied in this experiment [40]. They used imidazole as the source of N, Phosphoric acid as a source of P and polyethene glycol as a carbon precursor [40] and explored the anti-cancer activity of Nitrogen phosphorus-doped carbon dots (NPCDs) in mouse melanoma cell line B16F10 as well as cellular bioimaging properties in vitro system. Nitrogen phosphorus-doped carbon dots showed highly anticancer activity in different doses (1–120 $\mu\text{l/ml}$) as per the experiment by this group. At 30.01 $\mu\text{l/ml}$ dose of NPCDs showed 50% cell death so, it was the inhibitory concentration (IC_{50}) in B16F10 cell of this NPCDs. The chromatin fragmentation and DNA damage are the important phenomena of apoptotic cell death which was justified by them, 3030.01 $\mu\text{l/ml}$ dose of NPCDs showed chromatin fragmentation. In some normal cells like human keratinocytes (HCATs) and lung epithelial cells (BEAS-2B), these NPCDs had no adverse effects than melanoma cells (B16F10). Another important phenomenon which was found that autophagy induced by NPCDs, after the treatment of NPCDs autophagosome was formed. Thus their works also demand that cytotoxicity had happened in B16F10 melanoma cells. The expression of some important markers and their level has been also recorded by them, like LC3 (microtubule-associated protein 1A/1B-light chain 3), it was noticed that dose-dependent elevation of the LC3-phosphatidylethanolamine (LC3-II) expression.

4.9.1 Applications of QDs in the Direct Biological Approach

i. **QDs are a good drug delivery agent: pharmaceutical research**

Doxorubicin hydrochloride (Dox) is a known agent as a breast cancer drug; this was targeted to conjugate with CQDs for the delivery of the drug as an in-vitro model. Here the CQDs were synthesized by citric acid carbonization and modified by transferrin TF, here TF has a crucial role to increase the interaction of target cell receptors and increasing water solubility so that it can use in the biological process. To understand the cytotoxicity potential of Dox-TF-CQDs complex, the MCF-7 cell line was used by MD. Mahani et al. [41], showed that the MTT assay responds as more decrease the cell viability than TF-CQDs or Dox alone. The study also confirmed that the TF-CQDs have more efficiently endocytosed by MCF-7 cell line than the Dox alone. The study suggests that the CQDs induced by TF are a good drug delivery agent for Dox to in-vitro level delivery.

ii. **In life science research**

QDs are biologically functional when this is treated by some favourite ways to achieve some of the basic properties of Long-period stability in water [15, 42], 1. Presence of sterically active group for biological molecule combinations 2. It should have consisted of biologically compatible and non-immunogenicity property 3. There should be an interference lack of biomolecules with the basic properties of QDs.

Long-term observation of cellular trafficking, high resolution of cellular imaging [39]. intracellular process study of single-molecule level. Study of tumour trafficking and propagations as a part of tumour diagnostics also as in other animals.

ECL i.e. electrochemiluminescence of functional QDs in the application of DNA analysis, immunoassay, cytosensing also finding of different biomolecules in samples of a variety of origins.

A wide range of applications of QDs has emerged in modern sciences including biological and medical filed in imaging, flow cytometry, photodynamic therapy, drug delivery tissue mapping and demarcation etc.

Environment and bio-defence fields are also growing on the technologies of quantum dots nanoparticles based responses. However, the main focus of this chapter is to discuss the applications of quantum dots mainly in biomedical science, here some modern applications have been discussed for the readers.

Bio defence: In the traditional way involves identifying the pathogen by isolation and multiplication is requires time. In-vivo method of streptavidin quoted quantum dots that identify the pathogen very quickly a recent study has been found. The bacterial like Mycobacterium, *Bacillus Anthracis* are highly infectious, which can detect by the streptavidin quoted QDs from a sample very quickly and even more than one pathogen by the respective pathogen each

quoted with different QDs of different emission colours simultaneously [42] i.e. broad of applicability with good sensitivity also.

iii. **Biomedical imaging applications**

QDs-based immune fluorescence histochemistry (QDs-IHC) and conventional immune-histochemistry (IHC) techniques to perform a retrospective analysis on paraffin-embedded tissues of gastric biopsies of different patients were HP positive and negative as well. The HP i.e. *Helicobacter pylori* detection goes to the success of 99.1 to 100% success, QDs IHC based method has high sensitivity than that of other traditional methods which makes easier the diagnosis [43].

In the field of biomedical science, why it is emerging important to use QDs as there is a great extent of advantages over the traditional one like as it has (a) High bright photoelectron emission (b) Highly resistant to photobleaching (c) Emission spectra having the quality to optimize size quantization effect d. Simultaneous detection of multiple signals using a single excitation source. In the very precise and specifically it is can be mentioned that QDs are characterized by broad absorption spectra, composition tunable, size-tunable finally shows light fluorescence with a challenging disadvantage of the same is its property of biotoxicity.

Traditional OLEDs of fluorescent or phosphorescent emitters cannot emit the intensity of light in various wavelength windows of photomedicine than newly developed ultrabright and more active quantum dots light-emitting devices (QLEDs). A recently developed quantum dot light-emitting device QLED-based photo medical approach proves increased cell metabolism in a control system of PBK (PBZ binding kinase) and kills cancer cells effectively for PDT (photodynamic therapy) [44].

Modern photodynamic therapy is becoming a more important therapeutic for localized cancer proliferation in the body. The mechanism of PDT induced treatment of cancer cells is simply killing through oxidative stress produced by highly cytotoxic Reactive Oxygen Species (RSO), which is created by PS at its activated state.

iv. **Carbon quantum dots CQDs**

Carbon dot nanoparticles are now in tremendous interest in the various sectors of science including the energy sector as a large quantity. The Se, Ga, Cd, mediated QDs are not biologically compatible and the applications of the same in biology or medical science has proven cell cytotoxicity at a particular level of concentration into the cell is very low even. To avoid this limitation CQDs is one of the best alternative agents to the QDs filed. These CQDs has been various advanced properties which have already been discussed here earlier and the device or drug whichever it is required to improve and develop more precisely, therefore the field attracts rapid high-quality research in this area to well understand the optical property of CQDs.

v. **CQDs are potentially used in biomedical science**

Carbon dot nanoparticles are now in tremendous interest in the various sectors of science including the energy sector as a large quantity. The Se, Ga, Cd,

mediated QDs are not biologically compatible and the applications of the same in biology or medical science has proven cell cytotoxicity at a particular level of concentration into the cell is very low even. To avoid this limitation CQDs is one of the best alternative agents to QDs filed. These CQDs has been various advanced properties which have already been discussed here earlier and the device or drug whichever it is required to improve for the development of more precisely, therefore the field attracts rapid high-quality research in this area to well understand the optical property of CQDs.

Carbon-based quantum dots to the treatment of haemorrhage. A recent study has been established that Pollen Typhae Carbonisata PTC is a typically calcine drug used as a treatment of haemorrhage. These PTC quantum dots are prepared by using air drying at 50 °C for 2 h followed by heating with a muffle furnace for 1 h at 350 °C then cooled to normal temperature and grounded to fine particles. To ensure the effectiveness of this PTC quantum dots effect to haemorrhage treatment mouse tail amputation and liver scratch model was used by the workers and they found a significant decrease in bleeding time while the PTC based QDs applied to the mouse injury.

The study admits that the PTC based QDs are a very excellent agent for controlling the haemorrhage in the outer epithelial aperture of skins in different places of the body. A preliminary evaluation of the finding behind the coagulation of blood to the haemorrhage was justified on the basis of PTC based CQDs coagulation parameters were measured which admits that it was both endogenous coagulation pathway and exogenous coagulation pathway of binding PTC with blood serum. It is worthy to mention here that the carbon-based QDs have some advantages to their biological compatibility like non-toxic to a biological system, inert to chemicals of not under interest to the applications, it is very cheap.

In the aim of modern medical biology, scientists are focusing the applications of CQDs are mainly on the objectives of bio-imaging systems and drug delivery systems due to the biocompatibility and inert to a biological system that acts as a non-toxic substance. Here the understanding of the binding and delivery mechanism of CQDs is important to work more in this field.

vi. **Disease detection and diagnostics using CQDs**

An in-vivo biomedical application is new in the field of QDs nano-particles. The major goal of biological imaging is to build up the image contrast due to the molecular dissimilarities in the different tissues or organs and even species to species.

Use of hydrophilic silicon quantum dots as a biological imaging agent in an in-vivo imaging agent. For a tumour containing imaging system, a specific antibody coupled with near-IR QDs having a polymer layer is efficient to give a particular image with good resolutions, such QDs are extensively used for in-vivo imaging techniques. The present challenge of scientists to create a good resolution image for macro and microstructures using the QDs, for this quantity of CD released in the region of the cell is reduced.

Imaging of tissues into the deep of the body for better diagnostics of disease: The development of early detection methods stimulates the prevention of several kinds of tumours that are a threat to health.

5-FU (5-fluorouracil) is a well-known chemotherapeutic drug for colorectal cancer (CRC) also this is possible to combine easily with β -cyclodextrin so that it forms an effective inclusion complex [45]. 5-FU can be combined effectively to form an inclusion complex with β -cyclodextrin and mi-R34a (m) into a TCPI-CD quantum dot nanocarrier effective to inhibit the growth of patient drive tumorigenic graft, a type of tumour growth in human [46] a recent study has been found, the drug can be effectively administered to the collateral cancer cells. The drug invades in this process to use QDs has been found more efficient target delivery. A collateral cancer cell targeting QDs was designed by the self-assembly of host-guest based interaction.

vii. **Applications of QDs in medical science**

This section is a volatile area of continuously under development and challenges in new threats of health concern of not only mankind but the other planetary inhabitant as well. In medical science, early detection of pathogens is an important key to the health management of patients. The integration of QDs and gene identification is a brilliant approach here.

Viral infection diagnosis by nano-particles of Quantum Dot

SarS-CoV-2 was a major threat there was at the time an urgent need emerged for the scientists to detect the virus rapidly to individuals so that major precaution may be taken. The normal process was going through antibody-based detection i.e., ELISA test. Now carbon-based QDs has been developed to detect the pathogen even within 5 min, this QDs have moderate sensitivity and selectivity so that it can be done easily on another side it has a very low cost also afford all concern. The process of detection of microbes using Carbon QDs based nanomaterial is very simple and there are no chances of shortage of the materials for the purpose. Several methods have been developed for the preparation of carbon base QDs like electrochemical carbonization, microwave base irradiation, hydrothermal solvo-thermal based treatments.

The carbonaceous aggregation is one of the major hurdles during the synthesis of the material for this kind of experiment. This Carbon-based QDs have good quality over the materials are it is an excellent water solvent so easy to use biologically, there is no effect of photo-bleaching over this CQDs, it is a good chemical resistant i.e. inert to the chemicals, high-quality luminescence signals which can be treated the virus and use to detection also [47].

Challenges of QDs: Removal of QDs after the application to the body is a big problem as mentioned earlier in this article, besides that some QDs are very toxic at a certain level like CdQDs, CuQDs, ZnQDs which may restrict the metabolic functions after a certain level of its invasion. A more rigorous study is required to fabricate the non-toxic like CQDs agent to replace a toxic effect of QDs. Some of the QDs have limitations of biological tagging and overlapping of the molecular property of target molecules.

5 Conclusions

QDs are an emerging new therapeutic in medical sciences and in biology research it also can reveal a new horizon especially imaging of the tissues, cells etc. Carbon quantum dots are an alternate way to overcome the challenges of the biocompatibility of QDs. More research is required to the quantum dots to find out more effective utilization to biology and medical science. More modern techniques and methods can be used to formulate, characterization, and selection of target molecules, selection of QDs to be used for bio conjugate that can go successfully to the target cell.

References

1. Gao H, Sapelkin AV, Titirici MM, Sukhorukov GB. In situ synthesis of fluorescent carbon dots/polyelectrolyte nanocomposite microcapsules with reduced permeability and ultrasound sensitivity. *ACS Nano*. 2016;10:9608–15. <https://doi.org/10.1021/acsnano.6b05088>.
2. Gaponik N, Radtchenko IL, Sukhorukov GB, Rogach AL. Luminescent polymer microcapsules addressable by a magnetic field. *Langmuir*. 2004;20:1449–52. <https://doi.org/10.1021/la035914o>.
3. Luo PG, Sahu S, Yang ST, Sonkar SK, Wang J, Wang H, LeCroy GE, Cao L, Sun YP. Carbon “quantum” dots for optical bioimaging. *J Mater Chem B* 2013; 1:116–2127.
4. Huang G, Lin Y, Zhang L, Yan Z, Wang Y, Liu Y. Synthesis of Sulfur-Selenium Doped Carbon Quantum Dots for Biological Imaging and Scavenging Reactive Oxygen Species *Scientific Reports*, 2019 9:19651.
5. Kerr JF, Wyllie AH, Currie AR. Apoptosis: A basic biological phenomenon with wide ranging implications in tissue kinetics. *Br J Cancer*. 1972;26:239–57.
6. Marx J. Cell death studies yield cancer clues. *Science* (Washington DC). 1993;259:760–2.
7. Thompson CB. Apoptosis in the pathogenesis and treatment of disease. *Science*. 1995;267:1456–62.
8. Saraste A, Pulkki K. Morphological and biochemical hall marks of apoptosis. *Cardiovasc Res*. 2000;45:528–37.
9. Sartorius U, Schmitz I, Krammer PH. Molecular mechanisms of death-receptor-mediated apoptosis. *ChemBioChem*. 2001;2(1):20–9.
10. Enari M, Talanian RV, Wong WW, Nagata S. Sequential activation of ICE-like and CPP32-like proteases during Fas-mediated apoptosis. *Nature*. 1996;380(6576):723–6.
11. Wajant H, Pathway TFS. More than a paradigm. *Science*. 2002;296:1635.
12. Murphy KM, Ranganathan V, Farnsworth ML, Kavallaris M, Lock RB. Bcl-2 inhibits Bax translocation from cytosol to mitochondria during drug-induced apoptosis of human tumour cells. *Cell Death Differ*. 2000;7(1):102–11.
13. Rich T, Allen RL, Wylie AH. Defying death after DNA damage. *Nature*. 2000;407:777–83.
14. Cotran, Kumar, Collins. Robbins pathologic basis of disease, 7th ed. Philadelphia: W.B Saunders Company; 2005. 0-7216-7335-X.
15. Choi AO, Cho SJ, Desbarats J, Lovrić J, Maysinger D. *J Nanobiotechnol*. 2007.
16. Elmore S. Apoptosis: A review of programmed cell death. *Toxicol Pathol*. 2007;35:495–516.
17. Kesharwani P, Mishra V, Jain NK. Validating the anticancer potential of carbon-nanotube-based therapeutics through cell line testing. *Drug Discovery Today*. 2015;20(9):1049–60.
18. Sinha K, Das J, Pal PB, Sil PC. Oxidative stress: the mitochondria-dependent and mitochondria-independent pathways of apoptosis. *Arch Toxicol*. 2013;87(7):1157–80.
19. Jiao Y, Guo Y, Fan Y, Wang R, Li X, Wu H, Meng Z, Yang X, Cui Y, Liu H, Pan L. Triggering of apoptosis in osteosarcoma 143B cell line by carbon quantum dots via the mitochondrial apoptotic signal pathway. 2020.

20. Liu B, Jian Z, Li Q, Li K, Wang Z, Liu L, Tang L, Yi X, Wang H, Li C, Gao T. Baicalein protects human melanocytes from H₂O₂-induced apoptosis via inhibiting mitochondria-dependent caspase activation and the p38 MAPK pathway. *Free Radical Biol Med.* 2012;53(2):183–93.
21. Danial NN. BCL-2 family proteins: Critical checkpoints of apoptotic cell death. *Clin Cancer Res.* 2007;13(24):7254–63.
22. Şimşek S, Şüküroğlu AA, Yetkin D, Özbek B, Battal D, Genç R. DNA-damage and cell cycle arrest initiated anti-cancer potency of super tiny carbon dots on MCF7 cell line. *Sci Rep.* 2020;10:13880. Published online 2020 Aug 17. <https://doi.org/10.1038/s41598-020-70796-3>.
23. Chan WH, Shiao NH, Lu PZ. CdSe quantum dots induce apoptosis in human neuroblastoma cells via mitochondrial-dependent pathways and inhibition of survival signals; 2006.
24. Shen S, Ren J, Zhu X, Pang Z, Lu X, Deng C, Zhang R, et al. Monodisperse magnetites anchored onto carbon nanotubes: A platform for cell imaging, magnetic manipulation and enhanced photothermal treatment of tumors. *J Mater Chem B.* 2013;1(14):1939–46.
25. Mocan T, Matea CT, Cojocaru I, Ilie I, Tabaran FA, Zaharie F, Cornel I, Dana B, Mocan L. Photothermal treatment of human pancreatic cancer using PEGylated multi-walled carbon nanotubes induces apoptosis by triggering mitochondrial membrane depolarization mechanism. *J Cancer.* 2014;5(8):679.
26. Michalet X, Pinaud FF, Bentolila LA, Tsay JM, Doose S, Li JJ, Sundaresan G, Wu AM, Gambhir SS, Weiss S. Quantum dots for live cells, in vivo imaging, and diagnostics. *Science.* 2005;307:538–44.
27. Dollwet HHA, Sorenson JRJ. Historic uses of copper compounds in medicine. *Trace Elem Med.* 1985;2(2):80–7.
28. Lakhani SA, Masud A, Kuida K, Porter GA Jr, Booth GJ, Mehal WZ, Inayat I, Flavell RA. Caspases 3 and 7: Key mediators of mitochondrial events of apoptosis. *Science.* 2006;311:847–51.
29. Amna T, Van Ba H, Vaseem M, Hassan MS, Khil MS, Hahn YB, Lee HK, Hwang IH. 2013.
30. Kang SJ, Kim BM, Lee YJ, Hong SH, Chung HW. Titanium dioxide nanoparticles induce apoptosis through the JNK/p38-caspase-8-Bid pathway in phytohemagglutinin-stimulated human lymphocytes. *Biochem Biophys Res Commun.* 2009;386:682–7.
31. Fahmy B, Cormier SA. Copper oxide nanoparticles induce oxidative stress and cytotoxicity in airway epithelial cells. *Toxicol In Vitro.* 2009;23:1365–71.
32. Burg MB, Dmitrieva NI. Secretion of von Willebrand factor by endothelial cells links sodium to hypercoagulability and thrombosis. *Proc Natl Acad Sci U S A.* 2014;111(17):6485–90.
33. Yan M, Zhang Y, Qin H, Liu K, Guo M, Ge Y, Xu M, Sun Y, Zheng X. Cytotoxicity of CdTe quantum dots in human umbilical vein endothelial cells: The involvement of cellular uptake and induction of pro-apoptotic endoplasmic reticulum stress. *Int J Nanomed.* 2016.
34. Badiola N, Penas C, Miñano-Molina A, et al. Induction of ER stress in response to oxygen-glucose deprivation of cortical cultures involves the activation of the PERK and IRE-1 pathways and of caspase-12. *Cell Death Dis.* 2011;2: e149.
35. Apalla Z, Lallas A, Sotiriou E, Lazaridou E, Ioannides D. Epidemiological trends in skin cancer. *Dermatol Pract Concept.* 2017;7:1.
36. Sun Y-P, Zhou B, Lin Y, Wang W, Fernando KS, Pathak P, et al. Quantum-sized carbon dots for bright and colourful photoluminescence. *J Am Chem Soc.* 2006;128:7756–7.
37. Wang Z-X, Yu X-H, Li F, Kong F-Y, Lv W-X, Fan D-H, et al. Preparation of boron-doped carbon dots for fluorometric determination of Pb(II), Cu(II) and pyrophosphate ions. *Microchim Acta.* 2017;184:4775–83.
38. Tian T, He Y, Ge Y, Song G. One-pot synthesis of boron and nitrogen co-doped carbon dots as the fluorescence probe for dopamine based on the redox reaction between Cr(VI) and dopamine. *Sensors Actuators B: Chem.* 2017;240:1265–71.
39. Aswathy RG, Yoshida Y, Mwkawa T, Sakti Kumar D. Near infrared quantum dots for deep tissue imaging. *Anal Bio-analy Chem.* 397:1417–35 2010 Mar 29.
40. Bajpai VK, Khan I, Shukla S, Kang SM, Aziz F, Tripathi KM, Saini D, Cho HJ, Heo NS, Sonkar SK, Chen L, Huh YS, Han YK, Multifunctional N-P-doped carbon dots for regulation

- of apoptosis and autophagy in B16F10 melanoma cancer cells and in vitro imaging applications. 2020;10(17):7841–7856.
41. Mahani Md, Pourrahmani-Sarbanani M, Yoosefian M, Divsar F, Mosavi SM, Nomani A. Doxorubicin delivery to breast cancer cells with transferrin-targeted carbon quantum dots: An in vitro and in silico study. *J Drug Deliv Sci Technol.* 2021; 62: 102342
 42. Edgar R, McKinsty M, Hwang J, Oppenheim AB, Fekete RA, Giulian G, Merrill C, Nagashima K, Adhya S. High-sensitivity bacterial detection using biotin-tagged phage and quantum-dot nanocomplexes. *PNAS*, 2006, vol. 103, no. 13, p. 4841–45, 20. <https://doi.org/10.1073/pnas.0601211103>.
 43. Wan W, Pu Q, Huang X, Luo D, Hu Y, Liu Y. Comparison of quantum dot immunofluorescence histochemistry with conventional immunohistochemistry in detecting *Helicobacter pylori* infection in paraffin-embedded tissues of gastric biopsy. *J Mol Histol.* 2021; 52:461–466
 44. Triana MA, Restrepo AA, Lanzafame RJ, Polomaki P, Dong Y. Quantum dot light-emitting diodes as light sources in photomedicine: photodynamic therapy and photobiomodulation. *J Phys Mater.* 2020; 3:032002
 45. Gamelin EC, Danquechin-Dorval EM, Dumesnil YF, Maillart PJ, Goudier MJ, Burtin PC, Delva RG, Lortholary AH, Gesta PH, Larra FG. Relationship between 5-fluorouracil (5FU) dose intensity and therapeutic response in patients with advanced colorectal cancer receiving infusional therapy containing 5FU. *Cancer: Interdisc Int J Am Cancer Soc.* 1996;77(3):441–51.
 46. Xu J, Zhang G, Luo X, Wang D, Zhou W, Zhang Y, Zhang W, Chen J, Meng Q, Chen E, Chen H, Song Z. Co-delivery of 5-fluorouracil and miRNA-34a mimics by host-guest self-assembly nanocarriers for efficacious targeted therapy in colorectal cancer patient-derived tumor xenografts 2021;11(5):2475–89. <https://doi.org/10.7150/thno.52076>.
 47. Chang SJ, Meen TH, Prior SD, Ji LW, Young SJ. Applications of advanced nanomaterials to microelectronic and photonic devices. *J Nanomater.* 2015;1:2015.

Fluorescent Quantum Dots, A Technological Marvel for Optical Bio-imaging: A Perspective on Associated In Vivo Toxicity



Santosh Podder

Abstract Semiconductor quantum dots (QDs) are one of the technological wonders, known for their excellent photo-physical properties. The recent advances in nanotechnology have made QDs a robust and readily available fluorescent probe for both in vitro and in vivo bio-imaging research. QDs offer great advantages over traditional organic fluorescent dyes and present a number of beneficial characteristics such as size-tunable emission spectra, signal brightness, long life time, photostability, longer multiphoton cross sectioning capabilities and so on. Since its inception, it is being used as excellent fluorescent probe for a wide range of fluorescence microscopy technologies ranging from conventional epifluorescence, confocal, multiphoton to super-resolution microscopy for in vitro cell and tissue imaging to in vivo deep tissue and whole animal imaging. Hence, QDs have opened up plethora of exciting possibilities in bio-imaging research by enabling the researchers to probe and visualize the invisible biological processes from the whole organism level (macroscale) down to the cellular and in molecular level (nanoscale). Despite its enormous potential in bio-imaging, the involvement of heavy metals and the colloidal instability of QDs have led to legitimate concerns about toxicity. These issues have impeded the widespread adoption of QDs, especially in biomedical and in vivo bio-imaging. This chapter mainly focuses on the QD-based fluorescence bio-imaging applications from biological point of view and discuss relevant toxicity issues associated with using QDs in in vivo investigations.

Keywords Quantum dots · Bio-imaging · Fluorescence · In vivo toxicity

1 Introduction

The discovery of green fluorescence protein (GFP) by Osamu Shimomura in the hydroid jellyfish *Aequorea Victoria* followed by its successful expression in living organisms and development of different variants of GFP by Martin Chalfie and Roger

S. Podder (✉)

Indian Institute of Science Education and Research (IISER) Pune, Dr. Homi Bhabha Road, Pune 411008, India

e-mail: santosh.p@iiserpune.ac.in

Tsien, indeed revolutionized the field of optical microscopy and fluorescence imaging [1]. Subsequently, a panel of fluorescent proteins is now available covering almost the entire visible spectrum, each possessing different biochemical characteristics. Today, fluorescent labelling is of paramount importance to biological studies and a great number of chemical dyes are used extensively to label biological specimens [2] for high resolution and noninvasive imaging of live organisms. Quantum dots (QDs) technology has influenced other several technologies. One of the major beneficiaries of QDs is optical bio-imaging technology (which includes conventional fluorescence, laser scanning confocal, two-photon excitation, super-resolution microscopy and so on) which is rigorously used both in *in vitro* and *in vivo* bio-investigations [3]. QDs are nanoparticles which emit very narrow spectrum of lights after being illuminated by lights. QDs derive its fluorescent properties from the bandgap between its inner core material and the capsule shell, and display size dependent fluorescent properties (Fig. 1a). The size of this bandgap determines the QD's fluorescent properties and thus the QD's emission can be directly tuned by their physical size of the band gap [4]. In addition, it was recently shown that the size of the QD also determines the lifetime, which increases with size [5]. QDs have a relatively long lifetime, which provides the possibility to correct for background signals from short-lived fluorescent species by time-gating techniques [6].

Obviously, optical imaging is benefitted by several unique properties displayed by QDs. Their resultant emitted fluorescence can be tuned with high precision by varying the size and composition of the fluorescent core (Fig. 1b). As for example, QDs with cadmium selenide (CdSe) core, varying the core size (in the range of 2–8 nm) a gradual shift of emission peak from 480 to 660 nm is possible [7]. This is clearly an advantage of QDs over conventional fluorochromes in multiplex imaging applications [8, 9]. So, a single excitation light source can be used to detect the different antigens in the same biological sample while using QD-based nanoprobos. Because a single light source can excite multiple QDs with different emission wavelengths simultaneously and simple fluorescence light sources such as arc lamps and commercially available lasers in microscopes (405 diode, 488 Argon lasers etc.) can serve this purpose to excite QDs with varying degree of efficiency. QDs display a broad absorption band and narrower and more symmetric emission spectra compared with other fluorochromes (Fig. 1c) with a typical full-width at half max (FWHM) of ~25–40 nm [10]. These extraordinary optical properties of QDs made them a potent bio-imaging tool.

QDs are stable light emitters. In comparison to the available organic fluorogenic dyes, QDs are reported to be 10–100 times brighter and almost 100–1000 times more resistant to photobleaching. This might be due to the shell and various coatings that form physical barriers which separate the excited state from surrounding biomolecules and molecular oxygen. Hence, this characteristic makes them less susceptible to photobleaching than other available organic dye molecules. This feature has been well documented in number of biological labelling experiments earlier and the photostability of QDs was compared with commonly used fluorophores such as rhodamine, fluorescein, and Alexa-Fluor etc. [9, 13–15]. Figure 2 shows the better photostability of QDs when compared with one of the most stable

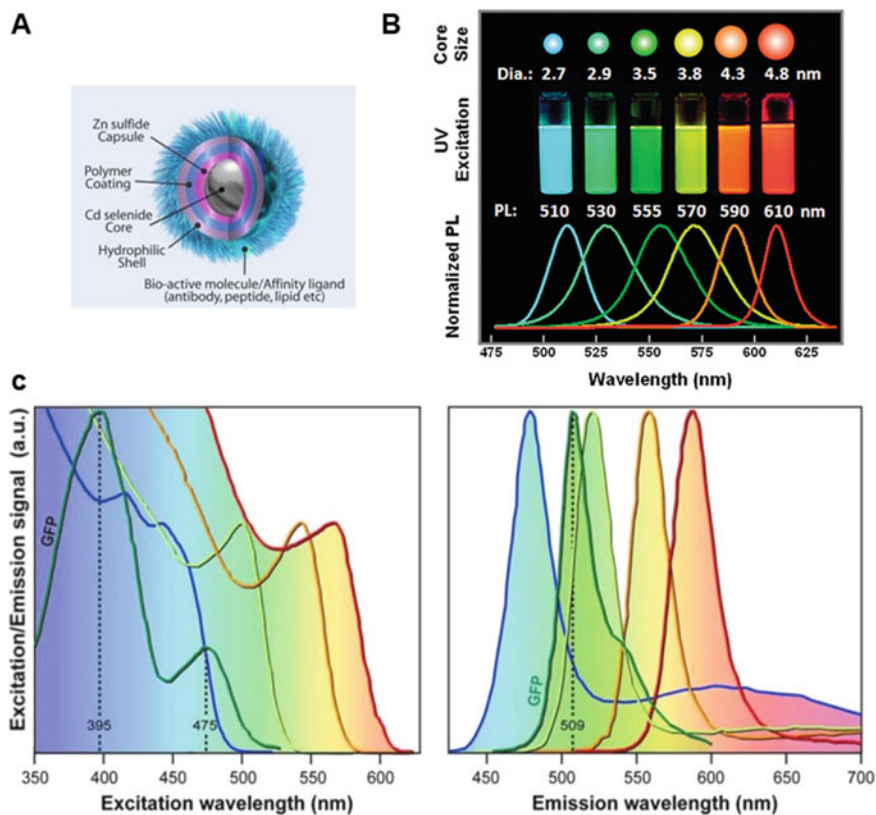


Fig. 1 **a** Schematic representation of the anatomy of a semiconductor QD. **b** QDs display physical size-tunable fluorescence properties. The spectral range of the six QD dispersions plotted against CdSe core size. **c** The comparison of the excitation and emission spectra of GFP (green lines) and QDs. The broad absorption windows of QDs allow the simultaneous excitation of all sizes QDs by a single excitation light source (UV to violet portion of the electromagnetic spectrum) making QDs suitable for multiplexing applications. **a**, **c** Adapted under the Creative Commons Attribution License from Ref. [11]. **b** Adapted with the permission from Ref. [12]. Copyright 2011 American Chemical Society

and commonly used organic dyes such as Alexa Fluor 488. When CdSe QDs were compared with fluorescein isothiocyanate (FITC), a very popular fluorescence probe in bio-imaging, CdSe were found to be a better alternative with safe, effective and convenient labelling procedures for cellular fluorescent imaging [16].

The QDs can be considered as a rising tool which can transform the paradigm of understanding the mystery of life processes otherwise invisible. This chapter mainly focuses on the immense potential of fluorescence QDs in different optical bio-imaging modalities and aims to provide an insight on the potential of QDs to enable the scientists dig deeper into the living biological processes. The different QDs synthesis processes and their modifications are out of the scope of this chapter.

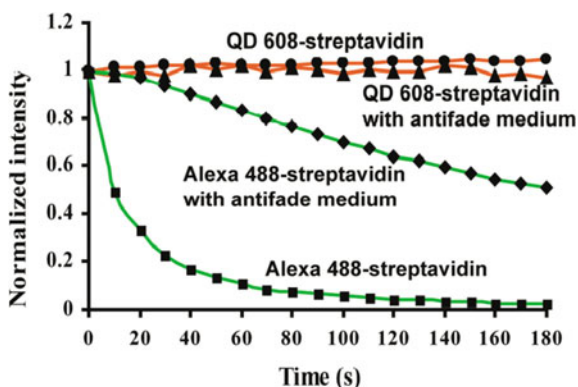


Fig. 2 A comparison of the photostability of QD 608 and Alexa 488. The fluorescence intensity changes of QD 608 and Alexa Fluor 488 was monitored simultaneously in the same mouse 3T3 fibroblast cell with the same excitation wavelength for 3 min. Adapted with permission from Ref. [9]

A foreign nanoparticle is always toxic in the living body because of its inability to assimilate in the body. As QDs are made up of different inorganic materials, their composition (e.g., heavy metals) and nanometric sizes have also opened a scope of extensive discussion about their toxicity issues before its widespread uses in bio-imaging research. Several studies have reported differential toxic effects of QDs ranging from completely harmless to very toxic. Therefore, it is relevant to address some of these toxicity issues in the light of its explicit potential in in vivo optical bio-imaging investigations.

1.1 QDs in Biological Applications

For biological application QDs need to be water soluble. Bruchez et al., added a third layer of silica on the core-shell system to make it water soluble and stable in buffer system. Hence for the first time, CdSe-CdS QDs enclosed in a silica shell were used to label the mouse fibroblasts. The biotin was covalently bound to the surface of the nanocrystals and this conjugated molecule was used to specifically mark F-actin on the cells. QDs were established as a class of fluorescent probes with a long fluorescence lifetime and higher tunability [13]. This was followed by others intensive efforts to produce biocompatible QDs [14] and their use for labelling biological samples [9]. In a fluorescence in situ hybridization (FISH) analysis of human metaphase chromosomes, CdSe-ZnS QDs were found to be significantly brighter and more photostable than conventional organic fluorophores such as Texas Red and FITC, thus offering a more stable and quantitative mode of FISH for research and clinical applications [15]. Zinc is already present in biological system. So, Zinc oxide (ZnO) is more biocompatible than Cd. Chan and Nie used semiconductor QDs

which were covalently attached to biomolecules for ultrasensitive detection at the single-dot level. Zinc oxide (ZnO) QDs surface functionalized with capping agent (mercaptoacetic acid) followed by covalent protein attachment (transferrin bioconjugate) were found to be biocompatible *in vitro* and with living cells. The presence of Transferrin facilitated the receptor-mediated endocytosis and transportation of these luminescent QDs into the cultured HeLa cell [14]. Subsequently, different Zinc compositions were used as core only or core-shell structures in QDs, e.g. Zinc Selenide (ZnSe), ZnS, CdSe-ZnS etc. These QDs were subsequently used for different biomedical applications, such as tumor imaging, monitoring of extracellular and intracellular trafficking and nanoparticle-mediated drug delivery etc. [17]. The lysine-coated CdSe/CdS/ZnS QDs were bioconjugated with Transferrin (Tf), an iron-transporting protein and used as targeted optical probes for live pancreatic cancer cell imaging using confocal microscopy [18]. Table 1 tabulated few studies which used different QDs with varied functionalization strategies and optical imaging modalities.

As a necessity, these nanoparticles went through different surface modification approaches with different biomolecules to avoid potential toxic release of shell atoms [19]. In recent years Graphene QDs (GQDs) are spreading in life science applications for their great photophysical properties as well as good biocompatibility and more “molecule-like” character than other QDs [20, 21].

1.2 A Tool for Deep Tissue Imaging

Imaging thick biological specimens such as thick tissue samples over long period of time always necessitates multiple optical sections to be collected without damaging the specimen. This has always remained as a challenging task for biologists using visible light. Hence, the multiphoton microscopy has become the primary fluorescence imaging technique in thick specimens because it allows deep imaging of a variety of biological samples with less overall photobleaching in comparison with wide field or confocal microscopy. The extreme photostability and the significantly higher two-photon action cross section of QDs make them a prominent choice of *in vivo* imaging using multiphoton excitation [23, 32–34] in demanding biological environments such as thick specimens and living tissues.

The water soluble CdSe-ZnS QDs enabled deep tissue multiphoton imaging of skin vasculature of live mice at greater depths with less laser power in comparison to the conventional fluorophores such as fluorescein. This successful application was critically dependent on its prominent and large two-photon action cross section of the CdSe-ZnS QDs (almost 3 orders of magnitude larger than fluorescein) [23]. The commercial red QD, Qtracker 655 are reported to be suitable for both cell and tissue two photon microscopy [35, 36]. A recent study demonstrated and characterized the three-photon action cross section and emission spectrum of Qtracker 655 QDs at the 1700 nm window. The imaging depth of 2100 μm mouse brain vasculature (Fig. 3) and 1600 μm for hemodynamic were reached setting a record depth

Table 1 A list of different QDs along with their functionalization strategies and usage in different bio-imaging research

QDs	Functionalization	Model/cell type	Cell type	Imaging modalities/permeability studies	Excitation/emission	Refs.
ZnS-capped CdSe	Coated with a lung-targeting peptide	In vitro	Lung, brain endothelial cells	Epifluorescence microscope	λ_{Exc} : 425/40-nm λ_{Em} : 515 nm long-pass filter	[22]
ZnS-capped CdSe	F3-coated and LyP-1	In vivo MDA-MB-435 breast carcinoma xenograft	Human breast carcinoma MDA-MD-435 cells	Confocal microscope	λ_{Exc} : UV excitation and λ_{Em} : 585 nm long-pass filter λ_{Em} : 550 nm and 625 nm	[22]
CdSe/ZnS	Mixed with neutralized amphiphilic polymer and cross-linked by EDC (1-ethyl-3-(3-dimethylamino propyl)carbodiimide)-mediated coupling to lysine (or PEG-lysine)	In vitro: live and fixed cells	Human breast cancer cell SK-BR-3 and mouse 3T3 fibroblasts, mammary tumor tissue sections	Epifluorescence microscope	Not mentioned	[9]
CdSe-ZnS	Encapsulated within an amphiphilic polymer	In vivo: mouse	Skin vasculature	Multiphoton microscopy	MP λ_{Exc} : 880 nm	[23]
InP-ZnS	SCH ₂ COOH conjugated with folic acid	In vitro: live cell	Human nasopharyngeal epidermal carcinoma cell line (KB) and a human lung carcinoma cell line (A549)	Confocal and multiphoton microscopy	λ_{Exc} : 420 nm MPM λ_{Exc} : 800 nm	[24]

(continued)

Table 1 (continued)

QDs	Functionalization	Model/cell type	Cell type	Imaging modalities/permeability studies	Excitation/emission	Refs.
CdSe/CdS/ZnS QDs	Transferrin conjugation	In vitro	Human pancreatic cancer cells	Confocal microscopy	Not mentioned	[18]
CdSe/CdS/ZnS QRs	Transferrin conjugation	In vitro: transwell blood brain barrier (BBR) model	Endothelial cells; astrocytes	Confocal microscopy	λ_{Exc} : 405 nm λ_{Em} : 580–620 nm and 640–690 nm	[25]
CdSe/ZnS commercial QDs	Nonfunctionalized, covered with Topo and PEG	In vitro: live cell	Frog muscle fibers, Macrophage (J774), HeLA cells	Confocal microscopy	$\lambda_{Exc}/\lambda_{Em}$: 488/550–580	[26]
CdSe/ZnS commercial QDs	Carboxylate functionalized	In vivo male C57BL/6 mice	Transplanted adipose-derived stem cells	In vivo imaging system	$\lambda_{Exc}/\lambda_{Em}$: 605 nm \pm 15 nm/660 nm \pm 10 nm at QDs655 $\lambda_{Exc}/\lambda_{Em}$: 745 nm \pm 15 nm/800 nm \pm 10 nm at QDs800	[27]
CdSe/ZnS commercial QDs	Carboxylate functionalized	In vivo male C57BL/6 mice	Transplanted adipose-derived stem cells	In vivo imaging system	$\lambda_{Exc}/\lambda_{Em}$: 635/670 nm long pass at QDs655; $\lambda_{Exc}/\lambda_{Em}$: 690/810 nm long pass at QDs705; $\lambda_{Exc}/\lambda_{Em}$: 785/845 nm long pass at QDs800	[28]
CdSe/ZnS	Biotinylated NGR peptide-conjugated	In vitro: fixed cells Transwell BBR and BTP model	Primary rat astrocytes, BCECs, C6 glioma cells	Confocal microscopy	$\lambda_{Exc}/\lambda_{Em}$: 488/525 nm	[29]

(continued)

Table 1 (continued)

QDs	Functionalization	Model/cell type	Cell type	Imaging modalities/permeability studies	Excitation/emission	Refs.
	NGR-conjugated	In situ rat brain glioma	C6 glioma cells	The living image system	$\lambda_{Exc}/\lambda_{Em}$: 488/525 nm	[29]
CdSe QDs	NA	In vitro: fixed cells	Human cervix cancer cells (HeLa)	Confocal microscopy	λ_{Exc} : 405, 488 and 633 nm λ_{Em} : not mentioned	[16]
CdTe/CdS	Mercaptosuccinic acid (MSA) capped	In vivo mouse model	Hepatocellular carcinoma	Multiphoton microscopy coupled with fluorescence lifetime imaging	MP $\lambda_{Exc}/\lambda_{Em}$: 900/515 to 620 nm; FLIM- $\lambda_{Exc}/\lambda_{Em}$: 740/350 to 450 nm	[30]
Qtracker655 (Commercial)	NA	Mouse	In vivo brain vasculature and hemodynamic	Multiphoton microscopy	MP $\lambda_{Exc}/\lambda_{Em}$: 1665/593 nm	[31]

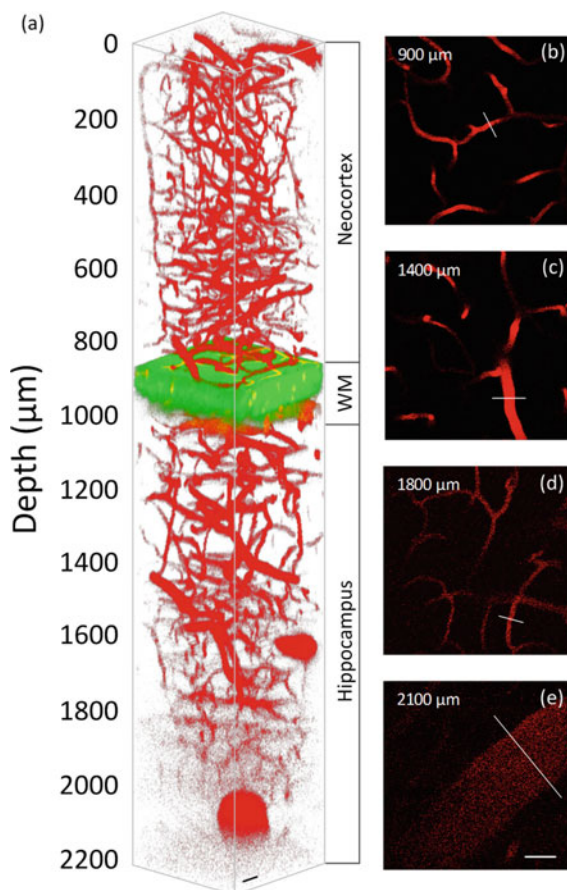


Fig. 3 The 3PM image of the deep-brain vasculature in adult mouse (in vivo) labelled with Qtracker655. **a** The 3D reconstructed 3PM images of the mouse brain showing Qtracker655 labelled vasculature (red); white matter (WM) layer extending from 860 to 1000 μm below the surface of the brain (THG signals; green). **b–e** The 2D images showing blood vessels at different depths; depths of 900 μm (**b**, in WM), 1400 μm (**c**, in hippocampus), 1800 μm (**d**, in hippocampus), and 2100 μm (**e**, in hippocampus) below the surface of the brain. Scale bars: 50 μm . Adapted with permission from Ref. [31]. Copyright 2019 American Chemical Society

among all the multiphoton microscopy modalities. In addition, the three-photon action cross section of Qtracker655 was recorded to be 4–5 orders of magnitude higher than the commonly used exogenous fluorophores in three-photon microscopy (3PM) excitation at 1700 nm window such as Texas Red dextran and SR101 [31].

QDs offers several advantages over traditional fluorophores. QDs emit light in the infrared and near-infrared regions. The absorption of tissues is minimal in this region and this is a great advantage of using QDs for deep tissue imaging compared to the classical fluorophore. In order to apply QDs in biomedical imaging, studies

focused on developing near-infrared (NIR) luminescent QDs which exhibit an emission wavelength ranging from 700 to 900 nm [37]. The most popular types of QDs include CdSe, CdTe and ZnSe. The most commonly studied and used QD is CdSe [38]. In last years, QDs with NIR emission suitable for in vivo imaging have been developed and made commercially available. In an in vivo imaging study of mouse model of acute liver failure, the labelling ability of commercial QDs655 and QDs800 to adipose-derived stem cells (ASCs) transplanted into QDs was assessed and organ-specific accumulation of transplanted ASCs labelled with IR QDs were investigated [27]. Although the excitation and emission wavelengths were in the red region of the visible light spectrum, all the transplanted labelled ASCs were detected efficiently in an in vivo imaging system because of the strong fluorescence of QDs. The transplanted ASCs with QDs800 were detected efficiently with NIR fluorescence for at least 5 days [28].

Most of the tissue chromophores such as haemoglobin and water weakly absorb light in the infrared range of wavelengths due to the lower absorption coefficient and scattering effects in the near-infrared (NIR) region (650–900 nm). Here the use of the NIR photons is beneficial for bio-imaging in living tissue due to their longer attenuation distances and a better tissue staining capabilities. These does not even interfere much with sample autofluorescence. Hence, QDs are advantageous because their emission can be set to a NIR area by adjusting its size or by incorporating rare-earth activators. Apart from QD's robust optical characteristics, their surface properties easily allow bioconjugation. The fluorescence lifetime of QDS (in the range of 10–40 ns) is significantly longer than typical organic dyes or autofluorescent flavin proteins which decay in the order of a few nanoseconds [39–41]. Therefore, with a combined pulsed laser and time-gated detection method using QD labels sample's images can be produced with significantly reduced background noise levels. The NIR-QDs arose as an attractive bio-imaging tool for picturing biological events because of their ability to provide deep imaging penetration and low fluorescence background. A recent study demonstrated the suitability of a NIR-far red emission two photon fluorescent probe GQD-MnO₂ (the surface covered with MnO₂ nanosheets) for the direct two photon excited fluorescence imaging of intracellular GSH levels in living HeLa cells and deep tissue imaging in rat liver frozen slices [42]. This raises a potential prospect of this multifunctional nanoprobe to become a new platform for bio-imaging and diagnosis in biomedical fields.

1.3 Imaging Beyond Diffraction Limit

As per Abbe's optical diffraction-limited theory, the resolution of conventional far-field (optical) fluorescence microscopy is limited to half of the imaging wavelength (~ 200 nm) [43]. The super-resolution microscopy techniques opened up a new dimension in cytobiological research by enabling the biologist to see the life processes in nano scale for the first time. Among all the available super-resolution

imaging methods such as structure illumination microscopy (SIM) [44, 45], photoactivated localization microscopy (PALM) [46] and stochastic optical reconstruction microscopy (STORM) [47, 48], the stimulated emission depletion (STED) is a pure-optical measure that can be applied with a variety of dyes, while being free from complex post imaging calculation. These advantages make STED favourable for super-resolution imaging in a real-time mode. However, the improvement in resolution in STED also comes with a price: the depletion of most conventional fluorescent labels, such as molecular probes and fluorescent proteins (FPs) because STED technique requires a very high depletion light intensity [49, 50]. As a result, STED bio-imaging suffers from severe photobleaching and phototoxicity [51], thus hampering the development of their long-term imaging applications with live samples.

The widely popular class of quantum dot molecular labels could so far not been utilized as standard fluorescent probes in STED nanoscopy. This is because, the broad quantum dot excitation spectra extend deeply into the spectral bands used for STED, thus compromising the transient fluorescence silencing required for attaining super-resolution. Reports on the usability of QDs in STED imaging is scanty. Hanne and co-workers recently reported the successful STED nanoscopic imaging by popular 775 nm STED laser using commercially available and widely used red-emitting ZnS/CdSe or ZnS/CdTe QDs. A resolution ~ 50 nm was achieved for single quantum dots. While Qds705-labelled vimentin filaments in fibroblasts was imaged, a 2.7-fold reduction in the measured filament diameter was recorded (Fig. 4). The high photostability of the QDs enabled repeated STED recordings of more than 1000 frames [52]. Commercial QD705 was efficaciously applied in a series of commercial super-resolution systems, including STED, SIM and single-molecule localization microscopy. QD705 was successfully used in STED with a careful choice of the depletion conditions (continuous-wave depletion laser 775 nm rather than a pulsed picosecond laser) to avoid the large two-photon excitation of QDs. A 85 nm FWHM super-resolution was recorded on a QD705-labelled microtubule network of HeLa cells by STED nanoscopy [53]. Very high lateral resolution (42 nm) was demonstrated for a single QDs (green emitted commercial CdSe/ZnS QDs) at relatively low-power depletion laser. For the first time these QDs were successfully used for labelling the lysosomes of living HeLa cells and 81.5 nm lateral resolution was obtained. Apart from that, living Eca-109 cells labelled with the CdSe/ZnS QDs was observed with fluorescence lifetime imaging microscope (FLIM) and served as a satisfactory probe in further FLIM-STED experiments [54]. In a recent report, a high resolution of 21.0 nm for a single QD was obtained when water soluble green emitting CdSe/ZnS QDs coated on a glass slide were imaged in a STED nanoscopy under irradiation with a 529 nm STED depletion laser. This is clearly a ten-fold enhancement compared to the resolution achieved in a laser scanning confocal microscopy imaging [55].

Apart from the group II–VI QDs stated above, recently, novel halide perovskite (CsPbX_3 , $X = \text{Cl, Br, or I}$) quantum dots also displayed their potential as future STED probes. For the first time, CsPbBr₃-based STED nanoscopic imaging was described and the lateral resolution of a single CsPbBr₃ QDs was recorded as low as 20.6 nm with a 27.5 mW depletion laser [56].

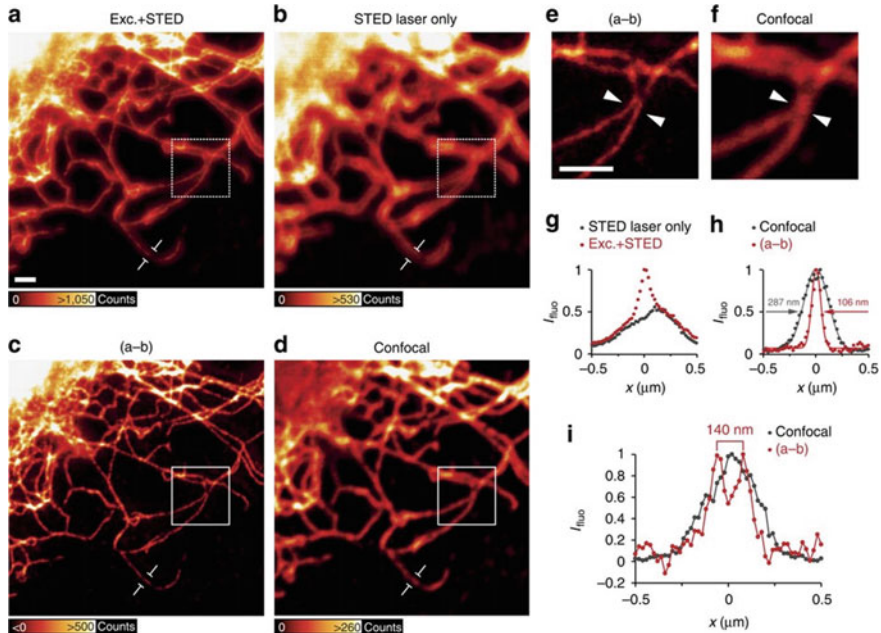


Fig. 4 STED imaging of immunostained cellular samples (REF cells) labelled with Qdot705. Vimentin fibres were labelled with Qdot705 and **a** imaged with the excitation (Exc.) plus the STED laser beam; **b** imaged with the STED laser beam only; **c** subtraction of the image (**b**) from the (**a**); **d** confocal image. **e** and **f** insets from white squares in (**c**) and (**d**), respectively. **g** Intensity profile of a single vimentin fibre as indicated in (**a**) and (**b**). **h** Intensity profile for the subtracted image (**c**) and the confocal image (**d**) as indicated. **i** Line profile of the position indicated by arrow heads in (**e**) and (**f**). The two fibres which appear as a single blurred object in the confocal reference image found to be resolved to a distance of 140 nm in the super-resolved image. Scale bar, 1 μm . Adapted with permission from Ref. [52]

The structured illumination super-resolution imaging microscopy (generally known as SIM) improves the resolution by modulating the spatial frequency domain of captured images by using structured illumination patterns [44]. For a single image to capture in 2D SIM, typically 9 images with 3 different illumination orientations in 3 sequential phases are necessary while 3D SIM requires the acquisition of 15 images. Hence, sample stability during the entire image acquisition process is the paramount requirement of this imaging technique. The photobleaching of available organic dyes introduce artificial effect during SIM reconstruction. QDs can be the better choice because of their superior photostability but point of concerns are the intermittency or blinking features of QDs' emission. This can introduce another source of artificial effect in SIM [57]. The artefact caused by the blinking of QDs can be decreased either by collecting several SIM images with each collection condition and averaging these data to form one frame or increasing the acquisition time for each frame and averaging out the blinking. In a subdiffractional imaging approach of microtubules on fixed HeLa cells, the spatial resolution (FWHM) of the microtubule

network were measured to be ~ 94 nm in the x - y plane. In comparison to wide-field imaging where artefacts were primarily appeared to be discontinuous, SIM imaging (acquired using above-mentioned strategies) worked well in preserving the connectivity of microtubule networks (Fig. 5).

STORM [47] and its close relative PALM [46, 58] utilizes the intensity blinking properties (“on” and “off” of fluorescence intensity) of fluorophores. Many fluorescence images are collected, wherein in each image has a random subset of the fluorophores that are “on” and precise localization of each isolated emitter in each image frame is determined. The final super-resolution image is reconstructed by combining the emitter localizations from every individual frame [46, 58]. Most commonly used organic dyes and photoactivatable fluorescent proteins require suitable oxygen-reducing buffer systems (this can be cytotoxic over time), high laser excitation powers (can be both phototoxic to cells resulting an increase in the

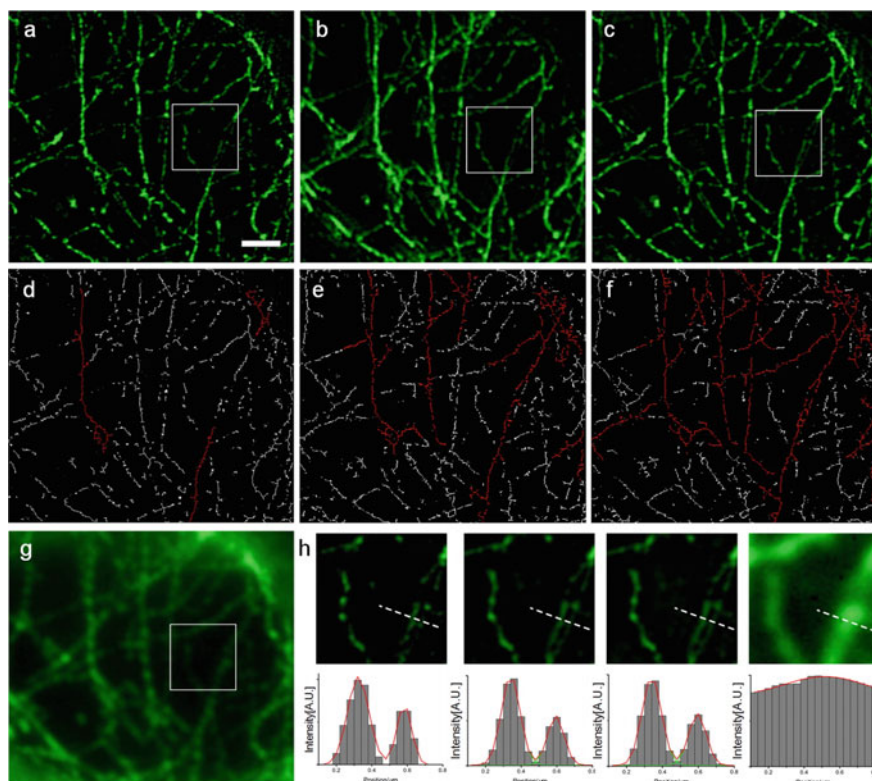


Fig. 5 SIM images of the microtubules in HeLa cells. **a** One SIM image; **b** summation of 10 reconstructed SIM images; **c** one SIM image with $10\times$ extended frame exposure time; **d-f** the morphological analysis of the **(a)-(c)** images; **g** wide-field microscopy image. Scale bar: $2\ \mu\text{m}$. **h** Resolution of SIM results **(a)-(c)** and wide-field image **(g)**. Adapted with permission from Ref. [53]. Copyright 2016 American Chemical Society

photobleaching rate), and/or the use of multiple excitation lasers to achieve this blinking property. These can be expensive and complicated [59, 60]. QDs naturally exhibit inherent fluorescence blinking. So, this inherent, fast blinking along with extremely photostable fluorescence properties of individual QD eliminate the need for multiple photoactivation lasers or oxygen-reducing buffers (required by other organic dyes and fluorescent proteins) in order to enable the fluorescence intensity blinking required for super-resolution imaging applications [61]. The neuropeptide namely bradykinin (BK) functionalized CdSe/CdS QDs (BKQD) were found to be a fundamentally superior STORM imaging probe to BK labelled with an organic fluorophore, 5-carboxytetra-methylrhodamine (TAMRA). Higher localization accuracy was remarkable in the super-resolution images of primary rat hippocampal neuronal cultures labelled with BKQD probes in comparison to the images obtained using TAMRA-BK. The BKQD treated cultures were imaged in physiologically relevant conditions: using PBS or neurobasal media whereas The TAMRA required a buffer that contain oxygen scavengers [62].

Table 2 tabularized some of the studies where QDs were successfully used in different super-resolution imaging modalities.

Table 2 Usage of QDs for super-resolution imaging

QDs	Functionalization	Model	Cell type	Imaging modalities	Excitation/emission	Refs.
ZnS/CdSe (Commercial) QDs	Antibody-coupled	In vitro	Rat embryonic fibroblasts	Confocal and STED microscopy	$\lambda_{Exc}/\lambda_{Em}$: 628 nm/650–770 nm; λ_{STED} : 775 nm (red)	[52]
CdSeTe/ZnS (Commercial) QDs	Streptavidin conjugates	In vitro fixed cells	Human cervix cancer cells	Confocal, STED and SIM microscopy	$\lambda_{Exc}/\lambda_{Em}$: 532 nm; λ_{STED} : 775 nm for SIM λ_{Exc} : 488 nm	[53]
CsPbBr ₃	Colloidal dispersed QDs in octane	Coated on glass slide	NA	Confocal and STED microscopy	$\lambda_{Exc}/\lambda_{Em}$: 488 and 510–570 nm λ_{STED} : 592 nm	[56]
CdSe/ZnS QDs (Commercial)	PEG-COOH	In vitro live cell	Human cervix and oesophageal cancer cells	Confocal FLIM and STED microscopy	$\lambda_{Exc}/\lambda_{Em}$: 488 nm/BP 520–550 nm λ_{STED} : 592 nm	[54]
CdSe/ZnS QDs	PEG-COOH	Coated on glass slide	NA	Confocal and STED microscopy	λ_{Exc} : 488 nm λ_{Em} : 592 nm (centred) λ_{STED} : 775 nm	[55]
CdSe/CdS QDs	Bradykinin	In vitro fixed cells	Primary mixed rat hippocampal neuronal and glial cultures	STORM imaging	λ_{Exc} : 532 nm	[62]

2 Concerns on Associated Toxicity

Most of the current studies rigorously emphasized on its physicochemical properties and underscored its immense potential as a bio-imaging probe but unfortunately QDs induced toxicity issues are not systematically documented yet [63]. Majority of the studies from which the toxicity aspects of QDs have been derived or cited in reference were mainly performed by nanotechnology researchers rather than toxicologists or health scientists [64]. A clear disparity exists on the available QD induced toxicity reports. No discernible toxicity was recorded in live animals when QDs were injected into *Xenopus* embryo [65], bloodstream of pigs [66] and for up to 4 months in mice [23, 67, 68] or cells grown *in vitro* with QDs for more than two weeks [69]. Negligible cytotoxicity of CdSe QDs was reported in a typical fluorescent cell imaging procedure (10 nmol/L, 12 h) using HeLa cells and labelling effect to microtubule was guaranteed satisfactorily [16]. However, most QDs are composed of heavy metals which are known to be toxic in their soluble form [70]. Hence, biocompatible surface coatings are paramount requirements in the *in vivo* bio-imaging applications of QDs to prevent intrinsic toxicity of QD constituent like Cd, lead (Pb), or arsenic (As). The stability QDs and their resistance to metabolic degradation in the biological system is an important aspect of their potential use in bio-imaging. QDs should not be acutely toxic as long as their coating is stable enough to detain the release of cadmium. These toxicity concerns are still valid *in vivo* applications and crucial for long-term imaging experiments using QD labelling. Therefore, both short- and long-term safety of QDs will need to be established in toxicological studies in clinically relevant animal models [63]. No apparent histopathological abnormalities were recorded in liver kidney and spleen of mice after 7 or 30 days of intravenous injection of injected with CdTe/Cds QDs [30] and the extent of lower toxicity of these QDs to the mice organs was attributed to the CdS shell on the core CdTe of QDs [71]. Core-shell QDs with an outer ZnS shell, are chemically more stable whereas an unadorned QD core is highly reactive and toxic. The degradation of the QD coating may result in undesirable reactions *in vivo* systems as the toxic heavy metal ions can be easily leaked out into biological systems [64]. Cytotoxicity of QDs has been observed in a large number of *in vitro* studies [72]. Cytotoxicity of the cultured cells were correlated with the liberation of Cd²⁺ ions [73]. The UV irradiation induced surface oxidation may trigger the breakage of shells and surface coatings of QDs instigating the release of free Cd²⁺ and lethal damage to the cell [74, 75]. The involvement of both Cd²⁺ and reactive oxygen species (ROS) accompanied by lysosomal enlargement and intracellular redistribution were reported in CdTe QDs induced cell death of MCF-7 [76]. Table 3 tabulated some of the QD toxicity studies.

The blood circulation system is considered one of the important barriers against foreign intruders, including nanomaterials *in vivo* investigations, different biomedical applications or environmental exposure. CdTe/SnS QDs are reported to be readily engulfed by macrophages and posed great damage to macrophages through intracellular accumulation coupled with ROS generation and inhibited macrophage cell proliferation. Particularly, QDs coated with PEG-NH₂ had a greater capability

Table 3 QD toxicity studies

QDs	Functionalization	Model and cell type	Toxicity documented	Refs.
CdSe	Tri-n-octylphosphine oxide capping	Rat hepatocytes	High cytotoxicity due to release of Cd ²⁺ ions	[75]
CdSe	ZnS capping	Rat hepatocytes	Low, no release of Cd	[75]
CdSe and CdSe/ZnS	Mercaptopropionic acid (MPA), silica shell bearing phosphonate groups (phos-silane) and polyethylene groups (PEG-silane)	In vitro: NRK fibroblasts, MDA-MB-435S breast cancer cells, CHO and RBL cells	Cytotoxic to the cells and poisoning is due to release of Cd ²⁺ ions	[73]
CdTe and CdSe/ZnS	MPA and NAC conjugated	Human breast cancer cells	CdTe QDs capped with small organic ligands are cytotoxic-induces oxidative stress releases Cd ²⁺ ions and photooxidation processes. CdSe/ZnS QDs are less cytotoxic	[76]
CdSe/Cds	MPA-conjugated	Intraperitoneal injection into BALB/c mice	The levels of lactate dehydrogenase, nicotinamide adenine dinucleotide phosphate oxidase, pro-inflammatory marker such as interleukin-6 increased in the plasma, liver and spleen	[78]
CdTe/SnS	PEG, PEG-NH ₂ , or PEG-COOH	J774A.1 Macrophage cells	Caused great damage to macrophages through intracellular accumulation, reactive oxygen species generation and inhibited macrophage cell proliferation	[77]

for entering the cells and revealed a robust ability to repress the proliferation of macrophages [77]. Intraperitoneal injection of CdSe/CdS-MPA QDs into BALB/c mice increased the lactate dehydrogenase, nicotinamide adenine dinucleotide phosphate oxidase, pro-inflammatory marker such as interleukin-6 increased in the plasma, liver and spleen [78]. Hence, optimization of surface modification and its biocompatibility is a critical parameter to ensure the function and the safety of QDs. The molecules used for surface functionalization of the QDs might also be a concern for toxicity [64]. Given the highly intrinsic toxicity of Cd, the biological applications of Cd-QDs have been limited. This is worth mentioning that the toxicity of QDs depends on various factors and varies in a complex manner. These factors may

include the nature of the biological environment where QDs are applied, physiological parameters, the extent of cellular uptake, and finally the physicochemical properties of QDs employed [79]. Hence, each type of QDs requires to be characterized individually for its potential toxicity because each type possesses own unique physicochemical properties such as sizes, charges, concentrations, outer coating materials and functional groups, oxidation and mechanical stability. Hence, all these characteristics along with environmental factors have been implicated as contributing factors to QDs toxicity [64] and making it quite difficult to generalize the toxicity aspects. If the metals are safely contained in QDs using more and more stable coating, still the relevant issue will be the metabolic clearance of the QDs before successful use in vivo bio-imaging experiments. Unfortunately, hardly anything is known about how these particles will be cleared by the body [72].

In recent years extensive efforts has been made to explore alternative strategies to develop more efficient QDs with high biocompatibility using nontoxic elements [80] such as InP-based QDs (III–V semiconductors), silicon (Si) QDs etc. in order to lower the potential toxicity of the fluorescent probes for biological applications. Very little studies reported the use of InP or other III–V QDs in bio-imaging applications because they are difficult to prepare on a competitive time scale, and their quantum efficiencies tend to be much lower [81]. Owing to their nontoxic nature, SiQDs showed a great potential to be used as an excellent fluorescent probe for bio-imaging. But the aqueous solubility remains the common problem in SiQDs too as in all types of QDs when they are employed in vitro and in vivo imaging experiments [63].

Proper knowledge of the biological fate and toxicity of QDs is very essential for the successful application of QDs in bioscience research [78]. An increase in QD usage in bio-imaging research will lead to the undeniable dumping of a lot of QDs directly into the environment. In due course, this may ultimately result in environmental toxicity [82, 83]. Till date no thorough study is available on the transport, elimination and biodegradation mechanisms of QDs.

3 Conclusion and Future Perspectives

The ongoing development in QD research made them a useful arsenal in the bio-imaging toolbox having immense potential for diverse bio-imaging studies (including live deep tissue imaging, intracellular life processes at the single-molecule level, high-resolution cellular imaging, tumour targeting and so on) in different scales (macro to nanoscales). QDs are suitable for use as probe in heterogenous fluorescence imaging modalities to visualize life processes. In spite of different physical strategies, the in vivo investigation of single-molecule dynamics in living cells by delivering QDs across the plasma membrane into the cytosol always remained a challenge. This is because of the absence of versatile delivery approaches. New approaches such as the cell-penetrating poly(disulfide)s based technology [84] and freeze-concentration strategy [85] are proficiently delivering QDs in the cell and increasing the chances of endosomal escape of QDs. This can be an important development in the field of

QD research by enabling the researcher to capture the single molecular dynamics in cells and living animals and probe biophysical properties of the cytosol. Despite of all these strategic advances, QDs are far from their exhaustive application in bio-imaging research due to their hydrophobicity and toxicity. Continuous efforts have been taken to make them more water soluble and suitable for bio-imaging research through different synthesis strategies, surface functionalization techniques and conjugating them with different biomolecules to facilitate the interactions with living biological systems. Still QDs may not be considered as a complete replacement of the widely used contemporary fluorescent dyes but they have the ample potential to complement the dye deficiencies in different bio-imaging applications. Nevertheless, their potential use in routine in vivo investigations will only be possible only when investigations on long-term QDs toxicity and its clearance mechanisms in bio-organisms are fully addressed.

Acknowledgements The author wishes to thank Prof. Aurnab Ghose, IISER Pune for reading the manuscript and valuable inputs.

Conflicts of Interest There is no conflict of interest.

References

1. Zimmer M. GFP: from jellyfish to the Nobel prize and beyond. *Chem Soc Rev.* 2009;38(10).
2. Chudakov DM, Lukyanov S, Lukyanov KA. Fluorescent proteins as a toolkit for in vivo imaging. *Trends Biotechnol.* 2005;23.
3. Wegner KD, Hildebrandt N. Quantum dots: bright and versatile in vitro and in vivo fluorescence imaging biosensors. *Chem Soc Rev.* 2015;44.
4. Drummen GPC. Quantum dots—from synthesis to applications in biomedicine and life sciences. *Int J Mol Sci.* 2010;11.
5. van Driel AF, Allan G, Delerue C, Lodahl P, Vos WL, Vanmaekelbergh D. Frequency-dependent spontaneous emission rate from CdSe and CdTe nanocrystals: influence of dark states. *Phys Rev Lett.* 2005;95(23).
6. Mitchell AC, Dad S, Morgan CG. Selective detection of luminescence from semiconductor quantum dots by nanosecond time-gated imaging with a colour-masked CCD detector. *J Microsc.* 2008;230(2):172–6.
7. Han M, Gao X, Su JZ, Nie S. Quantum-dot-tagged microbeads for multiplexed optical coding of biomolecules. *Nat Biotechnol.* 2001;19(7).
8. Bentolila LA, Ebenstein Y, Weiss S. Quantum dots for in vivo small-animal imaging. *J Nucl Med.* 2009;50.
9. Wu X, Liu H, Liu J, Haley KN, Treadway JA, Larson JP, et al. Immunofluorescent labeling of cancer marker Her2 and other cellular targets with semiconductor quantum dots. *Nat Biotechnol.* 2003;21(1).
10. Medintz IL, Mattoussi H. Quantum dot-based resonance energy transfer and its growing application in biology. *Phys Chem Chem Phys.* 2009;11.
11. Ishikawa-Ankerhold HC, Ankerhold R, Drummen GPC. Advanced fluorescence microscopy techniques-FRAP, FLIP, FLAP, FRET and FLIM. *Molecules.* 2012;17.
12. Algar WR, Susumu K, Delehanty JB, Medintz IL. Semiconductor quantum dots in bioanalysis: crossing the valley of death. *Anal Chem.* 2011;83(23).

13. Bruchez M, Moronne M, Gin P, Weiss S, Alivisatos AP. Semiconductor nanocrystals as fluorescent biological labels. *Science*. 1998;281(5385).
14. Chan WCW, Nie S. Quantum dot bioconjugates for ultrasensitive nonisotopic detection. *Science*. 1998;281(5385).
15. Xiao Y, Barker PE. Semiconductor nanocrystal probes for human metaphase chromosomes. *Nucleic Acids Res*. 2004;32(3).
16. Li X, Yan Z, Xiao J, Liu G, Li Y, Xiu Y. Cytotoxicity of CdSe quantum dots and corresponding comparison with FITC in cell imaging efficiency. *Int J Clin Exp Med*. 2017;10(1).
17. Delehanty JB, Mattoussi H, Medintz IL. Delivering quantum dots into cells: strategies, progress and remaining issues. *Anal Bioanal Chem*. 2009;393.
18. Qian J, Yong KT, Roy I, Ohulchanskyy TY, Bergey EJ, Lee BH, et al. Imaging pancreatic cancer using surface-functionalized quantum dots. *J Phys Chem B*. 2007;111(25).
19. Bailey RE, Smith AM, Nie S. Quantum dots in biology and medicine. *Phys E Low-Dimension Syst Nanostruct*. 2004;25.
20. Palmieri V, Papi M, Conti C, Ciasca G, Maulucci G, de Spirito M. The future development of bacteria fighting medical devices: the role of graphene oxide. *Expert Rev Med Dev*. 2016;13.
21. Bacon M, Bradley SJ, Nann T. Graphene quantum dots. In: Particle and particle systems characterization, vol. 1. Germany: Wiley-VCH Verlag; 2014. p. 415–28.
22. Åkerman ME, Chan WCW, Laakkonen P, Bhatia SN, Ruoslahti E. Nanocrystal targeting in vivo. *Proc Nat Acad Sci USA*. 2002;99(20).
23. Larson DR, Zipfel WR, Williams RM, Clark SW, Bruchez MP, Wise FW, et al. Water-soluble quantum dots for multiphoton fluorescence imaging in vivo. *Science*. 2003;300(5624).
24. Bharali DJ, Lucey DW, Jayakumar H, Pudavar HE, Prasad PN. Folate-receptor-mediated delivery of InP quantum dots for bioimaging using confocal and two-photon microscopy. *J Am Chem Soc*. 2005;127(32).
25. Xu G, Yong KT, Roy I, Mahajan SD, Ding H, Schwartz SA, et al. Bioconjugated quantum rods as targeted probes for efficient transmigration across an in vitro blood-brain barrier. *Bioconjug Chem*. 2008;19(6).
26. Belyaeva TN, Salova AV, Leontieva EA, Mozhenok TP, Kornilova ES, Krolenko SA. Untargeted quantum dots in confocal microscopy of living cells. *Cell Tissue Biol*. 2009;3(6).
27. Yukawa H, Watanabe M, Kaji N, Okamoto Y, Tokeshi M, Miyamoto Y, et al. Monitoring transplanted adipose tissue-derived stem cells combined with heparin in the liver by fluorescence imaging using quantum dots. *Biomaterials*. 2012;33(7).
28. Yukawa H, Watanabe M, Kaji N, Baba Y. Influence of autofluorescence derived from living body on in vivo fluorescence imaging using quantum dots. *Cell Med*. 2015;7(2).
29. Huang N, Cheng S, Zhang X, Tian Q, Pi J, Tang J, et al. Efficacy of NGR peptide-modified PEGylated quantum dots for crossing the blood–brain barrier and targeted fluorescence imaging of glioma and tumor vasculature. *Nanomed Nanotechnol Biol Med*. 2017;13(1).
30. Wang H, Yang H, Xu ZP, Liu X, Roberts MS, Liang X. Anionic long-circulating quantum dots for long-term intravital vascular imaging. *Pharmaceutics*. 2018;10(4).
31. Liu H, Deng X, Tong S, He C, Cheng H, Zhuang Z, et al. In vivo deep-brain structural and hemodynamic multiphoton microscopy enabled by quantum dots. *Nano Lett*. 2019;19(8).
32. Alivisatos AP, Gu W, Larabell C. Quantum dots as cellular probes. *Ann Rev Biomed Eng*. 2005;7.
33. Gao X, Nie S. Molecular profiling of single cells and tissue specimens with quantum dots. *Trends Biotechnol*. 2003;21.
34. Gao X, Cui Y, Levenson RM, Chung LWK, Nie S. In vivo cancer targeting and imaging with semiconductor quantum dots. *Nat Biotechnol*. 2004;22(8).
35. Maestro LM, Rodríguez EM, Rodríguez FS, de la Cruz MCI, Juarranz A, Naccache R, et al. CdSe quantum dots for two-photon fluorescence thermal imaging. *Nano Lett*. 2010;10(12).
36. Podgorski K, Ranganathan G. Brain heating induced by near-infrared lasers during multiphoton microscopy. *J Neurophysiol*. 2016;116(3).
37. Liu L, Jin S, Hu Y, Gu Z, Wu HC. Application of quantum dots in biological imaging. *J Nanomater*. 2011;2011.

38. Bera D, Qian L, Tseng TK, Holloway PH. Quantum dots and their multimodal applications: a review. *Materials*. 2010;3.
39. Dahan M, Laurence T, Pinaud F, Chemla DS, Alivisatos AP, Sauer M, et al. Time-gated biological imaging by use of colloidal quantum dots. *Opt Lett*. 2001;26(11).
40. Michalet X, Pinaud F, Lacoste TD, Dahan M, Bruchez MP, Alivisatos AP, et al. Properties of fluorescent semiconductor nanocrystals and their application to biological labeling. *Single Mol*. 2001;2.
41. Lounis B, Bechtel HA, Gerion D, Alivisatos P, Moerner WE. Photon antibunching in single CdSe/ZnS quantum dot fluorescence. *Chem Phys Lett*. 2000;329(5–6).
42. Meng HM, Zhao D, Li N, Chang J. A graphene quantum dot-based multifunctional two-photon nanoprobe for the detection and imaging of intracellular glutathione and enhanced photodynamic therapy. *Analyst*. 2018;143(20).
43. Rayleigh XV. On the theory of optical images, with special reference to the microscope. *Lond Edinb Dublin Philos Mag J Sci*. 1896;42(255).
44. Gustafsson MGL. Surpassing the lateral resolution limit by a factor of two using structured illumination microscopy. *J Microsc*. 2000;198(2).
45. Gustafsson MGL. Nonlinear structured-illumination microscopy: wide-field fluorescence imaging with theoretically unlimited resolution. *Proc Nat Acad Sci USA*. 2005;102(37).
46. Betzig E, Patterson GH, Sougrat R, Lindwasser OW, Olenych S, Bonifacino JS, et al. Imaging intracellular fluorescent proteins at nanometer resolution. *Science*. 2006;313(5793).
47. Rust MJ, Bates M, Zhuang X. Sub-diffraction-limit imaging by stochastic optical reconstruction microscopy (STORM). *Nat Methods*. 2006;3(10).
48. Huang B, Wang W, Bates M, Zhuang X. Three-dimensional super-resolution imaging by stochastic optical reconstruction microscopy. *Science*. 2008;319(5864).
49. Meyer L, Wildanger D, Medda R, Punge A, Rizzoli SO, Donnert G, et al. Dual-color STED microscopy at 30-nm focal-plane resolution. *Small*. 2008;4(8).
50. Hein B, Willig KI, Hell SW. Stimulated emission depletion (STED) nanoscopy of a fluorescent protein-labeled organelle inside a living cell. *Proc Nat Acad Sci USA*. 2008;105(38).
51. Wildanger D, Medda R, Kastrop L, Hell SW. A compact STED microscope providing 3D nanoscale resolution. *J Microsc*. 2009;236(1).
52. Hanne J, Falk HJ, Görlitz F, Hoyer P, Engelhardt J, Sahl SJ, et al. STED nanoscopy with fluorescent quantum dots. *Nat Commun*. 2015;6.
53. Yang X, Zhanghao K, Wang H, Liu Y, Wang F, Zhang X, et al. Versatile application of fluorescent quantum dot labels in super-resolution fluorescence microscopy. *ACS Photonics*. 2016;3(9).
54. Zhao M, Ye S, Peng X, Song J, Qu J. Green emitted CdSe@ZnS quantum dots for FLIM and STED imaging applications. *J Innov Opt Health Sci*. 2019;12(5).
55. Ye S, Guo J, Song J, Qu J. Achieving high-resolution of 21 nm for STED nanoscopy assisted by CdSe@ZnS quantum dots. *Appl Phys Lett*. 2020;116(4).
56. Ye S, Yan W, Zhao M, Peng X, Song J, Qu J. Low-saturation-intensity, high-photostability, and high-resolution STED nanoscopy assisted by CsPbBr₃ quantum dots. *Adv Mater*. 2018;30(23).
57. Killingsworth MC, Lai K, Wu X, Yong JLC, Lee CS. Quantum dot immunocytochemical localization of somatostatin in somatostatinoma by widefield epifluorescence, superresolution light, and immunoelectron microscopy. *J Histochem Cytochem*. 2012;60(11).
58. Hess ST, Girirajan TPK, Mason MD. Ultra-high resolution imaging by fluorescence photoactivation localization microscopy. *Biophys J*. 2006;91(11).
59. Pereira PM, Almada P, Henriques R. High-content 3D multicolor super-resolution localization microscopy. *Methods Cell Biol*. 2015;125.
60. Waldchen S, Lehmann J, Klein T, van de Linde S, Sauer M. Light-induced cell damage in live-cell super-resolution microscopy. *Sci Rep*. 2015;5.
61. Nirmal M, Dabbousi BO, Bawendi MG, Macklin JJ, Trautman JK, Harris TD, et al. Fluorescence intermittency in single cadmium selenide nanocrystals. *Nature*. 1996;383(6603).
62. Urban JM, Chiang W, Hammond JW, Cogan NMB, Litzburg A, Burke R, et al. Quantum dots for improved single-molecule localization microscopy. *J Phys Chem B*. 2021;125(10).

63. Brkić S. Applicability of quantum dots in biomedical science. In: *Ionizing radiation effects and applications*. 2018.
64. Hardman R. A toxicologic review of quantum dots: toxicity depends on physicochemical and environmental factors. *Environ Health Perspect*. 2006;114.
65. Dubertret B, Skourides P, Norris DJ, Noireaux V, Brivanlou AH, Libchaber A. In vivo imaging of quantum dots encapsulated in phospholipid micelles. *Science*. 2002;298(5599).
66. Kim S, Lim YT, Soltész EG, de Grand AM, Lee J, Nakayama A, et al. Near-infrared fluorescent type II quantum dots for sentinel lymph node mapping. *Nat Biotechnol*. 2004;22(1).
67. Hoshino A, Hanaki KI, Suzuki K, Yamamoto K. Applications of T-lymphoma labeled with fluorescent quantum dots to cell tracing markers in mouse body. *Biochem Biophys Res Commun*. 2004;314(1).
68. Ballou B, Lagerholm BC, Ernst LA, Bruchez MP, Waggoner AS. Noninvasive imaging of quantum dots in mice. *Bioconjug Chem*. 2004;15(1).
69. Jaiswal JK, Mattoussi H, Mauro JM, Simon SM. Long-term multiple color imaging of live cells using quantum dot bioconjugates. *Nat Biotechnol*. 2003;21(1).
70. Lovrić J, Cho SJ, Winnik FM, Maysinger D. Unmodified cadmium telluride quantum dots induce reactive oxygen species formation leading to multiple organelle damage and cell death. *Chem Biol*. 2005;12(11).
71. Zhu Y, Li Z, Chen M, Cooper HM, Lu GQ, Xu ZP. One-pot preparation of highly fluorescent cadmium telluride/cadmium sulfide quantum dots under neutral-pH condition for biological applications. *J Colloid Interface Sci*. 2013;390(1).
72. Medintz IL, Uyeda HT, Goldman ER, Mattoussi H. Quantum dot bioconjugates for imaging, labelling and sensing. *Nat Mater*. 2005;4.
73. Kirchner C, Liedl T, Kudera S, Pellegrino T, Javier AM, Gaub HE, et al. Cytotoxicity of colloidal CdSe and CdSe/ZnS nanoparticles. *Nano Lett*. 2005;5(2).
74. Tsay JM, Michalet X. New light on quantum dot cytotoxicity. *Chem Biol*. 2005;12.
75. Derfus AM, Chan WCW, Bhatia SN. Probing the cytotoxicity of semiconductor quantum dots. *Nano Lett*. 2004;4(1).
76. Cho SJ, Maysinger D, Jain M, Röder B, Hackbarth S, Winnik FM. Long-term exposure to CdTe quantum dots causes functional impairments in live cells. *Langmuir*. 2007;23(4).
77. Qu G, Wang X, Wang Z, Liu S, Jiang G. Cytotoxicity of quantum dots and graphene oxide to erythroid cells and macrophages. *Nanoscale Res Lett*. 2013;8(1).
78. Haque MM, Im HY, Seo JE, Hasan M, Woo K, Kwon OS. Acute toxicity and tissue distribution of CdSe/CdS-MPA quantum dots after repeated intraperitoneal injection to mice. *J Appl Toxicol*. 2013;33(9).
79. Nikazar S, Sivasankarapillai VS, Rahdar A, Gasmi S, Anumol PS, Shanavas MS. Revisiting the cytotoxicity of quantum dots: an in-depth overview. *Biophys Rev*. 2020;12.
80. Jin S, Hu Y, Gu Z, Liu L, Wu H-C. Application of quantum dots in biological imaging. *J Nanomater*. 2011;2011:13.
81. Yong K-T, Ding H, Roy I, Law W-C, Bergey EJ, Maitra A, et al. Imaging pancreatic cancer using bioconjugated InP quantum dots. 2009. Available from: www.acsnano.org.
82. Zhang S, Jiang Y, Chen CS, Spurgin J, Schwehr KA, Quigg A, et al. Aggregation, dissolution, and stability of quantum dots in marine environments: importance of extracellular polymeric substances. *Environ Sci Technol*. 2012;46(16).
83. Rocha TL, Mestre NC, Sabóia-Morais SMT, Bebianno MJ. Environmental behaviour and ecotoxicity of quantum dots at various trophic levels: a review. *Environ Int*. 2017;98.
84. Derivery E, Bartolami E, Matile S, Gonzalez-Gaitan M. Efficient delivery of quantum dots into the cytosol of cells using cell-penetrating poly(disulfide)s. *J Am Chem Soc*. 2017;139(30).
85. Ahmed S, Nakaji-Hirabayashi T, Rajan R, Zhao D, Matsumura K. Cytosolic delivery of quantum dots mediated by freezing and hydrophobic polyampholytes in RAW 264.7 cells. *J Mater Chem B*. 2019;7(46).

Quantum Dots in Biosensing, Bioimaging, and Drug Delivery



Somrita Mondal and Animesh Pan

Abstract Semiconductor quantum dots have been a matter of significant research interest owing to their potential biomedical applications, especially in drug delivery, biosensing, and, bioimaging. Practical biomedical applications of quantum dots require high fluorescence quantum yield, good aqueous solubility, narrow size distribution, and crystallinity of as-synthesized nano-sized particles. Several types of nanocarriers have been investigated for drug delivery. Out of different nanocarriers, semiconductor quantum dots have been favored due to their distinctive size-dependent optical, electrical, and, other physico-chemical characteristics. QDs have been explored for a wide variety of biomedical applications, e.g., detection of disease, drug delivery, biosensing, bioimaging, different type of therapeutic applications, including cancer therapeutics, tissue engineering, etc. QDs have excellent surface functionalization properties as well as biocompatibility. Encapsulation of QD core with different metal, metal oxides, polymers, or biomolecules facilitates core-shell structure, which, in turn, improves the efficacy of QDs for biomedical applications. The main advantage of using QDs as a nanocarrier for delivery of different types of drugs is its high surface to volume ratio, biocompatibility, and its cell-membrane permeability, which allows multiple sites for attachment of drug molecules. Moreover, surface functionalization of QDs enables loading of drug molecules to the QD surface through covalent as well as non-covalent bonding. On the other hand, bright photoluminescence ranging up to NIR region, excellent photostability, compressed light scattering, low tissue absorption, and unique size-tunable optical and electrical properties enable quantum dots for a wide range of biosensing as well as bioimaging applications. Furthermore, QDs provide a suitable platform for engineering of multi-functional nanodevices with capabilities of exploiting multiple imaging modalities or merging imaging and therapeutic functionalities within a single nanoparticle. Altogether, QDs have been a potential candidate for next-generation clinical and

S. Mondal (✉)

College of Pharmacy, Southwestern Oklahoma State University, Weatherford, OK, USA
e-mail: somrita.chem@gmail.com

A. Pan

Department of Chemical Engineering, University of Rhode Island, Kingstown, RI, USA

diagnostics research. In this book chapter, we aim to cover applications of different types of quantum dots in drug delivery, biosensing, and bioimaging.

Keywords Quantum dots · Biosensing · Bioimaging · Drug delivery

1 Introduction to Quantum Dots (QDs)

Nanoparticles are nano-sized particles having a dimension in the nanometer range (1–100 nm). Nanomaterials can be classified into different types. Based on the dimensional approach, there are zero-dimensional, one-dimensional, two-dimensional, and three-dimensional nanoparticles. QDs are the most popular example of 3-D semiconductor nanoparticles. Semiconductor nanomaterials, which has dimension less than their Bohr exciton radius, are termed as quantum dot. Thus, quantum dots, in general, have a dimension between 1 and 10 nm. Mark Reed introduced the term “quantum dot” [1]. QD excitons are confined within a small dimension. Due to this confinement, quantum dots behave like a particle in a 3-D box and follow quantum mechanics, hence the name “quantum dot.” Quantum confinement in quantum dot creates discrete energy levels, which, in turn, broadens the band-gap and enhances band-gap energy. QDs have unique size-tunable optical, electrical, and, magnetic properties. They possess size-tunable absorption and emission, broad absorption and narrow emission covering UV–Vis region (sometimes extending up to NIR region), large molar extinction coefficients, appreciable photostability, large surface area, high fluorescence quantum yield, flexible surface chemistry, and, biocompatibility. These properties enable them for diverse applications in biomedical field, specifically, in biosensing, bioimaging, and, drug delivery [2–7].

The main criterion for successful biological applications of QDs are narrow and symmetric photoluminescence profile, high fluorescence quantum yield, size uniformity and narrow size distribution of the particles, good crystallinity, aqueous solubility, and, biocompatibility of the particles [8]. Over the past decade, different types of QDs have been studied for biomedical applications, (1) group II–VI: e.g., ZnX, CdX (X = S/Se/Te), (2) group IV–VI: e.g., SiX, GeX (X = S/Se/Te), (3) group III–V: e.g., GaAs, InAs (4) graphene and graphene oxide quantum dots (GQDs or GOQDs) (5) carbon quantum dots (CQDs), etc. Broadly, quantum dots can be classified into two categories: (1) traditional QDs: group III/V, II/VI, IV/VI core or core/shell QDs and, (2) emerging QDs: non-toxic QDs, e.g., SiQDs, GQDs, GOQDs, some metallic hybrid (other than toxic heavy metals) quantum dots.

Over the past few years, core–shell quantum dots have also been popular in biomedical applications. Core–shell materials have distinct “core” and “shell” materials, giving rise to synergistic properties of core and shell, or, giving rise to some innovative property due to the core–shell interaction. Size tunable optoelectronic properties can be more prominent in core–shell quantum dot nanomaterials. Thus, core–shell quantum dots exhibit better optical properties compared to core only QDs, which, in turn, augments the photostability and photoluminescence quantum yield

[9–12]. One major problem in dealing with the core only quantum dots is the inherent toxicity of the quantum dots due to some heavy metals like cadmium, selenide, telluride, etc. This toxicity can limit their biological applications. This limitation can be overcome by putting a non-toxic shell (mostly ZnS) on top of a toxic core. Core-shell QDs like AgInS₂/ZnS have been a popular candidate for bio-applications [13]. Usage of non-toxic capping agents like sulfated bacterial polysaccharide has also been explored to address the toxicity concern of quantum dots [14].

2 Different Synthetic Routes for Biocompatible QDs

In general, there are two different routes for the synthesis of colloidal quantum dots: top-down method and bottom-up method. Top-down method is breaking down larger dimension precursor materials into nanoscale objects, ex., ball-milling method. Bottom-up method is the reverse, building up nanoscale dimension starting from atoms or molecules. In the chemical synthesis lab, generally bottom-up approach is followed for synthesis of quantum dots, as this is a better method for obtaining nanomaterials with size uniformity and narrow size distribution [15]. Typical chemical colloidal synthesis of semiconductor quantum dots consists of multiple steps, e.g., non-equilibrium nucleation followed by nanoparticle growth known as Ostwald ripening [16]. Some popular colloidal synthetic routes are: reverse micellar synthesis [17], thermolysis using organometallic reagents [18], aqueous synthesis using biomolecules as capping agent [19]. Reverse micellar synthesis is performed by combining two similar type of reverse micelle solutions consisting of hydrophilic reactant substances. Kwon et al. reported synthesis of fluorescent graphene quantum dots (GQDs) in reverse micelle method, the typical method involves simple carbonization of sugar in water-in-oil reverse micelle [20].

Zhang et al. reported synthesis of Co₃O₄ QDs through reverse micelle method. Typically, Cobalt nitrate was solubilized in butanol-dodecanol solvent mixture in an autoclave, followed by transfer of the autoclave in a microwave reactor [21]. This method involves mild reaction conditions, also, the synthesized nanoparticles are stable. However, photoluminescence of nanoparticles is not good enough as required for fruitful biological applications [22]. High-temperature organometallic thermolysis method is a very widespread method for synthesizing nanomaterials [23]. In this method, the anionic counterpart of the QD (e.g. S, Se, Te, etc.) is first reduced using some reducing agent, e.g. tri-octyl-phosphine (TOP). Next, salt or oxide of cationic counterpart is dissolved in mixture of some organic solvent and capping agents (usually long chain hydrocarbons like oleic acid, octadecane, TOPO, etc.). Next step is quick injection of previously prepared anionic part into the cationic part solution in nitrogen atmosphere on a heating system. Size tunability of the QDs can be achieved using different injection temperature and varying reaction time. For synthesis of core-shell QDs in this method, first, core QD is made, followed by injection of shell counterpart. There are numerous reports on synthesis of QDs using this method [24, 25]. This method gives very good quality nanomaterials with bright

fluorescence. Nevertheless, induced toxicity due to organometallic precursors and aqueous insolubility is the drawback for biological applications. Later on, several research groups worked to remove these limitations through surface exchange of the synthesized nanomaterials with some aqueous soluble and biocompatible ligands. Surface functionalization of the QDs made through organic route with water-soluble non-toxic ligands (mostly small chain thiols) reduces the toxicity to a significant amount, but the fluorescence of QDs after surface exchange usually drops a bit.

Another way for making biocompatible quantum dots is the aqueous colloidal synthesis using water-soluble capping agents [26–28]. In this method, the anionic counterpart of the QD (e.g. S, Se, Te) is first reduced using some reducing agent like sodium borohydride. Next, salt of cationic counterpart of QDs is dissolved in water and mixed with a water-soluble capping agent (e.g., cysteine, glutathione etc.), followed by injection of anionic precursor. Size tunability can be achieved through variation of injection time. There are a few examples reported on this aqueous synthesis procedure of QDs [18, 29]. QDs synthesized in this method generally give satisfactory fluorescence required for biological applications; however, particle size distribution is not very good and fluorescence spectra are generally broader. Synthesis of core–shell QDs in this method can be performed by first synthesizing the core counterpart, followed by injection of shell; however, synthesis of core–shell QDs in this method does not result in very stable QDs.

Thus, depending upon the application, synthesis method can be selected. Probably, the finest way to get the best quality biocompatible quantum dots with long-term stability and very bright photoluminescence with narrow spectra is to synthesize quantum dots via high-temperature thermolysis method using organometallic precursors, following surface functionalization with some water-soluble capping agents. If the application does not demand very long-term stability or good size distribution and a little broader spectral profile is good enough, then direct aqueous synthesis can be performed.

For carbon-based QDs, different synthetic routes can be carried out, e.g. hydrothermal synthesis [30]. Hummer's method consisting direct oxidation of graphite with KMnO_4 and H_2O_2 , followed by particle size reduction using particle size homogenizer or ultrasonication and centrifugation [31] and, pyrolysis of citric acid consisting heating and melting of citric acid, followed by addition of base like NaOH [32].

3 QDs in Biosensing

Sensing means detection. Biosensing refers to the detection of physiologically essential biomolecules. For almost every sensor probe, a very low detection limit, wide linear range of detection, high sensitivity, and specificity are the foremost criteria for sensing. QD-based sensors have been widely studied for biosensing applications over the past years. Here, we will focus on sensing of proteins, nucleic acids, and vitamins.

The sensing of protein is important in biomedical research. The presence, absence, or change in concentration of a particular protein within the human body helps with detection of diseases. Cancer has been one of the most deadly diseases. However, early detection and treatment significantly increases the chance of recovery. In vitro assays of cancer biomarkers are useful tools in cancer detection. Proteins are one of those significant cancer biomarkers, as well as, targeting species for many biomedical applications.

Nucleic acids are another vital type of bio-macromolecules, found in all living cells, as well as, viruses. Nucleic acids work on the storage and expression of genetics. Deoxyribonucleic acid (DNA) codes the information necessary for making protein in cells. Ribonucleic acid (RNA) contributes to the synthesis of protein within cells. These DNA and RNA are also a different class of biomarkers for many ailments, including cancer. Thus, sensing of nucleic acids is of paramount importance.

Vitamins are physiologically significant organic molecules, which are necessary for sustaining human health. Vitamins are required for cell function, cell growth and development, and for healthy metabolism. However, vitamins are not synthesized within the human body, they have to be taken from external diet. Insufficiency of vitamins in human body causes various diseases. Thus, detection of vitamins is extremely significant for detection of diseases.

3.1 Role of Traditional QDs in Biosensing

3.1.1 Sensing of Protein

Protein sensing with QD probes has been very popular in the past decade over conventional sensors [33]. Merkoci et al. reported that core-shell CdSe/ZnS QD-based sensor was able to detect Alzheimer's disease biomarker apolipoprotein E (ApoE) with a detection limit far lower than the detection limit using conventional sensors, e.g., dye Alexa or ELISA [34]. Goldman et al. designed QD-antibody-based sensor for detection of cholera toxin, ricin, shiga-like toxin, and staphylococcal enterotoxin B [35, 36].

Array-based sensing, i.e., chemical nose sensing, has also been reported using quantum dot-based sensor array. Array-based sensing denotes sensing of multiple species simultaneously with a single sensor. Yan et al. designed pH-dependent CdSe/ZnS quantum dot sensor array for sensing 12 proteins, namely, Pep, Cas, BSA, α -Amy, HSA, Lip, Hb, Myo, Pap, Try, Cyt-C, and, Lys. The pH-dependent sensor was able to differentiate multiple proteins based on surface charge. Further, concentration of HSA in real samples, like water and human urine, was also successfully detected, leading to clinical applications [37].

FRET-based ratiometric QD sensors have also been developed for multiple protein sensing. Tyrakowski et al. reported CdSe/ZnS QD-Rhodamine B piperazine-Biotin FRET pair ratiometric sensor for detection of protein Streptavidin and Thrombin. The quantum dot acts as an energy donor, whereas the synthesized dye Rhodamine

B piperazine acts as an energy acceptor in the FRET-couple sensor. The aforesaid FRET sensor couple was reported to sense proteins with a detection limit as low as a few pmol/mL. Sensing with this QD-dye FRET couple sensor is very fast compared to the conventional ELISA-based assay method. Further, the applicability of the protein sensor was also extended using DNA oligonucleotide aptamers. Thus, using different protein-binding agents and aptamers, this type of QD-dye-based sensor can be used for sensing series of proteins [38].

Qiu et al. developed another QD-dye FRET-based protein sensor. The sensor was designed with glutathione capped CdSe/ZnS QD coupled with antibody IgG and dye Cy5. Here, FRET occurs between QD and IgG-Cy5. However, with the addition of protein A, the FRET signals drop. This is the simple methodology for sensing of protein A, a surface-bound protein, obtained in the cell wall of staphylococcus aureus bacteria. The sensor also established good sensitivity in the detection range 0–2 μ M [39].

Manganese doped ZnS QDs have been extensively studied due to their unique defect and dopant-related fluorescence emissions. Wu et al. reported design of a multichannel array-based sensor utilizing fluorescence, phosphorescence, and, light scattering of Mn-doped ZnS QDs concurrently for detection of different proteins. They took eight proteins with different molecular weight and isoelectric points, namely, Cytochrome C (Cyt C), Hemoglobin (Hb), Human Serum Albumin (HSA), Lysozyme (Lys), Myoglobin (Mb), Papain (Pap), Transferrin (Tf), and Ovalbumin (Ob) as analyte. Fluorescence intensity, phosphorescence intensity, and, light scattering intensity of mercaptopropionic acid capped Mn-doped ZnS QDs were monitored in the absence or presence of different proteins at 440 nm, 595 nm, and, 500 nm, respectively. The change in fluorescence, phosphorescence, and, light-scattering properties of Mn-doped ZnS QDs after interaction with each protein was distinct, based on which the sensor array was fabricated, sensor model is illustrated in Fig. 1. The detection limit for distinct determination of all eight proteins using this sensor

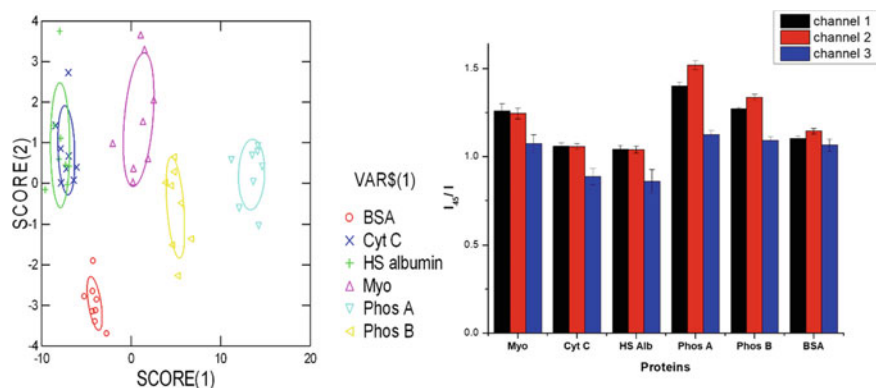


Fig. 1 Sketch of multichannel protein sensing with six different proteins; left: LDA analysis graph, right: plot of intensity ratio at different wavelengths versus concentration of different proteins

was reported to be 0.5 μM . The sensor was also tested for unknown samples, the sensing accuracy was 93.8% and 96.3% at 0.5 μM and 0.75 μM concentrations, respectively [40].

3.1.2 Sensing of Vitamins

Traditional QD-based nanosensors have been widely used for detection of vitamins. Pramanik et al. reported sensing of vitamin B₁₂ using a Manganese doped ZnS QD-based sensor. The working principle of the sensor is based on the fact that vitamin B₁₂ quenched the fluorescence of Manganese doped ZnS QDs. Stern–Volmer constant was calculated to be $5.2 \times 10^{10} \text{ M}^{-1}$. The mechanism behind this quenching is assumed to be Förster Resonance Energy Transfer (FRET) between Mn-doped ZnS QDs and vitamin B₁₂, Förster distance (R_0) and FRET efficiency were determined to be 2.33 nm and, 79.3%, respectively. This QD-based sensor showed good selectivity toward vitamin B₁₂ in the presence of various proteins, amino acids, and metal ions. The detection limit for this sensor was $(1.15 \pm 0.06) \text{ pM}$, with a detection range of 4.9–29.4 pM [41]. Vaishnavi et al. reported another vitamin B₁₂ sensor using CdTe quantum dot. Fluorescence of CdTe QDs was quenched in the presence of different derivatives of vitamin B₁₂. Stern–Volmer quenching constants, quenching rate constants, and binding constants for the binding interaction between CdTe QDs and different derivatives of vitamin B₁₂ were calculated to be in the order of 10^{-7} M^{-1} , $10^{-13} \text{ M}^{-1} \text{ s}^{-1}$, and 10^{-4} M^{-1} , respectively. The mechanism behind the fluorescence quenching is depicted as Förster Resonance Energy Transfer (FRET) between CdTe QDs and vitamin B₁₂. Critical energy transfer distance (R_0) for the interaction was calculated to be in the range of 2.7–4.2 nm for different derivatives of vitamin B₁₂. The limit of detection using this sensor was 0.15 $\mu\text{g/mL}$. The detection range, in which a linear plot can be obtained, was 1–14 $\mu\text{g/mL}$. Further, this sensor was also applied in pharmaceutical samples with a recovery range of ~100% [42].

Koneswaran et al. reported vitamin B₆ sensor using L-cysteine capped CdS/ZnS core–shell quantum dots. Fluorescence of CdS/ZnS QDs was quenched in the presence of vitamin B₆, quenching followed Stern–Volmer equation. A good linear Stern–Volmer quenching plot was obtained for 0.05 mg L^{-1} to 6.5 mg L^{-1} of vitamin B₆ concentration. The Stern–Volmer quenching constant (K_{sv}) was calculated to be 1.24 mg L^{-1} . The limit of detection using this sensor was found to be 0.015 mg L^{-1} . The sensor was pH and temperature-sensitive. Fluorescence intensity increased with pH enhancement until saturation at pH 6–6.5. At higher pH than 6.5, fluorescence intensity decreased. The fluorescence intensity of CdS/ZnS quantum dots diminished with increasing temperature due to thermal quenching as well as dissociation of the capping agent at a higher temperature. The optimum pH and temperature for the usage of the vitamin B₆ sensor were 6.25 and 25 °C, respectively. A possible mechanism behind this sensor fluorescence quenching was attributed to electron transfer from QDs to vitamin B₆. This sensor displayed good selectivity towards vitamin B₆ in the presence of several other physiologically essential vitamins, amino acids, and, metal ions [43].

Ghosh et al. reported detection of ascorbic acid (vitamin C) using dendrimer capped CdS quantum dot-based sensor. Fluorescence of different varieties of dendrimer capped CdS quantum dots was quenched with the addition of vitamin C. Quenching followed linear plot in Stern–Volmer equation and quenching was static by nature. A good linear plot was obtained over a wide range of concentrations of vitamin C, 16.6–100 μM . The limit of detection using this sensor was calculated to be 3.3 μM . The fluorescence quenching was dependent on the size of QDs. Further, this sensor was also applied for the determination of ascorbic acid concentration in vitamin C tablets; sample recovery was almost $\sim 100\%$. The CdS-dendrimer nanocomposite sensor also exhibited good selectivity in the presence of interference like uric acid, tartaric acid, and, citric acid [44].

3.1.3 Sensing of Nucleic Acid

Quantum dot-based sensors have also been reported for successful sensing applications of nucleic acids.

Lu et al. reported CdS quantum dot-based fluorescence sensor for the detection of nucleic acid DNA. This sensor works via a two-step process. In the first step, a fluorescent-labeled single-stranded DNA is attached to CdS QDs; this attachment quenches the fluorescence of CdS QDs, i.e., “turn-off” of QD fluorescence. In the second step, the DNA coupled QD probe is attached to its target single-stranded DNA forming a double-stranded DNA; this causes detachment of QD from the probe leading to recovery, i.e., “turn-on” of QD fluorescence. The detection limit for this sensor system is 1 nm. Moreover, the sensor system had exhibited good selectivity and sensitivity [45].

He et al. reported design of octa(3-aminopropyl) octasilsequioxane octahydrochloride (OA-POSS) and 3-mercaptopropionic acid (MPA)-capped Mn-doped ZnS QDs (MPA-1)-based sensor for quantitative detection of DNA. The sensing strategy was based on monitoring the RTP intensity of MPA-1/OA-POSS nanohybrids at 590 nm with respect to DNA concentration. A linear plot was obtained in DNA concentration range 0.125–10 μM . The detection limit using this sensor was obtained 54.9 nM. Further, this probe can be used for quantitative detection of different types of DNA, e.g., double-strand calf thymus DNA (dctDNA), double-strand hsDNA (dhsDNA), single strand calf thymus DNA (sctDNA), single-strand hsDNA (shsDNA), etc. Moreover, this sensor system also exhibited good selectivity toward DNA in the presence of interfering metal ions, macromolecules, and, small molecules [46].

Li et al. reported design of a photoelectrochemical sensor comprised of CdS quantum dot sensitized TiO_2 nanorod for sensing of DNA. The fabrication involved in-situ growth of TiO_2 nanorods on fluorine-doped tin oxide (FTO coated) substrate, followed by CdS QD labeled capturing DNA hairpin immobilized on FTO substrate. When target DNA is not present, direct interaction between TiO_2 and CdS enhances photocurrent density. When target DNA is present within the system, conformational change triggers diminishment in photocurrent density. The sensor gives a linear plot

of photocurrent versus logarithm of DNA concentration for the DNA concentration range of 10 aM to 100 pM. The limit of detection (LOD) using this sensor was calculated to be 5.2 aM. This sensor also showed good specificity and high stability, which is useful in clinical studies [34].

Zhao et al. reported gold nanoparticle (AuNPs)-CdTe QD Förster Resonance Energy Transfer (FRET)-based sensor probe for DNA detection. The sensor design strategy involves the linkage of 5'-NH₂-DNA and 3'-SH-DNA to CdTe QD surface and AuNP surface, respectively, using 1-ethyl-3-(dimethylaminopropyl)carbodiimide hydrochloride (EDC) as a linker. The ratio of AuNPs-DNA and CdTe QDs-DNA played an important role in determining the FRET efficiency of the probe; FRET efficiency was observed to be maximum at AuNP-DNA: QD-DNA: 10:1 ratio. The fluorescence of AuNP-DNA-CdTe system decreased due to FRET between CdTe QDs and AuNPs. In the presence of a complementary single-stranded DNA, the quenched fluorescence of the system was recovered due to decreased FRET caused by distance enhancement between CdTe QDs and AuNPs. The sensor probe displayed an excellent selectivity toward complementary base-pair DNA in presence of mismatching base-pair DNAs [47].

Wang et al. designed a sensor probe comprised of g-C₃N₄, CdS QDs, and, Avidin-CuO for detection of messenger RNA N⁶-methyladenosine (m⁶A). The sensor was designed with several moieties: g-C₃N₄/CdS QDs as photoactive substance, anti-m⁶A antibody as a recognition element, phos-tag-biotin as link component, and avidin-CuO as PEC signal indicator element. The sensor gave a linear range for detection at 0.01–10 nM concentration of RNA, the detection limit was determined to be 3.53 pM. Moreover, this sensor probe has the potential for recognition of m⁶A RNA expression level in breast cancer serum [48].

3.2 Role of Emerging CQDs in Biosensing

In recent years, carbon-based non-toxic quantum dots, e.g., carbon dots, graphene, and graphene oxide quantum dots, have been extensively studied for biosensing applications.

3.2.1 Sensing of Protein

Freire et al. reported fabrication of a CQD-based sensor for multichannel sensing of proteins. The sensor array was designed in combination of NH₂ rich, polyethyleneimine, ethylenediamine branched-capped carbon quantum dots (CQDs.BPEI), copper acetate, and ethylenediaminetetraacetic acid (EDTA). The chemical nose sensor exhibited good efficiency in simultaneous sensing of 8 proteins, namely, bovine serum albumin (BSA), human serum albumin (HSA), acid phosphatase (PhosA, from potato) and alkaline phosphatase (PhosB, from bovine intestinal mucosa), hemoglobin (Hem, from human), myoglobin (Myo, from equine

heart), α -amylase (α -Am, from *Bacillus licheniformis*) and cytochrome c (Cyt. C, from equine heart) at a concentration of 40 nM. The detection limit for this sensor was 5–40 nM depending upon protein. This sensor array was able to detect 40 samples in a random unknown set of 48 samples. Thus, the identification accuracy for this system was calculated to be 83% [49].

Han et al. designed another carbon quantum dot-based sensor probe for the detection of human protein IgG (HIgG). They synthesized nitrogen-doped carbon QDs, which exhibited excellent electro-chemiluminescent (ECL) activity on glassy carbon electrode (GCE). The immunosensor probe for HIgG was fabricated as GCE/Nitrogen-doped Carbon quantum dots (NCQDs)/anti-HIgG/Bovine Serum Albumin (BSA). For sensing of human IgG, different concentrations of HIgG solutions were dropped on the sensor electrode and kept for incubation. Next, the electrodes were kept in an electro-chemiluminescent (ECL) cell in pH 7.5 PBS buffer, and ECL signals were recorded for each electrode with scanning potential range –2 to 0 V and scanning rate 100 mV s⁻¹. The ECL-based sensor system showed the linear range at 0.1–4.0 ng mL⁻¹ of protein concentration, the limit of detection was calculated to be 0.05 ng mL⁻¹. Moreover, the sensor was stable, reproducible, and showed good selectivity in the presence of interfering substances [50].

Wang et al. reported fluorescence assay for the activity measurement of protein kinase (CK2) using phosphorylated peptide graphene quantum dots. The sensor was designed through the addition of different concentrations of protein CK2 and ATP to peptide-graphene quantum dot (GQD) in tris buffer of pH 7.5, followed by phosphorylation of peptide-GQDs and addition of Zr⁴⁺ ion. Steady-state and time-resolved fluorescence spectra and light scattering spectra of the solutions were measured for sensing. A linear plot was obtained for quenched fluorescence intensity versus concentration of protein casein kinase II (CK2) in a concentration ranging from 0.1 to 1 U mL⁻¹. The detection limit for the sensor was determined to be 0.03 U mL⁻¹. Further, the sensor system was also successfully applied for screening protein kinase inhibitors in real samples [51].

Liang et al. fabricated an electrochemiluminescence resonance energy transfer (ECL-RET)-based sensor probe for determining activity of protein kinase. In the sensor system, GQD acted as donor, and graphene oxide (GO) acted as acceptor. GQDs were functionalized with peptide on chitosan film electrode. When protein kinase (CK2) along with adenosine 5'-triphosphate (ATP) was added to the system followed by phosphorylation of peptides, graphene—anti-phosphoserine antibody nanocomposite got absorbed into the surface of phosphorylated peptide-GQD electrode, which quenched the electrochemiluminescence of GQDs. Protein kinase activity was measured as a function of the ECL quenching. The ECL sensor exhibited high specificity towards CK2 in the presence of bovine serum albumin (BSA), glucose oxidase (GOx), and alcohol dehydrogenase (ADH). The sensor was stable and gave reproducible results up to four weeks. Further, the sensor gave recoveries of 97–103% in complex clinical samples [52].

Song et al. reported simple fluorescence-based protein sensing using AgInZnS (AIZS)-GOQDs. Fluorescence of AIZS-GOQDs was quenched in the presence of protein human serum albumin (HSA); quenching was static in nature. Both of the

Stern–Volmer quenching constant (K_{SV}) and the amendatory Stern–Volmer effective quenching constant (K_a) were found in the order of 10^5 L mol^{-1} . Both constants were temperature dependent and decreased with an increase in temperature. The binding constant for the AIZS QD-GO and HSA binding was also in the order of 10^5 L mol^{-1} . However, the binding constant increased with an increase in temperature. Moreover, this AIZS-GO sensor also successfully interacted with protein lysozyme, but the fluorescence characteristics were distinct as compared to protein HSA. This fact established the selectivity of the sensor system towards protein HSA. Further, the cytotoxicity of the AIZS-GO system was found to be very low. The low cytotoxicity combined with biocompatibility makes this sensor an appropriate candidate for biomedical research applications [53].

3.2.2 Sensing of Vitamins

Sinduja et al. reported fabrication of graphene quantum dot-gold nanoparticle (Au-GQD) composite-based sensor for sensing of vitamin B1. Thiamine (vitamin B1) was detected both calorimetrically and spectrophotometrically using this sensor. Colorimetric detection allows qualitative sensing, whereas, spectrophotometric detection allows quantitative determination of thiamine. The color of AuNP-GQD changed from wine red to violet upon addition of colorless vitamin B1 solution of concentration $0.5 \mu\text{M}$; the change was visible in naked eye. However, the color of AuNP-GQD solution did not change with the addition of a huge concentration of other vitamins. Therefore, the AuNP-GQD sensor is specific towards thiamine only in the presence of other vitamins. Further, the absorbance intensity of AuNP-GQD decreased with increasing concentration of thiamine. The quenching followed Schott's equation, where the absorbance intensity of AuNP-GQD was correlated to vitamin B1 concentration. This equation allows quantitative determination of vitamin B1 concentration. Further, this sensor selectively detected thiamine in the presence of vitamin B2, B3, B6, B7, B12, C, and metal ions Cu^{2+} , Ca^{2+} , Zn^{2+} . The detection limit was calculated to be $0.16 \mu\text{g mL}^{-1}$ [54].

Wadhwa et al. reported detection of vitamin D₃ using graphene quantum dot-gold hybrid nanoparticles (GQD-AuNP)-based sensor probe. The electrochemical sensor was designed by immobilizing Au- μE electrodes with 1:1 ratio of MU: MUA, followed by EDC-NHS coupling. GQD-AuNP nanocomposite was further immobilized on the electrode through $-\text{CO}$ and $-\text{OH}$ functional groups on GQD and MU, respectively. This conjugation of GQD-AuNP to the surface was followed by conjugation of aptamer for complete formation of a sensor system. The aforesaid sensor exhibited linear range of detection for 1–500 nM concentration of vitamin D₃. The detection limit, limit of quantification, and sensitivity for sensing vitamin D₃ were calculated to be 0.70 nM, 2.09 nM, and $0.90 \Omega \text{ nM}^{-1} \text{ mm}^{-2}$, respectively. Further, the nanoparticle aptasensor was stable and selective toward vitamin D₃ in the presence of interfering substances. The sensor was also tested in serum samples with 98% recovery [55].

Du et al. designed a carbon quantum dot (carbon nanodot)-based ratiometric FRET nanosensor for detection of vitamin B₂. The fluorescence intensity of carbon dots at 470 nm decreased, while fluorescence intensity at 532 nm increased upon addition of vitamin B₂ solution to carbon dot solution. The fluorescence intensity ratio gave a linear relationship with the concentration of vitamin B₂ in the concentration range of 0.35–35.9 μM at pH 7.4. The limit of detection was found to be 37.2 nM. The ratiometric sensor exhibited excellent selectivity toward, vitamin B₂ only, in the presence of various metal ions and anions e.g., Na⁺, Ca²⁺, K⁺, Zn²⁺, CO₃²⁻, NO₃⁻, Cl⁻, different amino acids e.g., glycine, alanine, L-cysteine, L-tyrosine, L-glutamate, L-serine, valine, and other vitamins, e.g., vitamin C, B₁, B₃, B₁₂. Further, this sensor was also successfully applied for detection of vitamin B₂ inside live cells and in real samples, e.g., orange beverage, soybean milk, milk, honey, multivitamin tablet, and VB complex tablet with recovery ranging from 85 to 110% [56].

Wang et al. reported a zwitterion modified carbon quantum dot-based sensing platform for sensing of vitamin B₁₂. The absorption intensity of carbon quantum dots increased with the addition of vitamin B₁₂ solution, whereas, fluorescence intensity was quenched. Stern–Volmer quenching constant for the interaction was calculated to be 2.87×10^5 L/mol. The linear range was obtained for concentration range 0.5–3 μM concentration of vitamin B₁₂. The limit of detection was calculated to be 81 nM. The mechanism behind this quenching was explained as non-radiative electron transfer from carbon dots to Co²⁺ present in vitamin B₁₂. This carbon dot-based sensor exhibited excellent selectivity towards vitamin B₁₂ and Co²⁺ in the presence of interfering substances. Moreover, the sensor was stable over a wide range of pH, salt concentration, and various UV radiation environments [57].

3.2.3 Sensing of Nucleic Acids

Qian et al. reported GQDs and graphene oxide FRET-based sensor system for detection of DNA. First, graphene quantum dots were reduced with sodium borohydride to form reduced graphene quantum dots (rGQDs). Next, single-stranded DNA (ssDNA) was attached to the rGQDs. The ssDNA-rGQDs were further absorbed on graphene oxide (GO) surface, enabling FRET between GO and rGQDs leading to the diminishment of fluorescence. When target DNA is added to the ssDNA-rGQD-GO assembled system, the dsDNA-rGQD system is formed via complementary base pairing. Formation of dsDNA-rGQD ruptures interaction between GO and ssDNA-rGQDs thus liberates dsDNA-rGQD from GO, which, in turn, recovers the lost fluorescence. The as-proposed sensor gave a linear range of detection in the range 0–46 nM concentration of target DNA. The limit of detection was calculated to be 75 pM. Moreover, the GQD-based sensor exhibited excellent selectivity towards sensing of DNA [58].

Li et al. designed a GQD-based sensor probe for the detection of RNA both optically and electrochemically. The as-synthesized GQDs were functionalized with HVC-6. The optical sensor was prepared by simply adding RNA to HVC-6 functionalized GQD solution and monitoring the fluorescence upon excitation at 365 nm. The electrochemical sensor was designed by coating a glassy carbon electrode (GCE)

with HVC-6 modified QDs. For sensing, RNA solution was added to the electrode followed by surface coverage of the electrode with chitosan. The fluorescence intensity of HVC-6 functionalized QDs at 470 and 610 nm enhanced in the presence of RNA, the change in color was also visible in naked eye. The ratio of fluorescence intensities at 470 and 610 nm gave linear relation with the concentration of RNA, following which concentration of RNA can be determined. The optical sensor exhibited good selectivity in presence of other analytes. On the other hand, HVC-6 modified QDs gave a distinct change in cyclic voltammetry signal in the presence of RNA, which allows detection of RNA [59].

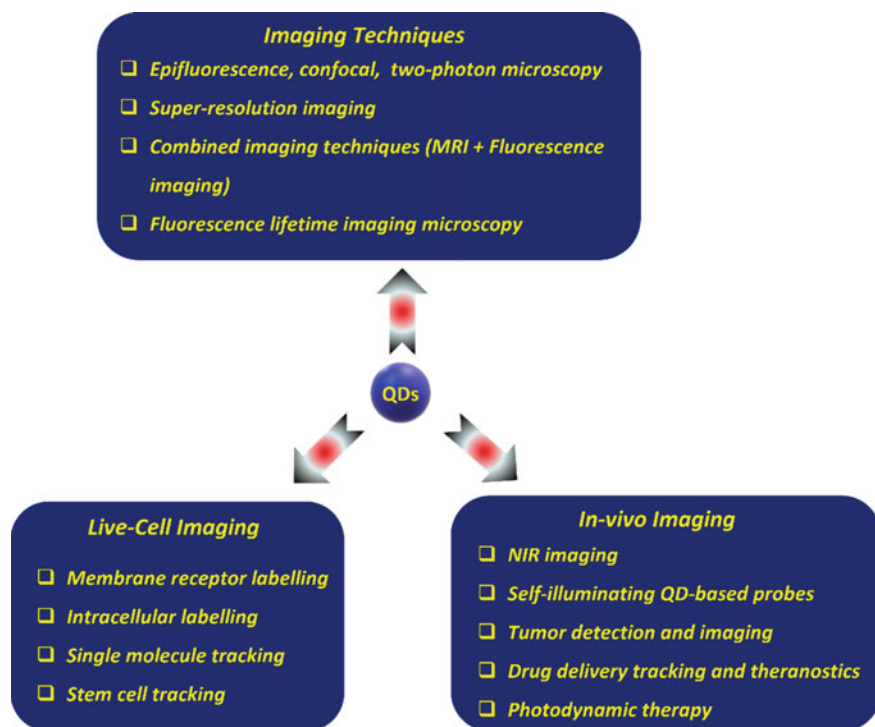
Loo et al. reported a carboxylic acid carbon quantum dot (cCQD)-based sensor for sensing of DNA. The optical sensor was designed by coupling a fluorescent-labeled single-stranded DNA (ssDNA) to carboxylic carbon quantum dots. The fluorescence of cCQDs was quenched due to interaction between ssDNA and cCQDs. In the presence of target DNA, ssDNA reacts with complementary base pair forming dsDNA, following which lost fluorescence of cCQDs is recovered. Two different types of cCQDs were tested for sensing, malic acid CQD and citric acid CQD. The linear range of detection using malic acid CQD and citric acid CQD was determined to be 0.04–400 nM and 0.4–400 nM, respectively. The limit of detection was calculated to be 45.6 nM and 17.4 nM for citric acid CQD and malic acid CQD, respectively. Both of the CQD-based sensor systems showed good selectivity for DNA detection [60].

Liu et al. designed an electrochemiluminescence (ECL) sensor for the detection of microRNA using DNA functionalized nitrogen-doped carbon quantum dots (N-CQDs). N-CQDs-hairpin probe composites were synthesized by activating N-CQDs with EDC and NHS, followed by combination of the amino-functionalized hairpin with N-CQDs. The sensor probe was designed as: MCH/Hairpin Probe-N-C QD/GO (graphene oxide)-Au (Gold NPs)/GCE (glassy carbon electrode). The ECL signal intensity enhanced in the presence of microRNA in the system. The sensor gave a linear range of detection for 10 aM– 10^4 fM concentration of microRNA. The detection limit using this sensor was determined to be 10 aM. Selectivity studies established the fact that the sensor was selective towards miR-21 compared to control RNA. Moreover, the sensor system was reasonably stable and gave reproducible results for five reduplicate measurements [61].

4 Emerging Carbon-Based QDs for Bioimaging Applications

4.1 Traditional QDs in Bioimaging

The discovery of semiconductor QDs has also led to significant breakthroughs in bioimaging methods (Scheme 1). Compared to conventional molecular-scale labels, QDs offer the advantage of cell labeling, unique optical and electrical properties,



Scheme 1 Current and perspective applications of semiconductor quantum dots (QDs) in bioimaging

surface functionalization and multimeric binding capacities, and a wide choice of multiplexing strategies [62, 63]. However, potential cytotoxicity of traditional QDs is the main barrier to their introduction as clinical labels and contrast agents in bioanalytical or medical diagnostics [64]. Nevertheless, over the past decade, several research groups have reported bioimaging modalities involving traditional QD-based studies. The detailed discussion on traditional QD-based bioimaging has been specified in some other chapter.

4.2 Emerging Carbon-Based QDs in Bioimaging

To overcome the limitations related to cytotoxicity of traditional QDs, various bio-applications [65, 66] of non-toxic carbon-based quantum dots have been extensively investigated. Carbon-based quantum dots have been evaluated for optical bioimaging applications, including cellular uptakes and the fluorescence brightness in the cellular environment, and, in vivo imaging in mice models in reference to the traditional QDs in the same models.

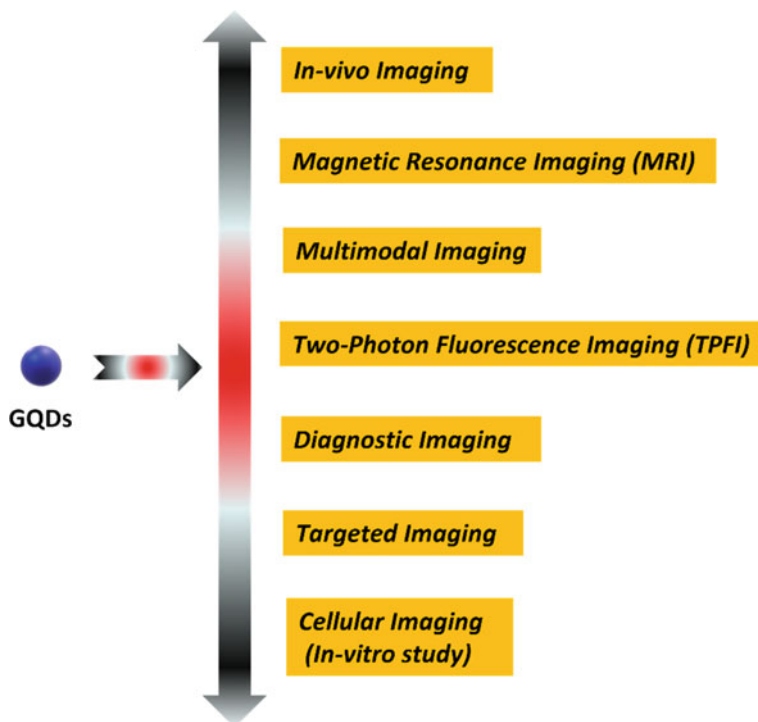
Carbon quantum dots (CQDs) have been successfully demonstrated for the fluorescence imaging of cells [67, 68], since its original discovery in 2004 [69], taking advantage of their non-toxicity, visible excitation and emission wavelengths, fluorescence brightness, and high photostability. The pioneering work on CQDs for bioimaging in vitro [68] and in vivo [70] was reported by Sun's group. The confocal microscopy imaging revealed that the endocytosed carbon dots were mainly in the cytoplasm, with only minor penetration into the cell nucleus [68]. The same approach was applied in several subsequent studies, including the one by Liu et al. on the labeling of *E. coli* cells and also murine P19 progenitor cells [71]. Zboril et al. reported the synthesis of ultrafine Gd(III)-doped CQDs with a dual fluorescence/MRI character [72]. It is possible to combine a T1 MRI agent with CQDs via robust covalent bonding, which increases the rotational correlation time (τ_R) of the T1-imaging probes [73]. Pandey et al. [74] used CQDs functionalized gold nanorods to deliver of doxorubicin in a multi-modality fashion, including drug delivery, photothermal therapy, and, bioimaging using the same platform.

Over the past decade, non-toxic carbon-based graphene quantum dots (GQDs) have shown potential application in the horizon of the biomedical research field owing to its intriguing and tailorable fluorescence properties comprising excellent biocompatibility. Apart from that GQDs exhibit low in vitro and in vivo toxicity, promising physiological stability, high permeability membranes, ultrahigh specific surface area, and, surface functionalization abilities [75–77]. The early-stage diagnosis of diseases helps to increase the survival rate of patients, which has motivated researchers to develop highly sensitive, low-toxicity QDs with excellent specificity. Conventional imaging techniques that have implemented GQDs-based bioimaging studies are shown in Scheme 2.

Researchers proposed targeted imaging as a potential alternative to the recognition and detection of cells. It is achieved via surface modification of GQDs with targeted groups and polymers. The most widely used cell-targeting agents are folic acid (FA), arginine-glycine-aspartic acid (RGD), hyaluronic acid (HA), and even proteins [78–81]. In addition, the targeting capability of the FA-N-GQDs is confirmed by the live-cell line imaging.

GQDs are used to fabricate multifunctional theragnostic platforms that integrated fluorescence imaging and therapeutic studies, such as photothermal therapy (PTT) and photodynamic therapy (PDT). For example, Cao and coworkers designed a novel theragnostic platform consisting of PEGylated and aptamer-functionalized GQDs loaded with porphyrin derivatives (P) photosensitizer [82]. The resulted system exhibited good feasibility for intracellular cancer-related microRNA detection and fluorescent imaging of cancer cells. GQDs with superior physicochemical and NIR-responsive properties can be used for combined PTT and PDT coupled with cancer cell tracking applications [83]. The GQDs exhibited potent therapeutic activity in treatment of MDA-MB-231 breast cancer cells.

Recent advances in the two-photon fluorescence behavior, photostability, and biocompatibility of GQDs have demonstrated the feasibility of two-photon fluorescence imaging (TPFI) as a powerful tool [84]. These findings open the door to new opportunities for GQDs in the bioimaging fields. Among various fluorescent



Scheme 2 Conventional imaging techniques that used graphene quantum dots (GQDs)

carbonaceous materials such as carbon dots (C-dots), GOs, and their derivatives, GQDs have garnered much attention in deep-tissue imaging due to (1) their tunable fluorescence properties via doping through heteroatoms, (2) their strong fluorescence behavior without passivation, and (3) their enhanced TP absorption towards deep imaging in TPFI due to their stacked π -electrons. The boron-doped magnetic GQDs (B-GODs) were shown convenient for TPFI and near-infrared (NIR) imaging contrast agent [85]. MRI technique can be coupled with the two-photon fluorescence imaging (TPFI) GQDs. Wang and coworkers developed an excellent and MR suitable contrast agent (GQD-conjugated Gd_2O_3) in which both one-photon and two-photon diagnostics were possible [86].

The application of GQDs for in vivo bioimaging has demonstrated by some research using model animals (mouse and zebrafish) [80, 87]. For instance, Zhu et al. carried out the in vivo bioimaging of mice with wide ranges of excitation light wavelengths varying from 465 to 500 nm, and they observed light emission from 580 to 620 nm [88]. Nurunnabi et al. also investigated the relationship between the emission light wavelengths and the fluorescence quality for bioimaging using carboxylate functionalized GQDs [89]. On the other hand, the NIR-GQDs could be detected around the heart, liver, spleen, and kidneys at 8-h post-injection [90].

However, it is challenging to synthesize NIR emitting GQDs, and the fluorescent quantum yields of these GQDs are often low, which significantly limited the development of the GQD-based bioimaging application in recent years. Therefore, *in vivo* application of GQDs has been little explored so far.

5 QDs for Drug Delivery Applications

A drug delivery carrier is a substance that enables a drug reaching its target cells selectively without affecting non-target healthy cells, tissues, or organs. A suitable drug carrier should have properties like decent drug loading capacity, sustained and controlled drug release at specific pH, low cytotoxicity to healthy organs. Conventional drug delivery vehicles suffer from many limitations, e.g., low water solubility, non-specific cytotoxicity, multi-drug resistance, non-specificity, low drug loading capability, etc. Nanomaterial-based drug delivery carriers were able to overcome the aforesaid restrictions. In the past decades, QD-based nano-drug carrier system has been successfully used for delivery of multiple drugs, both *in vitro* and *in vivo*.

5.1 Traditional QDs for Drug Delivery

Aswathy et al. studied 5-fluorouracil (5-FU) drug delivery prospects using Mn-doped ZnS quantum dot-Zein nanoparticle conjugate. TEM studies revealed the size of Mn-doped ZnS QD to be 5 nm; zein nanoparticles were of 600–700 nm size. After loading of the drug, the size of nano-conjugates increased to 800–900 nm. The nanocarrier was studied for delivery of drug 5-FU in L929 mouse fibroblast cell line and MCF-7 breast cancer cell line. Drug loading capacity of Mn-doped ZnS QDs-Zein NP was calculated to be 60%. The drug was released slowly over 24 h; drug release was 70% in 8 h. Cell viability studies revealed that 80% cells were viable with QD-Zein NP, whereas, cell viability significantly decreased with drug-loaded NPs. This fact suggests that QD-NP conjugate has very low cytotoxicity, but in the presence of drug, cytotoxicity increased in both of the cell lines [91]. Abdelhamid et al. reported TGA-capped CdTe quantum dot coupled with gelatin/chondroitin nano-assembly for delivery of hydrophobic drug celecoxib (CXB) and rapamycin (RAP) in human breast cancer MCF-7 and MDA-MB-231 cell lines. The gelatin-QD composite was synthesized using EDC and NHS as activating agent, gelatin-QD nano-conjugate was further covered with negatively charged chitosan (CS), thus forming gelatin-QD-CS (G-QD-CS) nanocarrier. TEM analysis revealed the size of QDs in 2.77–4.75 nm range. The size of drug-loaded G-QD-CS was measured to be 269.7 nm. The as-synthesized nanocarrier gave high loading efficiency for both drugs, 93.77% and 94% for CXB and RAP, respectively. Drug release from nanocarrier was prolonged for both drugs. The release of CXB from nanocarrier was 9.77% in 48 h. In case of RAP, 0.76% drug released in 30 min, the same pattern continued until 48 h. The

nanocarriers were stable up to 3 months without considerable aggregation. The as-synthesized nanocarriers did not exhibit any significant cytotoxicity toward both cell lines; cell viability was about 94%. In addition, a high cellular uptake was observed with this nanocarrier after 24 h of incubation. Further, the drug-loaded nanocarrier was also tested in tumor-bearing mice; it was successful in reducing tumor volume and, at the same time, inhibited tumor angiogenic marker VEGF-1. Further, effective localization of drug was observed in tumor tissues, however, mouse kidney, and liver were safe [92].

Abdelhamid et al. reported another chitosan (CS) functionalized (Lactoferrin) LF-MPA capped CdTe QD nanocomposite for dual targeting of drugs Celecoxib (CXB) and Honokiol (HNK) in breast cancer therapy. LF-CdTe QD conjugate was synthesized by carbodiimide reaction using EDC and NHS for activation. TEM studies revealed the size of the QDs in the range of 3.7–4.2 nm, the quantum yield was calculated as 34%. The size of the LF-QD-CS-NP nanocarriers increased up to 201.7 nm. The as-synthesized nanocarriers were stable up to three months with much aggregation; size increased to 236.3 nm after 3 months. The effect of drug-loaded nanocarrier was studied *in vitro* on MCF-7 and MDA-MB-23 breast cancer cell lines. Release of drug CXB from nano-vehicle was very slow, 14.76% and 19.87% drug was released in 48 h and 96 h, respectively. Release of drug HNK from the nano-vehicle was slower, 1.2% and 3.8% in 24 h and 96 h, respectively. MTT assays suggested that the blank nanocarriers did not exhibit any significant cytotoxicity. However, cytotoxicity values increased synergistically with dual drug-loaded nanocarrier compared to single drug-loaded nanocarrier. The LF-QD-CS-NC exhibited high cellular uptake to MCF-7 breast cancer cell line and mainly concentrated in the perinuclear region. Further, the effect of dual drug-loaded nanocarrier was studied *in vivo* on EAT model. Combined dual drug therapy without a nanocarrier caused 172.3% increase in tumor volume, while LF-QD-CS-NC loaded dual drug synergistic therapy increased only 48.12% increase in tumor volume in the mice model. Thus, the efficacy of QD-based nanocarrier was proved both *in vitro* and *in vivo* [93].

Olerile et al. reported CdTe/CdS/ZnS quantum dot loaded with anti-cancer drug paclitaxel (PTX) for cancer therapy. Two different types of nanocarriers were designed for study, co-loaded PTX and CdTe/CdS/ZnS QDs (NLC) and blank NLC without drug. The mean size of co-loaded NLC and NLC was calculated to be 115.93 nm and 113.23 nm, respectively. TEM studies suggested spheroid geometry with a smooth surface. Encapsulation efficiency and drug loading efficiency for PTX using this nanocarrier were calculated to be 80.7% and 4.68% respectively. The drug release was in a slow but uninterrupted manner; 27.9% and 59.78% PTX drug was released in 24 h and 72 h, respectively. *In vitro* cytotoxicity study was performed with human liver cancer HepG2 cell line. IC₅₀ values of PTX co-loaded NLC and blank NLC were determined to be 1.05 μ M and 0.07 μ M, respectively, which suggested almost no cytotoxicity with blank nanocarriers but a considerable increase in cytotoxicity with drug-loaded NLC. *In vivo* studies were carried out with tumor-bearing mice. After three weeks of administering into mice, the tumor volume of mice was determined to be 1065 mm³ and 549 mm³ with blank NLC and PTX drug co-loaded NLC, respectively. Moreover, body weight was almost constant in

mice after loading drug co-loaded, quantum dot nanocarriers, indicating negligible cytotoxicity to the animal at the given dose. Thus, the drug co-loaded QD system was proved to be efficient both in vivo and in vitro [94].

5.2 Emerging QDs in Drug Delivery

Iannazzo et al. reported a GQD-based nano-vehicle for the delivery of anti-cancer drug doxorubicin (DOX) on human lung epithelial cancer A549 cell line. GQD was modified with BTN, a synthetic derivative of biotin. GQD-BTN was used as a nanocarrier for the delivery of anti-cancer drug DOX. TEM studies suggested homogeneous circular nanoparticles with a size less than 5 nm. The drug DOX was loaded on GQD-BTN surface by taking advantage of π - π interaction between GQD surface functional groups and DOX aromatic structure; drug loading efficiency was 16.6 wt%. The drug release was pH-sensitive. No drug release was observed at basic pH (pH 9) or neutral pH (pH 7.4). However, at acidic pH 5.3, a huge drug release was observed from the nanocarrier in just 5 min. Cell viability studies exhibited 85% cell viability in 48 h with cell lines treated with GQD-BTN nanocarrier, which indicated negligible cytotoxicity. Further, GQD-BTN-DOX-loaded system was efficient in 27% more cellular uptake compared to free drug DOX only. Interestingly, cell mortality was delayed with GQD-BTN-DOX-loaded system compared to free DOX. Thus, GQD-BTN can be efficiently used as a nanocarrier for anti-cancer drug delivery [95].

Ruzycka Ayoush et al. reported a Folic acid (FA) functionalized Ag-In-Zn-S QD-based nano-vehicle for delivery of anti-cancer drug DOX in treatment of lungs cancer. Different types of nanocarriers were synthesized by further surface functionalization of FA modified Ag-In-Zn-S QD, e.g., QD-(Mercaptoundecanoic acid) MUA-FA, QD-(Cysteine) Cys-FA, QD-(Lipoic acid) LA-FA, and also their drug-loaded analogues, e.g., QD-MUA-FA-DOX, QD-Cys-FA-DOX, QD-LA-FA-DOX. Drug DOX was loaded in the nanocarriers through a chemical reaction with EDC/NHS as activating agent, successful attachment of DOX was confirmed through FTIR analysis. The size of the as-synthesized QDs was around 3 nm. Size of QD-MUA, QD-MUA-FA, and drug-loaded QD-MUA-FA-DOX was 11.5 nm, 14.2 nm, and 15.1 nm, respectively. The size of QD-Cys, QD-Cys-FA and QD-Cys-FA-DOX was 14 nm, 16.6 nm, and 17.6, nm respectively. The size of QD-LA, QD-LA-FA and QD-LA-FA-DOX was 18.8 nm, 21.3 nm, and 22.5 nm, respectively. The zeta potential of all three drug-loaded nanocarriers, QD-Cys-FA-DOX, QD-MUA-FA-DOX, and QD-LA-FA-DOX, are small, which suggests promising drug release from the nanocarriers in cell medium. A study on human alveolar basal epithelial cells (A549) revealed that QD-Cys-FA and QD-MUA-FA nanocarriers carried more DOX, thus facilitating more DOX release in the cells. Among the three nanocarriers, QD-MUA-FA-DOX was most cytotoxic against A549 cells, which is due to the mild cytotoxicity of MUA. The cytotoxicity order was: QD-MUA-FA-DOX > QD-LA-FA-DOX > QD-Cys-FA-DOX, while the nanocarriers themselves without drug were

not significantly cytotoxic. Thus, the three different ligand-modified FA attached Ag–In–Zn–S QD-based nanocarriers can be considered as a promising drug delivery system for cancer therapy [96].

Samimi et al. designed quinic acid-functionalized nitrogen-doped carbon quantum dots (CQDs) nano-vehicles for delivery of anti-cancer chemotherapeutic drug Gemcitabine (GEM) for treatment of breast cancer. SEM and TEM analysis suggested quinic acid-modified nitrogen-doped carbon quantum dots were of spherical shape with an average size of ~ 7 nm. Zeta potential values of the as-synthesized nitrogen-doped CQDs (NCQDs) and quinic acid-modified NCQDs were -1.73 mV and -0.1 mV, respectively. The zeta potential values of quinic acid NCQDs were 0.1 mV and 0.3 mV, which suggests moderate stability of the nanocarrier. The drug encapsulation efficiency varied with drug concentration. Encapsulation efficiency was calculated to be 15%, 13%, 21%, 16.5% and 18% with GEM concentration of $125 \mu\text{g/mL}$, $250 \mu\text{g/mL}$, $500 \mu\text{g/mL}$, $750 \mu\text{g/mL}$, and $1000 \mu\text{g/mL}$, respectively. The nanocarrier gave pH-dependent drug release profile. In physiological pH (7.4), 54.01% drug was released from nanocarrier in 72 h; at acidic pH 5, 81.01% drug was released from nanocarrier in 72 h. Cell viability studies were done on the human breast cancer MCF-7 cell line. MTT assay revealed 80–100% cell viability after 48 h with the nanocarriers, which suggested no substantial cytotoxicity. For GEM-loaded nanocarriers, cell viability dropped with increasing concentration. The cytotoxicity on MCF-7 cell lines suggested almost similar antitumor activity of GEM-loaded nanocarriers as free drug. In vivo biodistribution studies using tumor-bearing mice suggested accumulation of drug-loaded nanocarriers on tumor mostly; no significant accumulation was detected on heart, lungs, and spleen of the mouse. Accumulation was also observed on prostate, testis, and bladder, suggesting clearance of drug-loaded nanocarriers through the urinary tract of the mouse [97].

Su et al. reported a red emissive CQD-based system for nuclear drug delivery of anti-cancer drug doxorubicin in cancer stem cells. The as-synthesized CQDs exhibited emission at 620 nm, quantum yield was 20.1%. This NIR-emitting fluorescence as well as the nitrogen functional group on the surface of CQDs enabled the CQDs to be cancer stem cell-permeable. TEM analysis revealed a mean size of 3.3 nm of the QDs, AFM predicted thickness of 0.7–1.2 nm. Anti-cancer drug DOX was loaded to the nanocarrier through π - π stacking interaction; drug loading efficiency was 71%. In vitro cytotoxicity studies on HeLa cells showed 93% cell viability in 12 h after treating the HeLa cells with CQD-based nano-drug carrier, which suggested no cytotoxicity of the nanocarrier itself. 50% and 21% cell viability were observed with free DOX and drug-loaded nanocarrier respectively in 12 h. This observation suggested that drug-loaded nanocarrier was more efficient in killing cancer cells than the free drug. In vivo studies revealed accumulation of drug on tumor site without harming major organs of mice upon injection of drug-loaded nanocarriers to tumor-bearing mice. Further, it was observed from in vivo fluorescence imaging that drug DOX-loaded nanocarriers were able to pass in the nuclei of cancer stem cells. Thus, nanocarrier enabled drug delivery exhibited a better anti-cancer therapeutic effect compared to free drug [98].

6 Conclusion and Future Perspectives

QDs have unique size-tunable optical and photophysical properties, as well as, biocompatibility and flexible surface chemistry. Their properties are superior to traditional dyes. Therefore, they have been widely used for biosensing, bioimaging, and drug delivery applications over the past decade.

The main concern which limited the *in vivo* application of QDs was its inherent cytotoxicity, which is introduced in QDs due to the presence of heavy metal ions like Cd, Hg, Se, Te, As, Pb, etc. This cytotoxicity can be harmful for living cells and animals, which limits its *in vivo* as well as clinical application. It is a necessary practice to check the cytotoxicity of QDs before working with any of its bio-applications. In most cases, the concentration of QDs needed for bio-applications is so low that the low concentration cannot really kill the healthy living cells. However, it is a good practice to eliminate even the slight cytotoxicity effect of QDs, which may prove harmful. With advancing time, usage of non-toxic carbon-based quantum dot materials (like CDots, GQDs) has been popular for biological applications instead of traditional heavy metal QDs. Also, putting a non-toxic shell (e.g. ZnS, ZnO) on toxic core QDs can reduce the cytotoxicity of QDs to a significant extent, extending their role for successful *in vivo* bio-applications.

Doping and putting a shell on core only QDs also help generating near-infrared (NIR) fluorescence emission. NIR emitting QDs are promising candidate for biomedical applications, as they can decrease phototoxicity and penetrate deep tissue, empowering deep tissue imaging. Coupling QDs with other nanomaterials or biomaterials create nanocomposite of nano-bio hybrid structure, which allows improved physicochemical properties and biocompatibility, leading to better biomedical applications. Despite several promises, clinical applications of QDs are still limited. Challenges may be attributed to reproducibility performance in preparation of QDs and relevant setting standard quality controls to ensure the lack of batch-to-batch variations. In addition, the administration routes of produced QDs into the body and their regimes should be carefully considered and examined to provide required standards in the clinic. It is highlighted that current knowledge in the understanding of the interactions in molecular levels in the body sheds light on the potential use of QDs for personalized medicine. Still, the non-specific binding of QDs to molecular compartments (e.g., proteins) of cells and tissues remains a challenge. Research is going on for better application of QD composites towards clinical approach. Also, ongoing research aims to engineer QD multifunctional devices, that can perform biosensing, bioimaging, and drug loading simultaneously. Achieving this goal could pave the way towards a milestone in biomedical research.

References

1. Reed MA, Randall JN, Aggarwal RJ, Matyi RJ, Moore TM, Wetsel AE. Observation of discrete electronic states in a zero-dimensional semiconductor nanostructure. *Phys Rev Lett*.

- 1988;60(6):535–7.
- Wong C, Stylianopoulos T, Cui J, Martin J, Chauhan VP, Jiang W, et al. Multistage nanoparticle delivery system for deep penetration into tumor tissue. *PNAS*. 2011;108(6):2426–31.
 - Chen O, Zhao J, Chauhan VP, Cui J, Wong C, Harris DK, et al. Compact high-quality CdSe–CdS core–shell nanocrystals with narrow emission linewidths and suppressed blinking. *Nat Mater*. 2013;12(5):445–51.
 - Mashford BS, Stevenson M, Popovic Z, Hamilton C, Zhou Z, Breen C, et al. High-efficiency quantum-dot light-emitting devices with enhanced charge injection. *Nat Photon*. 2013;7(5):407–12.
 - Chuang C-HM, Brown PR, Bulović V, Bawendi MG. Improved performance and stability in quantum dot solar cells through band alignment engineering. *Nat Mater*. 2014;13(8):796–801.
 - Hsueh H-Y, Yao C-T, Ho R-M. Well-ordered nanohybrids and nanoporous materials from gyroid block copolymer templates. *Chem Soc Rev*. 2015;44(7):1974–2018.
 - Chauhan VP, Stylianopoulos T, Martin JD, Popović Z, Chen O, Kamoun WS, et al. Normalization of tumour blood vessels improves the delivery of nanomedicines in a size-dependent manner. *Nat Nanotech*. 2012;7(6):383–8.
 - Chakrabarty A, Marre S, Landis RF, Rotello VM, Maitra U, Guerso AD, et al. Continuous synthesis of high quality CdSe quantum dots in supercritical fluids. *J Mater Chem C*. 2015;3(29):7561–6.
 - Park HH, Woo K, Ahn J-P. Core-shell bimetallic nanoparticles robustly fixed on the outermost surface of magnetic silica microspheres. *Sci Rep*. 2013;3(1):1497.
 - Adijanto L, Bennett DA, Chen C, Yu AS, Cargnello M, Fornasiero P, et al. Exceptional thermal stability of Pd@CeO₂ core-shell catalyst nanostructures grafted onto an oxide surface. *Nano Lett*. 2013;13(5):2252–7.
 - Wang H, Guo H, Dai Y, Geng D, Han Z, Li D, et al. Optimal electromagnetic-wave absorption by enhanced dipole polarization in Ni/C nanocapsules. *Appl Phys Lett*. 2012;101(8):083116.
 - Cha W, Jeong NC, Song S, Park H, Thanh Pham TC, Harder R, et al. Core–shell strain structure of zeolite microcrystals. *Nat Mater*. 2013;12(8):729–34.
 - Kang X, Huang L, Yang Y, Pan D. Scaling up the aqueous synthesis of visible light emitting multinary AgInS₂/ZnS core/shell quantum dots. *J Phys Chem C*. 2015;119(14):7933–40.
 - Liu S, Tamura M, Nakagawa Y, Tomishige K. One-pot conversion of cellulose into n-hexane over the Ir-ReOx/SiO₂ catalyst combined with HZSM-5. *ACS Sustain Chem Eng*. 2014;2(7):1819–27.
 - Sweeney RY, Mao C, Gao X, Burt JL, Belcher AM, Georgiou G, et al. Bacterial biosynthesis of cadmium sulfide nanocrystals. *Chem Biol*. 2004;11(11):1553–9.
 - Stürzenbaum SR, Höckner M, Panneerselvam A, Levitt J, Bouillard J-S, Taniguchi S, et al. Biosynthesis of luminescent quantum dots in an earthworm. *Nat Nanotechnol*. 2013;8(1):57–60.
 - Jin T, Fujii F, Komai Y, Seki J, Seiyama A, Yoshioka Y. Preparation and characterization of highly fluorescent, glutathione-coated near infrared quantum dots for in vivo fluorescence imaging. *Int J Mol Sci*. 2008;9(10):2044–61.
 - Samanta A, Deng Z, Liu Y. Aqueous synthesis of glutathione-capped CdTe/CdS/ZnS and CdTe/CdSe/ZnS Core/shell/shell nanocrystal heterostructures. *Langmuir*. 2012;28(21):8205–15.
 - Mattoussi H, Mauro J, Goldman E, Green T, Anderson G, Sundar V, et al. Bioconjugation of highly luminescent colloidal CdSe–ZnS quantum dots with an engineered two-domain recombinant protein. *Phys Status Solidi (B)*. 2001;224(1):277–83.
 - Kwon W, Rhee S-W. Facile synthesis of graphitic carbon quantum dots with size tunability and uniformity using reverse micelles. *Chem Commun*. 2012;48(43):5256–8.
 - Zhang N, Shi J, Mao SS, Guo L. Co₃O₄ quantum dots: reverse micelle synthesis and visible-light-driven photocatalytic overall water splitting. *Chem Commun*. 2014;50(16):2002–4.
 - Lee W-B, Weng C-H, Cheng F-Y, Yeh C-S, Lei H-Y, Lee G-B. Biomedical microdevices synthesis of iron oxide nanoparticles using a microfluidic system. *Biomed Microdevices*. 2009;11(1):161–71.

23. Zhang Y, Schnoes AM, Clapp AR. Dithiocarbamates as capping ligands for water-soluble quantum dots. *ACS Appl Mater Interfaces*. 2010;2(11):3384–95.
24. Bae WK, Char K, Hur H, Lee S. Single-step synthesis of quantum dots with chemical composition gradients. *Chem Mater*. 2008;20(2):531–9.
25. Ramalingam G, Saravanan KV, Vizhi TK, Rajkumar M, Baskar K. Synthesis of water-soluble and bio-taggable CdSe@ZnS quantum dots. *RSC Adv*. 2018;8(16):8516–27.
26. Debnath R, Bakr O, Sargent EH. Solution-processed colloidal quantum dot photovoltaics: a perspective. *Energy Environ Sci*. 2011;4(12):4870–81.
27. Yang H, Luan W, Tu S, Wang ZM. Synthesis of nanocrystals via microreaction with temperature gradient: towards separation of nucleation and growth. *Lab Chip*. 2008;8(3):451–5.
28. Yen BKH, Günther A, Schmidt MA, Jensen KF, Bawendi MG. A microfabricated gas-liquid segmented flow reactor for high-temperature synthesis: the case of CdSe quantum dots. *Angew Chem Int Ed*. 2005;44(34):5447–51.
29. Mondal S, Ghosh S, Ghosh D, Saha A. Physico-chemical aspects of quantum dot-vasodilator interaction: implications in nanodiagnosics. *J Phys Chem C*. 2012;116(17):9774–82.
30. Gu J, Hu MJ, Guo QQ, Ding ZF, Sun XL, Yang J. High-yield synthesis of graphene quantum dots with strong green photoluminescence. *RSC Adv*. 2014;4(91):50141–4.
31. Zhu Y, Wang G, Jiang H, Chen L, Zhang X. One-step ultrasonic synthesis of graphene quantum dots with high quantum yield and their application in sensing alkaline phosphatase. *Chem Commun*. 2014;51(5):948–51.
32. Naik JP, Sutradhar P, Saha M. Molecular scale rapid synthesis of graphene quantum dots (GQDs). *J Nanostruct Chem*. 2017;7(1):85–9.
33. Goldman ER, Medintz IL, Mattoussi H. Luminescent quantum dots in immunoassays. *Anal Bioanal Chem*. 2006;384(3):560–3.
34. Morales-Narváez E, Montón H, Fomicheva A, Merkoçi A. Signal enhancement in antibody microarrays using quantum dots nanocrystals: application to potential Alzheimer's disease biomarker screening. *Anal Chem*. 2012;84(15):6821–7.
35. Goldman ER, Clapp AR, Anderson GP, Uyeda HT, Mauro JM, Medintz IL, et al. Multiplexed toxin analysis using four colors of quantum dot fluororeagents. *Anal Chem*. 2004;76(3):684–8.
36. Li J, Zhu J-J. Quantum dots for fluorescent biosensing and bio-imaging applications. *Analyst*. 2013;138(9):2506–15.
37. Yan P, Li X, Dong Y, Li B, Wu Y. A pH-based sensor array for the detection and identification of proteins using CdSe/ZnS quantum dots as an indicator. *Analyst*. 2019;144(9):2891–7.
38. Tyrakowski CM, Snee PT. Ratiometric CdSe/ZnS quantum dot protein sensor. *Anal Chem*. 2014;86(5):2380–6.
39. Qiu L, Bi Y, Wang C, Li J, Guo P, Li J, et al. Protein A detection based on quantum dots-antibody bioprobe using fluorescence coupled capillary electrophoresis. *Int J Mol Sci*. 2014;15(2):1804–11.
40. Wu P, Miao L-N, Wang H-F, Shao X-G, Yan X-P. A multidimensional sensing device for the discrimination of proteins based on manganese-doped ZnS quantum dots. *Angew Chem Int Ed*. 2011;50(35):8118–21.
41. Pramanik S, Roy S, Bhandari S. The quantum dot-FRET-based detection of vitamin B12 at a picomolar level. *Nanoscale Adv*. 2020;2(9):3809–14.
42. Vaishnavi E, Renganathan R. CdTe quantum dot as a fluorescence probe for vitamin B12 in dosage form. *Spectrochim Acta Part A Mol Biomol Spectrosc*. 2013;1(115):603–9.
43. Koneswaran M, Narayanaswamy R. RETRACTED: ultrasensitive detection of vitamin B6 using functionalised CdS/ZnS core-shell quantum dots. *Sens Actuators B Chem*. 2015;1(210):811–6.
44. Ghosh S, Bhattacharya SC, Saha A. Probing of ascorbic acid by CdS/dendrimer nanocomposites: a spectroscopic investigation. *Anal Bioanal Chem*. 2010;397(4):1573–82.
45. Lu W, Qin X, Luo Y, Chang G, Sun X. CdS quantum dots as a fluorescent sensing platform for nucleic acid detection. *Microchim Acta (Online)*. 2011;175(3–4):355–9.
46. He Y, Wang H-F, Yan X-P. Self-assembly of Mn-doped ZnS quantum dots/octa(3-aminopropyl)octasilsequioxane octahydrochloride nanohybrids for optosensing DNA. *Chem A Eur J*. 2009;15(22):5436–40.

47. Dai Z, Zhang J, Dong Q, Guo N, Xu S, Sun B, et al. Adaption of Au nanoparticles and CdTe quantum dots in DNA detection. Supported by the Natural Science Foundation of Tianjin (Nos. 06TXTJJC14400, 07JCYBJC15900) and Young Teacher Foundation of Tianjin Polytechnic University (No. 029624). *Chin J Chem Eng.* 2007;15(6):791–4.
48. Wang H, Zhang Q, Yin H, Wang M, Jiang W, Ai S. Photoelectrochemical immunosensor for methylated RNA detection based on g-C₃N₄/CdS quantum dots heterojunction and Phos-tag-biotin. *Biosens Bioelectron.* 2017;15(95):124–30.
49. Freire RM, Le NDB, Jiang Z, Kim CS, Rotello VM, Fechine PBA. NH₂-rich carbon quantum dots: a protein-responsive probe for detection and identification. *Sens Actuators B Chem.* 2018;255:2725–32.
50. Han T, Yan T, Li Y, Cao W, Pang X, Huang Q, et al. Eco-friendly synthesis of electrochemiluminescent nitrogen-doped carbon quantum dots from diethylene triamine pentacetate and their application for protein detection. *Carbon.* 2015;1(91):144–52.
51. Wang Y, Zhang L, Liang R-P, Bai J-M, Qiu J-D. Using graphene quantum dots as photoluminescent probes for protein kinase sensing. *Anal Chem.* 2013;85(19):9148–55.
52. Liang R-P, Qiu W-B, Zhao H-F, Xiang C-Y, Qiu J-D. Electrochemiluminescence resonance energy transfer between graphene quantum dots and graphene oxide for sensitive protein kinase activity and inhibitor sensing. *Anal Chim Acta.* 2016;21(904):58–64.
53. Song C, Luo H, Lin X, Peng Z, Weng L, Tang X, et al. Study on AgInZnS-graphene oxide non-toxic quantum dot for biomedical sensing. *Front Chem.* 2020;8:331.
54. Sinduja B, John SA. Highly selective naked eye detection of vitamin B1 in the presence of other vitamins using graphene quantum dots capped gold nanoparticles. *New J Chem.* 2019;43(5):2111–7.
55. Wadhwa S, John AT, Nagabooshanam S, Mathur A, Narang J. Graphene quantum dot-gold hybrid nanoparticles integrated aptasensor for ultra-sensitive detection of vitamin D3 towards point-of-care application. *Appl Surf Sci.* 2020;15(521):146427.
56. Du F, Cheng Z, Wang G, Li M, Lu W, Shuang S, et al. Carbon nanodots as a multifunctional fluorescent sensing platform for ratiometric determination of vitamin B2 and “turn-off” detection of pH. *J Agric Food Chem.* 2021;69(9):2836–44.
57. Wang M, Liu Y, Ren G, Wang W, Wu S, Shen J. Bioinspired carbon quantum dots for sensitive fluorescent detection of vitamin B12 in cell system. *Anal Chim Acta.* 2018;22(1032):154–62.
58. Qian ZS, Shan XY, Chai LJ, Ma JJ, Chen JR, Feng H. A universal fluorescence sensing strategy based on biocompatible graphene quantum dots and graphene oxide for the detection of DNA. *Nanoscale.* 2014;6(11):5671–4.
59. Li G, Liu Y, Niu J, Pei M, Lin W. A ratiometric fluorescent composite nanomaterial for RNA detection based on graphene quantum dots and molecular probes. *J Mater Chem B.* 2018;6(26):4380–4.
60. Loo AH, Sofer Z, Bouša D, Ulbrich P, Bonanni A, Pumera M. Carboxylic carbon quantum dots as a fluorescent sensing platform for DNA detection. *ACS Appl Mater Interfaces.* 2016;8(3):1951–7.
61. Liu Q, Ma C, Liu X-P, Wei Y-P, Mao C-J, Zhu J-J. A novel electrochemiluminescence biosensor for the detection of microRNAs based on a DNA functionalized nitrogen doped carbon quantum dots as signal enhancers. *Biosens Bioelectron.* 2017;15(92):273–9.
62. Kairdolf BA, Smith AM, Stokes TH, Wang MD, Young AN, Nie S. Semiconductor quantum dots for bioimaging and bdiagnostic applications. *Annu Rev Anal Chem (Palo Alto Calif).* 2013;6:143–62.
63. Martynenko IV, Litvin AP, Purcell-Milton F, Baranov AV, Fedorov AV, Gun’ko YK. Application of semiconductor quantum dots in bioimaging and biosensing. *J Mater Chem B.* 2017;5(33):6701–27.
64. Derfus AM, Chan WCW, Bhatia SN. Probing the cytotoxicity of semiconductor quantum dots. *Nano Lett.* 2004;4(1):11–8.
65. Yuan F, Li S, Fan Z, Meng X, Fan L, Yang S. Shining carbon dots: synthesis and biomedical and optoelectronic applications. *Nano Today.* 2016;11(5):565–86.

66. Han M, Zhu S, Lu S, Song Y, Feng T, Tao S, et al. Recent progress on the photocatalysis of carbon dots: classification, mechanism and applications. *Nano Today*. 2018;1(19):201–18.
67. Cao L, Wang X, Mezziani MJ, Lu F, Wang H, Luo PG, et al. Carbon dots for multiphoton bioimaging. *J Am Chem Soc*. 2007;129(37):11318–9.
68. Sun Y-P, Zhou B, Lin Y, Wang W, Fernando KAS, Pathak P, et al. Quantum-sized carbon dots for bright and colorful photoluminescence. *J Am Chem Soc*. 2006;128(24):7756–7.
69. Xu X, Ray R, Gu Y, Ploehn HJ, Gearheart L, Raker K, et al. Electrophoretic analysis and purification of fluorescent single-walled carbon nanotube fragments. *J Am Chem Soc*. 2004;126(40):12736–7.
70. Yang S-T, Cao L, Luo PG, Lu F, Wang X, Wang H, et al. Carbon dots for optical imaging in vivo. *J Am Chem Soc*. 2009;131(32):11308–9.
71. Liu R, Wu D, Liu S, Koykov K, Knoll W, Li Q. An aqueous route to multicolor photoluminescent carbon dots using silica spheres as carriers. *Angew Chem Int Ed*. 2009;48(25):4598–601.
72. Bourlinos AB, Bakandritsos A, Kouloumpis A, Gournis D, Krysmann M, Giannelis EP, et al. Gd(III)-doped carbon dots as a dual fluorescent-MRI probe. *J Mater Chem*. 2012;22(44):23327–30.
73. Gong P, Chen Z, Chen Y, Wang W, Wang X, Hu A. High-relaxivity MRI contrast agents prepared from miniemulsion polymerization using gadolinium(III)-based metallosurfactants. *Chem Commun*. 2011;47(14):4240–2.
74. Pandey S, Thakur M, Mewada A, Anjarlekar D, Mishra N, Sharon M. Carbon dots functionalized gold nanorod mediated delivery of doxorubicin: tri-functional nano-worms for drug delivery, photothermal therapy and bioimaging. *J Mater Chem B*. 2013;1(38):4972–82.
75. Biswas MC, Islam MT, Nandy PK, Hossain MM. Graphene quantum dots (GQDs) for bioimaging and drug delivery applications: a review. *ACS Mater Lett*. 2021;3(6):889–911.
76. Chung S, Revia RA, Zhang M. Graphene quantum dots and their applications in bioimaging, biosensing, and therapy. *Adv Mater*. 2021;33(22):1904362.
77. Lu H, Li W, Dong H, Wei M. Graphene quantum dots for optical bioimaging. *Small*. 2019;15(36):1902136.
78. Zhang D, Wen L, Huang R, Wang H, Hu X, Xing D. Mitochondrial specific photodynamic therapy by rare-earth nanoparticles mediated near-infrared graphene quantum dots. *Biomaterials*. 2018;1(153):14–26.
79. Zheng XT, Than A, Ananthanaraya A, Kim D-H, Chen P. Graphene quantum dots as universal fluorophores and their use in revealing regulated trafficking of insulin receptors in adipocytes. *ACS Nano*. 2013;7(7):6278–86.
80. Li S, Zhou S, Li Y, Li X, Zhu J, Fan L, et al. Exceptionally high payload of the IR780 iodide on folic acid-functionalized graphene quantum dots for targeted photothermal therapy. *ACS Appl Mater Interfaces*. 2017;9(27):22332–41.
81. Abdullah-Al-Nahain, Lee JE, In I, Lee H, Lee KD, Jeong JH, et al. Target delivery and cell imaging using hyaluronic acid-functionalized graphene quantum dots. *Mol Pharm*. 2013;10(10):3736–44.
82. Cao Y, Dong H, Yang Z, Zhong X, Chen Y, Dai W, et al. Aptamer-conjugated graphene quantum dots/porphyrin derivative theranostic agent for intracellular cancer-related MicroRNA detection and fluorescence-guided photothermal/photodynamic synergetic therapy. *ACS Appl Mater Interfaces*. 2017;9(1):159–66.
83. Thakur M, Kumawat MK, Srivastava R. Multifunctional graphene quantum dots for combined photothermal and photodynamic therapy coupled with cancer cell tracking applications. *RSC Adv*. 2017;7(9):5251–61.
84. Liu Q, Guo B, Rao Z, Zhang B, Gong JR. Strong two-photon-induced fluorescence from photostable, biocompatible nitrogen-doped graphene quantum dots for cellular and deep-tissue imaging. *Nano Lett*. 2013;13(6):2436–41.
85. Wang H, Mu Q, Wang K, Revia RA, Yen C, Gu X, et al. Nitrogen and boron dual-doped graphene quantum dots for near-infrared second window imaging and photothermal therapy. *Appl Mater Today*. 2019;1(14):108–17.

86. Wang FH, Bae K, Huang ZW, Xue JM. Two-photon graphene quantum dot modified Gd₂O₃ nanocomposites as a dual-mode MRI contrast agent and cell labelling agent. *Nanoscale*. 2018;10(12):5642–9.
87. Some S, Gwon A-R, Hwang E, Bahn G, Yoon Y, Kim Y, et al. Cancer therapy using ultrahigh hydrophobic drug-loaded graphene derivatives. *Sci Rep*. 2014;4(1):6314.
88. Zhu S, Song Y, Zhao X, Shao J, Zhang J, Yang B. The photoluminescence mechanism in carbon dots (graphene quantum dots, carbon nanodots, and polymer dots): current state and future perspective. *Nano Res*. 2015;8(2):355–81.
89. Nurunnabi M, Khatun Z, Huh KM, Park SY, Lee DY, Cho KJ, et al. In vivo biodistribution and toxicology of carboxylated graphene quantum dots. *ACS Nano*. 2013;7(8):6858–67.
90. Nurunnabi M, Khatun Z, Reeck GR, Lee DY, Lee Y. Near infra-red photoluminescent graphene nanoparticles greatly expand their use in noninvasive biomedical imaging. *Chem Commun*. 2013;49(44):5079–81.
91. Aswathy RG, Sivakumar B, Brahatheeswaran D, Fukuda T, Yoshida Y, Maekawa T, et al. Biocompatible fluorescent zein nanoparticles for simultaneous bioimaging and drug delivery application. *Adv Nat Sci Nanosci Nanotechnol*. 2012;3(2):025006.
92. Abdelhamid AS, Helmy MW, Ebrahim SM, Bahey-El-Din M, Zayed DG, Zein El Dein EA, et al. Layer-by-layer gelatin/chondroitin quantum dots-based nanotheranostics: combined rapamycin/celecoxib delivery and cancer imaging. *Nanomedicine*. 2018;13(14):1707–30.
93. Abdelhamid AS, Zayed DG, Helmy MW, Ebrahim SM, Bahey-El-Din M, Zein-El-Dein EA, et al. Lactoferrin-tagged quantum dots-based theranostic nanocapsules for combined COX-2 inhibitor/herbal therapy of breast cancer. *Nanomedicine*. 2018;13(20):2637–56.
94. Olerile LD, Liu Y, Zhang B, Wang T, Mu S, Zhang J, et al. Near-infrared mediated quantum dots and paclitaxel co-loaded nanostructured lipid carriers for cancer theragnostic. *Colloids Surf B*. 2017;1(150):121–30.
95. Iannazzo D, Pistone A, Salamò M, Galvagno S, Romeo R, Giofrè SV, et al. Graphene quantum dots for cancer targeted drug delivery. *Int J Pharm*. 2017;518(1):185–92.
96. Ruzycka-Ayoush M, Kowalik P, Kowalczyk A, Bujak P, Nowicka AM, Wojewodzka M, et al. Quantum dots as targeted doxorubicin drug delivery nanosystems in human lung cancer cells. *Cancer Nanotechnol*. 2021;12(1):8.
97. Samimi S, Ardestani MS, Dorkoosh FA. Preparation of carbon quantum dots-quinic acid for drug delivery of gemcitabine to breast cancer cells. *J Drug Deliv Sci Technol*. 2021;61:102287.
98. Su W, Guo R, Yuan F, Li Y, Li X, Zhang Y, et al. Red-emissive carbon quantum dots for nuclear drug delivery in cancer stem cells. *J Phys Chem Lett*. 2020;11(4):1357–63.

Quantum Dots: Potential Cell Imaging Agent



Tamanna Mallick, Abhijit Karmakar, and Zinnia Sultana

Abstract Fluorescent semiconductor nanocrystals (also known as quantum dots or QDs) have become monumental over the past two decades in the material science as well as biomedical field due to their tunable optical properties. Moreover, the exclusive nature of QDs has always kept it one step ahead of conventional organic fluorophores, particularly in cell imaging. QDs exhibit extremely bright multi-color fluorescence behaviour, high photo-stability, larger extinction co-efficient and lesser photo bleaching tendencies inside the cellular environment which make them as advanced labelling agents. Here we have depicted the supreme characteristics features of different types of QDs and their applications in the in vitro and in vivo cell imaging. Recently, QDs are safely used in the advanced clinical research as promising diagnostic tool that will surely open up a new direction.

Keywords Quantum dots · Bioimaging · Fluorescence · In vitro and in vivo cell imaging

1 Introduction

The worldwide on-going pandemic situation again reminded us that progressive research in the health science for mankind is worthy enough. Basic medical care and the improvement in the biomedical field are the most prominent signs of developing countries. These are only possible with the rapid diagnosis of diseases to find their cures [1]. A cell is a tiny chemical factory of the enormous number of biochemical reactions for conveying the life processes and within the shadow of those bio-processes, it also hides the pro-diseases factors inside its core biomolecule [2]. Hence, it has become a noteworthy challenge for the researchers to improve

T. Mallick (✉) · A. Karmakar

Department of Chemistry, Visva-Bharati (Central University), Santiniketan, WB 731235, India
e-mail: mallickchemistry717@gmail.com

Z. Sultana

Department of Botany, Visva-Bharati (Central University), Santiniketan, WB 731235, India

novel cell imaging agents for the insightful analyses of the abnormal cellular activities related to the diseases. Cell imaging biomarkers possess immense capabilities in diagnosing of diseases, monitoring the disease progression and tracking the drug response [3].

Moreover, target specific imaging agents can be utilized in the precise assessments of the pathophysiology of cell not only in the *in vitro* environment but also in an *in vivo* environment. It is a bitter truth that correct prediction of cellular structures and the dynamic behaviour of the biomolecules with the progression of diseases is critical in cell biology. This problem can only be overcome by giving an insight into the development of live cell imaging techniques. Live cell imaging helps us to visualize the dynamic changes of internal structures and cellular processes more accurately than imaging studies of fixed cells [4]. Nowadays, it is a significant concern for researchers to develop sensitive, reliable, cost-effective cell imaging-based technologies for the diagnosis of various fatal diseases. Among the existing techniques, fluorescent-based detection techniques are the most widely explored and promising methods in imaging as well as biosensing applications [5–7].

Organic compounds with high fluorophoric character have become prevalent and potential for cell imaging due to their superior optical activities [8]. But there are some major drawbacks of the application of small molecule-based fluorescent organic compounds in cell imaging, such as low biocompatibility, low photo-stability, poor water solubility and photo bleaching tendencies [9]. Moreover, aggregation caused quenching of fluorescence intensity of the organic fluorophores in the interior of the cell is also a major concern [7, 10–13]. Besides this, comparatively short lifetimes of the small molecule based fluoroprobes adversely affect the imaging process in fluorescence microscopy [14]. Such shortcomings in handling the organic fluorophores as an *in vitro/in vivo* cell imaging agent provoked the world to improve in the fluorescent based diagnostic application. In this regard, nanotechnology is one of the utmost focusing areas in the upgradation of the biomedical field for the early diagnosis of diseases and delivery of therapeutics in the targeted cells and tissues. Fluorescent nanoparticles (NPs) are widely used in the fluorescence guided imaging and biosensing applications due to their unique features such as improved brightness, high image contrast, and inertness to their microenvironment. Moreover, visualization of structures at high spatial and temporal resolutions and a more even distribution within the intracellular medium are also beneficial for using nanomaterials as imaging agents [5].

In comparison with organic compounds, NPs are better suited as they are relatively resistant to degradation in the interior of cells [15]. About ten years back, nanoparticles were first reported for the biological imaging of proteins in cells with an evaluation in the bio-medical field [16, 17]. Nowadays, researchers are dealing with nanomaterials in almost every dimension and exploiting their unique features in the bio-medical fields. A new avenue opens up for the imaging and labelling techniques by utilizing the superior characteristic features of biocompatible fluorescent NPs.

2 Exclusive Features of Quantum Dots (QDs) as Bio-imaging Tool

A few years back, a new generation fluorescent nanoparticle appeared as the finest item for imaging cells and organs which was the semiconductor nanocrystals (Quantum dots, QDs) [18]. Engagement of Quantum dots (QDs) with biology has changed the shape of modern generation hybrid biomedical research area that can profoundly influence clinical diagnosis/therapeutic actions. QDs are arguably the most potential moieties for acting as the highly advanced tools in the biomedical imaging techniques [19]. After introducing the QDs as cell imaging agents, a wide improvement of optical potentials was observed, making them superior to the common organic fluorophores in single and multi-color experiments [16]. Fluorescence-based techniques, i.e., fluorescence imaging, are progressively raised towards the diagnosis of chronic diseases where QDs may play a key role and can be utilized as probes in the cellular medium [20]. QDs display extremely bright fluorescence behaviour, long fluorescence lifetime, high photo-stability and extreme quantum yield, and larger extinction co-efficient in the interior of cell which prove them as advanced labelling agents [21]. In such a rapid development of nanotechnology, QDs are used as active cellular probes and have the potential to fulfill all the characteristic properties of standard imaging agents [22]. In addition to this, exceptionally unique properties of QDs made them surmounted in cell imaging techniques in comparison with the conventional fluorescent dyes. The most challenging and promising aspect of QDs is to use them in different organs of animals as diagnostic/therapeutic agents. Hence it is necessary to reduce the toxicity of nanocrystals by coating them with more biocompatible compounds. At the very beginning, quantum dots were effectively applied in the clinical diagnostic field as fluorescent labelling agents of cells and tissues as well as immunostaining agents of live cell's membrane proteins. Hence, surface modification of QDs by conjugation with biomolecules is a basic requirement to achieve selective targeting without any injury of the cells. QDs with emission in the near infra-red (NIR) region can be potential enough for using them to restrict the interference of the auto fluorescence.

There is an impressive progression of the story of QDs in biological research field. An admirable glimpse comes from this story which raised questions about how and why QDs were improved as imaging tools for biomedical research. Evolution of quantum dots in cell imaging technology along with the time lapse has been depicted in Fig. 1.

QDs are luminescent semiconductor nanocrystals with a size range falling between 1.5 and 10 nm [23]. In a simple thought, QDs are the groups of atoms that collectively form a semiconductor crystalline material that assures advanced transformation in bio-medical fields. In addition to this, it is also used as lights, computer displays and solar cells. These ultra small nanocrystals are sometimes described as 'artificial atoms' which display size and composition-dependent optical properties [23, 24]. These tiny materials are usually composed of groups II–VI, III–V and IV–VI atoms of periodic table [25]. The QDs were discovered first by Russian

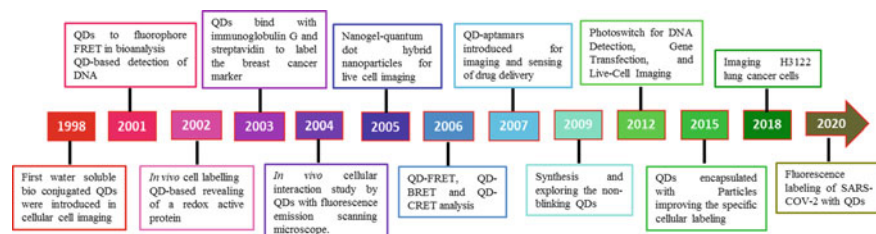


Fig. 1 The years of progress in cell imaging through the eyes of quantum dots

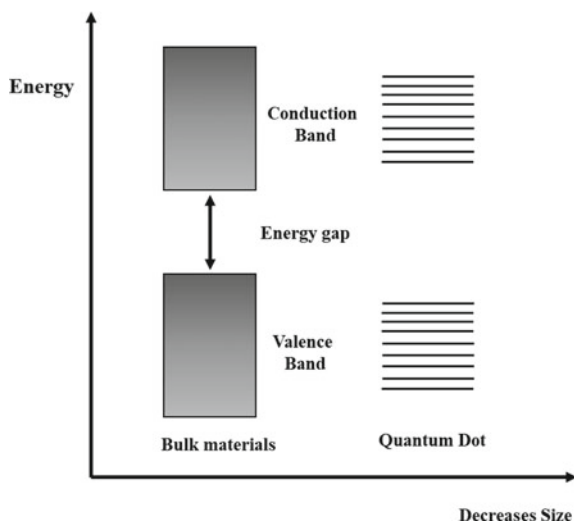
physicist Alexei Ekimov in 1970 whereas Alexander Efros explained the theory of the nanocrystal QDs, 1982 [26, 27]. The term ‘quantum dot’ was first coined by Mark Reed in 1986 [28].

The name ‘quantum dot’ arises as these materials are too small, basically compared with a tip of the pen, i.e., a single dot. Semiconductor nanocrystals have zero-dimensional materials that emit fluorescence i.e., glowing after irradiation of external light sources. Nearly about 10–50 atoms are included in a single QD that monitors their sizes and further control the intensity of their color. There is a basic relationship between the size and color of the QDs i.e., larger size QDs give light with a higher wavelength and smaller sizes produce light with a small wavelength. According to the basic concept of quantum mechanics i.e., theory of wave-particle duality of the famous physicist de Broglie, it is accounted that the particle can be characterized by using quantum mechanical calculation when the size of the particle becomes comparable to the wavelength [29]. Hence, behavior of nanocrystals can only be explained with the help of quantum mechanics i.e., the concept of ‘wave-particle duality’. The bulk material has free electrons in the conduction band which are movable throughout the materials. The movement of the free electrons all over the bulk materials can be described by a linear combination of plane waves [30]. Hence, when the size of a QD is comparable with these wavelengths, the free electrons are confined within this nanocrystal acts like a particle in a 1-D box [31]. The energy alignment of a particle shows discrete energy states when compared with the waves restricted in the potential well. A simple energy profile diagram of QDs in comparison with bulk materials are shown in Fig. 2.

The unique fluorescence character of semiconductor nanocrystals arises after the excitation of the electron which comes from the conduction band to the valence band. Mostly, the emission of QDs falls within the wavelength range from UV–Vis to the infrared regions. QDs exhibit broad UV–Vis spectra but narrow emission spectra [16, 33]. When the randomly moving carriers of the particle with a comparable size of waves are confined to restrict their movements in the discrete energy levels then it is referred to as quantum-confinement.

The quantum-confinement effect has a great role in the extraordinary electronic structures of the QDs. This quantum-confinement effect arises when the physical diameter of QDs are less than twice their exciton Bohr radius [34]. The term quantum-confinement effect of the semiconductor QD was first introduced by Weller in 1993

Fig. 2 Electronic energy levels alignments of bulk materials and quantum dots. [32] Reproduced from Ref. under a Creative Commons Attribution-NonCommercial-NoDerivatives 4.0 International License



[35]. Due to the quantum-confinement effects, the energy states of individual atom remain discrete. The energy gap of these discrete energy levels depends on the size of the QDs. With the decreases in the size of the QDs, the energy gap of the discrete energy level increases that results in the size-depended multi colors of QDs [36].

3 Types of QDs Used in the Cell Imaging Techniques

Generally, the QDs are typically divided into three major categories. One of the most famous types is metal-based semiconductor nanocrystals. Another recent demanding group is the carbon-based QDs. The last one is the silicon QDs. Semiconductor QDs have high photochemical stability with unique size-dependent optical properties that make them well recognized in the Nano world [37, 38]. Metallic semiconductor QDs are the heavy metal containing like, II-IV (CdSe, ZnS, and CdTe), IV-VI (PbSe and PbS) and III-V (InP and InAs) QDs [39–41]. Metallic semiconductor QDs can be prepared in various methods. Depending on the chemical compositions and arrangements, they can be subdivided into three main types: core type, core-shell, and alloyed-type QDs [Fig. 3] [42].

Core-type is one of the class of metallic semiconductor QD which is composed of a uniform single material including metallic chalcogenide (chalcogenide: S, Se and Te) [43]. There is a problem regarding the high toxicity of the II-IV QDs (such as CdTe and CdSe) which limits their potential use in the bio-medical field. But it has already been reported that cytotoxicity of cadmium-containing QDs depends on the size, charge and variation of coating ligands [44]. Hence, these problems raise concerns about the biocompatibility of QDs, which initiated a search for an alternative way to safely use the semiconductor QDs in the cellular medium [45].

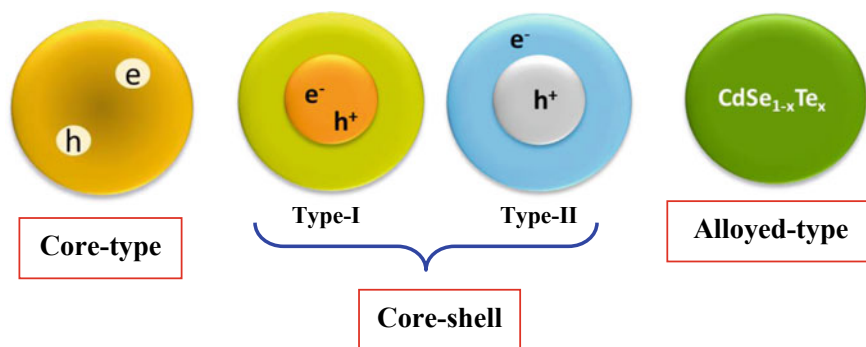


Fig. 3 Simple subdivision of metallic semiconductor QDs

Another types of semiconductors QDs is the core–shell QDs which have the ability to enter into the clinical research as a promising agent for the diagnosis. Core–shell QDs are produced when one semiconducting material acts as shell and encapsulate other materials within its core. The core and the shell of the core–shell type QDs are mainly consist of groups (notation: core/shell) CdS/ZnS, CdSe/ZnS, and InAs/CdSe semiconductors QDs [46]. The enhancement in the fluorescence quantum yield of the core–shell QDs over the simple core-typed QDs or organic capped QDs is due to the large confinement of the electron and hole to the core and shell [47]. Core–shell QDs displayed the increase of the absorption coefficients, high brightness, stability against photo bleaching, small fluorescence lifetime and extreme brightness, variation of the refractive index and red shifting in the threshold energy with an increase in the shell width [48]. This beautiful core–shell pattern triggered their availability and usefulness in bioimaging, biosensing and bio diagnostic [49]. Remarkably core–shell QDs perform as multicolor imaging agents due to their narrow fluorescence emission characteristics. In another aspect core–shell QDs have a wide absorption spectrum that permits multiple excitations at the same wavelength. Hence, at the same time, multiple core–shell QDs would be useful in cell imaging. The short lifetime of the core–shell QDs allow them for the time-resolved bioimaging. The best-suited and widespread core/shell pair is the CdSe/ZnS or CdSe/CdS, which enhanced their optical properties and had high stability [50].

Alloyed QDs are the last types of QDs, produced by alloying multiple materials with both homogeneous and gradient internal structures. These alloyed types of novel QDs with composition gradients did not display blinking; hence strong fluorescence emission was observed continuously [51].

The conventional QDs containing the toxic heavy metals (Cd, Pb or As) have created major disadvantages in their biomedical applications such as in vivo or even in vitro uses [39, 45, 52, 53]. When the shells or organic capping agents do not suitably enclose the surface of these QDs, they easily forsake into the cellular medium. Such problems regarding the toxic metal-based QDs triggered the research interest in searching for alternative approaches in the improvement of QDs as biocompatible

fluorescence imaging agents. Another class of QDs is the carbon-based QDs pursued safer at the forefront of various in vivo or in vitro clinical resolutions in comparison with metal-based QDs [51, 54, 55]. Carbon-based QDs generally have two major groups with intense emission including carbon QDs (CQDs) and graphene QDs (GQDs) [56–58]. CQDs were first introduced in 2004 and are familiarly termed carbon dots (CDots) [59]. CQDs are naturally carbon containing NPs with average diameter of less than 10 nm, mainly prepared from organic compounds or natural sources that are noteworthy from a biological point of view [60–62]. GQDs are typically referred to as zero-dimensional novel fluorescent NPs which contain a single or few layers of graphene sheet [63].

CQDs and GQDs have notable properties like higher biocompatibility, better chemical stability, and high-water solubility, increased photoluminescence with green and facial synthesis fascinated them towards replacing conventional semiconductor QDs [64]. Hence, these materials are suggested for bioimaging and fluorescence sensing applications. Such promising features make CQDs and GQDs perfectly suited in several fields of electronics, optics, photo-electrochemistry, catalysis and particularly in the most challenging areas of biology [65]. CQDs are especially developed to persuade various exciting applications, like imaging of cells and tissues.

Silicon QD is another and last type of QDs with many important features that make them attractive towards the biomedical research field. Silicon quantum dots (SiQDs) are the semiconductor silica nanoparticles (SiNPs) within the size range from 1 to 10 nm [66]. SiQDs have potentials applicability towards fluorescent biomarker and optoelectronic devices as it has high resistance to photo bleaching, high quantum yields and broad emission range from visible to IR region [67].

The molecular and cellular events that can be studied by using fluorescent probes have been impacted in many areas of biomedical research. Over the traditional fluorophores, QDs have certain excellent properties which are suitable for cell imaging techniques. Conventional organic fluorophores have some limitations; hence, these molecules pose a lack of sensitivity or specificity of the desired targets in comparison with QDs [68]. In 1998, Chan and Nie and Bruchez et al. individually first applied QDs for successful fluorescence labelling and staining of fixed or live cells [69].

4 Application of QDs in Cell Imaging

4.1 In vitro Imaging

Initially, QDs were used for in vitro imaging to label cells. Li et al. reported that CdS capped with 3-mercaptopropionic acid (3-MPA) having a quantum yield comparable to that of the commercial core-shell QDs. They utilized the photoluminescence behaviour of CdS QDs as an imaging tool to label *Salmonella typhimurium* cells [70]. Electrostatic self-assembly over the QD surface offers a greater scope of functionalization with particular biomolecules for specific labelling [67]. Jaiswal

et al. reported generalized long-term labelling of HeLa cells with dihydrolipoic acid (DHLA)-capped multicolor CdSe/ZnS QDs. Interestingly, labelling of HeLa cells with QDs did not affect the cell growth and cells remained stably labelled for over a week. Furthermore, they attached an antibody (clone 4E3) to the QD surface and utilized it for the specific labelling of extracellular P-glycoprotein (Pgp) of HeLa cells [71]. Gac et al. have used QDs for staining of cells undergoing apoptosis and for this purpose, they have developed CdSe@ZnS QDs conjugated with Annexin V for specific targeting of apoptotic cells. They have also shown that the functionalized fluorescent QDs are specific towards the phosphatidylserine (PS) moieties present on the outer membrane of apoptotic cells and not on healthy or necrotic cells [67]. Liu et al. reported that Core-shell (CdSe/CdS/ZnS) semiconductor QDs conjugated with phenylboronic acid (PBA) enables specific and efficient labelling of Sialic acids (SA) on living cells [72]. Sun et al. demonstrated a new kind of magnetic, fluorescent multifunctional, thiol-capped Fe_3O_4 nanoparticles and prepared a nanocomposite with CdTe QDs i.e., $\text{Fe}_3\text{O}_4/\text{CdTe}$. These magnetic/fluorescent nanocomposites conjugated with anti-CEACAM8 antibody were successfully employed for immuno-labelling and fluorescence imaging of HeLa cells [73]. Bagalkot et al. demonstrated CdSe/ZnS core-shell QD conjugated with aptamer (Apt) and utilized for differential uptake and imaging of prostate cancer cells that express the prostate specific membrane antigen (PSMA) protein. It was also used for the loading of doxorubicin (Dox), an anticancer drug to prepare a nano conjugate system [QD-Apt(Dox)] as a targeted cancer imaging, therapy, and sensing system. From their study, it was observed that functionalized QD has the immense possibility of delivering the doxorubicin (Dox) as well as imaging the cancer cells in vitro [74]. QD-conjugated biomolecules are very selective and effective for tracking the structures and functions of biological systems. Biju et al. reported that a neuropeptide, allatostatin 1, Ala-Pro-Ser-Gly-AlaGln-Arg-Leu-Tyr-Gly-Phe-Gly-Leu-NH₂, conjugated to streptavidin-coated CdSe-ZnS QDs that can transfect living human carcinoma cells and transports QDs inside the cytoplasm and even the nucleus of the cells for targeted imaging purposes. This method proved that biomolecules conjugated QDs have the higher efficacy for DNA gene delivery, cell labelling and photodynamic therapy [75, 76].

Fluorescent carbon-based nanomaterials, such as carbon dots (CDots) and the emerging graphene quantum dots (GQDs) are also drawing considerable interest in the field of biosensing and bioimaging for their high aqueous solubility, stable photoluminescence (PL), low cytotoxicity, good biocompatibility as well as superior resistivity to photo bleaching [77]. Especially, the quantum-confinement and edge effects of the carbon dots and graphene quantum dots show incredible optoelectronic properties. Moreover, due to their unique surface features, they offer a platform for the functionalization of several small molecules as well as large biomolecules which enable researchers for their use as bio-imaging tools. Aiyer et al. reported that folic acid (FA) functionalized green fluorescent carbon quantum/nano dots GCQDs (GCQDs-FA) is highly specific towards the imaging of MCF-7 breast cancer cells [78]. Meena et al. reported a green route for the preparation of fluorescent carbon quantum dots (CQDs) from ayurvedic medicinal plant leaves such as *Azadirachta Indica*, *Ocimum Tenuiflorum* and *Tridax Procumbens*. The synthesized

CQDs are observed to be green fluorescent in nature, photo-stable, decently water dispersible and biocompatible. The potentiality of synthesized CDots was evaluated when they were applied directly to the imaging of MC3T3-E1 mouse preosteoblasts cells without further functionalization [79]. Jana et al. demonstrated the efficiency of pH-dependent, fluorescent carbon dots for sensing hazardous anions in aqueous media. They also used it as a cell-imaging probe for HeLa cell [80]. One of the major advances about the graphene QDs is its layer structure and high quantum yield as compared with the carbon dots [81]. Sheng et al. doped graphene quantum dots with nitrogen (N-GQDs) for sensing and bio-imaging purposes. Their prepared graphene based quantum dot showed a 64.2% quantum yield. They also demonstrated that the nitrogen-doped GQDs can be used for imaging of MCF-7 cells and the detection of Cr(VI) [82]. In other work, Fan et al. synthesized GQDs-tetraphenylporphyrin (TPP) and GQDs-polyethyleneimine (PEI) conjugate systems by green method for imaging of the mitochondria or cell nucleus in a target-specific way. According to their report, they also claimed that the synthesized GQDs did not exhibit the photobleaching and cytotoxicity compared to common fluorescent dyes [83]. The development of multicolor imaging agents is one of the high demanding goals for researchers. Graphene quantum dots exhibit astounding attributes in cell imaging, specific sensing activities, drug delivery and various types of bio applications. Hai et al. conjugated the graphene quantum dots with folic acid and utilized this nanoconjugate system (FA-GQDs) as the cellular probe and pH sensor [84]. The synthesized FA-GQDs showed multicolor emission characteristics and it has been used for the pH determination of cell suspensions. Broad emission properties of FA-GQDs offer a great potential for application in living cell multicolor imaging [84]. Increasing the fluorescence intensity of graphene quantum dots GQDs is also a cherished goal for the researchers and among varieties of methods sulphur doping within the GQDs layer is very effective. Jin et al. selected a nontoxic and cost-effective way to prepare sulphur doped-GQDs with high luminescence behaviour. They further utilized it as the imaging agent and targeted the membranes of the HeLa cell [85]. Mondal et al. synthesized heteroatom (N and S) doped graphene quantum dot (NS-GQD) with unique fluorescence properties [86]. They reported that the fluorescence characterization of NS-GQD was enhanced due to the trapping of heteroatoms (N and S) within the surface of the GQDs. The NS-GQD fluorescent probe showed higher efficacy in the field of intracellular imaging, which is comparable to the available commercial dyes. Moreover, antibacterial drug streptomycin was conjugated with the NS-GQD to form a drug conjugated quantum dot (DCQD) for enhancing the drug activity [86]. In the work of Su et al., a novel multifunctional protein nanofiber (PNF) was prepared from a peptide with trifunctional motif. They further conjugated the protein nanofiber (PNF) profoundly with fluorescent GQDs via noncovalent interaction. The GQDs exhibited their good optical properties in the PNF-GQDs nanohybrids. These PNF-GQD nanohybrids possess higher biocompatibility as well as the capability of targeting and imaging fluorescence imaging of HeLa tumor cells simultaneously [80]. All of these investigations illustrate the fact that GQDs are either conjugated with specific molecules or alone have extraordinary potential as a multifunctional material for biomedical cell imaging applications. Figure 4 represents the biomedical

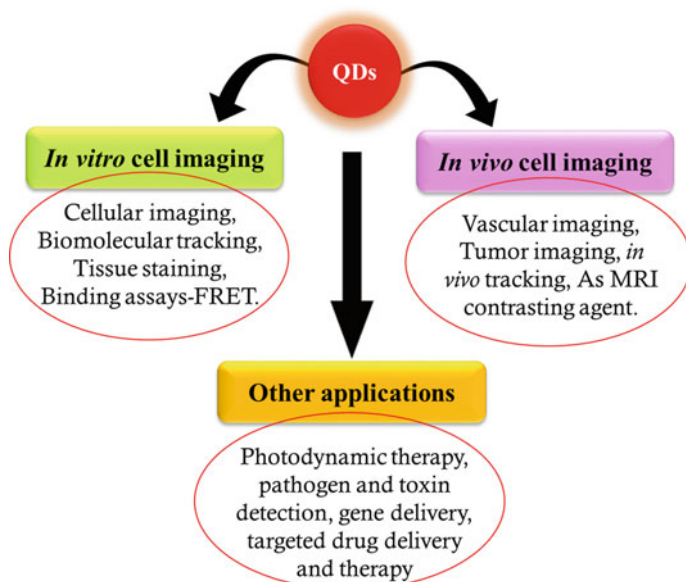


Fig. 4 Applications of QDs in the biomedical field

applications of QDs.

In vitro experiments which have several beneficial effects but have also some limitations, i.e., laboratory set up for the using of test tubes, Petri dishes etc. In vivo studies are paramount over in vitro experiments due to its well suited for detecting the overall effects on living subject.

4.2 In vivo imaging

Dubertret et al. encapsulated CdSe/ZnS QDs in phospholipid block-copolymer micelles and demonstrated them as both in vitro and in vivo imaging agents. For this purpose, they further modified the QD by DNA. These multi-functionalized DNA-QD-micelles were utilized as in vitro fluorescent probes to hybridize to specific complementary sequences. Moreover, they performed in vivo imaging study by microinjecting the DNA-QD-micelles system into the early-stage *Xenopus* embryos [87]. Yong et al. demonstrated highly luminescent CdSe/CdS/ZnS quantum rods (QRs) coated with PEGylated phospholipids and RGD peptides for tumor targeting and imaging in live animals. This conjugate was demonstrated to be a bright, photo stable, and biocompatible luminescent probe and showed no adverse effects even at a dose roughly 6.5 times higher than reported in vivo imaging studies using quantum dots [88]. Zimmer et al. synthesized a series of InAs/ZnSe core/shell quantum dots with a size less than 10 nm that offer a range of size tunable emission wavelengths,

between 750–920 nm. They further conjugated dihydrolipoic acid (DHLA) to the quantum dots and utilized it in the in vivo imaging study of the interstitial fluid in rats. This visualization of the extravasation sites gave an idea about the delivery mechanism of quantum dots to tumor cells [89]. Angiogenesis is the process by which new blood vessels are formed from preexisting vasculature and it is essential for the supply of nutrients from the blood stream into tumor cells. Receptors, such as integrin, are highly expressed in tumor cells during angiogenesis. So, targeting the receptor like integrin can be a crucial factor for cancer diagnosis and therapy. Cai et al. reported the in vivo targeting and imaging of arginine-glycine-aspartic acid (RGD) peptide labeled QDs for imaging of tumor vasculature in a murine xenograft model. This work widens the possibility of application of QDs as in vivo imaging of tumor vasculature in living subjects [90].

Carbon dots (CDots) have the most attractive luminescent features that emerging them as fluorescent labelling agents in the range of various biomedical research fields [59].

There are several studies regarding cell imaging with carbon QDs (CQDs). Here we represent some of the current examples; Sun et al. reported the synthesis of CDots doped with ZnS salt which were potentially used in in vivo cell imaging study in mice model [51] (Fig. 5). Zhang et al. synthesized the CQDs from poly-dopamine (PDA-FONs) for the specific fluorescence imaging in the cytoplasm but not a nucleus [91]. After one year, Yan et al. prepared CDs from cellulose and cyclodextrin and used them as cell imaging agents [92]. Mouse melanoma B16-F10 cell lines were incubated for five hours with quantum dots and within this time

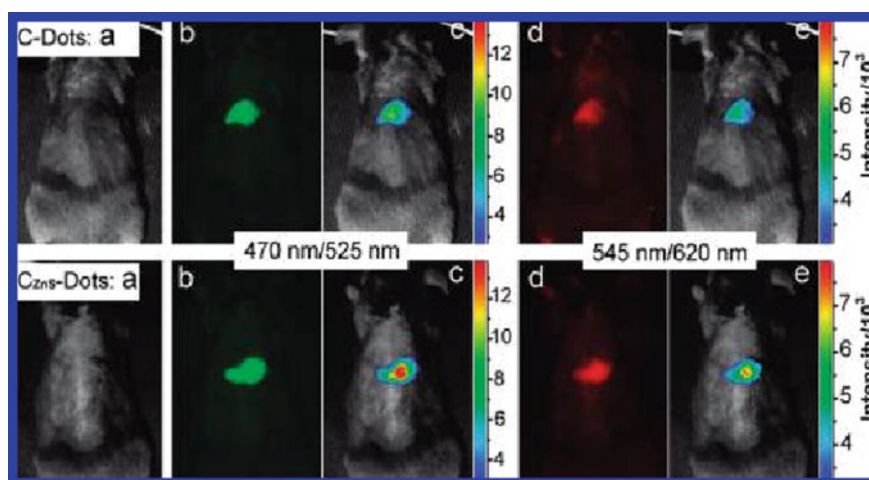


Fig. 5 Subcutaneous injection of C-Dots and CZnS-Dots: bright field **a**, fluorescence excitation/emission wavelength, 470/525 nm **b** and 545/620 nm **d** and color-coded images (**c**, **e**), adapted with permission from Ref. [51]. Copyright 2022 American Chemical Society

maximum QDs penetrated the cells and displayed bright red, yellow and blue fluorescence emissions [92]. In the same year, Zhang et al. obtained the CDots by one-pot hydrothermal synthesis of nanodiamond [93]. Upon incubation of CDots with NIH-3T3 cells, it was observed that cytoplasm specifically exhibited green and yellow fluorescence emissions at 405 nm and 458 nm excitations respectively [93]. Huang et al. reported the synthesis of admirable photoluminescent CDots decorated with dye ZW800 which were applied in the *in vivo* imaging and for the better understanding of the blood circulation and specific tumor detection [94]. Recently, F. Hashemi et al. reported the synthetic method of N-doped green CDots from lemon and tomato extractions. These QDs displayed a deep blue fluorescence under UV light at 360 nm excitation and were explored as cell detection and labelling agents [95].

The most attractive novel GQDs-based QDs have many characteristic features that make them ideal compared to conventional imaging tools. Mostly, GQDs are used as contrast agents for *in vivo* imaging and are highly explored for the labelling of deep tissue samples [96]. Tan and coworkers reported that near IR GQDs have the ability to detect the endogenous ascorbic acids in live cells. P. Roy et al. reported a novel preparation method of the GQDs from plant leaf, modified with Annexin V antibody (AbA5), useful for labelling apoptotic cells in live zebrafish [97]. Wang et al. reported the red fluorescent GQDs and investigated the NIR-I *in vivo* imaging [98]. Chen and co-workers investigated the whole distribution of cell surface carbohydrate receptors with the help of the monosaccharide sugar functionalized GQDs [99].

5 Conclusion

Owing to the preliminary success of fluorescent QDs in the biomedical field for *in vitro* and *in vivo* imaging, these materials soon explored themselves as the superior agents for cellular imaging and diagnoses, along with the vast progression in material science. The swift increase in the utilization of QDs is mainly due to their unique properties e.g., extreme emission intensity, high quantum yield and photo bleaching resistance, and easy fabrication or modification strategies. Although the metallic semiconductor QDs have few restrictions (low biocompatibility) over the core-shell or carbon-based QDs towards the interior of cells immense capabilities of single and multicolor image development are appreciable. A new avenue has already opened in medical science where QDs are being used as bio-imaging or diagnostic tools.

In future, conjugated QDs will be purposefully designed to focus on the early detection of cancer cells, which points out metastasis. These conjugated QDs can also be explored for targeting solid tumor tissues. The day is not so far when QDs will be used as highly reliable diagnostic and imaging tools for most acute diseases.

References

1. Peabody JW, Taguiwalo MM, Robalino DA, Frenk J. Improving the quality of care in developing countries. 2006.
2. Barr AJ. The biochemical basis of disease. *Essays Biochem.* 2018;62(5):619–42.
3. Weaver O, Leung JW. Biomarkers and imaging of breast cancer. *Am J Roentgenol.* 2018;210(2):271–8.
4. Sun D, Liu Y, Liu D, Zhang R, Yang X, Liu J. Stabilization of G-quadruplex DNA, inhibition of telomerase activity and live cell imaging studies of chiral ruthenium (II) complexes. *Chem–Eur J.* 2012;18(14):4285–95.
5. Wolfbeis OS. An overview of nanoparticles commonly used in fluorescent bioimaging. *Chem Soc Rev.* 2015;44(14):4743–68.
6. Resch-Genger U, Grabolle M, Cavaliere-Jaricot S, Nitschke R, Nann T. Quantum dots versus organic dyes as fluorescent labels. *Nat Methods.* 2008;5(9):763.
7. Wang L, Wang K, Santra S, Zhao X, Hilliard LR, Smith JE, et al. Watching silica nanoparticles glow in the biological world. ACS Publications; 2006.
8. Ronda CR, Jüstel T. Quantum dots and nanophosphors. *Luminescence: From Theory to Applications/CR Ronda, T Justel.* 2008:35–59.
9. Jensen EC. Use of fluorescent probes: their effect on cell biology and limitations. *Anat Rec Adv Integr Anat Evol Biol.* 2012;295(12):2031–6.
10. Ansari AA, Labis JP, Manthrammel MA. Designing of luminescent GdPO₄: Eu@ LaPO₄@ SiO₂ core/shell nanorods: Synthesis, structural and luminescence properties. *Solid State Sci.* 2017;71:117–22.
11. Cantelli A, Battistelli G, Guidetti G, Manzi J, Di Giosia M, Montalti M. Luminescent gold nanoclusters as biocompatible probes for optical imaging and theranostics. *Dyes Pigm.* 2016;135:64–79.
12. Hu F-l, Shi Y-X, Chen H-H, Lang J-P. A Zn (II) coordination polymer and its photocycloaddition product: syntheses, structures, selective luminescence sensing of iron (III) ions and selective absorption of dyes. *Dalton Trans.* 2015;44(43):18795–803.
13. Liu M, Huang H, Wang K, Xu D, Wan Q, Tian J, et al. Fabrication and biological imaging application of AIE-active luminescent starch based nanoprobe. *Carbohydr Polym.* 2016;142:38–44.
14. Walling MA, Novak JA, Shepard JR. Quantum dots for live cell and in vivo imaging. *Int J Mol Sci.* 2009;10(2):441–91.
15. Behzadi S, Serpooshan V, Tao W, Hamaly MA, Alkawareek MY, Dreaden EC, et al. Cellular uptake of nanoparticles: Journey inside the cell. *Chem Soc Rev.* 2017;46(14):4218–44.
16. Bruchez M, Moronne M, Gin P, Weiss S, Alivisatos AP. Semiconductor nanocrystals as fluorescent biological labels. *Science.* 1998;281(5385):2013–6.
17. Chan WC, Nie S. Quantum dot bioconjugates for ultrasensitive nonisotopic detection. *Science.* 1998;281(5385):2016–8.
18. Pierobon P, Cappello G. Quantum dots to tail single bio-molecules inside living cells. *Adv Drug Deliv Rev.* 2012;64(2):167–78.
19. Wegner KD, Hildebrandt N. Quantum dots: Bright and versatile in vitro and in vivo fluorescence imaging biosensors. *Chem Soc Rev.* 2015;44(14):4792–834.
20. Larramendy M, Soloneski S. Green nanotechnology: Overview and further prospects. 2016.
21. Li J, Zhu J-J. Quantum dots for fluorescent biosensing and bio-imaging applications. *Analyst.* 2013;138(9):2506–15.
22. Vu TQ, Lam WY, Hatch EW, Lidke DS. Quantum dots for quantitative imaging: from single molecules to tissue. *Cell Tissue Res.* 2015;360(1):71–86.
23. Daniel M-C, Astruc D. Gold nanoparticles: Assembly, supramolecular chemistry, quantum-size-related properties, and applications toward biology, catalysis, and nanotechnology. *Chem Rev.* 2004;104(1):293–346.
24. Kastner MA, Klein O, Lyszczyk TM, Mankiewich PM, Shaver DC, Wind S, et al. Artificial atoms. Research Laboratory of Electronics (RLE) at the Massachusetts Institute of ...; 1994.

25. Schaming D, Remita H. Nanotechnology: from the ancient time to nowadays. *Found Chem.* 2015;17(3):187–205.
26. Ęfros AL, Lockwood D, Tsybeskov L. Semiconductor nanocrystals: from basic principles to applications: Springer Science & Business Media; 2003.
27. Ekimov AI, Onushchenko AA. Quantum size effect in three-dimensional microscopic semiconductor crystals. *Jetp Lett.* 1981;34(6):345–9.
28. Reed M, Bate R, Bradshaw K, Duncan W, Frenslay W, Lee J, et al. Spatial quantization in GaAs–AlGaAs multiple quantum dots. *J Vacuum Sci Technol B: Microelectron Process Phenom.* 1986;4(1):358–60.
29. Emory SR, Haskins WE, Nie S. Direct observation of size-dependent optical enhancement in single metal nanoparticles. *J Am Chem Soc.* 1998;120(31):8009–10.
30. Mokari T, Habas SE, Zhang M, Yang P. Synthesis of lead chalcogenide alloy and core–shell nanowires. *Angew Chem.* 2008;120(30):5687–90.
31. Masala O, Seshadri R. Synthesis routes for large volumes of nanoparticles. *Annu Rev Mater Res.* 2004;34:41–81.
32. Adlim A. Preparations and application of metal nanoparticles. *Indonesian J Chem.* 2006;6(1):1–10.
33. Yen F-L, Wu T-H, Tzeng C-W, Lin L-T, Lin C-C. Curcumin nanoparticles improve the physicochemical properties of curcumin and effectively enhance its antioxidant and antihepatoma activities. *J Agric Food Chem.* 2010;58(12):7376–82.
34. Chukwuocha E, Onyeaju M. Simulation of quantum dots (QDs) in the confinement regime. *Ijaser Int J Appl Sci Eng Res.* 2012;1(6).
35. Weller H. Colloidal semiconductor q-particles: Chemistry in the transition region between solid state and molecules. *Angew Chem, Int Ed Engl.* 1993;32(1):41–53.
36. Ghaffari M, Dolatabadi JEN. Nanotechnology for pharmaceuticals. Industrial applications of nanomaterials: Elsevier; 2019. p. 475–502.
37. Haverinen HM, Myllylä RA, Jabbour GE. Inkjet printing of light emitting quantum dots. *Appl Phys Lett.* 2009;94(7): 073108.
38. Tekin E, Smith PJ, Hoepfener S, Van Den Berg AM, Susha AS, Rogach AL, et al. Inkjet printing of luminescent CdTe nanocrystal–polymer composites. *Adv Func Mater.* 2007;17(1):23–8.
39. Michalek X, Pinaud F, Bentolila L, Tsay J, Doose S, Li J, et al. Quantum dots for live cells, in vivo imaging, and diagnostics. *Science.* 2005;307(5709):538–44.
40. Prasad PN. Introduction to biophotonics: Wiley; 2003.
41. Wittcoff HA, Reuben BG, Plotkin JS. Industrial organic chemicals: Wiley; 2012.
42. Farzin MA, Abdoos H. A critical review on quantum dots: From synthesis toward applications in electrochemical biosensors for determination of disease-related biomolecules. *Talanta.* 2020:121828.
43. Kershaw SV, Susha AS, Rogach AL. Narrow bandgap colloidal metal chalcogenide quantum dots: synthetic methods, heterostructures, assemblies, electronic and infrared optical properties. *Chem Soc Rev.* 2013;42(7):3033–87.
44. Derfus AM, Chan WC, Bhatia SN. Probing the cytotoxicity of semiconductor quantum dots. *Nano Lett.* 2004;4(1):11–8.
45. Hardman R. A toxicologic review of quantum dots: Toxicity depends on physicochemical and environmental factors. *Environ Health Perspect.* 2006;114(2):165–72.
46. Loukanov AR, Dushkin CD, Papazova KI, Kirov AV, Abrashev MV, Adachi E. Photoluminescence depending on the ZnS shell thickness of CdS/ZnS core-shell semiconductor nanoparticles. *Colloids Surf, A.* 2004;245(1–3):9–14.
47. Vasudevan D, Gaddam RR, Trinchì A, Cole I. Core–shell quantum dots: Properties and applications. *J Alloy Compd.* 2015;636:395–404.
48. Carrillo-Carrión C, Cárdenas S, Simonet BM, Valcárcel M. Quantum dots luminescence enhancement due to illumination with UV/Vis light. *Chem Commun.* 2009;35:5214–26.
49. Kairdolf BA, Smith AM, Stokes TH, Wang MD, Young AN, Nie S. Semiconductor quantum dots for bioimaging and biodiagnostic applications. *Annu Rev Anal Chem.* 2013;6:143–62.

50. Wang X, Yu J, Chen R. Optical characteristics of ZnS passivated CdSe/CdS quantum dots for high photostability and lasing. *Sci Rep.* 2018;8(1):1–7.
51. Yang S-T, Cao L, Luo PG, Lu F, Wang X, Wang H, et al. Carbon dots for optical imaging in vivo. *J Am Chem Soc.* 2009;131(32):11308–9.
52. Gao X, Cui Y, Levenson RM, Chung LW, Nie S. In vivo cancer targeting and imaging with semiconductor quantum dots. *Nat Biotechnol.* 2004;22(8):969–76.
53. Geys J, Nemmar A, Verbeke E, Smolders E, Ratoi M, Hoylaerts MF, et al. Acute toxicity and prothrombotic effects of quantum dots: impact of surface charge. *Environ Health Perspect.* 2008;116(12):1607–13.
54. Cao L, Wang X, Meziani MJ, Lu F, Wang H, Luo PG, et al. Carbon dots for multiphoton bioimaging. *J Am Chem Soc.* 2007;129(37):11318–9.
55. Luo PG, Sahu S, Yang S-T, Sonkar SK, Wang J, Wang H, et al. Carbon “quantum” dots for optical bioimaging. *J Mater Chem B.* 2013;1(16):2116–27.
56. Sun Y-P, Zhou B, Lin Y, Wang W, Fernando KS, Pathak P, et al. Quantum-sized carbon dots for bright and colorful photoluminescence. *J Am Chem Soc.* 2006;128(24):7756–7.
57. Pan D, Zhang J, Li Z, Wu M. Hydrothermal route for cutting graphene sheets into blue-luminescent graphene quantum dots. *Adv Mater.* 2010;22(6):734–8.
58. Li L, Wu G, Yang G, Peng J, Zhao J, Zhu J-J. Focusing on luminescent graphene quantum dots: Current status and future perspectives. *Nanoscale.* 2013;5(10):4015–39.
59. Xu X, Ray R, Gu Y, Ploehn HJ, Gearheart L, Raker K, et al. Electrophoretic analysis and purification of fluorescent single-walled carbon nanotube fragments. *J Am Chem Soc.* 2004;126(40):12736–7.
60. Hutton GA, Martindale BC, Reisner E. Carbon dots as photosensitizers for solar-driven catalysis. *Chem Soc Rev.* 2017;46(20):6111–23.
61. Wang J, Qiu J. A review of carbon dots in biological applications. *J Mater Sci.* 2016;51(10):4728–38.
62. Lim SY, Shen W, Gao Z. Carbon quantum dots and their applications. *Chem Soc Rev.* 2015;44(1):362–81.
63. Dong Y, Shao J, Chen C, Li H, Wang R, Chi Y, et al. Blue luminescent graphene quantum dots and graphene oxide prepared by tuning the carbonization degree of citric acid. *Carbon.* 2012;50(12):4738–43.
64. Wang L, Zhu S-J, Wang H-Y, Qu S-N, Zhang Y-L, Zhang J-H, et al. Common origin of green luminescence in carbon nanodots and graphene quantum dots. *ACS Nano.* 2014;8(3):2541–7.
65. Liu Y, Huang H, Cao W, Mao B, Liu Y, Kang Z. Advances in carbon dots: from the perspective of traditional quantum dots. *Mater Chem Front.* 2020;4(6):1586–613.
66. Morozova S, Alikina M, Vinogradov A, Pagliaro M. Silicon quantum dots: synthesis, encapsulation, and application in light-emitting diodes. *Front Chem.* 2020;8:191.
67. Jin S, Hu Y, Gu Z, Liu L, Wu H-C. Application of quantum dots in biological imaging. *J Nanomater.* 2011;2011.
68. Rosenthal SJ, Wright DW. *Nanobiotechnology protocols*: Springer; 2005.
69. Zhou L, Yan J, Tong L, Han X, Wu X, Guo P. Quantum dot-based immunohistochemistry for pathological applications. *Cancer Transl Med.* 2016;2(1):21.
70. Li H, Shih WY, Shih W-H. Synthesis and characterization of aqueous carboxyl-capped CdS quantum dots for bioapplications. *Ind Eng Chem Res.* 2007;46(7):2013–9.
71. Jaiswal JK, Mattoussi H, Mauro JM, Simon SM. Long-term multiple color imaging of live cells using quantum dot bioconjugates. *Nat Biotechnol.* 2003;21(1):47–51.
72. Liu A, Peng S, Soo JC, Kuang M, Chen P, Duan H. Quantum dots with phenylboronic acid tags for specific labeling of sialic acids on living cells. *Anal Chem.* 2011;83(3):1124–30.
73. Sun P, Zhang H, Liu C, Fang J, Wang M, Chen J, et al. Preparation and characterization of Fe₃O₄/CdTe magnetic/fluorescent nanocomposites and their applications in immuno-labeling and fluorescent imaging of cancer cells. *Langmuir.* 2010;26(2):1278–84.
74. Bagalkot V, Zhang L, Levy-Nissenbaum E, Jon S, Kantoff PW, Langer R, et al. Quantum dot–aptamer conjugates for synchronous cancer imaging, therapy, and sensing of drug delivery based on bi-fluorescence resonance energy transfer. *Nano Lett.* 2007;7(10):3065–70.

75. Walther C, Meyer K, Rennert R, Neundorf I. Quantum dot—carrier peptide conjugates suitable for imaging and delivery applications. *Bioconjug Chem.* 2008;19(12):2346–56.
76. Biju V, Muraleedharan D, Nakayama K-i, Shinohara Y, Itoh T, Baba Y, et al. Quantum dot-insect neuropeptide conjugates for fluorescence imaging, transfection, and nucleus targeting of living cells. *Langmuir.* 2007;23(20):10254–61.
77. Fan Z, Li S, Yuan F, Fan L. Fluorescent graphene quantum dots for biosensing and bioimaging. *RSC Adv.* 2015;5(25):19773–89.
78. Aiyer S, Prasad R, Kumar M, Nirvikar K, Jain B, Kushwaha OS. Fluorescent carbon nanodots for targeted in vitro cancer cell imaging. *Appl Mater Today.* 2016;4:71–7.
79. Meena R, Singh R, Marappan G, Kushwaha G, Gupta N, Meena R, et al. Fluorescent carbon dots driven from ayurvedic medicinal plants for cancer cell imaging and phototherapy. *Heliyon.* 2019;5(9): e02483.
80. Su Z, Shen H, Wang H, Wang J, Li J, Nienhaus GU, et al. Motif-designed peptide nanofibers decorated with graphene quantum dots for simultaneous targeting and imaging of tumor cells. *Adv Func Mater.* 2015;25(34):5472–8.
81. Iravani S, Varma RS. Green synthesis, biomedical and biotechnological applications of carbon and graphene quantum dots. A Review. *Environ Chem Letters.* 2020;18(3):703–27.
82. Sheng L, Huangfu B, Xu Q, Tian W, Li Z, Meng A, et al. A highly selective and sensitive fluorescent probe for detecting Cr (VI) and cell imaging based on nitrogen-doped graphene quantum dots. *J Alloy Compd.* 2020;820: 153191.
83. Li H, Zhang Y, Wang L, Tian J, Sun X. Nucleic acid detection using carbon nanoparticles as a fluorescent sensing platform. *Chem Commun.* 2011;47(3):961–3.
84. Hai X, Wang Y, Hao X, Chen X, Wang J. Folic acid encapsulated graphene quantum dots for ratiometric pH sensing and specific multicolor imaging in living cells. *Sens Actuators, B Chem.* 2018;268:61–9.
85. Jin K, Gao H, Lai L, Pang Y, Zheng S, Niu Y, et al. Preparation of highly fluorescent sulfur doped graphene quantum dots for live cell imaging. *J Lumin.* 2018;197:147–52.
86. Mondal MK, Mukherjee S, Joardar N, Roy D, Chowdhury P, Babu SPS. Synthesis of smart graphene quantum dots: A benign biomaterial for prominent intracellular imaging and improvement of drug efficacy. *Appl Surf Sci.* 2019;495: 143562.
87. Dubertret B, Skourides P, Norris DJ, Noireaux V, Brivanlou AH, Libchaber A. In vivo imaging of quantum dots encapsulated in phospholipid micelles. *Science.* 2002;298(5599):1759–62.
88. Yong K-T, Hu R, Roy I, Ding H, Vathy LA, Bergey EJ, et al. Tumor targeting and imaging in live animals with functionalized semiconductor quantum rods. *ACS Appl Mater Interfaces.* 2009;1(3):710–9.
89. Zimmer JP, Kim S-W, Ohnishi S, Tanaka E, Frangioni JV, Bawendi MG. Size series of small indium arsenide—zinc selenide core—shell nanocrystals and their application to in vivo imaging. *J Am Chem Soc.* 2006;128(8):2526–7.
90. Cai W, Shin D-W, Chen K, Gheysens O, Cao Q, Wang SX, et al. Peptide-labeled near-infrared quantum dots for imaging tumor vasculature in living subjects. *Nano Lett.* 2006;6(4):669–76.
91. Zhang X, Wang S, Xu L, Feng L, Ji Y, Tao L, et al. Biocompatible polydopamine fluorescent organic nanoparticles: Facile preparation and cell imaging. *Nanoscale.* 2012;4(18):5581–4.
92. Yan H, Tan M, Zhang D, Cheng F, Wu H, Fan M, et al. Development of multicolor carbon nanoparticles for cell imaging. *Talanta.* 2013;108:59–65.
93. Zhang X, Wang S, Zhu C, Liu M, Ji Y, Feng L, et al. Carbon-dots derived from nanodiamond: Photoluminescence tunable nanoparticles for cell imaging. *J Colloid Interface Sci.* 2013;397:39–44.
94. Huang X, Zhang F, Zhu L, Choi KY, Guo N, Guo J, et al. Effect of injection routes on the biodistribution, clearance, and tumor uptake of carbon dots. *ACS Nano.* 2013;7(7):5684–93.
95. Hashemi F, Heidari F, Mohajeri N, Mahmoodzadeh F, Zarghami N. Fluorescence intensity enhancement of green carbon dots: Synthesis, characterization and cell imaging. *Photochem Photobiol.* 2020;96(5):1032–40.
96. Miao P, Han K, Tang Y, Wang B, Lin T, Cheng W. Recent advances in carbon nanodots: Synthesis, properties and biomedical applications. *Nanoscale.* 2015;7(5):1586–95.

97. Roy P, Periasamy AP, Lin C-Y, Her G-M, Chiu W-J, Li C-L, et al. Photoluminescent graphene quantum dots for in vivo imaging of apoptotic cells. *Nanoscale*. 2015;7(6):2504–10.
98. Ge J, Lan M, Zhou B, Liu W, Guo L, Wang H, et al. A graphene quantum dot photodynamic therapy agent with high singlet oxygen generation. *Nat Commun*. 2014;5(1):1–8.
99. Chen J, Than A, Li N, Ananthanarayanan A, Zheng X, Xi F, et al. Sweet graphene quantum dots for imaging carbohydrate receptors in live cells. *FlatChem*. 2017;5:25–32.

Quantum Dot: A Boon for Biological and Biomedical Research



Palash Pandit and Arpita Chandra

Abstract Quantum dots (QDs) are mostly semiconductor nanocrystals, having properties in between bulk semiconductors and discrete atoms or molecules. Quantum dots can be synthesised using several methods from colloidal synthesis to chemical vapor deposition, for QDs synthesis, but the cheapest and the convenient method is benchtop colloidal synthesis. Due to exceptional optical and chemical behavior, QDs are broadly used in different areas, including light-emitting diodes, laser technology and solar cells, as well as in the biological and biomedical fields. This chapter provides the brief idea about QDs, including their synthetic approaches, biological relevance, and potentials in clinical applications like bio-imaging (cancer cell imaging), and targeted molecular therapy (drug delivery), as well as the leftover issues and future perspectives.

Keywords Quantum dots · Bioimaging · Drug delivery · Cancer cell

Abbreviations

2D	Two dimensional
3D	Three dimensional
ACE	Angiotensin I-converting enzyme
BSA	Bovine serum albumin
CPPs	Cell-penetrating peptide
DDS	Drug delivery system
DOX	Doxorubicin
EPR	Enhanced permeability retention

P. Pandit

Department of Chemistry, Saheed Nurul Islam Mahavidyalaya, Gokulpur-Harishpur, Tentulia, North 24 Parganas, West Bengal 743286, India

A. Chandra (✉)

In Vitro Carcinogenesis and Cellular Chemotherapy, Chittaranjan National Cancer Institute, 37 S.

P. Mukherjee Road, Kolkata, West Bengal 700026, India

e-mail: arpitancnci@gmail.com

GFP	Green-fluorescent protein
MUA	11-Mercaptoundecanoic acid
NIR	Near infrared
NPs	Nanoparticles
OSCC	Oral squamous cell carcinoma
PAR ₁	Protease-activated receptor ₁
PC3	Prostate cancer cells
PEG	Polyethylene glycol
PL	Photoluminescence
QDs	Quantum dots
QY	Quantum yield
SLNs	Sentinel lymph nodes
UV	Ultraviolet
VCAM-1	Vascular cell adhesion molecule 1
VEGFR2	Vascular endothelial growth factor receptor 2

1 Introduction

Crystalline semiconductor nanoparticle (NP) QDs are attractive candidate in the biological and biomedical research field due to their several unique features. NPs are different from bulk materials due to their exceptional structural and functional properties. Their unique quantum features, like quantum size, small surface and quantum tunneling effects, are responsible for their outstanding electrical and optical features [1]. There are several types of inorganic NPs like quantum dots (QDs; e.g., CdSe, CdS, CdTe/CdS, PbS and InP), carbon NPs, silica nanoparticles, magnetic compounds (e.g., Fe₃O₄, CoFe₂O₄, and CoPt), prompted the development of nanotechnology. Among them, QDs have the most exceptional features to be applied in the field of biology and medicine [2–5]. Quantum dots (QDs) are a heterogeneous class of inorganic NPs, having physical size close to or smaller than exciton Bohr radius [6]. QDs are zero dimension NPs having particle sizes <10 nm. The quantum confinement effects and reduced size make QDs an intermediate between a molecule and bulk solids. This confinement effect of QDs is also responsible for their extraordinarily attractive photophysical property like intensive photoluminescence (PL) [7]. In comparison with the usual organic dyes, QDs have better sensitivity, 100-fold more photostability, excellent biocompatibility and less invasiveness, and these features made them superior candidates for bio-imaging, bio-sensing, cell targeting and drug delivery applications [8–10]. QDs also behave as a good candidate for multicolor imaging in cellular and molecular label because of their exceptional optical features, like size-tunable broad absorption spectra, narrow emission spectra and large stokes shift [11]. Relying upon their size and composition, the optical properties of QDs can be tuned from ultraviolet (UV) to near-infrared (NIR) region. Mainly NIR emitted QDs are the promising candidates for both in vitro and in vivo deep-tissue imaging, in

the biological and biomedical purposes [12–14]. Having high molar adsorption coefficients and high quantum yields (QY), QDs do not require intense photon beams for their photochemical excitation purpose, which in turn avoid photo-damaging. QDs require functionalization with antibodies, proteins, peptides or drugs to enhance their water solubility and biocompatibility [15]. Regardless of the above-mentioned exclusive features of QDs, their extensive use in biomedical purposes is restricted due to their toxic side effects and biodegradability [16, 17]. Therefore, researchers paid attention to design non-toxic and biocompatible high-quality QD-based fluorescent probes, and some successful solution has been achieved in this context [18]. Herein, we discussed the properties and synthesis of QDs for their biological relevance or potentials in clinical applications like bio-imaging, cancer cell imaging, cancer cell targeting, drug delivery and their perspectives and shortcoming for in vivo biological and biomedical applications.

2 Quantum Dots (QDs)

Quantum dots are solid spherical-shaped (may exist with other shapes, for example, rods and tetra-pods) nano-size crystals, having diameter <10 nm (10–50 atoms). QDs consist of only a few numbers of free electrons and 10^2 – 10^6 numbers of atoms. The conventional type colloidal semiconductor QDs comprise mainly atoms of groups II–VI, III–V or IV–VI (e.g., CdSe, PbSe, CdTe, GaAs, InP, etc.) of the periodic table, among which Cd-based QDs have received more attention in biomedical uses. QDs contain a semiconductor core [e.g., cadmium selenide (CdSe)], covered with a semiconductor outer shell (e.g., ZnS) (Fig. 1).

First traditional lithography-based QDs were synthesized in 1980s by Louis E. Brus and Alexei Ekimov, which shows exceptional electronic and optical properties [20]. QDs being very tiny in size exhibit attractive photophysical behavior like they

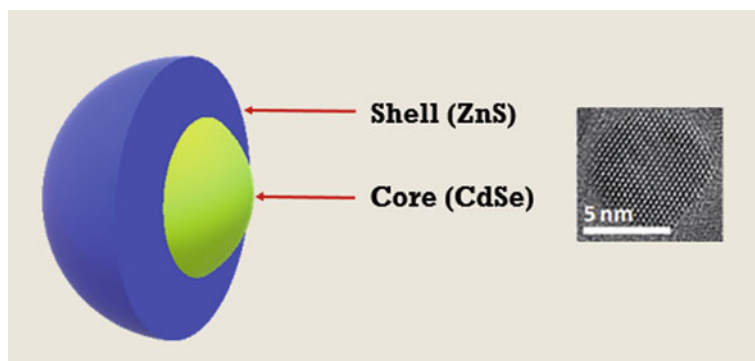


Fig. 1 Schematic representation of a core/shell QD and TEM image of the QD core. Reproduced with permission from Ref. [19]. Copyright 2015, The Royal Society of Chemistry

have narrow emission peak and broad excitation range, and their emission wavelength is also dependent on their particle size [21–23]. The size-tunable properties and high molar excitation coefficients of QDs made them a good fluorophore for biological, biomedical research and pharmaceutical industries [24–26]. Although a bare nanocrystal core is highly reactive and toxic, cap-enabled (using ZnS or SiO₂) and surface-modified QDs (adding biomolecules) have improved optical properties, water solubility, reduced toxicity and enhanced biocompatibility [27]. Although Carbon Quantum dots (C-QDs) are widely applied in electronics, sensors and catalysis due to their excellent electrical and electronic properties, but now a days they are also used in biomedical research [28] (detailed discussions about C-QDs fall beyond the scope of this chapter).

3 Properties of QDs

QDs, small crystalline semiconductor NPs, contain a few hundred to a few million atoms having size <10 nm with excellent optical and electronic properties due to their quantum confinement effect. Lower and higher energy levels of the semiconductors are called valance and conduction band, respectively. The resultant energy difference between the two bands is called band gap. After absorbing heat or light energy, electrons move from the lower energy level to the higher energy level, and thus, a hole is created at the valance band. The separation distance or gap between electron and hole is known as the exciton Bohr radius. If the exciton Bohr radius is greater than double of QDs size, then they will experience quantum confinement, and the particle in a box model can be used to evaluate their energy level. The energy involved with QDs is comprised of band gap energy, confinement energy and bound exciton energy. Since the electron of a semiconductor NPs is confined by the exciton Bohr radius, so their properties are dependent on the properties of electron and hole pair. Electrical conductive properties of semiconductor NPs can be changed by changing their size and shape; that is, lower the particle size, higher will be the band gap and vice-versa (Fig. 2) [29, 30].

That is to say, the photon's emission wavelength is directed by the size of the band gap, which can vary from UV to NIR region (400–1350 nm). For example, QDs with larger particle sizes have smaller band gaps and release red light, whereas QDs with smaller particle sizes and larger band gap release blue light (Fig. 3) [31, 32]. A quantum confinement effect of QDs is not only dependent on the size of the core, but also the chemical composition of the same. QDs are very similar to electron-bound nuclei; therefore, QDs act as an artificial atom, and it can excite and emit light together with sharp signal intensity. Compared to conventional organic fluorophores, inorganic QDs have very high fluorescence efficiency, elongated fluorescence lifetime of >10 ns and less photobleaching tendency. QDs also have a high molar excitation coefficient, large stokes shift, longer signal acquisition times and good photostability [33]. The diameter tunability and brightness (emission wavelength) properties of QDs make them suitable for multiplex detection [34]. Highly

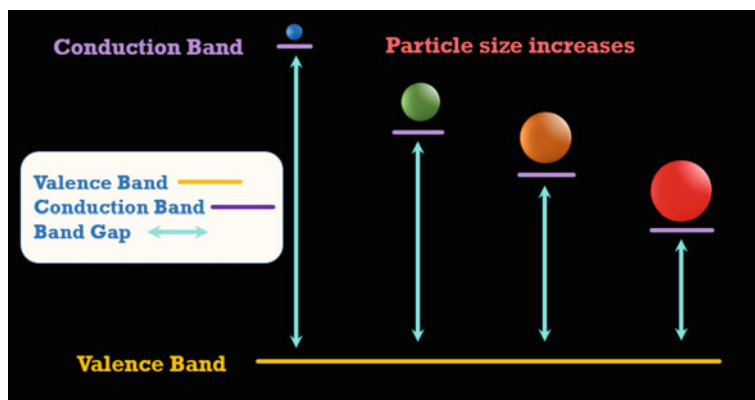


Fig. 2 Schematic representation of the size changes of the semiconductor NPs with band gap

luminescent, stable colloidal QDs are promising candidates for biological research and biomedical studies *in vivo*. The major drawback of heavy metal-containing QDs is their toxicity, which can be reduced by the modification of the QDs surface.

4 Surface Modifications of QDs

Semiconductor QDs required surface modification to reduce their toxic effects and to improve the optical property. Surface modification is a synthetic technique where the hydrophobic surface of the QDs is modified by attaching a variety of inorganic and organic or biological materials through sequential physical and chemical reactions. The surface of QDs can be modified by using thiol group coupling, multimodal ligand, cavity chain, group coupling and dendrimer (Fig. 4). For instance, polyethylene glycol (PEG) coatings are used to increase circulation time and stability and to minimize non-specific deposition of QDs for *in vivo* imaging [35].

Another advancement of surface modification of QDs is electrostatic interaction of the charged surfaces of QDs with a protein through polylysine chain. Encapsulation of a phospholipid micelle inside the QDs surface, through hydrophobic interaction, is also another effective strategy of surface modification. Here, hydrophilic part of micelle is attached to biomolecules and effectively improves efficiency of QDs for biological and biomedical experiments [37].

5 Synthesis of QDs

To synthesize QDs for biological purpose, one should pay attention to the material with high water solubility, less toxicity and having a wide range of emission

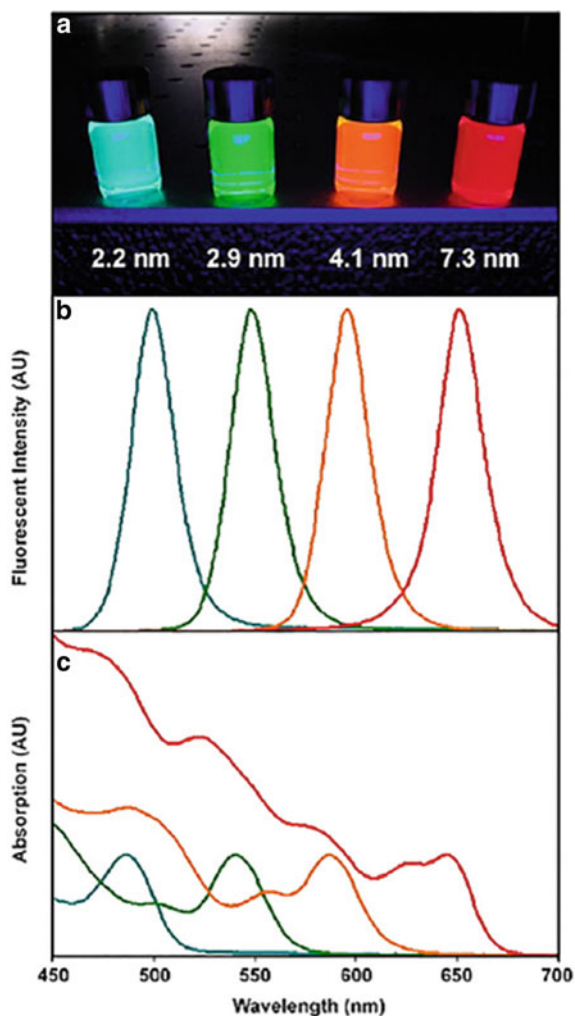


Fig. 3 Schematic representation of the change in fluorescent image (a), emission wavelength (b) and absorption spectrum (c) with the size of QDs. Reprinted with permission from Ref. [23]. Copyright 2019, Acta Materialia Inc., Elsevier Ltd.

wavelengths, ranging from ultraviolet to the infrared region. Among the frequently reported QDs like CdS, CdSe, ZnSe, ZnS, PbS, PbSe or CdTe, typically CdSe/ZnS, core/shell QDs are mainly used in the biological and biomedical purposes [38]. QDs that are usually used for biological and biomedical applications are prepared in such a way that they must have a semiconductor core such as CdSe, which is then shelled by another semiconductor material like ZnS. These core/shell QDs have improved optical properties and reduced toxicity [39].

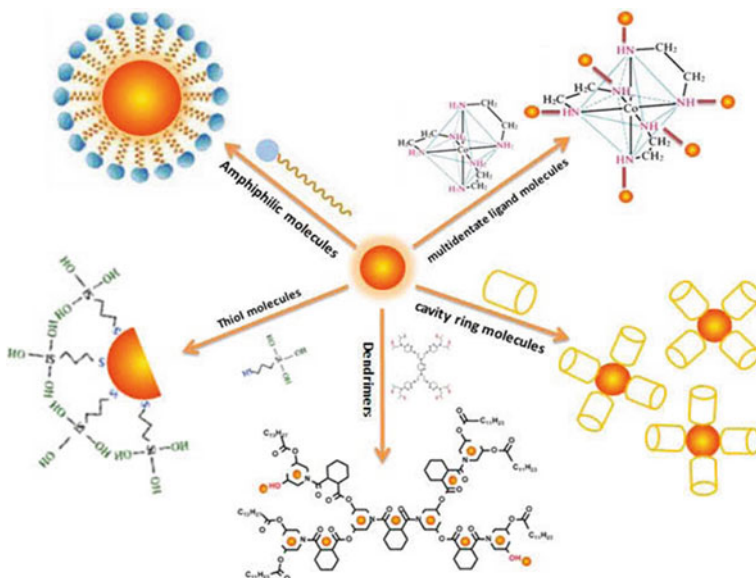


Fig. 4 Schematic representation of different surface modification techniques of QDs. Reprinted with permission from Ref. [36]. Copyright © 2014, Elsevier B.V.

General synthetic approaches for QDs are classified into two classes: one is the ‘top-down’ approach, and another is the ‘bottom-up’ approach (Fig. 5). Top-down synthetic methods consist of processing techniques such as X-ray lithography, molecular beam epitaxy (MBE), electron beam lithography and ion implantation [40]. In bottom-up approach, the colloidal QDs prepared in the solution phase via self-assembly of precursor materials [41–43].

5.1 ‘Top-Down’ Approach

A bulk semiconductor is thinned by the top-down approach for making the QDs. These synthetic routes are fundamentally more straightforward and depending upon either on the removal or division of bulk material or on the tininess of bulk fabrication procedures to manufacture the desired structure with suitable properties. Commonly used methods to achieve QDs via this approach are electron beam lithography, high-energy wet ball milling, atomic force manipulation, gas-phase condensation, wet chemical etching, etc. This approach also suffers from some disadvantages such as low yield, incorporation of impurities, non-controllable size, shapes and structural imperfections *and so on* [44]. Uniformly shaped small nanoparticle preparation maintaining their proper crystallographic pattern is very difficult using conventional top-down techniques.

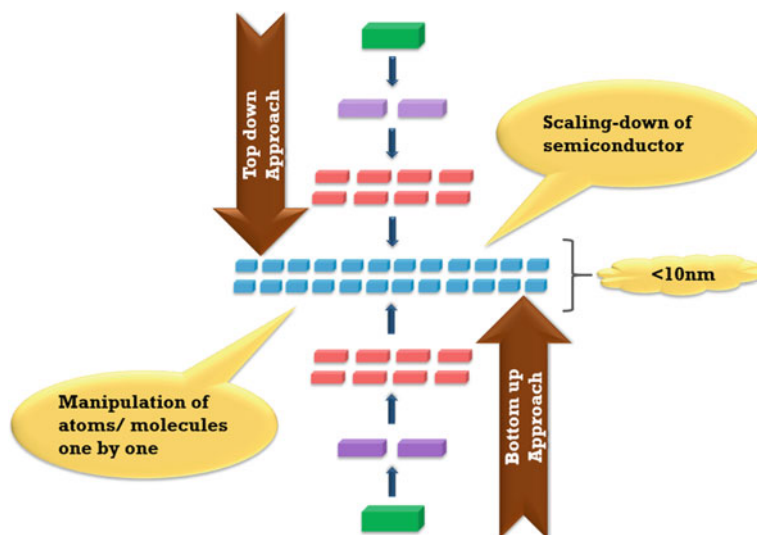


Fig. 5 Cartoon representation of general synthetic methods ('top-down' and 'bottom-up') of quantum dots

5.2 'Bottom-Up' Approach

In bottom-up synthesis, semiconductors QDs were build up of material from the bottom following atom-by-atom, molecule-by-molecule or cluster-by-cluster approach. This cost-effective approach produces less waste material. Some familiar techniques of QDs preparation using bottom-up routes are sol-gel synthesis, colloidal precipitation, organometallic chemical route, reverse-micelle route, hydrothermal synthesis, template-assisted sol-gel, electro-deposition, etc. The major challenge in the applying inorganic semiconductor QDs for biological purposes was the reproducible synthesis of highly luminescent, mono-disperse water-soluble QDs. In 1993, Murray et al. developed a groundbreaking bottom-up synthetic methodology to synthesize uniform colloidal mono-disperse nanocrystal QDs with a relatively high polydispersity and moderate PL and QY [45]. This high-temperature organometallic-based method, which resulted in a CdSe/ZnS core/shell structure to widen the band gap, inactive the surface, stabilizes the photophysical properties of CdSe core QDs [46]. First, aqueous phase synthesis of thiol-stabilized CdTe with small particle size and excellent QY was reported by Rogach et al. in 1996 [47]. In 2001, Peng et al. reported safe and larger scale synthesis of QDs using CdO instead of toxic Cd(CH₃)₂ that reduces toxicity by restricting leaching of the Cd²⁺ metal ion [48]. In 2013, Au et al. evaluated that the aqueous phase-synthesized QDs have better conjugation efficiency and stability than organic-synthesized QDs in biological media [49]. CdTe QDs with altered emission wavelength and improved QYs can be produced using a milder reaction conditions, i.e., lower temperatures (~100 °C), green chemicals (viz.

cadmium acetate; $\text{Cd}(\text{Ac})_2$) and thiolated capping agent in aqueous solution [50, 51]. Nie et al. have even developed SeTe-alloyed QDs with different morphologies and unique optical properties independent of size by controlling the cadmium feed into the reaction mixture [52, 53].

6 Biological and Biomedical Applications

6.1 *Bio-imaging*

Bio-imaging is a non-invasive process that enables us to visualize, characterize and quantify biological processes taking place at the cellular and sub-cellular levels in a specific period within intact living subjects. It helps to depict different cellular and molecular mechanisms and pathways related to the disease of a living subject without inhibiting the various processes of life such as movement and respiration. It also helps to elucidate the 3D structure of specimens. QDs possess exceptional optical and electronic properties, viz broad absorption spectra, composition and size adjustable narrow emission spectra, high absorption extinction coefficients, increased quantum yields, large stokes shift, photochemical robustness which made them suitable for bio-imaging [54–57]. QDs show higher emission wavelength (near-IR > 650 nm) compared to the most commonly used optical organic probes [58–60]; for this reason, their depth of penetration into living tissue is maximum and are suitable for target specific sites [61, 62].

6.2 *In Vitro Imaging*

QDs NPs made of inorganic core material have unique photophysical properties that make them suitable for immune-fluorescent labeling. There is a big challenge to deliver them into the cell for cellular imaging. The core–shell structure and surface functionalization of QDs make them biocompatible, stable and soluble in the biomatrix. Specific tissues and cells can be targeted by QDs conjugated with antibodies, peptides and DNA [63–70]. In 1998, Bruchez and Chan et al. first demonstrated QDs application as immunofluorescent for antigen detection in fixed cellular monolayers [71, 72]. Osaki et al. revealed that QDs mainly transported within the eukaryotic cells by engulfing activity of the cells, where they consume external objects like, here, QDs along with the plasma membrane (Fig. 6) [73]. Another route for cell penetration of QDs is done via electrostatic interaction with the plasma membrane. Small size, amine surface, cationic charge, cell incubation media and human body temperature sometimes help cellular uptake. Libchaber et al. reported intracellular imaging of QDs by covalently conjugating mercaptoacetic acid-coated CdSe/ZnS QDs, which

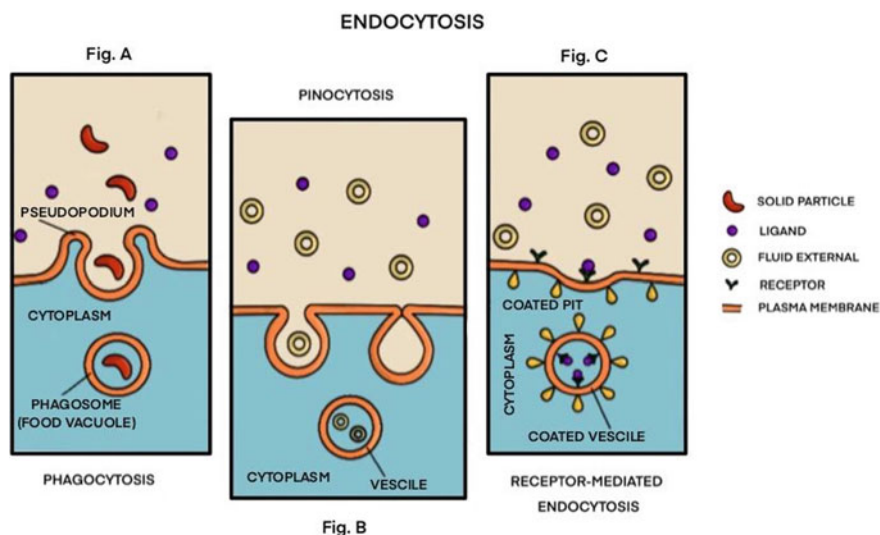


Fig. 6 Schematic representation of **a** phagocytosis, **b** pinocytosis, **c** receptor mediated endocytic pathway in mammal cell

spontaneously endocytosed by cancer cells and retained their bright fluorescence. PEG-coated CdSe/ZnS QDs used for intracellular staining of cells [37].

Non-invasive and invasive cancer cell lines can be distinguished by a quick-quantitative-easy *in vitro* 2D invasion assay using QDs, relying upon the process of phagocytosis (Fig. 6). In this 2D assay, cancer cells (both invasive and non-invasive) were seeded on top of a homogenous layer of QDs and are incubated. It was observed that the invasive cancer cells engulf (phagocytose) the QDs as they migrate. As the fluorescent QDs are engulfed by the aggressive cancer cells, this phenomenon leaves behind a non-fluorescent phagokinetic track, free of QDs [74]. Nisman et al. demonstrated to label the nuclear protein on cell sections. They also employed QDs in conjunction with immuno gold to co-localize proteins at the ultrastructural level [75]. A few different techniques that have been employed to deliver QDs into the cells are micro-injection, non-specific uptake of QDs via endocytosis or conjugation of QDs with translocating proteins or cationic peptides [37, 76, 77].

6.3 *In Vivo* Imaging

Size and composition tunable strong fluorescence signal made QDs a promising fluorescent probe for the *in vivo* imaging. In live mice, tissue-specific vascular markers were targeted using peptide conjugated QDs, by intravenous injection. The high *in vivo* specificity of these peptide conjugated QDs is attributed to the identifying of specific molecular markers expressed by blood vessels of organ/tissue/tumor by a

unique set of homing peptides. These peptides guide the QDs to the suitable vascular site in the live mice. So, when CdSe/ZnS QDs coated with a lung-targeting peptide are injected intravenously in live mice, it binds only in the lungs' blood vessels [78]. Stroh et al. demonstrated in vivo multi-photon imaging using semiconductor QDs. They also demonstrated the ability of QDs to monitor tumor vasculature and cell trafficking [79]. The lymphatic system can be called the drainage system of our body that helps our body to fight against infections and diseases, and it is made up of nodes, vessels and capillaries, containing lymphocytes. When tumor cells attack the local lymph node, they spread quickly over the whole body through extensive lymphatic network. Sentinel lymph nodes (SLNs) are the closest lymphatic nodes of the tumor cell. For effective cancer treatment and its surgery, it is essential to know the mapping of SLNs. The first demonstration of SLN mapping using NIR QDs was done by Kim et al. for image-directed surgery. The QDs entered into the animal lymphatic system through intradermal injection can be monitored through real-time images of lymphatic nodes and selectively identify the SLN for the surgical purposes [80]. Morgan et al. showed that the semiconductor nanocrystals of CdMnTe/Hg coated with bovine serum albumin (BSA) have significant photostability and cheaper than competing MRI technology [81]. Mapping of lymphatic drainage is problematic due their difficult accessibility and smaller size. NIR QDs can be used in non-invasive manner for imagining of multiple lymphatic drainage simultaneously as reported by Hema et al. and Kobayashi et al. Their study reveals the advantages of NIR QDs for in vivo multiplexed diagnostics [82, 83]. Noh et al. demonstrated NIR QDs guided non-invasive in vivo tracking of dendritic cells migration in the lymph nodes [84]. Their study helps to track immunotherapeutic cells. Accumulation of QDs inside the specific region of lymphatic nodes was demonstrated by Pic et al. [85]. Due to the lack of appropriate methods, it is difficult to track the real-time flow of lymph, which was resolved by Kosaka et al. combining macro-zoom fluorescence microscopy and QDs optical lymphatic imaging [86].

6.4 Tumor Cell Targeting and Imaging

In this century, cancer is a significant challenge for global public health. After several studies regarding cancer invasion, now it is clear that it is an adaptive process with the tumor microenvironment. For in vivo cancer imaging and its research are essential to know its biology, the location and distribution of tumors cell environments. Due to the unique optical and chemical properties of QDs over conventional organic fluorophores, they act as a promising candidate in biomedical imaging for cancer imaging, tracking, and diagnosis. Usually, antibodies tagged with QDs applied to target tumor cells [87, 88]. Antibody-labeled QDs entered into cell membrane through the blood vessels and are delivered to the perinuclear region [89]. Identifying the antibody delivery pathway significantly improves therapeutic efficacy. Membrane fluidity, morphology and membrane protein dynamics play a vital role in cancer metastasis. QDs-labeled metastasis-promoting factor [protease-activated

receptor₁ (PAR1)] inside cell membrane combined with anti-PAR1 antibody gives *in vivo* imaging of cancer cells and PAR1 during metastasis [90]. QDs (Qdot 800 QDs) functionalized with cell-penetrating peptide (CPPs) shows high sensitive image in oral carcinoma cell [91]. Another promising approach to improve cancer detection and treatment is multiplexed imaging. In this technique, green-fluorescent protein (GFP) coupled with QDs helps to distinguish tumor vessels from both perivascular cell and the matrix [79, 92]. An effective strategy for cancer treatment is cell-based cancer immunotherapy. Here, various therapeutic cells (e.g., lymphocytes, dendritic cells and natural killer cells) are tagged with QDs (e.g., Qdot 705, Life Technologies) and then systematically circulated into cancer patients' body. Since this is patient's own immune system-based therapy, so major advantage of this strategy is the effective tracking of injected therapeutic cells and less side effects on normal cells [93, 94]. The most effective method for cancer treatment is complete surgical resection of lymph nodes where high resolution image guidance is required. In image-guided surgery, NIR QDs (e.g., CdTe) attached with tumor-specific peptides (cyclic Arg-Gly-Asp peptide, cRGD) were injected into the U87 MG tumor xenografted mice through tail veins. This NIR QD-based bioconjugate shows significant enhancement of NIR signal within the vessels consequently, helps to locate the tumor cells and resects them [95]. QDs functionalization with vascular cell adhesion molecule 1 binding peptide (VCAM-1) enhances fluorescence intensity *in vivo* and *ex vivo* experiments which helps to visualize the VCAM-1 expressing endothelium *in vivo* [96]. Kwon et al. showed that how NIR QDs help to visualize anti-VEGFR2 (vascular endothelial growth factor receptor 2) antibody conjugated QDs for angiogenesis of cancer cell. Fluorescence enhancement at the tumor region of the prostate cancer (PC3) xenografted mouse after 12 h of injecting QD-conjugated antibody indicates that this technique can further be used to selectively monitor cells having up regulated expression of VEGFR2 [97].

7 Drug Delivery

A drug delivery system (DDS) is mainly used to enhance of the efficacy of the existing medication. It is an engineered technology to administer a pharmaceutical compound to achieve its therapeutic effect. It helps in selectively discharging the active constituent in the systemic circulation and thereby transferring them through the biological membranes to the operation site. The effectiveness of DDS can be optimized by controlling the time, rate, and site of release of drugs in the body. Currently, applications of QDs appear to be an emerging field of research as DDS, especially for cancer research. The preference of QD over other nano-carriers like dendrimer, micelles, silica nano-sphere, or nano-tube arises from its inimitable optical properties that make it a potential candidate as a carrier or delivery vehicle for biological applications. There are different techniques by which drugs can be laden into QD nano-carriers like adsorption, coupling, dispersion, dissolution, etc. The physical, chemical, or biological response of the drugs is altered due to their conjugation with

QDs and thus, the absorption, distribution, metabolism, and excretion of drugs are also affected. Eventually, QD nano-carriers for drugs can boost their effectiveness and decrease their harmful side effects to increase the therapeutic index. Ideally, any QD nano-carrier materials for the drugs should not react with drugs, should have high drug loading capacity and encapsulation efficiency, must be biocompatible, and less toxic, have longer dwelling time in biological systems, specific mechanical strength and stability and proper shape and particle size. Detectable drug delivery of therapeutics in vitro and in small animal models has a significant influence on biological research. In living systems, non-invasive recognition of any therapeutics tagged with drug carriers, in real-time requires specialized imaging techniques. QDs have the potential to elucidate the pharmacokinetics and pharmacodynamics of drug candidates. QDs can deliver a specific doses of the drug to the appropriate sites via enhanced permeability retention (EPR) effect. QDs being nanoscopic in size (<10 nm) and having a high surface-area-to-volume ratio can easily interact with biological molecules via surface adhesion and thereby found an exceptional opportunity as drug carriers in biomedical applications. Captopril, an antihypertensive drug, when conjugated with QDs, in vitro and in hypertensive rat model, reduces blood pressure by inhibiting the activity of angiotensin I-converting enzyme (ACE) [98]. CdSe/ZnS QD as DDS can reduce side effects and drug resistance of chemotherapeutic drug erlotinib used against non-small cell lung carcinoma [99]. Hypoxia-induced chemoresistance in oral squamous cell carcinoma (OSCC) overcome by the use of QD as DDS. Under hypoxia, PEG-modified graphene QDs loaded with platinum induce apoptosis via S phase cell cycle arrest in OSCC and a prominent tumor growth, inhibitory effect with less systemic drug toxicity was also reported in an OSCC xenograft mouse tumor model [100]. Carboxymethylcellulose hydrogel nanocomposite films conjugated with graphene QDs and doxorubicin (DOX) act as a pH-sensitive anticancer drug delivery system in blood cancer cell line K562 [101]. Despite having anti-cancerous properties and aqueous solubility sesamol was less bio available i.e, it has difficulties in penetrating cell membrane and thereby its cellular uptake is retarded. Its bio-availability and thereby cytotoxicity increase considerably after conjugation with CdS modified chitosan [52]. QD-based DDS have enormous prospects in treating cancer in terms of drug loading, targeting and enhanced efficacy. Many cancers (like breast, lung, kidney, ovarian, etc.) are known to express folate receptors in an appreciable quantity; folate receptor targeting DDS can be useful in treating these types of cancers with the existing chemotherapeutic drugs [102]. AgIn/ZnS QDs coupled with 11-mercaptoundecanoic acid (MUA)/L-cysteine/lipoic acid, when further loaded with folic acid and doxorubicin (a chemotherapeutic drug), behaved as targeted DDS to treat human lung cancer (A549 cell line) in vitro [103].

8 Conclusions

QDs, the tiny light-emitting nanocrystals of semiconductor materials, are a blessing for biological and biomedical research because of their numerous promising applications in real-time in vivo, cellular imaging, cell labeling and drug delivery. QDs have several advantages in comparison with usual organic dyes used for the bio-imaging purposes. They have exceptional optical and electronic properties, for example, size-tunable emission spectra, broad absorption range, narrow emission spectra, negligible photobleaching, better brightness, etc. In spite of QDs remarkable photochemical and photophysical properties, its in vivo applications are quite restricted owing to the relatively large size, degradation and toxicity. Typically, the toxicity of QDs is dependent on different parameters like their size, charge, coating, experimental conditions, surroundings, etc. Quantum dots that possess heavy metals like cadmium, arsenic, mercury or lead in the inner core may release toxic ions due to oxidation or photolysis [65, 104]. The escaped metal ion from the inner core may be enriched and stay for longer time inside the body that may cause a potential threat to that host [105]. Quick removal of QDs from the body circulatory system by phagocytic cells in systemically fixed tissues or entrapment QDs in the spleen or liver gives rise to heightened background noise or poor quality bio-image. Another challenge is the batch-to-batch variations or lack of reproducibility in the production of QDs. Clinical translation of QDs remains a challenging task because of the availability of less number of information in the literature regarding the relationship between physicochemical properties and pharmacokinetics/pharmacodynamics of QDs. Various synthetic techniques or strategies were adapted to enhance their effectiveness in different biological and biomedical applications. Finally, we hope that researchers will address these shortcomings and continue to move forward with modified QDs that may be suitable for human use.

Acknowledgements Dr. A. Chandra acknowledged Chittaranjan National Cancer Institute, Kolkata for facilities and research support.

Notes The authors declare no competing financial interest.

References

1. Zhang Y, Wei Q. The role of nanomaterials in electroanalytical biosensors: a mini review. *J Electroanal Chem.* 2016;781:401–9. <https://doi.org/10.1016/j.jelechem.2016.09.011>.
2. Jin Y, Kannan S, Wu M, Zhao JX. Toxicity of luminescent silica nanoparticles to living cells. *Chem Res Toxicol.* 2007;20:1126–33. <https://doi.org/10.1021/tx7001959>.
3. Lillemose M, Gammelgaard L, Richter J, Thomsen EV, Boisen A. Epoxy based photore-sist/carbon nanoparticle composites. *Compos Sci Technol.* 2008;68(7):1831–6. <https://doi.org/10.1016/j.compscitech.2008.01.017>.
4. Baldi G, Bonacchi D, Innocenti C, Lorenzi G, Sangregorio C. Cobalt ferrite nanoparticles: the control of the particle size and surface state and their effects on magnetic properties. *J Magn Magn Mater.* 2007;311(1):10–6. <https://doi.org/10.1016/j.jmmm.2006.11.157>.

5. Rogach AL, Eychmüller A, Hickey SG, Kershaw SV. Infrared-emitting colloidal nanocrystals: synthesis, assembly, spectroscopy, and applications. *Small*. 2007;3(4):536–57. <http://doi.org/10.1002/smll.200600625>.
6. Alivisatos AP. Semiconductor clusters, nanocrystals, and quantum dots. *Science*. 1996;271:933–7. <https://doi.org/10.1126/science.271.5251.933>.
7. Nair PS, Fritz KP, Scholes GD. Evolutionary shape control during colloidal quantum-dot growth. *Small*. 2007;3:481–7. <https://doi.org/10.1002/smll.200600558>.
8. Resch-Genger U, Grabolle M, Cavaliere-Jaricot S, Nitschke R, Nann T. Quantum dots versus organic dyes as fluorescent labels. *Nat Methods*. 2008;5:763–75. <https://doi.org/10.1038/nmeth.1248>.
9. Chen LD, Liu J, Yu X, He M, Pei X, Tang Z, Wang Q, Pang D, Li Y. The biocompatibility of quantum dot probes used for the targeted imaging of hepatocellular carcinoma metastasis. *Biomaterials*. 2008;29(31):4170–6. <https://doi.org/10.1016/j.biomaterials.2008.07.025>.
10. Bilan R, Nabiev I, Sukhanova A. Quantum dot-based nanotools for bioimaging, diagnostics, and drug delivery. *Chem Bio Chem*. 2016;17:2103–14. <https://doi.org/10.1002/cbic.201600357>.
11. Jaiswal J, Goldman E, Mattoussi H, Simon S. Use of quantum dots for live cell imaging. *Nat Methods*. 2004;1:73–8. <https://doi.org/10.1038/nmeth1004-73>.
12. Wang R, Zhang F. NIR luminescent nanomaterials for biomedical imaging. *J Mater Chem B*. 2014;2(17):2422–43. <https://doi.org/10.1039/C3TB21447H>.
13. Li C, Zhang Y, Wang M, Zhang Y, Chen G, Li L, Wu D, Wang Q. In vivo real-time visualization of tissue blood flow and angiogenesis using Ag₂S quantum dots in the NIR-II window. *Biomaterials*. 2014;35:393–400. <https://doi.org/10.1016/j.biomaterials.2013.10.010>.
14. Li Y, Liu Z, Hou Y, Yang G, Fei X, Zhao H, Guo Y, Su C, Wang Z, Zhong H. A multifunctional nanoplatform based on black phosphorus quantum dots for bioimaging and photodynamic/photothermal synergistic cancer therapy. *ACS Appl Mater Interfaces*. 2017;9(30):25098–106.
15. LeCroy GE, Yang ST, Yang F, Liu Y, Fernando KAS, Bunker CE, Hu Y, Luo PG, Sun YP. Functionalized carbon nanoparticles: syntheses and applications in optical bioimaging and energy conversion. *Coord Chem Rev*. 2016;320–321:66–81. <http://doi.org/10.1016/j.ccr.2016.02.017>.
16. Yong KT, Law WC, Hu R, Ye L, Liu L, Swihart MT, Prasad PN. Nanotoxicity assessment of quantum dots: from cellular to primate studies. *Chem Soc Rev*. 2013;42:1236–50. <https://doi.org/10.1039/C2CS35392J>.
17. Kim YSB, Jiang W, Oreopoulos J, Yip CM, Rutka JT, Chan WCW. Biodegradable quantum dot nanocomposites enable live cell labeling and imaging of cytoplasmic targets. *Nano Lett*. 2008;8(11):3887–92. <https://doi.org/10.1021/nl802311t>.
18. Yang ST, Wang X, Wang H, Lu F, Luo PG, Cao L, Mezziani MJ, Liu JH, Liu Y, Chen M, Huang Y, Sun YP. Carbon dots as nontoxic and high-performance fluorescence imaging agents. *J Phys Chem C Nanomater Interfaces*. 2009;113:18110–4. <https://doi.org/10.1021/jp9085969>.
19. David Wegner K, Hildebrandt N. Quantum dots: bright and versatile in vitro and in vivo fluorescence imaging biosensors. *Chem Soc Rev*. 2015;44:4792–834. <https://doi.org/10.1039/C4CS00532E>.
20. Brus LE. Electron-electron and electron-hole interactions in small semiconductor crystallites: the size dependence of the lowest excited electronic state. *J Chem Phys*. 1984;80:4403–9. <https://doi.org/10.1063/1.447218>.
21. Mazumder S, Dey R, Mitra MK, Mukherjee S, Das GC. Review: biofunctionalized quantum dots in biology and medicine. *J Nanomater*. 2009;38:1–17. <https://doi.org/10.1155/2009/815734>.
22. Ashoori RC. Electrons in artificial atoms. *Nature*. 1996;379:413–9. <https://doi.org/10.1038/379413a0>.
23. Wagner AM, Knipe JM, Orive G, Peppas NA. Quantum dots in biomedical applications. *Acta Biomater*. 2001;94:44–63. <https://doi.org/10.1016/j.actbio.2019.05.022>.

24. Trindade T, O'Brien P, Pickett NL. Nanocrystalline semiconductors: synthesis, properties, and perspectives. *Chem Mater*. 2001;13:3843–58. <https://doi.org/10.1021/cm000843p>.
25. Kuchibhatla SVNT, Karakoti AS, Bera D, Seal S. One dimensional nanostructured materials. *Prog Mater Sci*. 2007;52:699–913. <https://doi.org/10.1016/j.pmatsci.2006.08.001>.
26. Singh S, Dhawan A, Karhana S, Bhat M, Dinda AK. Quantum dots: an emerging tool for point-of-care testing. *Micromachines*. 2020;11:1058–81. <https://doi.org/10.3390/mi11121058>.
27. Dabbousi BO, Rodríguez-Viejo J, Mikulec FV, Heine JR, Mattoussi H, Ober R, Jensen KF, Bawendi MG. (CdSe)ZnS core–shell quantum dots: synthesis and characterization of a size series of highly luminescent nanocrystallites. *J Phys Chem B*. 1997;101:9463–75. <https://doi.org/10.1021/jp971091y>.
28. Mozafari M, Moztarzadeh F. Microstructural and optical properties of spherical lead sulphide quantum dots-based optical sensors. *Micro Nano Lett*. 2011;6:161–4. <https://doi.org/10.1049/mnl.2010.0203>.
29. Maksym AP, Chakraborty T. Quantum dots in a magnetic field: role of electron-electron interactions. *Phys Rev Lett*. 1990;65:108. <https://doi.org/10.1103/PhysRevLett.65.108>.
30. Bera D, Qian L, Tseng KT, Holloway PH. Quantum dots and their multimodal applications: a review. *Materials*. 2010;3:2260–345. <https://doi.org/10.3390/ma3042260>.
31. Byers RJ, Hitchman ER. Quantum dots brighten biological imaging. *Prog Histochem Cytochem*. 2011;45:201. <https://doi.org/10.1016/j.proghi.2010.11.001>.
32. Soloviev VN, Eichhöfer A, Fenske D, Banin U. Molecular limit of a bulk semiconductor: size dependence of the “band gap” in CdSe cluster molecules. *J Am Chem Soc*. 2000;122:2673–4. <https://doi.org/10.1021/ja9940367>.
33. Wu X, Liu H, Liu J, Haley KN, Treadway JA, Larson JP, Ge N, Peale F, Bruchez MP. Immunofluorescent labeling of cancer marker Her2 and other cellular targets with semiconductor quantum dots. *Nat Biotechnol*. 2003;21:41–6. <https://doi.org/10.1038/nbt764>.
34. Xing Y, Chaudry Q, Shen C, Kong KY, Zhou HE, Chung LW, Petros JA, O'Regan RM, Yezhelyev MV, Simons JW, Wang MD, Nie S. Bioconjugated quantum dots for multiplexed and quantitative immunohistochemistry. *Nat Protoc*. 2007;2:1152–65. <https://doi.org/10.1038/nprot.2007.107>.
35. Wang C, Gao X, Su X. In vitro and in vivo imaging with quantum dots. *Anal Bioanal Chem*. 2010;397:1397–415. <https://doi.org/10.1007/s00216-010-3481-6>.
36. Xing L, Yang L. Surface modifications technology of quantum dots based biosensors and their medical applications. *Chin J Anal Chem*. 2014;42(7):1061–9. [https://doi.org/10.1016/S1872-2040\(14\)60753-2](https://doi.org/10.1016/S1872-2040(14)60753-2).
37. Dubertret B, Skourides P, Norris DJ, Noireaux V, Brivanlou AH, Libchaber A. In vivo imaging of quantum dots encapsulated in phospholipid micelles. *Science*. 2002;298:1759–62. <http://doi.org/10.1126/science.1077194>.
38. Jin S, Hu Y, Gu Z, Liu L, Wu HC. Application of quantum dots in biological imaging. *J Nanomater*. 2011;2011:1–13. <https://doi.org/10.1155/2011/834139>.
39. Mathew S, Bhardwaj BS, Saran AD, Radhakrishnan P, Nampoori VPN, Vallabhan CPG, Bellare JR. Effect of ZnS shell on optical properties of CdSe-ZnS core-shell quantum dots. *Opt Mater*. 2015;39:46–51. <https://doi.org/10.1016/j.optmat.2014.10.061>.
40. Mattoussi H, Palui G, Na HB. Luminescent quantum dots as platforms for probing in vitro and in vivo biological processes. *Adv Drug Deliv Rev*. 2012;64:138–66. <https://doi.org/10.1016/j.addr.2011.09.011>.
41. Birudavolu S, Nuntawong N, Balakrishnan G, Xin YC, Huang S, Lee SC, Brueck SRJ. Selective area growth of InAs quantum dots formed on a patterned GaAs substrate. *Appl Phys Lett*. 2004;85(12):2337–9. <https://doi.org/10.1063/1.1792792>.
42. Nakata Y, Mukai K, Sugawara M, Ohtsubo K, Ishikawa H, Yokoyama N. Molecular beam epitaxial growth of InAs self-assembled quantum dots with light-emission at 1.3 μm . *J Cryst Growth*. 2000;208:93–9. [https://doi.org/10.1016/S0022-0248\(99\)00466-2](https://doi.org/10.1016/S0022-0248(99)00466-2).
43. Bertino MF, Gadipalli RR, Martin LA, Rich LE, Yamilov A, Heckman RB, Leventis N, Guha S, Katsoudas J, Divan R. Quantum dots by ultraviolet and x-ray lithography. *Nanotechnology*. 2007;18(31):315603. <http://doi.org/10.1088/0957-4484/18/31/315603>.

44. Valizadeh A, Mikaeili H, Samiei M, Farkhani SM, Zarghami N, Kouhi M, Akbarzadeh A, Davaran S. Quantum dots: synthesis, bioapplications, and toxicity. *Nanoscale Res Lett.* 2012;7:480. <https://doi.org/10.1186/1556-276X-7-480>.
45. Murray CB, Norris DJ, Bawendi MG. Synthesis and characterization of nearly monodisperse CdE (E = sulfur, selenium, tellurium) semiconductor nanocrystallites. *J Am Chem Soc.* 1993;115:8706–15. <https://doi.org/10.1021/ja00072a025>.
46. Burda C, Chen X, Narayanan R. Chemistry and properties of nanocrystals of different shapes. *Chem Rev.* 2005;105(4):1025–102. <https://doi.org/10.1021/cr030063a>.
47. Rogach AL, Katsikas L, Kornowski A, Su D, Eychmüller A, Weller H. Synthesis and characterization of thiol-stabilized CdTe nanocrystals. *Ber Bunsenges Phys Chem* 1996;100:1772–78. <http://doi.org/10.1002/bbpc.19961001104>.
48. Qu L, Peng ZA, Peng X. Alternative routes toward high quality cdse nanocrystals. *Nano Lett.* 2001;1:333–7. <https://doi.org/10.1021/nl0155532>.
49. Au GHT, Shih WY, Shih WH. High-conjugation-efficiency aqueous CdSe quantum dots. *Analyst.* 2013;138:7316–25. <https://doi.org/10.1039/C3AN01198D>.
50. Yong KT, Law WC, Roy I, Jing Z, Huang H, Swihart MT, Prasad PN. Aqueous phase synthesis of CdTe quantum dots for biophotonics. *J Biophotonics.* 2011;4(1–2):9–20. <http://doi.org/10.1002/jbio.201000080>.
51. Murray CB, Kagan CR, Bawendi MG. Synthesis and characterization of monodisperse nanocrystals and close-packed nanocrystal assemblies. *Annu Rev Mater Sci.* 2000;30:545–610. <http://doi.org/10.1146/annurev.matsci.30.1.545>.
52. Smith AM, Duan H, Mohs A, Nie S. Bioconjugated quantum dots for in vivo molecular and cellular imaging. *Adv Drug Delivery Rev.* 2008;60(11):1226–40. <http://doi.org/10.1016/j.addr.2008.03.015>.
53. Bailey RE, Nie S. Alloyed semiconductor quantum dots: tuning the optical properties without changing the particle size. *J Am Chem Soc.* 2003;125:7100–6. <https://doi.org/10.1021/ja035000o>.
54. Volkov Y. Quantum dots in nanomedicine: recent trends, advances and unresolved issues. *Biochem Biophys Res Commun.* 2015;3:419–27. <https://doi.org/10.1016/j.bbrc.2015.07.039>.
55. Matea CT, Mocan T, Tabaran F, Pop T, Mosteanu O, Puia C, Lancu C, Mocan L. Quantum dots in imaging, drug delivery and sensor applications. *Int J Nanomed.* 2017;12:5421–31. <https://doi.org/10.2147/IJN.S138624>.
56. Drummen GPC. Quantum dots-from synthesis to applications in biomedicine and life sciences. *Int J Mol Sci.* 2010;11:154–63. <https://doi.org/10.3390/ijms11010154>.
57. Kim S, Lim YT, Soltesz EG, De Grand AM, Lee J, Nakayama A, Parker JA, Mihaljevic T, Laurence RG, Dor DM, Cohn LH, Bawendi MG, Frangioni JV. Near-infrared fluorescent type II quantum dots for sentinel lymph node mapping. *Nat Biotechnol.* 2004;22:93–7. <https://doi.org/10.1038/nbt920>.
58. Contag CH, Ross DB. It's not just about anatomy: in vivo bioluminescence imaging as an eyepiece into biology. *J Magn Reson Imaging.* 2002;16:378–87. <https://doi.org/10.1002/jmri.10178>.
59. Klostranec J, Chan CW. Quantum dots in biological and biomedical research: recent progress and present challenges. *Adv Mater.* 2006;18:1953. <https://doi.org/10.1002/adma.200500786>.
60. Weissleder R. Scaling down imaging: molecular mapping of cancer in mice. *Nat Rev Cancer.* 2002;2E:11–8. <https://doi.org/10.1038/nrc701>.
61. Jiang W, Papa E, Fischer H, MardyTani S, Chan WC. Semiconductor quantum dots as contrast agents for whole animal imaging. *Trends Biotechnol.* 2004;22:607–9. <https://doi.org/10.1016/j.tibtech.2004.10.012>.
62. Weissleder R. A clearer vision for *in vivo* imaging. *Nat Biotechnol.* 2001;19:316–7. <https://doi.org/10.1038/86684>.
63. Pinaud F, King D, Moore HP, Weiss S. Bioactivation and cell targeting of semiconductor CdSe/ZnS nanocrystals with phytochelatin-related peptides. *J Am Chem Soc.* 2004;126:6115–23. <https://doi.org/10.1021/ja031691c>.

64. Michalet X, Pinaud FF, Bentolila LA, Tsay JM, Doose S, Li JJ, Sundaresan G, Wu AM, Gambhir SS, Weiss S. Quantum dots for live cells, in vivo imaging, and diagnostics. *Science*. 2005;307:538–44. <https://doi.org/10.1126/science.1104274>.
65. Derfus AM, Chan WCW, Bhatia SN. Probing the cytotoxicity of semiconductor quantum dots. *Nano Lett*. 2004;4:11–8. <https://doi.org/10.1021/nl0347334>.
66. Lidke DS, Nagy P, Heintzmann R, Arndt-Jovin DJ, Post JN, Grecco HE, Jares-Erijman EA, Jovin TM. Quantum dot ligands provide new insights into erbB/HER receptor-mediated signal transduction. *Nat Biotechnol*. 2004;22:198–203. <https://doi.org/10.1038/nbt929>.
67. Kaul Z, Yaguchi T, Kaul SC, Hirano T, Wadhwa R, Taira K. Mortalin imaging in normal and cancer cells with quantum dot immuno-conjugates. *Cell Res*. 2003;13:503–7. <https://doi.org/10.1038/sj.cr.7290194>.
68. Xiao Y, Barker PE. Semiconductor nanocrystal probes for human metaphase chromosomes. *Nucleic Acids Res*. 2004;32:e28. <http://doi.org/10.1093/nar/gnh024>.
69. Gerion D, Chen FQ, Kannan B, Fu AH, Parak WJ, Chen DJ, Majumdar A, Alivisatos AP. Room-temperature single-nucleotide polymorphism and multiallele DNA detection using fluorescent nanocrystals and microarrays. *Anal Chem*. 2003;75:4766–72. <https://doi.org/10.1021/ac034482j>.
70. Chen F, Gerion D. Fluorescent CdSe/ZnS nanocrystal-peptide conjugates for long-term, nontoxic imaging and nuclear targeting in living cells. *Nano Lett*. 2004;4:1827–32. <https://doi.org/10.1021/nl049170q>.
71. Bruchez JM, Moronne M, Gin P, Weiss S, Alivisatos PA. Semiconductor nanocrystals as fluorescent biological labels. *Science*. 1998;281(5385):2013–6. <https://doi.org/10.1126/science.281.5385.2013>.
72. Chan WCW, Nie S. Quantum dot bioconjugates for ultrasensitive nonisotopic detection. *Science*. 1998;281(5385):2016–8. <https://doi.org/10.1126/science.281.5385.2016>.
73. Osaki F, Kanamori T, Sando S, Sera T, Aoyama Y. A quantum dot conjugated sugar ball and its cellular uptake. On the size effects of endocytosis in the subviral region. *J Am Chem Soc*. 2004;126:6520–21. <http://doi.org/10.1021/ja048792a>
74. Pellegrino T, Parak WJ, Boudreau R, LeGros MA, Gerion D, Alivisatos AP, Larabell CA. Quantum dot-based cell motility assay. *Differentiation*. 71:542–8. <http://doi.org/10.1111/j.1432-0436.2003.07109006.x>.
75. Nisman R, Dellaire G, Ren Y, Li R, Bazett-Jones DP. Application of quantum dots as probes for correlative fluorescence, conventional, and energy-filtered transmission electron microscopy. *J Histochem Cytochem*. 2004;52:13–8. <https://doi.org/10.1177/002215540405200102>.
76. Jaiswal JK, Mattoussi H, Mauro JM, Simon SM. Long term multiple color imaging of live cells using quantum dot bioconjugates. *Nat Biotechnol*. 2003;21:47–51. <https://doi.org/10.1038/nbt767>.
77. Ballou B, Lagerholm BC, Ernst LA, Bruchez MP, Waggoner AS. Noninvasive imaging of quantum dots in mice. *Bioconjug Chem*. 2004;15:79–86. <https://doi.org/10.1021/bc034153y>.
78. Akerman ME, Chan WC, Laakkonen P, Bhatia SN, Ruoslahti E. Nanocrystal targeting in vivo. *Proc Natl Acad Sci*. 2002;99:12617–21. <https://doi.org/10.1073/pnas.152463399>.
79. Stroh M, Zimmer JP, Duda DG, Levchenko TS, Cohen KS, Brown EB, Scadden DT, Torchilin VP, Bawendi MG, Fukumura D, Jain RK. Quantum dots spectrally distinguish multiple species within the tumor milieu in vivo. *Nat Med*. 2005;11:678–82. <https://doi.org/10.1038/nm1247>.
80. Kim S, Lim YT, Soltesz FG, Grand AMD, Lee J, Nakayama A, Parker JA, Mihaljevic T, Laurence RG, Dor MD, Cohn HL, Bawendi GM, Frangioni VJ. Near-infrared fluorescent type II quantum dots for sentinel lymph node mapping. *Nat Biotechnol*. 2004;22:93–7. <https://doi.org/10.1038/nbt920>.
81. Morgan NY, English S, Chen W, Chernomordik V, Russo A, Smith PD, Gandjbakhche A. Real time in vivo non-invasive optical imaging using near-infrared fluorescent quantum dots. *Acad Radiol*. 2005;12:313–23. <https://doi.org/10.1016/j.acra.2004.04.023>.
82. Hama Y, Koyama Y, Urano Y, Choyke PL, Kobayashi H. Simultaneous two-color spectral fluorescence lymphangiography with near infrared quantum dots to map two lymphatic flows from the breast and the upper extremity. *Breast Cancer Res Treat*. 2007;103:23–8. <https://doi.org/10.1007/s10549-006-9347-0>.

83. Kobayashi H, Hama Y, Koyama Y, Barrett T, Regino CAS, Urano Y, Choyke PL. Simultaneous multicolor imaging of five different lymphatic basins using quantum dots. *Nano Lett.* 2007;7:1711–6. <https://doi.org/10.1021/nl0707003>.
84. Noh YW, Lim YT, Chung BH. Noninvasive imaging of dendritic cell migration into lymph nodes using near-infrared fluorescent semiconductor nanocrystals. *FASEB J.* 2008;22:3908–18. <http://doi.org/10.1096/fj.08-112896>.
85. Pic E, Pons T, Bezdtnaya L, Leroux A, Guillemin F, Dubertret B, Marchal F. Fluorescence imaging and whole-body biodistribution of near-infrared-emitting quantum dots after subcutaneous injection for regional lymph node mapping in mice. *Mol Imaging Biol.* 2010;12:394–405. <https://doi.org/10.1007/s11307-009-0288-y>.
86. Kosaka N, Mitsunaga M, Choyke PL, Kobayashi H. In vivo real-time lymphatic draining using quantum-dot optical imaging in mice. *Contrast Media Mol Imaging.* 2013;8:96–100. <https://doi.org/10.1002/cmmi.1487>.
87. Voura EB, Jaiswal JK, Mattoussi H, Simon SM. Tracking metastatic tumor cell extravasation with quantum dot nanocrystals and fluorescence emission-scanning microscopy. *Nat Med.* 2004;10:993–8. <https://doi.org/10.1038/nm1096>.
88. Ding H, Yong KT, Law WC, Roy I, Hu R, Wu F, Zhao W, Huang K, Erogbogbo F, Bergey EJ, Prasad PN. Non-invasive tumor detection in small animals using novel functional pluronic-nanomicelles conjugated with anti-mesothelin antibody. *Nanoscale.* 2011;3:1813–22. <http://doi.org/10.1039/C1NR00001B>.
89. Tada H, Higuchi H, Wanatabe TM, Ohuchi N. In vivo real-time tracking of single quantum dots conjugated with monoclonal anti-HER2 antibody in tumors of mice. *Can Res.* 2007;67:1138–44. <https://doi.org/10.1158/0008-5472.CAN-06-1185>.
90. Gonda K, Watanabe TM, Ohuchi N, Higuchi H. In vivo nano-imaging of membrane dynamics in metastatic tumor cells using quantum dots. *J Biol Chem.* 2010;285:2750–7. <https://doi.org/10.1074/jbc.M109.075374>.
91. Yang K, Cao YA, Shi C, Li ZG, Zhang FJ, Yang J, Zhao C. Quantum dot-based visual in vivo imaging for oral squamous cell carcinoma in mice. *Oral Oncol.* 2010;46:864–8. <http://doi.org/10.1016/j.oraloncology.2010.09.009>.
92. Kobayashi H, Longmire MR, Ogawa M, Choyke PL, Kawamoto S. Multiplexed imaging in cancer diagnosis: applications and future advances. *Lancet Oncol.* 2010;11:589–95. [https://doi.org/10.1016/S1470-2045\(10\)70009-7](https://doi.org/10.1016/S1470-2045(10)70009-7).
93. Lim YT, Cho MY, Noh YW, Chung JW, Chung BH. Near-infrared emitting fluorescent nanocrystals-labeled natural killer cells as a platform technology for the optical imaging of immunotherapeutic cells-based cancer therapy. *Nanotechnology.* 2009;20:475102.
94. Liu G, Swierczewska M, Niu G, Zhang X, Chen X. Molecular imaging of cell-based cancer immunotherapy. *Mol Biosyst.* 2011;7(4):993–1003. <https://doi.org/10.1039/C0MB00198H>.
95. Li Y, Li Z, Wang X, Liu F, Cheng Y, Zhang B, Shi D. In vivo cancer targeting and imaging-guided surgery with near infrared-emitting quantum dot bioconjugates. *Theranostics.* 2012;2(8):769–76. <https://doi.org/10.7150/thno.4690>.
96. Chen Y, Molnar M, Li L, Friberg P, Gan LM, Brismar H, Fu Y. Characterization of VCAM-1-binding peptide-functionalized quantum dots for molecular imaging of inflamed endothelium. *PLoS One.* 2013;8:e83805. <http://doi.org/10.1371/journal.pone.0083805>.
97. Kwon H, Lee J, Song R, Hwang SI, Lee J, Kim YH, Lee HJ. In vitro and in vivo imaging of prostate cancer angiogenesis using anti-vascular endothelial growth factor receptor 2 antibody-conjugated quantum dot. *Korean J Radiol.* 2013;14:30–7. <https://doi.org/10.3348/kjr.2013.14.1.30>.
98. Manabe N, Hoshino A, Liang Y, Goto T, Kato N, Yamamoto K. Quantum dot as a drug tracer in vivo. *IEEE Trans Nanobiosci.* 2006;5(4):263–7. <https://doi.org/10.1109/TNB.2006.886569>.
99. Kulkarni NS, Parvathaneni V, Shukla SK, Barasa L, Perron JC, Yoganathan S, Muth A, Gupta V. Tyrosine kinase inhibitor conjugated quantum dots for non-small cell lung cancer (NSCLC) treatment. *Eur J Pharm Sci.* 133:145–59. <http://doi.org/10.1016/j.ejps.2019.03.026>.

100. Wei J, Wu J, Xu W, Nie H, Zhou R, Wang R, Liu Y, Tang G, Wu J. Salvianolic acid B inhibits glycolysis in oral squamous cell carcinoma via targeting PI3K/AKT/HIF-1 α signaling pathway. *Cell Death Dis.* 2018;9:599. <https://doi.org/10.1038/s41419-018-0623-9>.
101. Javanbakht S, Namazi H. Doxorubicin loaded carboxymethyl cellulose/graphene quantum dot nanocomposite hydrogel films as a potential anticancer drug delivery system. *Mater Sci Eng C.* 2018;87:50–9. <https://doi.org/10.1016/j.msec.2018.02.010>.
102. Kulkarni NS, Guerro Y, Gupta N, Muth A, Gupta V. Exploring potential of quantum dots as dual modality for cancer therapy and diagnosis. *J Drug Deliv Sci Technol.* 2019;49:352–64. <https://doi.org/10.1016/j.jddst.2018.12.010>.
103. Ruzicka-Ayoush M, Kowalik P, Kowalczyk A, Bujak P, Nowicka AM, Wojewodzka M, Kruszewski M, Grudzinski IP. Quantum dots as targeted doxorubicin drug delivery nanosystems in human lung cancer cells. *Cancer Nanotechnol.* 2021;12:9. <https://doi.org/10.1186/s12645-021-00077-9>.
104. Guo GN, Liu W, Liang JG, Xu HB, He ZK, Yang XL. Preparation and characterization of novel CdSe quantum dots modified with poly (D, L-lactide) nanoparticles. *Mater Lett.* 2006;60:2565–8. <https://doi.org/10.1016/j.matlet.2006.01.073>.
105. Hardman R. A toxicologic review of quantum dots: toxicity depends on physicochemical and environmental factors. *Environ Health Perspect.* 2006;114:165–72. <https://doi.org/10.1289/ehp.8284>.

Upconversion and Downconversion Quantum Dots for Biomedical and Therapeutic Applications



Riya Dutta and Puspendu Barik

Abstract In recent years, upconversion (UC) and downconversion (DC) quantum dots (QDs) or nanoparticles (NPs) have shown excellent optical properties, which are helpful in various fields, including photonics, nanomedicine, biomedical, and therapeutic applications. This chapter summarizes the chemical and optical properties of different UC and DC QDs/NPs. Subsequently, luminescence mechanisms and modification of upconversion efficiency are discussed elaborately. Then the next section focuses on the application of UC and DC NPs in bioimaging biosensing, disease diagnostics, and light-controlled drug and gene delivery, which would enable researchers to help further research and development of both fundamental sciences and applications.

Keywords Quantum dots · Nanoparticles · Upconversion · Downconversion · Luminescence · Biomedical applications

1 Introduction

Luminescent materials, also called phosphors, are solids that can absorb (excitation) and convert certain types of energy, e.g., chemical, mechanical, photon, heat, into radiation of light (emission). During the last five decades and more, rare-earth (RE) elements with a unique combination of their partially filled $4f^n$ -electron shell ($1 < n < 14$) have remained the subject of intensive investigations due to the shielding from the $5s^25p^6$ subshells (makes them less affected by their microsurroundings, i.e., weakens the influence of external electric and magnetic field on the 4f-electrons) and their excellent photostability, a large anti-Stokes shift, long luminescence lifetime, and sharp-band emission [1–5]. RE elements are composed of the 15 lanthanides

R. Dutta (✉)

School of Advanced Materials Science and Engineering, Sungkyunkwan University, Suwon-si, Gyeonggi-do 16419, South Korea
e-mail: riyadutta@skku.edu

P. Barik

S. N. Bose National Centre for Basic Sciences, JD Block, Sector-III, Salt Lake City, Kolkata 700106, India

(Ln^{3+} , from lanthanum to lutetium), plus scandium and yttrium, which are generally exist as trivalent cations. However, the incorporation of a low concentration of Ln^{3+} atoms or ions into host lattices provides a steady microenvironment for Ln^{3+} emitter to emit efficient luminescence from the ultraviolet (UV), through visible, to the mid-infrared (MIR) light, as direct excitation of lanthanide ion (Ln^{3+}) is a relatively inefficient process [6]. Except for La^{3+} and Lu^{3+} , all of Ln^{3+} ions are luminescent, and their f–f emission lines cover the entire spectrum, from UV (Gd^{3+}) to visible (e.g., Pr^{3+} , Sm^{3+} , Eu^{3+} , Tb^{3+} , Dy^{3+} , Tm^{3+}) and near-infrared (NIR, e.g., Pr^{3+} , Nd^{3+} , Ho^{3+} , Er^{3+} , Yb^{3+}) [7]. Some ions are fluorescent, others are phosphorescent, and some are both. Luminescence from RE or RE doped material is of two kinds—upconversion (UC) and downconversion (DC)—based on the luminescence mechanism. They are nonlinear optical processes. Stokes' Law states that the fluorescence emission occurs at a longer wavelength (redshift) than the incident light wavelength (absorption), i.e., DC luminescence. However, the emission occurs at a lower wavelength (i.e., higher energy or blueshift) than the incident light wavelength (excitation) in UC luminescence via sequential adsorption and energy transfer steps [6]. A theoretical concept was first introduced by the Dutch-American physicist Nicolaas Bloembergen in 1959 [8] to develop an infrared photon detector using superexcitation to count infrared photons. The UC visible emission was reported in 1966 by François Auzel through the use of Yb^{3+} to sensitize Er^{3+} and Tm^{3+} [9].

At this present decade, the UC and DC QDs have attracted significant attention in the bioimaging field, including diagnostics, drug delivery, single-molecule probes. The multiplexing capacity and the resistance to photobleaching can boost these QDs to become an exceptional contender in this biomedical field [10]. Regarding the common luminescent proteins and dyes generally used in these applications, QDs have a broad range of excitation and emission spectra. It also possesses high quantum yield and stability. In most cases, various QDs of different optical properties are injected into a patient sample, excited with a single wavelength, and study the cross-talk between different channels and the spectral overlap between them [11, 12]. Recent biomedical applications have emphasized the Biotinylated QDs, prepared via the bioconjugation of semiconductor QDs with denatured bovine serum albumin (dBSA) attachment at the QD surface. Adding the ligands to the QDs stretches its applications beyond surface modification and ligand functionalization [13] and in competitive fluoroimmunoassay development for detecting human serum albumin (HSA) in human urine. Recently QDs have emerged as a new direction in real-time biomedical imaging. With the help of UC and DC properties of QDs, people can use spectral information-guided surgical probes to detect and perform deep-tissue imaging [14–18]. The obstacle to the path is the working range of the semiconductor quantum dot. QDs generally have the emission in the visible regime, which is not very compatible with penetrating in the deep tissues. In this process, the signal gets scattered due to various ligands, dopants, and other elements present in the tissue [16, 19]. The UC property of the QDs helps here to overcome the barrier that can work in the NIR range. This range is beneficial for imaging since tissue elements usually have significantly low absorption cross-section. The higher emission wavelength and high quantum yield assists the process.

Fluorescence resonance energy transfer (FRET) or resonance energy transfer (RET) is defined by the energy transfer mechanism between two active photo molecules. These light-sensitive molecules are referred to as acceptors and donors [20, 21]. The molecule absorbs the energy and gets into the excited state with incident excitation, known as a donor. Then it might transfer the excess energy to another molecule and come back to the ground state. The energy transfer process depends on physical parameters like distance and emission wavelength overlap. The biomolecule dynamics and interaction are susceptible to the intermolecular distance, owing to a power dependence law, inversely proportional to the sixth power of the distance between donor and acceptor. However, these processes may not be efficient due to the less spectral overlap between the acceptor and donors.

In 1996, Kagan et al. showed the resonance energy transfer between closely packed QDs [22, 23]. The particular UC and DC properties of QDs can overcome some of the existing obstruction of spectral overlap. More elaborately, lower-energy absorption can have the emission on the higher side. The properties of UC and DC QDs have contributed to many applications of the biomedical field. In the early work, Willard et al. have incorporated QDs as a FRET donor in a protein–protein binding assay [24]. Later on, researchers also used the QDs as a FRET donor and linked to BSA and tetramethylrhodamine (TMR), linked to the protein as the acceptor. This process enhances the TMR fluorescence that produces a better image. QDs are placed with maltose-binding protein (MBP) in several other works [25, 26]. On the other hand, Patolsky et al. demonstrated the process of DNA replication and sensitive DNA detection probed by the QD-based FRET mechanism [27].

This chapter focuses on the recent development of RE doped nanoparticles (NPs) or QDs (size below ~20 nm). First, we describe the basic concepts, theories, mechanisms for tuning, and enhancement of DC and UC luminescence. The hydrophilic modification and bioconjugation strategies of UC and DC QDs are discussed. Finally, we highlight the present status of UC and DC QDs in biomedical applications, including imaging, bio-detection, and clinical therapy. We also include a section for the perspectives, challenges, and future directions.

2 Luminescence Mechanism

UC process is categorized into two classes—(i) UC emission through RE ions (e.g., in Er^{3+} , Ho^{3+} , Tm^{3+}), and (ii) triplet–triplet annihilation (TTA) based UC emission in organic molecules. RE energy level schemes, absorption, and emission spectra were first experimentally determined by Dieke and Crosswhite [28] and summarized in the monograph by Dieke [29]. As a result of his outstanding work, a diagram of trivalent RE energy levels, i.e., the Dieke diagram, has been recognized, shown in Fig. 1. Triplet–triplet annihilation (TTA) is a promising upconversion approach and involves energy transfer between a sensitizer (donor) molecule and an acceptor/annihilator. TTA-UC or sensitized TTA-UC involves the sensitized population of metastable optically dark electronic states of a given system by a low excitation power density

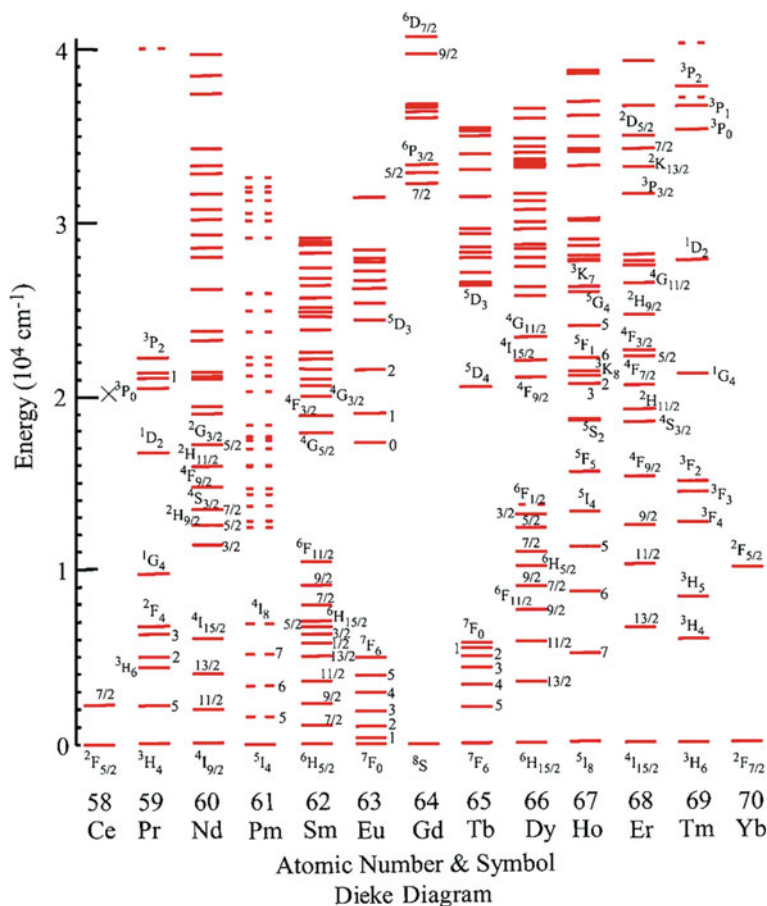


Fig. 1 Dieke diagram (energy levels of free RE^{3+} ions up to $42,000 \text{ cm}^{-1}$). Reproduced with permission from Ref. [30]. Copyright © 2007 Elsevier B.V.

requirement (a noncoherent radiation source like solar light is sufficient) and produces high UC quantum yield, readily tunable excitation/emission wavelength, and strong absorption of excitation light. The system consists of triplet donor (sensitizer, i.e., QDs or NPs) and acceptor (emitter) molecules. The triplet excited states are produced through intersystem crossing (ISC) from the singlet excited state after absorption of light by the sensitizer. Triplet–triplet energy transfer (TTET) from the sensitizer to an emitter occurs via a Dexter-type electron exchange mechanism producing upconverted delayed fluorescence. Quantum yield can be enhanced by minimizing the energy loss during ISC of triplet sensitizers or bypassing the ISC process.

2.1 Photon Upconversion Mechanism in Lanthanides

Photon is absorbed simultaneously during two-photon absorption (TPA) and second-harmonic generation (SHG), whereas photon absorption is sequential during the UC absorption process. The sequential absorption is pointed toward single or multiple intermediate states in the material and luminescence steps for a shorter-wavelength generation. UC emission process in lanthanide based system involves multiple mechanisms, i.e., ground state absorption (GSA)/excited-state absorption (ESA), energy transfer absorption (ETA), photon avalanche (PA), cooperative energy transfer (CET) based UC, and cross relaxation (CR) process. A schematics in Fig. 2 show the RE ions-doped nanoparticles (NPs) and photon UC process for different RE ions based systems. The UC NPs are composed of an inorganic crystalline host matrix and trivalent lanthanide ions (Ln^{3+}) embedded in the host lattice (Fig. 2a). The lanthanides' electronic configurations split into a rich energy level pattern owing to electronic repulsion and spin-orbit coupling [31], as depicted in Fig. 2b. The development of

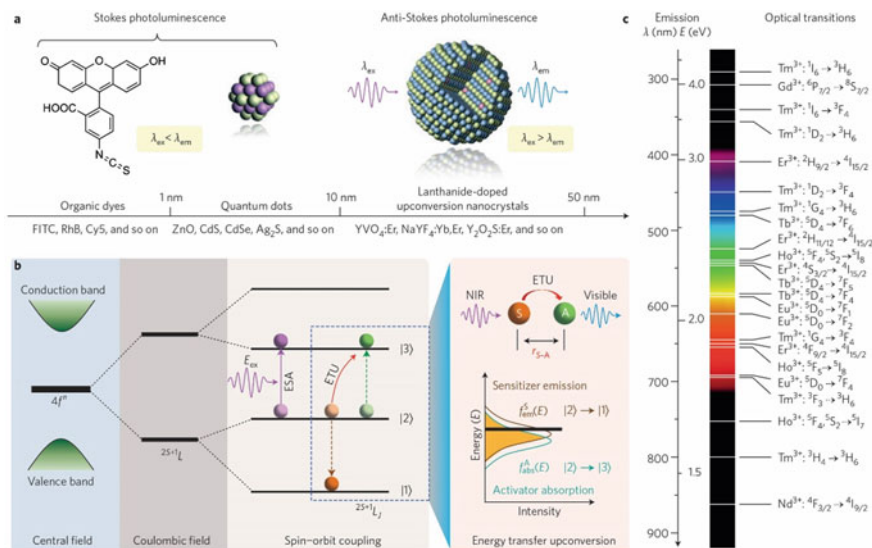


Fig. 2 Lanthanide-doped nanoparticles and photon upconversion. **a** Stokes ($\lambda_{\text{ex}} > \lambda_{\text{em}}$) and anti-Stokes ($\lambda_{\text{ex}} < \lambda_{\text{em}}$) emission from organic dyes, semiconductor QDs, and lanthanide-doped NPs. **b** Electronic energy level diagrams of trivalent Ln^{3+} ions in connection with the UC process. The Coulombic interaction, spin-orbit coupling, and weak crystal-field perturbation induce the electronic energy levels into many sublevels. The symbol $2S+1L_J$ represents the energy levels, where S, L, J are the electron's total spin, orbital, and angular momentum quantum numbers, respectively. [1], [2] and [3] represent the ground state, intermediate, and upper emitting levels, respectively. The excited-state absorption (ESA) process —|2⟩ → |3⟩. **c** Typical Ln^{3+} -based UC emission bands ranging from UV to NIR and their corresponding main optical transitions. Reproduced with permission from Ref. [31]. Copyright © 2015, Nature Publishing Group, a division of Macmillan Publishers Limited

research in UC leads to the tuning of emission wavelength ranging from the ultraviolet to the NIR region (Fig. 2c).

2.1.1 Excited-State Absorption (ESA)

Excited-state absorption (ESA) or ground state absorption (GSA) is the absorption of a photon from an intermediate excited state to a higher excited state of an atom, molecule, or ion rather than from the electronic ground state, as depicted in Fig. 3a. The preconditions for ESA to happen are: (i) a single or multiple higher-lying energy levels must exist which must coincide with the incident photon energy, (ii) existence of a metastable/intermediate state with a substantial lifetime, and (iii) the absorption cross-section of the excited state of atoms, molecules, or ions should be adequate to absorb the second pump photon (efficiency of absorption of second pump photon is very low). ESA can be possible only for a few lanthanide ions, e.g., Er^{3+} , Tm^{3+} , Ho^{3+} , and Nd^{3+} , which possess such energy levels structures. The ESA mechanism is a single ion absorption process, i.e., ESA involves a single ion and is thus independent of the RE doping concentration. During the ESA process, the phonons in the host materials also participate, and hence ESA can be possible without an exact match of the exciting source energy to the RE energy levels.

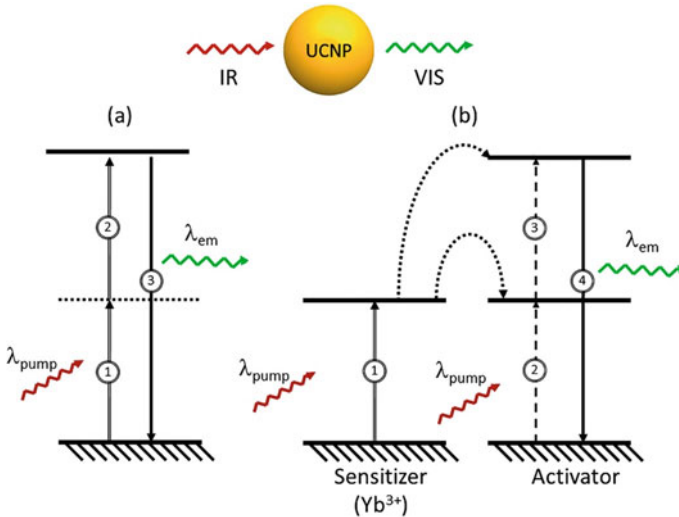


Fig. 3 Principal mechanisms for upconversion **a** excited-state absorption (ESA) involves sequential absorption of pump photons (λ_{pump}). 1. Excites a single lanthanide ion in the ground state to some intermediate excited level, 2. further absorption may take place, raising a single lanthanide ion to a higher excited state, 3. a single lanthanide ion relaxes back to the ground state. **b** Energy transfer (ET) upconversion—the dotted lines represent the energy transfer between the sensitizer and activator. Reproduced from Ref. [32] under Creative Common CC BY license

2.1.2 Energy Transfer Absorption (ETA)

Energy transfer absorption (ETA) involves sequential absorption of two photons similar to ESA to populate the energy level with a long lifetime. However, ETA involves two neighboring ions, rather a single ions as in ESA; a sensitizer and emitter/activator (typically two different rare-earth ions) are employed to create the UC process. The most straightforward ETA mechanism is shown in Fig. 3b. In the ETA process, the sensitizer is firstly excited from the ground state to its excited state (i.e., process ①, as depicted in Fig. 3b) after absorbing a pump photon (λ_{pump}). The energy is subsequently transferred to the activator. The activator is further pumped to higher energy levels by a pump photon or the transferred energy from the sensitizer to its highest energy levels (as depicted by the process ② and process ③). Finally, the exciting activator ions relax back to the ground state, emitting a higher energy photon (process ④). In contrast to the ESA process, the ETA process is highly contingent on the doping concentration as it determines the spatial distribution of neighboring doping ions. In general, an optimized UC system should contain Yb^{3+} less than 20 mol% (as sensitizer) and an activator with a concentration below two mol% to minimize the loss due to cross-relaxation processes. However, ESA and ETA are concurrent processes in many upconversion materials. Cooperative energy pooling (CEP) is an energy transfer mechanism, where two photoexcited sensitizers non-radiatively transfer their energy to a single higher energy state in an acceptor/activator ions [33] via a coupling of the emissive states of both sensitizers with the two-photon absorption (2PA) tensor of the acceptor [34] enabling UC with greater efficiency and at reduced excitation intensities.

2.1.3 Cooperative Sensitization and Luminescence

Cooperative sensitization (CS) or cooperative energy transfer (CET) is a process occurring by the interaction among three ions [35–38], where a pair of ions emit one photon by simultaneous depopulation from their excited states [39]. Ln^{3+} ions, e.g., Tb^{3+} and Eu^{3+} without metastable levels, are unfavorable for ESA and ETA. CS occurs for those Ln^{3+} ions as the energy storage reservoir. In a typical CS process, the excitation energy of two adjacent Yb^{3+} is simultaneously transferred to Tb^{3+} or Eu^{3+} ions, as depicted in Fig. 4. The efficiency of the CS process is $\sim 10^{-6}$, which is three order magnitude lower than ETA. The efficiency is exclusively related to the Yb^{3+} concentration as the activator requires two nearby excited Yb^{3+} [40]. The surface quenching effect of the UC process and CR process between RE ions limit the efficiency of the CS process to fabricate highly effective UC nanosystems. However, selecting proper host lattice and optimizing the doping concentrations of the sensitizer and the activator may enhance the efficiency. Cooperative luminescence (CL) is the radiative transition process, where two exciting ions simultaneously jump from excited states to emit one photon with the sum of their excitation energies.

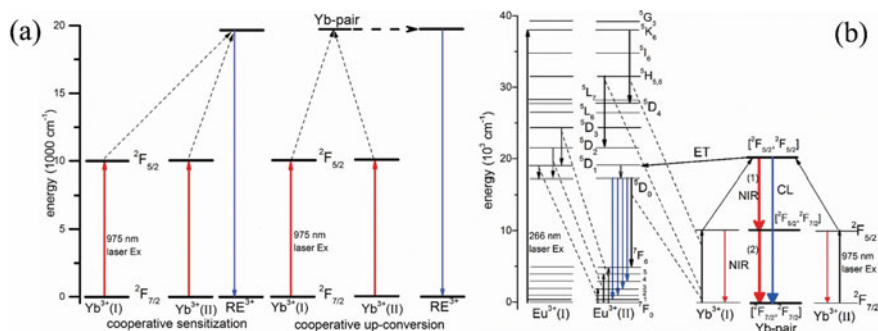


Fig. 4 **a** Schematic energy diagram of the CS and CU processes to emit the UC RE^{3+} emission. **b** Schematic energy level diagram of Yb^{3+} , Yb-pair , Eu^{3+} ions, and the relaxation processes in Yb^{3+} , Yb-pair . Straight broken lines represent the cross-relaxation (CR) processes. The thick blue arrow signifies CL, and the thin blue arrows indicate UC Eu^{3+} emission by ETA from the Yb-pair excited by 975 nm excitation. The thick red arrows indicate near-infrared (NIR) Yb^{3+} emission caused by the excited Yb-pair and thin red arrows NIR Yb^{3+} emission generated by radiative transition from the excited $^2F_{5/2}$ state. Reproduced with permission from Ref. [38]. Copyright © 2016 Elsevier B.V.

2.1.4 Cross-Relaxation

Cross-relaxation (CR) (also called self-quenching) is the same as the ETA process. It occurs between two identical ions, where one in its excited state transfers energy to the second ion in the ground state. The intermediate states for the two ions have equal energy and are energetically halfway between the initial excited state of the first ion and the ground state of the second ion. The ion-ion interaction is the fundamental reason behind it and requires a high concentration of ions. The mechanism of CR process is demonstrated with the help of three-level Yb^{3+} - Tb^{3+} system, as shown in Fig. 5.

2.1.5 Photon Avalanche (PA)

Photon avalanche (PA) is a process where multiple photons combine to create a single higher energy photon. The phenomenon of PA was first discovered by Chivian in 1979 in Pr^{3+} doped $\text{LaCl}_3/\text{LaBr}_3$ materials based on infrared quantum counters [42, 43]. Unlike ESA and ETA, PA is relatively complex compared as a threshold pump density is needed to start the process. In general, the energy of the pump photon is lower than the energy gap between the intermediate excited state and the ground state. The population in the intermediate state increases exponentially with repetition of CR beyond a threshold pump energy and hence, a multiple enhancement of population in highest level through strong ESA process. A strong UC emission occurs from the highest to the ground state through the avalanche process. The conditions for the PA process are (i) excitation energy should not be in resonance with the GSA, (ii) ESA

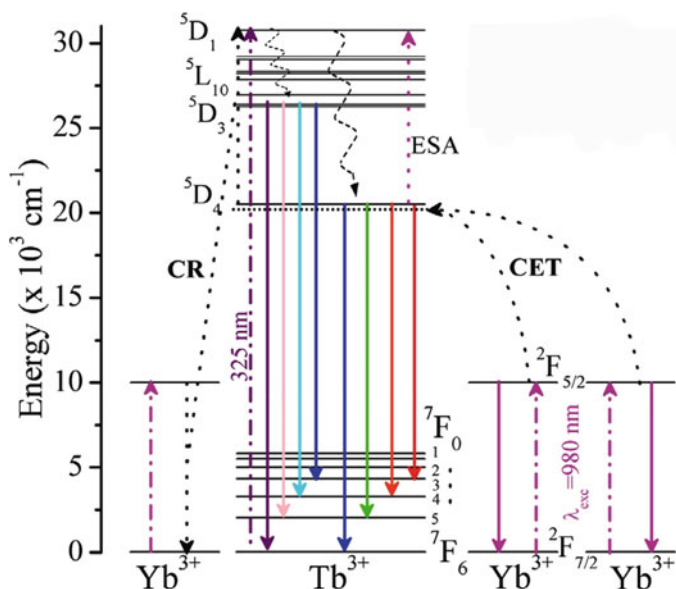


Fig. 5 Energy level diagrams of Yb³⁺ and Tb³⁺ ions. Dotted lines indicate the UC through CET, Yb³⁺-Tb³⁺ CR, and ESA processes. Dashed, dashed-dotted, and solid lines indicate the nonradiative relaxation processes, excitation, and emission transitions, respectively. Reproduced from Ref. [41] under the terms of the Creative Commons Attribution License

cross-section should be very high, and (iii) concentration of RE ions should be high enough for ion-ion interaction and efficient for the CR process.

2.2 Upconversion Mechanism Based on Triplet-Triplet Annihilation (TTA)

TTA-UC, also known as triplet fusion, produces one photon of higher energy from two lower-energy photons, i.e., two spin-triplet excitons combine to form a singlet exciton [44]. The efficient TTA-UC is performed by a two-component system, with a “triplet sensitizer” and “emitter,” as shown in Fig. 6. After absorbing incoming light, the triplet sensitizer produces the excited triplet state (T_1) via ISC. The triplet exciton transfers to the emitter through TET. Two emitters in their triplet excited states may annihilate to generate one emitter to return to the ground state and promote the other to the singlet excited state (S_1). Finally, the emitter emits a higher energy photon than the original incident photon used to excite the sensitizer, as depicted in Fig. 6. The energy gain in the TTA-UC process is defined as the difference between the absorption and emission wavelengths. The minimization of the energy gap of the triplet energy of the sensitizer and the emitter can lower the energy loss due to ISC till there will no back energy transfer from the emitter to the sensitizer. Recently,

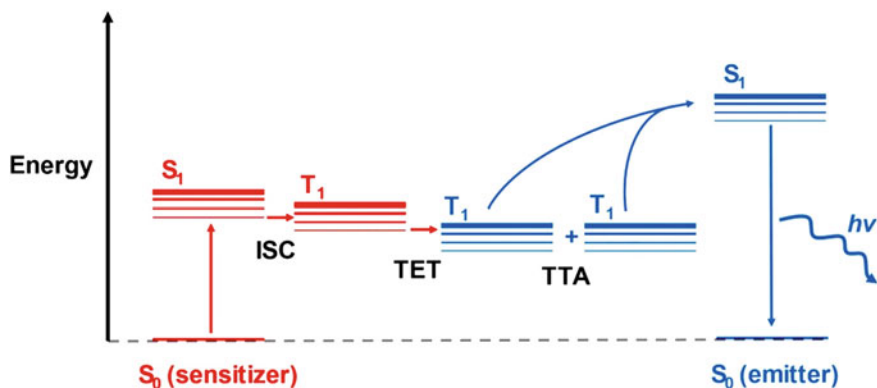


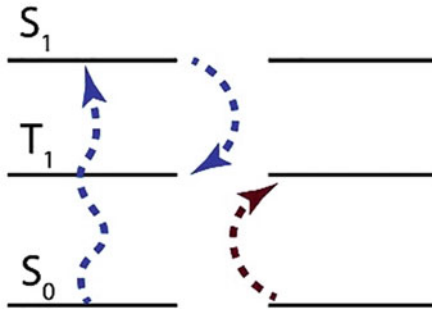
Fig. 6 Jablonski diagram depicting the processes involved in TTA-UC with a sensitizer-emitter pair. Reproduced from Ref. [54] under a Creative Commons Attribution 4.0 International License

nanocrystal (both quantum-confined and bulk semiconductors) sensitized TTA-UC processes have grown as a new strategy to overcome the main drawbacks of the molecular triplet sensitizers, i.e., significant loss due to ISC. In the QDs or NPs-based UC systems, the QD serves as the triplet sensitizer, and a proper ligand around the QD allows rapid harvesting of the excited state and the annihilator. In recent years, TTA-UC materials have been attracting attention in various fields, including bioimaging, biomedicines, photocatalysts, photovoltaics, and OLEDs, due to tunable spectral range and high UC efficiency ($>1\text{--}40\%$) at noncoherent incident light ($I_{\text{ex}} < 1 - 10^2 \text{ mW cm}^{-2}$) compared to conventional UC technologies [45]. Details description of the nanocrystal sensitized TTA-UC process is out of the scope of this chapter. However, readers may find several reviews for further reading [45–53].

2.3 DC Luminescence Mechanisms

Molecular downconversion (DC) or singlet fission (SF) (also known as quantum cutting) converts one single high-energy photon into two low-energy photons (theoretical quantum efficiency of 200%). This phenomenon has been demonstrated for QDs (multiple exciton generation, MEG) [55, 56], dye molecules (SF, where one singlet exciton is converted into two triplet excitons) [57], and ion pairs of $\text{Ln}^{3+}/\text{RE}^{3+}$ (DC) [58]. The most efficient DC can be possible in RE^{3+} -doped materials. A schematic for SF and DC process is shown in Fig. 7. Here, we consider examples of SF or DC of Ln^{3+} -based systems. Ln^{3+} -doped materials are most frequently investigated in the context of UC and have also proven helpful as DC photoluminescent agents, referring to reviews by Bünzli [7, 59]. DC occurs in a material or the inorganic matrix co-doped with appropriate Ln^{3+} ions via cooperative energy transfer, e.g., transparent glass–ceramics with embedded $\text{Pr}^{3+}/\text{Yb}^{3+}:\beta\text{-YF}_3$ nanocrystals, Yb^{3+} and

(a) Singlet Fission



(b) Rare-Earth Downconversion

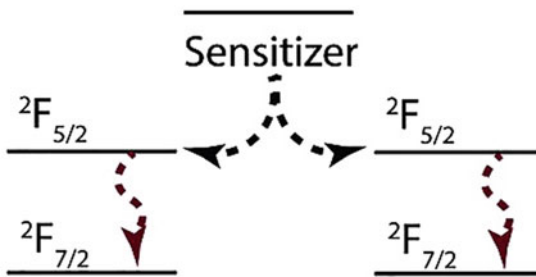


Fig. 7 Schematic representation of **a** singlet fission, the conversion of one singlet exciton into two triplet excitons, **b** rare-earth downconversion, emitting light (Yb^{3+} ions). Reproduced with permission from Ref. [44]. Copyrights managed by AIP Publishing

Tb^{3+} in polyborate $\text{La}_{0.99-x}\text{Yb}_x\text{BaB}_9\text{O}_{16}:\text{Tb}_{0.01}$, Yb^{3+} and Tb^{3+} doped into Zn_2SiO_4 thin films, $\text{Tm}^{3+}/\text{Yb}^{3+}$ co-doping into YPO_4 , oxyfluoride glass-ceramics containing LaF_3 nanocrystals, and $\text{Ce}^{3+}/\text{Yb}^{3+}$ co-doped borate glasses [7].

3 Enhancing Upconversion Efficiency

The UC emission of Ln-doped nanocrystals can be precisely controlled in terms of emission color, lifetime, and intensity for advanced research and diverse practical applications [31]. The enhancement of the UC luminescence intensity is the primary concern for the biomedical application of UC NPs due to the limited absorption

cross-section by the materials. Some predominant strategies to UC increase the luminescence intensity are (i) finding the optimal activator ions concentration in the host lattice, (ii) ensuring maximum transfer of energy between sensitizer and activator in the host matrix, (iii) a host with low vibrational energy to minimize loss, (iv) chemical and thermal stability, (v) choosing an effective solvent/reaction medium and capping agent to optimize the structure of the Ln^{3+} doped materials, (vi) co-doping of the sensitizer, (vii) doping of Ln^{3+} in the semiconductor matrix. Apart from these considerations, three fundamental strategies for enhancing upconversion efficiency and making them suitable for biomedical applications are (i) *surface passivation*—coating of shell material to minimize the surface defects and contaminations, (ii) *dye sensitization*—the antenna effect of dye molecules by increasing the excitation efficiency due to their broad absorption band and large absorption cross-sections, and (iii) *plasmonic modulation*—promoting the photon conversion processes by excitation enhancement or emission enhancement or both.

UC NPs are usually synthesized by reacting Ln-precursors in organic media in the presence of capping ligands for uniformity. Surface modification techniques can be employed to make hydrophilic and flexible for bioconjugation, e.g., layer-by-layer assembly, silanization, ligand exchange, and polymer encapsulation. However, one-pot processing of water-dispersible UC NPs is highly desirable for biomedical applications. Another approach, like direct doping of Ln^{3+} ions into the semiconductor nanocrystals, may produce additional functionalities and improved optical performance [31]. The core-shell approach for assembling UC NPs has proven effective in preparing multifunctional nanomaterials, e.g., magneto-UC NPs, SiO_2 , TiO_2 , CdS coated UC NPs, tailoring composite functions. Moreover, surface modification or coating with a non-toxic or biocompatible coating, like phospholipids, maleic anhydride, copolymers, Parylene C polymer, chitosan, bovine serum albumin (BSA), decreases the toxicity of UC and DC NPs for biological applications [60–64]. The coating of polyethylene glycol (PEG) (also called PEGylation) has been helpful to shield the surface of UC NPs, which is beneficial for in vivo use without toxicity [65, 66]. Similarly, silica encapsulation provides an efficient UC NPs surface, supporting a higher loading of therapeutic reagent suitable for therapeutic application [67, 68]. Bioconjugation (i.e., functionalization with biomolecules) is vital for target-based applications, including biosensing and specific cell tracking in cellular imaging. For example, bioconjugation with targeting molecules, such as folic acid, biotin, receptor-binding elements, including antibodies, aptamers, and small peptides, can improve cellular uptake, intracellular imaging, and therapy [69–71]. The nucleic acid-mediated assembly has been employed for bioimaging [72]. Ln^{3+} ions also bind oligonucleotides, and the resulting bioconjugates have been offered to monitor the hybridization reactions and phosphodiesterase activity by FRET technology.

The use of the effect of surface plasmon resonance (SPR) to enhance the efficiency using metal NPs (especially Au and Ag in the form of a metal shell or double shell on the surface of UC NPs) has been explored to tune and optimize the interaction between the metal and UC NPs [73, 74]. Localized surface plasmon resonance (LSPR) can promote the excitation and radiative recombination processes in UC NPs by intensifying the excitation light field and altering the local density of optical states (LDOS)

[75]. The localized electromagnetic (EM) field enhancement at the metal surface plays a vital role in the PEPL plasmon-enhanced photoluminescence effect. Modifying LDOS will enhance the absorption cross-section or radiative decay rate with an adequately configured luminous system. UC NPs exhibit a higher signal-to-noise ratio (SNR), superior photostability, deeper tissue penetration with the near-infrared excitation wavelengths, and lower photodamage to the biological sample. UC intensity will enhance by introducing a plasmonic nanostructure matching the plasmonic resonance to the absorption or emission wavelength. The anisotropic metal nanostructures, such as nanorod, nanostar are used to tune the maximal spectral overlap between SPR and the emitter absorption/emission wavelength [76]. With the careful fabrication of the metallic nanostructure and selectivity of the luminous center with the proper energy level, the plasmon-enhanced PL can be achieved [74]. Wu et al. described the significant improvements in UC efficiency using plasmon resonances [75]. Zong et al. discussed in their review the physical mechanism and principle of plasmon-enhanced UC luminescence with an emphasis on the potential applications [77]. Park et al. comprehensively described the plasmon-enhanced UC process, comparable classes of nanostructures, the effects of spacer layers and local heating, and the dynamics of the plasmon-enhanced UC process and significant impact on biomedical imaging [73]. Dong et al. demonstrated that the plasmonic nanostructure, including nonperiodic and periodic metallic nanostructures, has a critical effect on upconversion UC NPs [74].

4 Applications in Biomedical Fields

QDs have been widely used in biomedical fields compared to other alternatives such as organic fluorescent nanomaterials dye molecules. The exciting and flexible properties of QDs such as size-dependent tunable properties, high quantum yield, more extended stability, and lesser photobleaching effect [78]. The application of the QDs in the biomedical field has been grown up gradually since 1998. Chen's group has shown the application of QDs in bioimaging and nuclear targeting with great stability and biocompatibility in living cells [79–81].

4.1 Biosensing

Biosensing detects target molecules and is an integrated analytical technique that combines a biological recognition element and a detection method in a quantitative or semiquantitative manner. A simple example of biosensing is an immunoassay, where an antibody is employed to trap and detect the presence of the target antigen marker [5]. The signal acquisition involves detecting signals from detectors, such as photodiodes or charge-coupled devices (CCD). UC and DC QDs/NPs-based biosensing methods have gained interest in biosensing applications due to their high

signal-to-noise ratio, high quantum yield, and low detection limit during the last decade.

Temperature and pH: Sensing biological conditions such as temperature and pH is the primary concern in the biomedical field to monitor the individual cell to understand the mechanism of biological events or the progress of disease status. Here, UC and DC NPs have played an essential role as nanothermometers with a high resolution and a wide range within the nano-scale in the past few years [82–87]. Various metal ions, e.g., Li^+ , Mg^{2+} , were co-doped with Er in UC NPs to improve the luminescence intensity during temperature measurement. The development of a temperature sensor by UC and DC NPs shows the ability to detect temperature with a consistent sensitivity of 0.005–0.006 K from 303 to 573 K [88]. The variation of luminescence intensity or the emission maxima from a RE doped material may be used for temperature sensing in the biological environment. However, the UC emission in the visible range from RE doped materials limits the ability of the detection in the deep tissue. Here, the DC NPs may play an essential role in converting NIR-I to NIR-II and NIR-III with a better penetrating power for measuring the temperature of deep tissues.

Similarly, pH sensing is vital in the biomedical field due to its variation on a subcellular level caused by cancers and metabolic diseases, i.e., pH homeostasis. In this perspective, fluorescence-based pH sensors have a great advantage over common electrochemical sensors for monitoring intracellular pH in biomedical research. The resonance energy transfer UC process is the basic principle behind it. For example, fluorescein and a reference dye embedded in a polyacrylamide matrix, $\text{NaYF}_4:\text{Yb}$, Er UC NPs core, and silica shell are capable of effective pH monitoring and excellent light stability in various biological matrices [89, 90]. The conjugation of pH-responsive nanoprobe, e.g., pH-dependent fluorescence molecules, pH-dependent absorber (like polyethyleneimine), fluorescent dyes, with the UC NPs are of present focus of the research in recent years [91–93].

Electrolytes, heavy metals, small and macromolecules: The key idea for detecting metal ions, electrolytes, small and macromolecules is the mechanism of fluorescence/luminescence resonance energy transfer (FRET/LRET). Fluorescence sensing or optical recognition is essential for sensing biochemical substances owing to convenient detection systems, extraordinary sensitivity and selectivity, cost-effectiveness, fast response time, and reproducible results. FRET is a nonradiative process where donor and acceptor fluorophores transfer energy through the intermolecular long-range dipole–dipole coupling. The quantum efficiency of the energy transfer process can be expressed as $\eta = 1/\{1 + (R/R_0)^6\}$, R (~10–100 Å) is the distance between the donor and acceptor, and R_0 is the characteristic space with a 50% energy transfer efficiency [94]. UC NPs have been applied as an energy donor in FRET/LRET-based luminescent biosensing, where the luminescence intensity, FRET efficiency are dependent on the surface-functionalized materials, small and macromolecules, metal ions present in the environment. The proper understanding of luminescent Ln^{3+} with the host matrixes in the UC NPs may improve the emission efficiency with exceptional physicochemical properties for biosensing applications. The FRET

mechanism depends on the spectral overlap of the donor's emission spectrum with the absorption spectrum of the acceptor, the total coordination of the transition dipoles, and the spatial difference between the molecules of the donor and the acceptor. Most FRET-based luminescent probes emit emission upon the excitation of UV or visible light, which is not suitable for biological samples due to low penetration depth and harmful to biological tissue. Therefore, UC NPs are an effective alternative for FRET/LRET-based biological detection (LRET when UC NPs are involved). In most cases, the UC NPs act as energy donors, and the organic luminophores or plasmonic NPs/graphene/graphene oxide act as energy acceptors molecules/ions. Most of the UC NPs based LRET schemes in the literature report the fixed excitation bands in the NIR-I window (980 nm for Yb^{3+} and 800 nm for Nd^{3+}) to obtain the emission in the visible or NIR range. Ansari et al. describe functionalized UC NPs' role in FRET-based luminescence biosensing [94]. The review has included the recent advancement of UC NPs in optical biosensing applications, synthesis of UC NPs, surface functionalization, emission efficiency enhancement factors, and applications like detecting pathogenic diseases, free radicals, and biomarkers [94]. The review has discussed a detailed overview of functionalization techniques for UC NPs, i.e., the techniques for biological species-encapsulation/conjugation, organic ligands-functionalization, and Ln^{3+} doping. Sun et al. summarize the recent development of UC NPs through nanostructural design and emerging biomedical applications [4]. Lin et al. have discussed the latest development of UC NPs with cellular optogenetics and their biomedical applications, cancer therapy, cardiac optogenetics, and the latest strategies to optimize and advance UC-mediated optogenetics [37]. Yao et al. have introduced UC NPs for sensing, imaging, and therapy applications [3].

Functionalized Mn^{2+} -doped $\text{NaYF}_4:\text{Yb}$, Er UC NPs can be applied for detecting metabolites such as glucose, H_2O_2 , and uric acid in human serum to estimate the oxidation stress and detoxification inside the body [95]. A dual-mode UC and DC NPs were used to sensitively detect temperature and O_2 concentration [56]. Besides biomolecules, detecting small chemical molecules and the antibiotic residue is also possible by fluorescence-based UC NPs [96–98]. Moreover, UC NPs are extensively used for biosensing of nucleic acids, including DNA, RNA, small and circular DNA, or RNA as the fingerprint in target identification and the detection of disease-related RNA and small RNA [99–104]. LRET-based detection was commonly employed to target DNAs with UC NPs as donors [105]. UC NPs are also useful for detecting protein or peptides, well-known biomarkers for disease, and medical diagnosis [106–109]. LRET between UC NPs and metal nanostructure is advantageous for cancer diagnostics [110–112].

4.2 Bioimaging

UC NPs convert low-energy photon (NIR light) into a high-energy photon (Visible). NIR excitation can reduce cell damage and enhance the penetration depth into tissue.

Low auto-fluorescence is the prerequisite for biological imaging. In this perspective, UC NPs are perfect alternatives for *in vitro* or *in vivo* imaging to prove their promising applications in the living body [3, 59, 113–115]. UC NPs are highly resistant to photobleaching, and hence they can monitor live cells over more extended periods. The photostability of UC NPs is good over the dye molecules. Through proper doping or surface coupling, UC NPs can offer multiple imaging modalities, including Magnetic resonance imaging (MRI), computed tomography (CT), positron emission tomography (PET), single-photon emission computed tomography (SPECT), photothermal (PT), and photoacoustic (PA) imaging. For example, PEG-phospholipid-coated UC NPs are essential for the high contrast cellular imaging, the entire intracellular pathway, including endocytosis, active transport, and exocytosis [116, 117]. UC NPs provide a long emission lifetime and produce a clear microscopic image.

Moreover, lifetime tuning is possible for UC NPs without affecting their emission brightness, beneficial to the super-fast laser scanning for real-time superresolution imaging [5, 118–121]. UC NPs and DCNPs are attractive for the high contrast deep-tissue optical imaging owing to the absence of auto-fluorescence and higher intrinsic quantum yield, as they possess a high NIR optical transmission range in biological tissue and culture media [122, 123]. UC NPs with various surface functional groups coatings such as $-\text{COOH}$, $-\text{PEG}$, produce bright UCL the tumor site in tissue model and *in vivo* mouse model [124]. In addition, UC NPs support multimodal imaging in the simultaneous observation of multiple targets [125–128]. $\text{LiYF}_4:\text{Yb}^{3+}/\text{Tm}^{3+}@\text{SiO}_2$ UC NPs can track biodegradable hydrogel in living tissues. During prolonged high contrast deep-tissue imaging (~ 980 nm, absorbed by water molecules), an increase of temperature in the local tissue environment is observed, consequently inducing temperature-stress-induced tissue damage. Therefore, excitation by 800–1000 nm for Yb^{3+} and 1522 nm for Er^{3+} , prohibit possible heating effects during imaging [129]. NIR-II spectral range of 1000–1400 nm and beyond 1550 nm have attracted much attention in recent years for *in vivo* imaging of the living mice to a noninvasive brain angiography, real-time tracking of the NPs flow in the blood vessel of the whole organism without interference from skeletons [130–136]. Chapter 8 describes in detail fluorescence imaging by UC NPs.

4.3 Gene and Drug Delivery

The main obstacle to cancer gene therapy is the availability of therapeutic agents with target-specific properties. On the other hand, therapeutic agents must have minimum toxic side effects on healthy cells and tissues. UC NPs are an excellent alternative to provide comprehensive transport of genes such as DNA and siRNA. However, the tricky problem of gene delivery is how the engineered system protects genes from the complex physiological environment and increases the delivered expression effect. Researchers have employed FRET [137–139], hydrophobic interaction [140–142],

pH [143, 144], NIR excitation [145–147] for the release of drugs, genes, stimulating multifunctional targeting, and cell imaging.

UC NPs have unique and fascinating optical properties that convert NIR to visible and UV, allowing them to be employed as efficient nanocarrier materials in drug/gene delivery systems owing to photoinduced reactions, e.g., photocleavage and photoisomerization. NIR-triggered drug delivery systems are desirable in applications requiring a drug at a specific location and time, such as anesthetics, post wound healing, cardiothoracic surgery, and cancer treatment. The light-triggered delivery with appropriate excitation wavelengths is noninvasive, spatially precise, and safe. Moreover, photoinduced drug and gene delivery systems minimize normal cell death, side effects, and tissue damage [148, 149]. UC NPs-based vehicle systems can be utilized to track and evaluate drug release efficiency and mechanism since the last decade [149–155]. UCNP-based drug delivery systems are consist of three primary methodologies: hydrophobic pockets, mesoporous silica shells, and hollow spheres with the mesoporous surface. A hydrophobic pocket constructed by conjugating poly (DL-lactic-co-glycolic acid) (PLGA) or PEGylated amphiphilic polymer onto the NaYF₄:Yb, Er@NaGdF₄, or oleic acid (OA)-capped NaYF₄:Yb³⁺/Er³⁺ UC NPs, respectively, carrying anticancer drug doxorubicin (DOX) [66, 156]. The pH can control the release to the target. UC NPs with mesoporous silica shell offers many advantages over others, like good water dispersibility, a high drug-loading capacity, low cytotoxicity, excellent cell imaging properties, and the ability to incorporate magnetic entity that can manipulate by the external magnetic field in vivo experiments [157, 158]. Tuneable release of Ibuprofen (IBU) can be possible by changing the silica shell thickness, and quantitative measurement of drug release can be achieved. Apart from the transport of drugs using hollow/mesoporous materials, hollow nanospheres, like PEGylated Y₂O₃:Yb³⁺/Er³⁺ hollow nanospheres [159], have emerged as promising drug carriers and enabled high contrast imaging of cell and tissue as well [3, 160–162].

4.4 Therapy

In recent years, photodynamic therapy (PDT) has advanced as a new alternative to chemotherapy and radiotherapy in the clinical treatment of diverse diseases. PDT has been employed in the therapy of head, neck, lung, prostate, or skin cancers and helps treat bacterial, fungal, and viral infections. PDT employs high-energy light to trigger chemical drugs (the photosensitizer, PS) accumulated in the tumor tissue to produce reactive oxygen species (ROS) that kill cancer cells. PDT controls the damage to healthy cells because the PS be likely to build up in cancer cells, and the exciting light is focused directly on them. PDT does not trigger scarring, making it suitable for skin cancers and precancers. PDT is less helpful in treating large tumors as the penetration depth for NIR light ranges from 0.5 to 5 mm. It has several side effects, including burns, swelling, pain, and scarring in the treatment area. However, proper selection of PS and engineering the PS-cell (e.g., immune protein) binding

may reduce the side effects drastically. Photothermal therapy (PTT) opens [163] the possibility of generating contactless and local heating when exposed to laser light using light-absorbing molecules or nanoparticles as microscopic heat sources and is expected to improve the therapeutic accuracy and reduce injury to normal tissues [163–167]. PTT using near-infrared (NIR) absorption agents (QDs or NPs) has been widely applied in medicine, especially cancer therapy [166].

4.4.1 Photodynamic Therapy

The primary prerequisite for PDT is the promising photosensitizer (PS) with strong absorption and high extinction coefficient in the NIR region, which allows deeper tissue penetration. PS must preferentially accumulate in the target cells and have negligible cytotoxicity in the absence of light. In this perspective, UC QDs are excellent candidates for the sensitizer due to their low toxicity [168]. NIR-excited UC NPs can be employed to activate the photosensitizers in deep tissues, compared to the traditional PDT by conventional photosensitizers, like chlorine e6 (Ce6), zinc phthalocyanine (ZnPc), and methylene blue (MB) induced by visible or UV light [5]. Combining the conventional photosensitizers with UC NPs has demonstrated its benefits in offering a complete solution to in vivo therapy [169]. UC NPs efficiently convert the deeply penetrating near-infrared light into visible wavelengths and excite the photosensitizer to produce ROS, which plays an essential role in treating deep tumors [170–174]. NIR light excites the UC NPs to emit intense visible light and hence, activate the PS (e.g., Rose Bengal (RB) and Phthalocyanine) to generate ROS to destroy target cancer cells or tissues [64, 175–180] and induces the suppression of the aggregation of Alzheimer's β -amyloid during the photodynamic reaction [181].

For in vitro and in vivo PDT, photosensitizer loading into UC and DC NPs effectively kills cancer cells. A few examples are 5,10,15,20-tetra-(*m*-hydroxyphenyl)chlorin (*m*-THPC, Temoporfin, Foscan[®]) functionalized $\text{LiYF}_4:\text{Yb}^{3+}/\text{Er}^{3+}$ [182], Graphene QDs [176, 178], UC NP/methylene blue (MB) mixed based PDT drug of $\text{NaYF}_4:\text{Er}/\text{Yb}/\text{Gd}@\text{SiO}_2(\text{MB})$ [183], DNA-mediated assembly of core-satellite structures composed of Zr (IV)-based porphyrinic metal-organic framework (MOF) and $\text{NaYF}_4, \text{Yb}, \text{Er}$ UC NPs [184], $\text{LiYbF}_4:\text{Yb}^{3+}/\text{LiYF}_4$ UC NPs [185], NIR-to-NIR via a core-shell structure of $\text{Y}_2\text{O}_3:\text{Nd}^{3+}/\text{Yb}^{3+}@\text{-SiO}_2@\text{Cu}_2\text{S}$ DC NPs for dual-mode imaging and PTT [186, 187], aminolevulinic acid-conjugated $\text{NaYF}_4:\text{Yb}, \text{Er}@\text{CaF}_2$ UC NPs [188], molybdenum disulfide (MoS_2) QDs [189], TiO_2 -coated UC NPs [190, 191] and many more [3, 5]. Recent applications of UC and DC NPs in PDT have limitations due to the sensitizer's uncontrolled loading amount; therefore, the design of controllable and stable sensitizer loading for reproducible optical observation and therapeutic efficiency is desirable.

4.4.2 Photothermal Therapy

In photothermal therapy (PTT), the energy supplied by the sensitizer is converted into thermal energy, killing the cancer cells [192, 193]. The carbon-coated core-shell upconversion nanocomposite (NaLuF₄:Yb, Er/NaLuF₄/Carbon or UCNPs@C) exhibits both UC emission and photothermal effect, as shown in Fig. 8. The figure illustrates the photothermal effect and shows the thermal images of nude mice with (+) and without (–) UCNP@C-labelled HeLa cell tumors under 730-nm irradiation. Common examples of UC and DC NPs systems for PTT in recent years: KLu(WO₄)₂:Ho³⁺, Tm³⁺ NPs [194], CuS-NP onto the surface of silica-coated UCNPs [195], polyaniline coated UC NPs [193], monosaccharide-UC NPs [196, 197], Y₂O₃:Nd³⁺/Yb³⁺ based UCNPs [192], UCNPs-DPA conjugated NGO-PEG-BPEI-DOX [198], polydopamine (PDA) modified UC NPs [199] and many more [3, 200–204]. In recent years, combined therapy, i.e., a combination of PDT and PTT, is now performing a significant role in tumor ablation, necrosis, and cancer therapy [205–210]. However, image guide therapy combined with PDT and PTT further enhances the cytotoxicity rate on cancer cells [211]. PDT and chemotherapy can reduce cancer recurrence, metastasis, and prognosis [212]. The PTT is limited outside in vitro environment as the high-temperature generation is not compatible with the biological environment. However, controlled heating may lead to the optimal application of PTT in cancer therapy.

4.5 Optogenetic Stimulation

Optogenetics, the optical control of neuronal activity by using light (“opto”) and genetically encoded photosensitive proteins (“genetics”), is developed in neuroscience to assess the roles of one specific type of neuron in neural circuits that control sensory, motor, memory, emotion, and Parkinson’s disease [213, 214]. Dissecting the function of each neuronal type needs cell-type-specific manipulation in multiple neuronal populations. The advantages of optogenetics in clinical application are epileptic suppression and pain relief. In this perspective, NIR-excited UC NPs with narrow emission bandwidths, deep-tissue penetration compared with visible lights, and anti-photo-bleaching are advantageous for noninvasive remote activation of neurons and NIR imaging [37, 215–218]. However, the conventional UC NPs generate multiple emission bands under single NIR excitation. Moreover, the excitation-responsive UC luminescence is still constrained to only two colors like green and blue emission under continuous wave (CW) light NIR excitations and pulse modulation of CW light for temporal control of spiking. Complex neuronal stimulation requires distinct monochromatic or trichromatic UC emission. Liu et al. reported a CW NIR excitable trichromatic UC NPs for remote

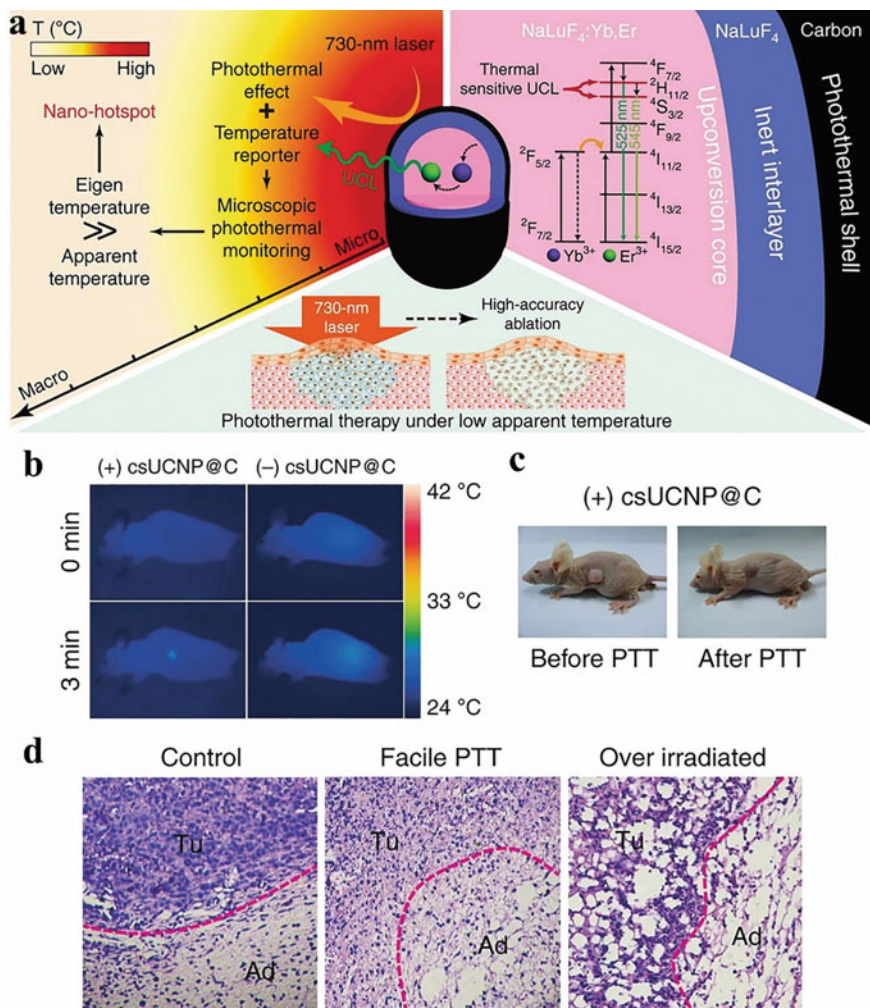


Fig. 8 **a** The carbon-coated core-shell upconversion nanocomposite (NaLuF₄:Yb,Er/NaLuF₄/Carbon or UCNP@C) exhibit both UC emission and photothermal effect. UCNP@C (acted as a nano-hotspot at the microscopic level) monitors the change in the microscopic temperature of the photoabsorber (carbon shell under 730-nm irradiation due to the temperature-sensitive UC emission (UCL represents UC luminescence in the picture)). **b** Thermal images of nude mice with (+) and without (-) UCNP@C-labelled HeLa cell tumors under 730-nm irradiation (0.3 W cm⁻²). **c** Representative images of nude mice transplanted with UCNP@C-labelled HeLa cells under 730-nm irradiation (0.3 W cm⁻²). **d** Hematoxylin and eosin (H&E) histopathological section of the tumor and normal fat tissue border. The figure presents the conditions of tumor region (Tu) and the adipocytes (Ad) in normal fat tissue of the mice without 730-nm irradiation (left, control), after photothermal treatment (middle, Facile PTT) under 730-nm irradiation (0.3 W cm⁻²), and high-power irradiation (right, Over irradiated) with the 730-nm laser (0.8 W cm⁻²). Reproduced from Ref. [86] under the terms of the Creative Commons CC BY license

optogenetic modulation of three distinct neuronal populations—channelrhodopsin-2 (ChR2)-expressing inhibitory parvalbumin (PV), ChrimsonR-expressing somatostatin (SOM) neurons, as well as C1V1-expressing excitatory Ca^{2+} /calmodulin-dependent protein kinase II α (CaMKII α) neurons in the primary visual cortex (V1) [213]. In most of the UC NPs-mediated NIR-activatable optogenetics, excitation wavelengths are 800 nm, 808 nm, and 980 nm, whereas UC NPs are mostly core/shell or core/shell/shell configuration with some different ligands, e.g., $\text{NaYF}_4\text{:Sc/Yb/Er}$, $\text{NaYF}_4\text{:Yb/Tm@NaYF}_4$, $\text{NaYF}_4\text{:Yb/Tm@SiO}_2$, $\text{NaYF}_4\text{:Yb/Tm}$, $\text{NaYF}_4\text{:Yb/Er}$, $\text{NaYF}_4\text{:Yb/Tm/Nd@NaYF}_4\text{:Nd}$ and many more [37].

5 Conclusion and Future Perspectives

This chapter offers a comprehensive discussion on understanding the fundamental photophysical processes leading to UC and DC luminescence process for the application in biomedical fields. Despite significant achievements made in the last decade, several challenges remain for its biomedical application and clinical translational research. Potential toxicity arises from chemical composition and the smaller size of UC NPs, enabling them to circumvent biological barriers and/or accumulate in the tissue. The focus of research on the UC and DC NPs to enhance desired optical properties is modifying the absorption efficiency and refining the energy transfer mechanism within NPs. In bioimaging, bright and multicolor emission from UC NPs enables them as suitable agents for multimodal imaging and in vivo animal imaging in medical diagnosis, and NIR emission from UC NPs may solve the limitation of penetrating power through the skeleton by the combination of fluorescence imaging, magnetic resonance imaging (MRI), CT scanning. Doping of paramagnetic material different kinds of UC NPs may introduce magnetic imaging, where the paramagnetic species can work as a contrast agent in MRI. Recent progress in NIR or mid-IR imaging and instrumentation for mid-IR sensing may develop label-free techniques for high-speed, hyperspectral bioimaging for medical diagnosis.

Acknowledgements Dr. P. Barik acknowledges the Technical Research Centre (TRC) [No. All1/64/SNB/2014(C)] of the S. N. Bose National Centre for Basic Sciences, Kolkata, for funding this work.

References

1. Gao C, Zheng P, Liu Q, Han S, Li D, Luo S, et al. Recent advances of upconversion nanomaterials in the biological field. *Nanomaterials*. 2021;11(10):2474. Available from: <https://www.mdpi.com/2079-4991/11/10/2474>.
2. Sun L-D, Dong H, Zhang P-Z, Yan C-H. Upconversion of rare earth nanomaterials. *Annu Rev Phys Chem*. 2015;66(1):619–42. Available from: <http://doi.org/10.1146/annurev-physchem-040214-121344>.

3. Yao J, Huang C, Liu C, Yang M. Upconversion luminescence nanomaterials: a versatile platform for imaging, sensing, and therapy. *Talanta*. 2020;208:120157. Available from: <https://linkinghub.elsevier.com/retrieve/pii/S0039914019307830>.
4. Sun T, Ai F, Zhu G, Wang F. Upconversion in nanostructured materials: from optical tuning to biomedical applications. *Chem Asian J*. 2018;13(4):373–85. Available from: <http://doi.org/10.1002/asia.201701660>.
5. Loo JF-C, Chien Y-H, Yin F, Kong S-K, Ho H-P, Yong K-T. Upconversion and downconversion nanoparticles for biophotonics and nanomedicine. *Coord Chem Rev*. 2019;400:213042. Available from: <https://linkinghub.elsevier.com/retrieve/pii/S0010854519301390>.
6. Gai S, Li C, Yang P, Lin J. Recent progress in rare earth micro/nanocrystals: soft chemical synthesis, luminescent properties, and biomedical applications. *Chem Rev*. 2014;114(4):2343–89. Available from: <http://doi.org/10.1021/cr4001594>.
7. Eliseeva SV, Bünzli J-CG. Lanthanide luminescence for functional materials and bio-sciences. *Chem Soc Rev*. 2010;39(1):189–227. Available from: <http://xlink.rsc.org/?DOI=B905604C>.
8. Bloembergen N. Solid state infrared quantum counters. *Phys Rev Lett*. 1959;2(3):84–5. Available from: <http://doi.org/10.1103/PhysRevLett.2.84>.
9. Auzel F. Upconversion and anti-stokes processes with f and d ions in solids. *Chem Rev*. 2004;104(1):139–74. Available from: <https://doi.org/10.1021/cr020357g>.
10. Wagner AM, Knipe JM, Orive G, Peppas NA. Quantum dots in biomedical applications. *Acta Biomater*. 2019;94:44–63. Available from: <https://linkinghub.elsevier.com/retrieve/pii/S1742706119303393>.
11. West JL, Halas NJ. Engineered nanomaterials for biophotonics applications: improving sensing, imaging, and therapeutics. *Annu Rev Biomed Eng*. 2003;5(1):285–92. Available from: <http://doi.org/10.1146/annurev.bioeng.5.011303.120723>.
12. Wang D, Rogach AL, Caruso F. Semiconductor quantum dot-labeled microsphere bioconjugates prepared by stepwise self-assembly. *Nano Lett*. 2002;2(8):857–61. Available from: <https://doi.org/10.1021/nl025624c>.
13. Hlavacek A, Bouchal P, Skládal P. Biotinylation of quantum dots for application in fluoroimmunoassays with biotin-avidin amplification. *Microchim Acta*. 2012;176(3–4):287–93. Available from: <http://doi.org/10.1007/s00604-011-0729-6>.
14. Aswathy RG, Yoshida Y, Maekawa T, Kumar DS. Near-infrared quantum dots for deep tissue imaging. *Anal Bioanal Chem*. 2010;397(4):1417–35. Available from: <http://doi.org/10.1007/s00216-010-3643-6>.
15. Resch-Genger U, Grabolle M, Cavaliere-Jaricot S, Nitschke R, Nann T. Quantum dots versus organic dyes as fluorescent labels. *Nat Methods*. 2008;5(9):763–75. Available from: <http://www.nature.com/articles/nmeth.1248>.
16. Mukherjee A, Shim Y, Myong Song J. Quantum dot as probe for disease diagnosis and monitoring. *Biotechnol J*. 2016;11(1):31–42. Available from: <https://doi.org/10.1002/biot.201500219>.
17. Bilan R, Nabiev I, Sukhanova A. Quantum dot-based nanotools for bioimaging, diagnostics, and drug delivery. *ChemBioChem*. 2016;17(22):2103–14. Available from: <https://doi.org/10.1002/cbic.201600357>.
18. Pohanka M. Quantum dots in the therapy: current trends and perspectives. *Mini Rev Med Chem*. 2017;17(8):650–6.
19. Frangioni J. In vivo near-infrared fluorescence imaging. *Curr Opin Chem Biol*. 2003;7(5):626–34. Available from: <https://linkinghub.elsevier.com/retrieve/pii/S1367593103001091>.
20. Helms V. Fluorescence resonance energy transfer. In: *Principles of computational cell biology: from protein complexes to cellular networks*. Hoboken: Wiley; 2008. p. 202.
21. Cheng P-C. The contrast formation in optical microscopy. In: *Handbook of biological confocal microscopy*. Boston, MA: Springer US; 2006. p. 162–206. Available from: http://doi.org/10.1007/978-0-387-45524-2_8.
22. Kagan CR, Murray CB, Nirmal M, Bawendi MG. Electronic energy transfer in CdSe quantum dot solids. *Phys Rev Lett*. 1996;76(9):1517–20. Available from: <https://doi.org/10.1103/PhysRevLett.76.1517>.

23. Kagan CR, Murray CB, Bawendi MG. Long-range resonance transfer of electronic excitations in close-packed CdSe quantum-dot solids. *Phys Rev B*. 1996;54(12):8633–43. Available from: <https://doi.org/10.1103/PhysRevB.54.8633>.
24. Willard DM, Carillo LL, Jung J, Van Orden A. CdSe–ZnS quantum dots as resonance energy transfer donors in a model protein–protein binding assay. *Nano Lett*. 2001;1(9):469–74. Available from: <https://doi.org/10.1021/nl015565n>.
25. Medintz IL, Clapp AR, Mattoussi H, Goldman ER, Fisher B, Mauro JM. Self-assembled nanoscale biosensors based on quantum dot FRET donors. *Nat Mater*. 2003;2(9):630–8. Available from: <http://www.nature.com/articles/nmat961>.
26. Clapp AR, Medintz IL, Mauro JM, Fisher BR, Bawendi MG, Mattoussi H. Fluorescence resonance energy transfer between quantum dot donors and dye-labeled protein acceptors. *J Am Chem Soc*. 2004;126(1):301–10. Available from: <https://doi.org/10.1021/ja037088b>.
27. Patolsky F, Gill R, Weizmann Y, Mokari T, Banin U, Willner I. Lighting-up the dynamics of telomerization and DNA replication by CdSe–ZnS quantum dots. *J Am Chem Soc*. 2003;125(46):13918–9. Available from: <https://doi.org/10.1021/ja035848c>.
28. Dieke GH, Crosswhite HM. The spectra of the doubly and triply ionized rare earths. *Appl Opt*. 1963;2(7):675. Available from: <https://www.osapublishing.org/abstract.cfm?URI=ao-2-7-675>.
29. Dieke GH. Spectra and energy levels of rare earth ions in crystals. New York, NY: Wiley; 1968. p. 401.
30. Ogasawara K, Watanabe S, Toyoshima H, Brik MG. Chapter 231 first-principles calculations of transition spectra. 2007. p. 1–59. Available from: <https://linkinghub.elsevier.com/retrieve/pii/S0168127307370311>.
31. Zhou B, Shi B, Jin D, Liu X. Controlling upconversion nanocrystals for emerging applications. *Nat Nanotechnol*. 2015;10(11):924–36. Available from: <http://www.nature.com/articles/nnano.2015.251>.
32. Naccache R, Rodríguez EM, Bogdan N, Sanz-Rodríguez F, de la Cruz MCI, de la Fuente ÁJ, et al. High resolution fluorescence imaging of cancers using lanthanide ion-doped upconverting nanocrystals. *Cancers (Basel)*. 2012;4(4):1067–105. Available from: <http://www.mdpi.com/2072-6694/4/4/1067>.
33. Weingarten DH, LaCount MD, van de Lagemaat J, Rumbles G, Lusk MT, Shaheen SE. Experimental demonstration of photon upconversion via cooperative energy pooling. *Nat Commun*. 2017;8(1):14808. Available from: <http://www.nature.com/articles/ncomms14808>.
34. LaCount MD, Weingarten D, Hu N, Shaheen SE, van de Lagemaat J, Rumbles G, et al. Energy pooling upconversion in organic molecular systems. *J Phys Chem A*. 2015;119(17):4009–16. Available from: <https://doi.org/10.1021/acs.jpca.5b00509>.
35. Ostermayer FW, Van Uitert LG. Cooperative energy transfer from Yb³⁺ to Tb³⁺ in YF₃. *Phys Rev B*. 1970;1(11):4208–12. Available from: <https://doi.org/10.1103/PhysRevB.1.4208>.
36. Auzel F. Upconversion processes in coupled ion systems. *J Lumin*. 1990;45(1–6):341–5. Available from: <https://linkinghub.elsevier.com/retrieve/pii/0022231390901891>.
37. Lin Y, Yao Y, Zhang W, Fang Q, Zhang L, Zhang Y, et al. Applications of upconversion nanoparticles in cellular optogenetics. *Acta Biomater*. 2021;135:1–12. Available from: <https://linkinghub.elsevier.com/retrieve/pii/S1742706121005614>.
38. Qiao X, Tsuboi T, Seo HJ. Correlation among the cooperative luminescence, cooperative energy transferred Eu³⁺-emission, and near-infrared Yb³⁺ emission of Eu³⁺-doped LiYb(MoO₄)₂. *J Alloys Compd*. 2016;687:179–87. Available from: <https://linkinghub.elsevier.com/retrieve/pii/S0925838816318485>.
39. Qin W-P, Liu Z-Y, Sin C-N, Wu C-F, Qin G-S, Chen Z, et al. Multi-ion cooperative processes in Yb³⁺ clusters. *Light Sci Appl*. 2014;3(8):e193. Available from: <http://www.nature.com/articles/lsa201474>.
40. Xue M, Zhu X, Qiu X, Gu Y, Feng W, Li F. Highly enhanced cooperative upconversion luminescence through energy transfer optimization and quenching protection. *ACS Appl Mater Interfaces*. 2016;8(28):17894–901. Available from: <https://doi.org/10.1021/acsami.6b05609>.

41. Terra I, Borrero-González L, Almeida J, Hernandez A, Nunes L. Judd-Ofelt analysis of Tb³⁺ and upconversion study in Yb³⁺-Tb³⁺ co-doped calibo glasses. *Quim Nova*. 2020. Available from: http://quimicanova.sbq.org.br/audiencia_pdf.asp?aid2=8023&nomeArquivo=AR20190342.pdf.
42. Chivian JS, Case WE, Eden DD. The photon avalanche: a new phenomenon in Pr³⁺-based infrared quantum counters. *Appl Phys Lett*. 1979;35(2):124–5. Available from: <http://doi.org/10.1063/1.91044>.
43. Kueny AW, Case WE, Koch ME. Nonlinear-optical absorption through photon avalanche. *J Opt Soc Am B*. 1989;6(4):639. Available from: <https://www.osapublishing.org/abstract.cfm?URI=josab-6-4-639>.
44. Ehrler B, Yanai N, Nienhaus L. Up- and down-conversion in molecules and materials. *J Chem Phys*. 2021;154(7):070401. Available from: <https://doi.org/10.1063/5.0045323>.
45. Seo SE, Choe H-S, Cho H, Kim H, Kim J-H, Kwon OS. Recent advances in materials for and applications of triplet–triplet annihilation-based upconversion. *J Mater Chem C*. 2022. Available from: <http://xlink.rsc.org/?DOI=D1TC03551G>.
46. Bharmoria P, Bildirir H, Moth-Poulsen K. Triplet–triplet annihilation based near infrared to visible molecular photon upconversion. *Chem Soc Rev*. 2020;49(18):6529–54. Available from: <http://xlink.rsc.org/?DOI=D0CS00257G>.
47. Okumura K, Mase K, Yanai N, Kimizuka N. Employing core-shell quantum dots as triplet sensitizers for photon upconversion. *Chem A Eur J*. 2016;22(23):7721–6. Available from: <http://doi.org/10.1002/chem.201600998>.
48. Ahmad W, Wang J, Li H, Ouyang Q, Wu W, Chen Q. Strategies for combining triplet–triplet annihilation upconversion sensitizers and acceptors in a host matrix. *Coord Chem Rev*. 2021;439:213944. Available from: <https://linkinghub.elsevier.com/retrieve/pii/S0010854521002186>.
49. Han Y, He S, Wu K. Molecular triplet sensitization and photon upconversion using colloidal semiconductor nanocrystals. *ACS Energy Lett*. 2021;6(9):3151–66. Available from: <https://doi.org/10.1021/acsenerylett.1c01348>.
50. Gray V, Allardice JR, Zhang Z, Rao A. Organic-quantum dot hybrid interfaces and their role in photon fission/fusion applications. *Chem Phys Rev*. 2021;2(3):031305. Available from: <https://doi.org/10.1063/5.0050464>.
51. Lai R, Sang Y, Zhao Y, Wu K. Triplet sensitization and photon upconversion using InP-based quantum dots. *J Am Chem Soc*. 2020;142(47):19825–9. Available from: <https://doi.org/10.1021/jacs.0c09547>.
52. Xu Z, Huang Z, Jin T, Lian T, Tang ML. Mechanistic understanding and rational design of quantum dot/mediator interfaces for efficient photon upconversion. *Acc Chem Res*. 2021;54(1):70–80. Available from: <https://doi.org/10.1021/acs.accounts.0c00526>.
53. Ronchi A, Brazzo P, Sassi M, Beverina L, Pedrini J, Meinardi F, et al. Triplet–triplet annihilation based photon up-conversion in hybrid molecule–semiconductor nanocrystal systems. *Phys Chem Chem Phys*. 2019;21(23):12353–9. Available from: <http://xlink.rsc.org/?DOI=C9CP01692A>.
54. O’shea R, Kendrick WJ, Gao C, Owyong TC, White JM, Ghiggino KP, et al. Revealing the influence of steric bulk on the triplet–triplet annihilation upconversion performance of conjugated polymers. *Sci Rep*. 2021;11(1):19585. Available from: <https://www.nature.com/articles/s41598-021-99179-y>.
55. Kagan CR, Lifshitz E, Sargent EH, Talapin DV. Building devices from colloidal quantum dots. *Science*. 2016;353(6302). Available from: <https://doi.org/10.1126/science.aac5523>.
56. McGuire JA, Sykora M, Joo J, Pietryga JM, Klimov VI. Apparent versus true carrier multiplication yields in semiconductor nanocrystals. *Nano Lett*. 2010;10(6):2049–57. Available from: <https://doi.org/10.1021/nl100177c>.
57. Smith MB, Michl J. Singlet fission. *Chem Rev*. 2010;110(11):6891–936. Available from: <https://doi.org/10.1021/cr1002613>.
58. Huang X, Han S, Huang W, Liu X. Enhancing solar cell efficiency: the search for luminescent materials as spectral converters. *Chem Soc Rev*. 2013;42(1):173–201. Available from: <http://xlink.rsc.org/?DOI=C2CS35288E>.

59. Bünzli J-CG. Lanthanide luminescence for biomedical analyses and imaging. *Chem Rev.* 2010;110(5):2729–55. Available from: <https://doi.org/10.1021/cr900362e>.
60. Van Duong H, Chau TTL, Dang NTT, Vanterpool F, Salmerón-Sánchez M, Lizundia E, et al. Biocompatible chitosan-functionalized upconverting nanocomposites. *ACS Omega.* 2018;3(1):86–95. Available from: <https://doi.org/10.1021/acsomega.7b01355>.
61. Plohl O, Kralj S, Majaron B, Fröhlich E, Ponikvar-Svet M, Makovec D, et al. Amphiphilic coatings for the protection of upconverting nanoparticles against dissolution in aqueous media. *Dalt Trans.* 2017;46(21):6975–84. Available from: <http://xlink.rsc.org/?DOI=C7DT00529F>.
62. Pokhrel M, Mimun LC, Yust B, Kumar GA, Dhanale A, Tang L, et al. Stokes emission in GdF₃:Nd³⁺ nanoparticles for bioimaging probes. *Nanoscale.* 2014;6(3):1667–74. Available from: <http://xlink.rsc.org/?DOI=C3NR03317A>.
63. Wang R, Li X, Zhou L, Zhang F. Epitaxial seeded growth of rare-earth nanocrystals with efficient 800 nm near-infrared to 1525 nm short-wavelength infrared downconversion photoluminescence for in vivo bioimaging. *Angew Chem.* 2014;126(45):12282–6. Available from: <https://doi.org/10.1002/ange.201407420>.
64. Sabri T, Pawelek PD, Capobianco JA. Dual activity of rose bengal functionalized to albumin-coated lanthanide-doped upconverting nanoparticles: targeting and photodynamic therapy. *ACS Appl Mater Interfaces.* 2018;10(32):26947–53. Available from: <https://doi.org/10.1021/acsomega.8b08919>.
65. Cheng L, Yang K, Zhang S, Shao M, Lee S, Liu Z. Highly-sensitive multiplexed in vivo imaging using pegylated upconversion nanoparticles. *Nano Res.* 2010;3(10):722–32. Available from: <https://doi.org/10.1007/s12274-010-0036-2>.
66. Wang C, Cheng L, Liu Z. Drug delivery with upconversion nanoparticles for multi-functional targeted cancer cell imaging and therapy. *Biomaterials.* 2011;32(4):1110–20. Available from: <https://linkinghub.elsevier.com/retrieve/pii/S0142961210012822>.
67. Lv R, Yang P, Chen G, Gai S, Xu J, Prasad PN. Dopamine-mediated photothermal theranostics combined with up-conversion platform under near infrared light. *Sci Rep.* 2017;7(1):13562. Available from: <http://www.nature.com/articles/s41598-017-13284-5>.
68. Ding B, Shao S, Yu C, Teng B, Wang M, Cheng Z, et al. Large-pore mesoporous-silica-coated upconversion nanoparticles as multifunctional immunoadjuvants with ultrahigh photosensitizer and antigen loading efficiency for improved cancer photodynamic immunotherapy. *Adv Mater.* 2018;30(52):1802479. Available from: <https://doi.org/10.1002/adma.201802479>.
69. Yang C, Wang Y, Ge MH, Fu YJ, Hao R, Islam K, et al. Rapid identification of specific DNA aptamers precisely targeting CD33 positive leukemia cells through a paired cell-based approach. *Biomater Sci.* 2019;7(3):938–50. Available from: <http://xlink.rsc.org/?DOI=C8BM01393D>.
70. Ellington AD, Szostak JW. In vitro selection of RNA molecules that bind specific ligands. *Nature.* 1990;346(6287):818–22. Available from: <http://www.nature.com/articles/346818a0>.
71. Hamula CLA, Peng H, Wang Z, Newbigging AM, Tyrrell GJ, Li X-F, et al. The effects of SELEX conditions on the resultant aptamer pools in the selection of aptamers binding to bacterial cells. *J Mol Evol.* 2015;81(5–6):194–209. Available from: <http://doi.org/10.1007/s00239-015-9711-y>.
72. He L, Mao C, Cho S, Ma K, Xi W, Bowman CN, et al. Experimental and theoretical photoluminescence studies in nucleic acid assembled gold-upconverting nanoparticle clusters. *Nanoscale.* 2015;7(41):17254–60. Available from: <http://xlink.rsc.org/?DOI=C5NR05035A>.
73. Park W, Lu D, Ahn S. Plasmon enhancement of luminescence upconversion. *Chem Soc Rev.* 2015;44(10):2940–62. Available from: <http://xlink.rsc.org/?DOI=C5CS00050E>.
74. Dong J, Gao W, Han Q, Wang Y, Qi J, Yan X, et al. Plasmon-enhanced upconversion photoluminescence: mechanism and application. *Rev Phys.* 2019;4:100026. Available from: <https://linkinghub.elsevier.com/retrieve/pii/S2405428318300030>.
75. Wu DM, García-Etxarri A, Salleo A, Dionne JA. Plasmon-enhanced upconversion. *J Phys Chem Lett.* 2014;5(22):4020–31. Available from: <https://doi.org/10.1021/jz5019042>.
76. Cao J, Sun T, Grattan KTV. Gold nanorod-based localized surface plasmon resonance biosensors: a review. *Sens Actuators B Chem.* 2014;195:332–51. Available from: <https://linkinghub.elsevier.com/retrieve/pii/S0925400514000732>.

77. Zong H, Mu X, Sun M. Physical principle and advances in plasmon-enhanced upconversion luminescence. *Appl Mater Today*. 2019;15:43–57. Available from: <https://linkinghub.elsevier.com/retrieve/pii/S2352940718305572>.
78. Alivisatos P. The use of nanocrystals in biological detection. *Nat Biotechnol*. 2004;22(1):47–52. Available from: <http://www.nature.com/articles/nbt927>.
79. Bruchez Jr. M, Bruchez M, Moronne M, Gin P, Weiss S, Alivisatos AP. Semiconductor nanocrystals as fluorescent biological labels. *Science*. 1998;281(5385):2013–6. Available from: <https://doi.org/10.1126/science.281.5385.2013>.
80. Chen F, Gerion D. Fluorescent CdSe/ZnS nanocrystal–peptide conjugates for long-term, nontoxic imaging and nuclear targeting in living cells. *Nano Lett*. 2004;4(10):1827–32. Available from: <https://doi.org/10.1021/nl049170q>.
81. Xiao D, Qi H, Teng Y, Pierre D, Kutoka PT, Liu D. Advances and challenges of fluorescent nanomaterials for synthesis and biomedical applications. *Nanoscale Res Lett*. 2021;16(1):167. Available from: <https://doi.org/10.1186/s11671-021-03613-z>.
82. Dong B, Cao B, He Y, Liu Z, Li Z, Feng Z. Temperature sensing and in vivo imaging by molybdenum sensitized visible upconversion luminescence of rare-earth oxides. *Adv Mater*. 2012;24(15):1987–93. Available from: <https://doi.org/10.1002/adma.201200431>.
83. Brites CDS, Martínez ED, Urbano RR, Rettori C, Carlos LD. Self-calibrated double luminescent thermometers through upconverting nanoparticles. *Front Chem*. 2019;7. Available from: <https://doi.org/10.3389/fchem.2019.00267/full>.
84. Kamimura M, Matsumoto T, Suyari S, Umezawa M, Soga K. Ratiometric near-infrared fluorescence nanothermometry in the OTN-NIR (NIR II/III) biological window based on rare-earth doped β -NaYF₄ nanoparticles. *J Mater Chem B*. 2017;5(10):1917–25. Available from: <http://xlink.rsc.org/?DOI=C7TB00070G>.
85. Sun X, Sun J, Dong B, Huang G, Zhang L, Zhou W, et al. Noninvasive temperature monitoring for dual-modal tumor therapy based on lanthanide-doped up-conversion nanocomposites. *Biomaterials*. 2019;201:42–52. Available from: <https://linkinghub.elsevier.com/retrieve/pii/S0142961219300997>.
86. Zhu X, Feng W, Chang J, Tan Y-W, Li J, Chen M, et al. Temperature-feedback upconversion nanocomposite for accurate photothermal therapy at facile temperature. *Nat Commun*. 2016;7(1):10437. Available from: <http://www.nature.com/articles/ncomms10437>.
87. Pang T, Wan W, Qian D, Liu Z. Calibration of optical temperature sensing of Ca_{1-x}NaxMoO₄:Yb³⁺,Er³⁺ with intense green up-conversion luminescence. *J Alloys Compd*. 2019;771:571–7. Available from: <https://linkinghub.elsevier.com/retrieve/pii/S092583881832043>.
88. Liu W, Pan G, Hao Z, Zhang L, Zhang X, Luo Y, et al. Highly efficient upconversion emission of Er³⁺ in δ -Sc₄Zr₃O₁₂ and broad-range temperature sensing. *Phys Chem Chem Phys*. 2018;20(21):14461–8. Available from: <http://xlink.rsc.org/?DOI=C8CP02217H>.
89. Arppe R, Näreoja T, Nylund S, Mattsson L, Koho S, Rosenholm JM, et al. Photon upconversion sensitized nanoprobe for sensing and imaging of pH. *Nanoscale*. 2014;6(12):6837–43. Available from: <http://xlink.rsc.org/?DOI=C4NR00461B>.
90. Clark HA, Hoyer M, Philbert MA, Kopelman R. Optical nanosensors for chemical analysis inside single living cells. 1. Fabrication, characterization, and methods for intracellular delivery of PEBBLE sensors. *Anal Chem*. 1999;71(21):4831–6. Available from: <https://doi.org/10.1021/ac990629o>.
91. Du S, Hernández-Gil J, Dong H, Zheng X, Lyu G, Bañobre-López M, et al. Design and validation of a new ratiometric intracellular pH imaging probe using lanthanide-doped upconverting nanoparticles. *Dalt Trans*. 2017;46(40):13957–65. Available from: <http://xlink.rsc.org/?DOI=C7DT02418E>.
92. Song X, Yue Z, Zhang J, Jiang Y, Wang Z, Zhang S. Multicolor upconversion nanoprobe based on a dual luminescence resonance energy transfer assay for simultaneous detection and bioimaging of [Ca²⁺]_i and pH_i in living cells. *Chem A Eur J*. 2018;24(24):6458–63. Available from: <https://doi.org/10.1002/chem.201800154>.

93. Mahata MK, Lee KT. Development of near-infrared sensitized core-shell-shell upconverting nanoparticles as pH-responsive probes. *Nanoscale Adv.* 2019;1(6):2372–81. Available from: <http://xlink.rsc.org/?DOI=C9NA00088G>.
94. Ansari AA, Thakur VK, Chen G. Functionalized upconversion nanoparticles: new strategy towards FRET-based luminescence bio-sensing. *Coord Chem Rev.* 2021;436:213821. Available from: <https://linkinghub.elsevier.com/retrieve/pii/S0010854521000552>.
95. Wu S, Kong X-J, Cen Y, Yuan J, Yu R-Q, Chu X. Fabrication of a LRET-based upconverting hybrid nanocomposite for turn-on sensing of H₂O₂ and glucose. *Nanoscale.* 2016;8(16):8939–46. Available from: <http://xlink.rsc.org/?DOI=C6NR00470A>.
96. Jin X, Fang G, Pan M, Yang Y, Bai X, Wang S. A molecularly imprinted electrochemiluminescence sensor based on upconversion nanoparticles enhanced by electrodeposited rGO for selective and ultrasensitive detection of clenbuterol. *Biosens Bioelectron.* 2018;102:357–64. Available from: <https://linkinghub.elsevier.com/retrieve/pii/S0956566317307315>.
97. Tang Y, Liu H, Gao J, Liu X, Gao X, Lu X, et al. Upconversion particle@Fe₃O₄@molecularly imprinted polymer with controllable shell thickness as high-performance fluorescent probe for sensing quinolones. *Talanta.* 2018;181:95–103. Available from: <https://linkinghub.elsevier.com/retrieve/pii/S003991401830002X>.
98. Hu W, Chen Q, Li H, Ouyang Q, Zhao J. Fabricating a novel label-free aptasensor for acetamiprid by fluorescence resonance energy transfer between NH₂-NaYF₄: Yb, Ho@SiO₂ and Au nanoparticles. *Biosens Bioelectron.* 2016;80:398–404. Available from: <https://linkinghub.elsevier.com/retrieve/pii/S0956566316301075>.
99. Gao R, Hao C, Xu L, Xu C, Kuang H. Spiny nanorod and upconversion nanoparticle satellite assemblies for ultrasensitive detection of messenger RNA in living cells. *Anal Chem.* 2018;90(8):5414–21. Available from: <https://doi.org/10.1021/acs.analchem.8b00617>.
100. Zhu D, Miao ZY, Hu Y, Zhang XJ. Single-step, homogeneous and sensitive detection for microRNAs with dual-recognition steps based on luminescence resonance energy transfer (LRET) using upconversion nanoparticles. *Biosens Bioelectron.* 2018;100:475–81. Available from: <https://linkinghub.elsevier.com/retrieve/pii/S0956566317306486>.
101. Zhang K, Yang L, Lu F, Wu X, Zhu J-J. A universal upconversion sensing platform for the sensitive detection of tumour-related ncRNA through an exo III-assisted cycling amplification strategy. *Small.* 2018;14(10):1703858. Available from: <https://doi.org/10.1002/smll.201703858>.
102. Qu A, Sun M, Xu L, Hao C, Wu X, Xu C, et al. Quantitative zeptomolar imaging of miRNA cancer markers with nanoparticle assemblies. *Proc Natl Acad Sci.* 2019;116(9):3391–400. Available from: <http://doi.org/10.1073/pnas.1810764116>.
103. Wu S, Duan N, Ma X, Xia Y, Yu Y, Wang Z, et al. Simultaneous detection of enterovirus 71 and coxsackievirus A16 using dual-colour upconversion luminescent nanoparticles as labels. *Chem Commun.* 2012;48(40):4866. Available from: <http://xlink.rsc.org/?DOI=c2cc00092j>.
104. Chen D, Mauk M, Qiu X, Liu C, Kim J, Ramprasad S, et al. An integrated, self-contained microfluidic cassette for isolation, amplification, and detection of nucleic acids. *Biomed Microdevices.* 2010;12(4):705–19. Available from: <http://doi.org/10.1007/s10544-010-9423-4>.
105. Mendez-Gonzalez D, Lahtinen S, Laurenti M, López-Cabarcos E, Rubio-Retama J, Soukka T. Photochemical ligation to ultrasensitive DNA detection with upconverting nanoparticles. *Anal Chem.* 2018;90(22):13385–92. Available from: <https://doi.org/10.1021/acs.analchem.8b03106>.
106. Zhang Y, Dong C, Su L, Wang H, Gong X, Wang H, et al. Multifunctional microspheres encoded with upconverting nanocrystals and magnetic nanoparticles for rapid separation and immunoassays. *ACS Appl Mater Interfaces.* 2016;8(1):745–53. Available from: <https://doi.org/10.1021/acsami.5b09913>.
107. Yuan F, Chen H, Xu J, Zhang Y, Wu Y, Wang L. Aptamer-based luminescence energy transfer from near-infrared-to-near-infrared upconverting nanoparticles to gold nanorods and its application for the detection of thrombin. *Chem A Eur J.* 2014;20(10):2888–94. Available from: <https://doi.org/10.1002/chem.201304556>.

108. Jo E-J, Byun J-Y, Mun H, Bang D, Son JH, Lee JY, et al. Single-step LRET aptasensor for rapid mycotoxin detection. *Anal Chem.* 2018;90(1):716–22. Available from: <https://doi.org/10.1021/acs.analchem.7b02368>.
109. Wu Z, Xu E, Chughtai MFJ, Jin Z, Irudayaraj J. Highly sensitive fluorescence sensing of zearalenone using a novel aptasensor based on upconverting nanoparticles. *Food Chem.* 2017;230:673–80. Available from: <https://linkinghub.elsevier.com/retrieve/pii/S0308814617304818>.
110. Chen H, Guan Y, Wang S, Ji Y, Gong M, Wang L. Turn-on detection of a cancer marker based on near-infrared luminescence energy transfer from NaYF₄: Yb, Tm/NaGdF₄ core–shell upconverting nanoparticles to gold nanorods. *Langmuir.* 2014;30(43):13085–91. Available from: <https://doi.org/10.1021/la502753e>.
111. Loo J, Lau P-M, Kong S-K, Ho H-P. An assay using localized surface plasmon resonance and gold nanorods functionalized with aptamers to sense the cytochrome-c released from apoptotic cancer cells for anti-cancer drug effect determination. *Micromachines.* 2017;8(11):338. Available from: <http://www.mdpi.com/2072-666X/8/11/338>.
112. Loo JF-C, Yang C, Tsang HL, Lau PM, Yong K-T, Ho HP, et al. An Aptamer Bio-barCode (ABC) assay using SPR, RNase H, and probes with RNA and gold-nanorods for anti-cancer drug screening. *Analyst.* 2017;142(19):3579–87. Available from: <http://xlink.rsc.org/?DOI=C7AN01026E>.
113. Yi Z, Li X, Xue Z, Liang X, Lu W, Peng H, et al. Remarkable NIR enhancement of multi-functional nanoprobess for in vivo trimodal bioimaging and upconversion optical/T2-weighted MRI-guided small tumor diagnosis. *Adv Funct Mater.* 2015;25(46):7119–29. Available from: <https://doi.org/10.1002/adfm.201503672>.
114. Yang B, Zhang Y, Chen B, He M, Yin X, Wang H, et al. A multifunctional probe for ICP-MS determination and multimodal imaging of cancer cells. *Biosens Bioelectron.* 2017;96:77–83. Available from: <https://linkinghub.elsevier.com/retrieve/pii/S0956566317302889>.
115. Jalani G, Naccache R, Rosenzweig DH, Lerouge S, Haglund L, Vetrone F, et al. Real-time, non-invasive monitoring of hydrogel degradation using LiYF₄: Yb³⁺/Tm³⁺ NIR-to-NIR upconverting nanoparticles. *Nanoscale.* 2015;7(26):11255–62. Available from: <http://xlink.rsc.org/?DOI=C5NR02482J>.
116. Askes SHC, Leeuwenburgh VC, Pomp W, Arjmandi-Tash H, Tanase S, Schmidt T, et al. Water-dispersible silica-coated upconverting liposomes: can a thin silica layer protect TTA-UC against oxygen quenching? *ACS Biomater Sci Eng.* 2017;3(3):322–34. Available from: <https://doi.org/10.1021/acsbiomaterials.6b00678>.
117. Bae YM, Park Y II, Nam SH, Kim JH, Lee K, Kim HM, et al. Endocytosis, intracellular transport, and exocytosis of lanthanide-doped upconverting nanoparticles in single living cells. *Biomaterials.* 2012;33(35):9080–6. Available from: <https://linkinghub.elsevier.com/retrieve/pii/S0142961212009428>.
118. Peng X, Huang B, Pu R, Liu H, Zhang T, Widengren J, et al. Fast upconversion super-resolution microscopy with 10 μ s per pixel dwell times. *Nanoscale.* 2019;11(4):1563–9. Available from: <http://xlink.rsc.org/?DOI=C8NR08986H>.
119. Cho U, Riordan DP, Ciepla P, Kocherlakota KS, Chen JK, Harbury PB. Ultrasensitive optical imaging with lanthanide lumiphores. *Nat Chem Biol.* 2018;14(1):15–21. Available from: <http://www.nature.com/articles/nchembio.2513>.
120. Teitelboim A, Tian B, Garfield DJ, Fernandez-Bravo A, Gotlin AC, Schuck PJ, et al. Energy transfer networks within upconverting nanoparticles are complex systems with collective, robust, and history-dependent dynamics. *J Phys Chem C.* 2019;123(4):2678–89. Available from: <https://doi.org/10.1021/acs.jpcc.9b00161>.
121. McLellan CA, Siefe C, Casar JR, Peng CS, Fischer S, Lay A, et al. Engineering bright and mechanosensitive alkaline-earth rare-earth upconverting nanoparticles. *J Phys Chem Lett.* 2022;13(6):1547–53. Available from: <https://doi.org/10.1021/acs.jpcclett.1c03841>.
122. Yu Z, Chan WK, Tan TTY. Neodymium-sensitized nanoconstructs for near-infrared enabled photomedicine. *Small.* 2020;16(1):1905265. Available from: <https://doi.org/10.1002/smll.201905265>.

123. Xu J, Zhou J, Chen Y, Yang P, Lin J. Lanthanide-activated nanoconstructs for optical multiplexing. *Coord Chem Rev.* 2020;415:213328. Available from: <https://linkinghub.elsevier.com/retrieve/pii/S0010854520301259>.
124. Tian R, Zhao S, Liu G, Chen H, Ma L, You H, et al. Construction of lanthanide-doped upconversion nanoparticle-Uelx Europaeus Agglutinin-I bioconjugates with brightness red emission for ultrasensitive in vivo imaging of colorectal tumor. *Biomaterials.* 2019;212:64–72. Available from: <https://linkinghub.elsevier.com/retrieve/pii/S0142961219302741>.
125. Yang D, Li C, Lin J. Multimodal cancer imaging using lanthanide-based upconversion nanoparticles. *Nanomedicine.* 2015;10(16):2573–91. Available from: <https://doi.org/10.2217/nmm.15.92>.
126. Santelli J, Lepoix C, Lechevallier S, Martinez C, Calise D, Zou Q, et al. Custom NIR imaging of new up-conversion multimodal gadolinium oxysulfide nanoparticles. *Part Part Syst Charact.* 2021;38(4):2000216. Available from: <https://doi.org/10.1002/ppsc.202000216>.
127. Shapoval O, Oleksa V, Šlouf M, Lobaz V, Trhlíková O, Filipová M, et al. Colloidally stable P(DMA-AGME)-Ale-coated Gd(Tb)F₃:Tb³⁺(Gd³⁺), Yb³⁺, Nd³⁺ nanoparticles as a multimodal contrast agent for down- and upconversion luminescence, magnetic resonance imaging, and computed tomography. *Nanomaterials.* 2021;11(1):230. Available from: <https://www.mdpi.com/2079-4991/11/1/230>.
128. Marin R, Jaque D, Benayas A. Switching to the brighter lane: pathways to boost the absorption of lanthanide-doped nanoparticles. *Nanoscale Horizons.* 2021;6(3):209–30. Available from: <http://xlink.rsc.org/?DOI=D0NH00627K>.
129. Shen J, Chen G, Vu A-M, Fan W, Bilsel OS, Chang C-C, et al. Engineering the upconversion nanoparticle excitation wavelength: cascade sensitization of tri-doped upconversion colloidal nanoparticles at 800 nm. *Adv Opt Mater.* 2013;1(9):644–50. Available from: <https://doi.org/10.1002/adom.201300160>.
130. Levy ES, Tajon CA, Bischof TS, Iafrati J, Fernandez-Bravo A, Garfield DJ, et al. Energy-looping nanoparticles: harnessing excited-state absorption for deep-tissue imaging. *ACS Nano.* 2016;10(9):8423–33. Available from: <https://doi.org/10.1021/acsnano.6b03288>.
131. Deng Z, Li X, Xue Z, Jiang M, Li Y, Zeng S, et al. A high performance Sc-based nanoprobe for through-skull fluorescence imaging of brain vessels beyond 1500 nm. *Nanoscale.* 2018;10(19):9393–400. Available from: <http://xlink.rsc.org/?DOI=C8NR00305J>.
132. Wu L, Hu J, Zou Q, Lin Y, Huang D, Chen D, et al. Synthesis and optical properties of a Y₃(Al/Ga)₅O₁₂: Ce³⁺, Cr³⁺, Nd³⁺ persistent luminescence nanophosphor: a promising near-infrared-II nanoprobe for biological applications. *Nanoscale.* 2020;12(26):14180–7. Available from: <http://xlink.rsc.org/?DOI=D0NR03269G>.
133. Zhang X, He S, Ding B, Qu C, Chen H, Sun Y, et al. Synergistic strategy of rare-earth doped nanoparticles for NIR-II biomedical imaging. *J Mater Chem B.* 2021;9(44):9116–22. Available from: <http://xlink.rsc.org/?DOI=D1TB01640G>.
134. Deng Z, Huang J, Xue Z, Jiang M, Li Y, Zeng S. A general strategy for designing NIR-II emissive silk for the in vivo monitoring of an implanted stent model beyond 1500 nm. *J Mater Chem B.* 2020;8(21):4587–92. Available from: <http://xlink.rsc.org/?DOI=C9TB02685A>.
135. Li Z, Ding X, Cong H, Wang S, Yu B, Shen Y. Recent advances on inorganic lanthanide-doped NIR-II fluorescence nanoprobes for bioapplication. *J Lumin.* 2020;228:117627. Available from: <https://linkinghub.elsevier.com/retrieve/pii/S0022231320315945>.
136. Liu Y, Teitelboim A, Fernandez-Bravo A, Yao K, Altoe MVP, Aloni S, et al. Controlled assembly of upconverting nanoparticles for low-threshold microlasers and their imaging in scattering media. *ACS Nano.* 2020;14(2):1508–19. Available from: <https://doi.org/10.1021/acsnano.9b06102>.
137. Isert L, Mehta A, Adams F, Merkel OM. Tracking siRNA–nanocarrier assembly and disassembly using FRET. 2021. p. 383–96. Available from: https://doi.org/10.1007/978-1-0716-1250-7_17.
138. Wang C, Liu Q, Zhang Z, Wang Y, Zheng Y, Hao J, et al. Tumor targeted delivery of siRNA by a nano-scale quaternary polyplex for cancer treatment. *Chem Eng J.* 2021;425:130590. Available from: <https://linkinghub.elsevier.com/retrieve/pii/S1385894721021768>.

139. Zhang S, Gan Y, Shao L, Liu T, Wei D, Yu Y, et al. Virus mimetic shell-sheddable chitosan micelles for siVEGF delivery and FRET-traceable acid-triggered release. *ACS Appl Mater Interfaces*. 2020;12(48):53598–614. Available from: <https://doi.org/10.1021/acsami.0c13023>.
140. Lostalé-Seijo I, Montenegro J. Synthetic materials at the forefront of gene delivery. *Nat Rev Chem*. 2018;2(10):258–77. Available from: <http://www.nature.com/articles/s41570-018-0039-1>.
141. Wang H, Miao W, Wang F, Cheng Y. A self-assembled coumarin-anchored dendrimer for efficient gene delivery and light-responsive drug delivery. *Biomacromolecules*. 2018;19(6):2194–201. Available from: <https://doi.org/10.1021/acs.biomac.8b00246>.
142. Wang H, Ding S, Zhang Z, Wang L, You Y. Cationic micelle: a promising nanocarrier for gene delivery with high transfection efficiency. *J Gene Med*. 2019;21(7). Available from: <https://doi.org/10.1002/jgm.3101>.
143. Jia X, Yin J, He D, He X, Wang K, Chen M, et al. Polyacrylic acid modified upconversion nanoparticles for simultaneous pH-triggered drug delivery and release imaging. *J Biomed Nanotechnol*. 2013;9(12):2063–72. Available from: <http://openurl.ingenta.com/content/xref?genre=article&issn=1550-7033&volume=9&issue=12&spage=2063>.
144. Xu C, Guan X, Lin L, Wang Q, Gao B, Zhang S, et al. pH-responsive natural polymeric gene delivery shielding system based on dynamic covalent chemistry. *ACS Biomater Sci Eng*. 2018;4(1):193–9. Available from: <https://doi.org/10.1021/acsbomaterials.7b00869>.
145. Zuo C, Guo Y, Li J, Peng Z, Bai S, Yang S, et al. A nanoprobe for fluorescent monitoring of microRNA and targeted delivery of drugs. *RSC Adv*. 2021;11(15):8871–8. Available from: <http://xlink.rsc.org/?DOI=D1RA00154J>.
146. Zhang F, Wu Q, Liu H. <sc>NIR</sc> light-triggered nanomaterials-based prodrug activation towards cancer therapy. *WIREs Nanomed Nanobiotechnol*. 2020;12(6). Available from: <https://doi.org/10.1002/wnan.1643>.
147. Le XT, Youn YS. Emerging NIR light-responsive delivery systems based on lanthanide-doped upconverting nanoparticles. *Arch Pharm Res*. 2020;43(1):134–52. Available from: <http://doi.org/10.1007/s12272-020-01208-3>.
148. Lee G, Park Y. Lanthanide-doped upconversion nanocarriers for drug and gene delivery. *Nanomaterials*. 2018;8(7):511. Available from: <http://www.mdpi.com/2079-4991/8/7/511>.
149. Jalani G, Tam V, Vetrone F, Cerruti M. Seeing, targeting and delivering with upconverting nanoparticles. *J Am Chem Soc*. 2018;140(35):10923–31. Available from: <https://doi.org/10.1021/jacs.8b03977>.
150. Tian G, Yin W, Jin J, Zhang X, Xing G, Li S, et al. Engineered design of theranostic upconversion nanoparticles for tri-modal upconversion luminescence/magnetic resonance/X-ray computed tomography imaging and targeted delivery of combined anticancer drugs. *J Mater Chem B*. 2014;2(10):1379. Available from: <http://xlink.rsc.org/?DOI=c3tb21394c>.
151. Chen Y, Ai K, Liu Y, Lu L. Tailor-made charge-conversional nanocomposite for pH-responsive drug delivery and cell imaging. *ACS Appl Mater Interfaces*. 2014;6(1):655–63. Available from: <https://doi.org/10.1021/am404761h>.
152. Yang Y. Upconversion nanophosphors for use in bioimaging, therapy, drug delivery and biosays. *Microchim Acta*. 2014;181(3–4):263–94. Available from: <http://doi.org/10.1007/s00604-013-1139-8>.
153. Chowdhuri AR, Laha D, Chandra S, Karmakar P, Sahu SK. Synthesis of multifunctional upconversion NMOFs for targeted antitumor drug delivery and imaging in triple negative breast cancer cells. *Chem Eng J*. 2017;319:200–11. Available from: <https://linkinghub.elsevier.com/retrieve/pii/S1385894717303455>.
154. Yuan Y, Xu L, Dai S, Wang M, Wang H. A facile supramolecular approach to fabricate multifunctional upconversion nanoparticles as a versatile platform for drug loading, in vivo delivery and tumor imaging. *J Mater Chem B*. 2017;5(13):2425–35. Available from: <http://xlink.rsc.org/?DOI=C6TB03381D>.
155. Wang F, Zhai D, Wu C, Chang J. Multifunctional mesoporous bioactive glass/upconversion nanoparticle nanocomposites with strong red emission to monitor drug delivery and stimulate

- osteogenic differentiation of stem cells. *Nano Res.* 2016;9(4):1193–208. Available from: <http://doi.org/10.1007/s12274-016-1015-z>.
156. Zhao J, Yang H, Li J, Wang Y, Wang X. Fabrication of pH-responsive PLGA(UCNPs/DOX) nanocapsules with upconversion luminescence for drug delivery. *Sci Rep.* 2017;7(1):18014. Available from: <http://www.nature.com/articles/s41598-017-16948-4>.
157. Yu S, Zhang R, Zhao J, Gao X, Li Z, Tan Z, et al. Synthesis and characteristic of the NaYF₄/Fe₃O₄@SiO₂@Tb(DBM)₃·2H₂O/SiO₂ luminomagnetic microspheres with core-shell structure. *J Nanosci Nanotechnol.* 2016;16(4):3791–5. Available from: <https://doi.org/10.1166/jnn.2016.11858>.
158. Kang X, Cheng Z, Li C, Yang D, Shang M, Ma P, et al. Core-shell structured up-conversion luminescent and mesoporous NaYF₄: Yb³⁺/Er³⁺@n SiO₂@m SiO₂ nanospheres as carriers for drug delivery. *J Phys Chem C.* 2011;115(32):15801–11. Available from: <https://doi.org/10.1021/jp203039t>.
159. Dong L, An D, Gong M, Lu Y, Gao H-L, Xu Y-J, et al. PEGylated upconverting luminescent hollow nanospheres for drug delivery and in vivo imaging. *Small.* 2013. Available from: <https://doi.org/10.1002/smll.201300433>.
160. Adhikari C, Mishra A, Nayak D, Chakraborty A. Drug delivery system composed of mesoporous silica and hollow mesoporous silica nanospheres for chemotherapeutic drug delivery. *J Drug Deliv Sci Technol.* 2018;45:303–14. Available from: <https://linkinghub.elsevier.com/retrieve/pii/S1773224717306184>.
161. Zhang K, Zhou D, Wang Z, Zhang Y, He P. Hybrid mesoporous silica nanospheres modified by poly (NIPAM-co-AA) for drug delivery. *Nanotechnology.* 2019;30(35):355604. Available from: <https://doi.org/10.1088/1361-6528/ab209d>.
162. Lin K, Gan Y, Zhu P, Li S, Lin C, Yu S, et al. Hollow mesoporous polydopamine nanospheres: synthesis, biocompatibility and drug delivery. *Nanotechnology.* 2021;32(28):285602. Available from: <https://doi.org/10.1088/1361-6528/abf4a9>.
163. Huang X, El-Sayed IH, Qian W, El-Sayed MA. Cancer cell imaging and photothermal therapy in the near-infrared region by using gold nanorods. *J Am Chem Soc.* 2006;128(6):2115–20. Available from: <https://doi.org/10.1021/ja057254a>.
164. Yang K, Zhang S, Zhang G, Sun X, Lee S-T, Liu Z. Graphene in mice: ultrahigh in vivo tumor uptake and efficient photothermal therapy. *Nano Lett.* 2010;10(9):3318–23. Available from: <https://doi.org/10.1021/nl100996u>.
165. Robinson JT, Tabakman SM, Liang Y, Wang H, Sanchez Casalongue H, Vinh D, et al. Ultra-small reduced graphene oxide with high near-infrared absorbance for photothermal therapy. *J Am Chem Soc.* 2011;133(17):6825–31. Available from: <https://doi.org/10.1021/ja2010175>.
166. Wang J, Wu X, Shen P, Wang J, Shen Y, Shen Y, et al. Applications of inorganic nanomaterials in photothermal therapy based on combinational cancer treatment. *Int J Nanomed.* 2020;15:1903–14. Available from: <https://www.dovepress.com/applications-of-inorganic-nanomaterials-in-photothermal-therapy-based-peer-reviewed-article-IJN>.
167. Xu D, Yang F, Qu D, Wang Z, Gu L, Wu W, et al. Transferred photothermal to photodynamic therapy based on the marriage of ultrathin titanium carbide and up-conversion nanoparticles. *Langmuir.* 2020;36(43):13060–9. Available from: <https://doi.org/10.1021/acs.langmuir.0c02521>.
168. Gnach A, Lipinski T, Bednarkiewicz A, Rybka J, Capobianco JA. Upconverting nanoparticles: assessing the toxicity. *Chem Soc Rev.* 2015;44(6):1561–84. Available from: <http://xlink.rsc.org/?DOI=C4CS00177J>.
169. Tian G, Ren W, Yan L, Jian S, Gu Z, Zhou L, et al. Red-emitting upconverting nanoparticles for photodynamic therapy in cancer cells under near-infrared excitation. *Small.* 2013;9(11):1929–38. Available from: <https://doi.org/10.1002/smll.201201437>.
170. Xu J, Xu L, Wang C, Yang R, Zhuang Q, Han X, et al. Near-infrared-triggered photodynamic therapy with multitasking upconversion nanoparticles in combination with checkpoint blockade for immunotherapy of colorectal cancer. *ACS Nano.* 2017;11(5):4463–74. Available from: <https://doi.org/10.1021/acsnano.7b00715>.

171. Hou Z, Deng K, Li C, Deng X, Lian H, Cheng Z, et al. 808 nm light-triggered and hyaluronic acid-targeted dual-photosensitizers nanoplatfrom by fully utilizing Nd³⁺-sensitized upconversion emission with enhanced anti-tumor efficacy. *Biomaterials*. 2016;101:32–46. Available from: <https://linkinghub.elsevier.com/retrieve/pii/S0142961216301971>.
172. Liang L, Care A, Zhang R, Lu Y, Packer NH, Sunna A, et al. Facile assembly of functional upconversion nanoparticles for targeted cancer imaging and photodynamic therapy. *ACS Appl Mater Interfaces*. 2016;8(19):11945–53. Available from: <https://doi.org/10.1021/acsami.6b00713>.
173. Liu B, Li C, Xing B, Yang P, Lin J. Multifunctional UCNPs@PDA-ICG nanocomposites for upconversion imaging and combined photothermal/photodynamic therapy with enhanced antitumor efficacy. *J Mater Chem B*. 2016;4(28):4884–94. Available from: <http://xlink.rsc.org/?DOI=C6TB00799F>.
174. Yin M, Li Z, Zhou L, Dong K, Ren J, Qu X. A multifunctional upconverting nanoparticle incorporated polycationic hydrogel for near-infrared triggered and synergistic treatment of drug-resistant bacteria. *Nanotechnology*. 2016;27(12):125601. Available from: <https://doi.org/10.1088/0957-4484/27/12/125601>.
175. Han R, Shi J, Liu Z, Wang H, Wang Y. Fabrication of mesoporous-silica-coated upconverting nanoparticles with ultrafast photosensitizer loading and 808 nm NIR-light-triggering capability for photodynamic therapy. *Chem Asian J*. 2017;12(17):2197–201. Available from: <https://doi.org/10.1002/asia.201700836>.
176. Zhang D, Wen L, Huang R, Wang H, Hu X, Xing D. Mitochondrial specific photodynamic therapy by rare-earth nanoparticles mediated near-infrared graphene quantum dots. *Biomaterials*. 2018;153:14–26. Available from: <https://linkinghub.elsevier.com/retrieve/pii/S0142961217306841>.
177. Sonali, Viswanadh MK, Singh RP, Agrawal P, Mehata AK, Pawde DM, et al. Nanotheranostics: emerging strategies for early diagnosis and therapy of brain cancer. *Nanotheranostics*. 2018;2(1):70–86. Available from: <http://www.ntno.org/v02p0070.htm>.
178. Kostiv U, Patsula V, Nocolak A, Podhorodecki A, Větvička D, Poučková P, et al. Phthalocyanine-conjugated upconversion NaYF₄:Yb³⁺/Er³⁺@SiO₂ nanospheres for NIR-triggered photodynamic therapy in a tumor mouse model. *ChemMedChem*. 2017;12(24):2066–73. Available from: <https://doi.org/10.1002/cmdc.201700508>.
179. Wang J, Zhong Y, Wang X, Yang W, Bai F, Zhang B, et al. pH-dependent assembly of porphyrin–silica nanocomposites and their application in targeted photodynamic therapy. *Nano Lett*. 2017;17(11):6916–21. Available from: <https://doi.org/10.1021/acs.nanolett.7b03310>.
180. Buchner M, García Calavia P, Muhr V, Kröninger A, Baeumner AJ, Hirsch T, et al. Photosensitiser functionalised luminescent upconverting nanoparticles for efficient photodynamic therapy of breast cancer cells. *Photochem Photobiol Sci*. 2019;18(1):98–109. Available from: <http://xlink.rsc.org/?DOI=C8PP00354H>.
181. Kuk S, Lee B II, Lee JS, Park CB. Rattle-structured upconversion nanoparticles for near-IR-induced suppression of Alzheimer's β -amyloid aggregation. *Small*. 2017;13(11):1603139. Available from: <https://doi.org/10.1002/smll.201603139>.
182. Yu Q, Rodriguez EM, Naccache R, Forgione P, Lamoureux G, Sanz-Rodríguez F, et al. Chemical modification of temoporfin—a second generation photosensitizer activated using upconverting nanoparticles for singlet oxygen generation. *Chem Commun*. 2014;50(81):12150–3. Available from: <http://xlink.rsc.org/?DOI=C4CC05867D>.
183. Chen F, Zhang S, Bu W, Chen Y, Xiao Q, Liu J, et al. A uniform sub-50 nm-sized magnetic/upconversion fluorescent bimodal imaging agent capable of generating singlet oxygen by using a 980 nm laser. *Chem A Eur J*. 2012;18(23):7082–90. Available from: <https://doi.org/10.1002/chem.201103611>.
184. He L, Brasino M, Mao C, Cho S, Park W, Goodwin AP, et al. DNA-assembled core-satellite upconverting-metal–organic framework nanoparticle superstructures for efficient photodynamic therapy. *Small*. 2017;13(24):1700504. Available from: <https://doi.org/10.1002/smll.201700504>.

185. Cheng T, Marin R, Skripka A, Vetrone F. Small and bright lithium-based upconverting nanoparticles. *J Am Chem Soc.* 2018;140(40):12890–9. Available from: <https://doi.org/10.1021/jacs.8b07086>.
186. Wang P, Fan Y, Lu L, Liu L, Fan L, Zhao M, et al. NIR-II nanoprobes in-vivo assembly to improve image-guided surgery for metastatic ovarian cancer. *Nat Commun.* 2018;9(1):2898. Available from: <http://www.nature.com/articles/s41467-018-05113-8>.
187. Yang Y, Wang P, Lu L, Fan Y, Sun C, Fan L, et al. Small-molecule lanthanide complexes probe for second near-infrared window bioimaging. *Anal Chem.* 2018;90(13):7946–52. Available from: <https://doi.org/10.1021/acs.analchem.8b00603>.
188. Punjabi A, Wu X, Tokatli-Apollon A, El-Rifai M, Lee H, Zhang Y, et al. Amplifying the red-emission of upconverting nanoparticles for biocompatible clinically used prodrug-induced photodynamic therapy. *ACS Nano.* 2014;8(10):10621–30. Available from: <https://doi.org/10.1021/nn505051d>.
189. Dong H, Tang S, Hao Y, Yu H, Dai W, Zhao G, et al. Fluorescent MoS₂ quantum dots: ultrasonic preparation, up-conversion and down-conversion bioimaging, and photodynamic therapy. *ACS Appl Mater Interfaces.* 2016;8(5):3107–14. Available from: <https://doi.org/10.1021/acsami.5b10459>.
190. Hou Z, Deng K, Wang M, Liu Y, Chang M, Huang S, et al. Hydrogenated titanium oxide decorated upconversion nanoparticles: facile laser modified synthesis and 808 nm near-infrared light triggered phototherapy. *Chem Mater.* 2019;31(3):774–84. Available from: <https://doi.org/10.1021/acs.chemmater.8b03762>.
191. Yin M, Ju E, Chen Z, Li Z, Ren J, Qu X. Upconverting nanoparticles with a mesoporous TiO₂ shell for near-infrared-triggered drug delivery and synergistic targeted cancer therapy. *Chem A Eur J.* 2014;20(43):14012–7. Available from: <https://doi.org/10.1002/chem.201403733>.
192. Zhang Z, Suo H, Zhao X, Sun D, Fan L, Guo C. NIR-to-NIR deep penetrating nanoplatforms Y₂O₃: Nd³⁺/Yb³⁺ @SiO₂ @Cu₂S toward highly efficient photothermal ablation. *ACS Appl Mater Interfaces.* 2018;10(17):14570–6. Available from: <https://doi.org/10.1021/acsami.8b03239>.
193. Xing Y, Li L, Ai X, Fu L. Polyaniline-coated upconversion nanoparticles with upconverting luminescent and photothermal conversion properties for photothermal cancer therapy. *Int J Nanomed.* 2016;11:4327–38. Available from: <https://www.dovepress.com/polyaniline-coated-upconversion-nanoparticles-with-upconverting-lumine-peer-reviewed-article-IJN>.
194. Savchuk OA, Carvajal JJ, Brites CDS, Carlos LD, Aguilo M, Diaz F. Upconversion thermometry: a new tool to measure the thermal resistance of nanoparticles. *Nanoscale.* 2018;10(14):6602–10. Available from: <http://xlink.rsc.org/?DOI=C7NR08758F>.
195. Xiao Q, Zheng X, Bu W, Ge W, Zhang S, Chen F, et al. A core/satellite multifunctional nanotheranostic for in vivo imaging and tumor eradication by radiation/photothermal synergistic therapy. *J Am Chem Soc.* 2013;135(35):13041–8. Available from: <https://doi.org/10.1021/ja404985w>.
196. Kanamori T, Sawamura T, Tanaka T, Sotokawa I, Mori R, Inada K, et al. Coating lanthanide nanoparticles with carbohydrate ligands elicits affinity for HeLa and RAW264.7 cells, enhancing their photodamaging effect. *Bioorg Med Chem.* 2017;25(2):743–9. Available from: <https://linkinghub.elsevier.com/retrieve/pii/S0968089616308367>.
197. Bazylińska U, Wawrzyńczyk D, Kulbacka J, Frąckowiak R, Cichy B, Bednarkiewicz A, et al. Polymeric nanocapsules with up-converting nanocrystals cargo make ideal fluorescent bioprobes. *Sci Rep.* 2016;6(1):29746. Available from: <http://www.nature.com/articles/srep29746>.
198. Gulzar A, Xu J, Xu L, Yang P, He F, Yang D, et al. Redox-responsive UCNPs-DPA conjugated NGO-PEG-BPEI-DOX for imaging-guided PTT and chemotherapy for cancer treatment. *Dalt Trans.* 2018;47(11):3921–30. Available from: <http://xlink.rsc.org/?DOI=C7DT04093H>.
199. Cen Y, Deng W-J, Yang Y, Yu R-Q, Chu X. Core-shell-shell multifunctional nanoplatform for intracellular tumor-related mRNAs imaging and near-infrared light triggered photodynamic-photothermal synergistic therapy. *Anal Chem.* 2017;89(19):10321–8. Available from: <https://doi.org/10.1021/acs.analchem.7b02081>.

200. Hou X, Tao Y, Pang Y, Li X, Jiang G, Liu Y. Nanoparticle-based photothermal and photodynamic immunotherapy for tumor treatment. *Int J Cancer*. 2018;143(12):3050–60. Available from: <https://doi.org/10.1002/ijc.31717>.
201. Bu L, Rao L, Yu G, Chen L, Deng W, Liu J, et al. Cancer stem cell-platelet hybrid membrane-coated magnetic nanoparticles for enhanced photothermal therapy of head and neck squamous cell carcinoma. *Adv Funct Mater*. 2019;29(10):1807733. Available from: <https://doi.org/10.1002/adfm.201807733>.
202. Suo H, Zhao X, Zhang Z, Wu Y, Guo C. Upconverting LuVO₄: Nd³⁺/Yb³⁺/Er³⁺ @SiO₂ @Cu₂S hollow nanoplatforms for self-monitored photothermal ablation. *ACS Appl Mater Interfaces*. 2018;10(46):39912–20. Available from: <https://doi.org/10.1021/acsami.8b18184>.
203. Li P, Yan Y, Chen B, Zhang P, Wang S, Zhou J, et al. Lanthanide-doped upconversion nanoparticles complexed with nano-oxide graphene used for upconversion fluorescence imaging and photothermal therapy. *Biomater Sci*. 2018;6(4):877–84. Available from: <http://xlink.rsc.org/?DOI=C7BM01113J>.
204. Xiang G, Xia Q, Liu X, Wang Y, Jiang S, Li L, et al. Upconversion nanoparticles modified by Cu₂S for photothermal therapy along with real-time optical thermometry. *Nanoscale*. 2021;13(15):7161–8. Available from: <http://xlink.rsc.org/?DOI=D0NR09115D>.
205. Lucky SS, Soo KC, Zhang Y. Nanoparticles in photodynamic therapy. *Chem Rev*. 2015;115(4):1990–2042. Available from: <https://doi.org/10.1021/cr5004198>.
206. Hou Y, Yang X, Liu R, Zhao D, Guo C, Zhu A, et al. Pathological mechanism of photodynamic therapy and photothermal therapy based on nanoparticles. *Int J Nanomed*. 2020;15:6827–38. Available from: <https://www.dovepress.com/pathological-mechanism-of-photodynamic-therapy-and-photothermal-therap-peer-reviewed-article-IJN>.
207. Li X, Kwon N, Guo T, Liu Z, Yoon J. Innovative strategies for hypoxic-tumor photodynamic therapy. *Angew Chem Int Ed*. 2018;57(36):11522–31. Available from: <https://doi.org/10.1002/anie.201805138>.
208. Han Y, Chen Z, Zhao H, Zha Z, Ke W, Wang Y, et al. Oxygen-independent combined photothermal/photodynamic therapy delivered by tumor acidity-responsive polymeric micelles. *J Control Release*. 2018;284:15–25. Available from: <https://linkinghub.elsevier.com/retrieve/pii/S0168365918303559>.
209. Wan G, Chen B, Li L, Wang D, Shi S, Zhang T, et al. Nanoscaled red blood cells facilitate breast cancer treatment by combining photothermal/photodynamic therapy and chemotherapy. *Biomaterials*. 2018;155:25–40. Available from: <https://linkinghub.elsevier.com/retrieve/pii/S0142961217307238>.
210. Sozmen F, Kucukoflaz M, Ergul M, Sahin Inan ZD. Nanoparticles with PDT and PTT synergistic properties working with dual NIR-light source simultaneously. *RSC Adv*. 2021;11(4):2383–9. Available from: <http://xlink.rsc.org/?DOI=D0RA09954F>.
211. Chen Q, Wang C, Cheng L, He W, Cheng Z, Liu Z. Protein modified upconversion nanoparticles for imaging-guided combined photothermal and photodynamic therapy. *Biomaterials*. 2014;35(9):2915–23. Available from: <https://linkinghub.elsevier.com/retrieve/pii/S0142961213015305>.
212. Han Y, An Y, Jia G, Wang X, He C, Ding Y, et al. Theranostic micelles based on upconversion nanoparticles for dual-modality imaging and photodynamic therapy in hepatocellular carcinoma. *Nanoscale*. 2018;10(14):6511–23. Available from: <http://xlink.rsc.org/?DOI=C7NR09717D>.
213. Liu X, Chen H, Wang Y, Si Y, Zhang H, Li X, et al. Near-infrared manipulation of multiple neuronal populations via trichromatic upconversion. *Nat Commun*. 2021;12(1):5662. Available from: <https://www.nature.com/articles/s41467-021-25993-7>.
214. Tye KM, Deisseroth K. Optogenetic investigation of neural circuits underlying brain disease in animal models. *Nat Rev Neurosci*. 2012;13(4):251–66. Available from: <http://www.nature.com/articles/nrn3171>.
215. Lin X, Wang Y, Chen X, Yang R, Wang Z, Feng J, et al. Multiplexed optogenetic stimulation of neurons with spectrum-selective upconversion nanoparticles. *Adv Healthc Mater*. 2017;6(17):1700446. Available from: <https://doi.org/10.1002/adhm.201700446>.

216. He L, Zhang Y, Ma G, Tan P, Li Z, Zang S, et al. Near-infrared photoactivatable control of Ca²⁺ signaling and optogenetic immunomodulation. *Elife*. 2015;4. Available from: <https://elifesciences.org/articles/10024>.
217. Ding H, Lu L, Shi Z, Wang D, Li L, Li X, et al. Microscale optoelectronic infrared-to-visible upconversion devices and their use as injectable light sources. *Proc Natl Acad Sci*. 2018;115(26):6632–7. Available from: <http://doi.org/10.1073/pnas.1802064115>.
218. Chen S, Weitemier AZ, Zeng X, He L, Wang X, Tao Y, et al. Near-infrared deep brain stimulation via upconversion nanoparticle-mediated optogenetics. *Science* (80). 2018;359(6376):679–84. Available from: <https://doi.org/10.1126/science.aaq1144>.

Present Status and Future Perspective



Samiran Mondal

Abstract The present chapter illustrates an overview of the application of quantum dots (QDs) and enlightens the future perspective on their potentiality in biology and medicine. The chapter highlights the critical aspects of QDs and the present state-of-the-art applications, both in vitro and in vivo.

Keywords Quantum dots (QDs) · Present status · Future perspective

The concept of artificial atoms or quantum dots (QDs) comes from the reduced dimensionality of semiconducting crystals, i.e., the size of semiconductor particles controls optical and electronic properties called the quantum size effect. QD synthesis, characterization, and applications are still highly active fields of interest to researchers despite being part of mature technologies. During the last three decades, researchers have synthesized QDs by improving monodispersity and size tunability to ameliorate the overall optical properties by exploring different reaction conditions such as solvents, salts, pH, and temperature. The size-dependent tunable emission is attractive for biomedical research since luminescence is commonly used in cell, tissue, and animal experiments, supporting biomedical researchers with many precursors for building tools to address important questions and diagnose and treat diseases. Many researchers convincingly described many optical advantages of QDs over organic fluorophores or dye molecules for biomedical research, owing to their high quantum yield, broad absorption spectra, large Stoke shift, and highly stable. The widely increased interest in QDs has been established as a technological revolution by the tremendous efforts of scientists in chemistry, physics, biology, medical engineering, and pharmaceutical sciences.

QDs present a versatile tool to obtain a series of remarkable results in the fields of cell labeling, cell migration tracking, multiplexed imaging, flow cytometry, fluorescence in situ hybridization, targeted tracing in living cells and animals, real-time in vivo and cellular process imaging, genomic and proteomic detection, pathogen

S. Mondal (✉)

Department of Chemistry, Rammohan College, 102/1-Raja Rammohan Sarani, Kolkata, West Bengal 700009, India

e-mail: samiran@rammohancollege.ac.in; samiran1985@gmail.com

detection, fluorescence resonance energy transfer, and high-throughput screening of biological molecules. However, QD-based agents or probes persist at the laboratory level, far from the commercial application, due to potential biotoxicity. Decades of research and advances in synthesis and bioconjugation strategies of QDs ensure the ability to control the size, polydispersity, colloidal stability, quantum yield, formation of more complex hybrid nanomaterials, and surface properties. However, the spatial distribution of functional groups is not well established in the present demonstrations. Therefore, researchers must address this issue to understand the biological complexity of the intended application. During the last decade, semiconductors nanocrystals with various dopants and hosts have been explored for therapeutic, imaging, biosensors, and drug/gene delivery. Though the doped nanocrystal shows superior results over others, however, straightforward, accessible, and precise manufacturing technology is still much needed. Due to doping, the uniform distribution of vacancies or ions on a large scale must be precisely controllable to achieve tunable optical and magnetic properties. In recent years, the synthesis and multiple surface modifications of NIR QDs with excellent optical performance have been achieved. Nevertheless, efficient synthesis strategies are needed to make NIR QDs (both NIR-I and NIR-II) less toxic, biocompatible, and suitable for *in vivo* applications.

Surface ligands play an important role in controlling the colloidal stability, tuning the fluorescence emission behaviors of QDs, and the energy transfer between QDs and acceptor/donor molecules. Thus, a proper understanding of the role of ligands is the prerequisite for applying QDs in the biomedical field. Still, many challenges remain unsolved in developing QDs-derived luminescent materials for biomedical applications, including the lack of selectivity inside the biological environment, low sensing/probing capabilities (i.e., less selectivity) for biomolecules, e.g., thiols, amino acids, peptides, and proteins, and other supramolecules, lowering the toxicity inside a living organism, even though the diversity of QDs with varieties of surface ligands will offer a promising future in the biomedical field.

Although, due to the toxic effects of semiconductor QDs, the potential applications of QDs in biology and medicine were limited, which have received enormous attention over the past few years. Tissue and cell toxicity of QDs have been studied in many *in vitro* and *in vivo* experiments. The toxicity of QDs depends on the physicochemical properties of individual QDs themselves and environmental conditions, which include size, charge, concentration, outer functional groups and oxidative, photolytic and mechanical stability of the QDs. At the same concentration, the smaller QDs are significantly more toxic than, the bigger QDs. On the other hand, the highly concentrated QDs are more toxic. The mechanism of QD-induced toxicity has been demonstrated in the model cell culture systems. The risk-to-benefit ratio is crucial for the clinical application of QDs before pushing them into the therapeutic and nanomedicine market. Still, several significant limitations and regulatory issues need to be tackled before applying QDs in medicine and *in vivo* imaging in human subjects. Some key issues must consider: the inefficient delivery from low biological specificity, poorly controlled biodistribution to target tissues, inadequate information of biodistribution for *in vivo* studies, assessment of the long-term accumulation

of QDs, and the risk of severe acute and long-term toxicity. Therefore, a comprehensive understanding of the effects owing to physicochemical properties of QDs and their pharmacokinetic and pharmacodynamic behavior, altering the dose, dosing frequency, and side effects are the prerequisite before applying QDs for in vivo study. Efficient risk assessment, risk management, and risk communication are the main challenges to assessing these risks arising from the QDs. Clinical trials or extrapolation of animal-based studies into humans can be detrimental even though the results were promising in animal subjects. Post-clinical trials must be monitored to avoid potential risks. Despite many challenges, the efficiency of QDs in nanomedicine and therapy will grow further in the coming years. Several regulatory agencies approve many nano carrier-related cancer drugs and nano-based drug delivery agents.

Researchers may focus on the heavy metal-free QDs, e.g., C-based QDs, 2D-QDs, as an alternative with lower toxicity. C-based QDs have great potential for bioimaging and have low toxicity in humans, with emissions maxima up to the NIR region of the light spectrum. The optical properties and biocompatibility of C-based QDs depend on surface coating and functionalizing, N-doping, and synthesis routes. Therefore, researchers must focus on the synthesis parameters and doping to obtain high QY with desired optical properties and biocompatibility so that these QDs can be used as an alternative to existing semiconductor QDs. Various approaches have been demonstrated to reduce the toxicity of QDs in recent years. However, the techniques are laboratory-based and need to be comprehensively explored in the biological environment to assess the biodistribution, metabolism, and excretion of QDs. In this perspective, more research is needed to explore hydrophilic QDs for their biological application and labeling of the cell.

Currently, suitable cell-based therapy approaches are required for dynamically targeting cells from the injected site to the final location for effective diagnosis and therapy. Non-immunogenic and non-toxic QDs are one of the most widely studied and used for tagging cells. Uptake dynamics, cytotoxicity, and subcellular and extracellular distribution of non-targeted carboxylated QDs in human bone marrow mesenchymal stem cells (MSCs) at different cell growing densities show promising results in fundamental stem cell biology as well as in cellular therapy, anticancer drug delivery and tissue engineering. QDs can be used to label neuronal proteins in a single-molecule imaging format to illuminate their dynamics and kinetics in their native membranes to understand their roles in the brain. Excellent photostability, prolonged circulation time, lower toxicity and tumor-specific solid homing property suggest its utility in precise tumor detection during surgery and lay a foundation for potential clinical translation of the probe. Development of black phosphorus QDs functionalized with PEG for cancer bioimaging and combined photothermal therapy (PTT) and photodynamic therapy (PDT) significantly promote the therapeutic efficacy of cancer treatment in comparison with PTT or PDT alone, which provides a potential platform for future clinical applications. Applications of QDs in cancer medicine have gained much attention in recent years because of remarkable enhancement in the development of chemotherapy and protein-based drugs. In addition, QDs could play a game-changer in future medicine because of their optical characteristics tailored for bioimaging and biosensing. Innovative surface

functionalization techniques focus on overcoming the long-term toxicity of QDs to reach a pharmaceutical QDs product in clinical and industrial use soon. To increase the quantum yields of the QDs, new method may be developed. Multiple functional groups attached to QD simultaneously will benefit from combined array-based detection systems. Better carriers and increased sensitivity of QDs will result in better-targeted delivery. In recent times, QD and biomolecule conjugates utilized for various in vitro and in vivo imaging are opening new avenues for future research, which focuses on the formation of QDs conjugation for cancer diagnosis and cell labeling. Peptides, antibodies, small molecule ligands, or nucleic acids are covalently bound to QDs because of their larger surface area and are potentially used as fluorescence probes. QDs will be used soon to promote personalized clinical treatment based on the molecular profiles of every patient individually. Additionally, more genome and proteome studies are required where QDs can be incorporated to detect diverse disease biomarkers. Although QDs are widely used in different applications, care should be taken as several concerns have yet to be answered, and the behavior of QDs is yet to be thoroughly characterized.

This book specifically described the story of QDs, from development in chemistry and physics laboratories to applications in biology and medicine. QDs demand more application in the biomedical field due to their unique properties that could substantially progress in vivo and in vitro imaging and gain significant achievement in nanomedicine research. With its potential beneficial role, there is great concern about their exposure to humans and the repercussions to human health, which need to be overcome.